Geologic Assessment of the Ohio Geological Survey CO_2 No. 1 Well in Tuscarawas County and Surrounding Vicinity

APPENDICES ONLY

By

Lawrence H. Wickstrom[1], Ronald A. Riley[1], Frank A. Spane[2], James McDonald[1], Ernie R. Slucher[1], Steven P. Zody[3], Joseph G. Wells[1], and Erica Howat[4]

[1]ODNR, Division of Geological Survey, Columbus, OH
[2]Battelle, Pacific Northwest Division, Richland, WA
[3]Zody Geoscience, Wooster, OH
[4]Battelle, Columbus, OH

Open-File Report 2011-3
Columbus 2011

NOTICE

This report was prepared by the Ohio Department of Natural Resources, Division of Geological Survey as a result of research performed under subcontract to Battelle Memorial Institute, 505 King Avenue, Columbus, OH 43201. This report was supported by the Ohio Air Quality Development Authority and the Ohio Coal Development Office (grant/agreement number CDO/D-05-13) and the U.S. Department of Energy, National Energy Technology Laboratory (NETL), DOE Cooperative Agreement DE-FC26-05NT42589.

Neither the Ohio Department of Natural Resources, nor any agency thereof, nor any of their employees, contractors, or subcontractors, make any warranty, express or implied, nor assume any legal liability or responsibility for the accuracy, completeness, or usefulness of this product. Any use thereof for a purpose other than for which said information or product was intended shall be solely at the risk of the user.

ACKNOWLEDGMENTS

The authors thank the Ohio Coal Development office (OCDO) within the Ohio Air Quality Development Authority (OAQDA) and the Ohio legislature for funding the bulk of this project. Some cost share funding was provided by the U.S. Department of Energy through the Midwest Regional Carbon Sequestration Partnership. We also thank Battelle Memorial Institute who served as project lead. Most importantly, we want to acknowledge Phillip Jagucki who performed as overall project manager during drilling. He was supported on site by Danielle Meggyessy and Matthew Place. Dr. Neeraj Gupta and Joel Sminchak provided technical support; David Ball provided contract management; and Judith Bradbury assisted with public outreach.

Thanks also go to Artex Oil Company and Northwood Energy Corporation, owners of the oil and gas mineral rights to the site, for allowing us to drill and test this very important stratigraphic well. Kilbarger Drilling Company was contracted to perform the drilling, Laurel Oil and Gas was contracted to oversee all site and drilling operations, Bill Rike was retained to perform well site geology, and mudlogging services were provided by Stratagraph, Inc.

Special thanks go to Lisa Van Doren, Donovan Powers, and Ed Kuehnle of the Technology Transfer Group at the ODNR Division of Geological Survey for their patience and skill in helping compile this report and their assistance to team members giving presentations related to this study.

DISCLAIMER

The information contained herein has not been reviewed for technical accuracy and conformity with current ODNR Division of Geological Survey standards for published or open-file materials. The ODNR Division of Geological Survey does not guarantee this information to be free from errors, omissions, or inaccuracies and disclaims any responsibility or liability for interpretations or decisions based thereon.

Cover photo: Thin section photomicrograph of the Beekmantown dolomite at the Ohio Geological Survey CO_2 No. 1 well site at a depth of 7,231 feet (see p. 50).

Recommended citation: Wickstrom, L.H., Riley, R.A., Spane, F.A., McDonald, James, Slucher, E.R., Zody, S.P., Wells, J.G., and Howat, Erica, 2011, Geologic assessment of the Ohio Geological Survey CO_2 No. 1 well in Tuscarawas County and surrounding vicinity: Ohio Department of Natural Resources, Division of Geological Survey Open-File Report 2011-3, 82 p., 5 appendices.

INTENTIONALLY BLANK

APPENDIX 1

DRILLING CHRONOLOGY OF THE OHIO GEOLOGICAL SURVEY CO_2 NO. 1 WELL

Battelle Memorial Institute was the prime contractor to the State of Ohio on this stratigraphic test well. Kilbarger Drilling Company's Rig #17 was contracted to perform the drilling, and Laurel Oil and Gas Corporation was contracted to oversee all site and drilling operations. William M. Rike was retained to perform wellsite geologic analysis, and mudlogging services were provided by Stratagraph, Inc. Other vendors involved included: Universal Well Services (cement); Eastern Reservoir Services (pressure and injection testing); Schlumberger (logging, sidewall cores); Stone Drilling (service rig); A & A Excavating (site preparation and restoration); Ken Miller Supply, Inc. and McJunkin Corporation (casing and tubing); Baker Oil Tools (packer assemblies); Omni Laboratories, Inc. (core analyses); Smith Technologies (drill bits); and Weatherford (drill tools rental, blow-out preventer, etc.).

The drill site was located in Tuscarawas County, Salem Township, just east of State Route 36 between the towns of Port Washington and Gnadenhutten, Ohio. The specific location is 4,360 feet from the north line and 70 feet from the east line of Salem Township at an elevation of 917 feet above sea level. The landowner of the site is Holmes Limestone Company; Northwood Energy Corporation held the lease rights to drill on this property. Further, Northwood Energy, by previous agreement, had a partnership arrangement with Artex Oil Company for all deep oil and gas rights, below the "Clinton" sandstone. All parties agreed to allow the state to drill the deep stratigraphic test well with provisions for turning the well over to the proper lessee in the event significant hydrocarbons were discovered.

A stratigraphic-test well permit was issued to the ODNR Division of Geological Survey by the ODNR Division of Mineral Resources Management on April 18, 2007. The issued American Petroleum Institute-compliant well permit number is 34157253340000.

Drilling commenced on May 5, 2007, with drilling a 20-inch hole to a depth of 32 feet—through all unconsolidated materials and into bedrock. On May 6, the hole was reamed and 22-inch casing was driven into place to 32 feet. Drilling continued on fluid with a 20-inch bit to a depth of 132 feet, at which point 16-inch casing was set and cemented in place on May 14. Cement with 100 sacks Class A cement, 3% CaCl, 1/4# Flake; 10 barrels returned. Drilling then resumed using air and 15-inch bits (both hammer and tri-cone) until a depth of 1,215 feet was reached on May 16, at which point the drilling was halted, the hole was cleaned with air and foam sweep, loaded with native fluid and circulated, and the first round of geophysical logs run (table 1). After logging, 11.75-inch casing was lowered into the well and cemented in place with circulation to surface (cement from 11,215 feet to surface). It was cemented with 260 sacks of Unfill lite 6% gel, 3% CaCl; 200 sacks Class A cement; 20 barrels returned. The well was drilled to this depth before casing to ensure all potential fresh water zones and known shallow aquifers were set behind the casing that was then cemented back to the surface. This protects these water-bearing zones from all future drilling fluids and seals the water zones from introducing water into the borehole while drilling continues.

Samples of the rock material drilled were collected every five feet from a depth of 40 feet through 1,215 feet. Because lithologic changes can occur faster in the shallow Mississippian strata, a smaller sample interval was taken. Throughout the rest of the drilling, samples were taken every 10 feet. All samples from the well are available for inspection at the Ohio Geological Survey H. R. Collins Core and Sample Repository.

Drilling resumed on May 18 using 11-inch bits on air. At this stage a blow out preventer was installed and pressure tested. These devices are used to shut down the flow of the well in case any large volumes of gas and/or oil are encountered. Drilling was halted again on May 22 at a depth of 4,964 feet, the hole cleaned and loaded with brine, and the second stage of geophysical logs were run (table 1, log run 2). It was also planned at this point to obtain approximately 50 sidewall cores of various stratigraphic intervals from 1,215 feet through 4,964 feet, to include the Ohio Shale, Oriskany Sandstone, Bass Islands Dolomite, Salina Group, Lockport Dolomite, and the Cataract Group ("Clinton" sandstone interval). Unfortunately, the logging/coring vendor's sidewall coring tool failed on the first run (retrieving only nine sidewall cores in the "Clinton" sandstone and overlying Rochester Shale), and the vendor was unable to repair or bring another tool in an economic amount of time. On May 24, an $8^5/_8$-inch casing was run in the hole and cemented in place with 130 sacks of thixotropic 10-4-2 cement.

On May 26, drilling on air was resumed with $7^7/_8$-inch bits. On May 28, drillers encountered significant natural gas shows at 6,926 feet (300 units) and 6,956 feet (700 units) in the Black River Group. The well was switched to drilling on fluid at 7,092 feet. The rate of penetration began to decrease significantly at these depths. On June 5, at a depth of 8,410 feet, after removing all drill pipe from the hole to replace a drill bit, the crown block bearings went out requiring repairs that took 2 days.

Drilling was resumed on June 7 and reached a total depth of 8,695 feet—65 feet into the crystalline Precambrian—on June 9. The hole was then cleaned and loaded with brine and the third stage, and the most extensive suite of geophysical logs were run followed by the Schlumberger Pressure Express tool—the first time this tool was used in the Appalachian Basin.

After logging, the $4^1/_2$-inch casing was installed and cemented. On June 13, the Kilbarger crew began to rig down and leave the site. A service rig arrived and began to rig up on July 14. A packer tubing string was used for perforated-zone isolation, and 850 gallons of hydrochloric (HCL) acid were subsequently injected into the composite basal sandstone perforated intervals for test zone development on July 19, 2007. Fluid was swabbed from the composite perforated zone after acid injection and continued to July 20, 2007. A total of 3,970 gal (94.5 bbl) of test system fluid were removed during the swabbing activity.

Following the development and subsequent hydraulic testing of the basal sandstone, a bridge was set above the basal sandstone at a depth of 7,530 feet, and the Rose Run sandstone was perforated. The bridge plug packer and a packer tubing string were used for perforated-zone isolation, and 800 gallons of HCL acid were subsequently injected into the composite Rose Run perforated intervals for test zone development on July 24, 2007. Swabbing of fluid from the composite perforated zone was initiated after acid injection and continued to July 25, 2007. Fluid weight density, pH, and chloride concentration were monitored within the discharge water removed during swabbing as a qualitative indicator of test zone development. A total of 10,330 gal (246 bbl) of test system fluid were removed during the swabbing activity.

After the reservoir testing, the well was then plugged with cement to the top of the Rose Run sandstone. After service rig was released, all remaining materials were removed from the drill site. The site was then graded to the specifications of the leaseholder and planted in grass. The well was then turned over to Artex Oil Company, per the pre-drill agreement with the leaseholders. Artex perforated the casing in the Beekmantown dolomite (7,229–7,246 ft), performed an acid job, ran tubing, and placed the well in production shortly after. In 2008, the well's first full year of production, the reported amounts were 338,291 MCFG and 1,768 BO. Through 2009 (the last full year that records are available), the well had reported total production of 553,311 MCFG, 3,770 BO, and 536 bbl of brine.

INTENTIONALLY BLANK

APPENDIX 2

PETROGRAPHIC STUDY
OF
ROTARY SIDEWALL CORES
FOR
OHIO DIVISION OF GEOLOGICAL SURVEY
CO_2 NO. 1
TUSCARAWAS COUNTY, OHIO

OMNI FILE NO.: HH-38266

Weatherford®
LABORATORIES

INTENTIONALLY BLANK

(832) 237-4000
8845 Fallbrook • Houston, Texas 77064

June 2, 2008

Mr. Phil Jagucki
Ohio Division of Geological Survey
505 King Avenue
Columbus, OH 43201-2693

SUBJECT: *Final Report - Petrographic Study of Rotary Sidewall Cores*
CO_2 No. 1
Tuscarawas County, Ohio
OMNI File No.: HH-38266

Dear Mr. Jagucki:

A petrographic study of selected rotary sidewall cores from the above referenced well was completed. A total of eighty-two (82) rotary sidewall cores were submitted for thin section preparation and photography (Table 1; attachment). Sixteen were selected (16) for detailed thin section analysis (including point count modal analysis), eight (8) for general thin section description, eighteen (18) for X-ray diffraction (XRD) analysis, and eighteen (18) for scanning electron microscopy (SEM) analysis.

It has been a pleasure to provide this study for Ohio Division of Geological Survey. Two (2) copies and two (2) CDs of this report have been prepared and provided. Additional copies can be prepared if you require them.

Please feel free to contact us if you have any questions concerning this report or if we can be of further service.

Sincerely,
OMNI LABORATORIES

Michael Dixon
Manager, Geologic Services

Douglas J. Schultz
Geologic Advisor

Nathan A. Treptow
Geologist

Charles Manske
Senior Geologist

The interpretations or opinions expressed represent the best judgment of OMNI Laboratories, Inc. and it assumes no responsibility and makes no warranty or representations, as to the productivity, proper operation, or profitableness of any oil, gas or any other mineral well. These analyses, opinions or interpretations are based on observations and materials supplied by the client for whom this report is made.

INTENTIONALLY BLANK

APPENDIX A

PETROGRAPHIC ANALYTICAL PROCEDURES

X-ray Diffraction (XRD) Analysis

A representative portion of each sample was dried, extracted if necessary, and then ground in a Brinkman MM-2 Retsch Mill to a fine powder (10-15 microns). This ground sample was next loaded into an alloy sample holder. This “bulk” sample mount was scanned with a Bruker AXS D4 Endeavor X-ray diffractometer using copper K-alpha radiation at standard scanning parameters. Computer analysis of the diffractograms provide identification of mineral phases and semiquantitative analysis of the relative abundance (in weight percent) of the various mineral phases. It should also be noted that X-ray diffraction **does not** allow the identification of non-crystalline (amorphous) material, such as organic material and volcanic glass.

An oriented clay fraction mount was also prepared for each sample from the ground powder. The samples were further size fractionated by centrifuge to separate the <4 micron fraction. Ultrasonic treatment was used to suspend the material, then a dispersant was used to prevent flocculation when noted. The solution containing the clay fraction was then passed through a Fisher filter membrane apparatus allowing the solids to be collected on a cellulose membrane filter. These solids were then mounted on a glass slide, dried, and scanned with the Bruker AXS diffractometer. The oriented clay mount was then glycolated and another diffractogram prepared to identify the expandable, water sensitive minerals. The slide is heat-treated and scanned with the same parameters to aid in distinguishing kaolinite and chlorite.

Standard Scanning Parameters:

For both bulk and clay
Cu K-alpha1 0.15406 nm and K-alpha2 0.1544390 nm, the ratio is 0.5
50kv
40ma
A primary soller slit
Radius 217 mm
A graphite monochromator
A 0.2 mm detection slit

For bulk
Divergence slit and antiscatter slit 1.5 degree or 3mm
Step 0.02 degree
1.2 second per step
From 5 to 70 degree 2 theta

For clay
Divergence slit and antiscatter slit 0.5 degree or 1mm
Step 0.025 degree
1.2 second per step
From 2 to 30 degree 2 theta

Thin Section Petrographic Analyses

Samples selected for thin section analysis were prepared by first vacuum impregnating with blue-dyed epoxy. The samples were then mounted on an optical glass slide and cut and lapped in water to a thickness of 0.03 mm (30 microns). The samples were stained for potassium (K-) feldspar using the method described by Bailey and Stevens in 1960, and by Laniz in 1964. First, hydrofluoric acid (HF) is used to etch the surface. Then sodium cobaltinitrite is used to stain any K-feldspar on that surface a yellow color. Next, the sections were stained using Alizarin Red S for calcite, and potassium ferricyanide for ferroan dolomite/calcite. When present, dolomite will appear clear, ankerite will appear turquoise blue, calcite will appear red, and ferroan calcite will appear purple.

Standard point count analysis was utilized to obtain the composition of framework grains, as well as abundance of diagenetic, and pore system components. A modal analysis consisting of ~300 point counts was completed for each thin section using magnifications ranging from 100X to 400X. Reflected light microscopy was utilized in the determination of opaque minerals, specifically iron/titanium oxides and pyrite. The modal analyses include a detailed evaluation of secondary pores and micropores; i.e., specifically counting the grain type or other rock components in which these pore types occur.

Scanning Electron Microscopy (SEM) Analysis

Samples selected for scanning electron microscopy analysis were first broken, or split, to expose fresh surfaces. The samples were then mounted on sample holders with a conductive carbon paste and coated with palladium gold in a “cool” sputter coater to prevent heat damage to sensitive clay minerals or friable samples. The samples were analyzed with a Quanta 200 Digital Scanning Electron Microscope and Oxford Inca X-sight Energy Dispersive Spectrometer (EDS).

Ohio Division of Geological Survey
CO 2 No. 1
Tuscarawas County, OH
HH-38266

Formation	Sample Number	Sample Depth (ft.)	Thin Section Preparation	General Thin Section Description	Detailed Thin Section Analysis	XRD (Bulk and Clay)	SEM Analysis
Rochester Shale	1-1R	4605.0	X				
Clinton Sandstone	1-2R	4760.0	X				
Clinton Sandstone	1-3R	4771.0	X		X	X	X
Clinton Sandstone	1-4R	4776.0	X				
Clinton Sandstone	1-5R	4790.0	X		X	X	X
Clinton Sandstone	1-6R	4816.0	X				
Clinton Sandstone	1-7R	4821.0	X				
Clinton Sandstone	1-8R	4834.0	X				
Clinton Sandstone	1-9R	4840.0	X		X	X	X
Cincinnati Group (Undiff.)	1-10R	6064.0	X	X			
Utica Shale	1-11R	6141.0	X	X			
Point Pleasant Formation	1-12R	6282.0	X	X			
Trenton Limestone	1-13R	6336.0	X	X			
Trenton Limestone	1-14R	6396.0	X	X			
Trenton Limestone	1-15R	6490.0	X				
Black River Group	1-16R	6524.0	X				
Black River Group	1-17R	6566.0	X				
Black River Group	1-18R	6620.0	X				
Black River Group	1-19R	6750.0	X				
Black River Group	1-20R	6794.0	X		X	X	X
Black River Group	1-21R	6808.0	X				
Black River Group	1-22R	6844.0	X		X	X	X
Black River Group	1-23R	6871.0	X				
Black River Group	1-24R	6936.0	X				
Black River Group	1-25R	6940.0	X		X	X	X
Black River Group	1-26R	7030.0	X				
Black River Group	1-27R	7128.0	X				
Black River Group	1-28R	7142.0	X				
Wells Creek Formation	1-29R	7192.0	X	X			
Beekmantown Dolomite	1-30R	7226.0	X		X	X	X
Beekmantown Dolomite	1-31R	7231.0	X		X	X	X
Beekmantown Dolomite	1-32R	7235.0	X		X	X	X
Beekmantown Dolomite	1-33R	7248.0	X				
Beekmantown Dolomite	1-34R	7296.0	X				
Beekmantown Dolomite	1-35R	7328.0	X				
Beekmantown Dolomite	1-36R	7365.0	X				
Rose Run Sandstone	1-37R	7377.0	X		X	X	X
Rose Run Sandstone	1-38R	7387.0	X				
Rose Run Sandstone	1-39R	7392.0	X		X	X	X
Rose Run Sandstone	1-40R	7414.0	X				
Rose Run Sandstone	1-41R	7426.0	X				
Rose Run Sandstone	1-42R	7434.0	X				
Rose Run Sandstone	1-43R	7441.0	X		X	X	X
Rose Run Sandstone	1-44R	7459.0	X				
Rose Run Sandstone	1-45R	7480.0	X				
Rose Run Sandstone	1-46R	7495.0	X				
Rose Run Sandstone	1-47R	7506.0	X		X	X	X

Formation	Sample Number	Sample Depth (ft.)	Thin Section Preparation	General Thin Section Description	Detailed Thin Section Analysis	XRD (Bulk and Clay)	SEM Analysis
Copper Ridge Dolomite	1-48R	7528.0	X				
Copper Ridge Dolomite	1-49R	7579.0	X	X			
Copper Ridge Dolomite	1-50R	7692.0	X		X	X	X
Copper Ridge Dolomite	1-51R	7730.0	X				
Copper Ridge Dolomite	1-52R	7742.0	X				
Copper Ridge Dolomite	1-53R	7818.0	X				
Copper Ridge Dolomite	1-54R	7868.0	X				
Conasauga group	1-55R	7931.0	X				
Conasauga group	1-56R	7991.0	X				
Conasauga group	1-57R	8014.0	X				
Conasauga group	1-58R	8066.0	X				
Conasauga group	1-59R	8138.0	X				
Conasauga group	1-60R	8176.0	X				
Conasauga group	1-61R	8274.0	X	X			
Conasauga group	1-62R	8350.0	X				
Conasauga group	1-63R	8421.0	X				
Conasauga group	1-64R	8451.0	X				
Conasauga group	1-65R	8467.0	X				
Conasauga group	1-66R	8495.0	X				
Cambrian Basal Sandstone	1-67R	8528.0	X				
Cambrian Basal Sandstone	1-68R	8538.0	X		X	X	X
Cambrian Basal Sandstone	1-69R	8544.0	X				
Cambrian Basal Sandstone	1-70R	8549.0	X				
Cambrian Basal Sandstone	1-71R	8555.0	X				
Cambrian Basal Sandstone	1-72R	8561.0	X		X	X	X
Cambrian Basal Sandstone	1-73R	8570.0	X				
Cambrian Basal Sandstone	1-74R	8583.0	X		X	X	X
Cambrian Basal Sandstone	1-75R	8585.0	X				
Cambrian Basal Sandstone	1-76R	8590.0	X				
Cambrian Basal Sandstone	1-77R	8603.0	X				
Cambrian Basal Sandstone	1-78R	8610.0	X				
Pre Cambrian Basement	1-79R	8628.0	X		X	X	X
Pre Cambrian Basement	1-80R	8643.0	X				
Pre Cambrian Basement	1-81R	8659.0	X				
Pre Cambrian Basement	1-82R	8688.0	X				

APPENDIX B

X-RAY DIFFRACTION DATA

INTENTIONALLY BLANK

OMNI LABORATORIES, INC.
X-RAY DIFFRACTION
(WEIGHT %)

Client: Ohio Division of Geological Survey
Well: CO_2 No. 1
Area: Tuscarawas County, OH
Sample Type: Rotary Sidewall Core

File No: HH-38266
Date: 3/28/2008
Analyst: G. Walker

Formation Name	Sample Number	Sample Depth (ft)	CLAYS				CARBONATES			OTHER MINERALS						TOTALS		
			Chlorite	Kaolinite	Illite	Mx I/S*	Calcite[1]	Dol/Ank	Siderite	Quartz	K-spar	Plag.	Pyrite	Hematite	Barite	Clays	Carb.	Other
Clinton Sandstone	1-3R	4771.0	1	1	3	Tr	Tr	0	Tr	92	1	1	1	Tr	0	5	Tr	95
Clinton Sandstone	1-5R	4790.0	3	1	8	1	Tr	Tr	Tr	85	1	1	Tr	0	0	13	Tr	87
Clinton Sandstone	1-9R	4840.0	1	Tr	4	Tr	0	2	Tr	90	1	1	1	0	0	5	2	93
Black River Group	1-20R	6794.0	1	Tr	1	Tr	91	4	Tr	2	Tr	Tr	1	0	0	2	95	3
Black River Group	1-22R	6844.0	Tr	Tr	Tr	Tr	96	3	Tr	1	Tr	Tr	Tr	0	0	Tr	99	1
Black River Group	1-25R	6940.0	Tr	Tr	Tr	Tr	98	2	Tr	Tr	Tr	Tr	Tr	0	0	Tr	100	Tr
Beekmantown Dolomite	1-30R	7226.0	Tr	Tr	Tr	Tr	1	99	Tr	Tr	Tr	Tr	Tr	0	0	Tr	100	Tr
Beekmantown Dolomite	1-31R	7231.0	Tr	Tr	Tr	Tr	1	99	Tr	Tr	Tr	Tr	Tr	0	0	Tr	100	Tr
Beekmantown Dolomite	1-32R	7235.0	Tr	Tr	Tr	Tr	Tr	100	Tr	Tr	Tr	Tr	Tr	0	0	Tr	100	Tr
Rose Run Sandstone	1-37R	7377.0	1	1	1	1	0	5	Tr	89	1	1	Tr	0	0	4	5	91
Rose Run Sandstone	1-39R	7392.0	1	1	1	1	0	8	Tr	85	1	1	1	0	0	4	8	88
Rose Run Sandstone	1-43R	7441.0	1	1	3	1	Tr	2	Tr	74	17	1	Tr	0	0	6	2	92
Rose Run Sandstone	1-47R	7506.0	1	1	2	1	Tr	1	Tr	89	4	1	Tr	0	0	5	1	94
Copper Ridge Dolomite	1-50R	7692.0	Tr	Tr	1	Tr	Tr	89	Tr	5	3	1	1	0	0	1	89	10
Cambrian Basal Sandstone	1-68R	8538.0	1	Tr	1	Tr	Tr	11	Tr	72	13	1	1	0	0	2	11	87
Cambrian Basal Sandstone	1-72R	8561.0	1	1	2	1	1	3	Tr	68	21	1	1	0	0	5	4	91
Cambrian Basal Sandstone	1-74R	8583.0	1	Tr	2	Tr	1	19	Tr	62	13	2	Tr	0	0	3	20	77
Crystalline Basement	1-79R	8628.0	11	22	3	Tr	2	2	Tr	18	16	23	3	0	0	36	4	60

* Ordered interstratified mixed-layer illite/smectite; Approximately 5-10% expandable interlayers

[1] May include the Fe-rich variety

INTENTIONALLY BLANK

APPENDIX C

THIN SECTION MODAL ANALYSIS

INTENTIONALLY BLANK

THIN SECTION MODAL ANALYSIS

Ohio Division of Geological Survey
CO_2 No. 1 Well
Tuscarawas County, Ohio

Sample Number	1-20R	1-22R	1-25R	1-30R
Depth (ft):	6794.0	6844.0	6940.0	7226.0
Formation:	Trenton Black River	Trenton Black River	Trenton Black River	Beekmantown
Rock Name (Dunham): Dolomite Fabric (Sibley and Gregg):	Skeletal Peloidal Lime Packstone / Grainstone	Skeletal Peloidal Lime Grainstone / Packstone	Skeletal Peloidal Lime Grainstone / Packstone	Medium Crystalline Dolostone
Sedimentary Structures	Discont. Clay Laminations; Microstylolites	Massive; Possibly Burrow-Mottled	Irregular Bedding; Microstylolites	Planar S Fabric
ALLOCHEMS				
Fossil Fragments	**26**	**19**	**23**	**0**
Pelecypod	20	19	18	0
Gastropod	0	0	0	0
Foraminifera	0	0	0	0
Brachipod	1	tr	1	0
Ostracod	0	0	1	0
Coral	0	0	0	0
Bryozoan	tr	tr	tr	0
Echinoid/Crinoid	tr	tr	0	0
Undifferentiated	5	4	3	0
Other Allochems	**42**	**40**	**39**	**0**
Ooids / Coated Grains	0	0	0	0
Peloids	42	40	39	0
Grapestone	0	0	0	0
OTHER DETRITAL GRAINS	**tr**	**tr**	**2**	**tr**
Siliciclastics	tr	0	0	0
Glauconite	0	0	0	0
Phosphate	0	0	0	0
Plant Fragments	tr	tr	2	tr
MATRIX	**11**	**tr**	**8**	**0**
Clay	0	0	0	0
Micrite (Lime Mud)	11	tr	8	0
Microsparite	0	0	0	0
CEMENT/REPLACEMENT	**14**	**32**	**27**	**94**
Authigenic Clay	tr	1	0	1
Silica	0	tr	0	0
Sparry Calcite	9	28	18	0
Dolomite	4	2	5	93
Fe-rich Dolomite	0	0	0	0
Ankerite	0	0	0	0
Pyrite	tr	1	1	tr
Calcite Fracture Fill	1	0	3	0
Fe / Ti Oxides	0	0	tr	0
Bitumen	0	0	tr	tr
POROSITY	**7**	**5**	**1**	**6**
Interparticle	tr	tr	tr	tr
Intercrystalline	tr	tr	tr	3
Intraparticle	3	2	tr	1
Intracrystalline	0	0	0	1
Moldic	tr	tr	tr	1
Vuggy	0	0	0	tr
Fenestral	0	0	0	0
Fracture	0	0	0	0
Microscopic	4	3	1	tr
TOTALS:	**100**	**100**	**100**	**100**

THIN SECTION MODAL ANALYSIS

Ohio Division of Geological Survey
CO_2 No. 1 Well
Tuscarawas County, Ohio

Sample Number	1-31R	1-32R	1-50R
Depth (ft):	7231.00	7235.00	7692.00
Formation:	Beekmantown	Beekmantown	Copper Ridge
Rock Name (Dunham): Dolomite Fabric (Sibley and Gregg):	Fine to Medium Crystalline Dolomite	Very Fine Crystalline Dolostone	Medium Crystalline Skeletal Peloidal Dolostone
Sedimentary Structures	Overprint of Breccia; Planar E Dolomite Fabric	Laminated; Planar S Dolomite Fabric	Massive; Non-Planar Dolomite Fabric
ALLOCHEMS	**tr**	**tr**	**0**
Fossil Fragments	**tr**	**tr**	**0**
Pelecypod (ghost)	tr	0	0
Gastropod	0	0	0
Foraminifera	0	0	0
Brachipod	0	0	0
Sponge	0	0	0
Coral	0	0	0
Bryozoan	0	0	0
Echinoid/Crinoid	0	0	0
Unidentified Fossil Fragments	tr	tr	0
Other Allochems	**0**	**0**	**0**
Ooids / Coated Grains	0	0	0
Peloids	0	tr	0
Grapestone	0	0	0
OTHER DETRITAL GRAINS	**tr**	**4**	**23**
Siliciclastics	0	tr	5
Glauconite	0	0	0
Phosphate	0	0	tr
Unidentified Ghost Grains	tr	3	17
Plant Fragments	tr	1	1
MATRIX	**tr**	**0**	**0**
Clay	0	0	0
Micrite (Lime Mud)	tr	0	0
Microsparite	0	0	0
CEMENT/REPLACEMENT	**86**	**95**	**76**
Authigenic Clay	tr	0	0
Silica	0	0	0
Sparry Calcite	0	tr	0
Dolomite	83	84	75
Fe-rich Dolomite	0	0	0
Ankerite	0	0	0
Pyrite	0	1	1
Calcite Fracture Fill	0	0	0
Fe / Ti Oxides	0	0	0
Bitumen	3	10	0
POROSITY	**14**	**1**	**0**
Interparticle	2	tr	tr
Intercrystalline	4	tr	0
Intraparticle	tr	0	tr
Intracrystalline	0	tr	0
Moldic	5	0	0
Vuggy	2	0	0
Fenestral	0	0	0
Fracture	0	0	0
Microscopic	1	1	1
TOTALS:	**100**	**100**	**100**

THIN SECTION MODAL ANALYSIS

Ohio Division of Geological Survey
CO_2 No. 1
Tuscarawas Co., Ohio
Sample Type: Rotary Sidewall Core Analyst: C. Manske

DEPTH (ft):	**4771.0**	**4790.0**	**4840.0**	**7377.0**
SAMPLE NO.:	**1-3R**	**1-5R**	**1-9R**	**1-37R**
Formation	**Clinton Sandstone**	**Clinton Sandstone**	**Clinton Sandstone**	**Rose Run Sandstone**
Grain Size Avg. (mm):	**0.10**	**0.11**	**0.15**	**0.48**
Grain Size Range (mm):	**<0.01-0.32**	**<0.01-0.38**	**0.03-0.32**	**0.09-1.09**
Sorting:	**Moderately Well**	**Moderate**	**Well**	**Moderately Well**
Fabric:	**Vaguely G.S.-zoned**	**Laminated**	**Near-Massive**	**Vaguely G.S.-zoned**
Rock Type:	**Quartzarenite**	**Sublitharenite**	**Sublith./Subark.**	**Quartzarenite**
FRAMEWORK GRAINS				
Quartz	**68**	**51**	**68**	**77**
Monocrystalline	63	48	61	70
Polycrystalline	5	3	7	7
Feldspar	**1**	**3**	**2**	**1**
K-Feldspar	1	1	1	1
Plagioclase	tr	2	1	tr
Lithic Fragments	**1**	**4**	**2**	**tr**
Plutonic	tr	tr	1	tr
Volcanic	tr	tr	tr	0
Metamorphic	1	2	1	0
Chert	tr	tr	tr	tr
Mudstone	tr	2	tr	0
Carbonate	0	0	0	0
Volcanic Glass	0	0	0	0
Accessory Grains	**tr**	**2**	**1**	**0**
Muscovite	tr	2	tr	0
Biotite	tr	tr	1	0
Heavy Minerals*	tr	tr	tr	0
ENVIRON. INDICATORS	**2**	**3**	**tr**	**tr**
Carbonaceous Material	2	3	tr	tr
Glauconite	0	0	tr	0
Phosphatic Grains	0	tr	tr	0
DETRITAL MATRIX	**5**	**16**	**0**	**0**
CEMENT/REPLACEMENT	**18**	**14**	**18**	**13**
Pore-lining Clay	2	2	2	1
Kaolinite	0	tr	0	0
Other Pore-filling Clay	tr	1	tr	tr
Quartz Overgrowths	9	10	13	12
Feldspar Overgrowths	tr	tr	tr	tr
Calcite	0	0	0	0
Dolomite	0	tr	2	0
Ankerite	0	tr	tr	0
Siderite	tr	tr	tr	tr
Pyrite	2	1	1	tr
Fe/Ti Oxides	5	tr	tr	tr
Bitumen	tr	tr	tr	0
POROSITY	**5**	**6**	**9**	**9**
Primary	1	tr	3	4
Secondary	2	3	4	5
Microscopic	2	3	2	tr
TOTALS:	**100**	**99**	**100**	**100**

*Epidote, Rutile, Sphene, Tourmaline, Zircon

THIN SECTION MODAL ANALYSIS

Ohio Division of Geological Survey
CO_2 No. 1
Tuscarawas Co., Ohio
Sample Type: Rotary Sidewall Core Analyst: C. Manske

DEPTH (ft):	**7392.0**	**7441.0**	**7506.0**	**8538.0**
SAMPLE NO.:	**1-39R**	**1-43R**	**1-47R**	**1-68R**
Formation	**Rose Run Sandstone**	**Rose Run Sandstone**	**Rose Run Sandstone**	**Cambrian Basal Sandstone**
Grain Size Avg. (mm):	**0.35**	**0.31**	**0.27**	**0.23**
Grain Size Range (mm):	**<0.01-1.06**	**0.06-1.23**	**0.03-0.97**	**0.05-1.01**
Sorting:	**Moderate**	**Moderate**	**Moderately Poor**	**Poor**
Fabric:	**Grain Size-zoned**	**Grain Size-zoned**	**Dolomite Cmt.-zoned**	**Grain Size-zoned**
Rock Type:	**Quartzarenite**	**Subarkose**	**Subarkose**	**Arkose**
FRAMEWORK GRAINS				
Quartz	**67**	**62**	**46**	**43**
Monocrystalline	61	54	41	37
Polycrystalline	6	8	5	6
Feldspar	**2**	**17**	**9**	**22**
K-Feldspar	2	16	8	20
Plagioclase	tr	1	1	2
Lithic Fragments	**1**	**1**	**tr**	**1**
Plutonic	1	1	tr	1
Volcanic	0	tr	0	0
Metamorphic	tr	0	0	tr
Chert	tr	tr	tr	tr
Mudstone	tr	0	0	tr
Carbonate	0	0	0	0
Volcanic Glass	0	0	0	0
Accessory Grains	**tr**	**tr**	**tr**	**tr**
Muscovite	tr	tr	tr	tr
Biotite	tr	0	tr	tr
Heavy Minerals*	tr	tr	0	tr
ENVIRON. INDICATORS	**1**	**tr**	**1**	**tr**
Carbonaceous Material	1	tr	1	tr
Glauconite	0	0	0	0
Phosphatic Grains	0	0	0	tr
DETRITAL MATRIX	**1**	**0**	**0**	**0**
CEMENT/REPLACEMENT	**17**	**10**	**33**	**25**
Pore-lining Clay	2	tr	1	1
Kaolinite	0	0	0	0
Other Pore-filling Clay	tr	tr	tr	tr
Quartz Overgrowths/Massive	14	8	5	8
Feldspar Overgrowths	0	2	1	2
Calcite	0	0	0	0
Dolomite	0	0	23	12
Ankerite	0	0	0	0
Siderite	0	0	0	0
Pyrite	1	0	1	1
Fe/Ti Oxides	tr	0	1	tr
Bitumen	0	0	1	1
POROSITY	**11**	**10**	**11**	**9**
Primary	5	6	3	2
Secondary	5	3	5	4
Microscopic	1	1	3	3
TOTALS:	**100**	**100**	**100**	**100**

*Tourmaline

THIN SECTION MODAL ANALYSIS

Ohio Division of Geological Survey
CO_2 No. 1
Tuscarawas Co., Ohio
Sample Type: Rotary Sidewall Core Analyst: C. Manske

DEPTH (ft):	**8561.00**	**8583.00**	**8628.00**
SAMPLE NO.:	**1-72R**	**1-74R**	**1-79R**
Formation	**Cambrian Basal Sandstone**	**Cambrian Basal Sandstone**	**Pre-Cambrian Basement**
Grain Size Avg. (mm):	**0.26**	**0.28**	**Altered**
Grain Size Range (mm):	**<0.01-0.99**	**0.03-0.90**	**Granoblastic Quartzo-**
Sorting:	**Moderate**	**Moderately Poor**	**Feldspathic Gneiss &**
Fabric:	**Vague.-Lam./G.S.-zon.**	**Grain Size-zoned**	**Foliated Chlorite/Biotite**
Rock Type:	**Arkose**	**Arkose**	**Schist**
FRAMEWORK GRAINS			
Quartz	**51**	**35**	**29**
Monocrystalline	44	30	29
Polycrystalline	7	5	0
Feldspar	**21**	**24**	**20**
K-Feldspar	18	21	8
Plagioclase	3	3	12
Lithic Fragments	**1**	**1**	**0**
Plutonic	1	1	0
Volcanic	tr	tr	0
Metamorphic	0	tr	0
Chert	tr	0	0
Mudstone	0	0	0
Carbonate	0	0	0
Volcanic Glass	0	0	0
Accessory Grains	**tr**	**tr**	**3**
Muscovite	tr	tr	0
Biotite	0	tr	39 [1]
Heavy Minerals*	tr	0	3
ENVIRON. INDICATORS	**tr**	**1**	**0**
Carbonaceous Material	tr	1	0
Glauconite	0	0	0
Phosphatic Grains	0	0	0
DETRITAL MATRIX	**tr**	**2**	**0**
CEMENT/REPLACEMENT	**13**	**27**	**2**
Pore-lining Clay	1	2	0
Kaolinite	0	tr	0
Other Pore-filling Clay	tr	1	0
Quartz Overgrowths	7	4	0
Feldspar Overgrowths	4	3	0
Calcite	0	6	2
Dolomite	tr	9	0
Ankerite	0	0	0
Siderite	0	0	0
Pyrite	1	1	tr
Fe/Ti Oxides	tr	1	6 [2]
Bitumen	tr	tr	0
POROSITY	**14**	**10**	**1**
Primary	9	3	0
Secondary	4	3	tr**
Microscopic	1	4	1
TOTALS:	**100**	**100**	**100**

[1] includes chlorite

[2] includes hematite and leucoxene

*Tourmaline

**Inlcudes fracture porosity

INTENTIONALLY BLANK

APPENDIX D

THIN SECTION PHOTOMICROGRAPHS WITH DESCRIPTIONS

Ohio Division of Geological Survey **OMNI File No: HH-38266**
CO_2 No. 1 Well
Tuscarawas County, Ohio
Rochester Shale Formation
Rotary Sidewall Core

THIN SECTION PHOTOMICROGRAPHS

SAMPLE DEPTH: 4605.0 FEET
SAMPLE NUMBER: 1-1R

Plate 1

Permeability (Klink.): N/A **Porosity (ambient): 6.4%** **Grain Density: 2.78 gm/cc**

Sample not selected for petrographic analysis.

Magnification: A: 40X B: 200X

Ohio Division of Geological Survey
CO2 No. 1
Tuscarawas County, Ohio

4605.0'
Plate 1

Weatherford LABORATORIES

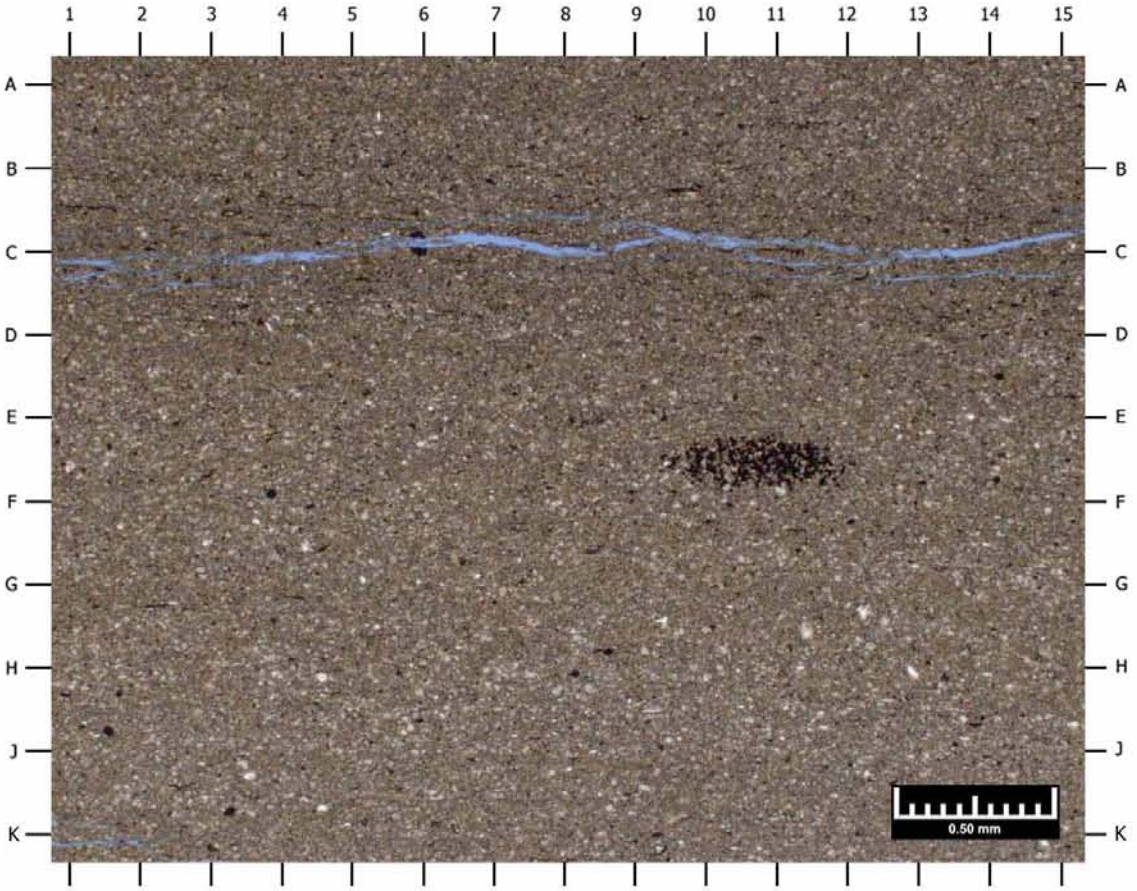

A

40X

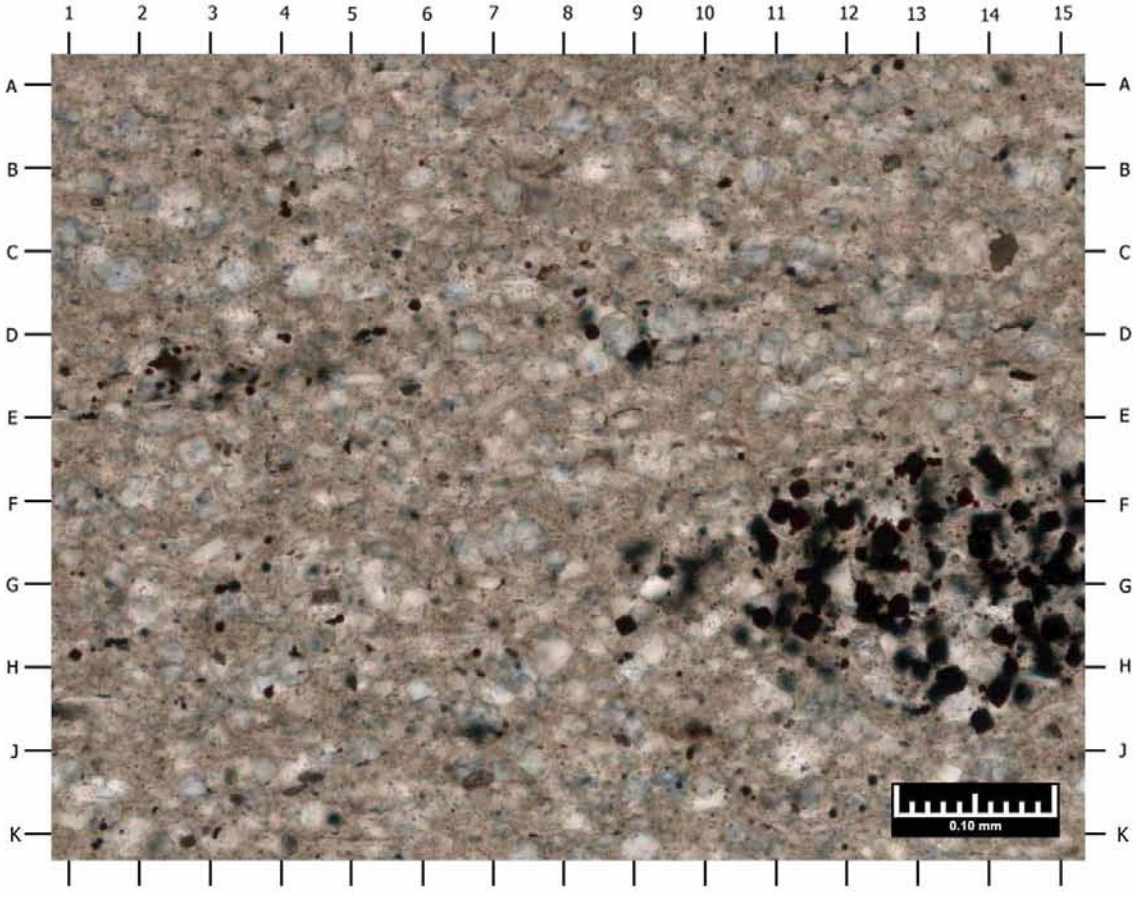

B

200X

Ohio Division of Geological Survey **OMNI File No: HH-38266**
CO_2 No. 1 Well
Tuscarawas County, Ohio
Clinton Sandstone Formation
Rotary Sidewall Core

THIN SECTION PHOTOMICROGRAPHS

SAMPLE DEPTH: 4760.0 FEET
SAMPLE NUMBER: 1-2R

Plate 2

Permeability (Klink.): N/A **Porosity (NCS): 5.7%** **Grain Density: 2.67 gm/cc**

Sample not selected for petrographic analysis.

Magnification: A: 40X B: 200X

Ohio Division of Geological Survey
CO2 No. 1
Tuscarawas County, Ohio

4760.0'
Plate 2

Weatherford LABORATORIES

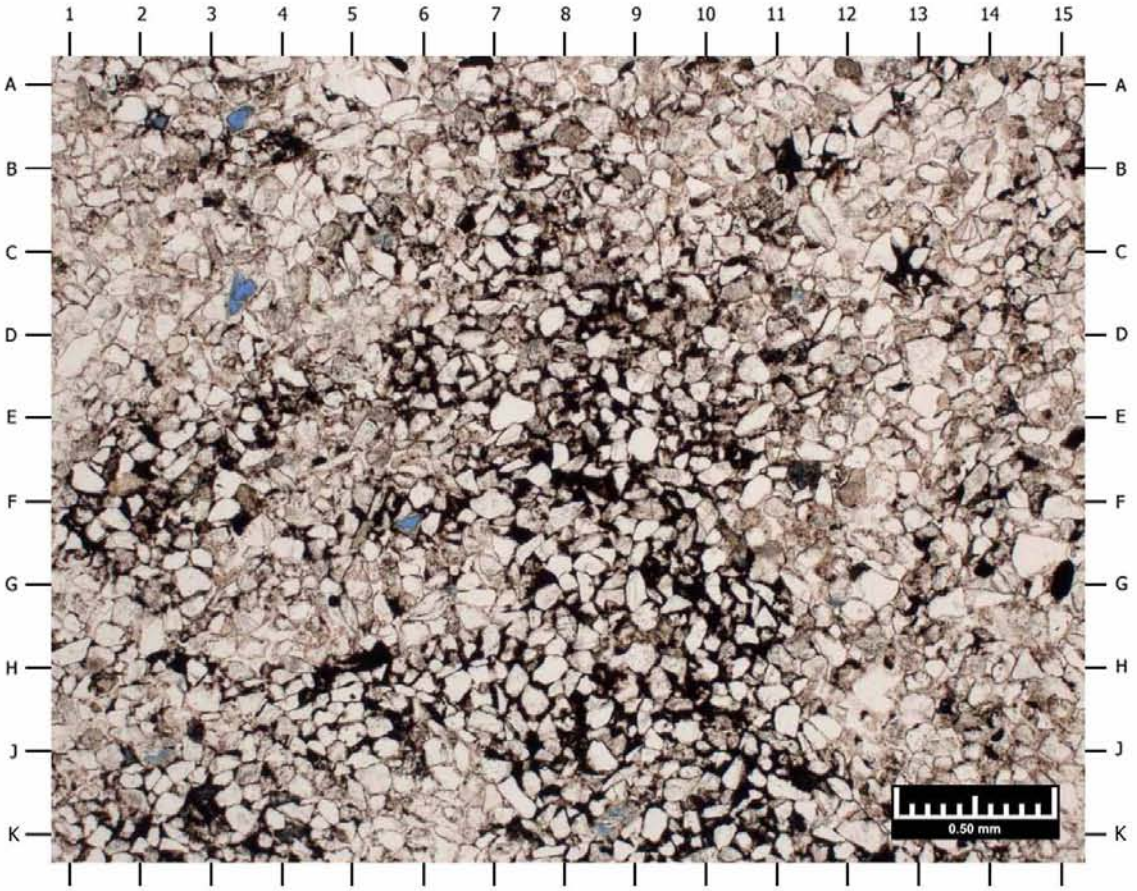

A

40X

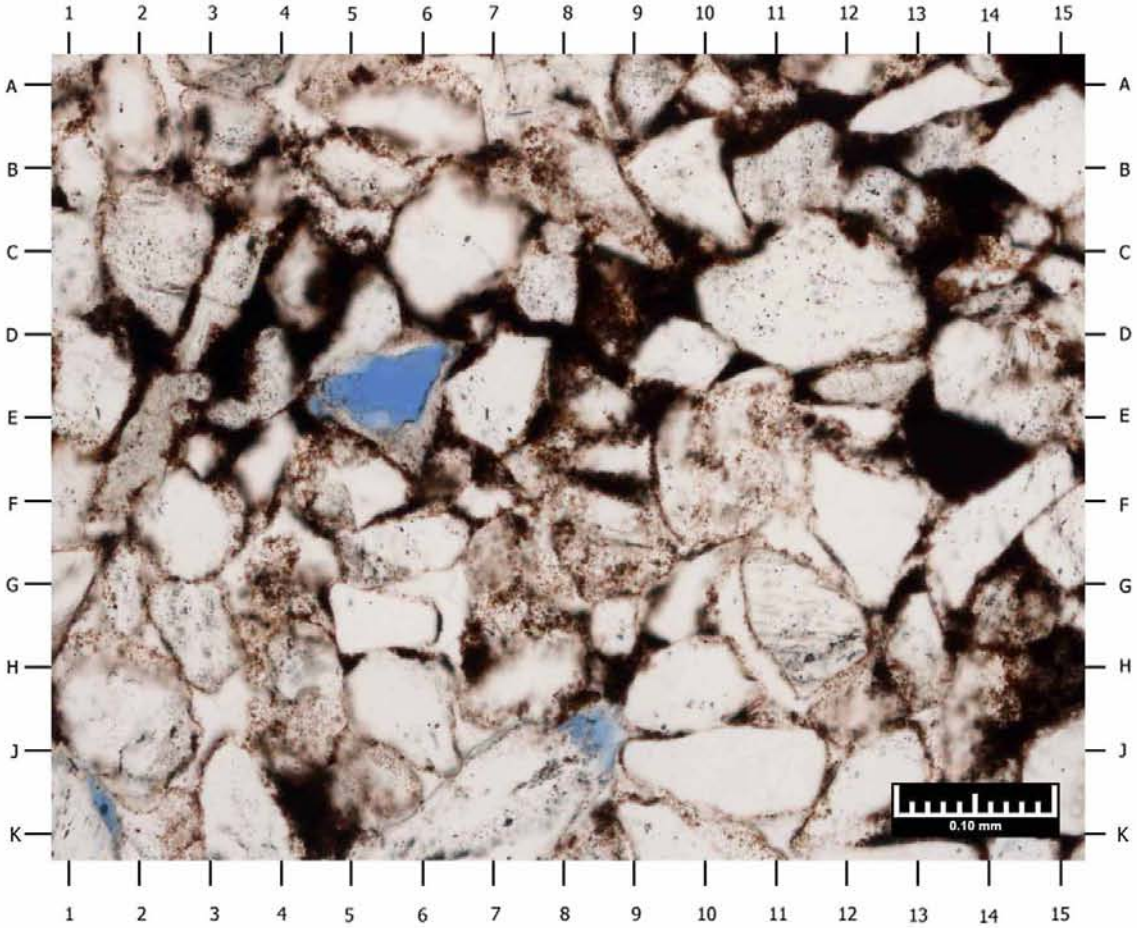

B

200X

Ohio Division of Geological Survey **OMNI File No: HH-38266**
CO_2 No. 1 Well
Tuscarawas County, Ohio
Clinton Sandstone Formation
Rotary Sidewall Core

THIN SECTION DESCRIPTION - DETAILED

SAMPLE DEPTH: 4771.0 FEET
SAMPLE NUMBER: 1-3R

Plate 3

Permeability (Klink.): 0.0069 mD Porosity (NCS): 6.8% Grain Density: 2.65 gm/cc

Lithology:	Quartzarenite
Sedimentary Fabric:	Vaguely grain size-zoned
Grain Size Range:	<0.01mm-0.32mm
Average Grain Size:	0.10mm
Compaction:	Moderate
Sorting:	Moderately well sorted
Framework Grains:	
Major:	Monocrystalline quartz
Minor:	Polycrystalline quartz, feldspar
Accessory:	Zircon, tourmaline, epidote, sphene, rutile
Matrix Content:	
Detrital Matrix:	Minor detrital clays and organics
Authigenic Clay:	Minor pore-filling clay (undifferentiated)
Cement Types:	Common quartz overgrowths; minor Fe/Ti oxides, and pyrite
Porosity Types:	Minor micropores and secondary intragranular pores
Reservoir Quality:	Poor

Magnification: A: 40X B: 200X

A) Subangular to subround monocrystalline quartz (F6, C1) is the predominant grain type in this sample. Organic material (G6) and detrital clay (A11) are scattered throughout the sample, and partially occlude the original intergranular pores. Quartz overgrowth cement also reduces the original pore volume (G3.5).

B) The majority of remaining pores in this sample consist of widely scattered, secondary intragranular pores (AB5, D2, GH6, J12) that result from the partial to nearly complete dissolution of unstable grains (i.e., lithic grains and feldspar). Low permeability results from the poor communication between these secondary pores.

Ohio Division of Geological Survey
CO2 No. 1
Tuscarawas County, Ohio

4771.0'
Plate 3

Weatherford LABORATORIES

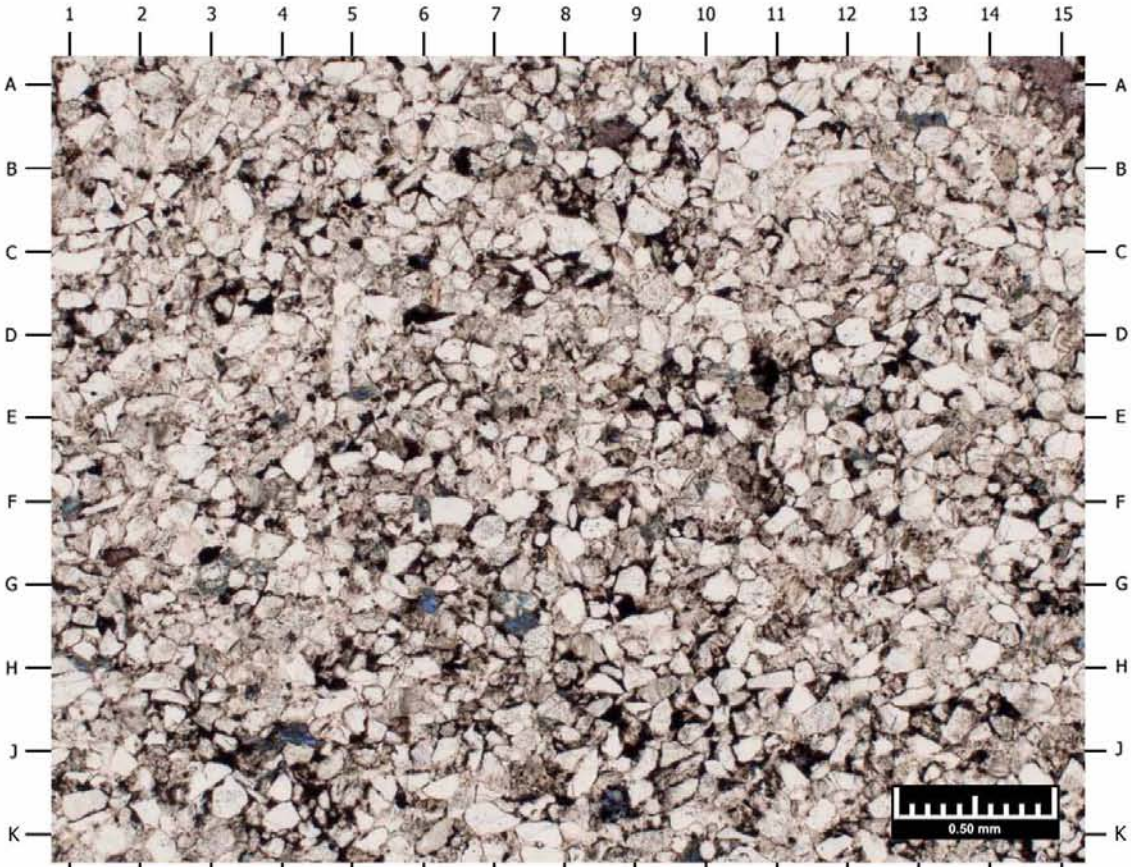

A

40X

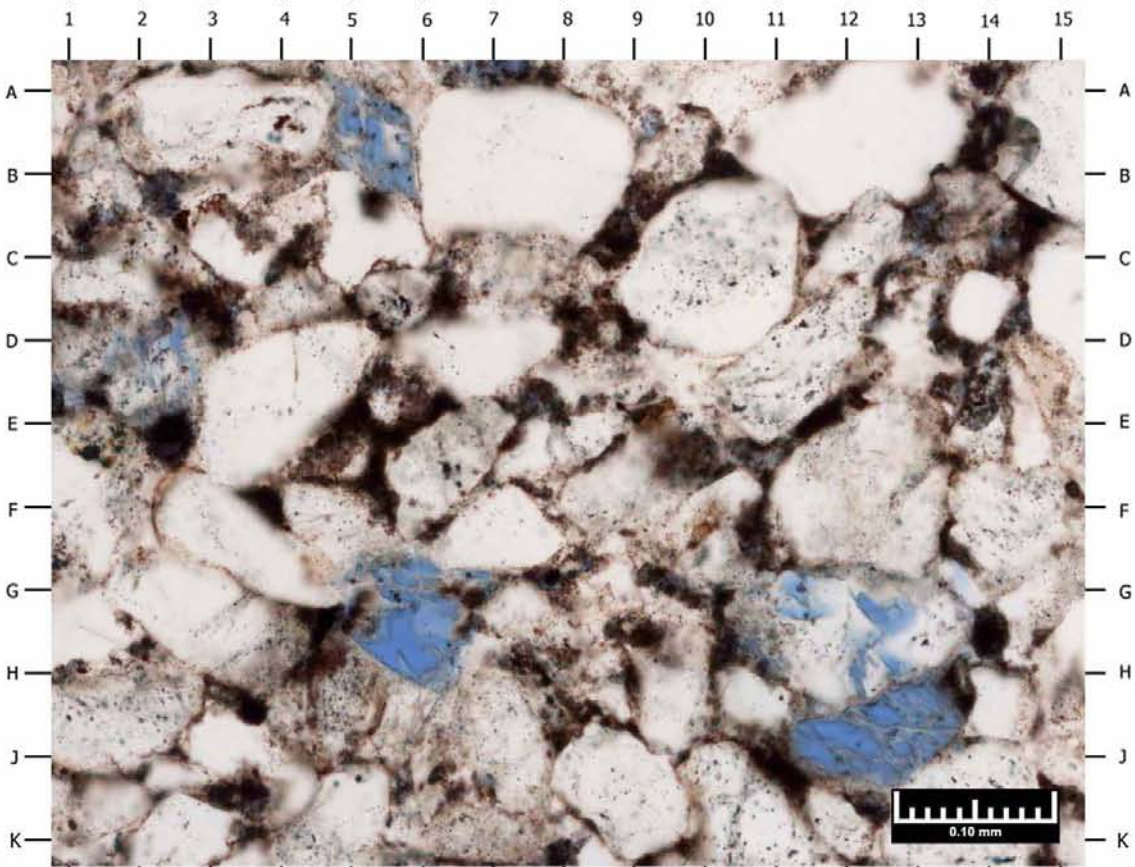

B

200X

Ohio Division of Geological Survey **OMNI File No: HH-38266**
CO_2 No. 1 Well
Tuscarawas County, Ohio
Clinton Sandstone Formation
Rotary Sidewall Core

THIN SECTION PHOTOMICROGRAPHS

SAMPLE DEPTH: 4776.0 FEET
SAMPLE NUMBER: 1-4R

Plate 4

Permeability (Klink.): N/A Porosity (ambient): 8.6% Grain Density: 2.67 gm/cc

Sample not selected for petrographic analysis.

Magnification: A: 40X B: 200X

Ohio Division of Geological Survey
CO2 No. 1
Tuscarawas County, Ohio

4776.0'
Plate 4

Weatherford LABORATORIES

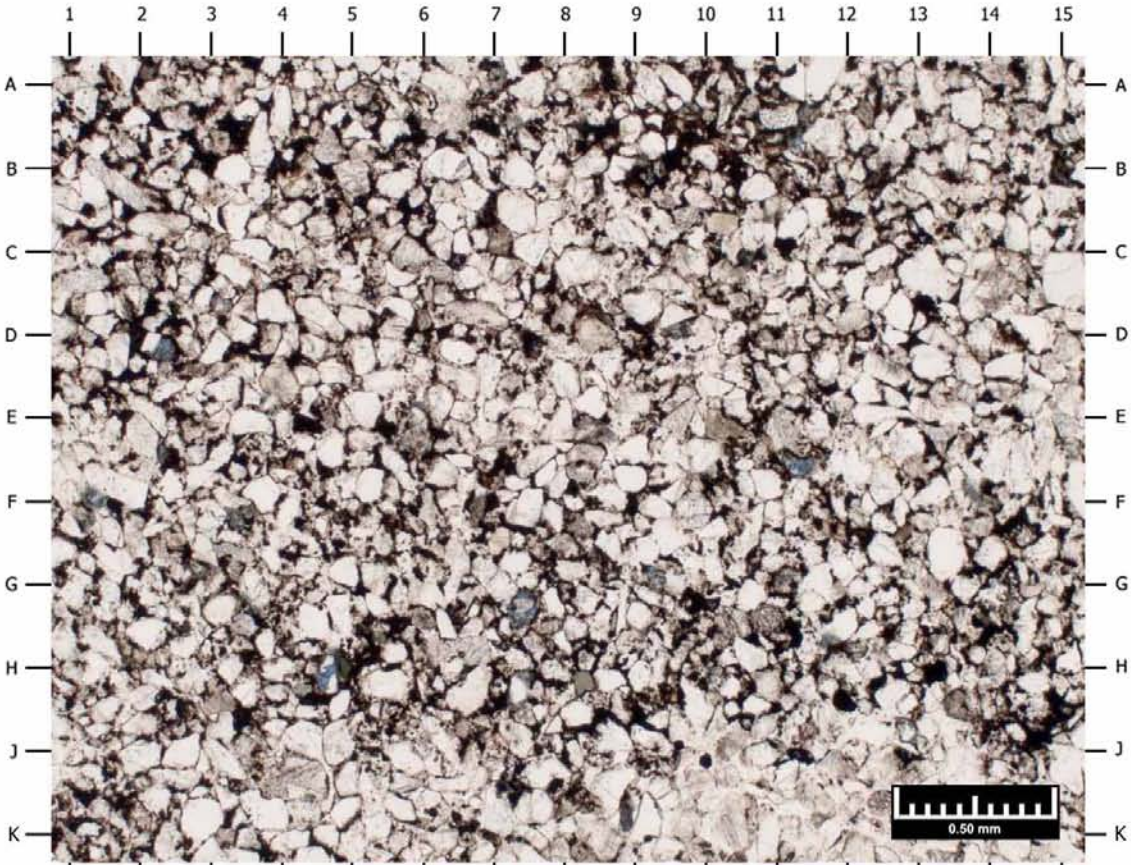

A

40X

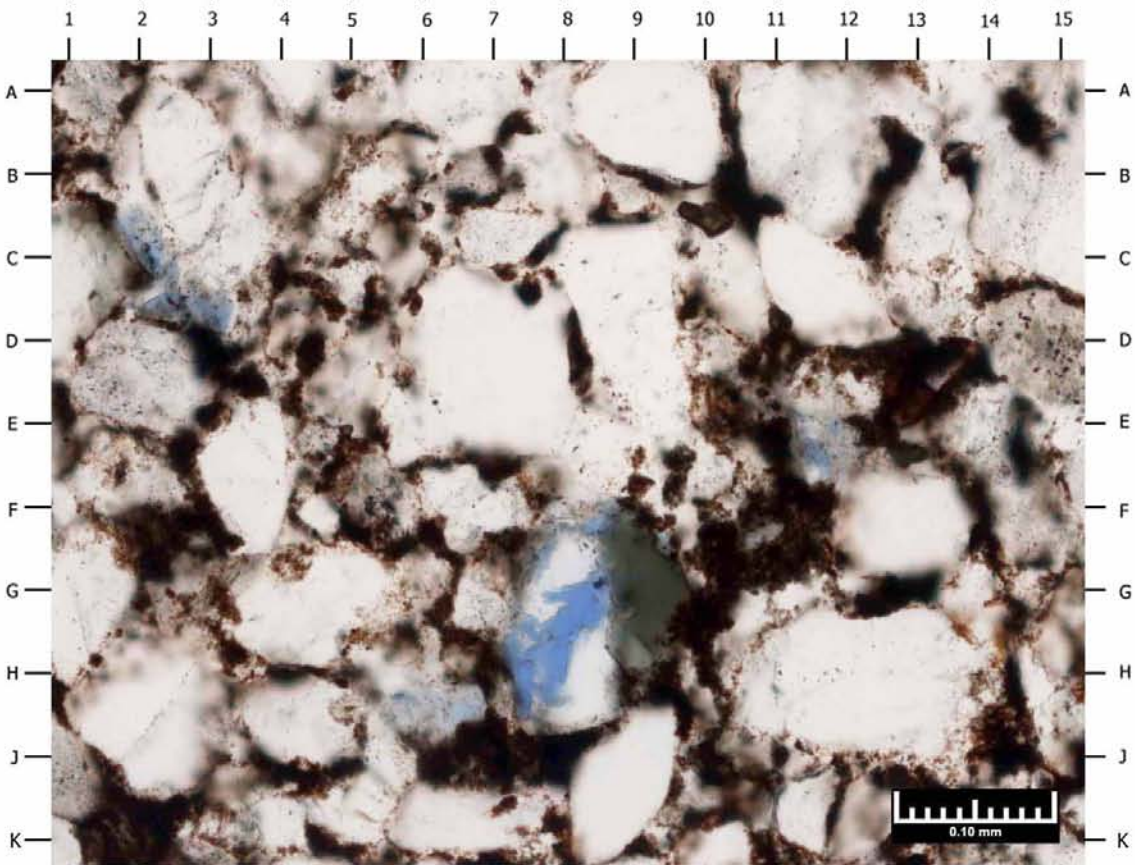

B

200X

Ohio Division of Geological Survey **OMNI File No: HH-38266**
CO_2 No. 1 Well
Tuscarawas County, Ohio
Clinton Sandstone Formation
Rotary Sidewall Core

THIN SECTION DESCRIPTION - DETAILED

SAMPLE DEPTH: 4790.0 FEET
SAMPLE NUMBER: 1-5R

Plate 5

Permeability (Klink.): N/A Porosity (NCS): 7.7% Grain Density: 2.70 gm/cc

Lithology:	Sublitharenite with deformed shale
Sedimentary Fabric:	Laminated; deformed bedding
Grain Size Range:	<0.01mm-0.38mm
Average Grain Size:	0.11mm
Compaction:	Moderate
Sorting:	Moderately sorted
Framework Grains:	
Major:	Monocrystalline quartz
Minor:	Polycrystalline quartz, feldspar, metamorphic lithic grains
Accessory:	Zircon, tourmaline, epidote, sphene, rutile
Matrix Content:	
Detrital Matrix:	Minor detrital clays and organics (in sandstone)
Authigenic Clay:	Minor grain-coating clay (undifferentiated)
Cement Types:	Common quartz overgrowths; minor pyrite and anhydrite
Porosity Types:	Minor micropores and secondary intragranular pores
Reservoir Quality:	Poor

Magnification: A: 40X B: 200X

A) Variably truncated and deformed shale encased in quartzose sandstone illustrates the irregular fabric associated with soft sediment deformation. Note that compaction results in the embedment of nearby quartz grains into the soft muddy sediment (J11.5).

B) Detailed view of the sample shows the absence of intergranular pore due to the presence of compacted mud matrix (G11.5) or due to pore-filling quartz overgrowth cement (E6.5). Note the authigenic pyrite that forms microcrystals (D7.5), partially replaces detrital grains (A4), and replaces organic material (A12.5)

Ohio Division of Geological Survey
CO2 No. 1
Tuscarawas County, Ohio

4790.0'
Plate 5

Weatherford LABORATORIES

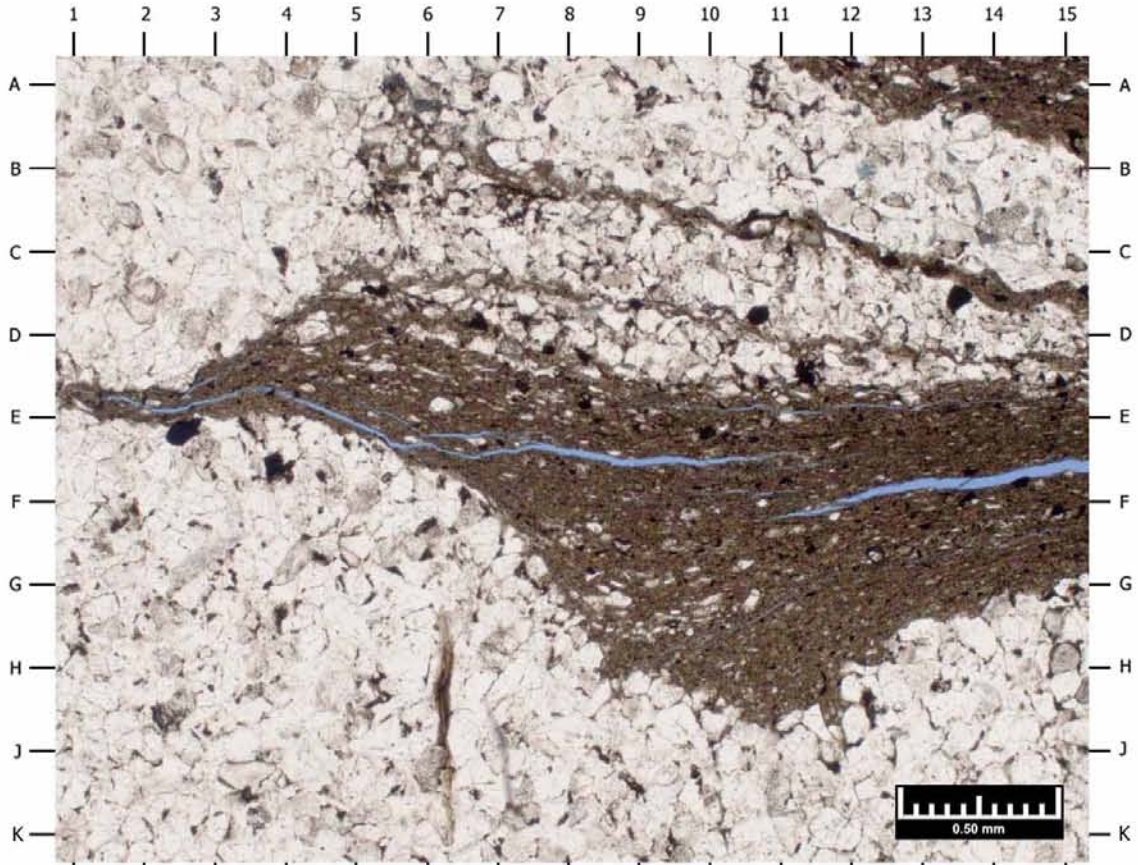

A

40X

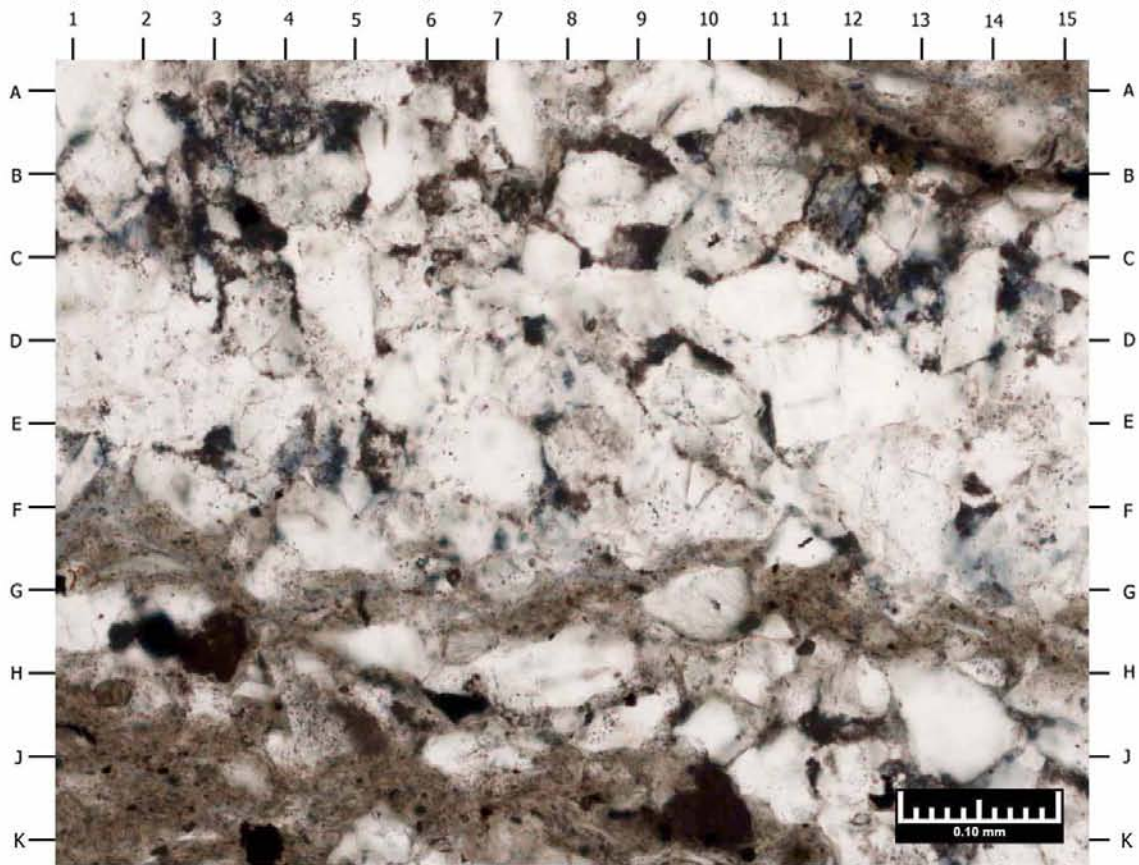

B

200X

Ohio Division of Geological Survey **OMNI File No: HH-38266**
CO_2 No. 1 Well
Tuscarawas County, Ohio
Clinton Sandstone Formation
Rotary Sidewall Core

Thin Section Description - General

SAMPLE DEPTH: 4816.0 FEET
SAMPLE NUMBER: 1-6R

Plate 6

Permeability (Klink.): N/A Porosity (ambient): 8.3% Grain Density: 2.80 gm/cc

Sample not selected for petrographic analysis.

Magnification: A: 40X B: 200X

Ohio Division of Geological Survey
CO2 No. 1
Tuscarawas County, Ohio

4816.0'
Plate 6

Weatherford LABORATORIES

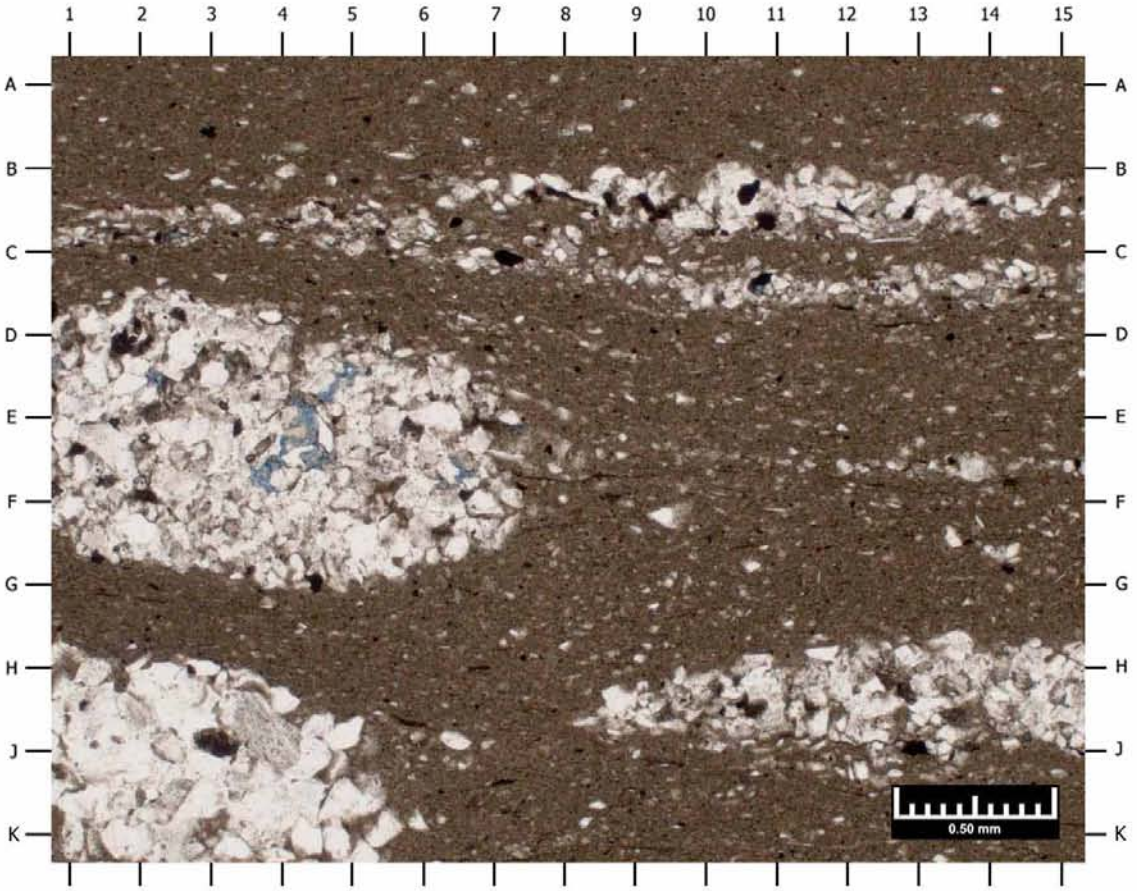

A

40X

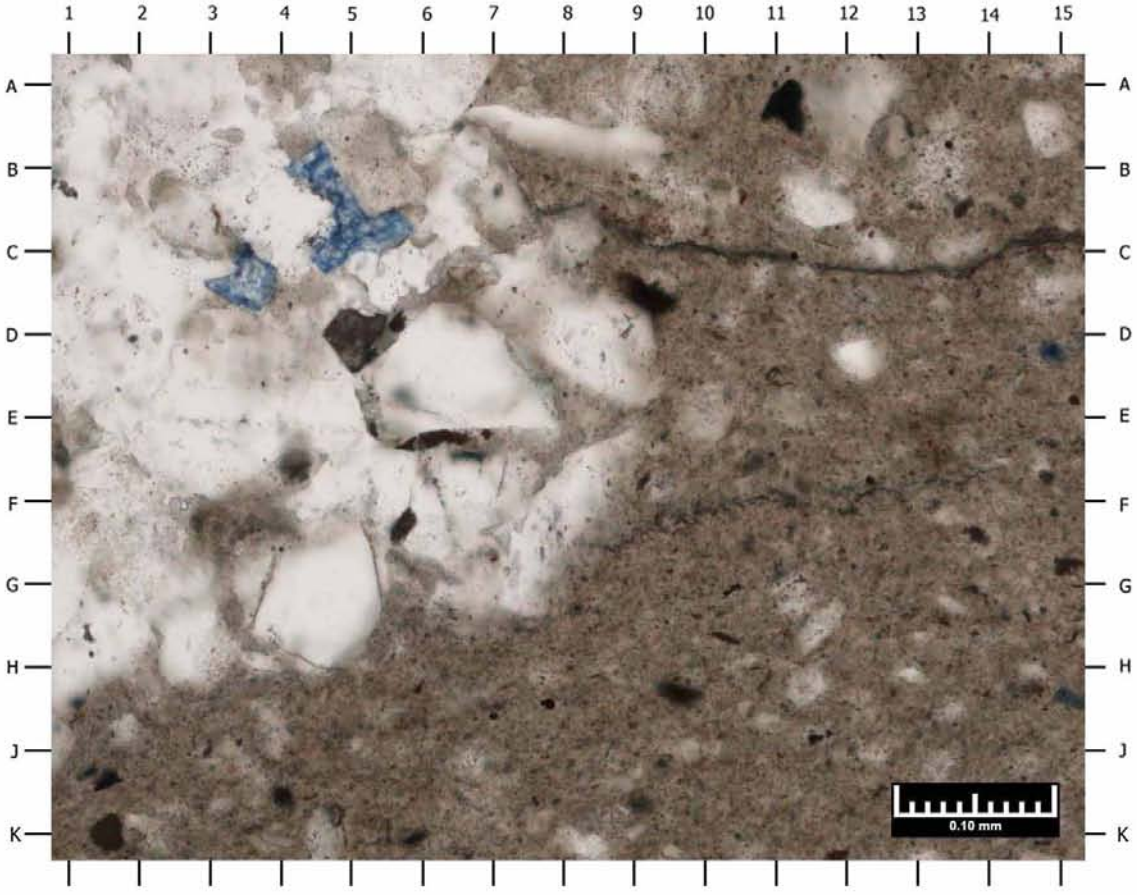

B

200X

Ohio Division of Geological Survey **OMNI File No: HH-38266**
CO_2 No. 1 Well
Tuscarawas County, Ohio
Clinton Sandstone Formation
Rotary Sidewall Core

Thin Section Description - General

SAMPLE DEPTH: 4821.0 FEET
SAMPLE NUMBER: 1-7R

Plate 7

Permeability (Klink.): N/A Porosity (NCS): 4.2% Grain Density: 2.72 gm/cc

Sample not selected for petrographic analysis.

Magnification: A: 40X B: 200X

Ohio Division of Geological Survey
CO2 No. 1
Tuscarawas County, Ohio

4821.0'
Plate 7

Weatherford LABORATORIES

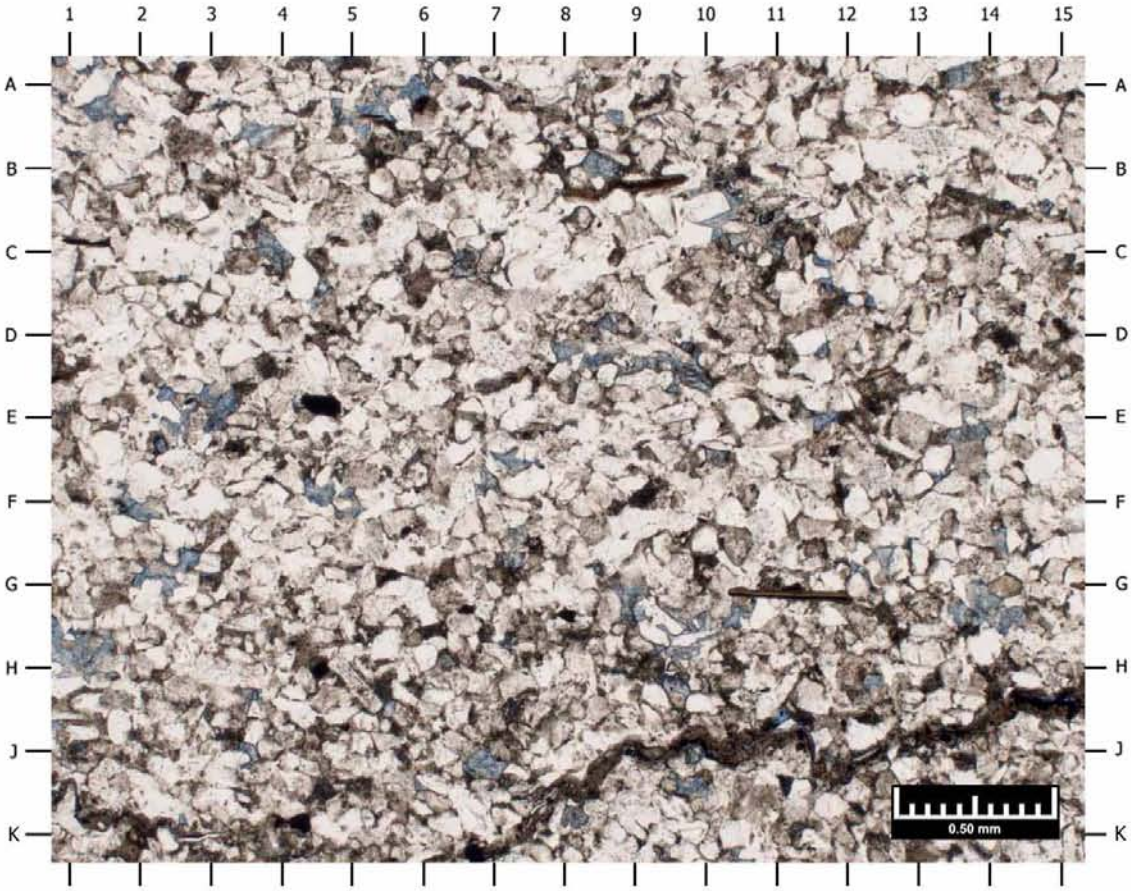

A

40X

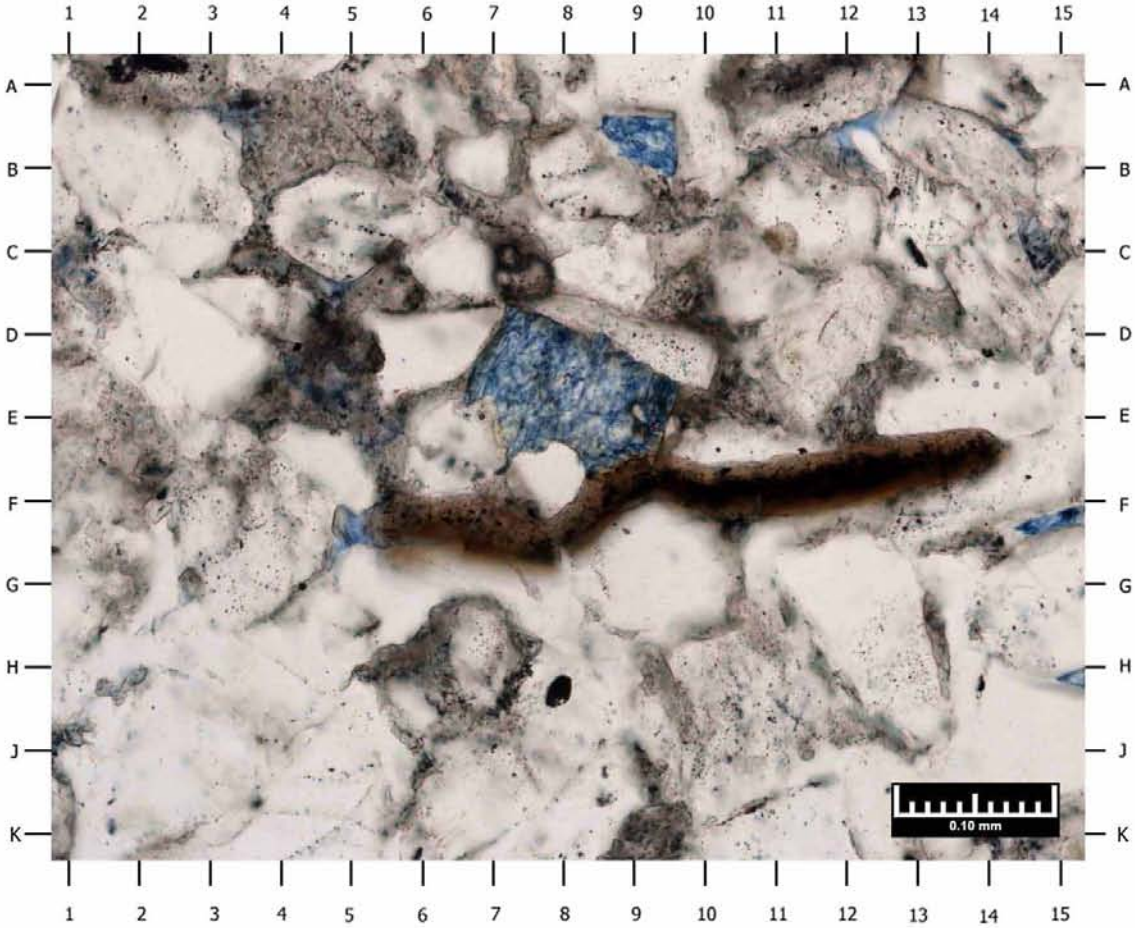

B

200X

Ohio Division of Geological Survey **OMNI File No: HH-38266**
CO_2 No. 1 Well
Tuscarawas County, Ohio
Clinton Sandstone Formation
Rotary Sidewall Core

Thin Section Description - General

SAMPLE DEPTH: 4834.0 FEET
SAMPLE NUMBER: 1-8R

Plate 8

Permeability (Klink.): N/A Porosity (NCS): 3.5% Grain Density: 2.66 gm/cc

Sample not selected for petrographic analysis.

Magnification: A: 40X B: 200X

Ohio Division of Geological Survey
CO2 No. 1
Tuscarawas County, Ohio

4834.0'
Plate 8

Weatherford LABORATORIES

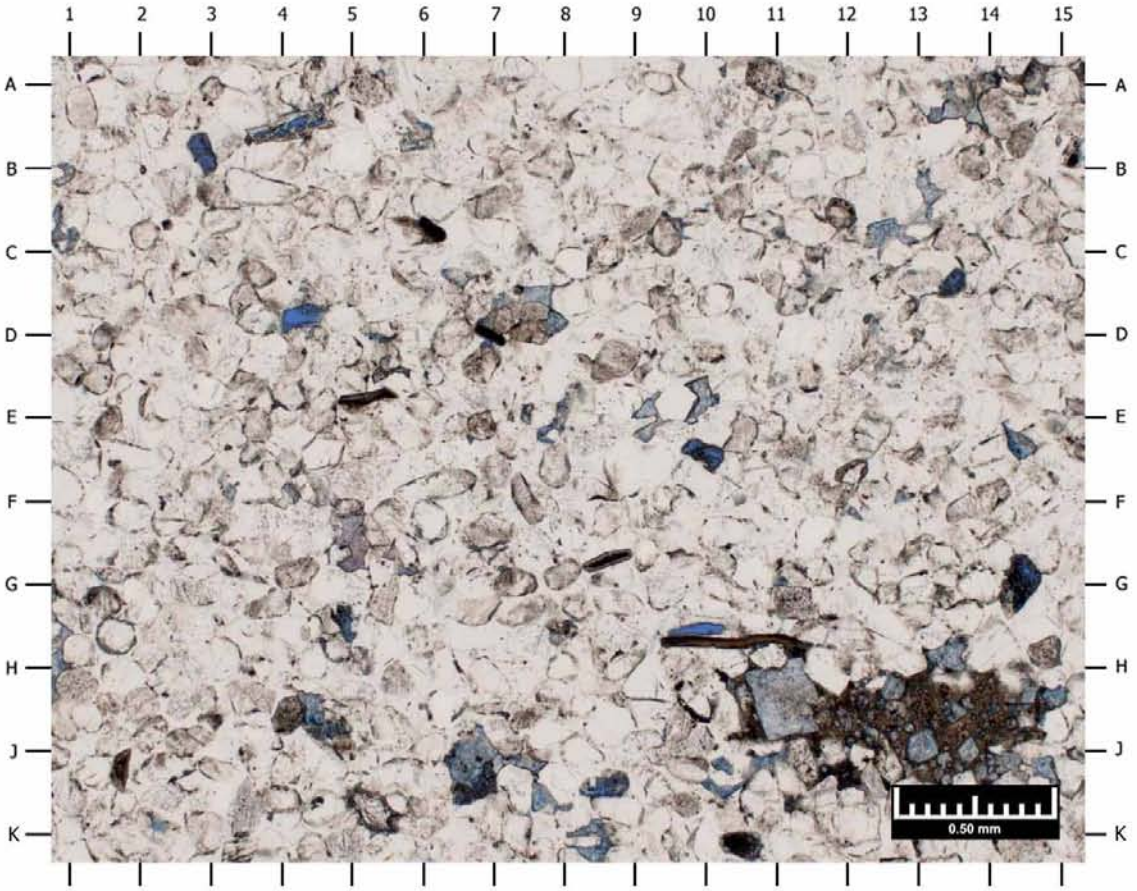

A

40X

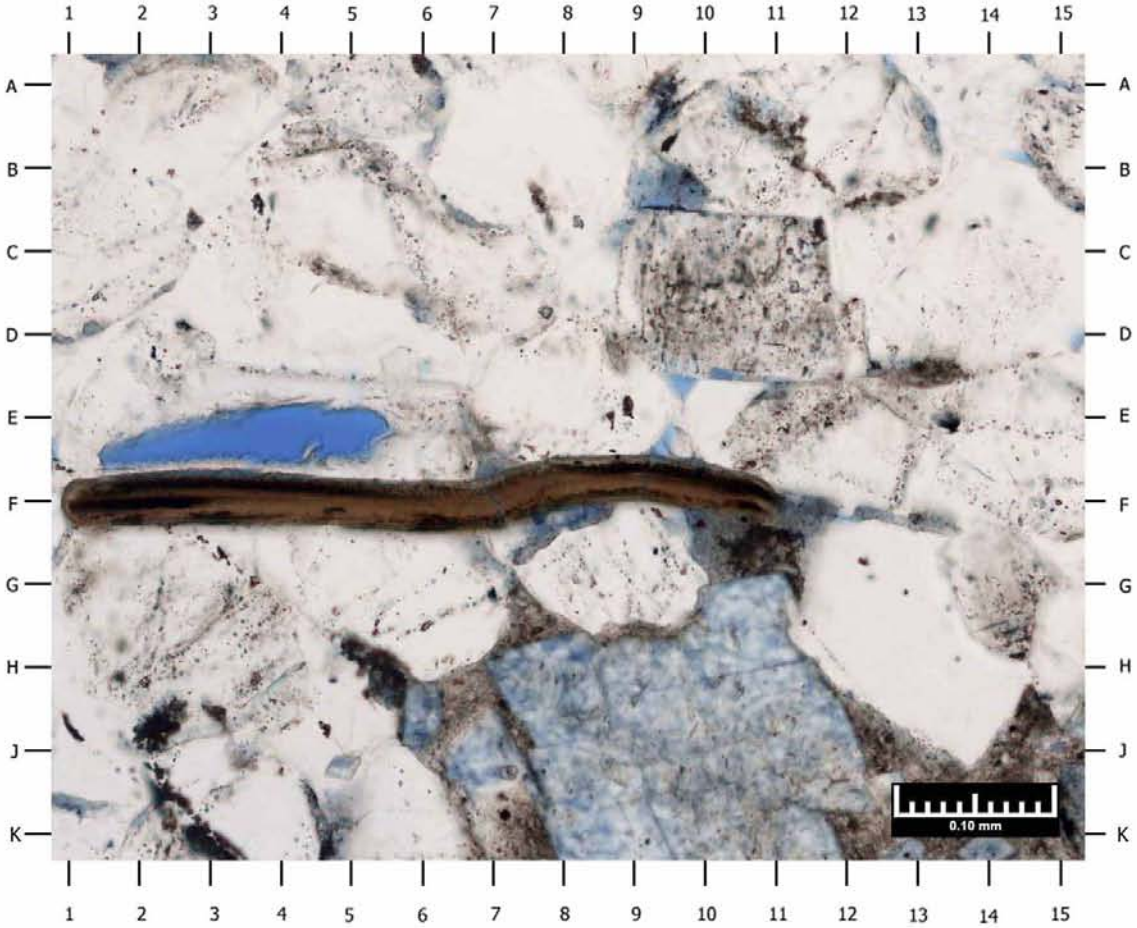

B

200X

Ohio Division of Geological Survey **OMNI File No: HH-38266**
CO_2 No. 1 Well
Tuscarawas County, Ohio
Clinton Sandstone Formation
Rotary Sidewall Core

Thin Section Description - Detailed

SAMPLE DEPTH: 4840.0 FEET
SAMPLE NUMBER: 1-9R

Plate 9

Permeability (Klink.): 0.0061 mD Porosity (NCS): 5.7% Grain Density: 2.66 gm/cc

Lithology:	Sublitharenite / Subarkose
Sedimentary Fabric:	Massive
Grain Size Range:	<0.03mm-0.32mm
Average Grain Size:	0.15mm
Compaction:	Moderate
Sorting:	Well sorted
Framework Grains:	
Major:	Monocrystalline quartz
Minor:	Polycrystalline quartz, feldspar, metamorphic and plutonic lithic grains
Accessory:	Zircon, tourmaline, epidote, sphene, rutile
Matrix Content:	
Detrital Matrix:	Trace of organic material
Authigenic Clay:	Minor grain-coating clay (undifferentiated)
Cement Types:	Common quartz overgrowths; minor dolomite and pyrite
Porosity Types:	Subequal, minor amounts of intergranular pores, micropores and secondary intragranular pores
Reservoir Quality:	Fair

Magnification: A: 40X B: 200X

A) This sandstone sample consists largely of detrital quartz with subequal amounts of feldspar and lithic fragments. Pore types consist predominantly of primary intergranular pores (DE12.5) secondary intragranular pores (J4) in partially altered and dissolved grains.

B) Two phosphatic shell fragments (DE3 to DE8; H5 to H10) are partially replaced by pyrite (black crystals). Note the pore-filling and grain-replacing ferroan dolomite cement (aka ankerite; B10, B13, J10). Quartz overgrowths project into partially reduced pores (GH11) and completely fill some pores (B4).

Ohio Division of Geological Survey
CO2 No. 1
Tuscarawas County, Ohio

4840.0'
Plate 9

Weatherford LABORATORIES

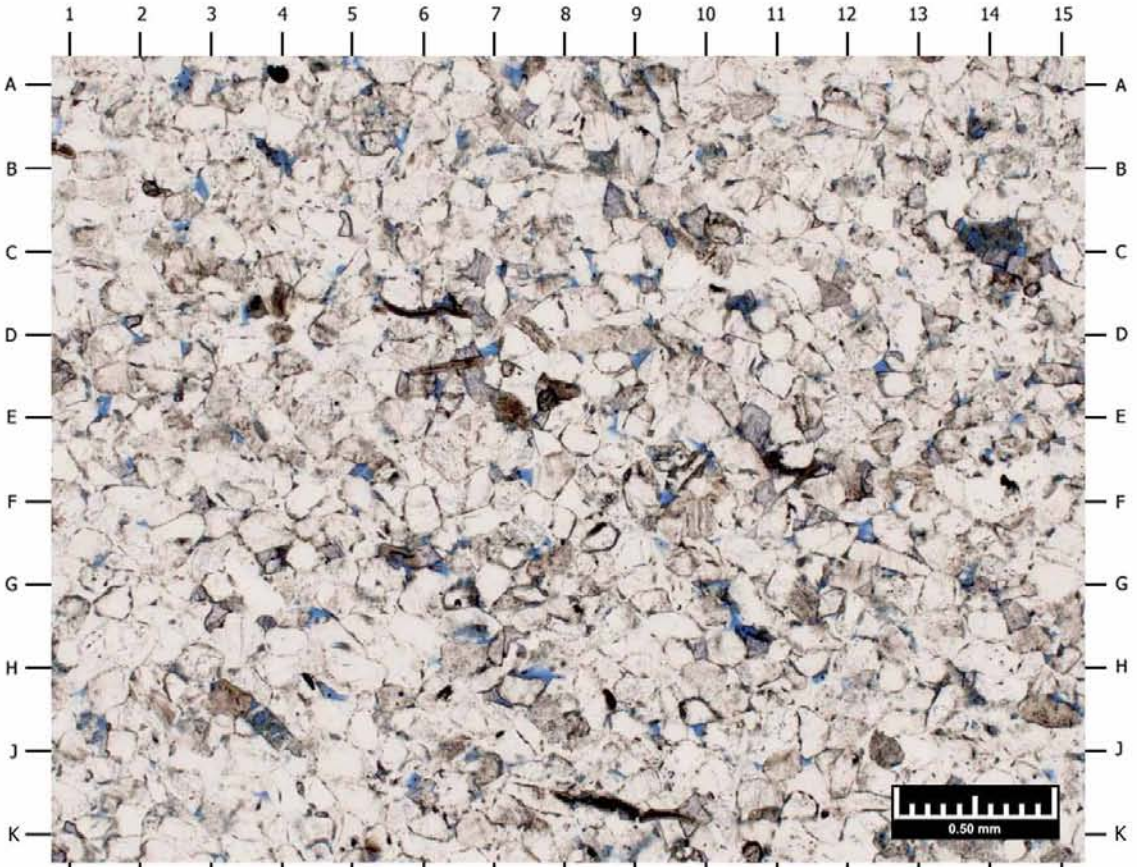

A

40X

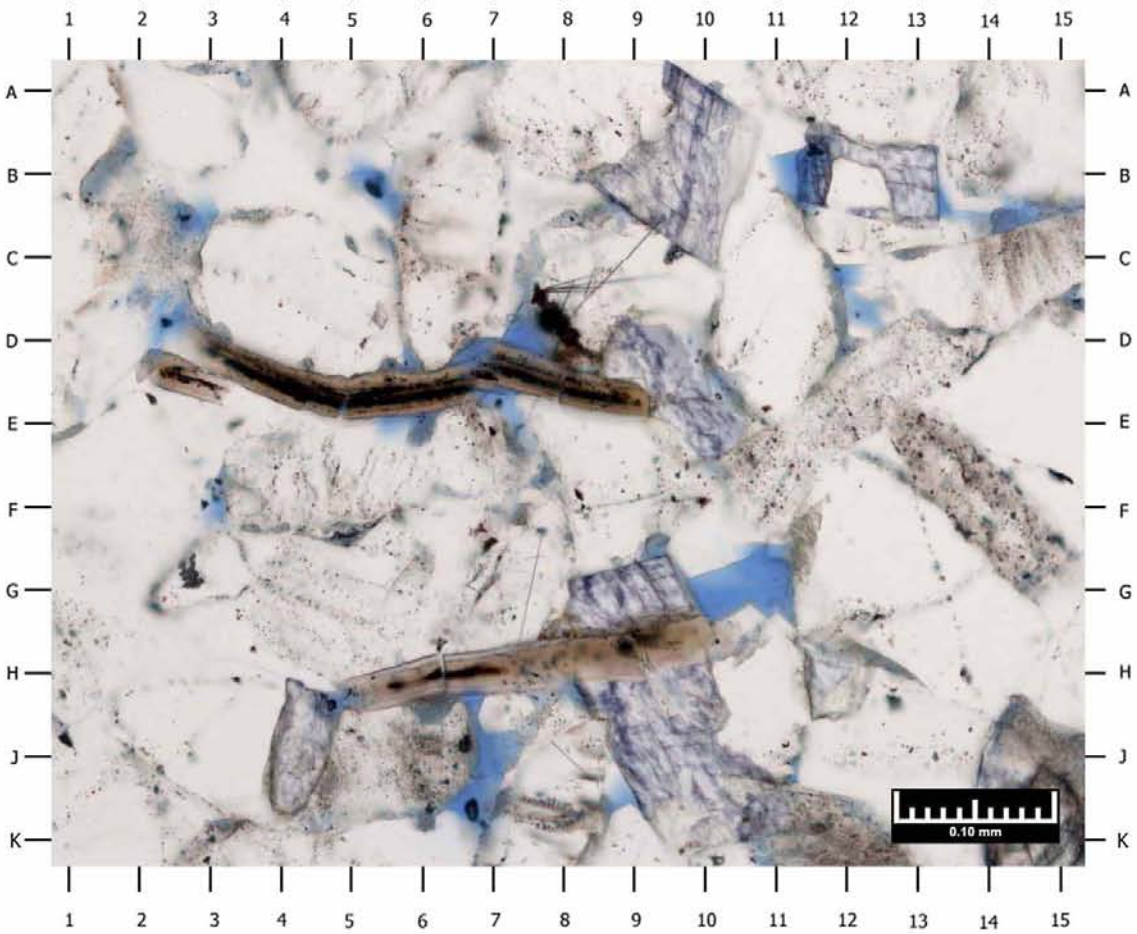

B

200X

Ohio Division of Geological Survey **OMNI File No: HH-38266**
CO_2 No. 1 Well
Tuscarawas County, Ohio
Cincinnati Group (Undifferentiated)
Rotary Sidewall Core

THIN SECTION DESCRIPTION - GENERAL

SAMPLE DEPTH: 6064.0 FEET
SAMPLE NUMBER: 1-10R

Plate 10

Permeability (Klink.): N/A Porosity (NCS): 4.8% Grain Density: 2.78 gm/cc

Lithology: Silty mudstone and muddy siltstone (silty shale and shaly siltstone)

Texture: Thinly laminated (millimeter scale); possible burrow traces

Framework Grains: Common silt-sized quartz and mica; scattered chambered calcareous fossil fragments (foraminifera?) and fine undifferentiated fragments; minor organic particles, with several thin organic layers.

Matrix: Variably abundant clay laminations

Cements and Replacement Minerals: Minor amount of calcite cement trace amount of microcrystalline pyrite occurring as a replacement of shell material, organic material, and mud matrix; several laminations cemented by calcite

Pore System: Minor amount of micropores associated with clay matrix

Reservoir Quality: Poor (may serve as a reservoir seal)

Magnification: A: 40X B: 200X

A) An overview of this sample shows the silty mudstone (C4) and muddy siltstone (E14) laminations. Subtle changes in fabric within the mudstone suggest the possibility of burrow traces (e.g., AB12).

B) The contact between the silty mudstone and muddy siltstone laminations extends from G1 to E15. Quartz silt (white grains) and detrital mud (brownish material) are the major constituents. Note the minor amount of calcite cement (stained red; K8) and ferroan dolomite cement (stained blue; B10.5).

Ohio Division of Geological Survey
CO2 No. 1
Tuscarawas County, Ohio

6064.0'
Plate 10

Weatherford LABORATORIES

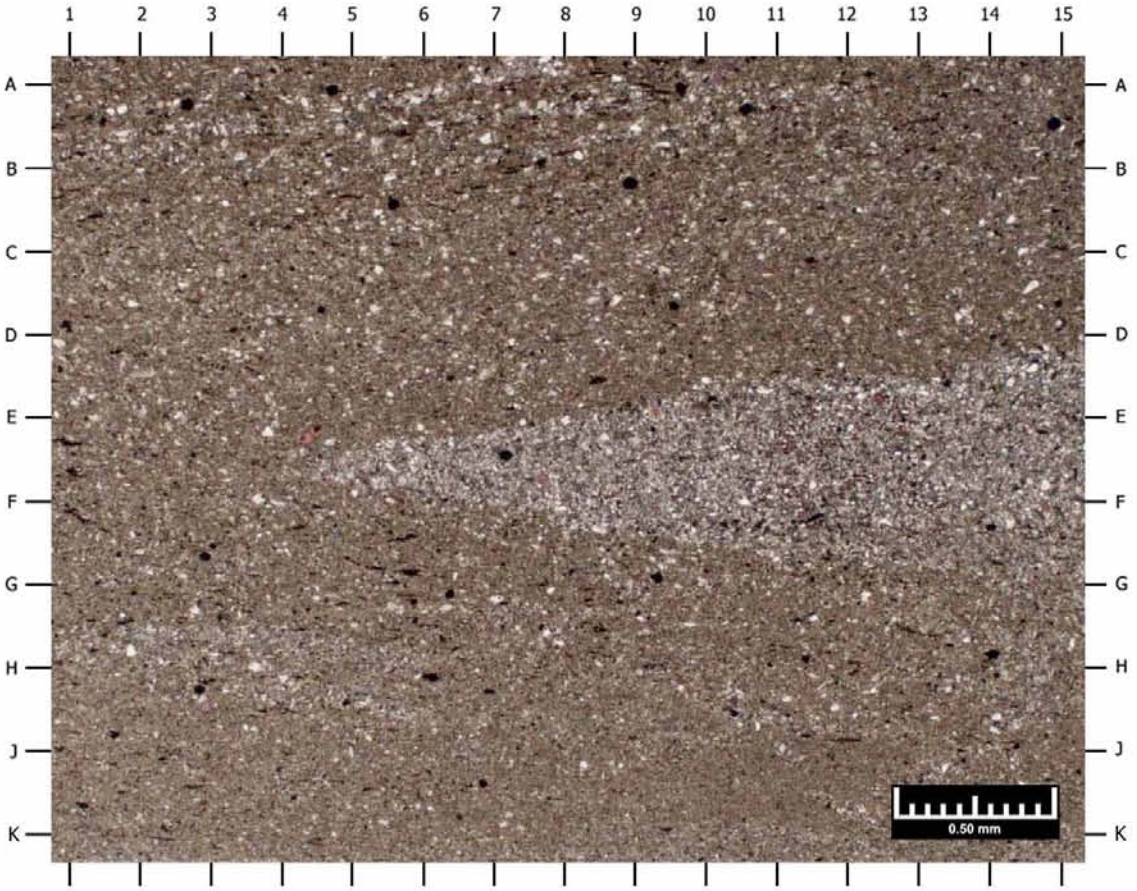

A

40X

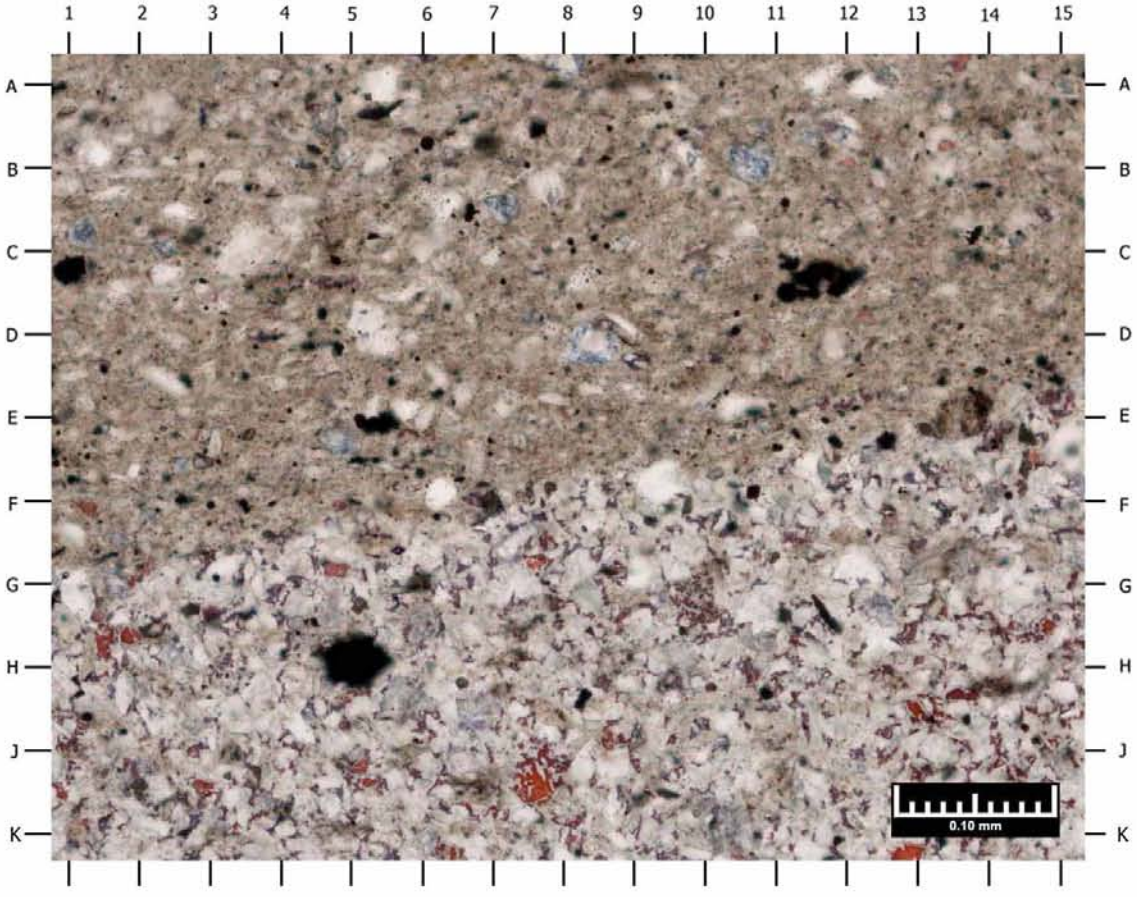

B

200X

Ohio Division of Geological Survey **OMNI File No: HH-38266**
CO_2 No. 1 Well
Tuscarawas County, Ohio
Utica Shale
Rotary Sidewall Core

THIN SECTION DESCRIPTION - GENERAL

SAMPLE DEPTH: 6141.0 FEET
SAMPLE NUMBER: 1-11R

Plate 11

Permeability (Klink.): 0.0002 mD Porosity (NCS): 5.1% Grain Density: 2.70 gm/cc

Lithology: Slightly fossiliferous, silty mudstone (silty shale)

Texture: Massive to vaguely laminated

Framework Grains: Common fine silt-sized to medium silt-sized quartz and mica; scattered chambered calcareous fossil fragments, including bivalves up to 1.3 mm in length, ostracods, rare phosphatic shell fragments, and fine undifferentiated fragments; common organic particles

Matrix: Abundant detrital clay

Cements and Replacem ent M inerals: Minor amount of patchy calcite cement and replacements; scattered ferroan dolomite crystals replacing clay matrix; trace amount of microcrystalline pyrite replacement of shell material, organic material, and mud matrix; rare framboidal pyrite

Pore System: Trace amount of micropores associated with clay matrix

Reservoir Quality: Poor (may serve as a reservoir seal)

Magnification: A: 40X B: 200X

A) This vaguely laminated silty mudstone contains several calcareous shell fossils (stained red; G14, J11) and less common phosphatic shell fragments (K6.5). Note the thin, silt-rich lamination C1 to C15).

B) Scattered quartz silt (white grains), mica (A13, J2.5), organic fragments (D15) and shell fragments (A8) are the predominant components in this mudstone. Most of the organic material has been partially to completely replaced by pyrite (H6).

Ohio Division of Geological Survey
CO2 No. 1
Tuscarawas County, Ohio

6141.0'
Plate 11

Weatherford LABORATORIES

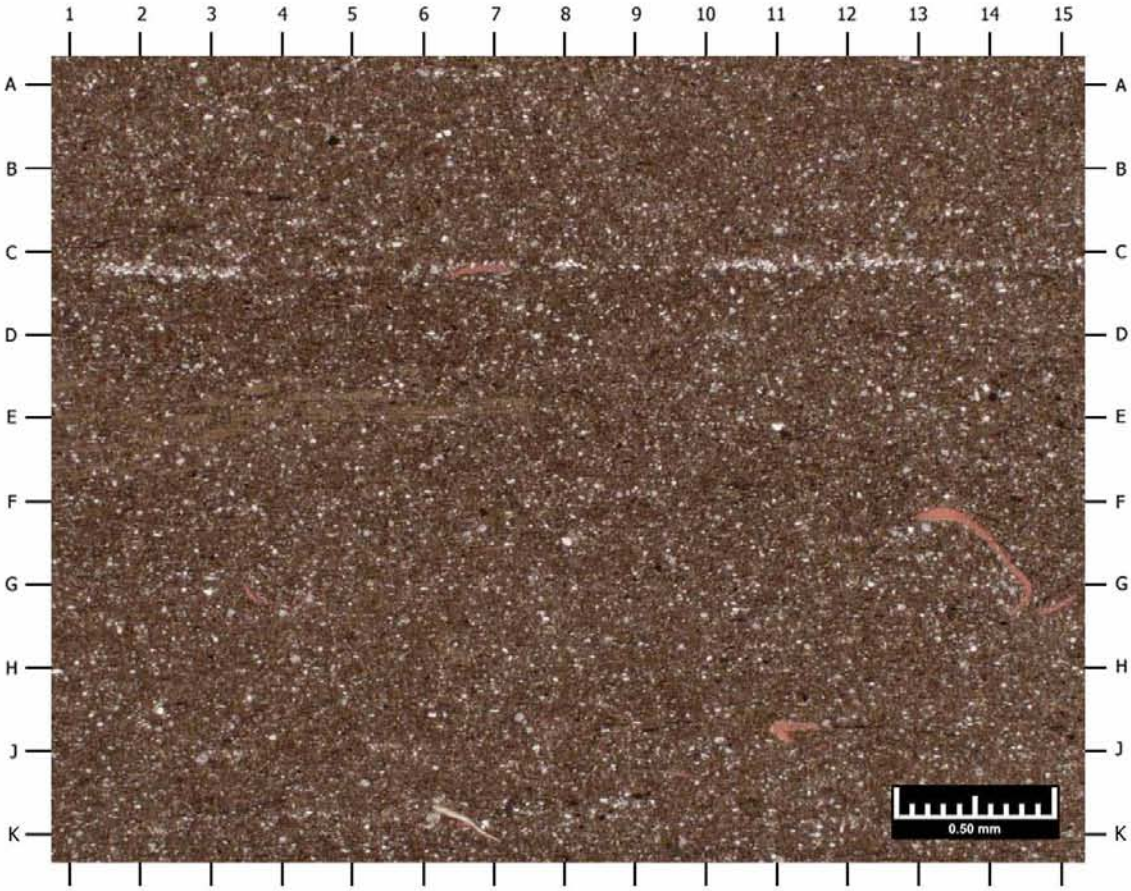

A

40X

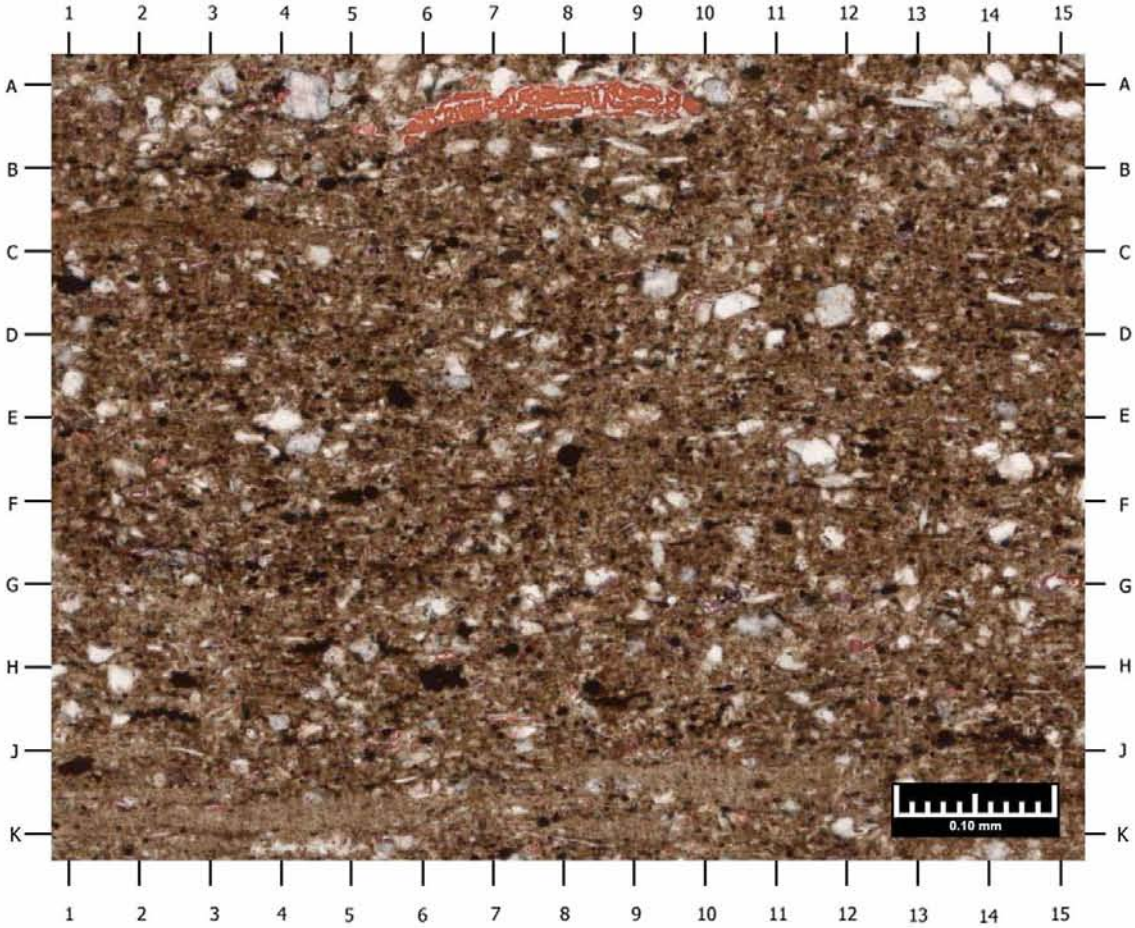

B

200X

Ohio Division of Geological Survey **OMNI File No: HH-38266**
CO_2 No. 1 Well
Tuscarawas County, Ohio
Point Pleasant Formation
Rotary Sidewall Core

THIN SECTION DESCRIPTION - GENERAL

SAMPLE DEPTH: 6282.0 FEET
SAMPLE NUMBER: 1-12R

Plate 12

Permeability (Klink.): 0.0003 mD Porosity (NCS): 4.2% Grain Density: 2.70 gm/cc

Lithology: Fossiliferous, slightly dolomitic mudstone (shale) to argillaceous skeletal wackestone (marlstone)

Texture: Variably disrupted laminations; rare pyrite-filled burrows

Framework Grains: Minor amount of fine silt-sized to medium silt-sized quartz and mica; abundant calcareous fossil fragments (typically concentrated in layers), including bivalves, echinoderm fragments up to 1.2 mm in length, ostracods, rare phosphatic shell fragments and brachiopod spines, and fine undifferentiated fragments; possible bryozoan and trilobite fragments; common organic particles

Matrix: Abundant detrital clay

Cements and Replacement Minerals: Minor amount of scattered, subhedral dolomite crystals replacing clay matrix; minor amount of microcrystalline pyrite replacement of shell material, organic material, mud matrix, and as framboids

Pore System: Trace amount of micropores associated with clay matrix; no visible macropores

Reservoir Quality: Poor

Magnification: A: 40X B: 200X

A) Common variably abraded and disarticulated calcareous fossil fragments (E4, C8) are scattered throughout the mud-rich matrix. The irregular fabric suggests the sediment was burrowed prior to lithification.

B) Authigenic pyrite partially replaces shells (B14) and matrix material (K9.5). The acicular morphology of pyrite at D8.5 suggests it represents a pseudomorph after marcasite. Note the dolomite crystals (G14,B9) that partially replace matrix and skeletal fragments.

Ohio Division of Geological Survey
CO2 No. 1
Tuscarawas County, Ohio

6282.0'
Plate 12

Weatherford LABORATORIES

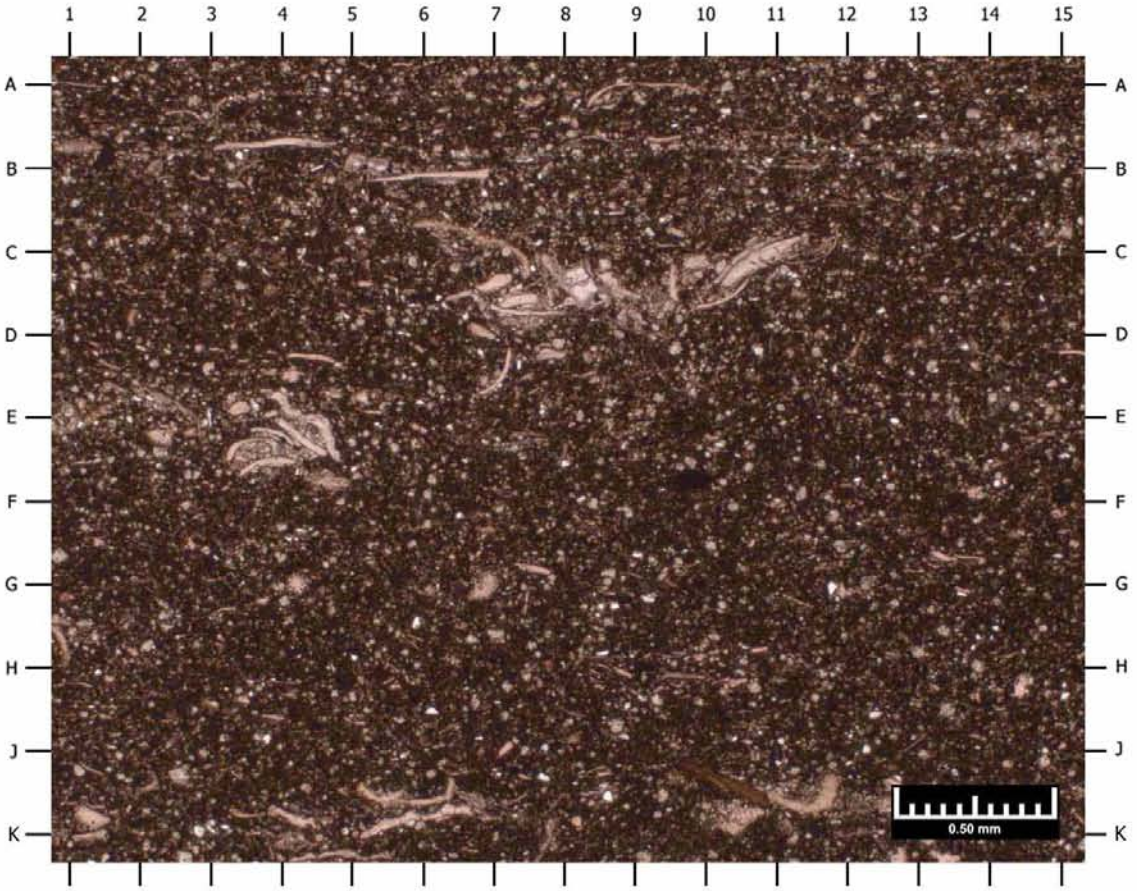

A

40X

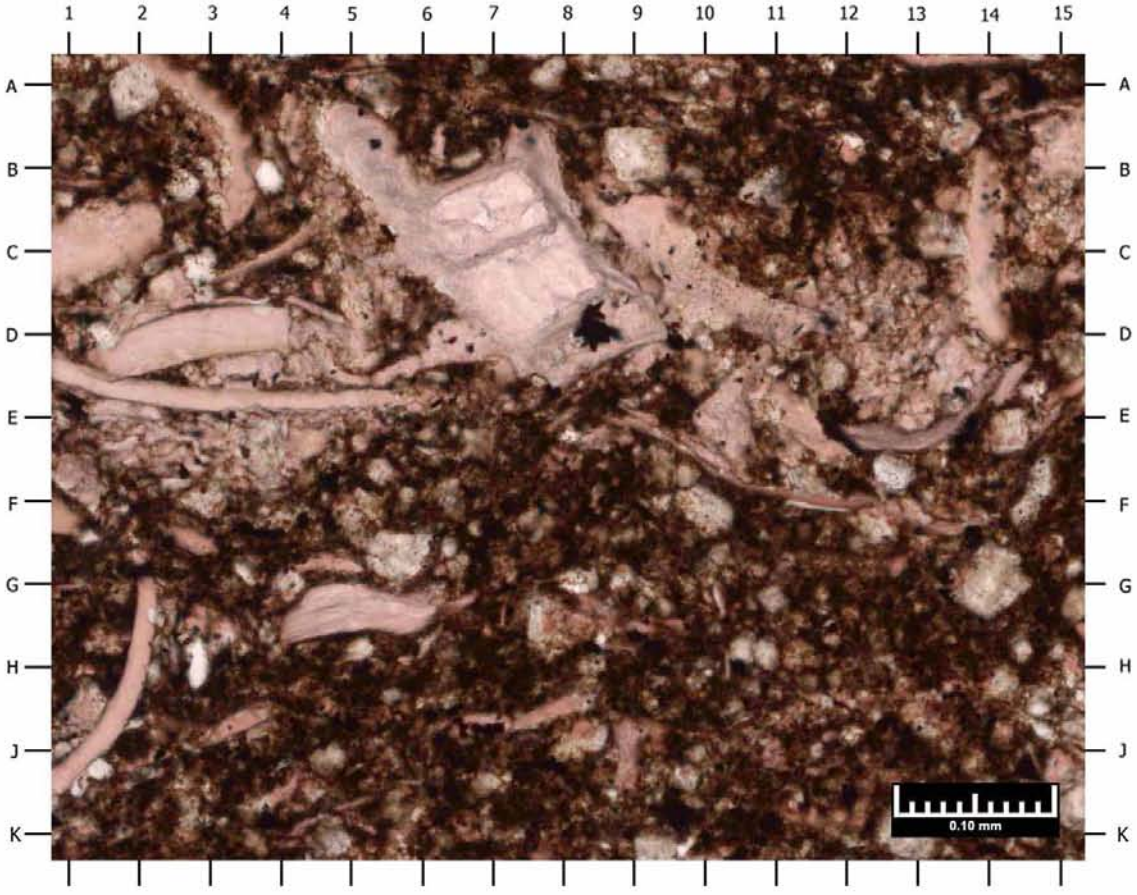

B

200X

Ohio Division of Geological Survey **OMNI File No: HH-38266**
CO_2 No. 1 Well
Tuscarawas County, Ohio
Trenton Limestone
Rotary Sidewall Core

THIN SECTION DESCRIPTION - GENERAL

SAMPLE DEPTH: 6336.0 FEET
SAMPLE NUMBER: 1-13R

Plate 13

Permeability (Klink.): 0.0001 mD Porosity (NCS): 5.0% Grain Density: 2.61 gm/cc

Lithology: Slightly silty, organic limestone

Texture: Skeletal peloidal packstone with minor thin laminations of skeletal packstone**;** minor bedding disruption by burrowing

Framework Grains: Allochems consist of abundant peloids, with a common broken and abraded shell fragments (pelecypods with a trace amount of ostracod fragments); rare intact shells have calcite-filled shelter voids; minor amount of silt-sized quartz; trace amount of fine organic debris and mica

Matrix: Minor recrystallized micritic mud matrix; trace amount of dispersed matrix clay; minor amount of finely divided organic material

Cements and Replacem ent M inerals: Minor microcrystalline calcite cement; recrystallized calcareous skeletal fragments; trace amount of microcrystalline pyrite replacement of shell material, organic material, and mud matrix; trace amount of medium crystalline calcite filling shelter voids

Pore System: No visible macropores; possible trace amount of micropores

Reservoir Quality: Poor

Magnification: A: 40X B: 200X

A) Thin laminations of skeletal-rich packstone (B1-15) overlie the massive (possibly burrow mottled) peloidal packstone below. Most allochems consist of dark peloids with only a minor amount of pelecypod (D14) and ostracod (B12) shell fragments.

B) The massive peloidal packstone includes common fine, highly abraded skeletal fragments (undifferentiated; J2, H15). Other components consists of silt-sized quartz (whit grains) and authigenic pyrite (B11, B9.5) There is no visible macroporosity.

Ohio Division of Geological Survey
CO2 No. 1
Tuscarawas County, Ohio

6336.0'
Plate 13

Weatherford LABORATORIES

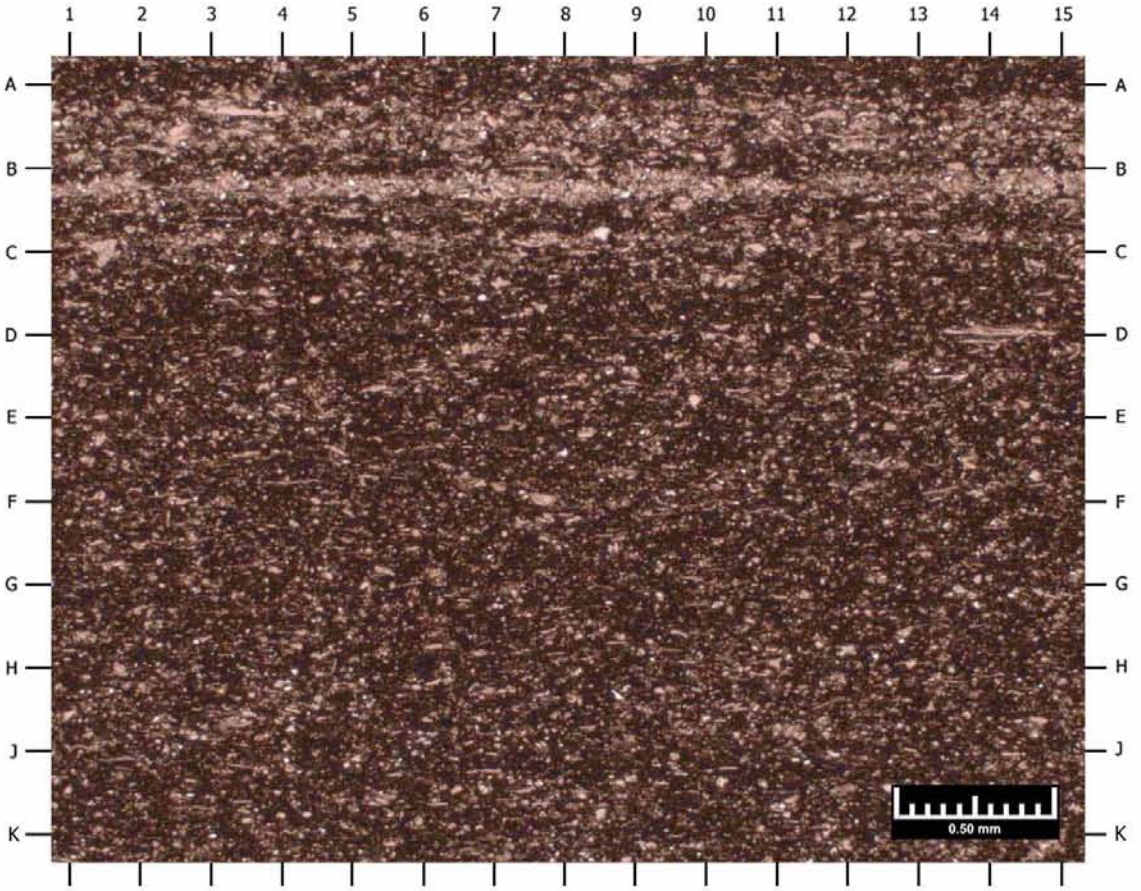

A

40X

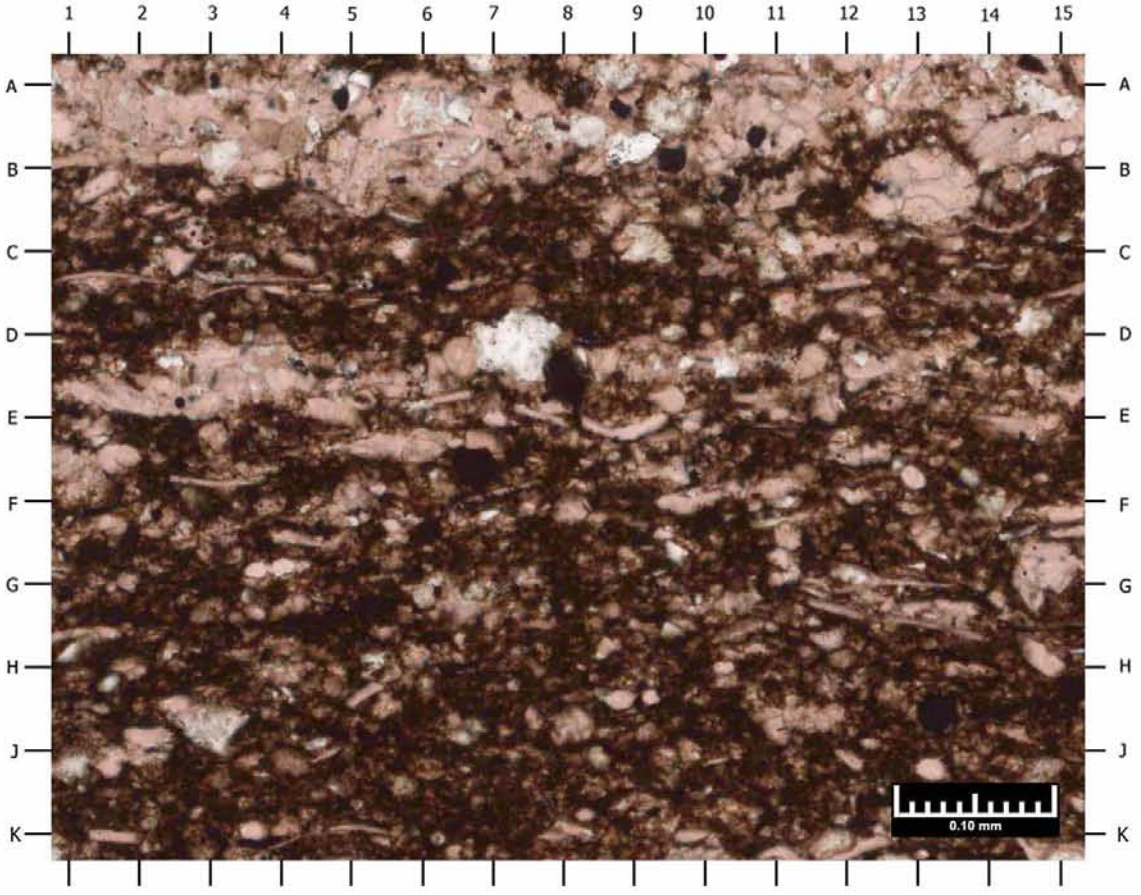

B

200X

Ohio Division of Geological Survey **OMNI File No: HH-38266**
CO_2 No. 1 Well
Tuscarawas County, Ohio
Trenton Limestone
Rotary Sidewall Core

THIN SECTION DESCRIPTION - GENERAL

SAMPLE DEPTH: 6396.0 FEET
SAMPLE NUMBER: 1-14R

Plate 14

Permeability (Klink.): 0.0002 mD Porosity (NCS): 2.8% Grain Density: 2.69 gm/cc

Lithology: Slightly Dolomitic Limestone

Texture: Skeletal Packstone / Wackestone

Framework Grains: Allochems consist of rare phosphatic peloids, with a common recrystallized skeletal shell fragments (pelecypods up to 1 cm) with a minor amount of trilobite, echinoderm, and ostracod fragments); trace amount of brachiopod spines and sponge spicules; minor amount of peloids; trace amount of phosphatic shell fragments; trace amount of silt-sized quartz and organic material

Matrix: Variable amounts of carbonate mud matrix; trace amount of dispersed clay

Cements and Replacement Minerals: Common calcite cement reduces interparticle pores; allochem particles have been partially replaced by pyrite; trace amount of dolomite; trace amount of microcrystalline pyrite replacement of organic material, and mud matrix

Pore System: No visible macropores

Reservoir Quality: Poor

Magnification: A: 40X B: 200X

A) Calcareous shell fragments are variably concentrated in laminations (skeletal packstone) and less abundant in the mud-rich portions of the sample (skeletal wackestone). Note the rather random orientation of shell fragments, suggesting rapid deposition or reworking of the sediment following deposition.

B) There are no visible macropores in this sample. The matrix consists of recrystallized micrite mud, compacted and replaced peloids (CD4), and authigenic pyrite (B11). Thin calcareous shells are commonly broken due to burial pressure (F11), whereas thicker shells are not broken.

Ohio Division of Geological Survey
CO2 No. 1
Tuscarawas County, Ohio

6396.0'
Plate 14

Weatherford LABORATORIES

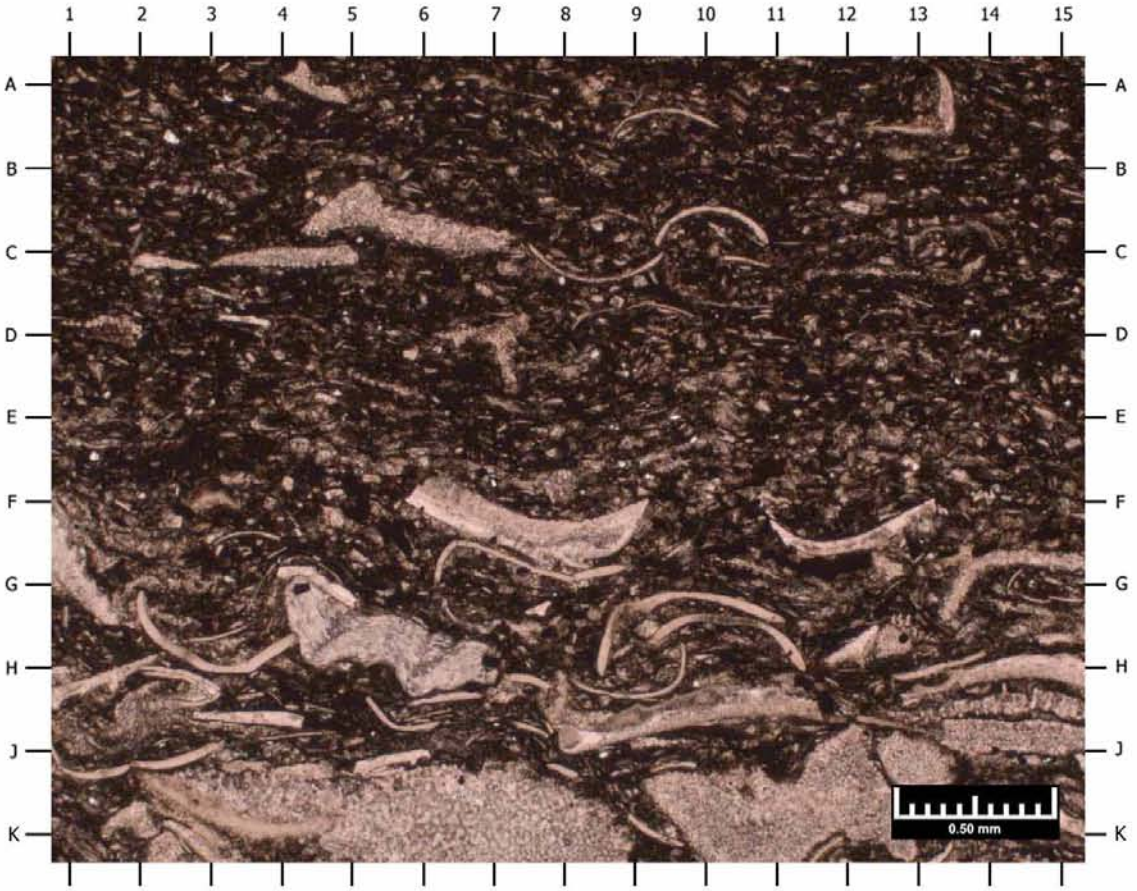

A

40X

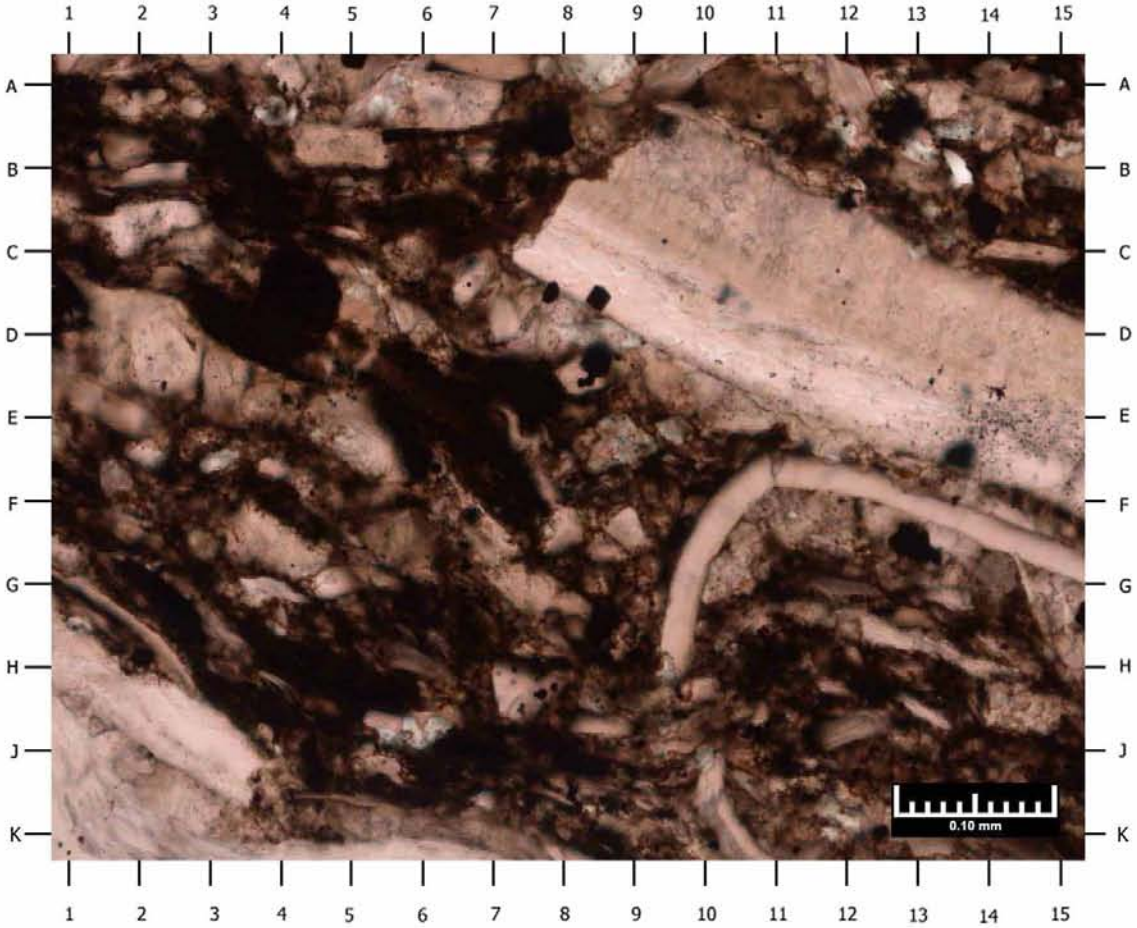

B

200X

Ohio Division of Geological Survey **OMNI File No: HH-38266**
CO_2 No. 1 Well
Tuscarawas County, Ohio
Trenton Limestone
Rotary Sidewall Core

THIN SECTION PHOTOMICROGRAPHS

SAMPLE DEPTH: 6490.0 FEET
SAMPLE NUMBER: 1-15R

Plate 15

Permeability (Klink.): 0.0003 mD Porosity (NCS): 3.1% Grain Density: 2.69 gm/cc

Sample not selected for petrographic analysis.

Magnification: A: 40X B: 200X

Ohio Division of Geological Survey
CO2 No. 1
Tuscarawas County, Ohio

6490.0'
Plate 15

Weatherford LABORATORIES

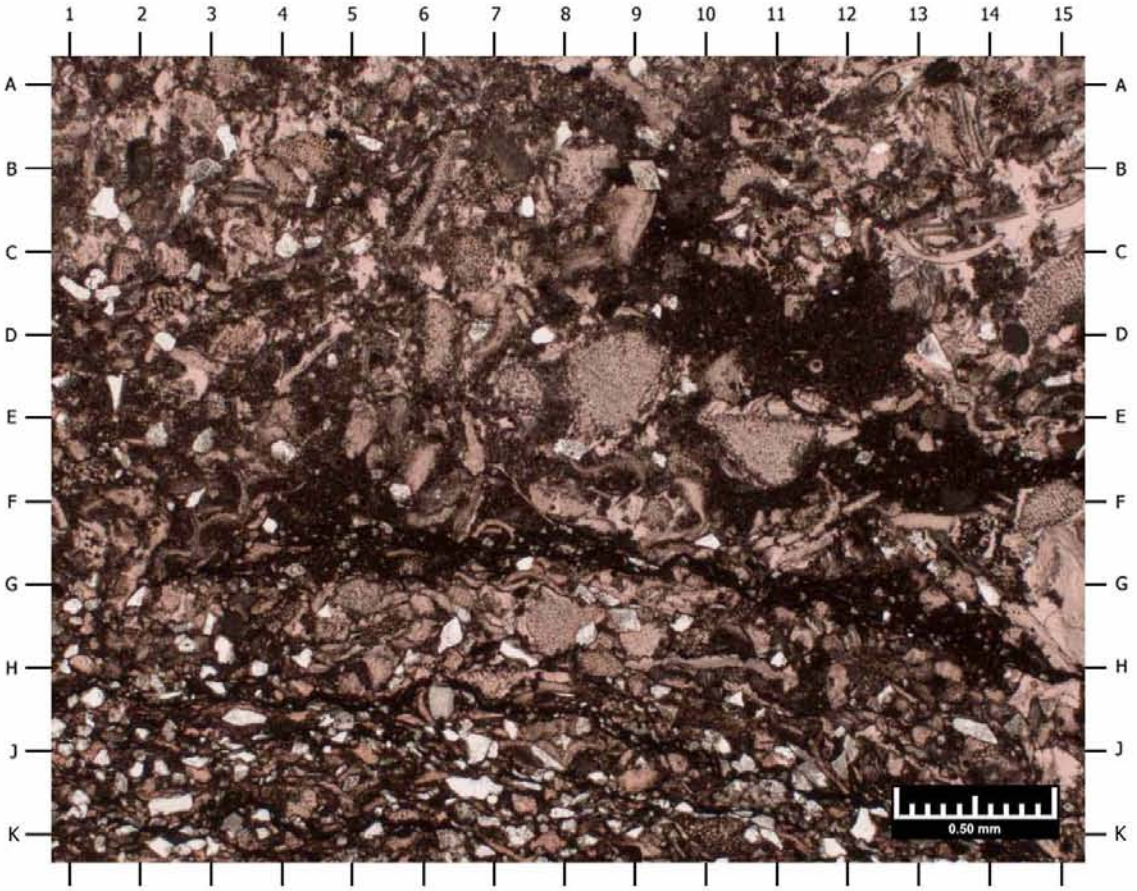

A

40X

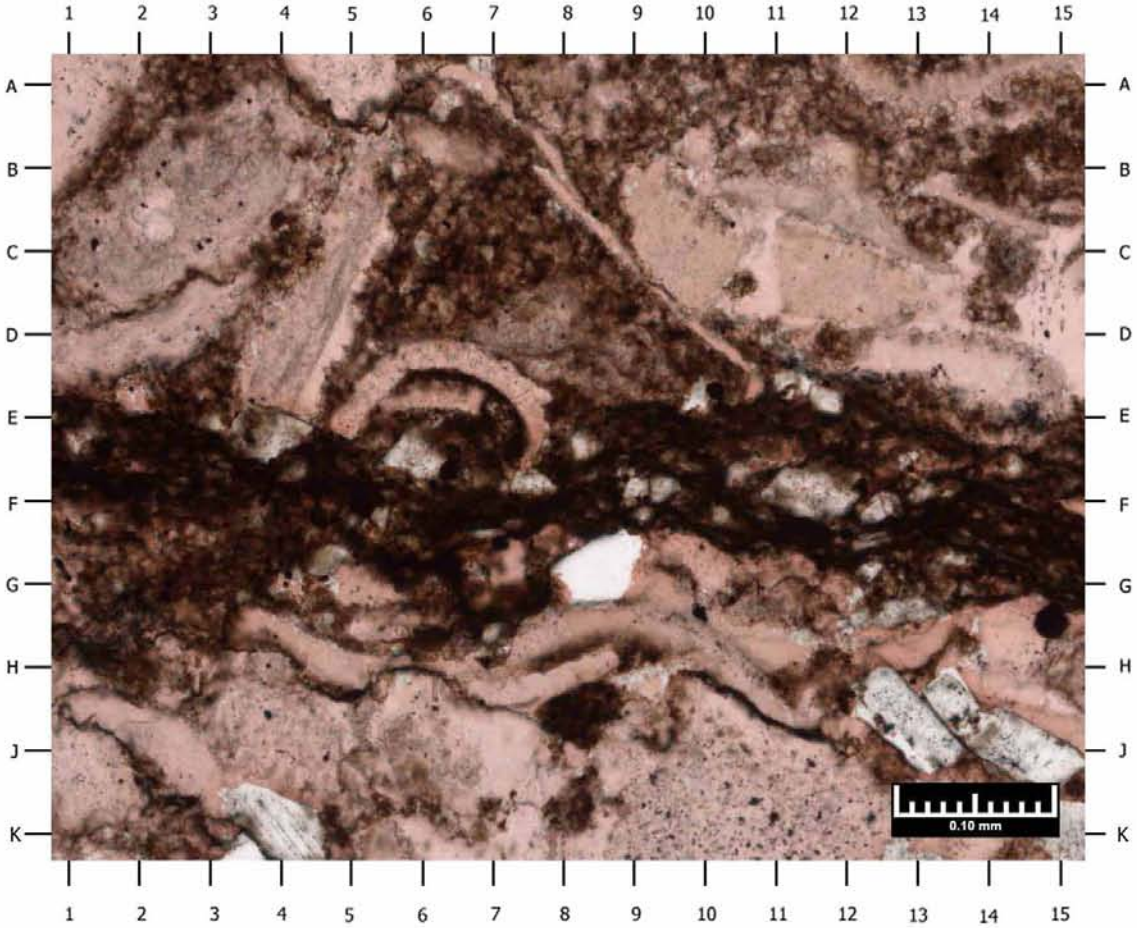

B

200X

Ohio Division of Geological Survey **OMNI File No: HH-38266**
CO_2 No. 1 Well
Tuscarawas County, Ohio
Black River Group
Rotary Sidewall Core

THIN SECTION PHOTOMICROGRAPHS

SAMPLE DEPTH: 6524.0 FEET
SAMPLE NUMBER: 1-16R

Plate 16

Permeability (Klink.): 0.0058 mD Porosity (NCS): 3.5% Grain Density: 2.75 gm/cc

Sample not selected for petrographic analysis.

Magnification: A: 40X B: 200X

Ohio Division of Geological Survey
CO2 No. 1
Tuscarawas County, Ohio

6524.0'
Plate 16

Weatherford LABORATORIES

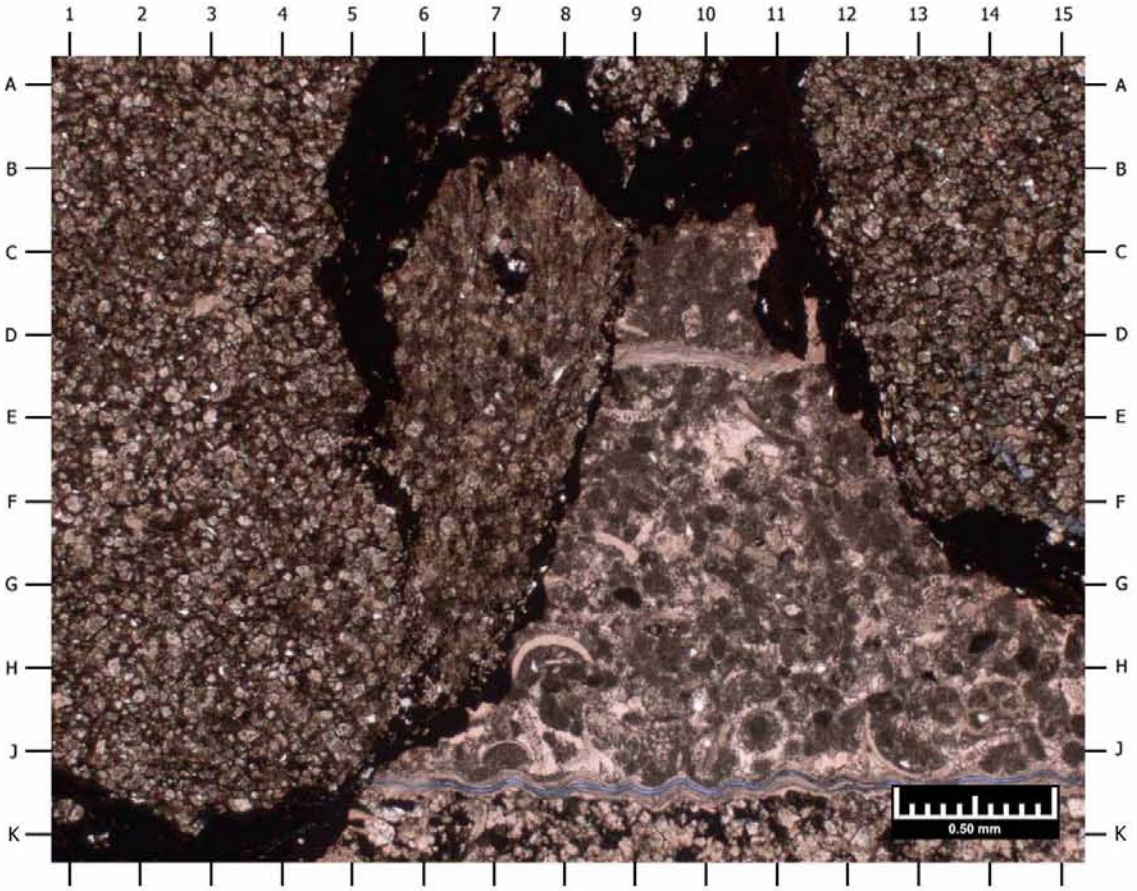

A

40X

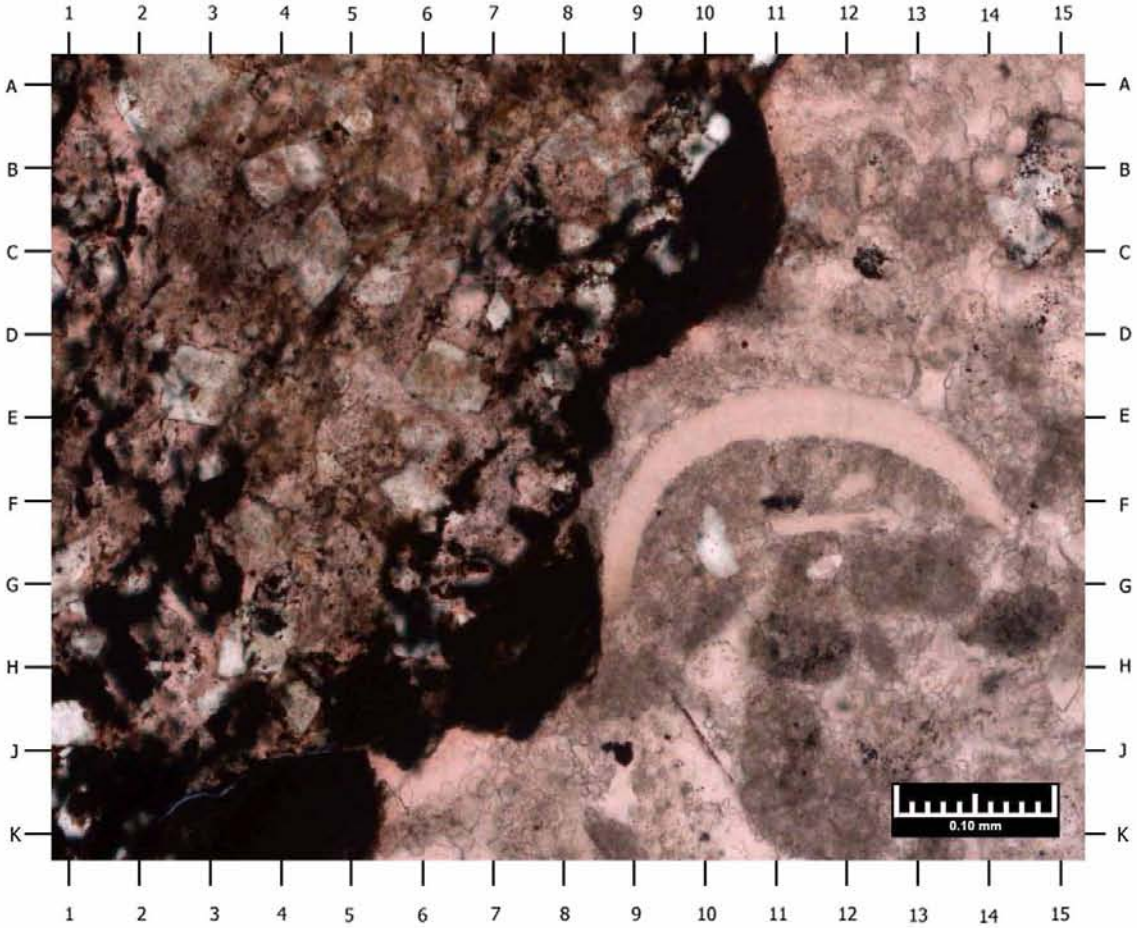

B

200X

Ohio Division of Geological Survey **OMNI File No: HH-38266**
CO_2 No. 1 Well
Tuscarawas County, Ohio
Black River Group
Rotary Sidewall Core

THIN SECTION PHOTOMICROGRAPHS

SAMPLE DEPTH: 6566.0 FEET
SAMPLE NUMBER: 1-17R

Plate 17

Permeability (Klink.): 0.0003 mD Porosity (NCS): 1.5% Grain Density: 2.73 gm/cc

Sample not selected for petrographic analysis.

Magnification: A: 40X B: 200X

Ohio Division of Geological Survey
CO2 No. 1
Tuscarawas County, Ohio

6566.0'
Plate 17

Weatherford LABORATORIES

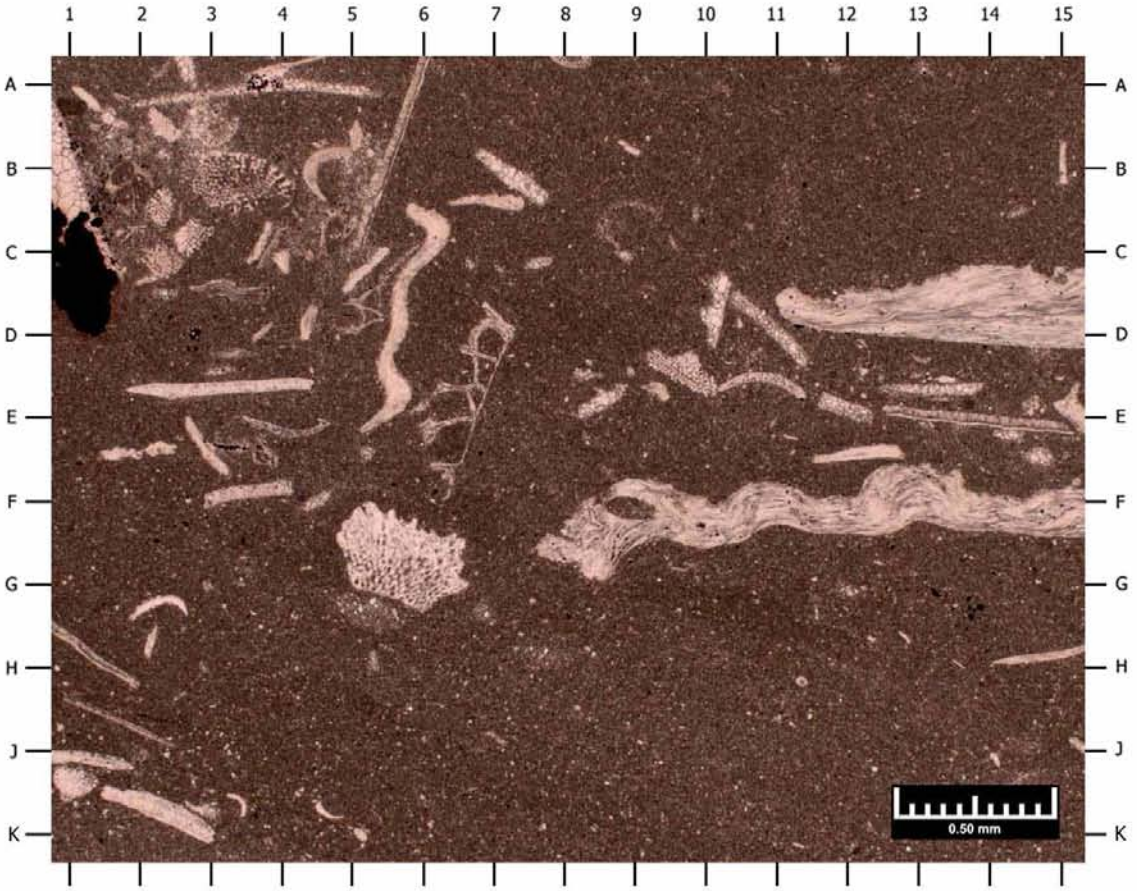

A

40X

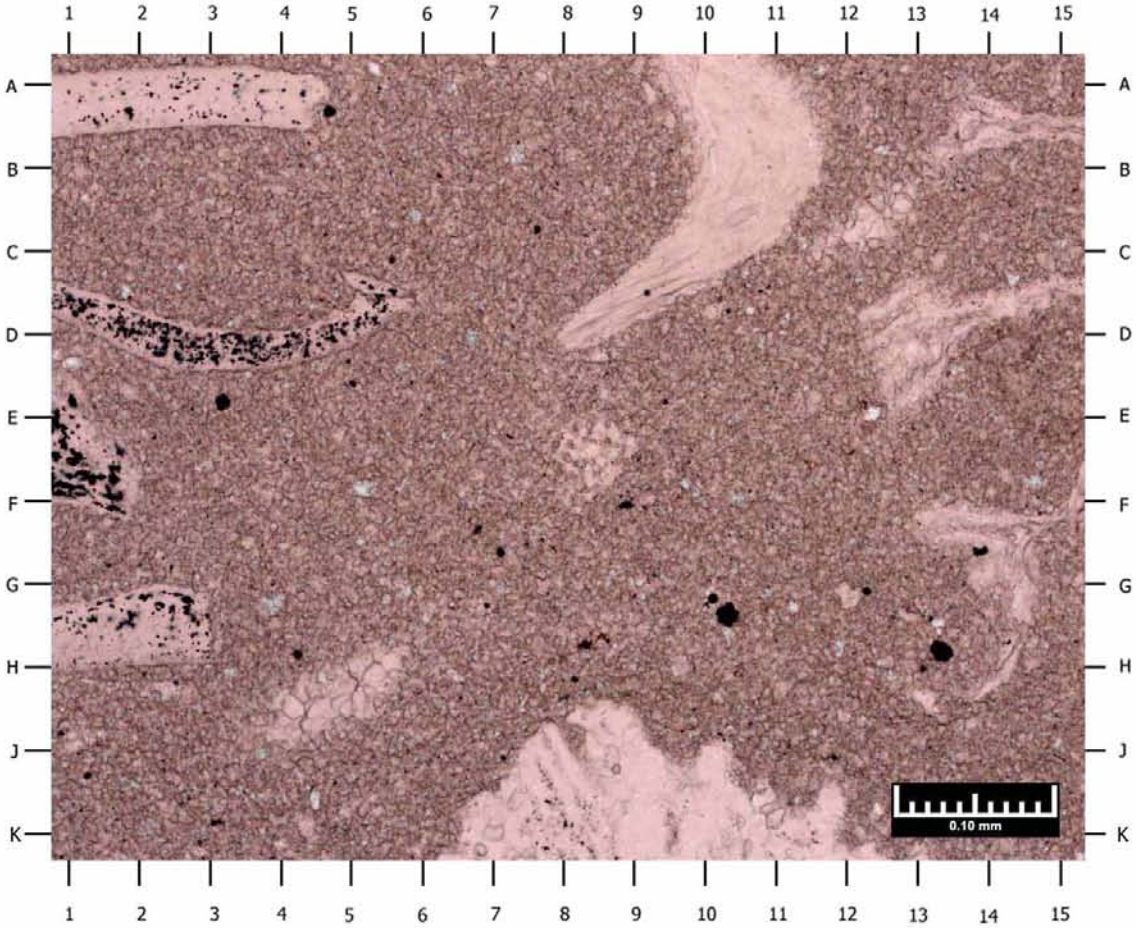

B

200X

Ohio Division of Geological Survey **OMNI File No: HH-38266**
CO_2 No. 1 Well
Tuscarawas County, Ohio
Black River Group
Rotary Sidewall Core

THIN SECTION PHOTOMICROGRAPHS

SAMPLE DEPTH: 6620.0 FEET
SAMPLE NUMBER: 1-18R

Plate 18

Permeability (Klink.): 0.0003 mD Porosity (NCS): 1.6% Grain Density: 2.71 gm/cc

Sample not selected for petrographic analysis.

Magnification: A: 40X B: 200X

Ohio Division of Geological Survey
CO2 No. 1
Tuscarawas County, Ohio

6620.0'
Plate 18

Weatherford LABORATORIES

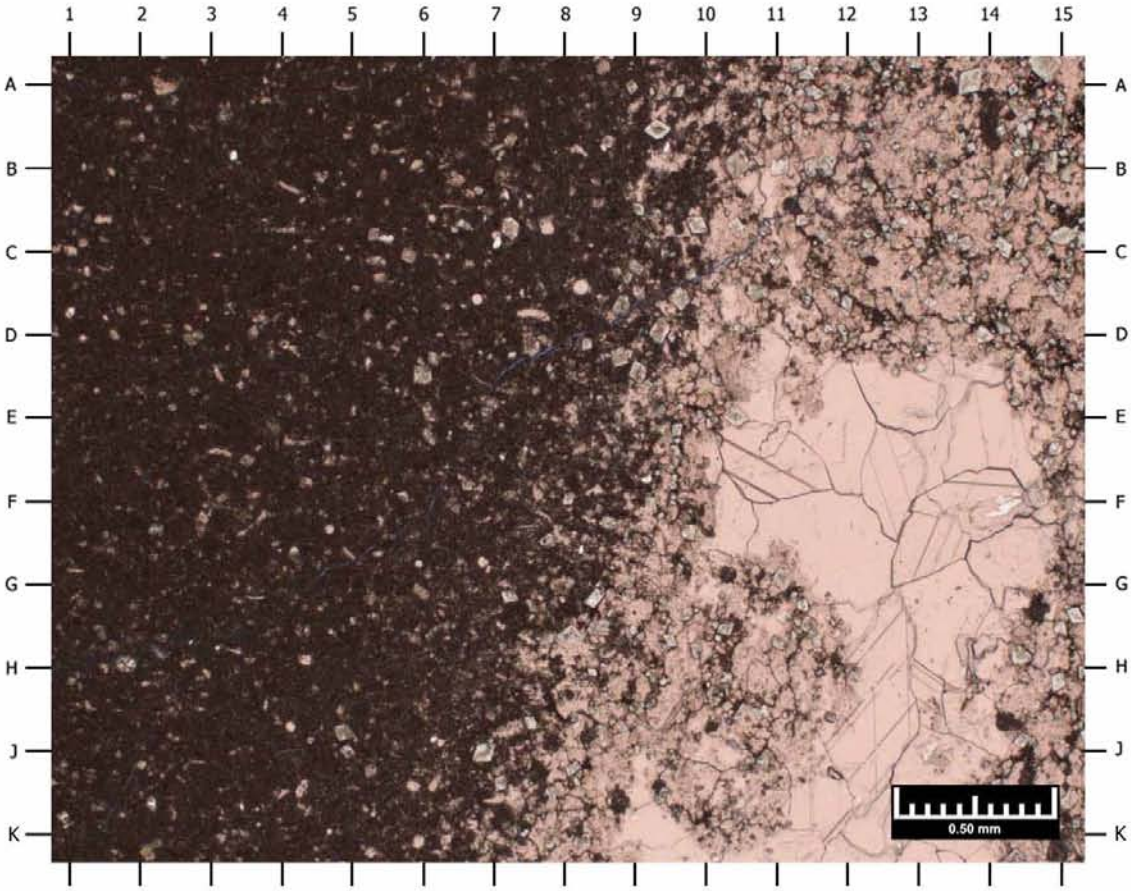

A

40X

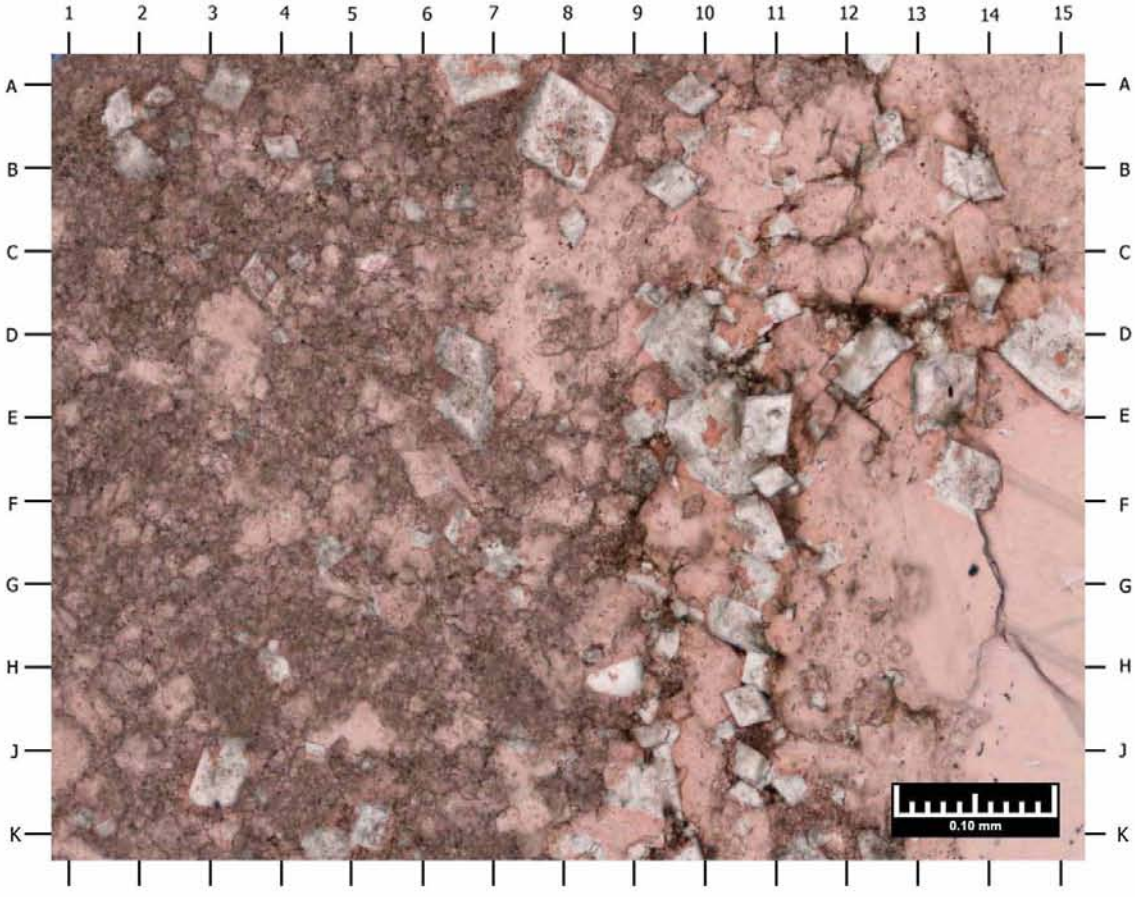

B

200X

Ohio Division of Geological Survey **OMNI File No: HH-38266**
CO_2 No. 1 Well
Tuscarawas County, Ohio
Black River Group
Rotary Sidewall Core

THIN SECTION PHOTOMICROGRAPHS

SAMPLE DEPTH: 6750.0 FEET
SAMPLE NUMBER: 1-19R

Plate 19

Permeability (Klink.): 0.0057 mD Porosity (NCS): 5.1% Grain Density: 2.71 gm/cc

Sample not selected for petrographic analysis.

Magnification: A: 40X B: 200X

Ohio Division of Geological Survey
CO2 No. 1
Tuscarawas County, Ohio

6750.0'
Plate 19

Weatherford LABORATORIES

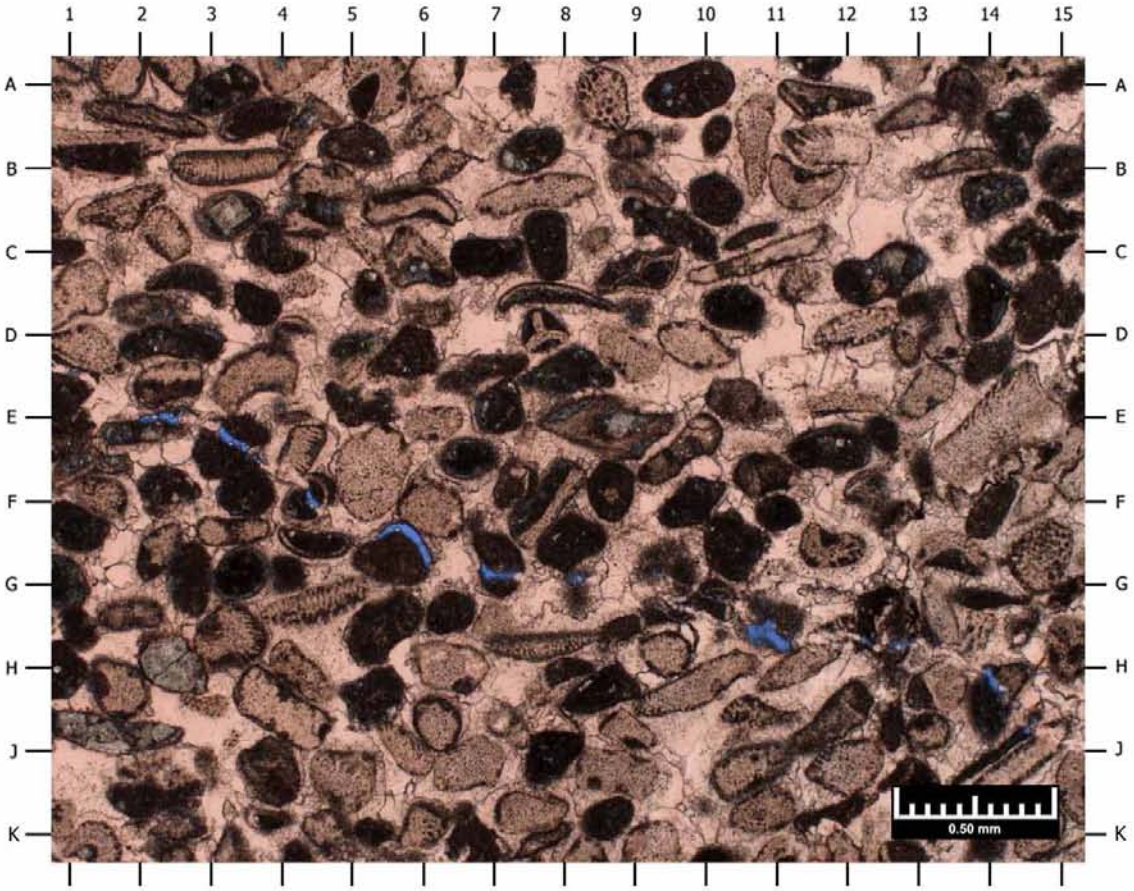

A

40X

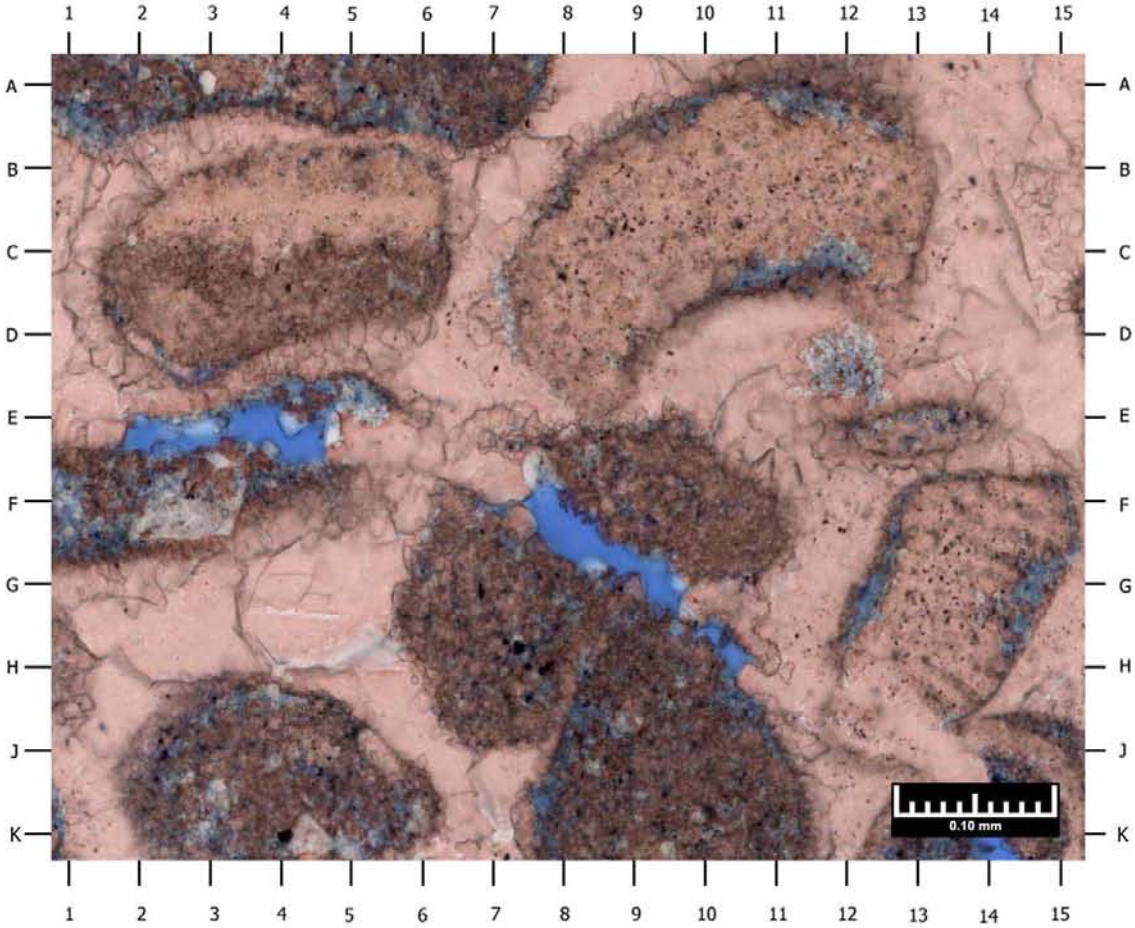

B

200X

Ohio Division of Geological Survey **OMNI File No: HH-38266**
CO_2 No. 1 Well
Tuscarawas County, Ohio
Black River Group
Rotary Sidewall Core

THIN SECTION DESCRIPTION - DETAILED

SAMPLE DEPTH: 6794.0 FEET
SAMPLE NUMBER: 1-20R

Plate 20

Permeability (Klink.): 0.286 mD Porosity (NCS): 8.3% Grain Density: 2.70 gm/cc

Lithology: Slightly dolomitic limestone

Texture: Skeletal peloidal packstone / grainstone; rare laminations with microstylolites

Framework Grains: Allochems consist of abundant peloids, with a minor amount of recrystallized skeletal shell fragments (pelecypods with a trace amount of brachiopod and bryozoan fragments); trace amount of silt-sized quartz; trace amount of organic material concentrated along microstylolites

Matrix: Minor amount of carbonate mud matrix; minor concentration of insoluble clay and organics along microstylolites; trace amount of authigenic clay

Cements and Replacement Minerals: Common micritic calcite cement in combination with sparry calcite cement reduces original interparticle pores; minor amount of dolomite replacing shell fragments, cement, and matrix; trace amount of microcrystalline pyrite replacement of shell material and organic material; trace amount of subhedral to euhedral dolomite; trace amount of calcite filling fractures

Pore System: Trace amount of interparticle macropores, intercrystalline micropores, and skeletal moldic pores; minor amount of intercrystalline micropores; trace amount of cement-filled fractures; minor amount of secondary intraparticle pores

Reservoir Quality: Fair (based on matrix micropores in combination with scattered macropores and fracture pores, and assuming fracture stimulation of the reservoir to enhance matrix permeability for dry gas storage or production)

Magnification: A: 40X B: 200X

A) Most allochems consist of peloids (G10) with a minor amount of calcareous shell fragments (C5, B11). The sample contains thin, anastomosing microstylolites (E1 to E15) with insoluble organic material and authigenic dolomite. Subvertical fractures partially healed with dolomite (G4.5) and quartz (F7) terminate at the microstylolite.

B) Detailed view shows dead oil in the fracture (E10, G6.5). Note the concentration of euhedral dolomite crystals (D4, C8, C10) along the stylolite.

Ohio Division of Geological Survey
CO2 No. 1
Tuscarawas County, Ohio

6794.0'
Plate 20

Weatherford LABORATORIES

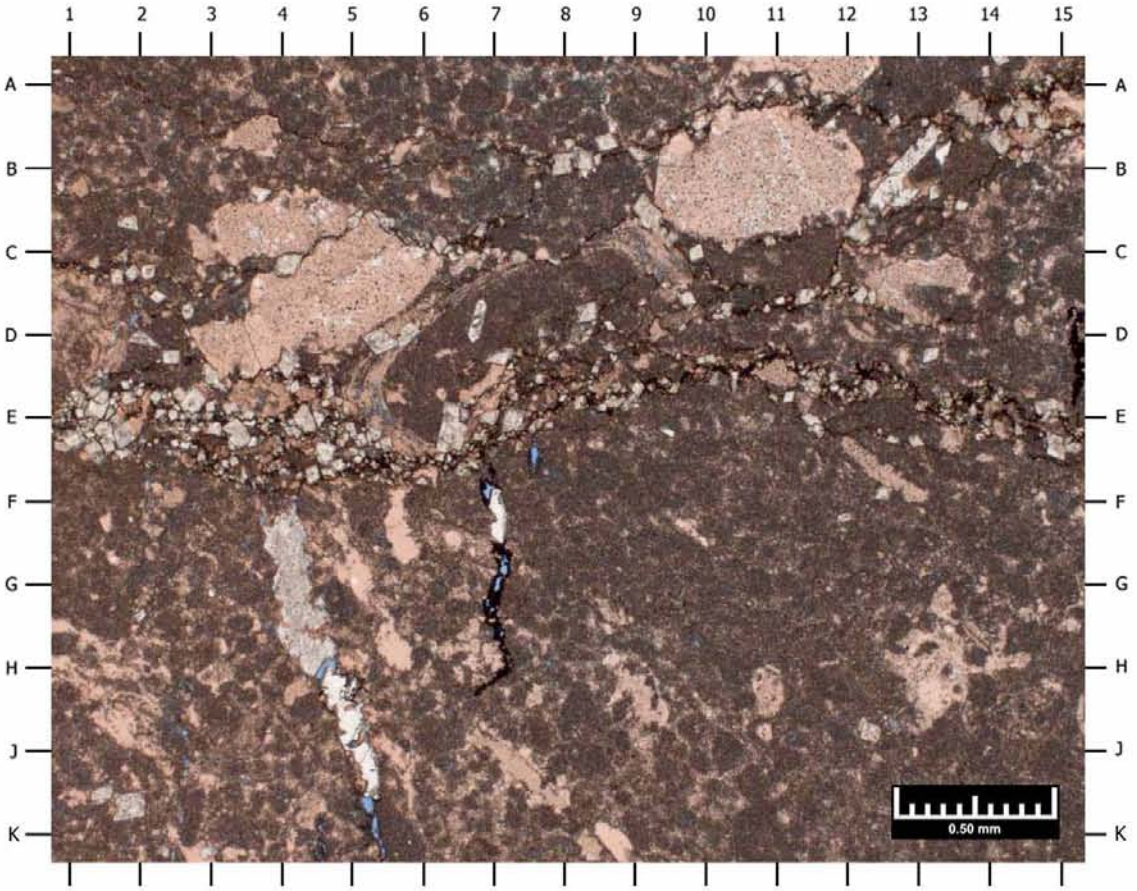

A

40X

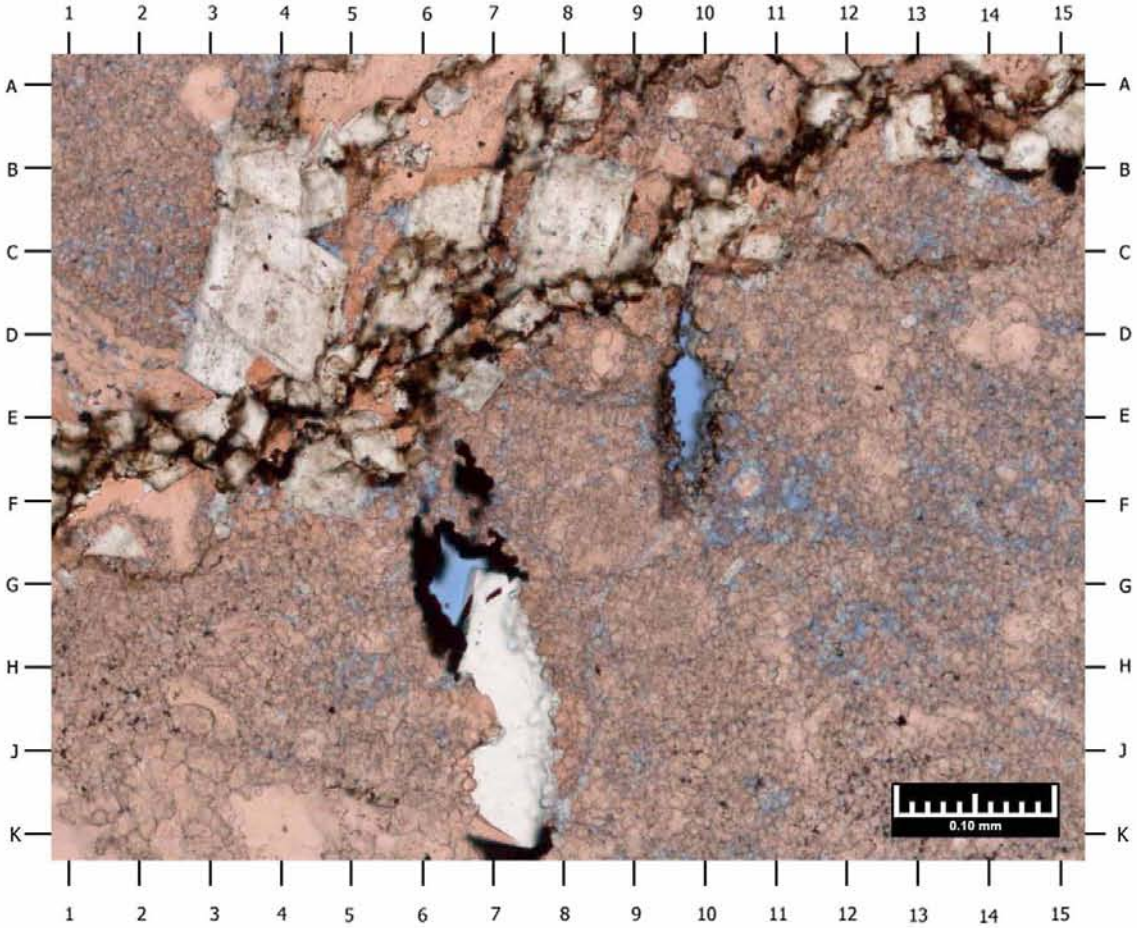

B

200X

Ohio Division of Geological Survey **OMNI File No: HH-38266**
CO_2 No. 1 Well
Tuscarawas County, Ohio
Black River Group
Rotary Sidewall Core

THIN SECTION PHOTOMICROGRAPHS

SAMPLE DEPTH: 6808.0 FEET
SAMPLE NUMBER: 1-21R

Plate 21

Permeability (Klink.): 0.027 mD Porosity (NCS): 4.7% Grain Density: 2.71 gm/cc

Sample not selected for petrographic analysis.

Magnification: A: 40X B: 200X

Ohio Division of Geological Survey
CO2 No. 1
Tuscarawas County, Ohio

6808.0'
Plate 21

Weatherford LABORATORIES

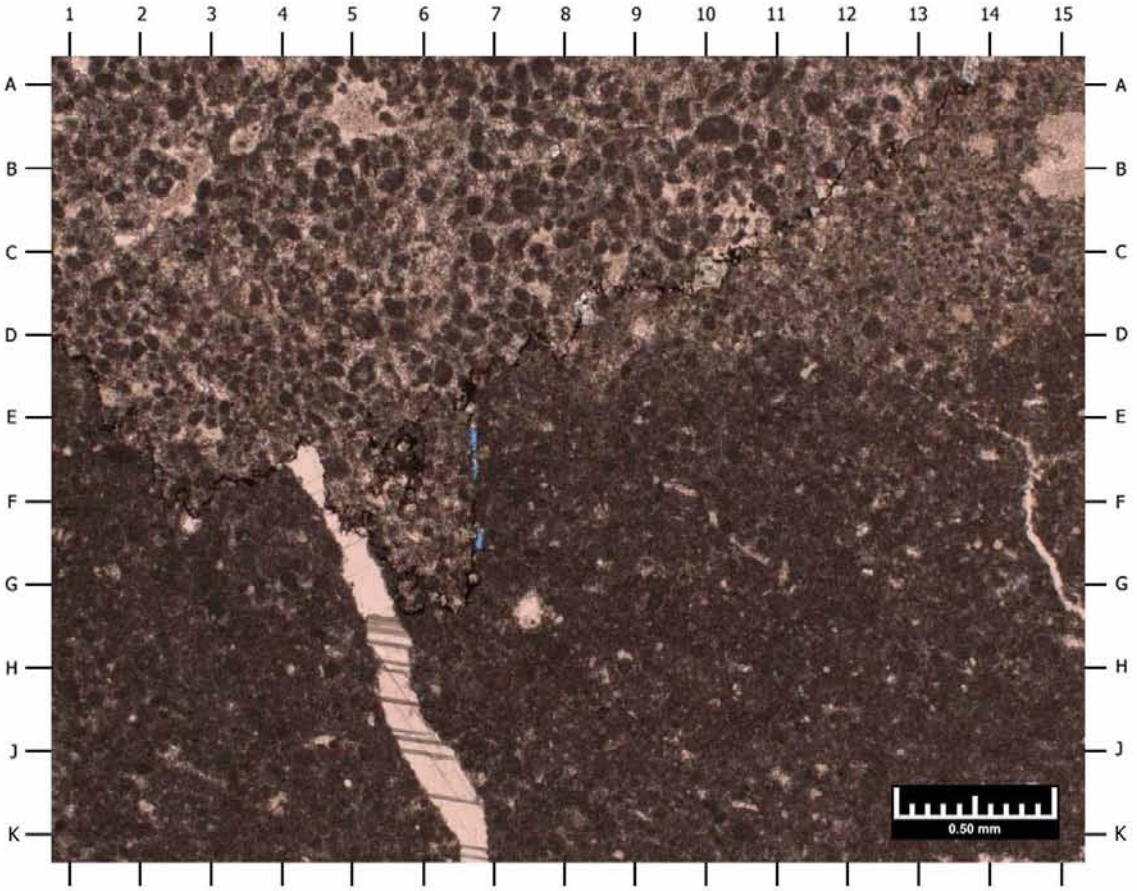

A

40X

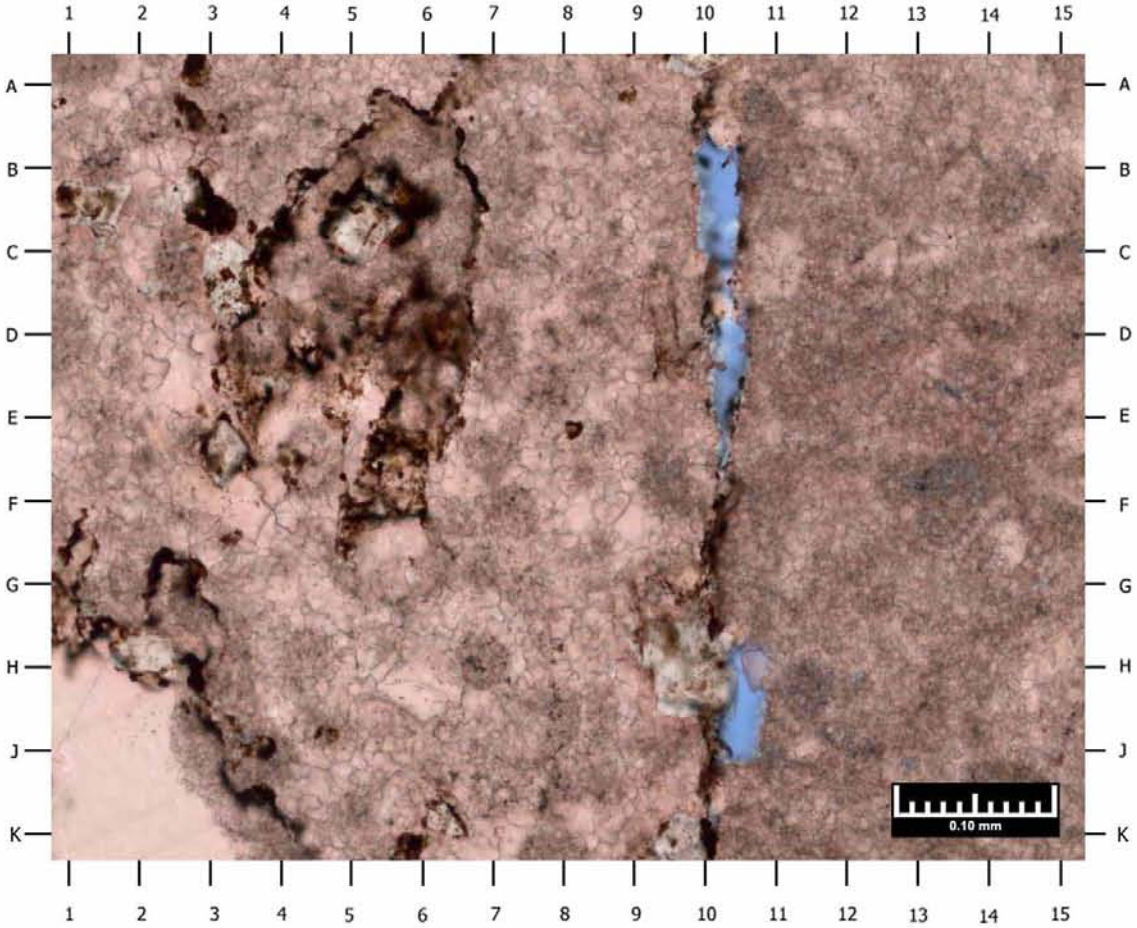

B

200X

Ohio Division of Geological Survey **OMNI File No: HH-38266**
CO_2 No. 1 Well
Tuscarawas County, Ohio
Black River Group
Rotary Sidewall Core

THIN SECTION DESCRIPTION - DETAILED

SAMPLE DEPTH: 6844.0 FEET
SAMPLE NUMBER: 1-22R

Plate 22

Permeability (Klink.): 0.0027 mD Porosity (NCS): 4.4% Grain Density: 2.71 gm/cc

Lithology: Limestone

Texture: Skeletal peloidal packstone / grainstone; massive; possible burrow mottling

Framework Grains: Allochems consist of abundant peloids, with a minor amount of recrystallized skeletal shell fragments (pelecypods with a trace amount of brachiopod , echinoderm, and bryozoan fragments); trace amount of organic material

Matrix: Trace amount of carbonate mud matrix; trace amount of authigenic clay

Cements and Replacement Minerals: Common sparry calcite cement reduces original interparticle pores; minor amount of dolomite replacing shell fragments, cement, and matrix; trace amount of microcrystalline pyrite replacement of shell material, and organic material; trace amount of subhedral to euhedral dolomite

Pore System: Trace amount of interparticle macropores, intercrystalline micropores, and skeletal moldic pores; minor amount of secondary intraparticle pores

Reservoir Quality: Poor

Magnification: A: 40X B: 200X

A) This sample consists of poorly sorted peloids (H3) and shell fragments (B8) with only scattered intraparticle pores (B10.5). Note the calcite syntaxial overgrowth on the echinoderm fragments (A6.5, B10.5).

B) A detailed view of the sample shows microporous peloids (D12.5) that are sometimes partially dissolved (H1) or replaced by dolomite (F6) or authigenic quartz (F13). Early cement includes isopachous rim cement (E13.5, H3) and sparry calcite that formed as a syntaxial overgrowth (A2). Most of the pores are not well connected, resulting in very low permeability.

Ohio Division of Geological Survey
CO2 No. 1
Tuscarawas County, Ohio

6844.0'
Plate 22

Weatherford LABORATORIES

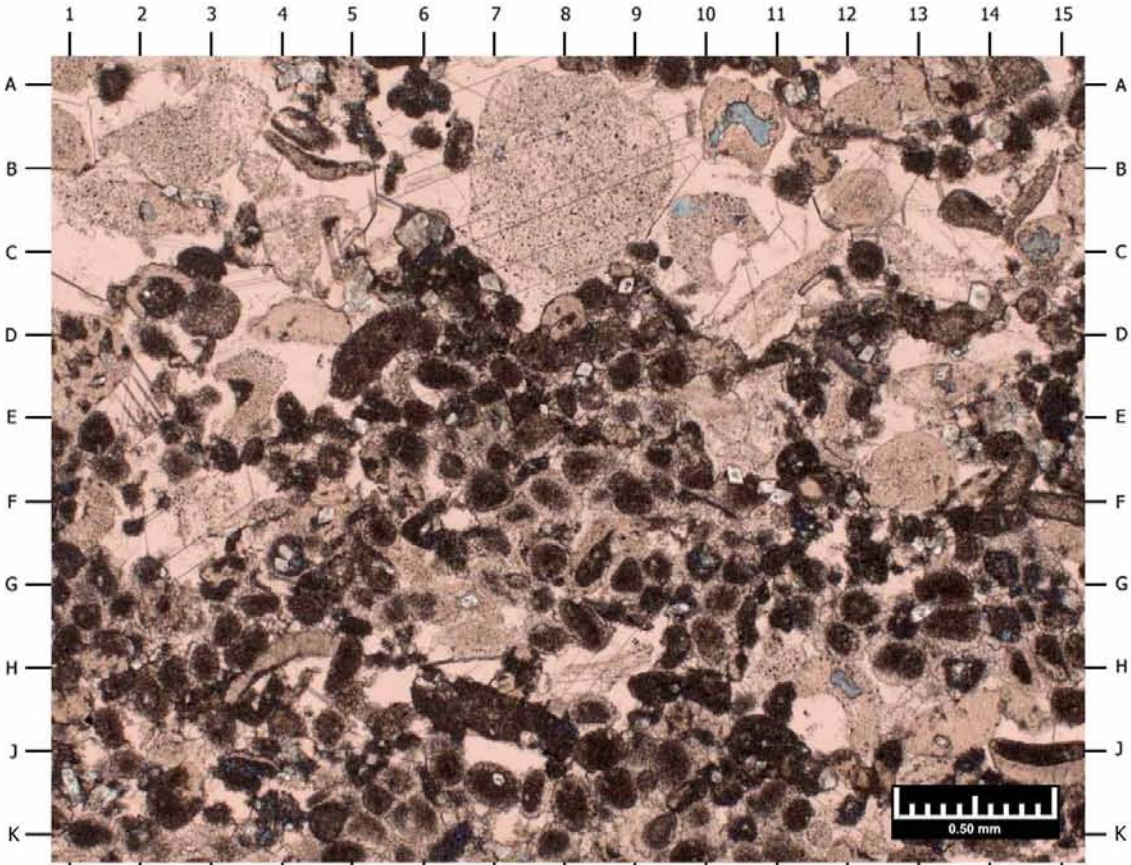

A

40X

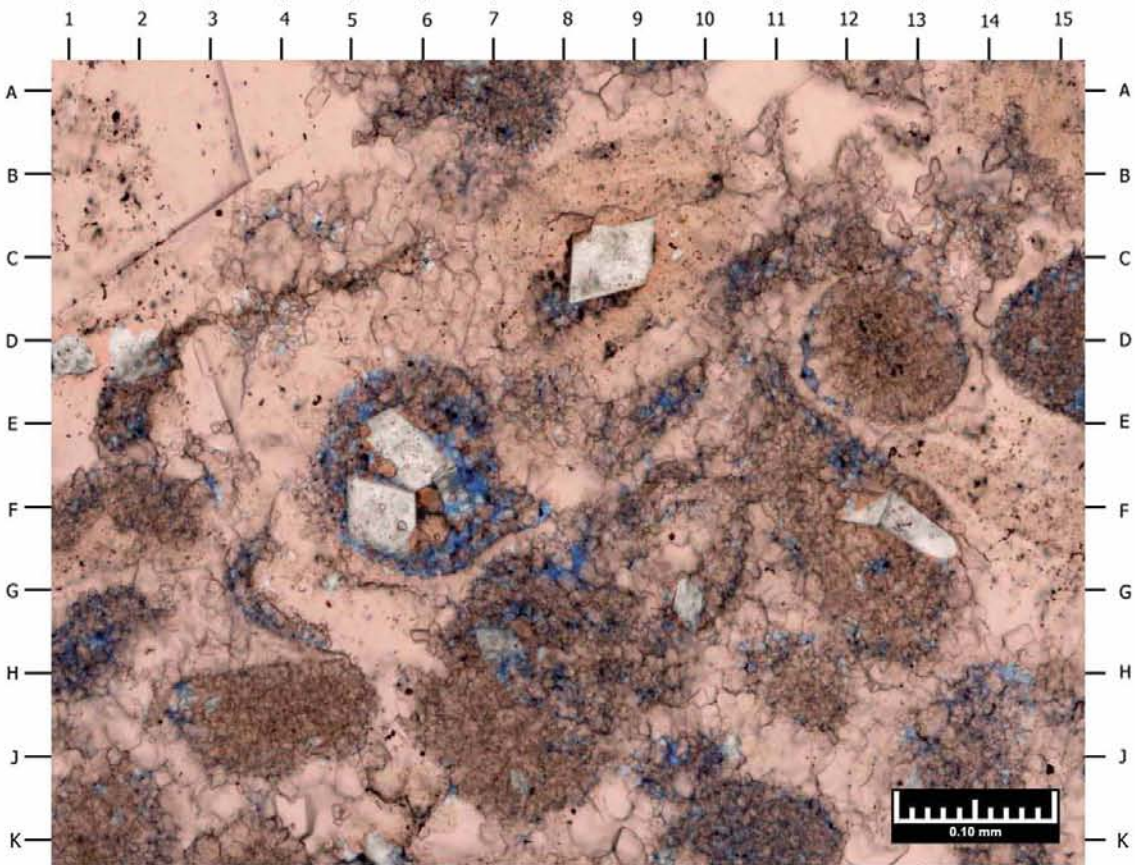

B

200X

Ohio Division of Geological Survey **OMNI File No: HH-38266**
CO_2 No. 1 Well
Tuscarawas County, Ohio
Black River Group
Rotary Sidewall Core

THIN SECTION PHOTOMICROGRAPHS

SAMPLE DEPTH: 6871.0 FEET
SAMPLE NUMBER: 1-23R

Plate 23

Permeability (Klink.): 0.482 mD Porosity (NCS): 13.0% Grain Density: 2.73 gm/cc

Sample not selected for petrographic analysis.

Magnification: A: 40X B: 200X

Ohio Division of Geological Survey
CO2 No. 1
Tuscarawas County, Ohio

6844.0'
Plate 23

Weatherford LABORATORIES

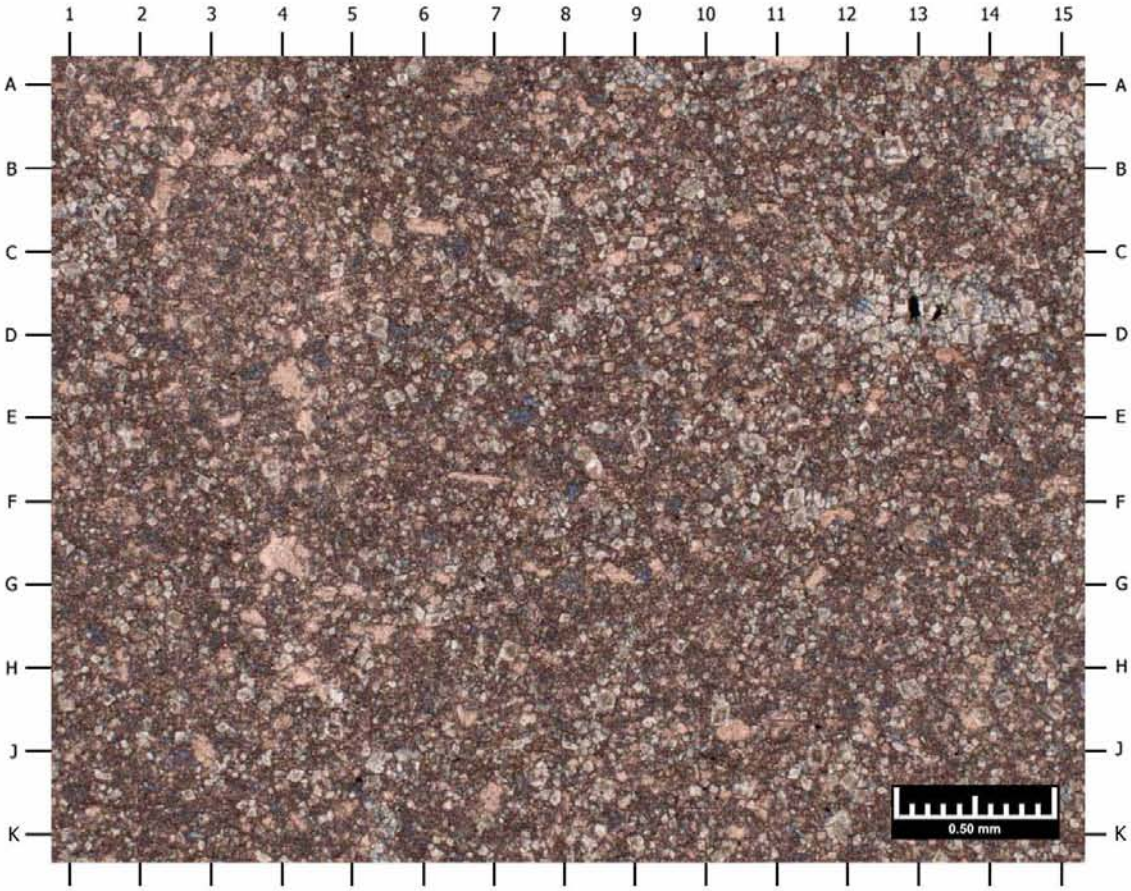

A

40X

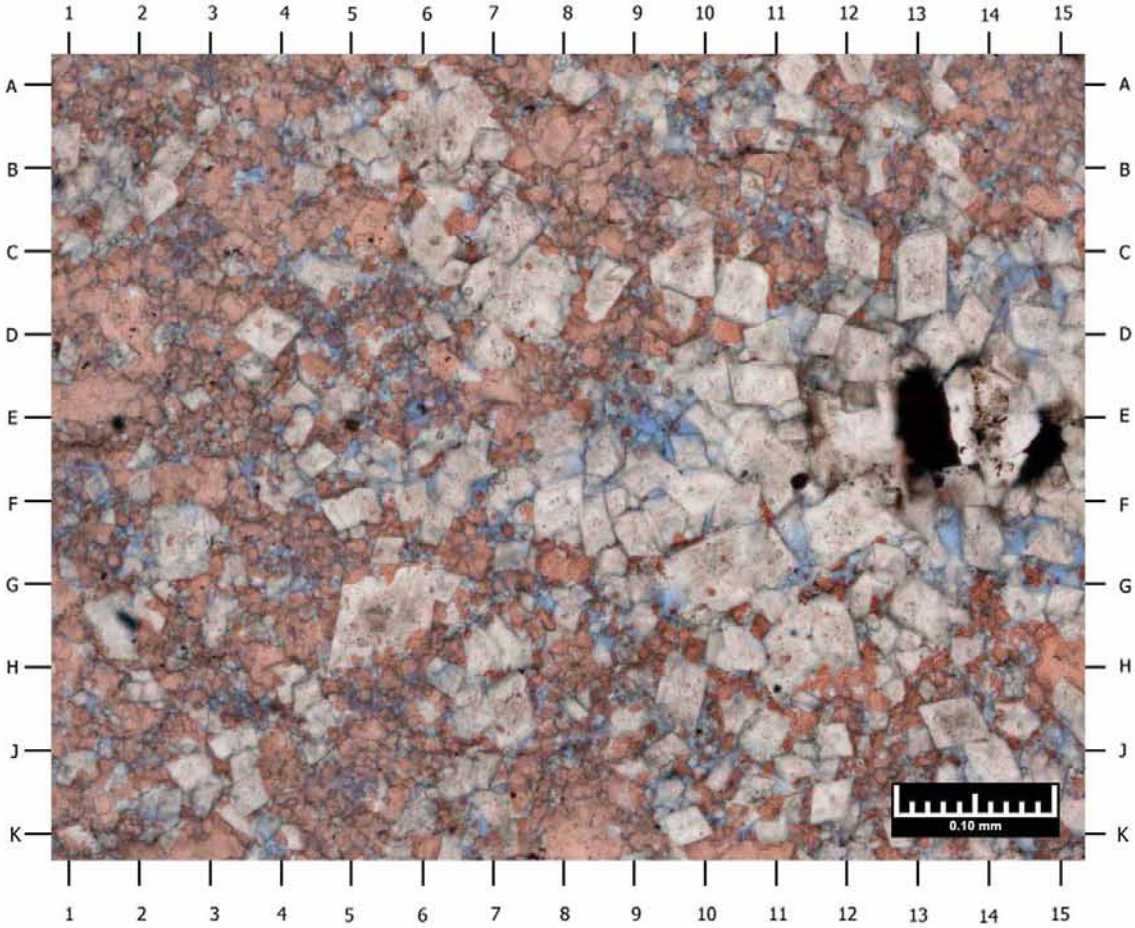

B

200X

Ohio Division of Geological Survey **OMNI File No: HH-38266**
CO_2 No. 1 Well
Tuscarawas County, Ohio
Black River Group
Rotary Sidewall Core

THIN SECTION PHOTOMICROGRAPHS

SAMPLE DEPTH: 6936.0 FEET
SAMPLE NUMBER: 1-24R

Plate 24

Permeability (Klink.): 0.032 mD Porosity (NCS): 8.3% Grain Density: 2.73 gm/cc

Sample not selected for petrographic analysis.

Magnification: A: 40X B: 200X

Ohio Division of Geological Survey
CO2 No. 1
Tuscarawas County, Ohio

6936.0'
Plate 24

Weatherford LABORATORIES

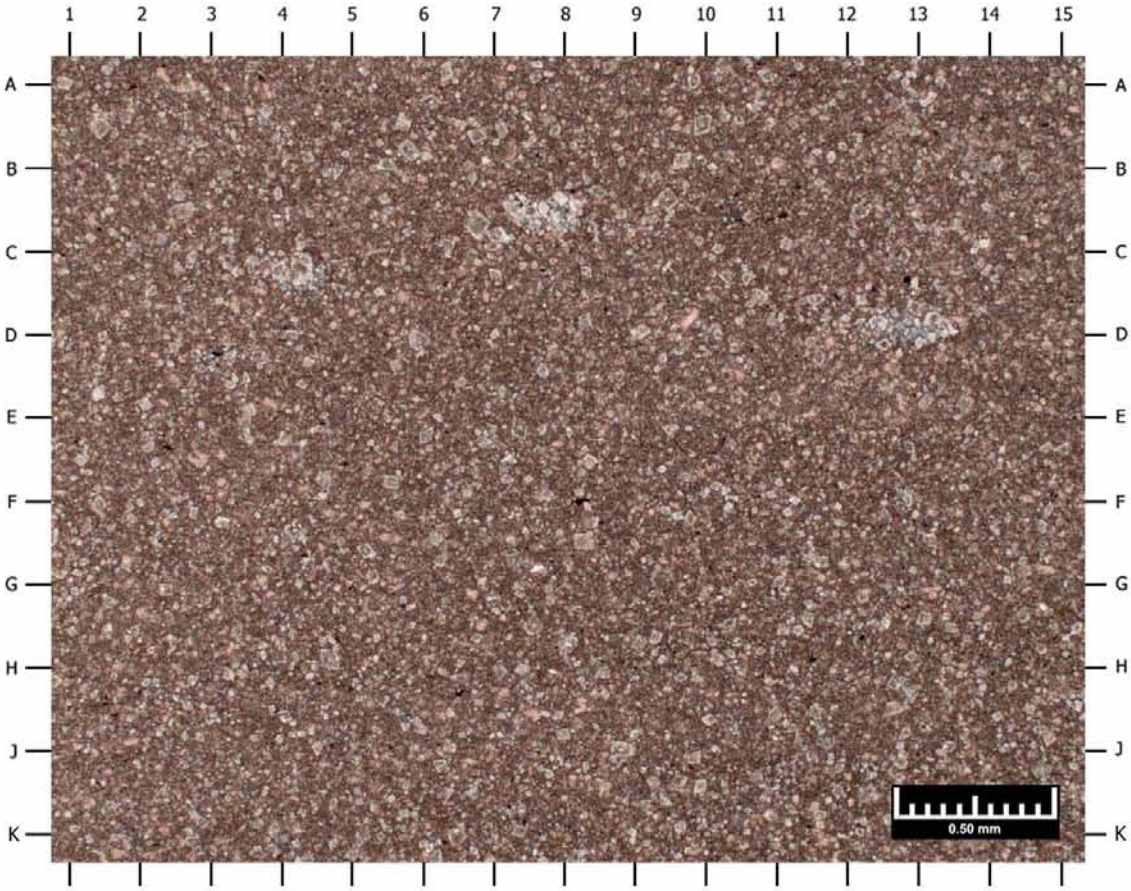

A

40X

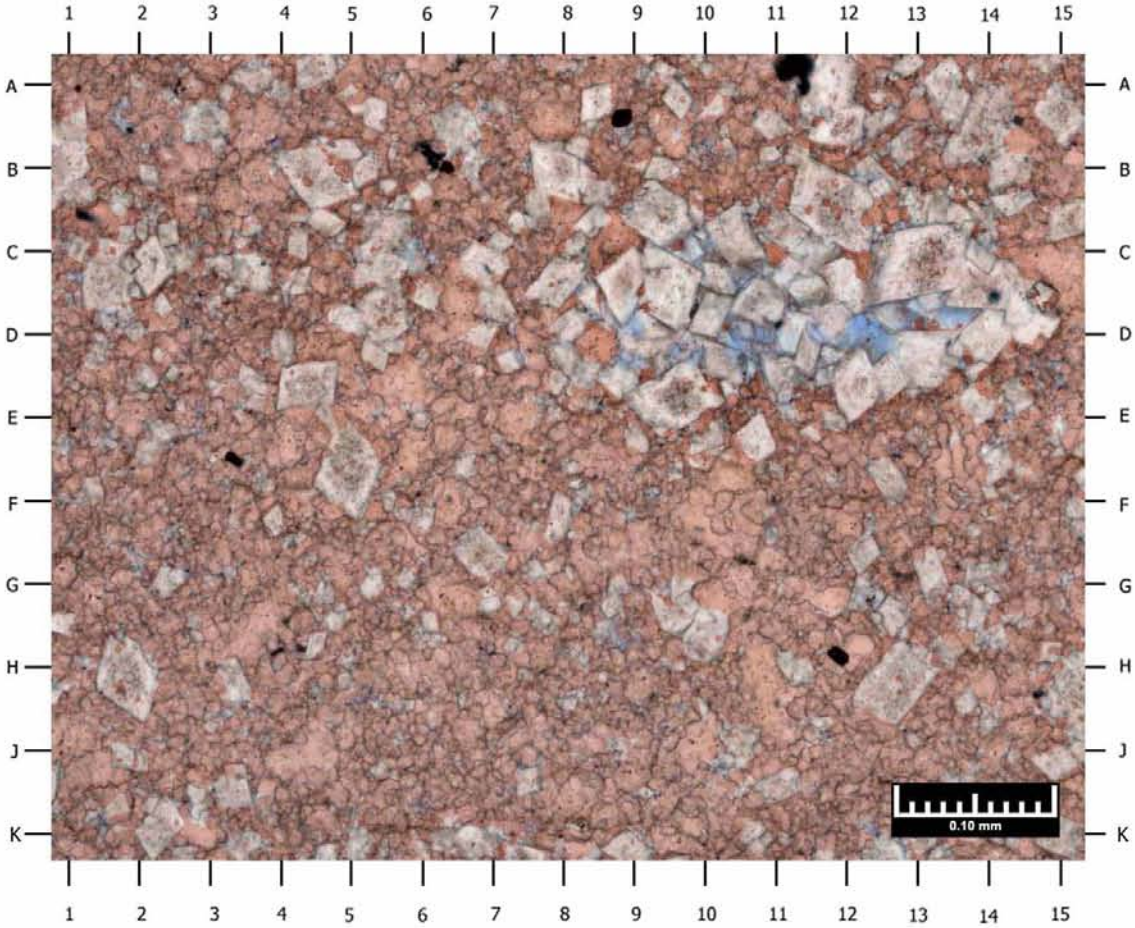

B

200X

Ohio Division of Geological Survey **OMNI File No: HH-38266**
CO_2 No. 1 Well
Tuscarawas County, Ohio
Black River Group
Rotary Sidewall Core

THIN SECTION DESCRIPTION - DETAILED

SAMPLE DEPTH: 6940.0 FEET
SAMPLE NUMBER: 1-25R

Plate 25

Permeability (Klink.): 0.0001 mD Porosity (NCS): 1.3% Grain Density: 2.71 gm/cc

Lithology: Limestone

Texture: Skeletal peloidal packstone / grainstone; thin, irregular shaly lamination containing authigenic dolomite; microstylolite

Framework Grains: Allochems consist of abundant peloids, with a minor amount of recrystallized skeletal shell fragments (pelecypods with a trace amount of brachiopod, ostracod, and echinoderm fragments); minor amount of organic material

Matrix: Minor amount of carbonate mud matrix; trace amount of clay

Cements and Replacement Minerals: Common sparry calcite cement reduces original interparticle pores; minor amount of dolomite filling interparticle pores and replacing shell fragments, cement, and matrix; small, euhedral dolomite concentrated in shaly lamination; trace amount of microcrystalline pyrite replacement of shell material, and organic material; minor amount of calcite-filled fractures

Pore System: Trace amount of interparticle macropores micropores; trace amount of secondary intraparticle pores; minor amount of intercrystalline micropores

Reservoir Quality: Poor

Magnification: A: 40X B: 200X

A) Most of the allochems consist of peloids (J5), with a minor amount of well worn skeletal fragments (B7, F4). The compaction of thin, clay-rich laminations resulted in the formation of microstylolites where authigenic dolomite is concentrated (F1 to G15).

B) Anastomosing microstylolites contain concentrations of insoluble clay and organic material (G4, J12.5). The peloids and shell fragments are cemented by fine crystalline calcite (J4), some of which appears to have formed as isopachous rim cements (K4).

Ohio Division of Geological Survey
CO2 No. 1
Tuscarawas County, Ohio

6940.0'
Plate 25

Weatherford LABORATORIES

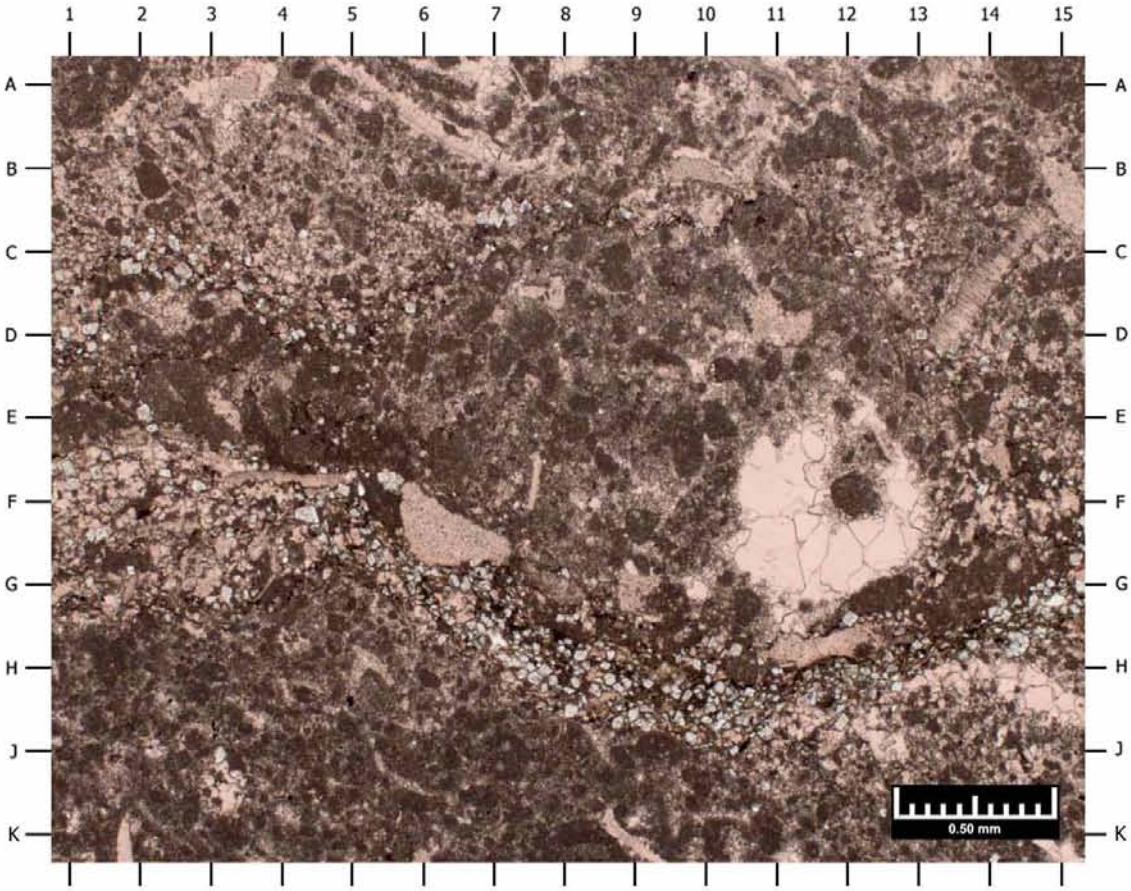

A

40X

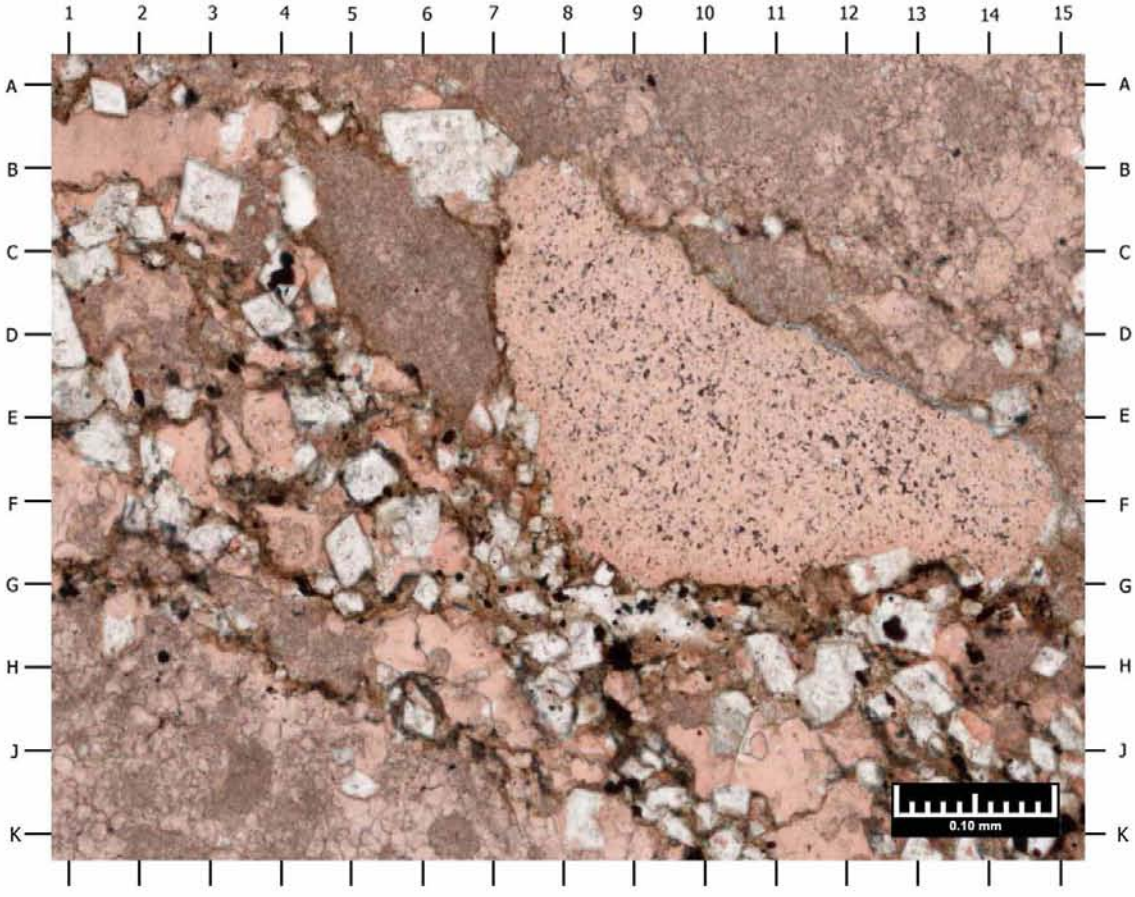

B

200X

Ohio Division of Geological Survey **OMNI File No: HH-38266**
CO_2 No. 1 Well
Tuscarawas County, Ohio
Black River Group
Rotary Sidewall Core

THIN SECTION PHOTOMICROGRAPHS

SAMPLE DEPTH: 7030.0 FEET
SAMPLE NUMBER: 1-26R

Plate 26

Permeability (Klink.): 0.0006 mD Porosity (NCS): 1.2% Grain Density: 2.73 gm/cc

Sample not selected for petrographic analysis.

Magnification: A: 40X B: 200X

Ohio Division of Geological Survey
CO2 No. 1
Tuscarawas County, Ohio

7030.0'
Plate 26

Weatherford LABORATORIES

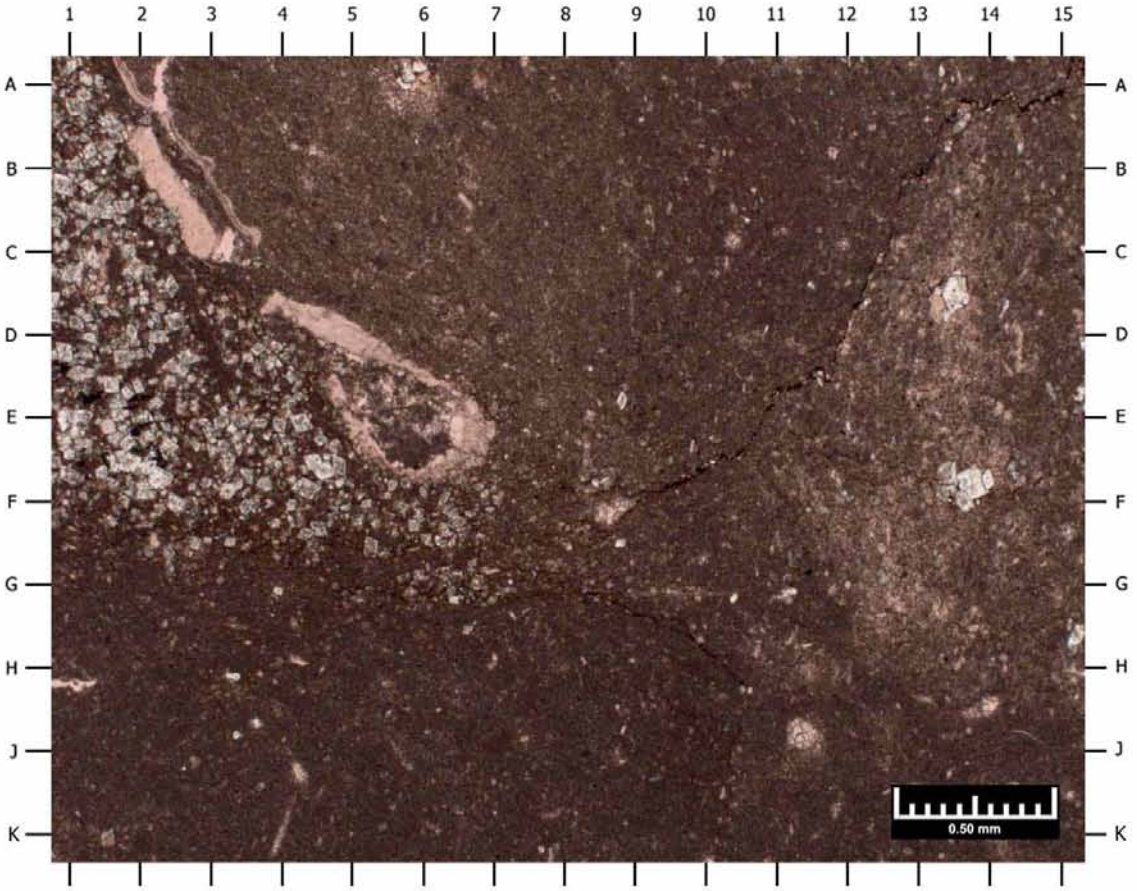

A

40X

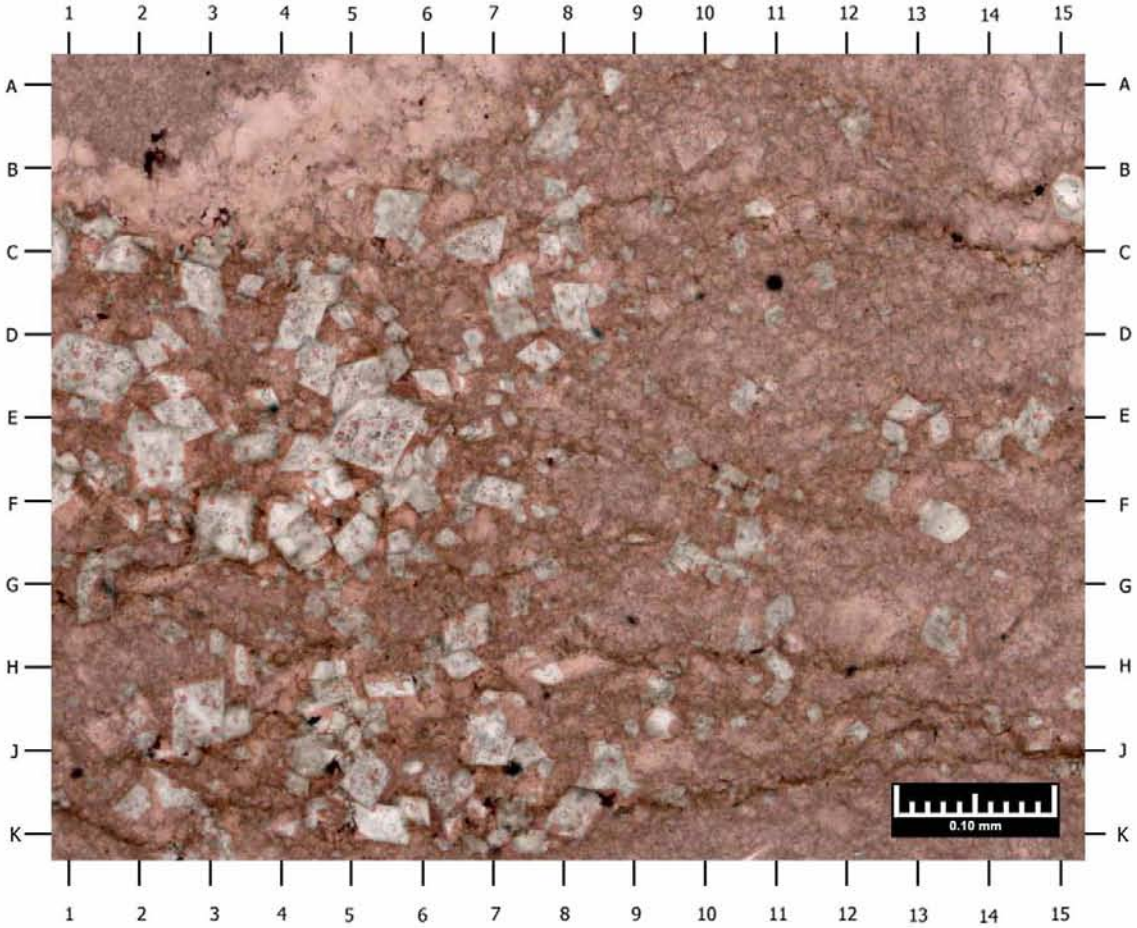

B

200X

Ohio Division of Geological Survey **OMNI File No: HH-38266**
CO_2 No. 1 Well
Tuscarawas County, Ohio
Black River Group
Rotary Sidewall Core

THIN SECTION PHOTOMICROGRAPHS

SAMPLE DEPTH: 7128.0 FEET
SAMPLE NUMBER: 1-27R

Plate 27

Permeability (Klink.): 0.016 mD Porosity (NCS): 5.4% Grain Density: 2.74 gm/cc

Sample not selected for petrographic analysis.

Magnification: A: 40X B: 200X

Ohio Division of Geological Survey
CO2 No. 1
Tuscarawas County, Ohio

7128.0'
Plate 27

Weatherford LABORATORIES

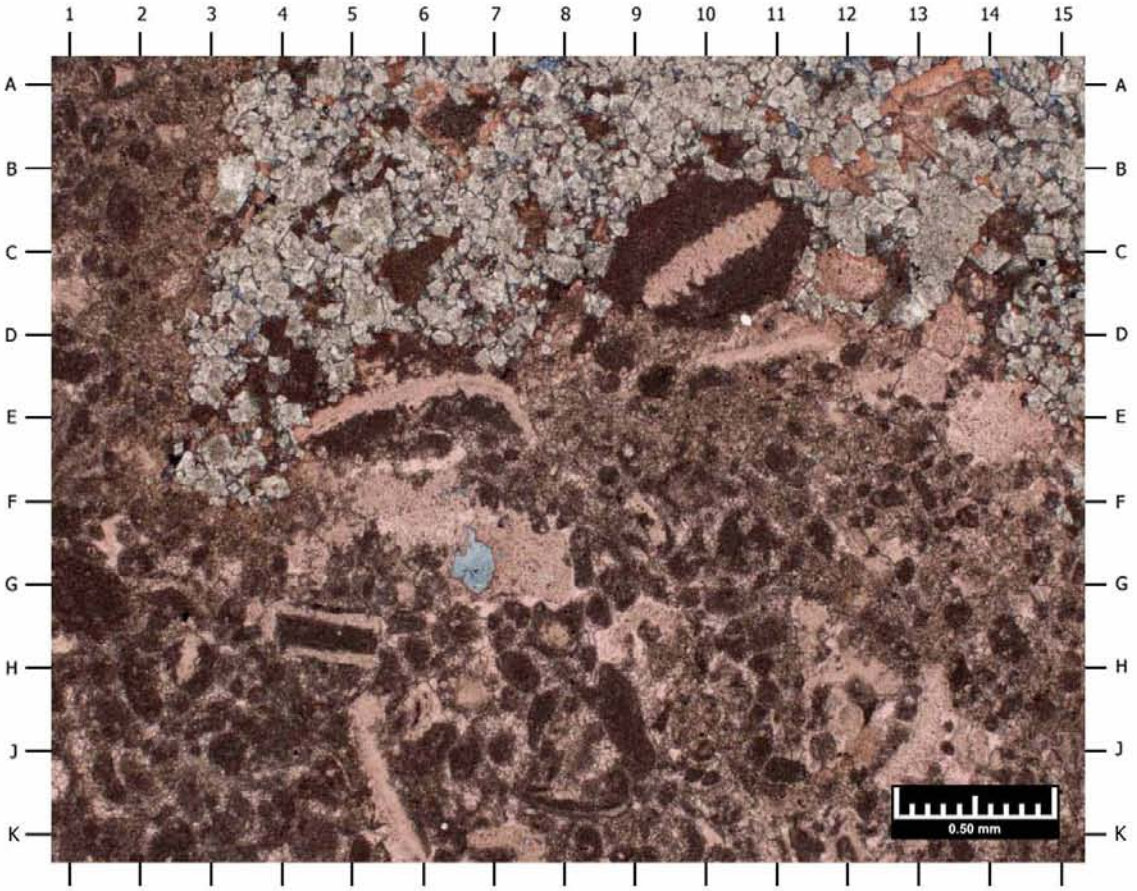

A

40X

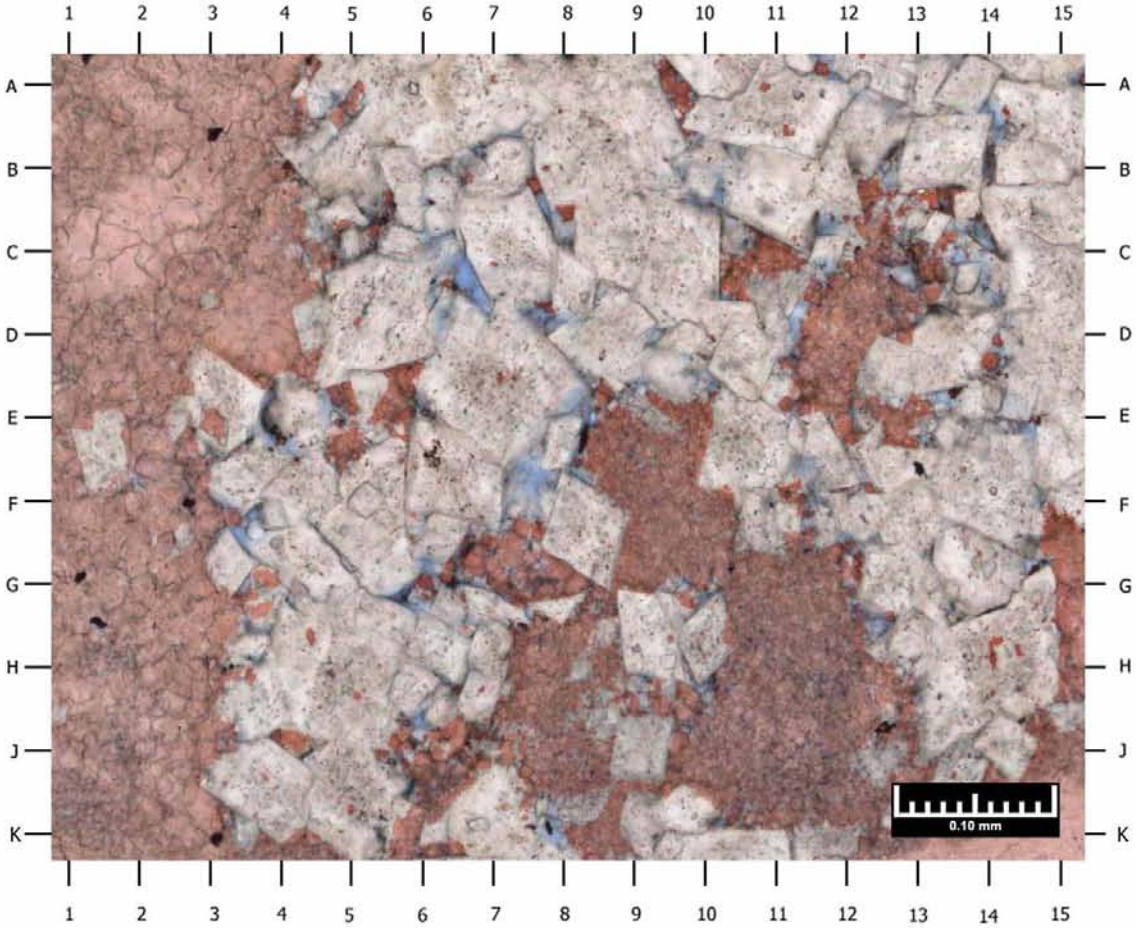

B

200X

Ohio Division of Geological Survey **OMNI File No: HH-38266**
CO_2 No. 1 Well
Tuscarawas County, Ohio
Black River Group
Rotary Sidewall Core

THIN SECTION PHOTOMICROGRAPHS

SAMPLE DEPTH:7142.0 FEET
SAMPLE NUMBER: 1-28R

Plate 28

Permeability (Klink.): 0.0002 mD Porosity (NCS): 2.2% Grain Density: 2.76 gm/cc

Sample not selected for petrographic analysis.

Magnification: A: 40X B: 200X

Ohio Division of Geological Survey
CO2 No. 1
Tuscarawas County, Ohio

7142.0'
Plate 28

Weatherford LABORATORIES

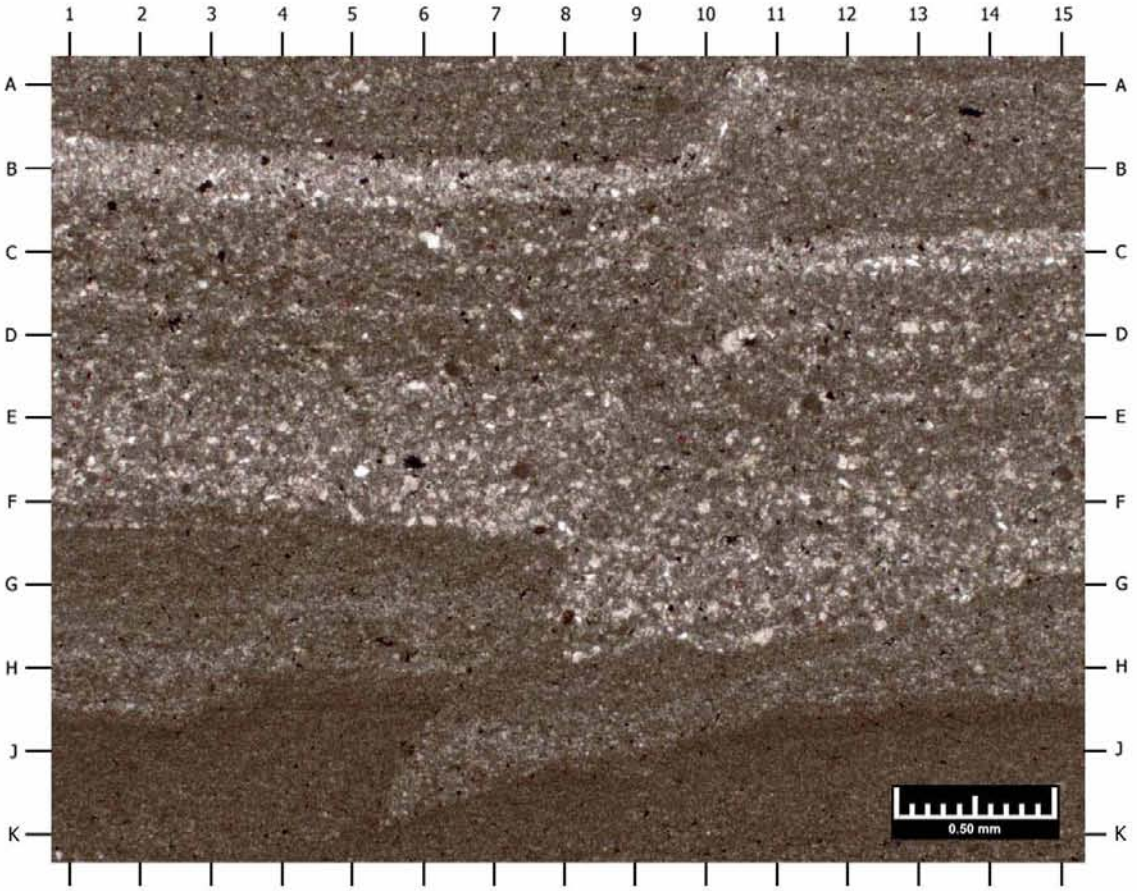

A

40X

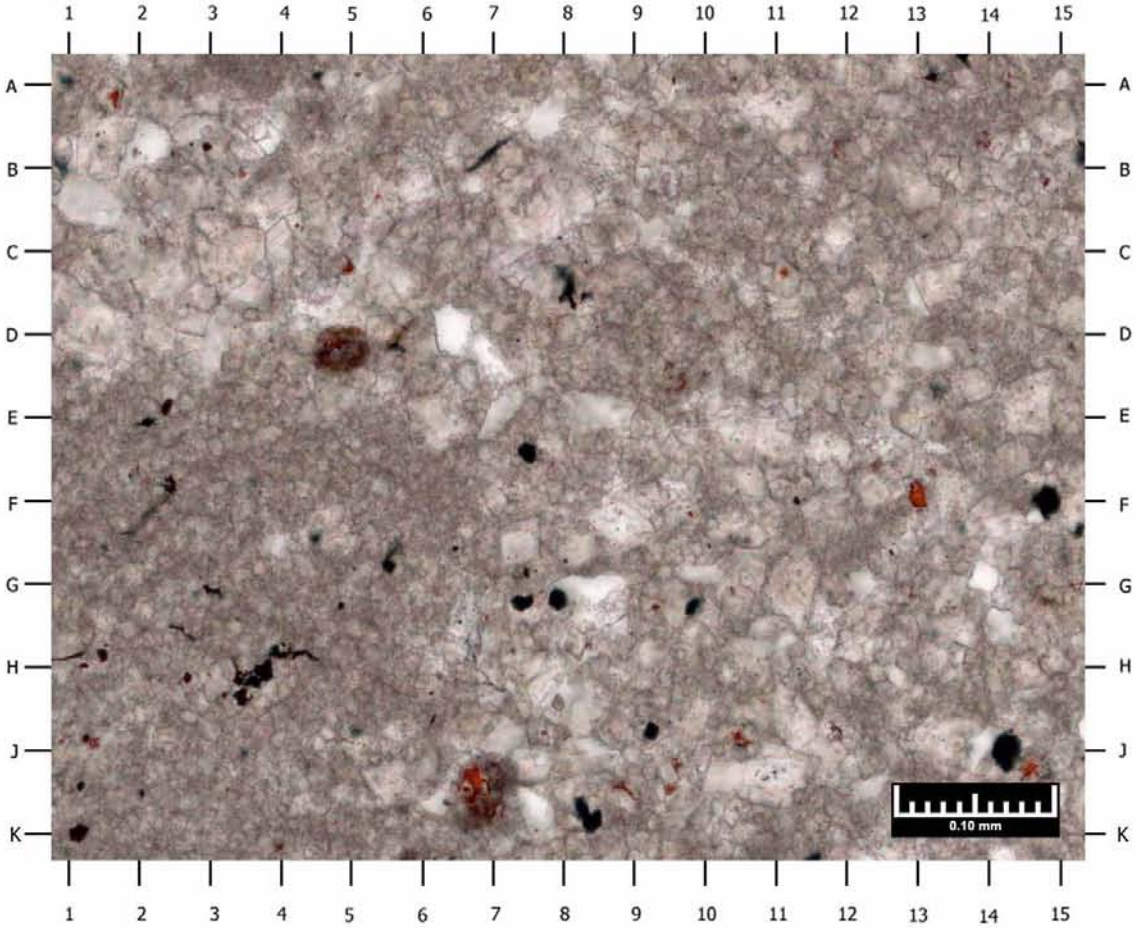

B

200X

Ohio Division of Geological Survey **OMNI File No: HH-38266**
CO_2 No. 1 Well
Tuscarawas County, Ohio
Wells Creek Formation
Rotary Sidewall Core

THIN SECTION DESCRIPTION – GENERAL

SAMPLE DEPTH: 7192.0 FEET
SAMPLE NUMBER: 1-29R

Plate 29

Permeability (Klink.): 0.0003 mD Porosity (NCS): 3.7% Grain Density: 2.82 gm/cc

Lithology: Dolomite

Texture: Packstone / wackestone; irregularly burrow-mottled

Framework Grains: Allochems consist of ghosts of skeletal shell fragments (pelecypods with a trace amount echinoderm fragments); possible ghosts of peloids; rare fine organic debris; minor amount of silt-sized quartz; rare glauconite

Matrix: Original carbonate mud matrix replaced by dolomite

Cements and Replacement Minerals: Pervasive dolomitization, with crystal size ranging from 5 to 40 microns; interlocking euhedral to subhedral crystals; dolomite replaced shell fragments; trace amount of microcrystalline pyrite replacement of shell material and organic material; trace amount of authigenic microquartz, chalcedony, and chert filling a vug (?) or replacing a fossil (?); trace amount of dead oil / bitumen

Pore System: Trace amount of intercrystalline micropores associated replacement of dolomite; rare secondary intraparticle pores

Reservoir Quality: Poor

Magnification: A: 40X B: 200X

A) Pervasive dolomitization of the allochems hinders their identification in this dolopackstone / dolowackestone. The sample contains scattered silt- and sand-sized quartz (white grains; B11, G4). Note the bimodal size distribution of the dolomite crystals, suggesting different episodes of dolomitization.

B) At high magnification, ghost of allochems are visible in some dolomite crystals (B11, J12, J5). Microcrystalline pyrite (black) occurs scattered grain replacements and cements, sometimes outlining allochem ghosts (C4).

Ohio Division of Geological Survey
CO2 No. 1
Tuscarawas County, Ohio

7192.0'
Plate 29

Weatherford LABORATORIES

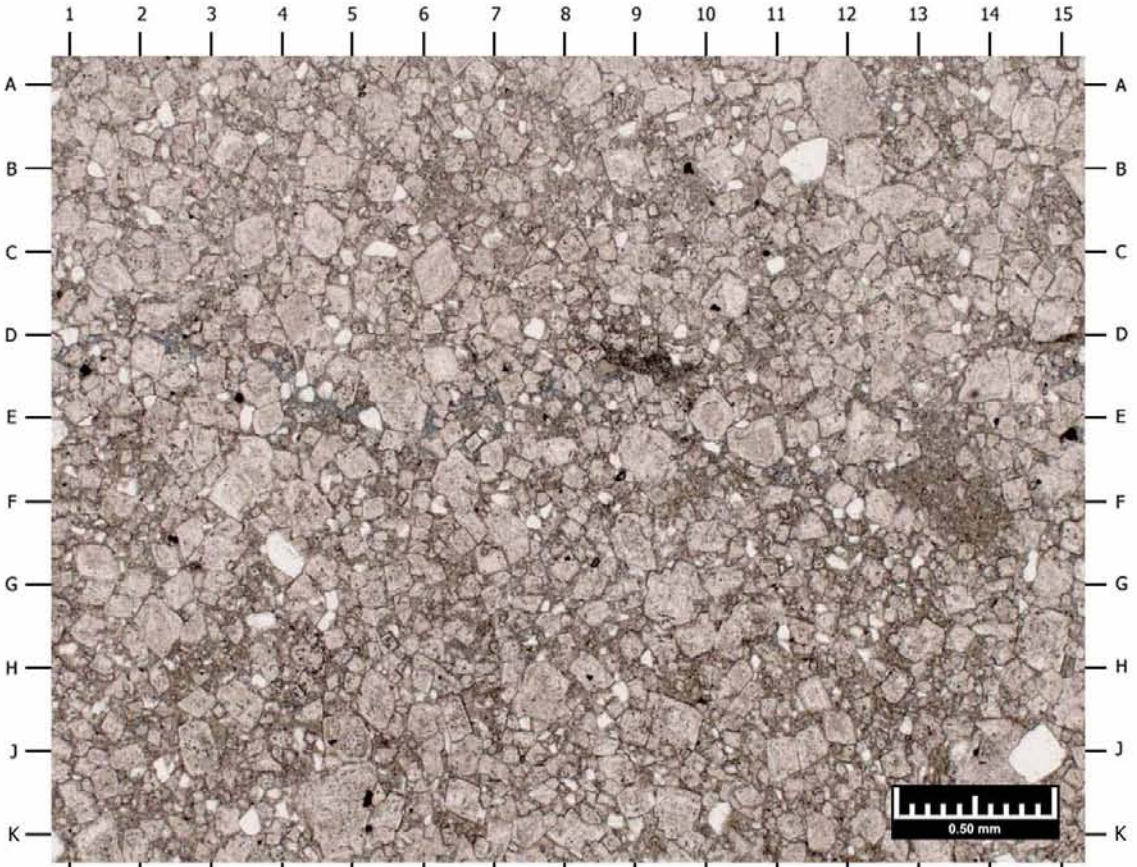

A

40X

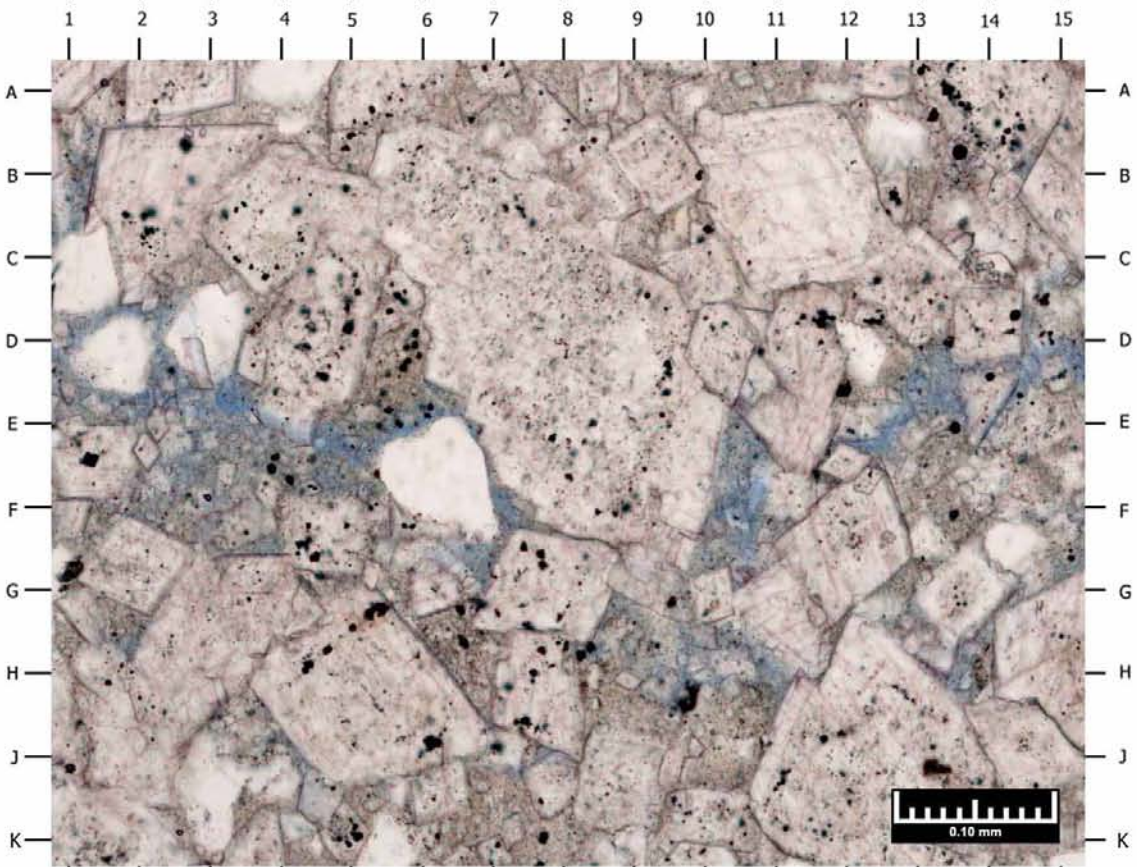

B

200X

Ohio Division of Geological Survey **OMNI File No: HH-38266**
CO_2 No. 1 Well
Tuscarawas County, Ohio
Beekmantown Dolomite
Rotary Sidewall Core

THIN SECTION PHOTOMICROGRAPHS

SAMPLE DEPTH: 7226.0 FEET
SAMPLE NUMBER: 1-30R

Plate 30

Permeability (Klink.): 0.0003 mD Porosity (NCS): 2.1% Grain Density: 2.83 gm/cc

Sample not selected for petrographic analysis.

Magnification: A: 40X B: 200X

Ohio Division of Geological Survey
CO2 No. 1
Tuscarawas County, Ohio

7226.0'
Plate 30

Weatherford LABORATORIES

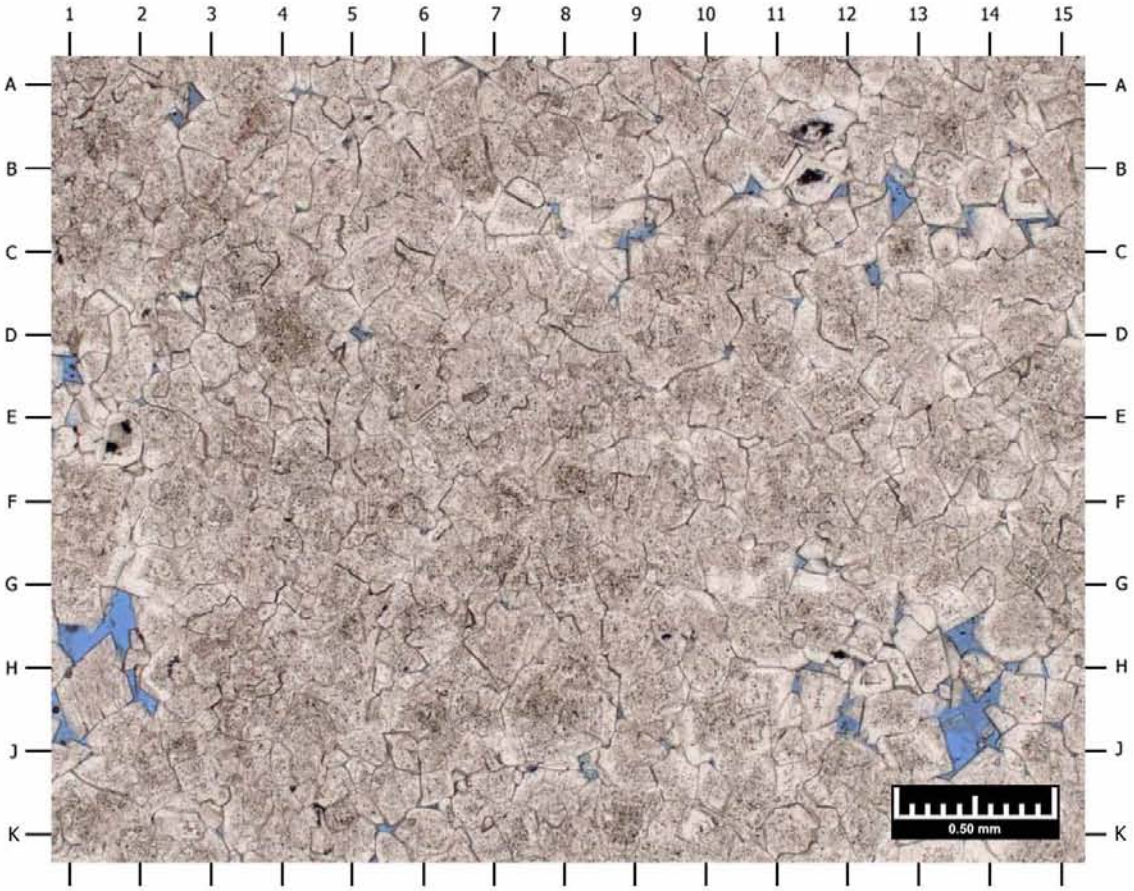

A

40X

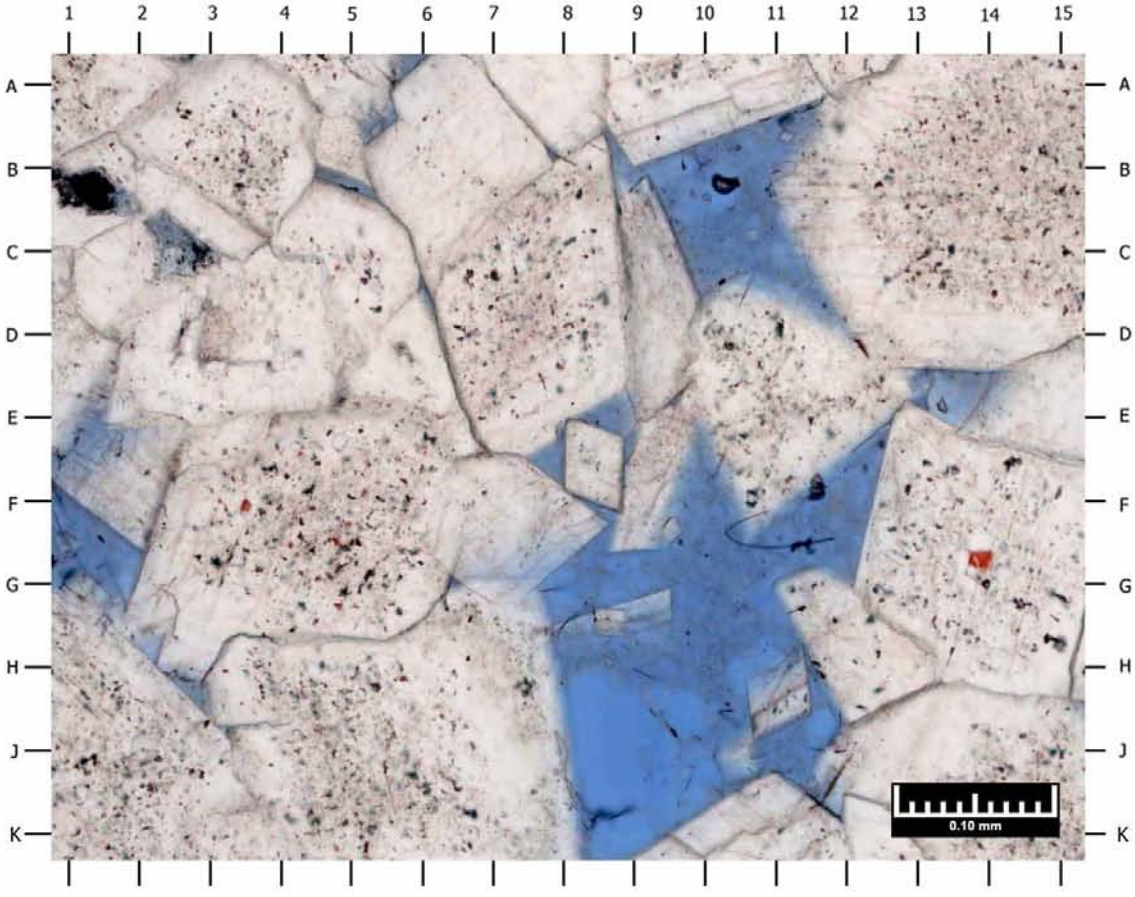

B

200X

Ohio Division of Geological Survey **OMNI File No: HH-38266**
CO_2 No. 1 Well
Tuscarawas County, Ohio
Beekmantown Dolomite
Rotary Sidewall Core

THIN SECTION DESCRIPTION - DETAILED

SAMPLE DEPTH: 7231.0 FEET
SAMPLE NUMBER: 1-31R

Plate 31

Permeability (Klink.): 0.726 mD Porosity (NCS): 9.2% Grain Density: 2.70 gm/cc

Lithology: Dolomite

Texture: Dolomite breccia; fractured and brecciated (possible karst feature)

Framework Grains: Original allochems (if any) cannot be recognized due to dolomitization overprint; trace amount of fine organic debris; trace amount of silt-sized quartz

Matrix: None

Cements and Replacement Minerals: All original fabric and allochems completely replaced by fine to medium crystalline, subhedral to euhedral dolomite; trace amount of microcrystalline pyrite replacement; minor amount of subhedral to euhedral dolomite rhombs partially occlude breccia voids and fracture pores; minor amount of dead oil / bitumen in matrix and fractures

Pore System: Minor amount of macropores consisting of cement-reduced intercrystalline pores; minor amount of fracture pores reduced by medium to coarse crystalline dolomite rhombs

Reservoir Quality: Fair to good (based on matrix micropores in combination with scattered macropores and fracture pores, assuming fracture stimulation of the reservoir to enhance matrix permeability and assuming dry gas is the likely fluid for storage or production)

Magnification: A: 40X B: 200X

A) The sample has well developed intercrystalline pores (D2) that are largely filled with dead oil (G14). Larger fracture voids (B5 to B13) are partially reduced by dolomite crystals (B7).

B) Detailed view of the area around B5 shows intercrystalline pores (J2,K3.5) and dolomite reduced fracture pores (E8, F15). Compare the euhedral crystal shape of the pore-filling dolomite (G11) with the anhedral shape of the dolomite in the matrix (G3).

Ohio Division of Geological Survey
CO2 No. 1
Tuscarawas County, Ohio

7231.0'
Plate 31

Weatherford LABORATORIES

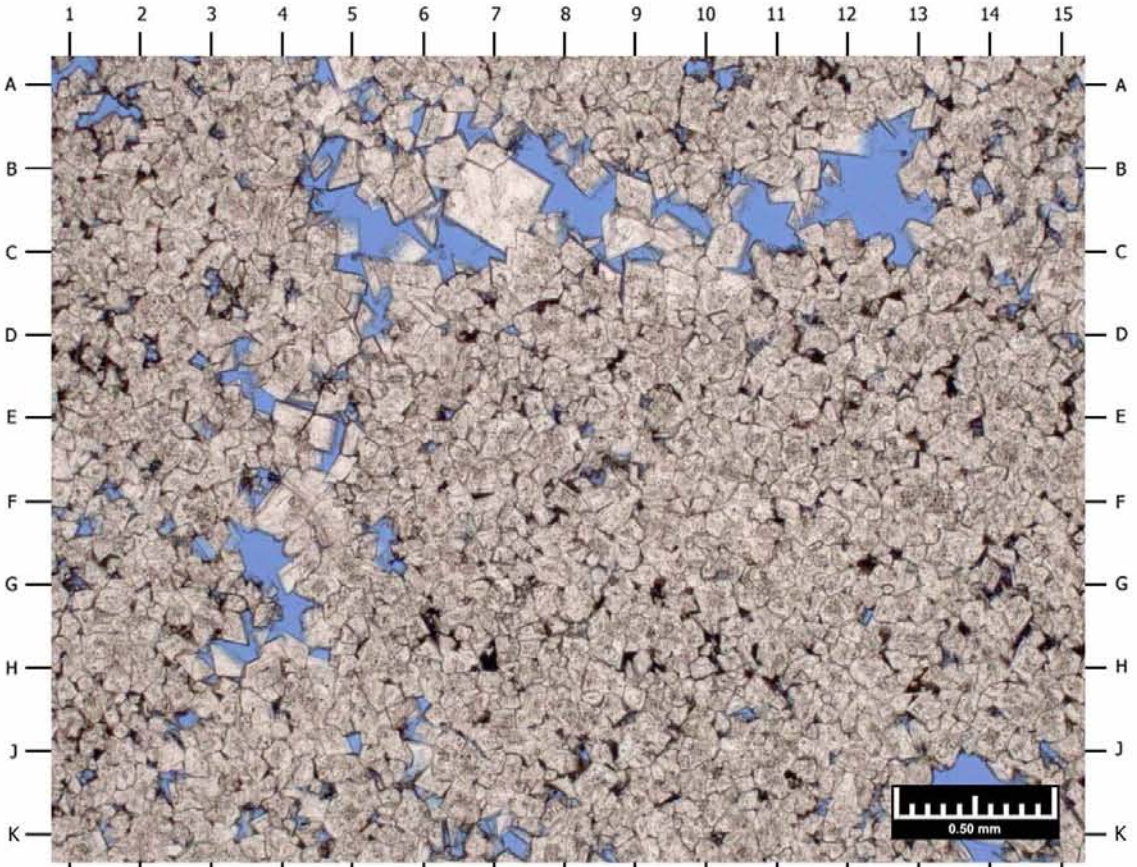

A

40X

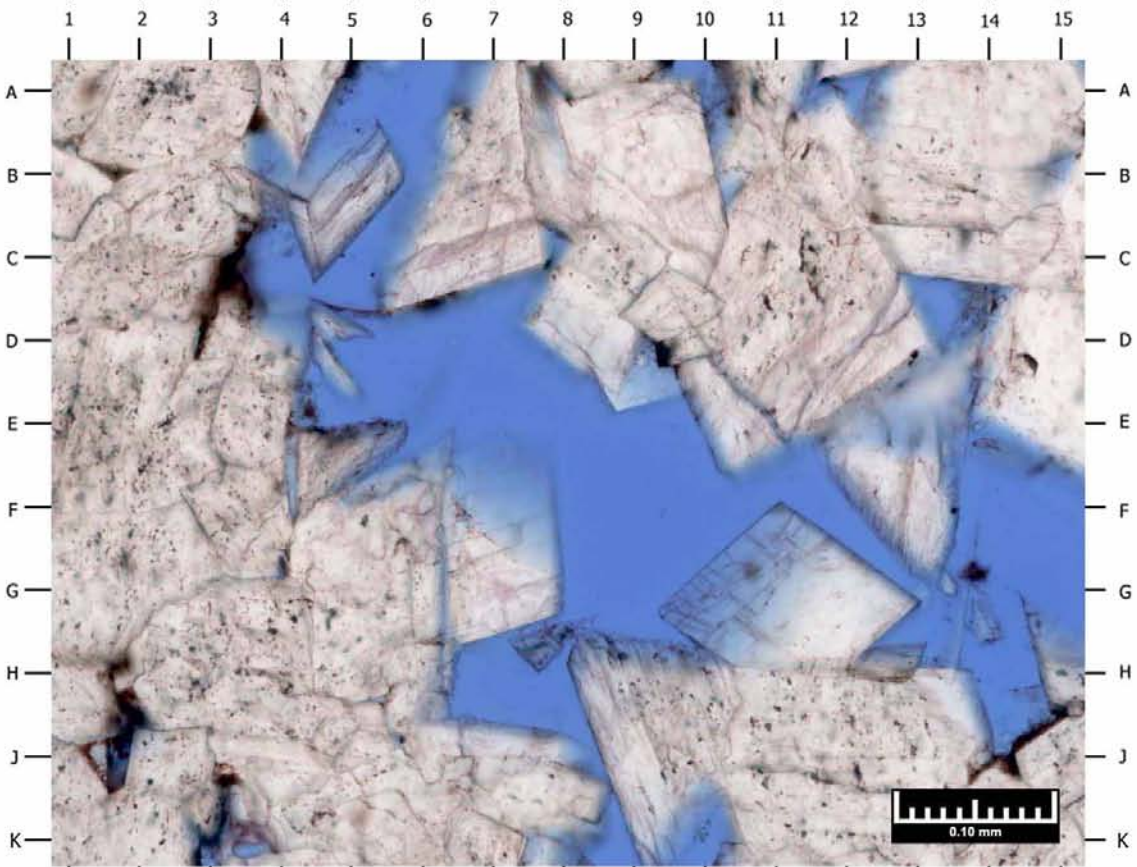

B

200X

Ohio Division of Geological Survey **OMNI File No: HH-38266**
CO_2 No. 1 Well
Tuscarawas County, Ohio
Beekmantown Dolomite
Rotary Sidewall Core

THIN SECTION DESCRIPTION - DETAILED

SAMPLE DEPTH: 7235.0 FEET
SAMPLE NUMBER: 1-32R

Plate 32

Permeability (Klink.): 0.0002 mD Porosity (NCS): 3.9% Grain Density: 2.85 gm/cc

Lithology: Dolomite

Texture: Dolomite; vague laminations

Framework Grains: Original allochems difficult to recognize due to dolomitization overprint; rare ghost allochems (possible peloids and other undifferentiated fragments); trace amount of fine organic debris; trace amount of silt-sized quartz; common bitumen

Matrix: Trace

Cements and Replacement Minerals: All original fabric and nearly all allochems completely replaced by fine to medium crystalline, subhedral to euhedral dolomite; trace amount of microcrystalline pyrite replacement; minor amount of subhedral to euhedral dolomite rhombs partially occlude breccia voids and fracture pores; trace amount of dead oil / bitumen in matrix and fractures

Pore System: Trace amount of macropores consisting of interparticle pores and intercrystalline pores; minor amount of intercrystalline micropores; trace amount of secondary intracrystalline pores

Reservoir Quality: Poor

Magnification: A: 40X B: 200X

A) The laminated fabric of the sample is defined by the variation in crystal size of the replacement dolomite, which is a proxy of the original limestone fabrics. Possible ghosts of peloids and undifferentiated calcareous fragments are the only visible allochems (A6.5, F3).

B) A detailed view of the area around D11 in Plate 32A shows the contact between the very fine crystalline dolomite and fine crystalline dolomite. Note the trace amount of calcite that fills a remnant interparticle void (F10). A possible peloid ghost is visible at B3. Microcrystalline pyrite (black specks) is scattered throughout the sample.

Ohio Division of Geological Survey
CO2 No. 1
Tuscarawas County, Ohio

7235.0'
Plate 32

Weatherford LABORATORIES

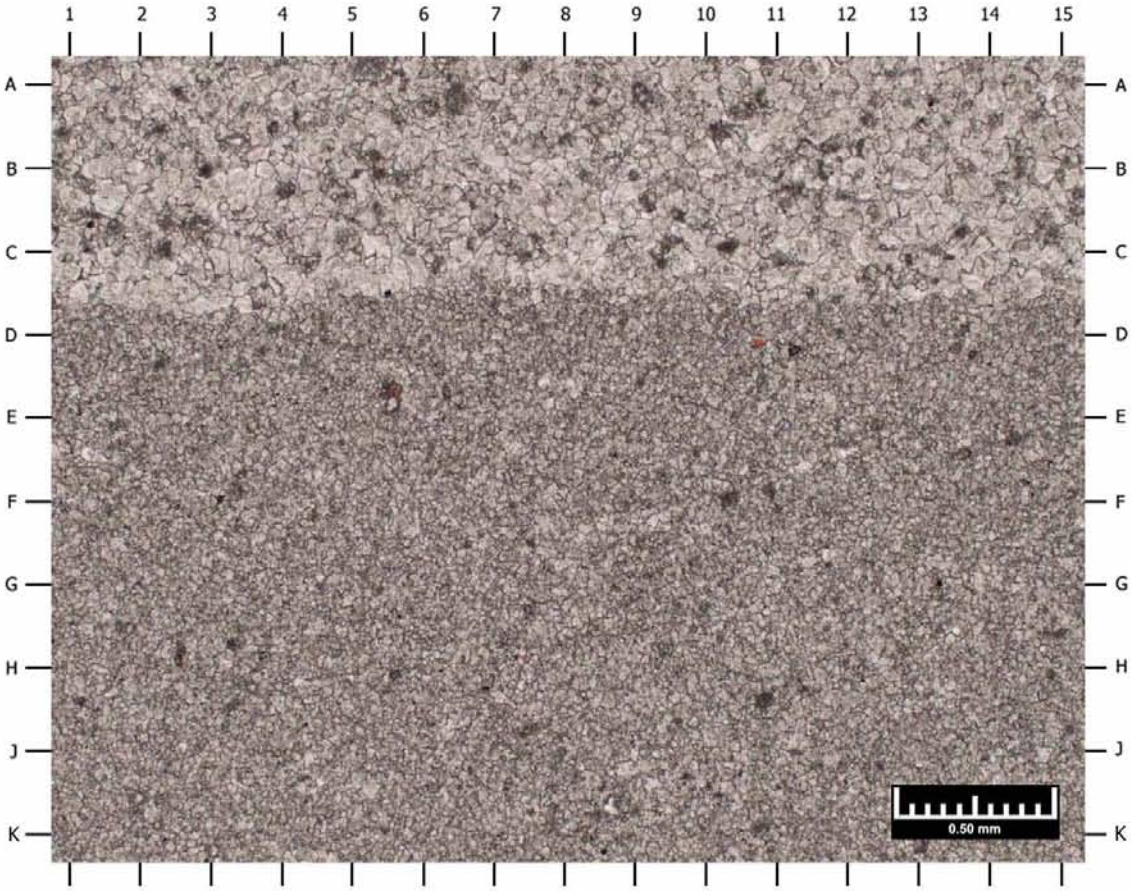

A

40X

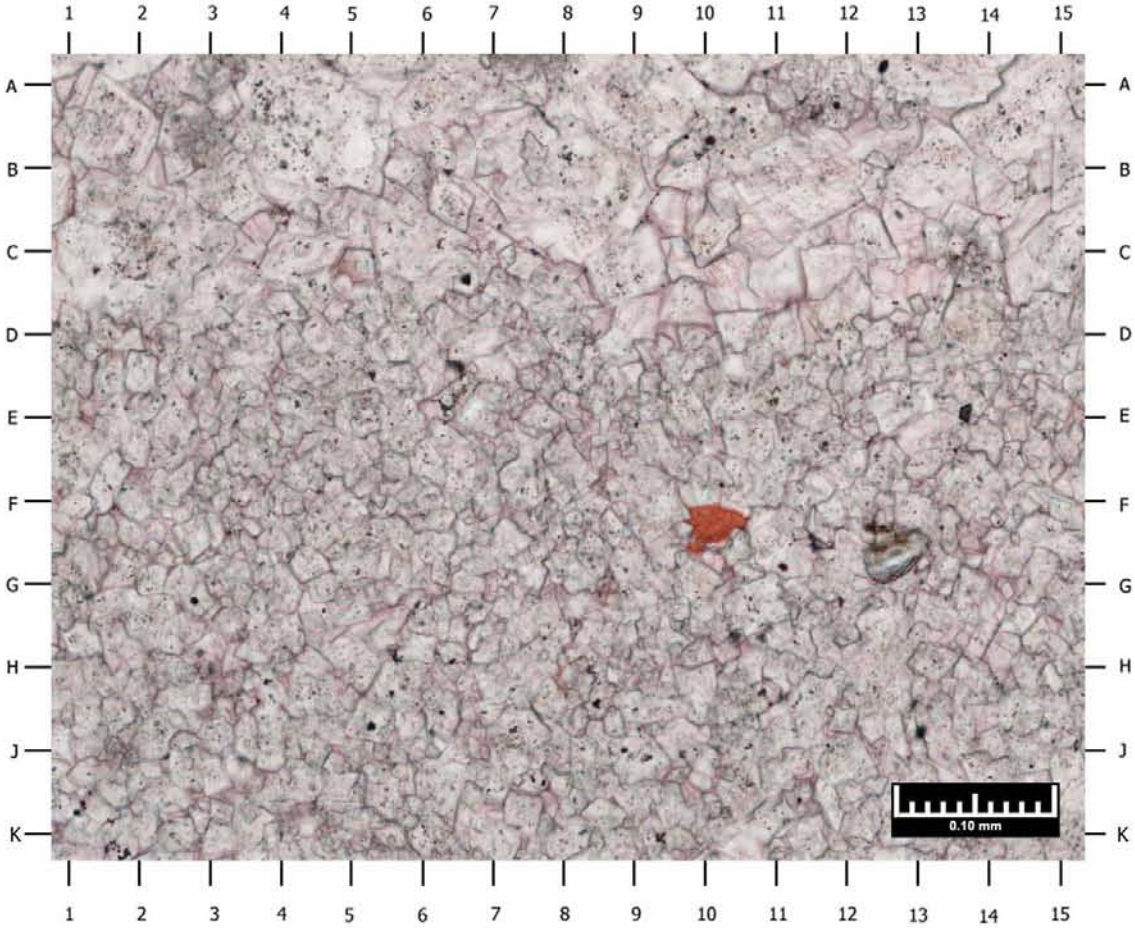

B

200X

Ohio Division of Geological Survey **OMNI File No: HH-38266**
CO_2 No. 1 Well
Tuscarawas County, Ohio
Beekmantown Dolomite
Rotary Sidewall Core

THIN SECTION PHOTOMICROGRAPHS

SAMPLE DEPTH: 7248.0 FEET
SAMPLE NUMBER: 1-33R

Plate 33

Permeability (Klink.): <0.0001 mD Porosity (NCS): 1.4% Grain Density: 2.80 gm/cc

Sample not selected for petrographic analysis.

Magnification: A: 40X B: 200X

Ohio Division of Geological Survey
CO2 No. 1
Tuscarawas County, Ohio

7248.0'
Plate 33

Weatherford LABORATORIES

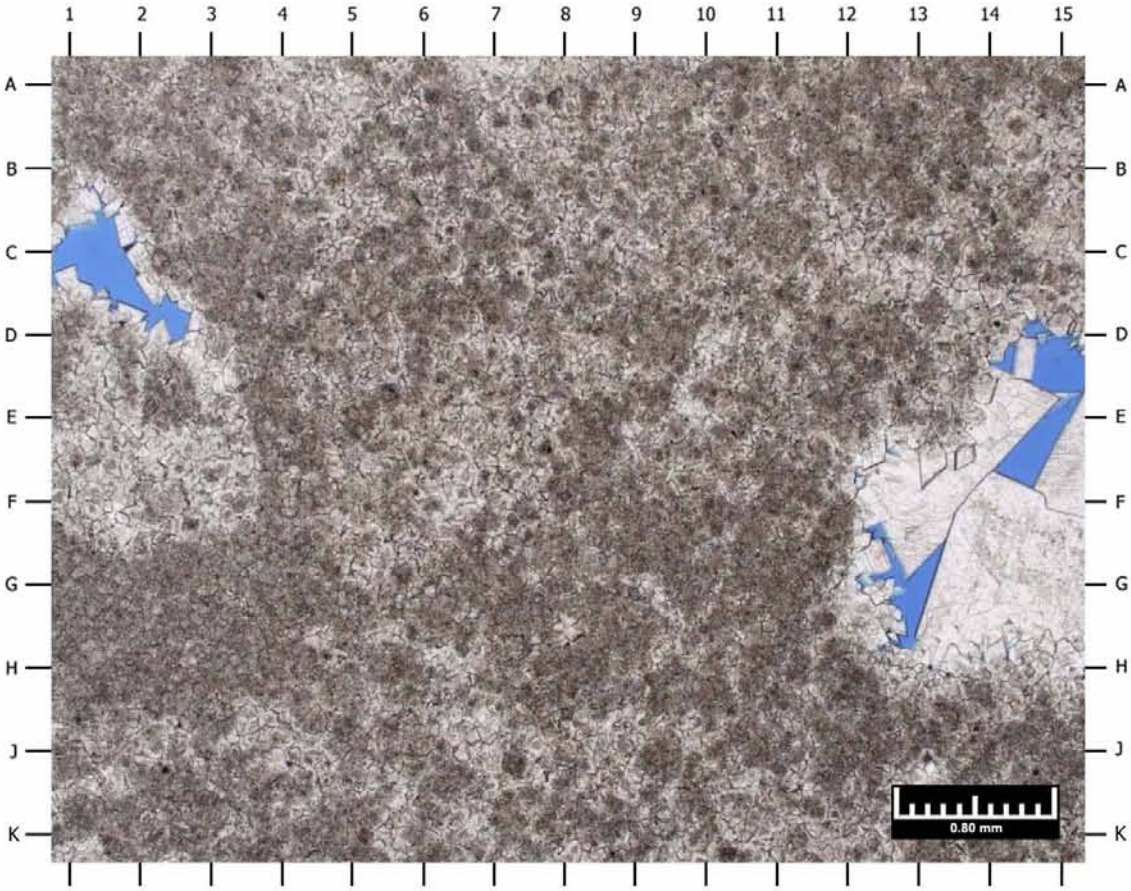

A

25X

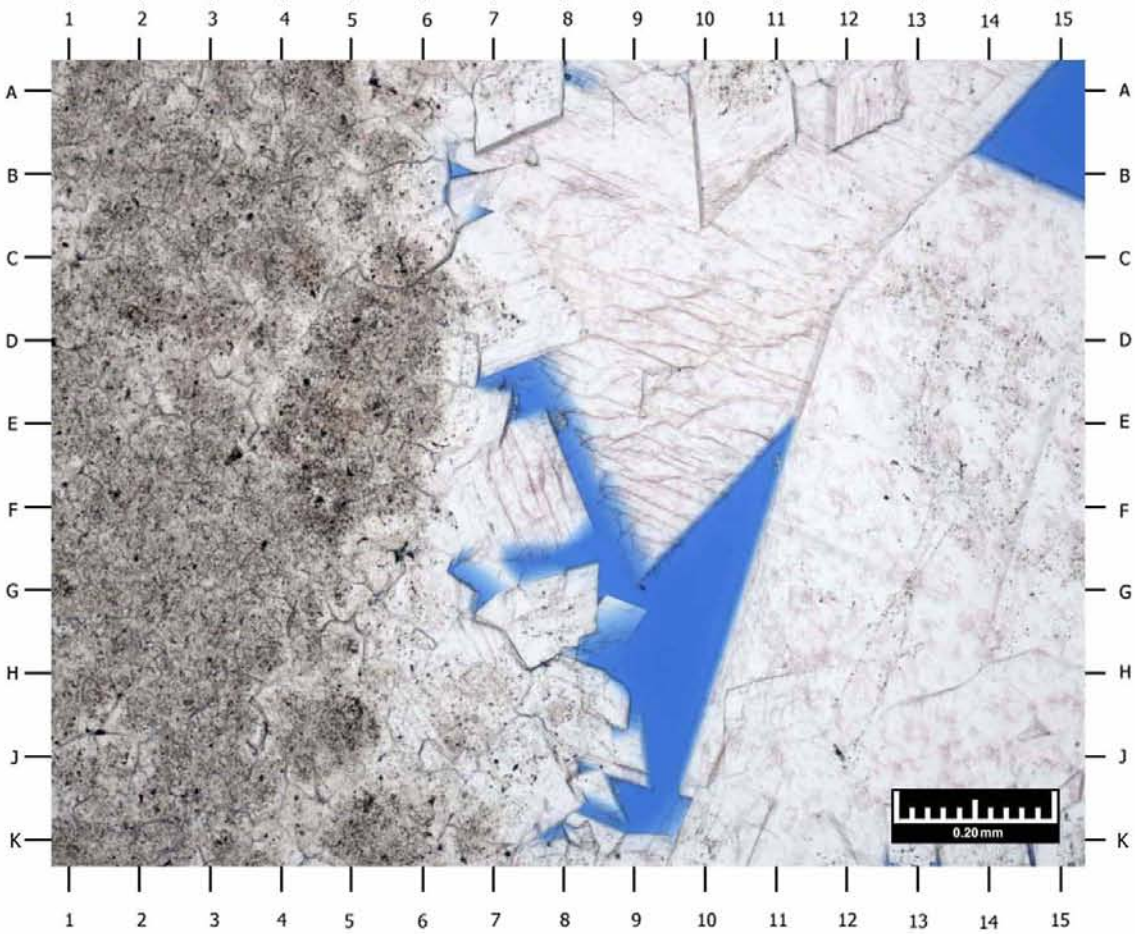

B

100X

Ohio Division of Geological Survey **OMNI File No: HH-38266**
CO_2 No. 1 Well
Tuscarawas County, Ohio
Beekmantown Dolomite
Rotary Sidewall Core

THIN SECTION PHOTOMICROGRAPHS

SAMPLE DEPTH: 7296.0 FEET
SAMPLE NUMBER: 1-34R

Plate 34

Permeability (Klink.): 0.0022 mD Porosity (NCS): 3.3% Grain Density: 2.84 gm/cc

Sample not selected for petrographic analysis.

Magnification: A: 40X B: 200X

Ohio Division of Geological Survey
CO2 No. 1
Tuscarawas County, Ohio

7296.0'
Plate 34

Weatherford LABORATORIES

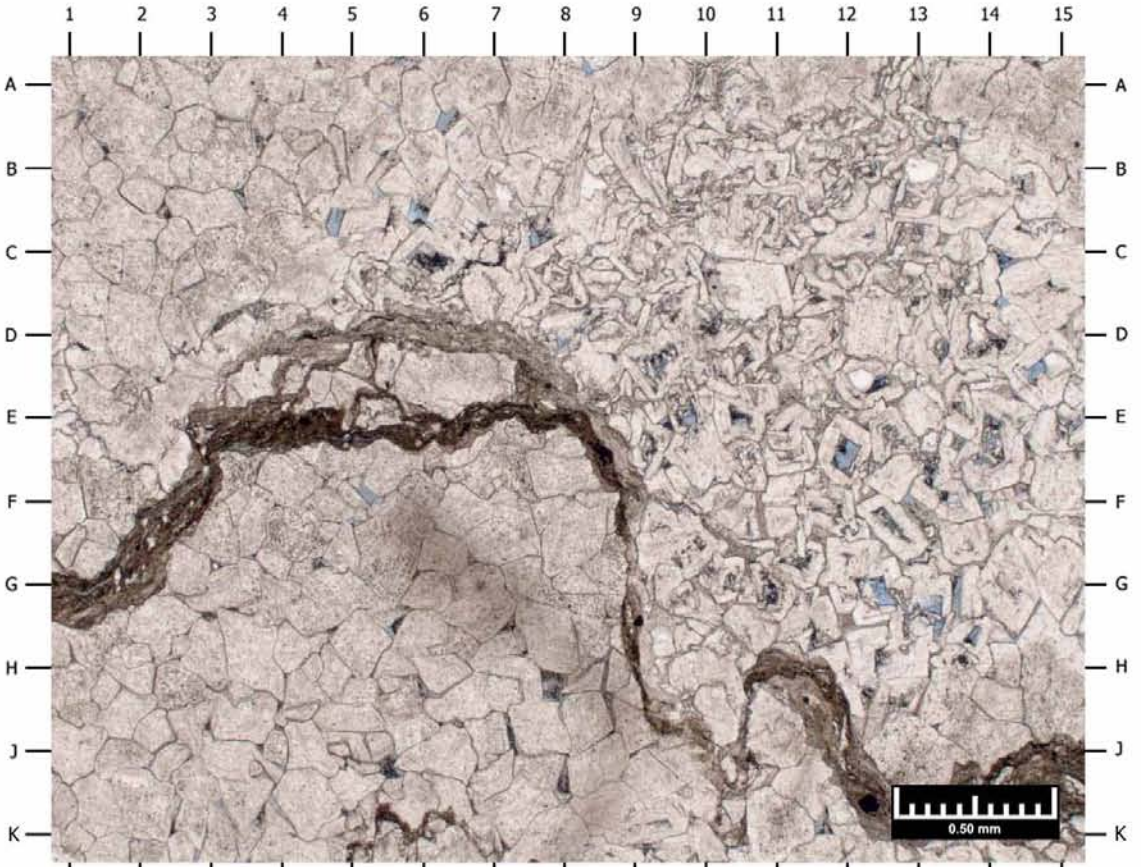

A

40X

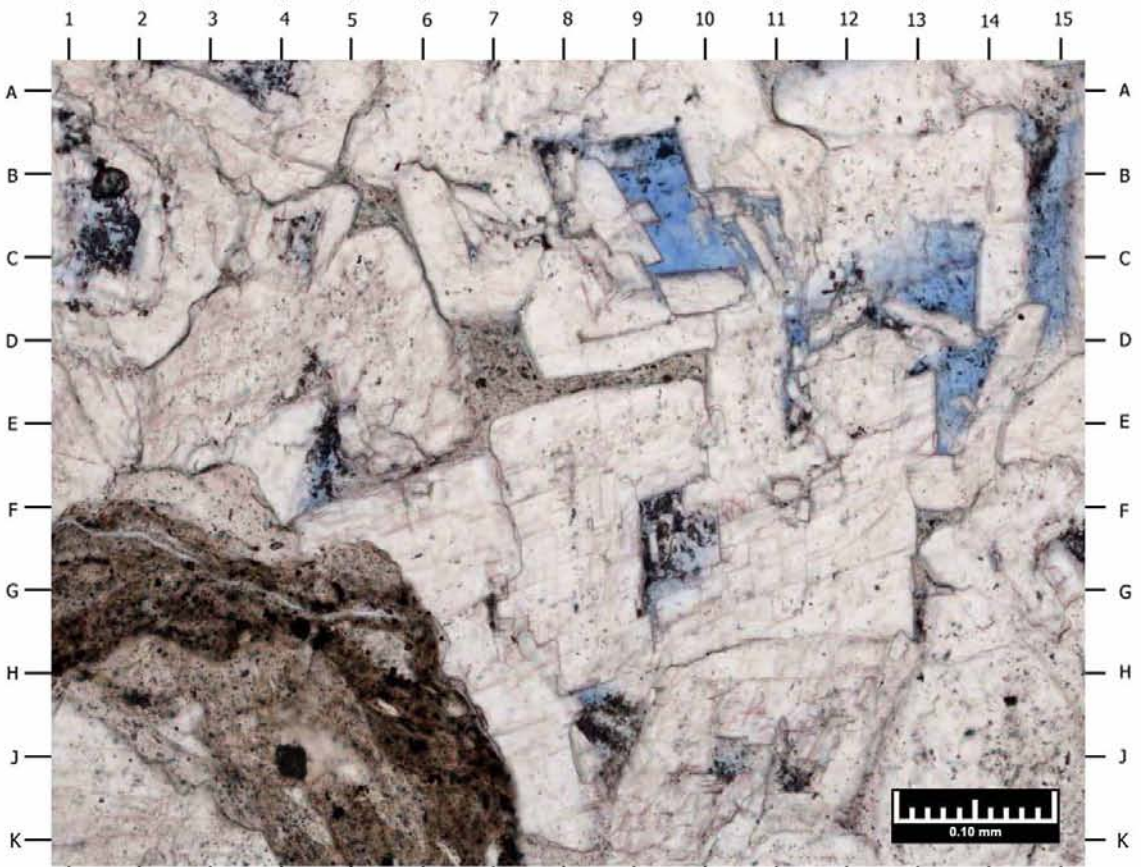

B

200X

Ohio Division of Geological Survey **OMNI File No: HH-38266**
CO_2 No. 1 Well
Tuscarawas County, Ohio
Beekmantown Dolomite
Rotary Sidewall Core

THIN SECTION PHOTOMICROGRAPHS

SAMPLE DEPTH: 7328.0 FEET
SAMPLE NUMBER: 1-35R

Plate 35

Permeability (Klink.): 0.0067 mD Porosity (NCS): 1.8% Grain Density: 2.83 gm/cc

Sample not selected for petrographic analysis.

Magnification: A: 40X B: 200X

Ohio Division of Geological Survey
CO2 No. 1
Tuscarawas County, Ohio

7328.0'
Plate 35

Weatherford LABORATORIES

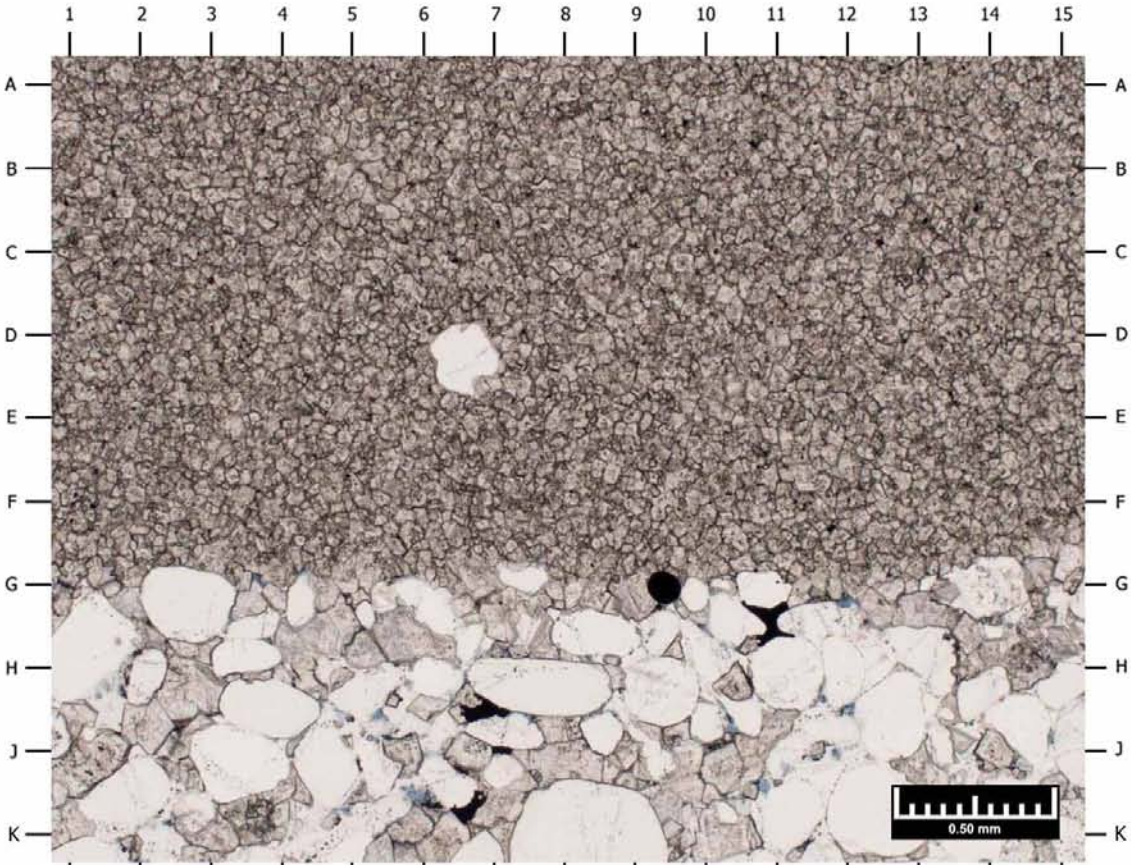

A

40X

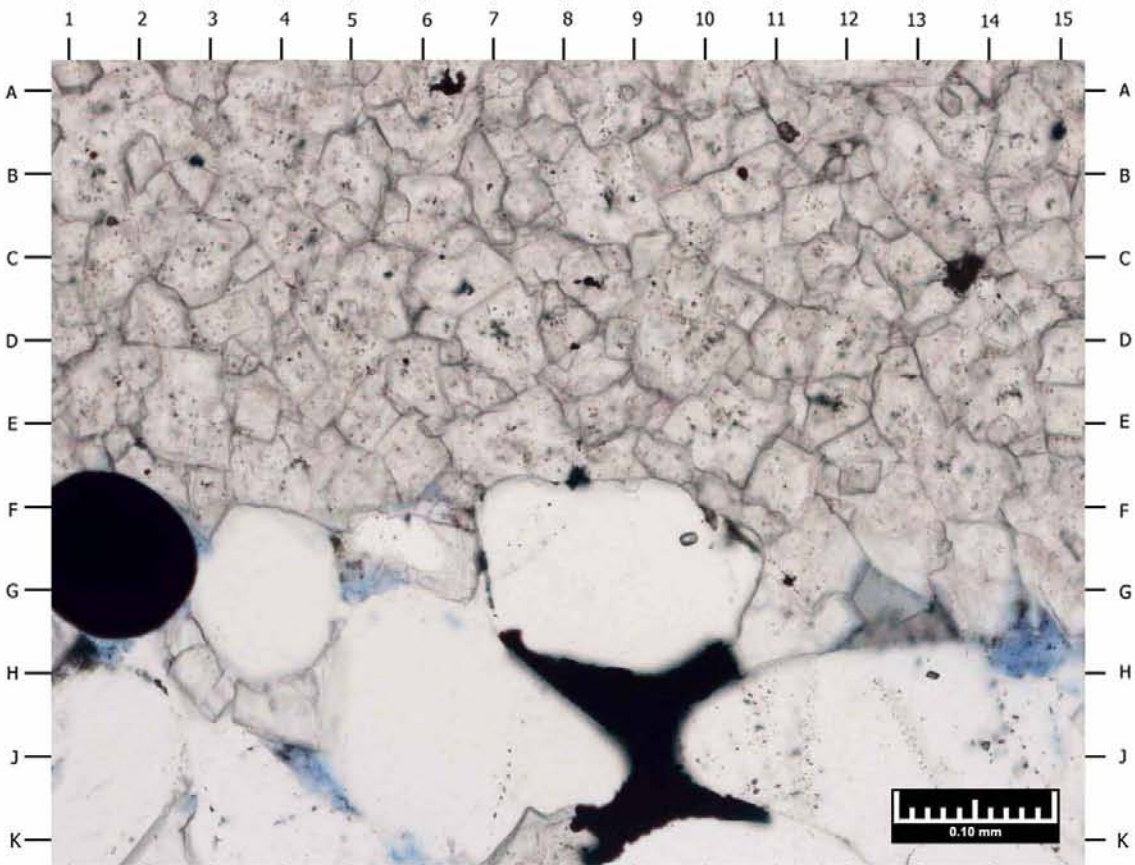

B

200X

Ohio Division of Geological Survey **OMNI File No: HH-38266**
CO_2 No. 1 Well
Tuscarawas County, Ohio
Beekmantown Dolomite
Rotary Sidewall Core

THIN SECTION PHOTOMICROGRAPHS

SAMPLE DEPTH: 7365.0 FEET
SAMPLE NUMBER: 1-36R

Plate 36

Permeability (Klink.): 0.0065 mD Porosity (NCS): 5.6% Grain Density: 2.66 gm/cc

Sample not selected for petrographic analysis.

Magnification: A: 40X B: 200X

Ohio Division of Geological Survey
CO2 No. 1
Tuscarawas County, Ohio

7365.0'
Plate 36

Weatherford LABORATORIES

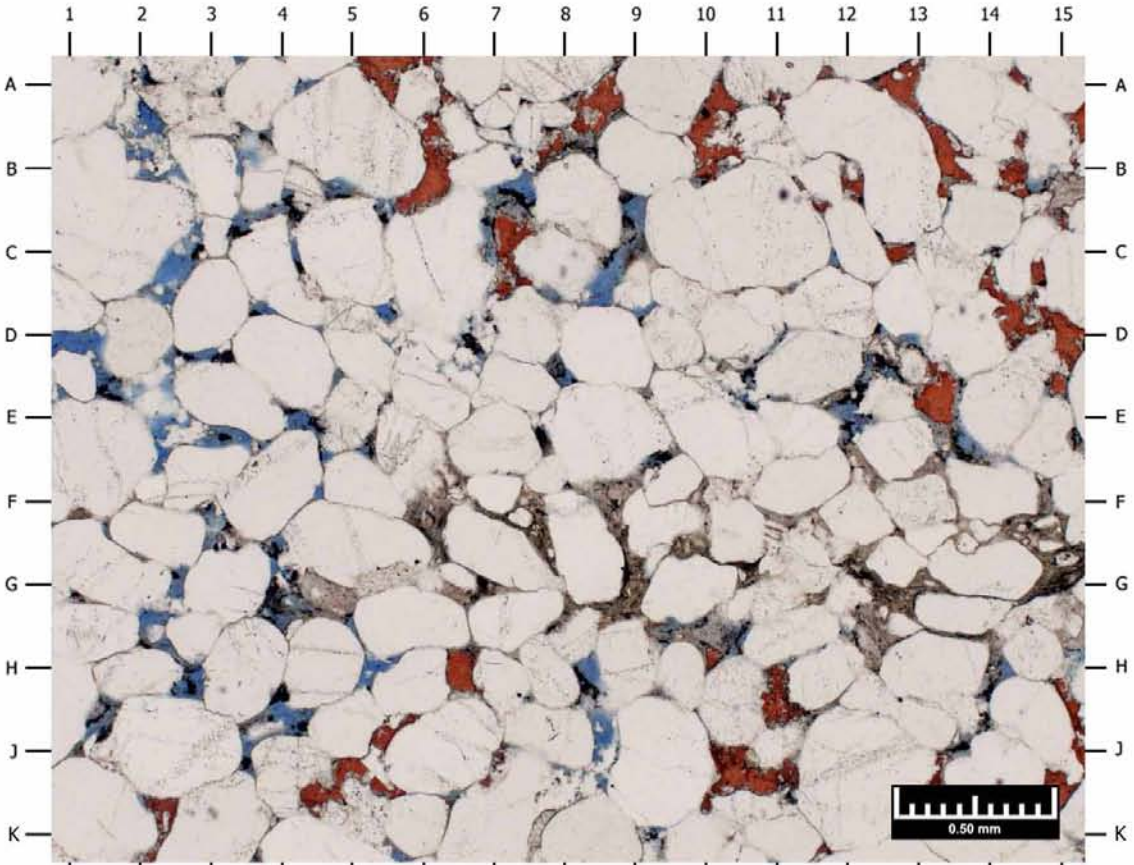

A

40X

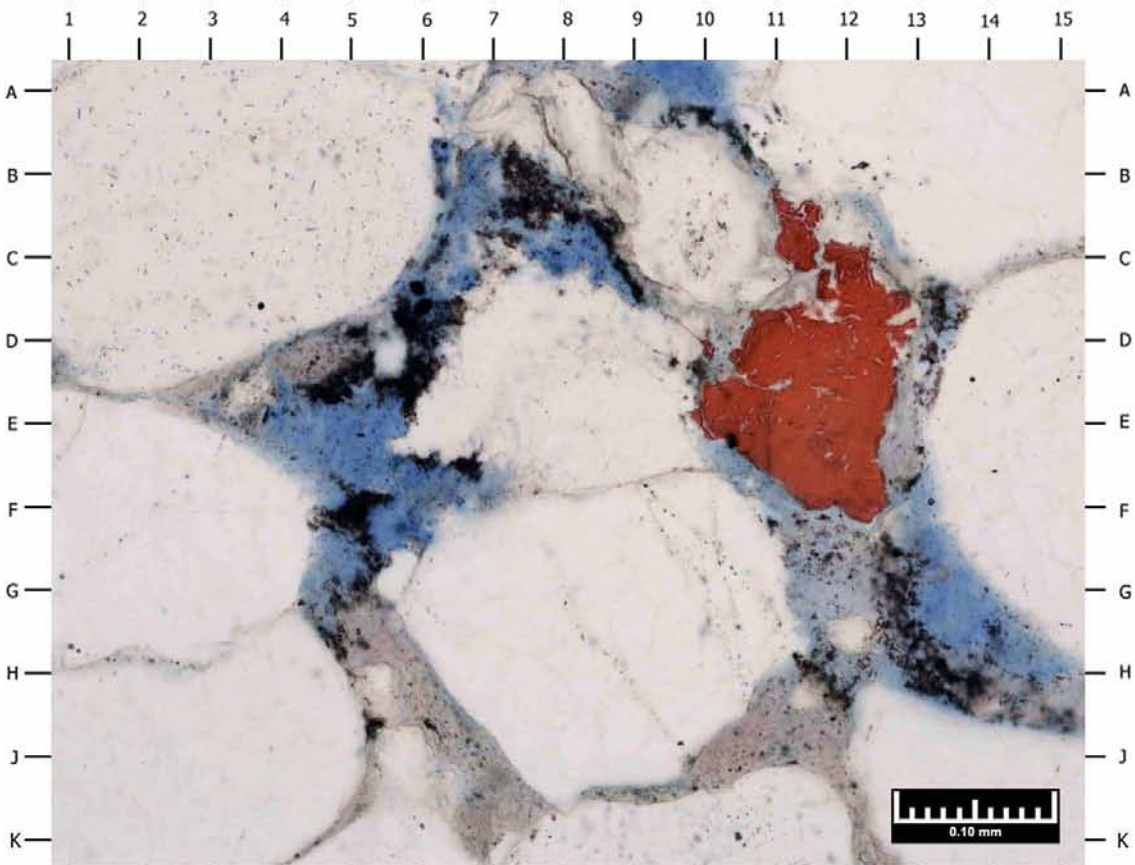

B

200X

Ohio Division of Geological Survey **OMNI File No: HH-38266**
CO_2 No. 1 Well
Tuscarawas County, Ohio
Rose Run Sandstone
Rotary Sidewall Core

THIN SECTION DESCRIPTION - DETAILED

SAMPLE DEPTH: 7377.0 FEET
SAMPLE NUMBER: 1-37R

Plate 37

Permeability (Klink.): 0.023 mD Porosity (NCS): 6.1% Grain Density: 2.64 gm/cc

Lithology:	Quartzarenite
Sedimentary Fabric:	Vague grain size-zoning
Grain Size Range:	<0.09mm-1.09mm
Average Grain Size:	0.48mm
Compaction:	Moderate
Sorting:	Moderately well sorted
Framework Grains:	
Major:	Monocrystalline quartz
Minor:	Polycrystalline quartz, feldspar
Accessory:	Tourmaline, sphene, rutile, zircon
Matrix Content:	
Detrital Matrix:	Trace of organic material
Authigenic Clay:	Minor pore-lining clay and pore-filling clay (undifferentiated)
Cement Types:	Common quartz overgrowths; trace feldspar, siderite, Fe/Ti oxides, and pyrite
Porosity Types:	Subequal, minor amounts of intergranular pores and secondary intragranular pores; trace amount of micropores
Reservoir Quality:	Fair to poor

Magnification: A: 40X B: 200X

A) Abundant quartz overgrowth cement (D4, E15) significantly reduces the intergranular pore volume. The detrital quartz grains commonly have healed microfractures (D10, J13). Oversized pores result from the dissolution of unstable lithic fragments (F3, F13).

B) The remnants of a partially dissolved and altered lithic fragment (E5) remain within the oversized, secondary intragranular pore. Quartz overgrowths (E12, G4) extend into adjacent intergranular pores, and commonly coalesce resulting in a significant reduction in permeability. An altered feldspar grain (A9) has feldspar overgrowth cement (A6).

Ohio Division of Geological Survey
CO2 No. 1
Tuscarawas County, Ohio

7377.0'
Plate 37

Weatherford LABORATORIES

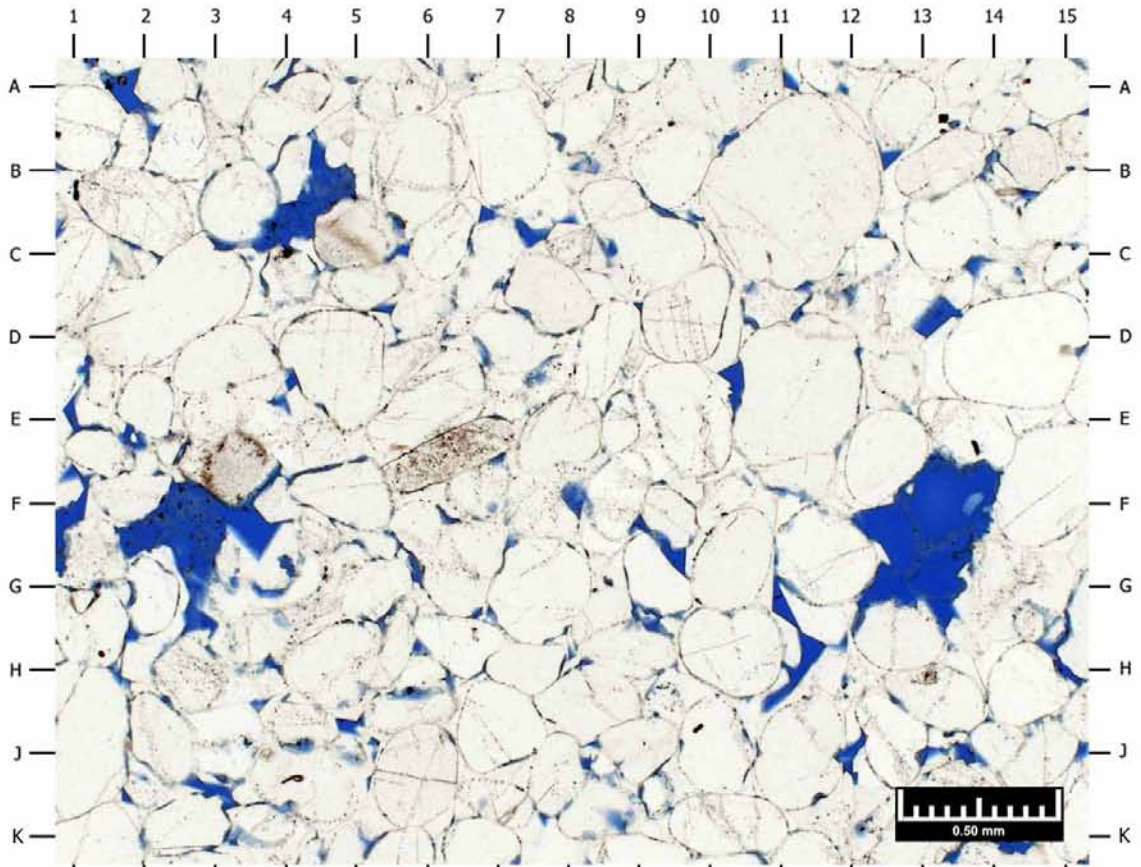

A

40X

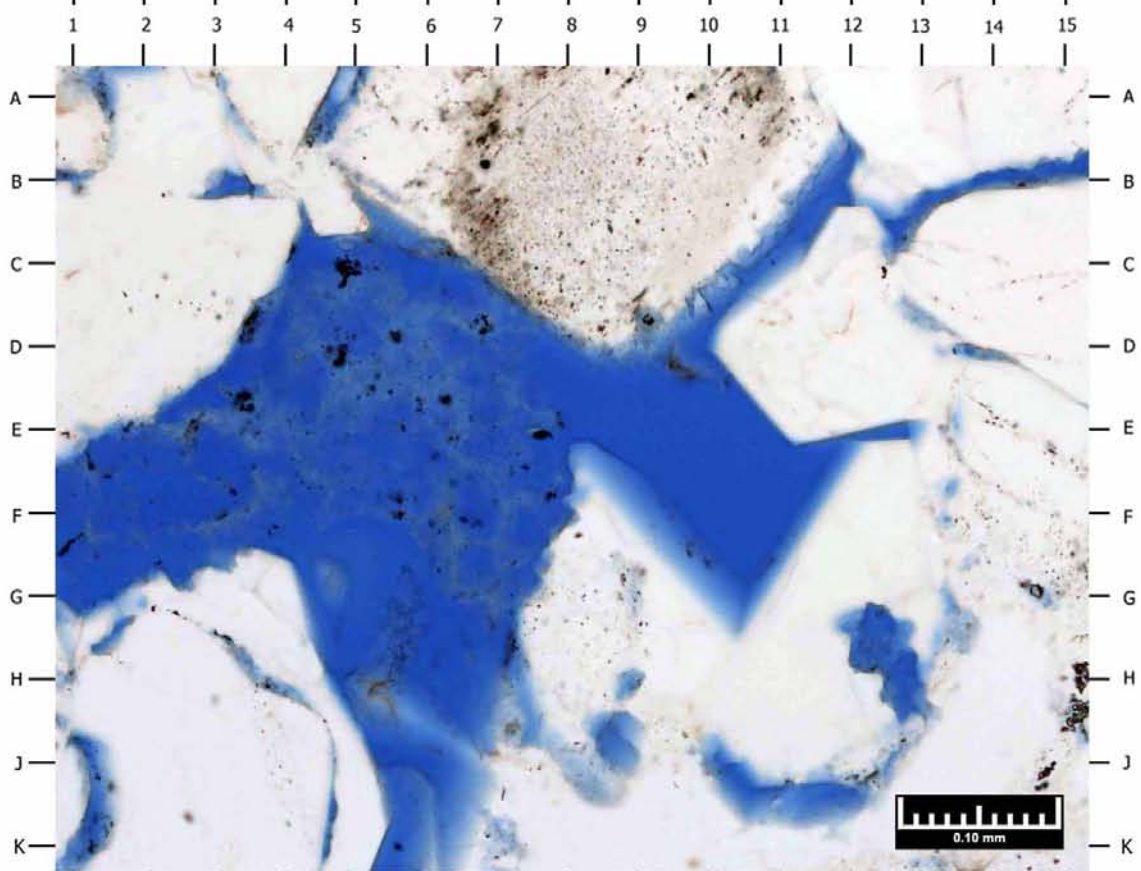

B

200X

Ohio Division of Geological Survey **OMNI File No: HH-38266**
CO_2 No. 1 Well
Tuscarawas County, Ohio
Rose Run Sandstone
Rotary Sidewall Core

THIN SECTION PHOTOMICROGRAPHS

SAMPLE DEPTH: 7387.0 FEET
SAMPLE NUMBER: 1-38R

Plate 38

Permeability (Klink.): 0.0044 mD Porosity (NCS): 5.9% Grain Density: 2.66 gm/cc

Sample not selected for petrographic analysis.

Magnification: A: 40X B: 200X

Ohio Division of Geological Survey
CO2 No. 1
Tuscarawas County, Ohio

7387.0'
Plate 38

Weatherford LABORATORIES

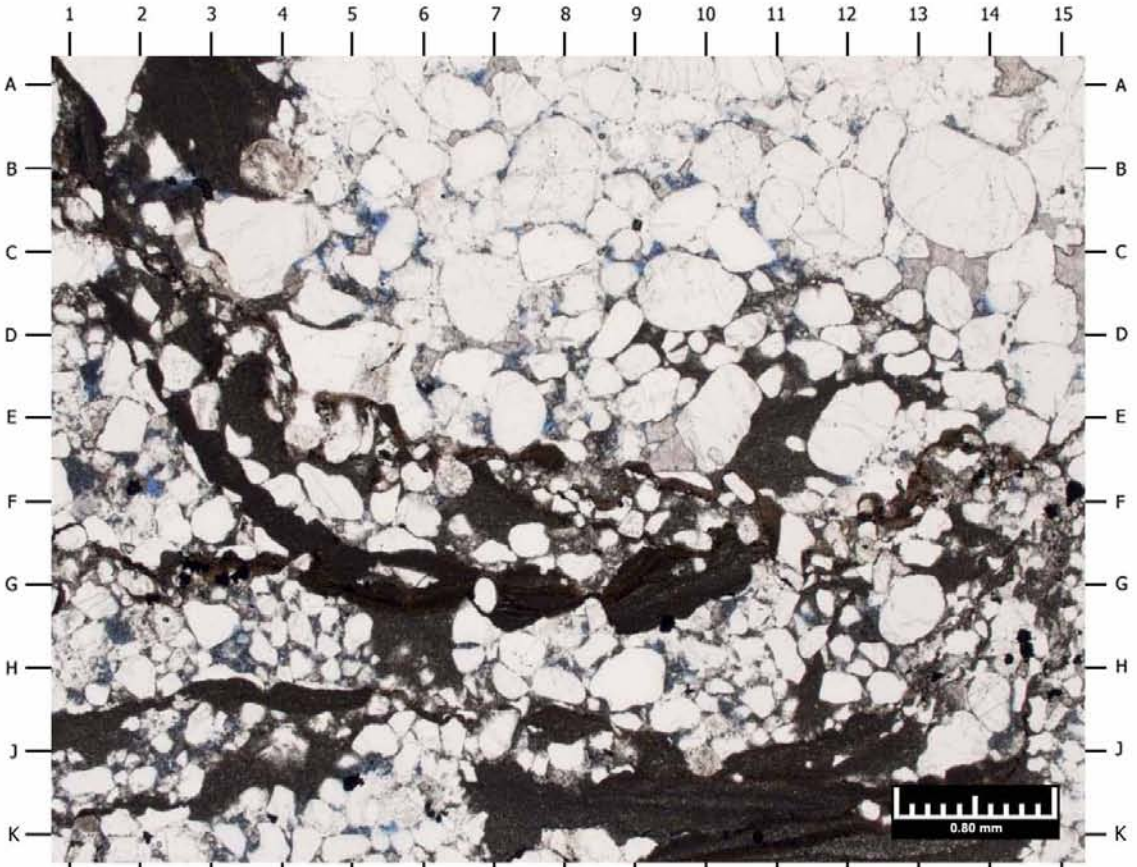

A

25X

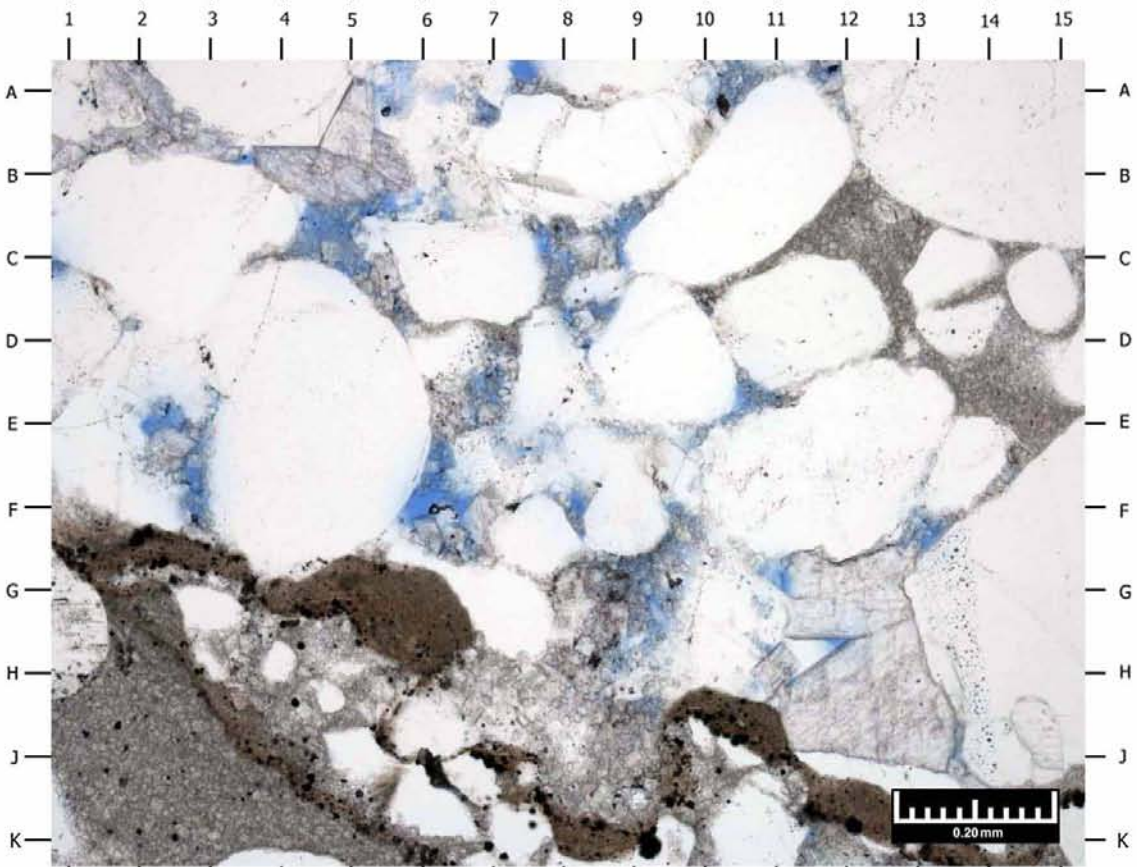

B

100X

Ohio Division of Geological Survey **OMNI File No: HH-38266**
CO_2 No. 1 Well
Tuscarawas County, Ohio
Rose Run Sandstone
Rotary Sidewall Core

THIN SECTION DESCRIPTION - DETAILED

SAMPLE DEPTH: 7392.0 FEET
SAMPLE NUMBER: 1-39R

Plate 39

Permeability (Klink.): 13.8 mD Porosity (NCS): 10.7% Grain Density: 2.64 gm/cc

Lithology:	Quartzarenite
Sedimentary Fabric:	Vague grain size-zoning
Grain Size Range:	<0.01mm-1.06mm
Average Grain Size:	0.35mm
Compaction:	Moderate
Sorting:	Moderately sorted
Framework Grains:	
Major:	Monocrystalline quartz
Minor:	Polycrystalline quartz, feldspar, lithic fragments (chert, mudstone, metamorphic fragments)
Accessory:	Tourmaline
Matrix Content:	
Detrital Matrix:	Minor of clay matrix and organic material
Authigenic Clay:	Minor pore-lining clay and pore-filling clay (undifferentiated)
Cement Types:	Common quartz overgrowths; minor pyrite; trace Fe/Ti oxides
Porosity Types:	Subequal, moderate amounts of intergranular pores and secondary intragranular pores; minor amount of micropores
Reservoir Quality:	Fair

Magnification: A: 40X B: 200X

A) Well developed quartz overgrowth cement (H6.5, E2.5) reduces intergranular pores (G8.5, H14.5). Most of the quartz grain exhibit healed microfractures (H9, K7). Oversized pores (F6) result from the partial to complete dissolution of unstable lithic fragments.

B) Dust rims mark the boundaries between the detrital quartz grainsA4, A7) and their quartz overgrowths (B5, C7, respectively). Hexagonal crystals represent euhedral quartz overgrowth terminations (D6, F10). Note the narrow pore throats between overgrowths (DE5, F11.5).

Ohio Division of Geological Survey
CO2 No. 1
Tuscarawas County, Ohio

7392.0'
Plate 39

Weatherford LABORATORIES

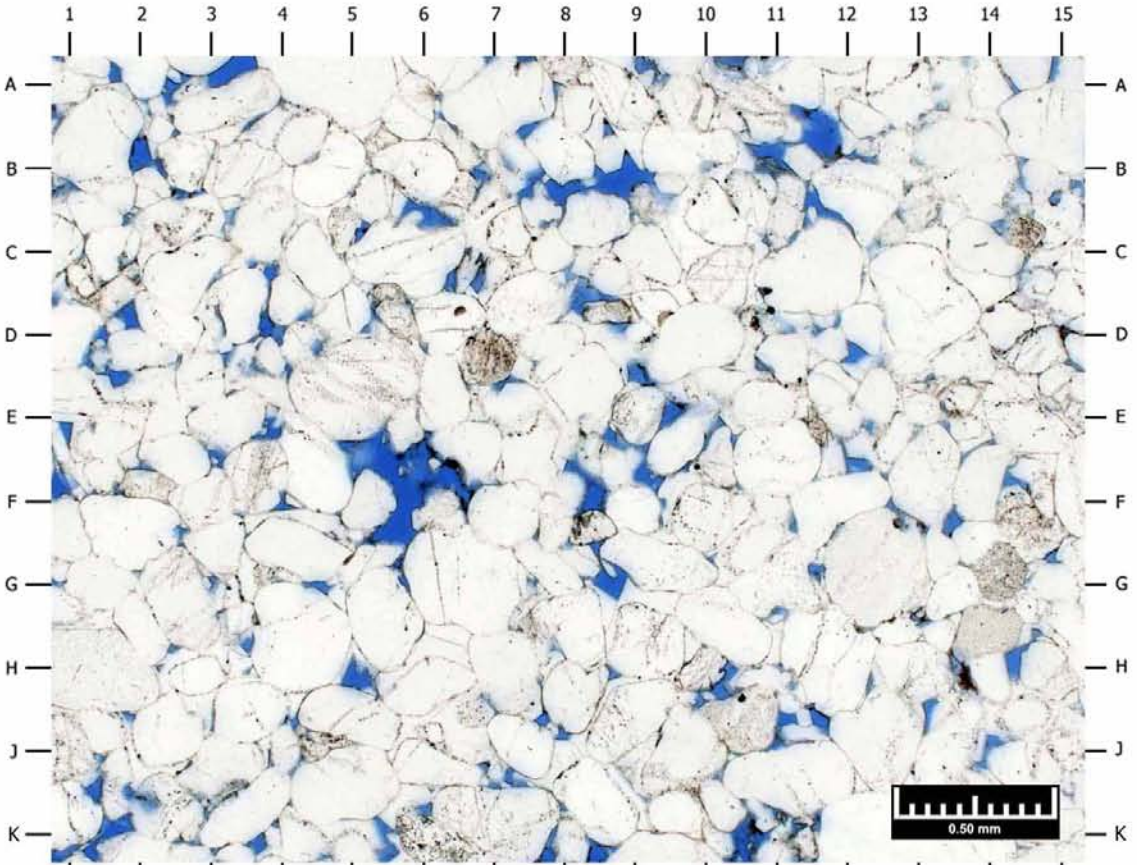

A

40X

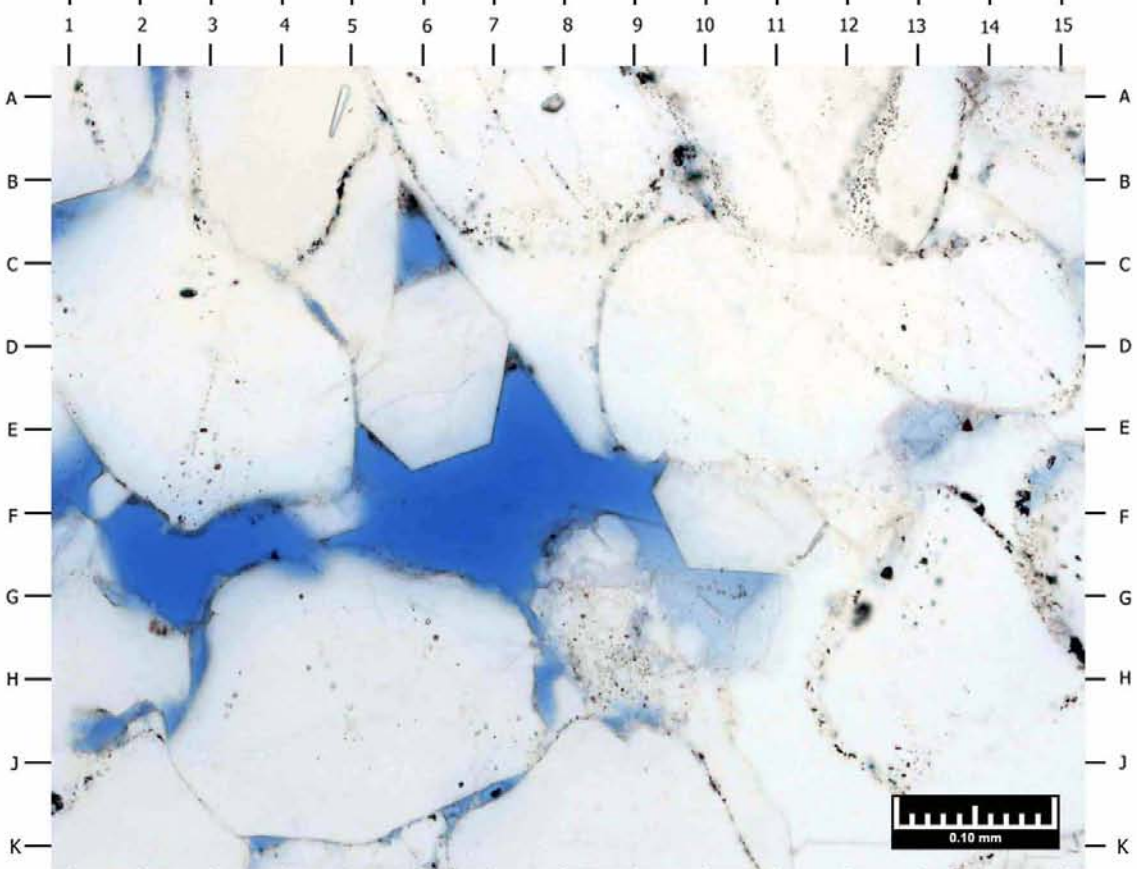

B

200X

Ohio Division of Geological Survey **OMNI File No: HH-38266**
CO_2 No. 1 Well
Tuscarawas County, Ohio
Rose Run Sandstone
Rotary Sidewall Core

THIN SECTION PHOTOMICROGRAPHS

SAMPLE DEPTH: 7414.0 FEET
SAMPLE NUMBER: 1-40R

Plate 40

Permeability (Klink.): 0.0009 mD Porosity (NCS): 3.3% Grain Density: 2.67 gm/cc

Sample not selected for petrographic analysis.

Magnification: A: 40X B: 200X

Ohio Division of Geological Survey
CO2 No. 1
Tuscarawas County, Ohio

7414.0'
Plate 40

Weatherford LABORATORIES

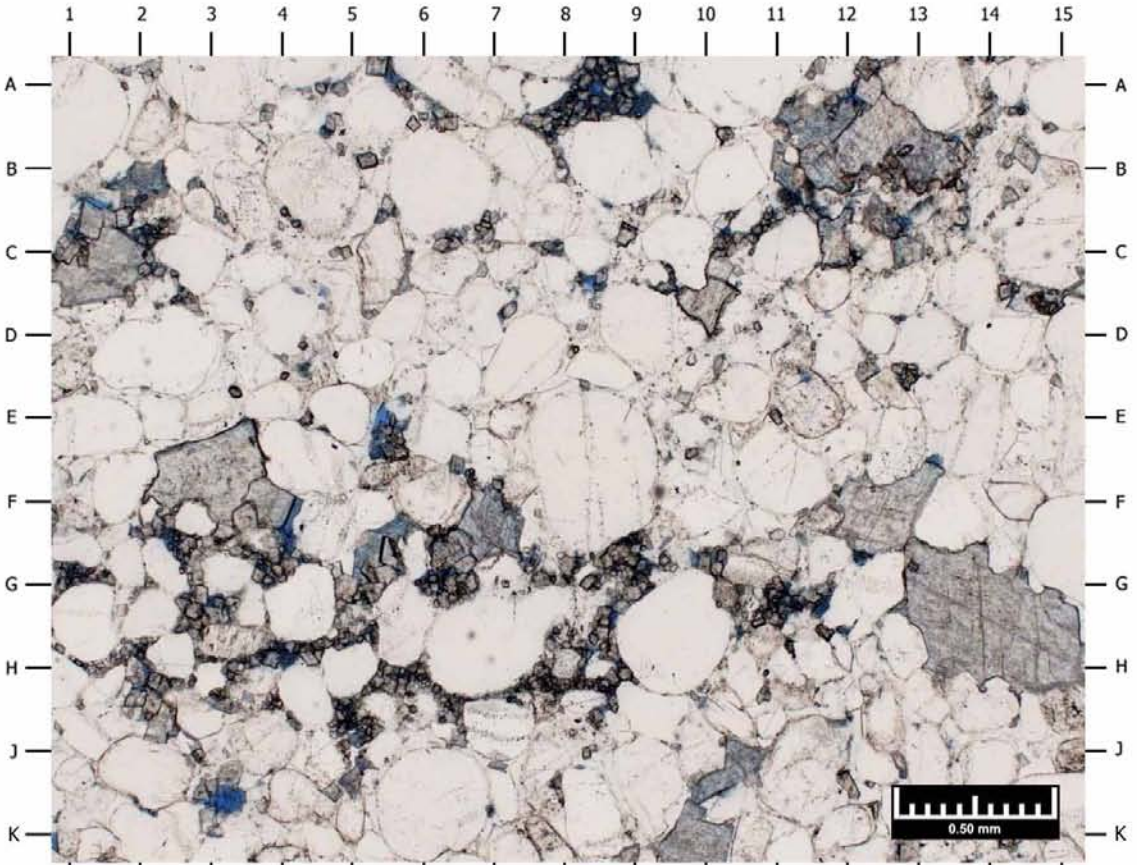

A

40X

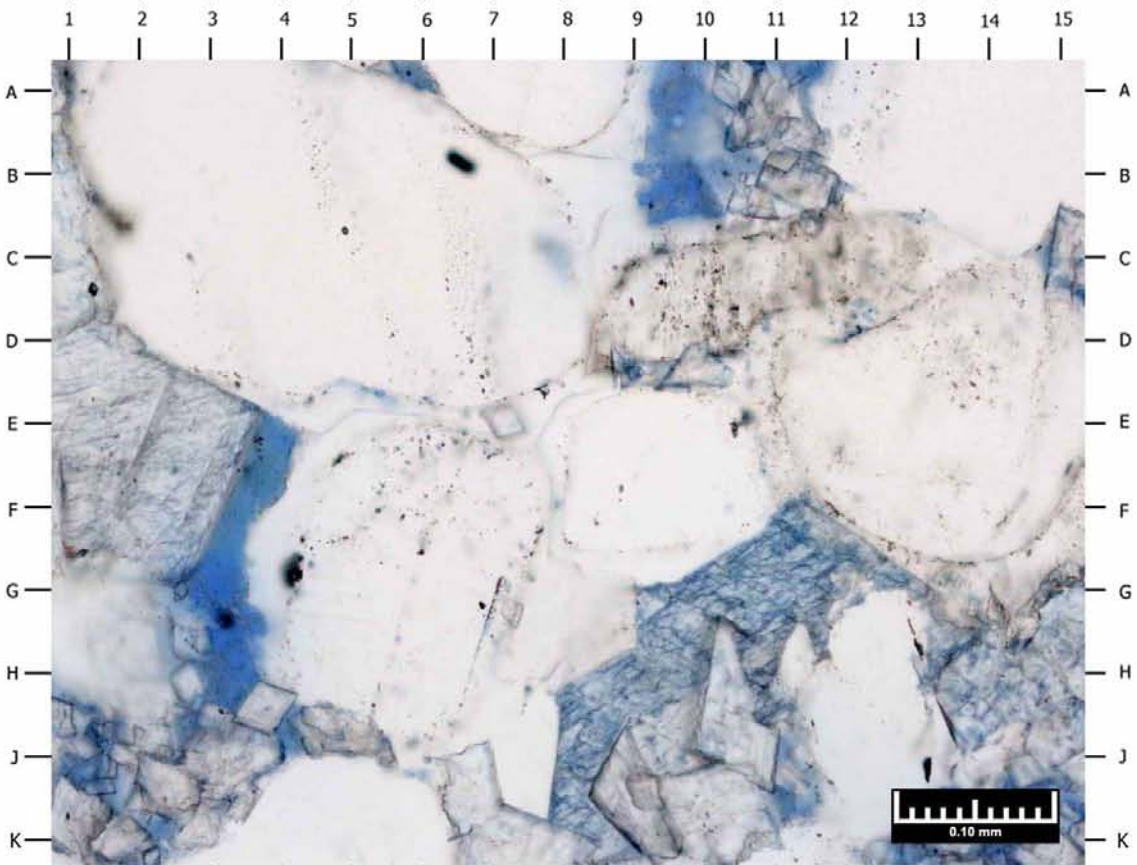

B

200X

Ohio Division of Geological Survey **OMNI File No: HH-38266**
CO_2 No. 1 Well
Tuscarawas County, Ohio
Rose Run Sandstone
Rotary Sidewall Core

THIN SECTION PHOTOMICROGRAPHS

SAMPLE DEPTH: 7426.0 FEET
SAMPLE NUMBER: 1-41R

Plate 41

Permeability (Klink.): 0.081 mD Porosity (NCS): 6.7% Grain Density: 2.62 gm/cc

Sample not selected for petrographic analysis.

Magnification: A: 40X B: 200X

Ohio Division of Geological Survey
CO2 No. 1
Tuscarawas County, Ohio

7426.0'
Plate 41

Weatherford LABORATORIES

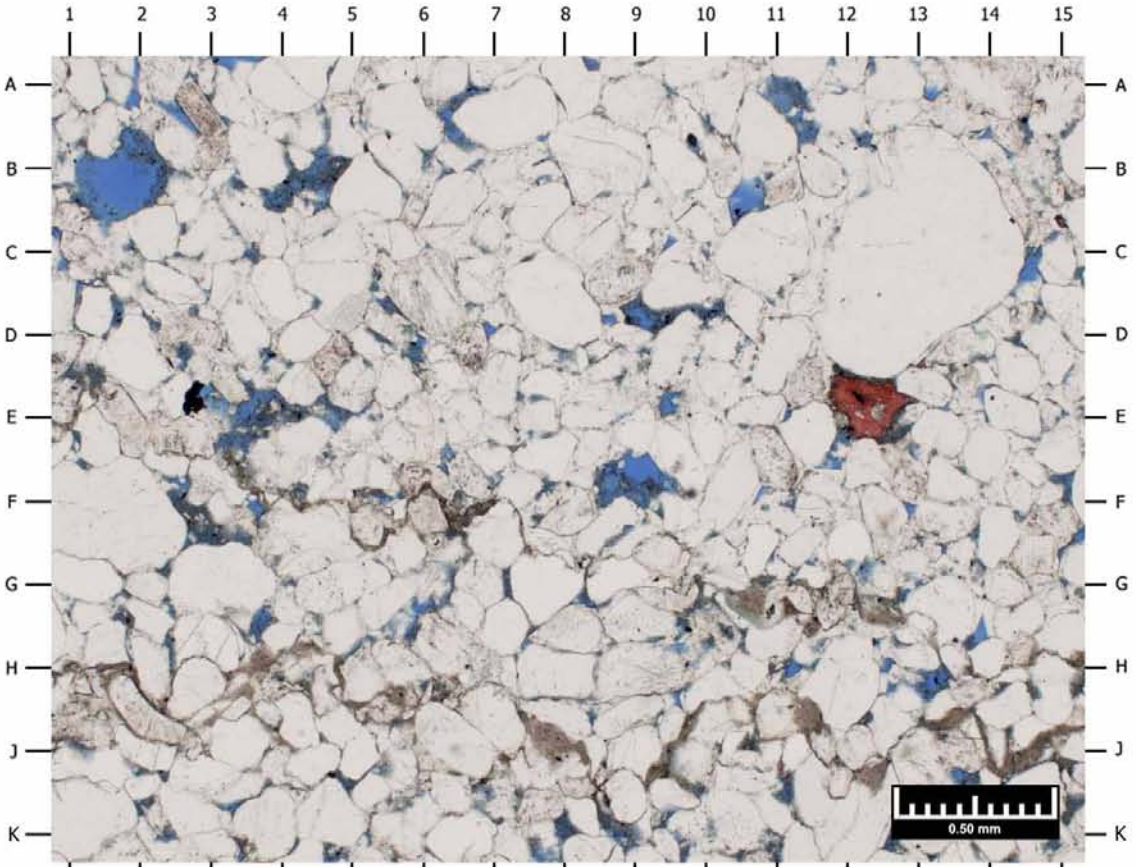

A

40X

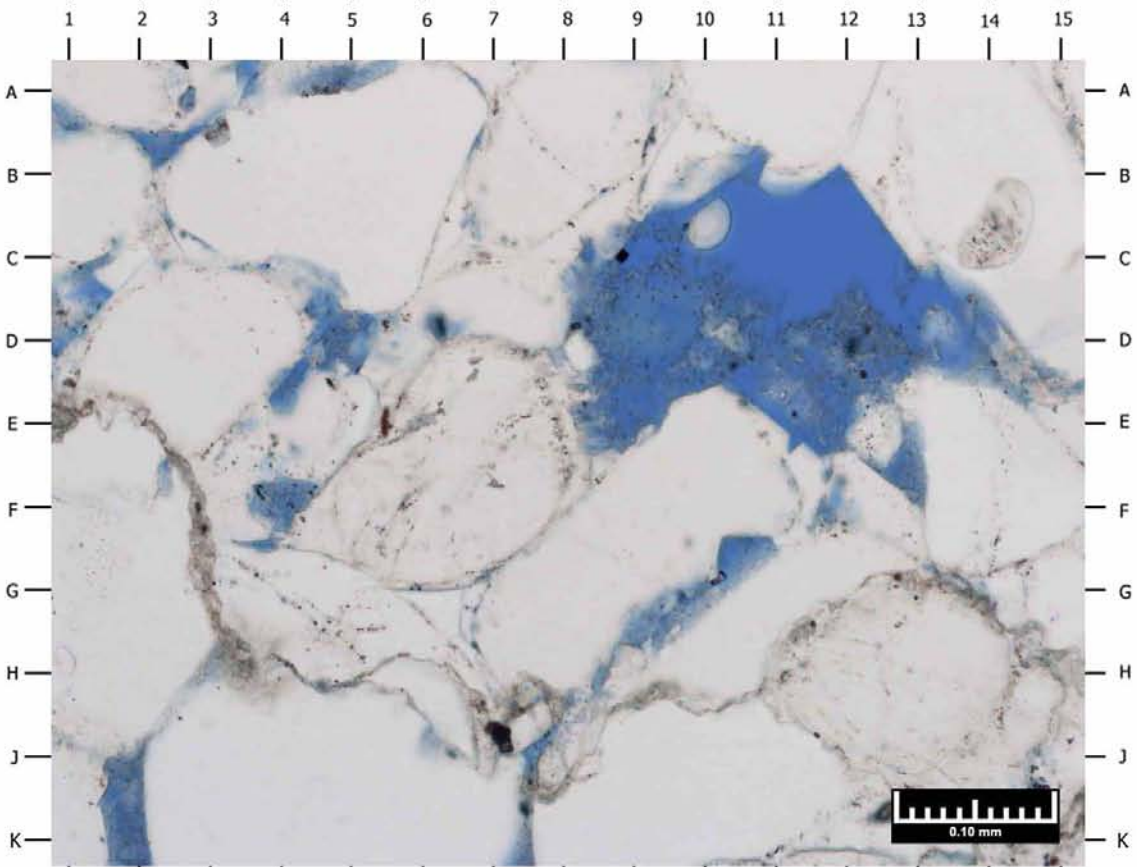

B

200X

Ohio Division of Geological Survey **OMNI File No: HH-38266**
CO_2 No. 1 Well
Tuscarawas County, Ohio
Rose Run Sandstone
Rotary Sidewall Core

THIN SECTION PHOTOMICROGRAPHS

SAMPLE DEPTH: 7434.0 FEET
SAMPLE NUMBER: 1-42R

Plate 42

Permeability (Klink.): 0.26.6 mD Porosity (NCS): 9.1% Grain Density: 2.68 gm/cc

Sample not selected for petrographic analysis.

Magnification: A: 40X B: 200X

Ohio Division of Geological Survey
CO2 No. 1
Tuscarawas County, Ohio

7434.0'
Plate 42

Weatherford LABORATORIES

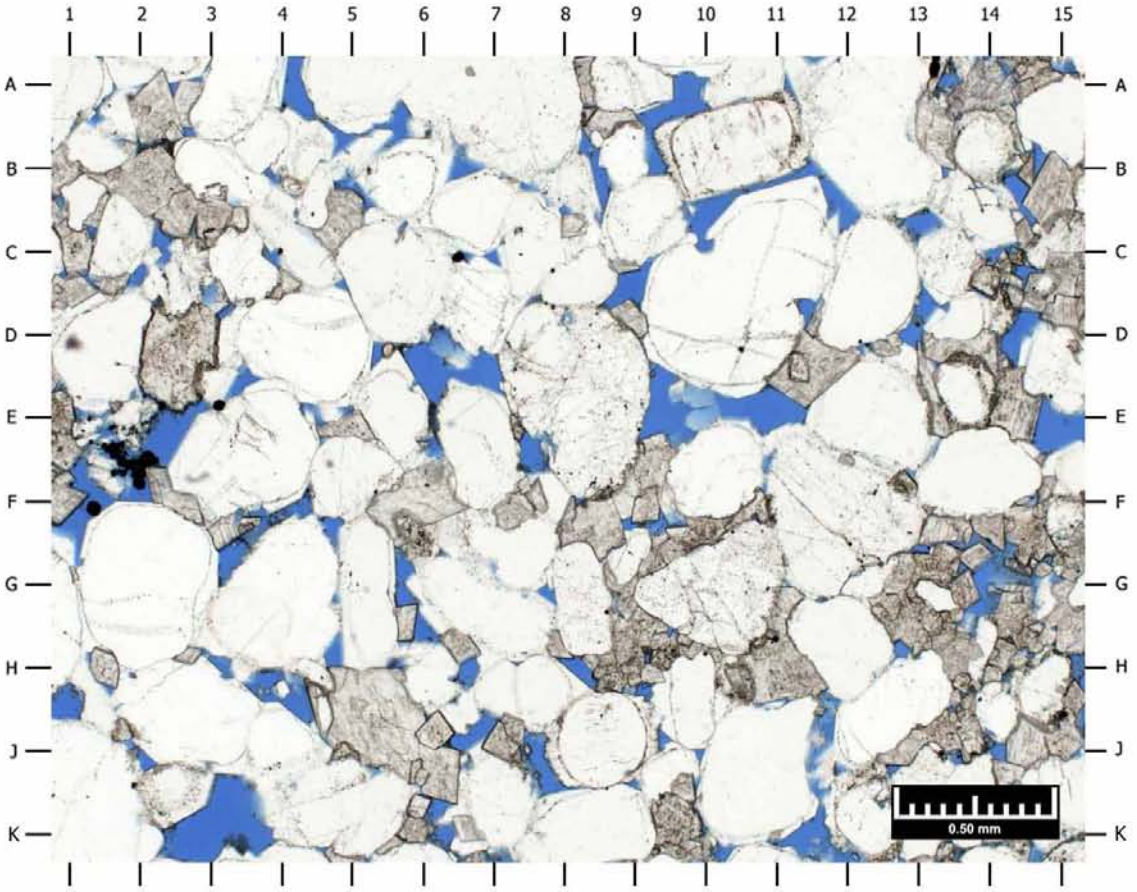

A

40X

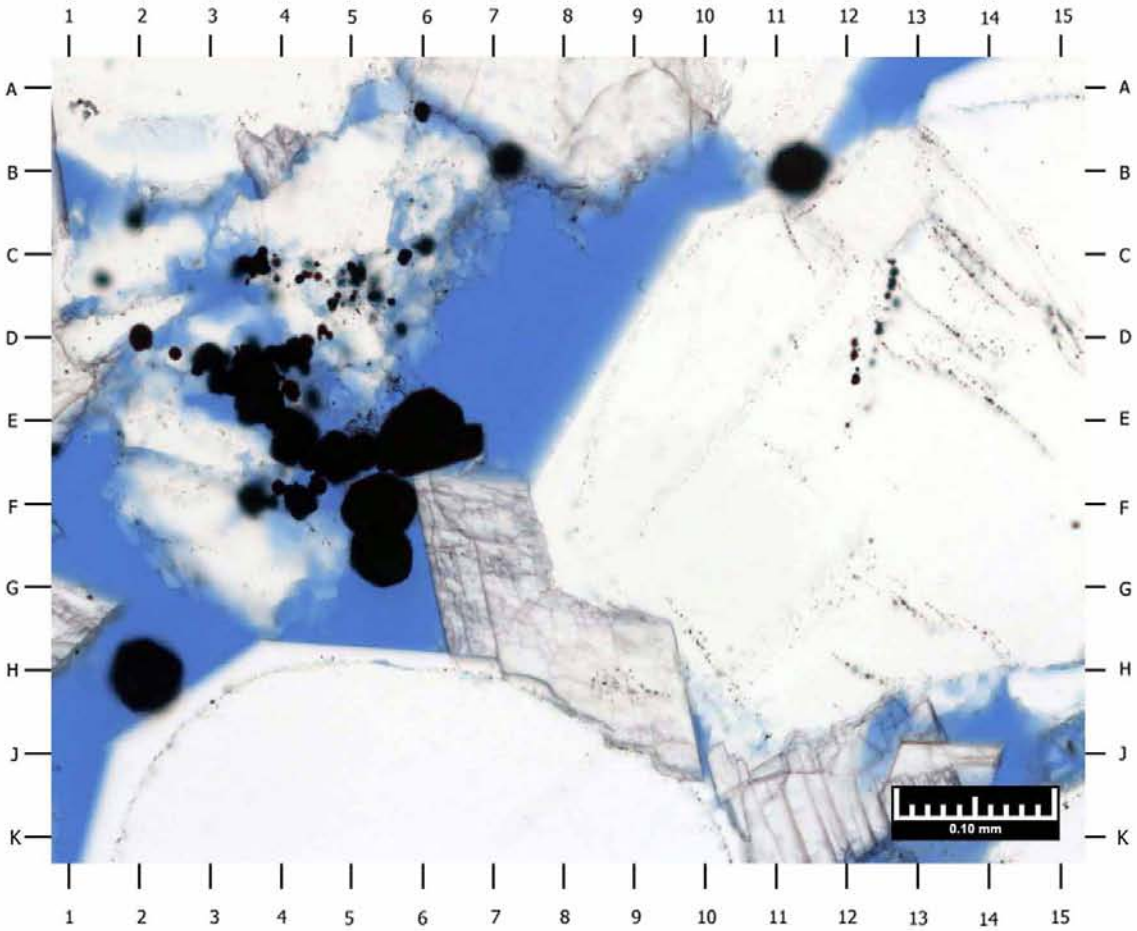

B

200X

Ohio Division of Geological Survey **OMNI File No: HH-38266**
CO_2 No. 1 Well
Tuscarawas County, Ohio
Rose Run Sandstone
Rotary Sidewall Core

THIN SECTION DESCRIPTION - DETAILED

SAMPLE DEPTH: 7441.0 FEET
SAMPLE NUMBER: 1-43R

Plate 43

Permeability (Klink.): 0.776 mD Porosity (NCS): 7.2% Grain Density: 2.61 gm/cc

Lithology:	Subarkose
Sedimentary Fabric:	Vague grain size-zoning
Grain Size Range:	<0.06mm-1.23mm
Average Grain Size:	0.31mm
Compaction:	High
Sorting:	Moderately sorted
Framework Grains:	
Major:	Monocrystalline quartz, potassium feldspar
Minor:	Polycrystalline quartz, plagioclase feldspar, lithic fragments (chert, mudstone, metamorphic fragments)
Accessory:	Tourmaline
Matrix Content:	
Detrital Matrix:	Trace of organic material
Authigenic Clay:	Trace of pore-lining clay (undifferentiated)
Cement Types:	Common quartz overgrowths; minor feldspar overgrowths
Porosity Types:	Common intergranular pores and minor amounts of secondary intragranular pores; minor amount of micropores
Reservoir Quality:	Fair

Magnification: A: 40X B: 200X

A) The feldspar grains in this subarkose are variably altered (C9,E0.5) and partially dissolved (B9, J13.5). Note the sutured boundaries between quartz grains (A3, F2) that result from burial compaction.

B) A combination of primary intergranular pores (C13) and secondary intragranular pores (C5, F7.5) results in good porosity but low permeability. Quartz overgrowth cement (K9, G12.5) and feldspar overgrowths (F8, G11) are the predominant cements. A tourmaline grain (H8.5) also shows evidence of healed fractures.

Ohio Division of Geological Survey
CO2 No. 1
Tuscarawas County, Ohio

7441.0'
Plate 43

Weatherford LABORATORIES

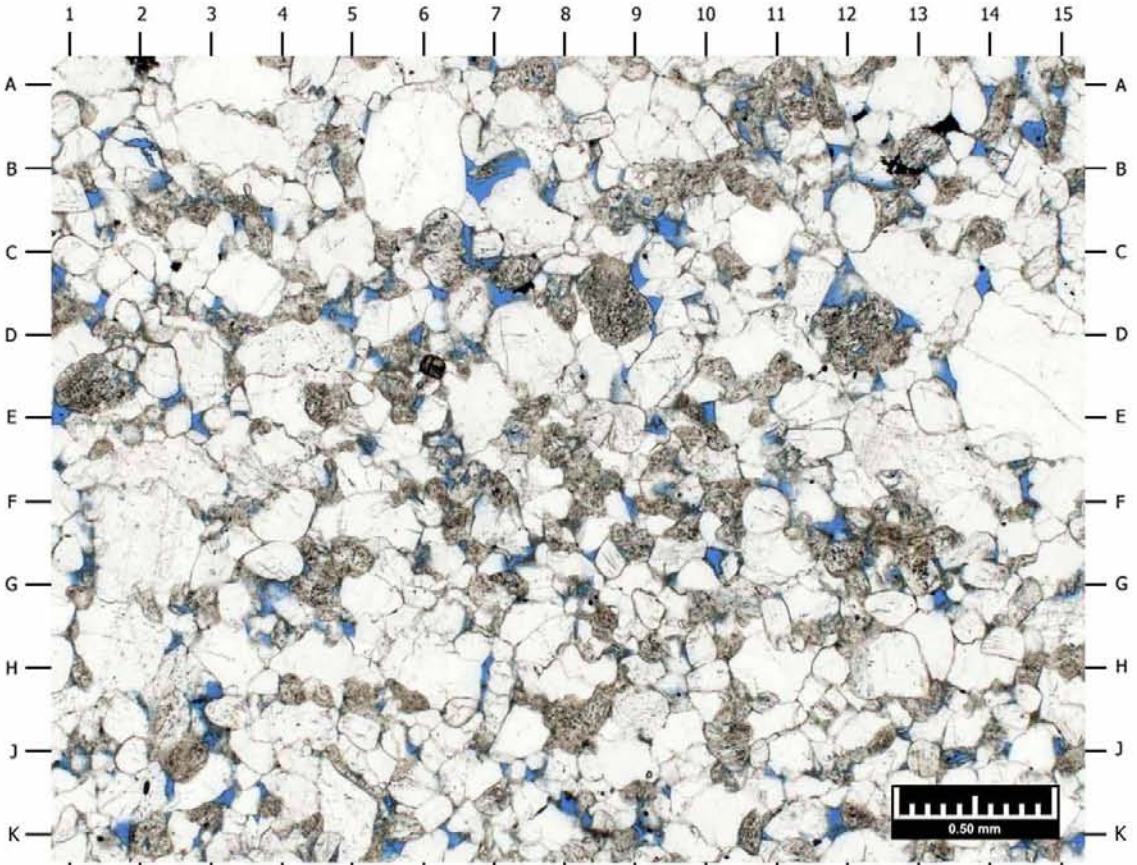

A

40X

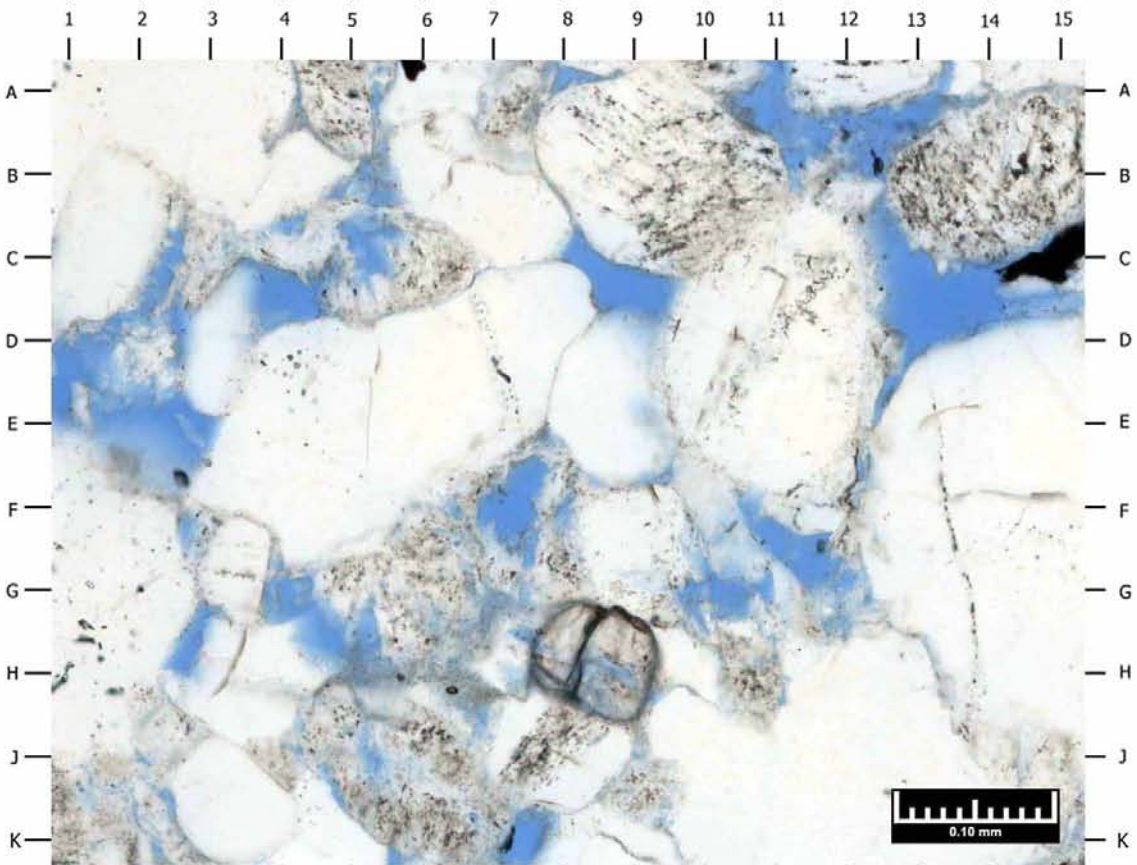

B

200X

Ohio Division of Geological Survey **OMNI File No: HH-38266**
CO_2 No. 1 Well
Tuscarawas County, Ohio
Rose Run Sandstone
Rotary Sidewall Core

THIN SECTION PHOTOMICROGRAPHS

SAMPLE DEPTH: 7459.0 FEET
SAMPLE NUMBER: 1-44R

Plate 44

Permeability (Klink.): 0.0002 mD Porosity (NCS): 1.2% Grain Density: 2.82 gm/cc

Sample not selected for petrographic analysis.

Magnification: A: 40X B: 200X

Ohio Division of Geological Survey
CO2 No. 1
Tuscarawas County, Ohio

7459.0'
Plate 44

Weatherford LABORATORIES

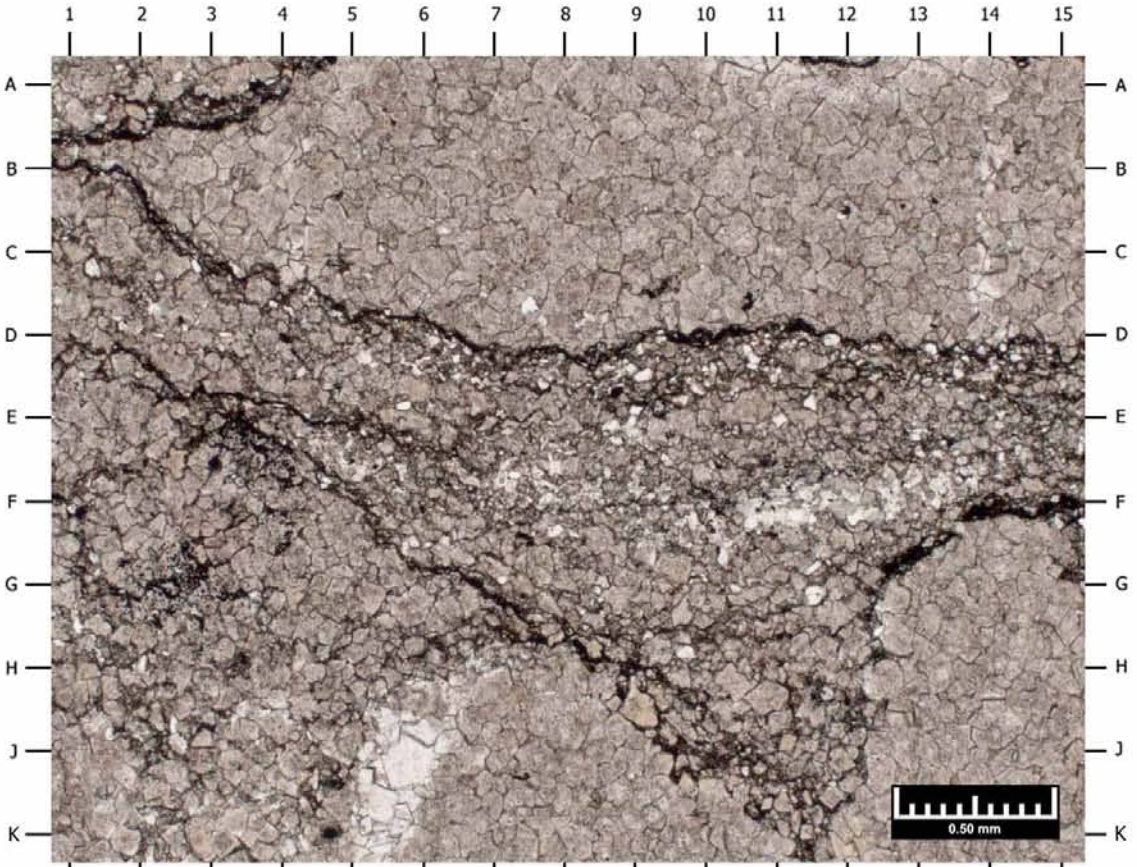

A

40X

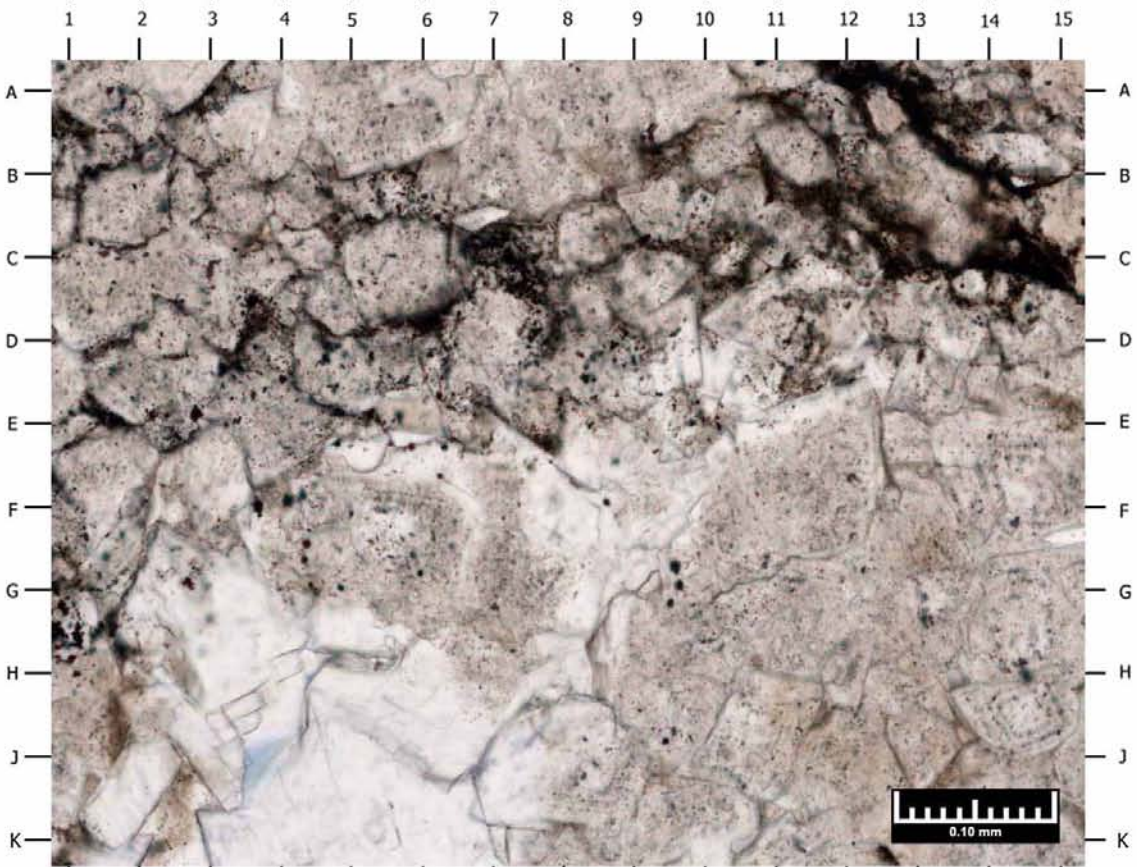

B

200X

Ohio Division of Geological Survey **OMNI File No: HH-38266**
CO_2 No. 1 Well
Tuscarawas County, Ohio
Rose Run Sandstone
Rotary Sidewall Core

THIN SECTION PHOTOMICROGRAPHS

SAMPLE DEPTH: 7480.0 FEET
SAMPLE NUMBER: 1-45R

Plate 45

Permeability (Klink.): 0.0029 mD Porosity (NCS): 4.2% Grain Density: 2.74 gm/cc

Sample not selected for petrographic analysis.

Magnification: A: 40X B: 200X

Ohio Division of Geological Survey
CO2 No. 1
Tuscarawas County, Ohio

7480.0'
Plate 45

Weatherford LABORATORIES

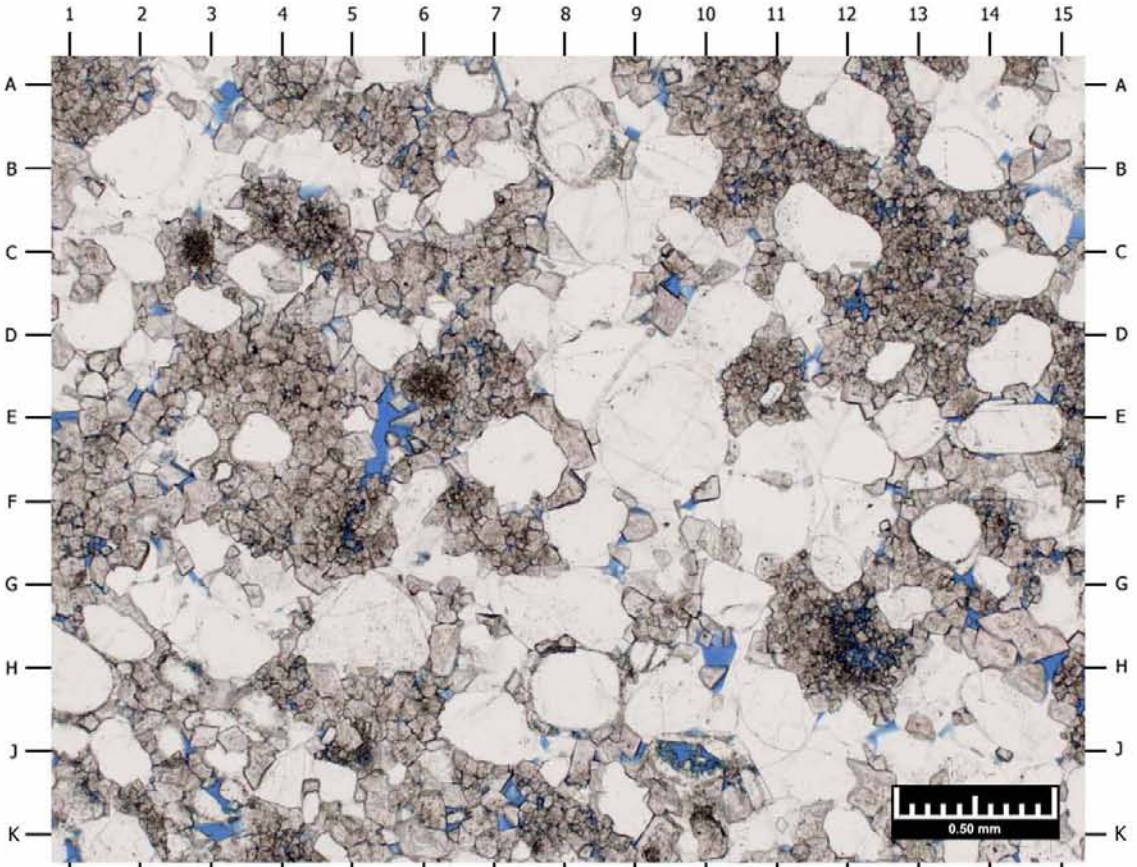

A

40X

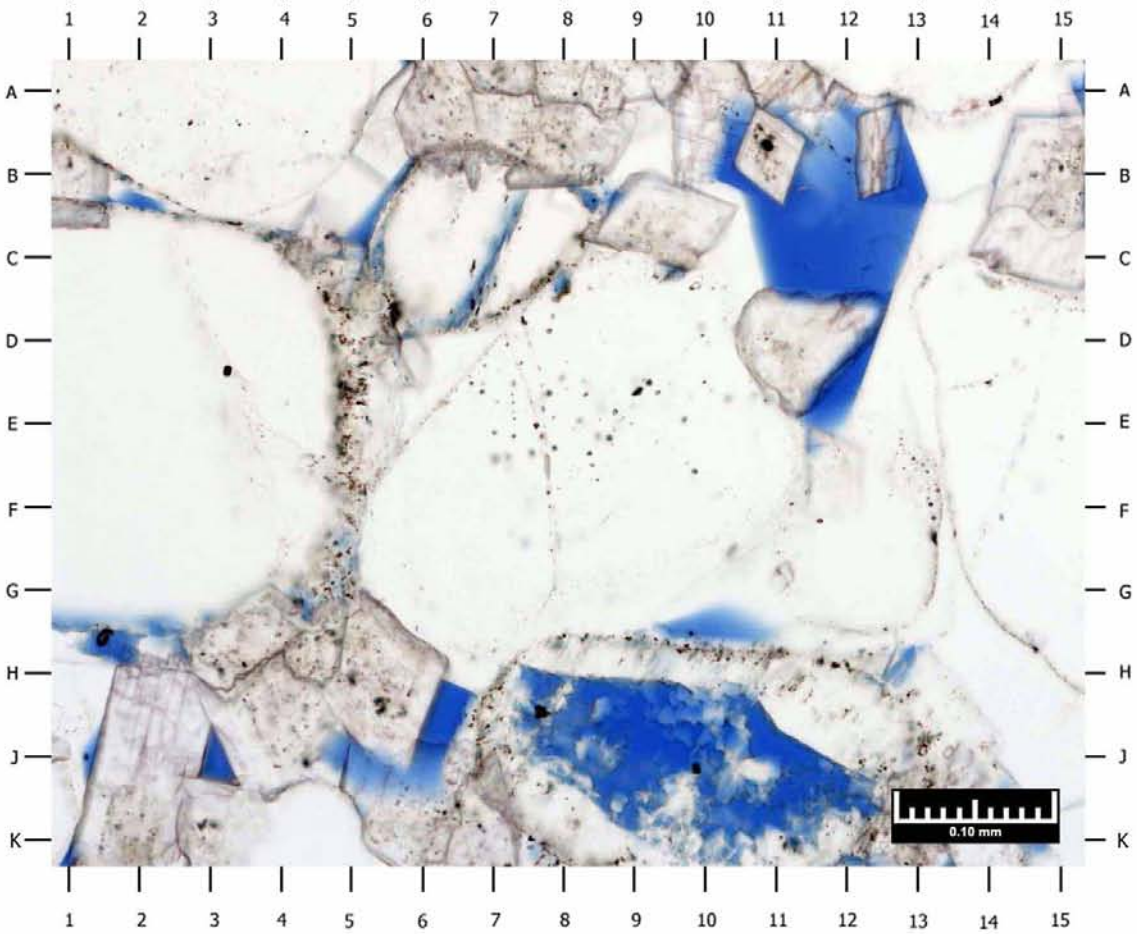

B

200X

Ohio Division of Geological Survey **OMNI File No: HH-38266**
CO_2 No. 1 Well
Tuscarawas County, Ohio
Rose Run Sandstone
Rotary Sidewall Core

THIN SECTION PHOTOMICROGRAPHS

SAMPLE DEPTH: 7495.0 FEET
SAMPLE NUMBER: 1-46R

Plate 46

Permeability (Klink.): 0.015 mD Porosity (NCS): 8.4% Grain Density: 2.62 gm/cc

Sample not selected for petrographic analysis.

Magnification: A: 40X B: 200X

Ohio Division of Geological Survey
CO2 No. 1
Tuscarawas County, Ohio

7495.0'
Plate 46

Weatherford LABORATORIES

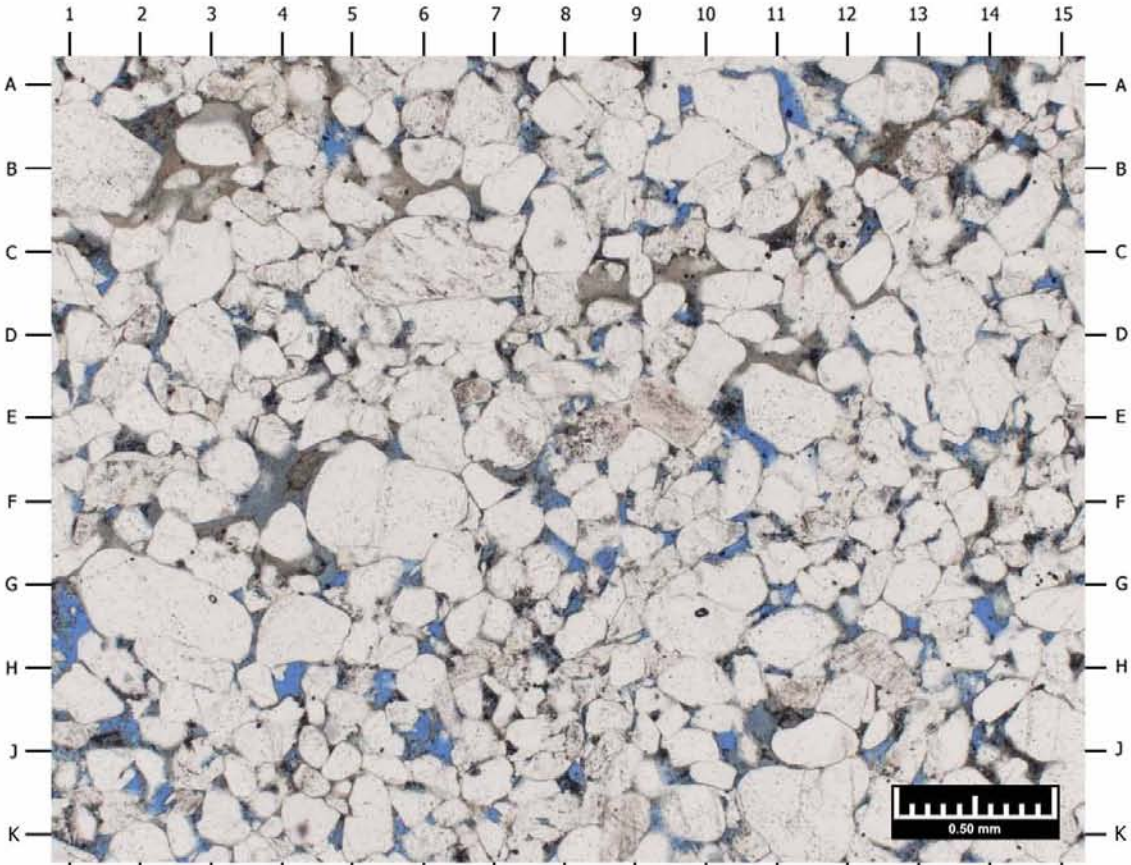

A

40X

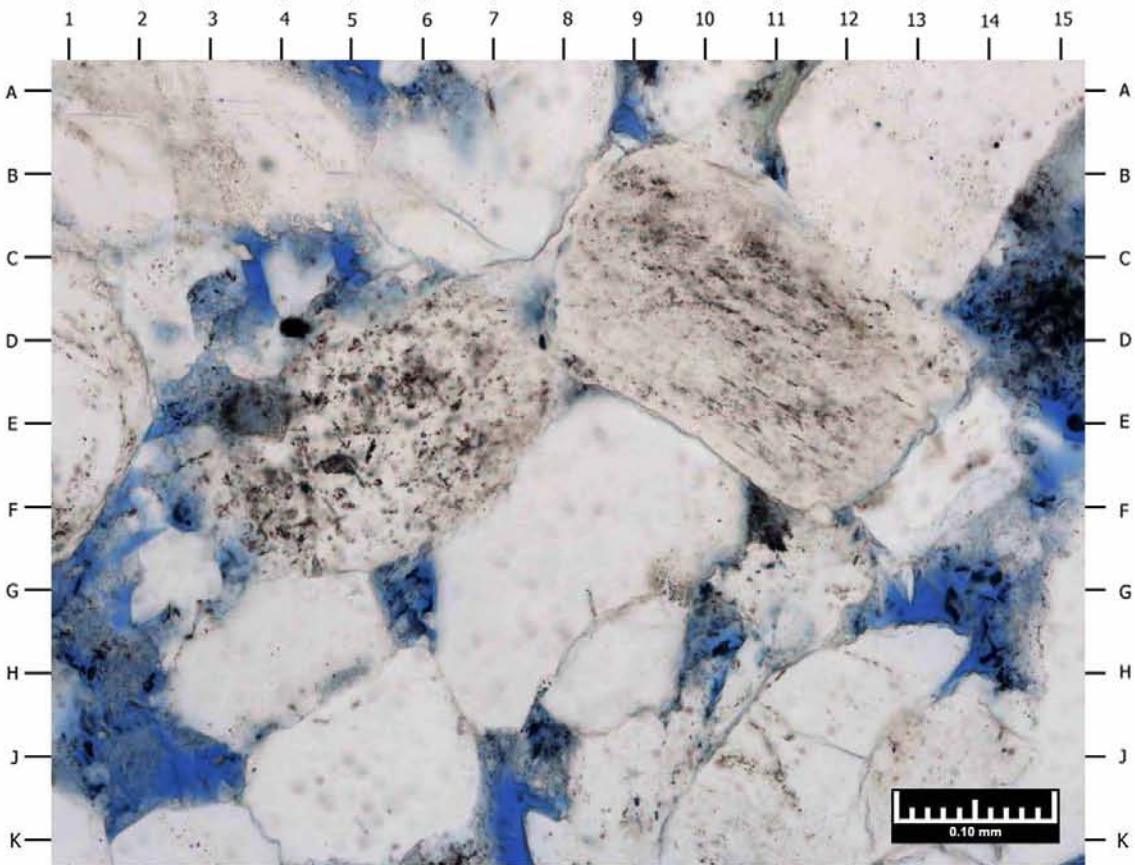

B

200X

Ohio Division of Geological Survey **OMNI File No: HH-38266**
CO_2 No. 1 Well
Tuscarawas County, Ohio
Rose Run Sandstone
Rotary Sidewall Core

THIN SECTION DESCRIPTION - DETAILED

SAMPLE DEPTH: 7506.0 FEET
SAMPLE NUMBER: 1-20R

Plate 47

Permeability (Klink.): 1.4 mD Porosity (NCS): 8.2% Grain Density: 2.71 gm/cc

Lithology:	Subarkose
Sedimentary Fabric:	Cement-zoning (dolomite)
Grain Size Range:	<0.03mm-0.97mm
Average Grain Size:	0.27mm
Compaction:	Moderate
Sorting:	Moderately poorly sorted
Framework Grains:	
Major:	Monocrystalline quartz, potassium feldspar
Minor:	Polycrystalline quartz, plagioclase feldspar, lithic fragments (plutonic and metamorphic fragments), shale
Accessory:	Tourmaline
Matrix Content:	
Detrital Matrix:	Minor organic material
Authigenic Clay:	Minor pore-lining clay and pore-filling clay (undifferentiated)
Cement Types:	Abundant dolomite cement; minor quartz overgrowths; trace feldspar, Fe/Ti oxides, and pyrite; minor bitumen
Porosity Types:	Minor amount of secondary intragranular pores; lesser amount of intergranular pores and micropores
Reservoir Quality:	Fair

Magnification: A: 40X B: 200X

A) Variably developed microcrystalline dolomite cement appears to mimic the original bedding in this subarkose. There are scattered outsized grains, including a metaquartzite grain (G6) and a shale clast (G4). Macropores in the poorly cemented layers include intergranular pores (A11) and secondary intragranular pores (A4.5).

B) A detailed view of the dolomite cemented layer shows common intercrystalline pores between dolomite crystals (D9), as well as secondary intragranular pores (C3.5, H6). Note the surfaces of quartz grains are etched by the dolomite crystals (H4.5, D8).

Ohio Division of Geological Survey
CO2 No. 1
Tuscarawas County, Ohio

7506.0'
Plate 47

Weatherford LABORATORIES

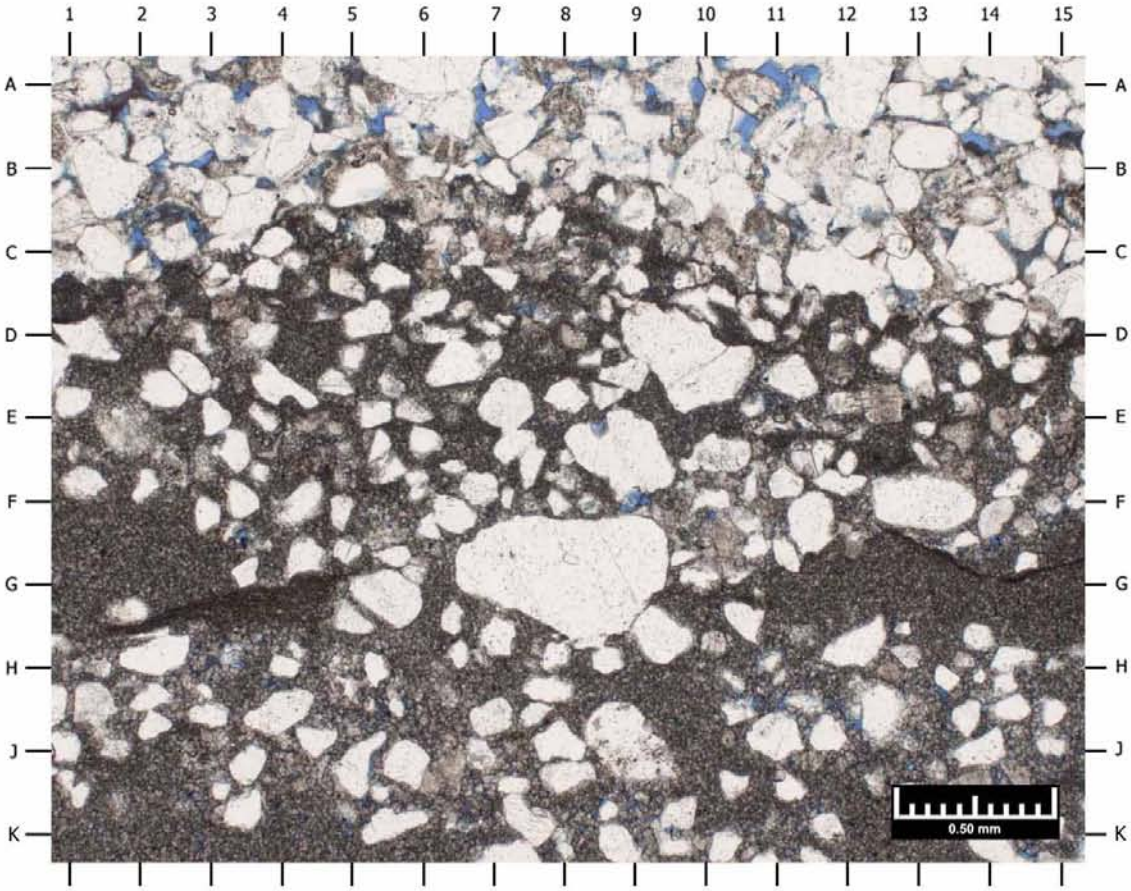

A

40X

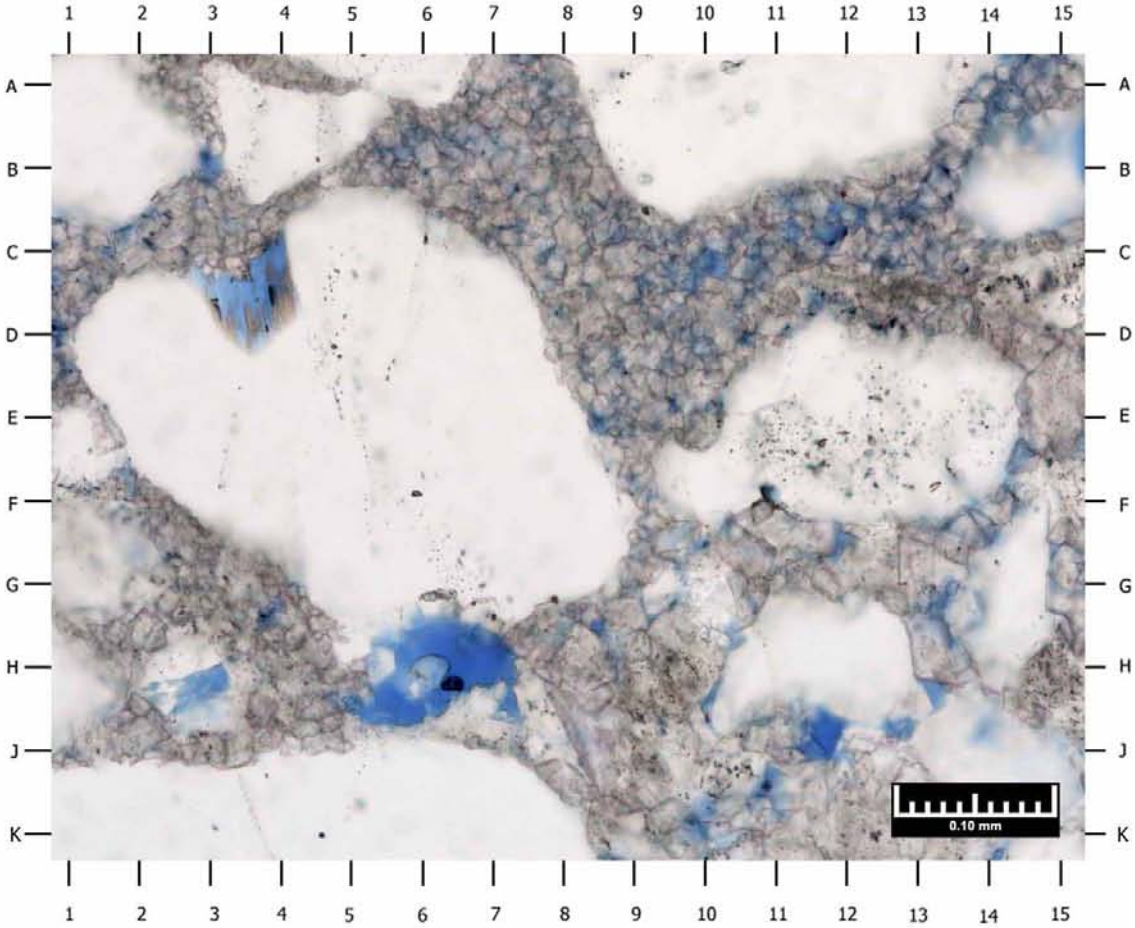

B

200X

Ohio Division of Geological Survey **OMNI File No: HH-38266**
CO_2 No. 1 Well
Tuscarawas County, Ohio
Copper Ridge Dolomite
Rotary Sidewall Core

THIN SECTION PHOTOMICROGRAPHS

SAMPLE DEPTH: 7528.0 FEET
SAMPLE NUMBER: 1-48R

Plate 48

Permeability (Klink.): 0.017 mD Porosity (NCS): 2.0% Grain Density: 2.83 gm/cc

Sample not selected for petrographic analysis.

Magnification: A: 40X B: 200X

Ohio Division of Geological Survey
CO2 No. 1
Tuscarawas County, Ohio

7528.0'
Plate 48

Weatherford LABORATORIES

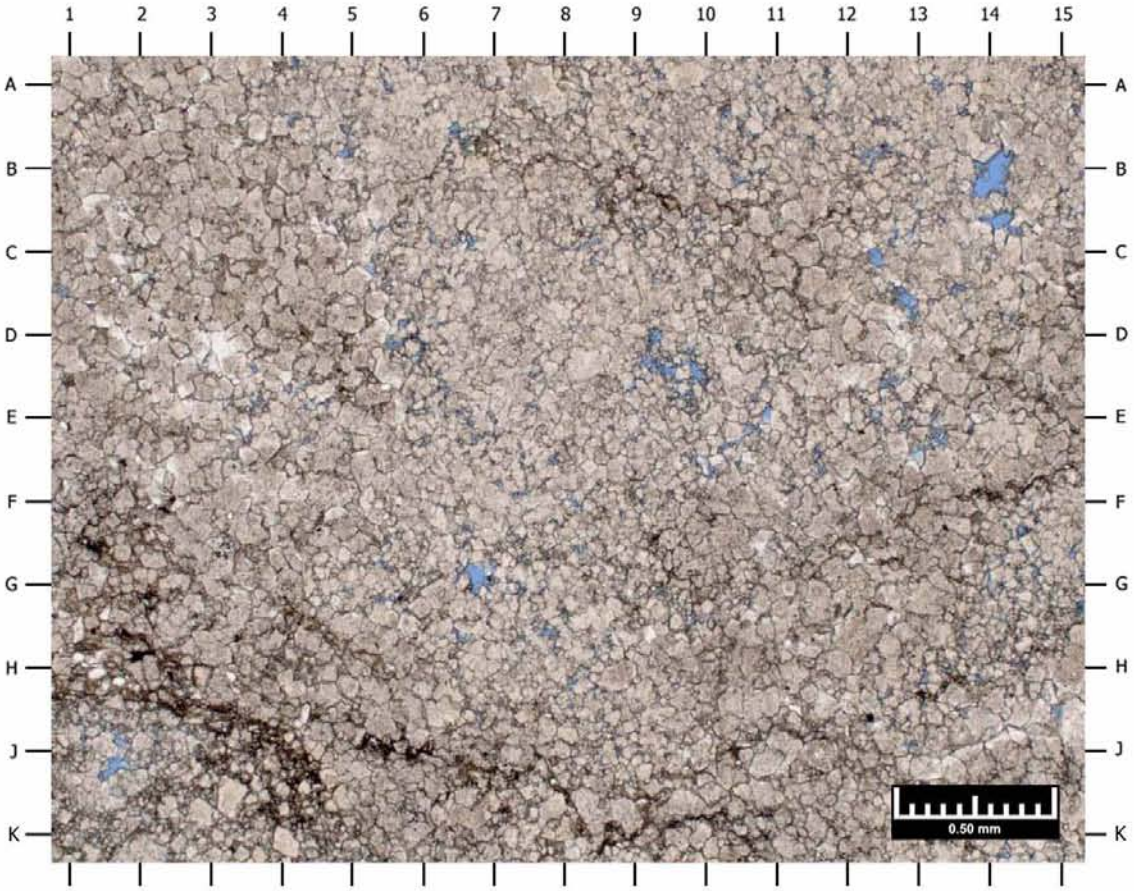

A

40X

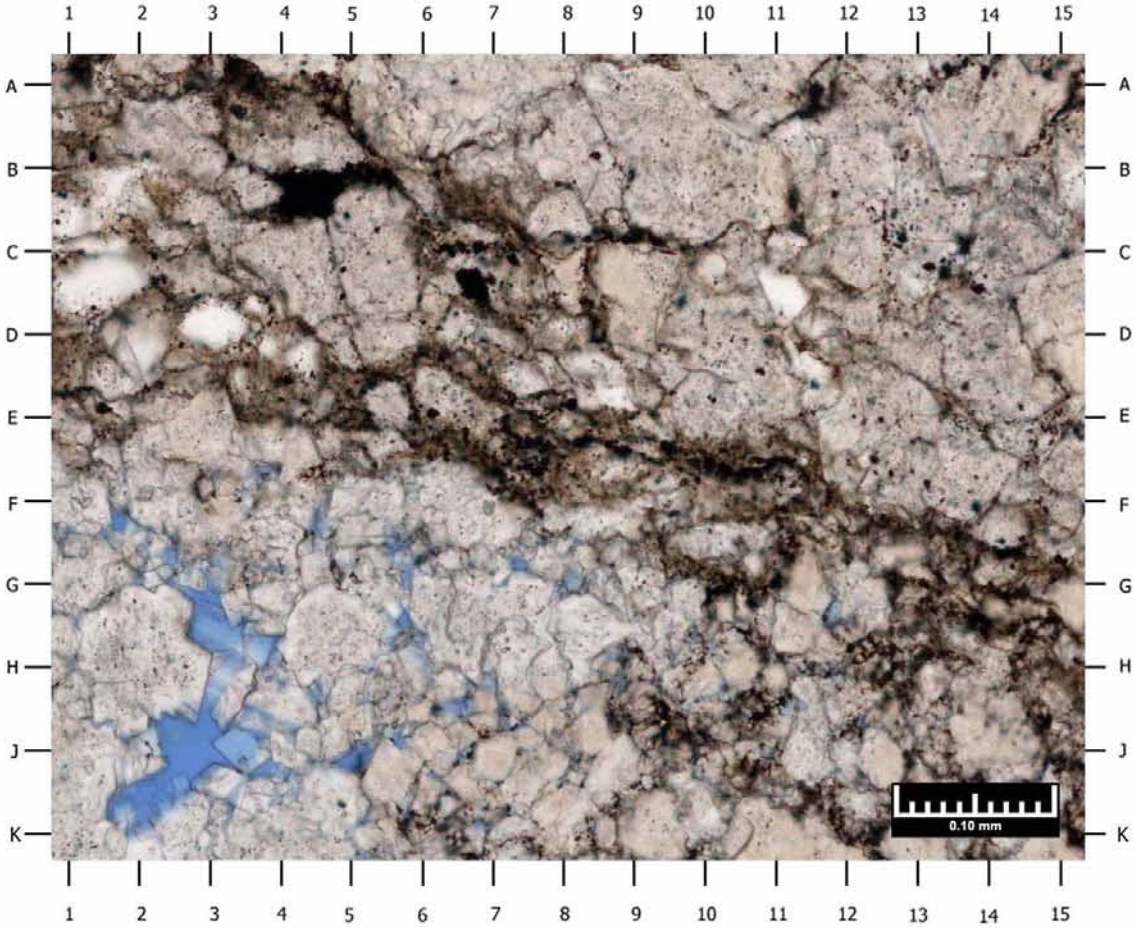

B

200X

Ohio Division of Geological Survey **OMNI File No: HH-38266**
CO_2 No. 1 Well
Tuscarawas County, Ohio
Copper Ridge Dolomite
Rotary Sidewall Core

THIN SECTION DESCRIPTION - GENERAL

SAMPLE DEPTH: 7579.0 FEET
SAMPLE NUMBER: 1-49R

Plate 49

Permeability (Klink.): 0.0005 mD Porosity (NCS): 1.9% Grain Density: 2.83gm/cc

Lithology: Dolomite

Texture: Dolomite; vague laminations defined by concentrations of quartz silt or clay; incipient microstylolites; possible burrow traces

Framework Grains: Original allochems difficult to recognize due to dolomitization overprint; rare ghost allochems undifferentiated); trace amount of fine organic debris and clay, especially concentrated along microstylolites; trace amount of silt-sized quartz

Matrix: Trace matrix clay

Cements and Replacement Minerals: All original fabric and nearly all allochems completely replaced by fine crystalline, subhedral to euhedral dolomite; minor amount of microcrystalline pyrite replacement

Pore System: No visible macropores; minor amount of intercrystalline micropores

Reservoir Quality: Poor

Magnification: A: 40X B: 200X

A) This dolomitized sediment contains only rare allochem ghosts (none visible in this view). The interlocking dolomite crystals result in very low porosity and permeability. Note the thin concentrations of clay (dark streaks; D4 to K12) that appear to represent original bedding.

B) The high magnification view shows the interlocking anhedral dolomite crystals, a rare sand-sized quartz grain (CD8), and scattered microcrystalline authigenic pyrite (black specks; A14.5, E8.5).

Ohio Division of Geological Survey
CO2 No. 1
Tuscarawas County, Ohio

7579.0'
Plate 49

Weatherford LABORATORIES

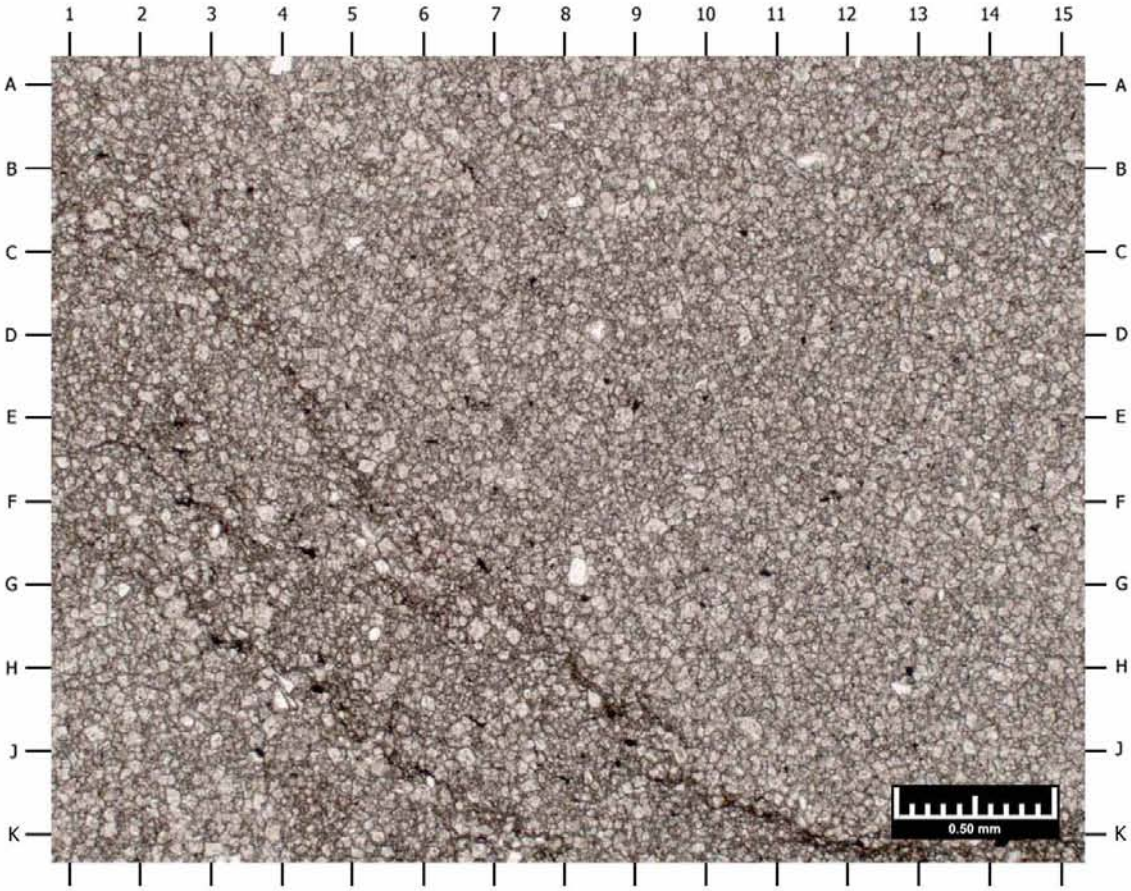

A

40X

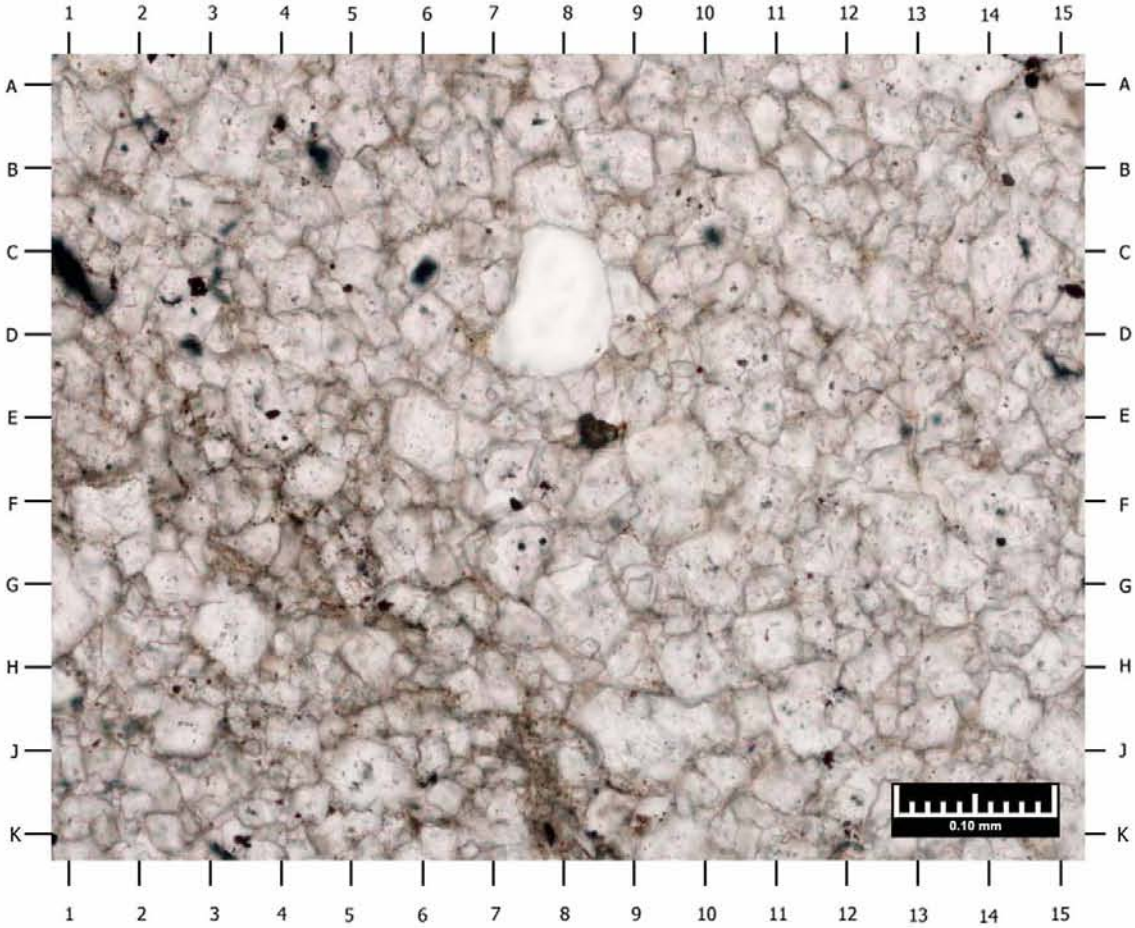

B

200X

Ohio Division of Geological Survey **OMNI File No: HH-38266**
CO_2 No. 1 Well
Tuscarawas County, Ohio
Copper Ridge Dolomite
Rotary Sidewall Core

THIN SECTION DESCRIPTION - DETAILED

SAMPLE DEPTH: 7692.0 FEET
SAMPLE NUMBER: 1-50R

Plate 50

Permeability (Klink.): 0.0001 mD Porosity (NCS): 1.3% Grain Density: 2.81 gm/cc

Lithology: Dolomite

Texture: Skeletal peloidal dolopackstone / dolowackestone; possible burrow traces

Framework Grains: Original allochems are difficult to recognize due to dolomitization overprint; common ghosts of peloids and echinoderm and undifferentiated fossil fragments; trace amount of phosphatic shell fragments; minor amount of silt-sized quartz trace amount of fine organic debris;

Matrix: Trace matrix clay

Cements and Replacement Minerals: All original fabrics and nearly all allochems completely replaced by fine crystalline, subhedral to euhedral dolomite; minor amount of microcrystalline pyrite replacement

Pore System: No visible macropores; minor amount of intercrystalline micropores, interparticle micropores, and intraparticle micropores.

Reservoir Quality: Poor

Magnification: A: 40X B: 200X

A) Peloid ghosts (C4, D8) and scattered phosphatic shell fragments (E3, E5, DE11) are the most common allochems in this dolomite sample. The irregular boundaries marked by color differences represent the original packstone (light color) and wackestone (dark color) textures.

B) A detailed photograph of a phosphatic shell fragment shows that it has been partially replaced by microcrystalline pyrite (D2) along its lower edge. Note the quartz silt in the wackestone (H7, J15) and the rare intercrystalline pores in the coarser crystalline dolomite in the packstone (DE8.5, C13).

Ohio Division of Geological Survey
CO2 No. 1
Tuscarawas County, Ohio

7692.0'
Plate 50

Weatherford LABORATORIES

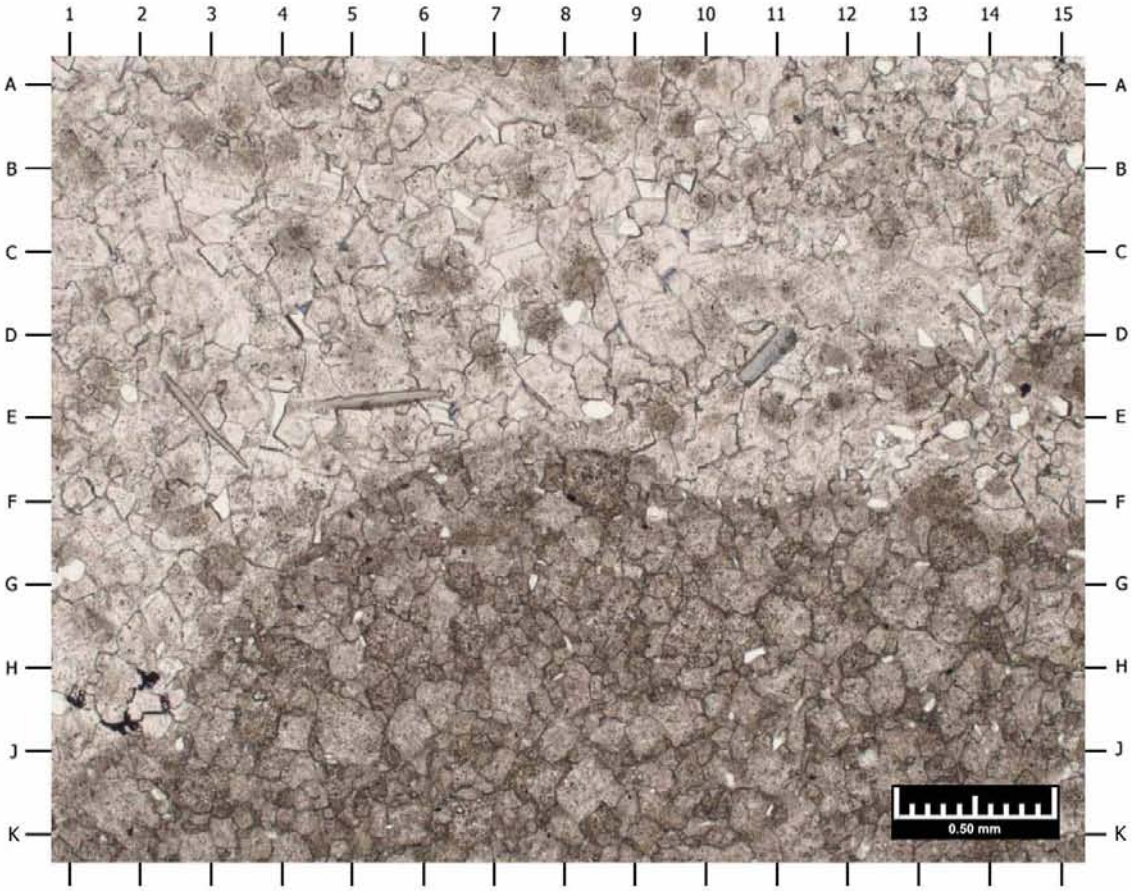

A

40X

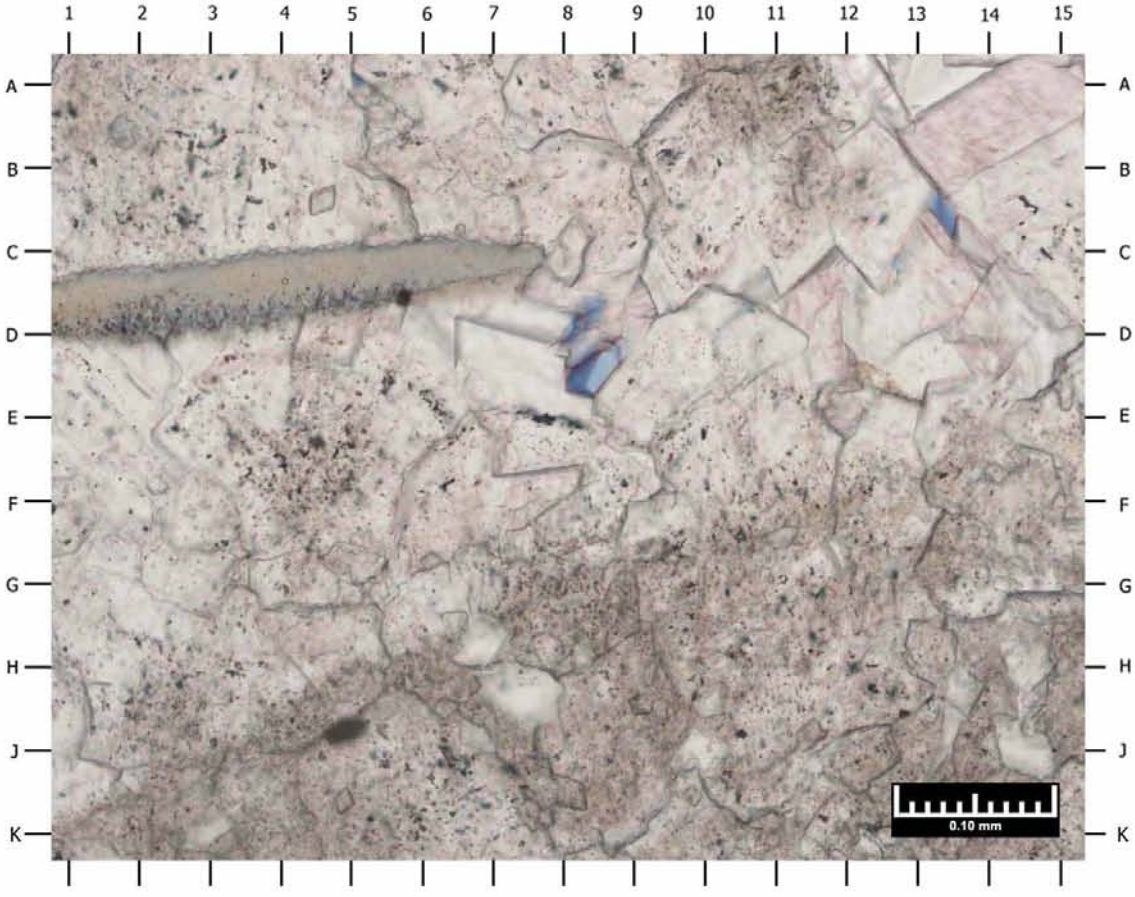

B

200X

Ohio Division of Geological Survey **OMNI File No: HH-38266**
CO_2 No. 1 Well
Tuscarawas County, Ohio
Copper Ridge Dolomite
Rotary Sidewall Core

THIN SECTION PHOTOMICROGRAPHS

SAMPLE DEPTH: 7730.0 FEET
SAMPLE NUMBER: 1-51R

Plate 51

Permeability (Klink.): 0.0001 mD Porosity (NCS): 1.3% Grain Density: 2.83 gm/cc

Sample not selected for petrographic analysis.

Magnification: A: 40X B: 200X

Ohio Division of Geological Survey
CO2 No. 1
Tuscarawas County, Ohio

7730.0'
Plate 51

Weatherford LABORATORIES

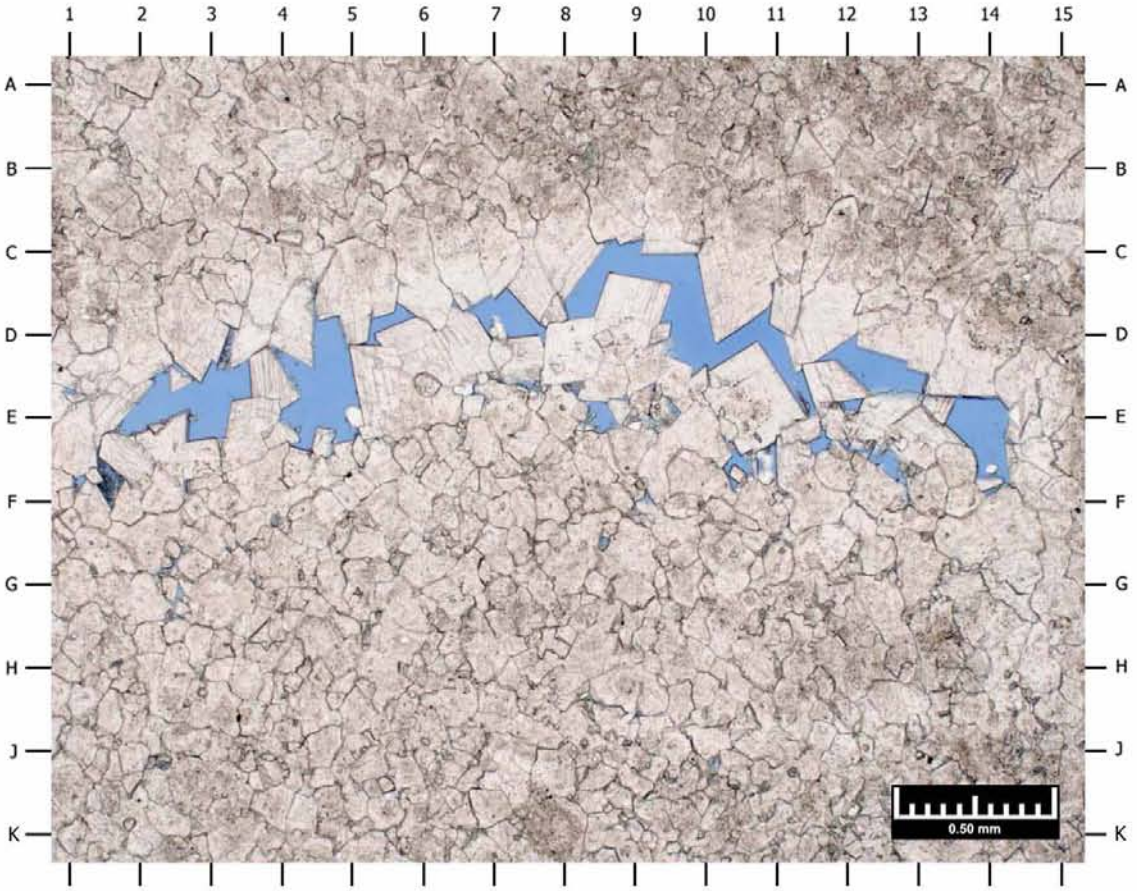

A

40X

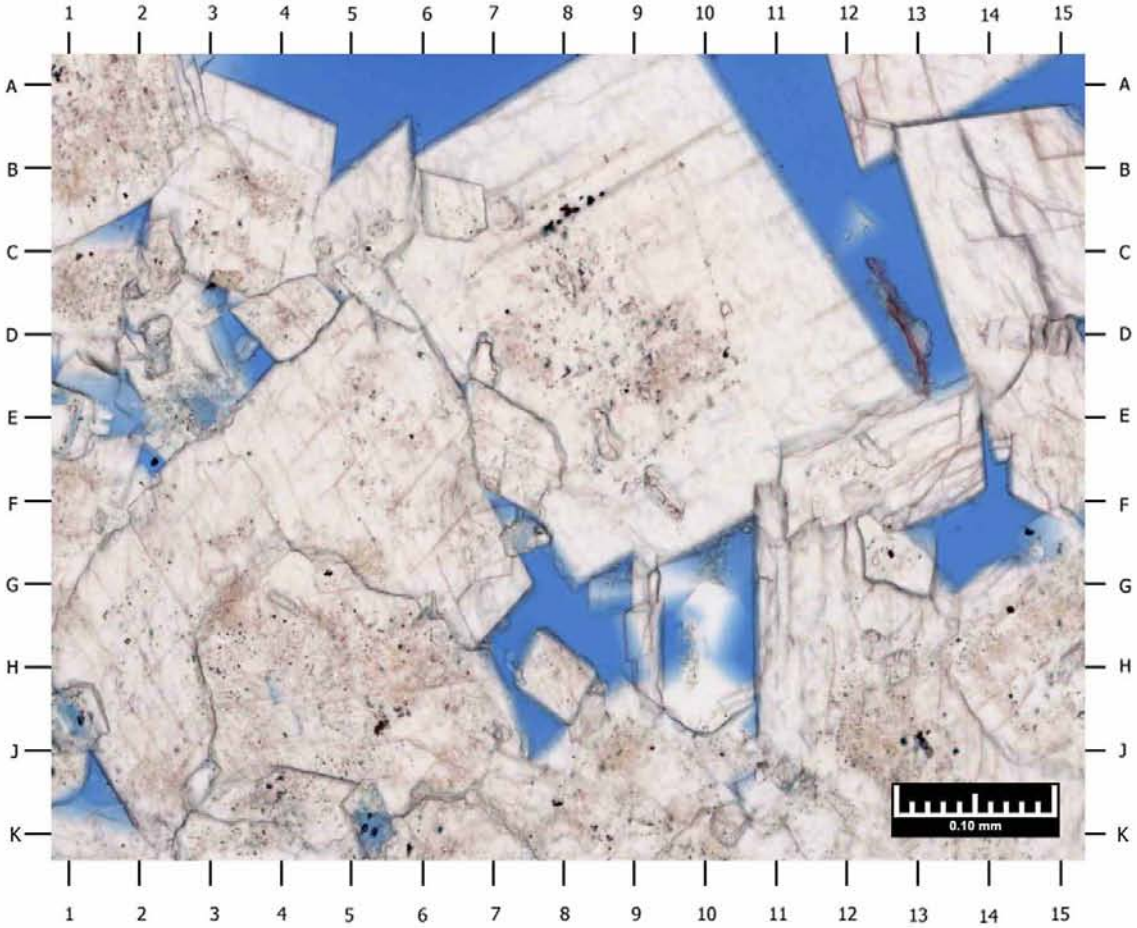

B

200X

Ohio Division of Geological Survey **OMNI File No: HH-38266**
CO_2 No. 1 Well
Tuscarawas County, Ohio
Copper Ridge Dolomite
Rotary Sidewall Core

THIN SECTION PHOTOMICROGRAPHS

SAMPLE DEPTH: 7742.0 FEET
SAMPLE NUMBER: 1-52R

Plate 52

Permeability (Klink.): 0.0004 mD Porosity (NCS): 0.9% Grain Density: 2.81 gm/cc

Sample not selected for petrographic analysis.

Magnification: A: 40X B: 200X

Ohio Division of Geological Survey
CO2 No. 1
Tuscarawas County, Ohio

7742.0'
Plate 52

Weatherford LABORATORIES

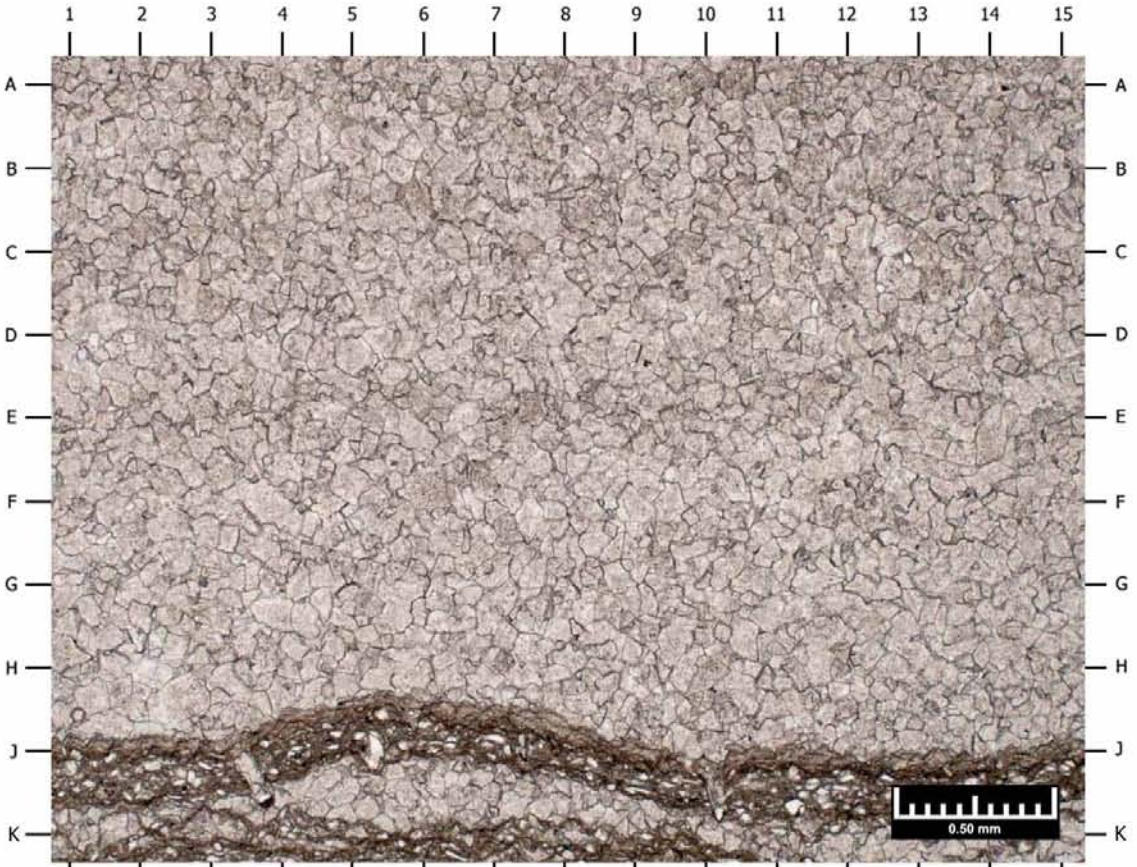

A

40X

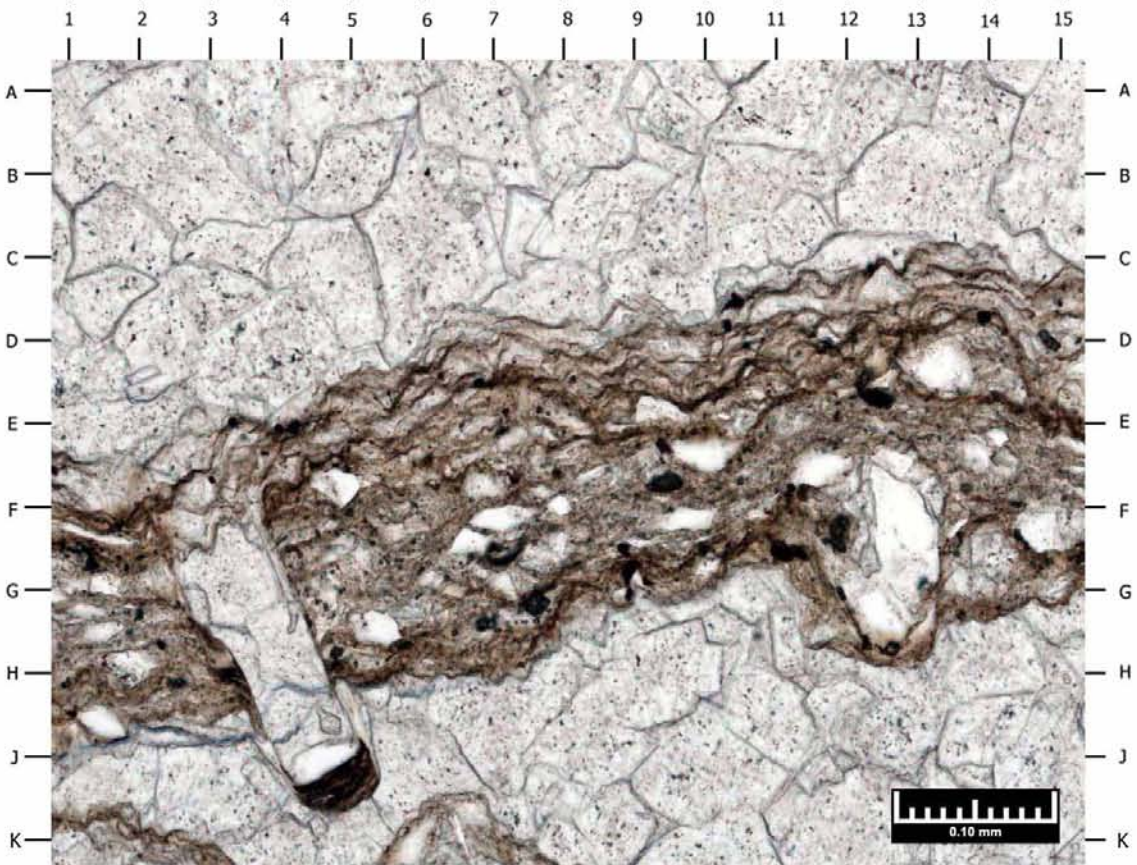

B

200X

Ohio Division of Geological Survey **OMNI File No: HH-38266**
CO_2 No. 1 Well
Tuscarawas County, Ohio
Copper Ridge Dolomite
Rotary Sidewall Core

THIN SECTION PHOTOMICROGRAPHS

SAMPLE DEPTH: 7818.0 FEET
SAMPLE NUMBER: 1-53R

Plate 53

Permeability (Klink.): 0.0011 mD Porosity (NCS): 3.7% Grain Density: 2.86 gm/cc

Sample not selected for petrographic analysis.

Magnification: A: 40X B: 200X

Ohio Division of Geological Survey
CO2 No. 1
Tuscarawas County, Ohio

7818.0'
Plate 53

Weatherford LABORATORIES

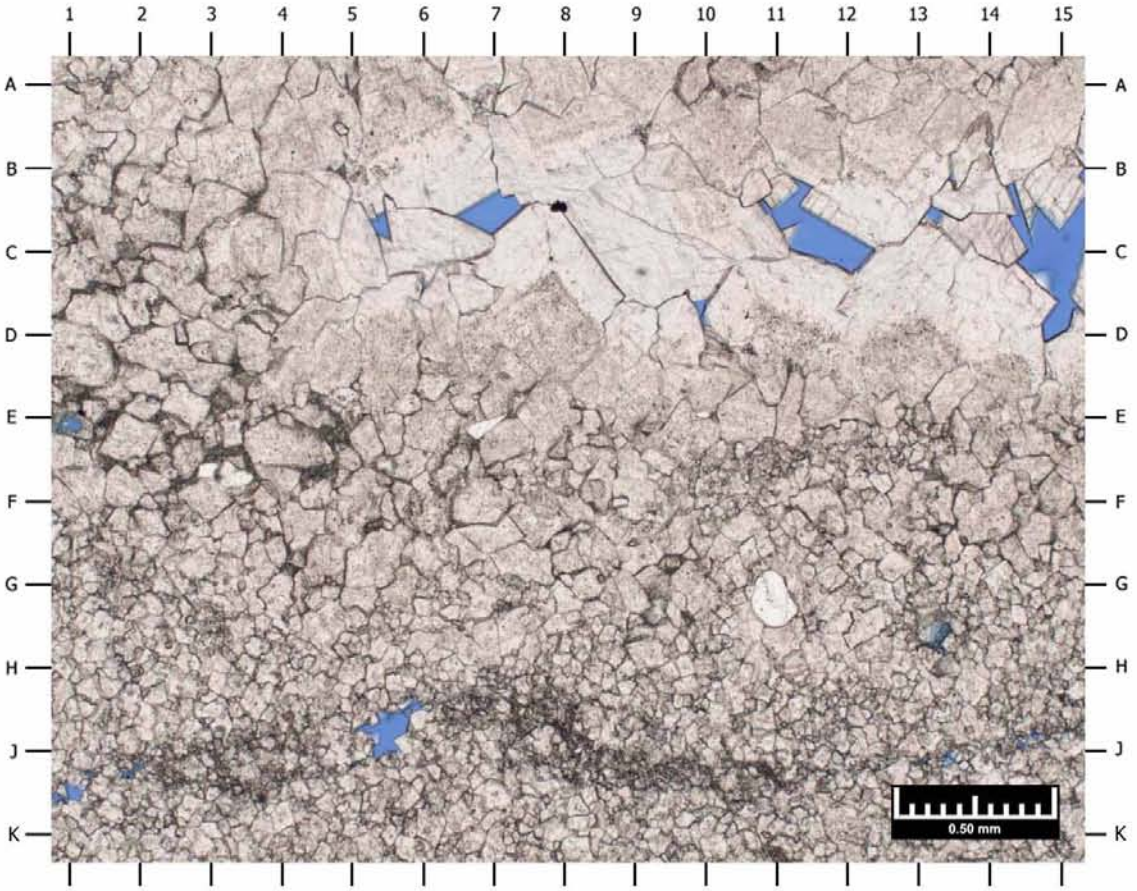

A

40X

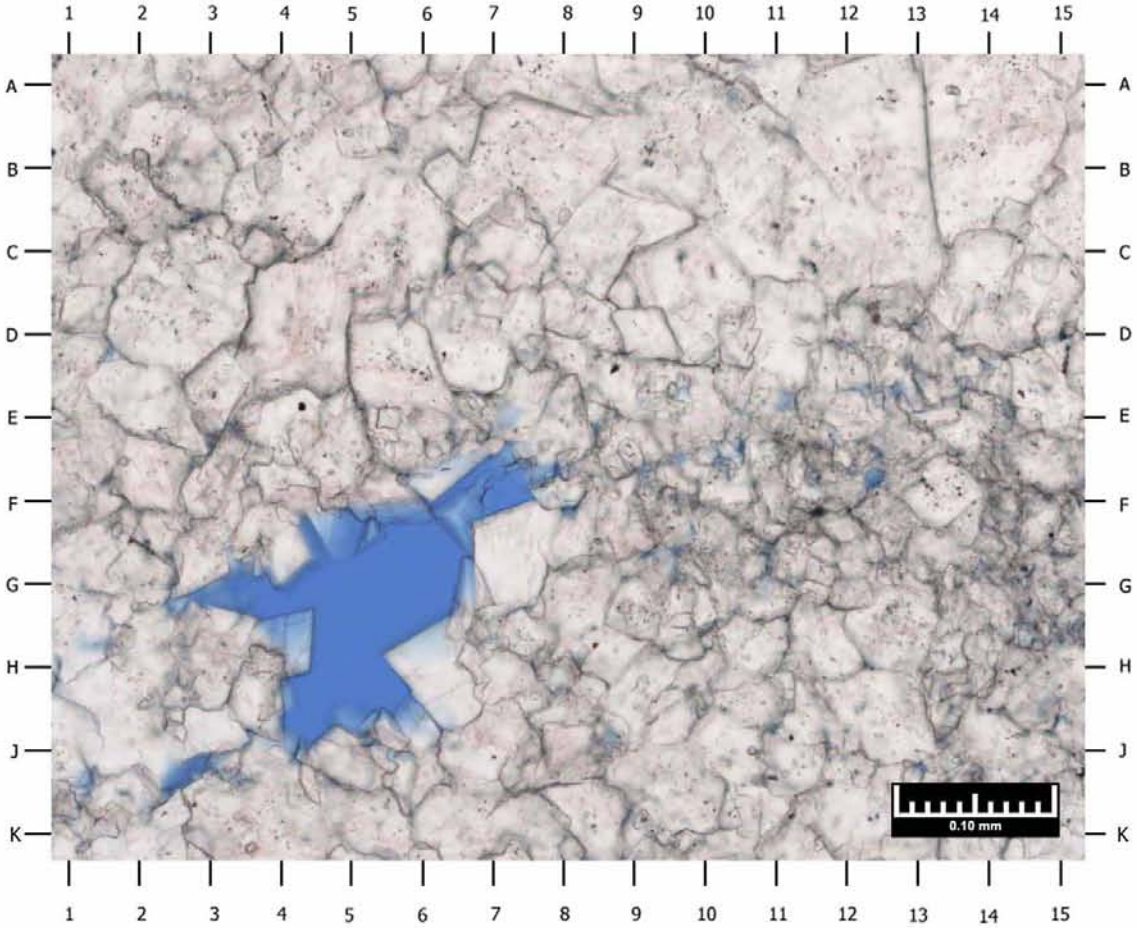

B

200X

Ohio Division of Geological Survey **OMNI File No: HH-38266**
CO_2 No. 1 Well
Tuscarawas County, Ohio
Copper Ridge Dolomite
Rotary Sidewall Core

THIN SECTION PHOTOMICROGRAPHS

SAMPLE DEPTH: 7868.0 FEET
SAMPLE NUMBER: 1-54R

Plate 54

Permeability (Klink.): <0.0001mD Porosity (NCS): 1.8% Grain Density: 2.84 gm/cc

Sample not selected for petrographic analysis.

Magnification: A: 40X B: 200X

Ohio Division of Geological Survey
CO2 No. 1
Tuscarawas County, Ohio

7868.0'
Plate 54

Weatherford LABORATORIES

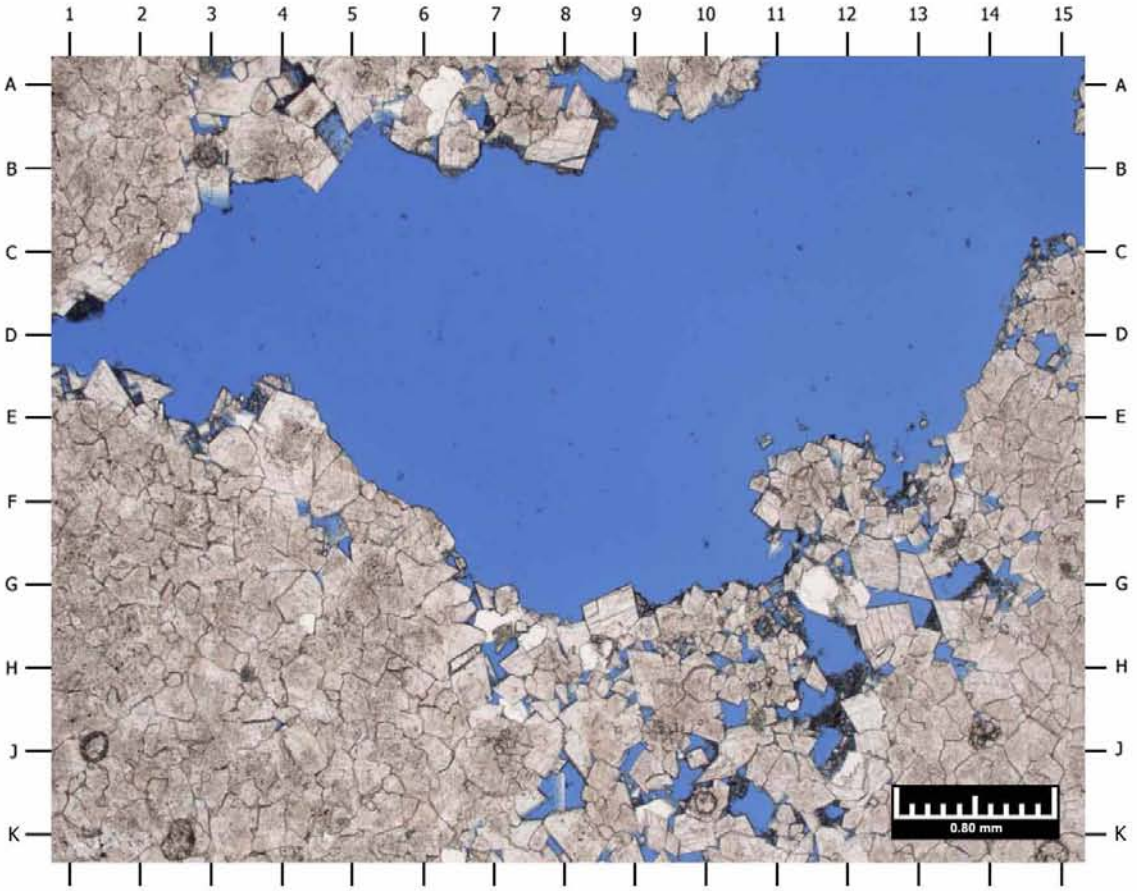

A

25X

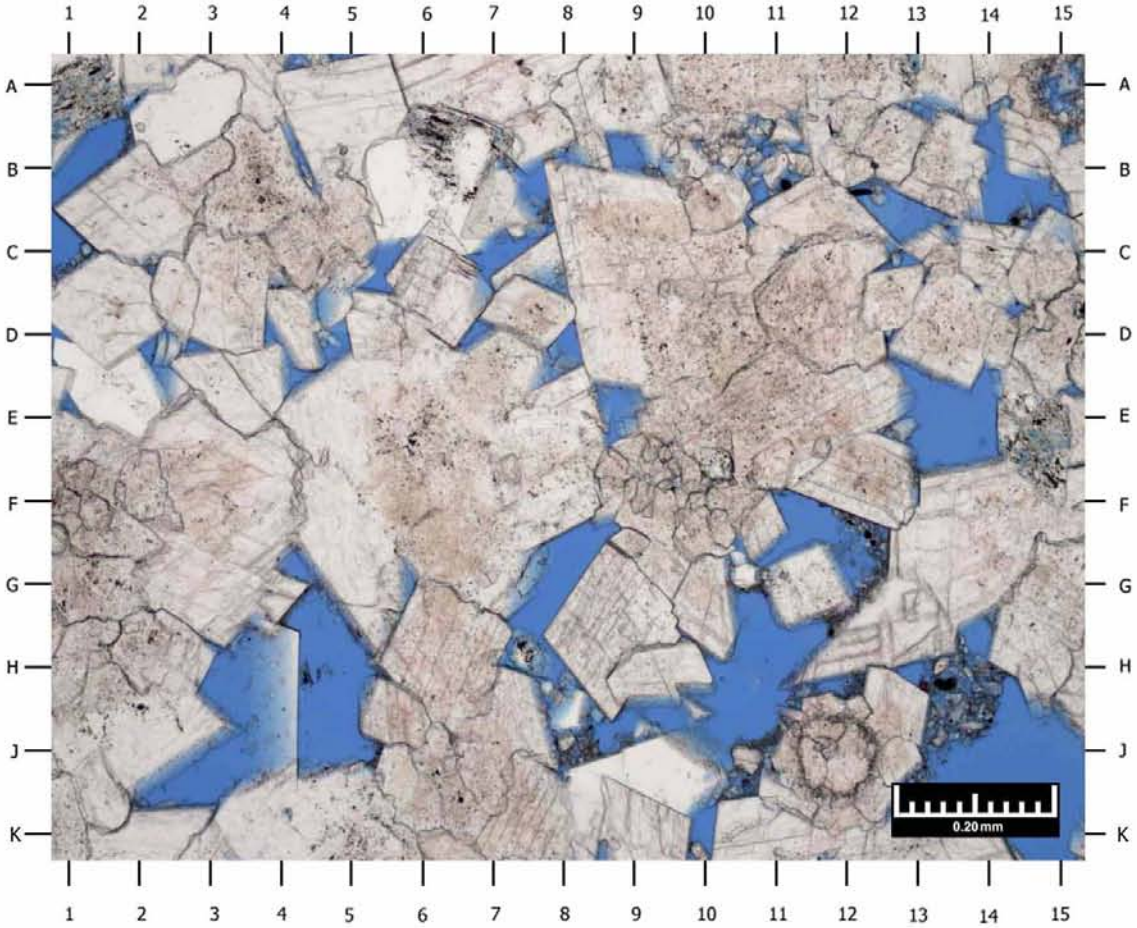

B

100X

Ohio Division of Geological Survey **OMNI File No: HH-38266**
CO_2 No. 1 Well
Tuscarawas County, Ohio
Conasauga group
Rotary Sidewall Core

THIN SECTION PHOTOMICROGRAPHS

SAMPLE DEPTH: 7931.0 FEET
SAMPLE NUMBER: 1-55R

Plate 55

Permeability (Klink.): 0.0007 mD Porosity (NCS): 1.0% Grain Density: 2.82 gm/cc

Sample not selected for petrographic analysis.

Magnification: A: 40X B: 200X

Ohio Division of Geological Survey
CO2 No. 1
Tuscarawas County, Ohio

7931.0'
Plate 55

Weatherford LABORATORIES

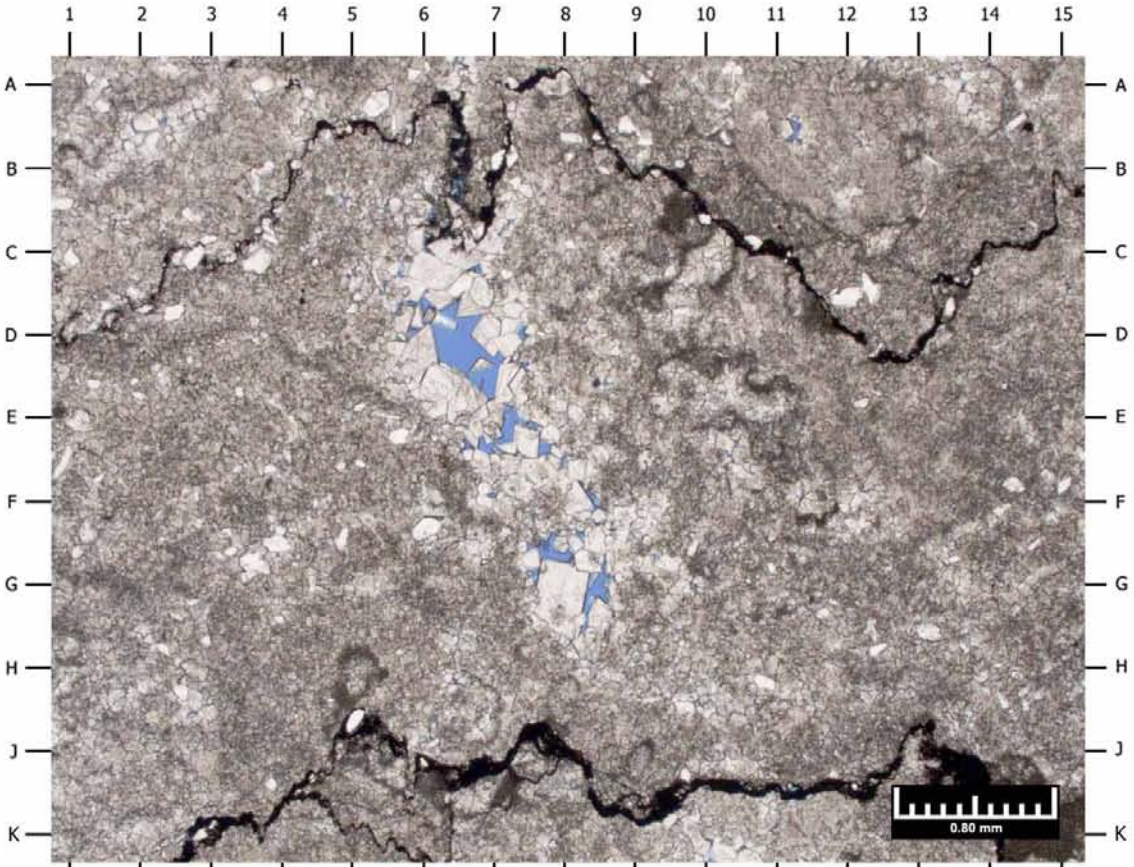

A

25X

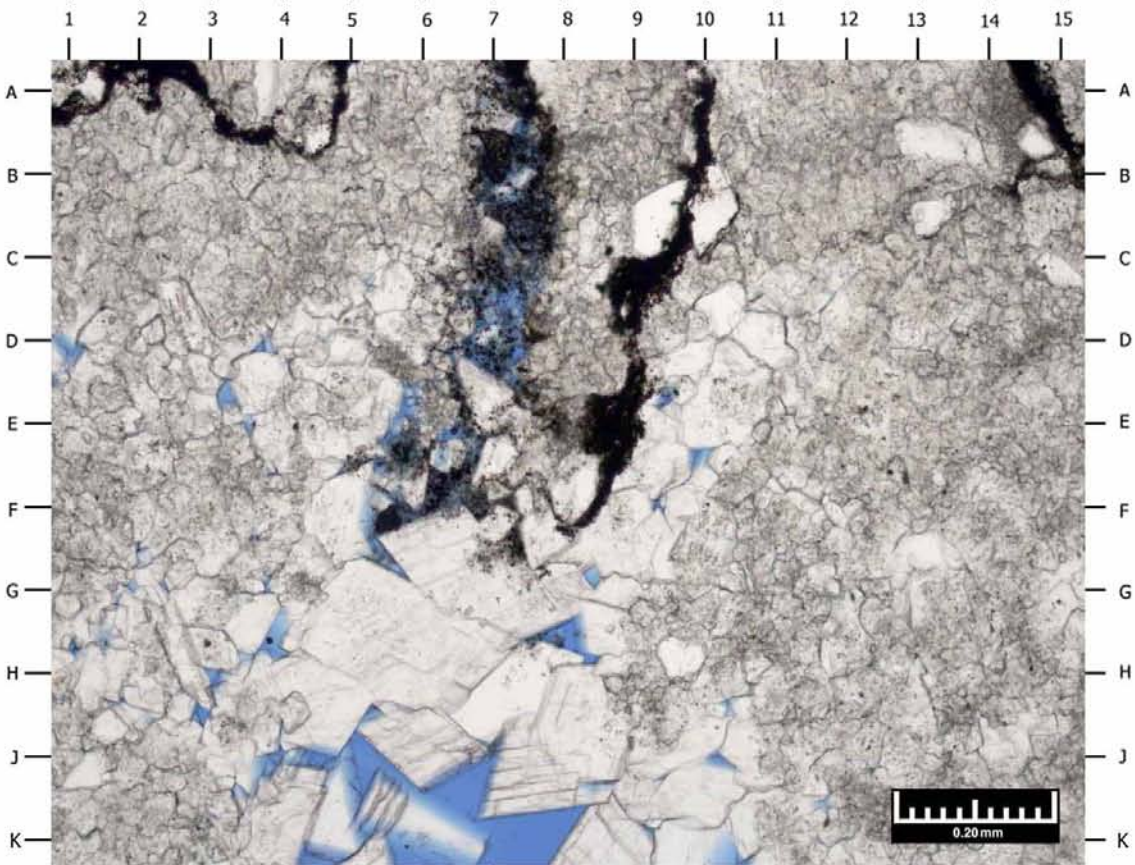

B

100X

Ohio Division of Geological Survey **OMNI File No: HH-38266**
CO_2 No. 1 Well
Tuscarawas County, Ohio
Conasauga group
Rotary Sidewall Core

THIN SECTION PHOTOMICROGRAPHS

SAMPLE DEPTH: 7991.0 FEET
SAMPLE NUMBER: 1-56R

Plate 56

Permeability (Klink.): 0.0016 mD Porosity (NCS): 1.6% Grain Density: 2.84 gm/cc

Sample not selected for petrographic analysis.

Magnification: A: 40X B: 200X

Ohio Division of Geological Survey
CO2 No. 1
Tuscarawas County, Ohio

7991.0'
Plate 56

Weatherford LABORATORIES

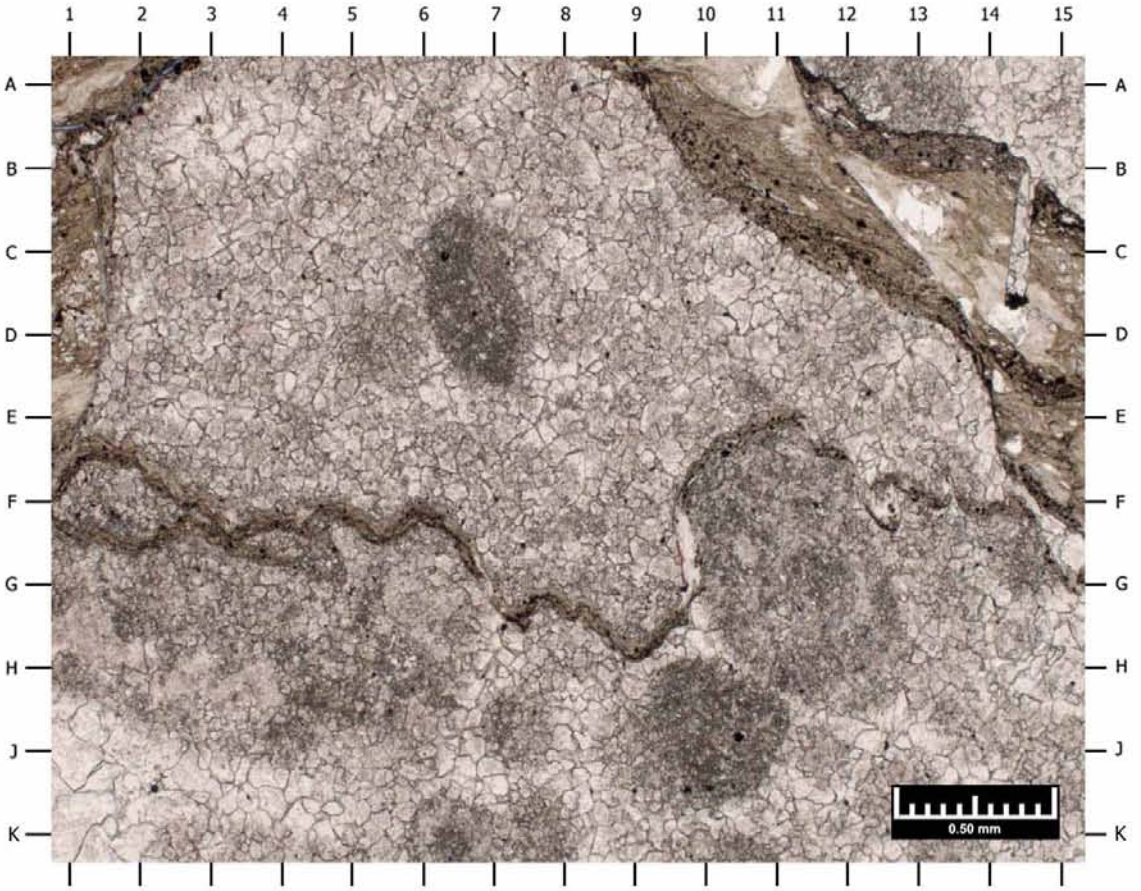

A

40X

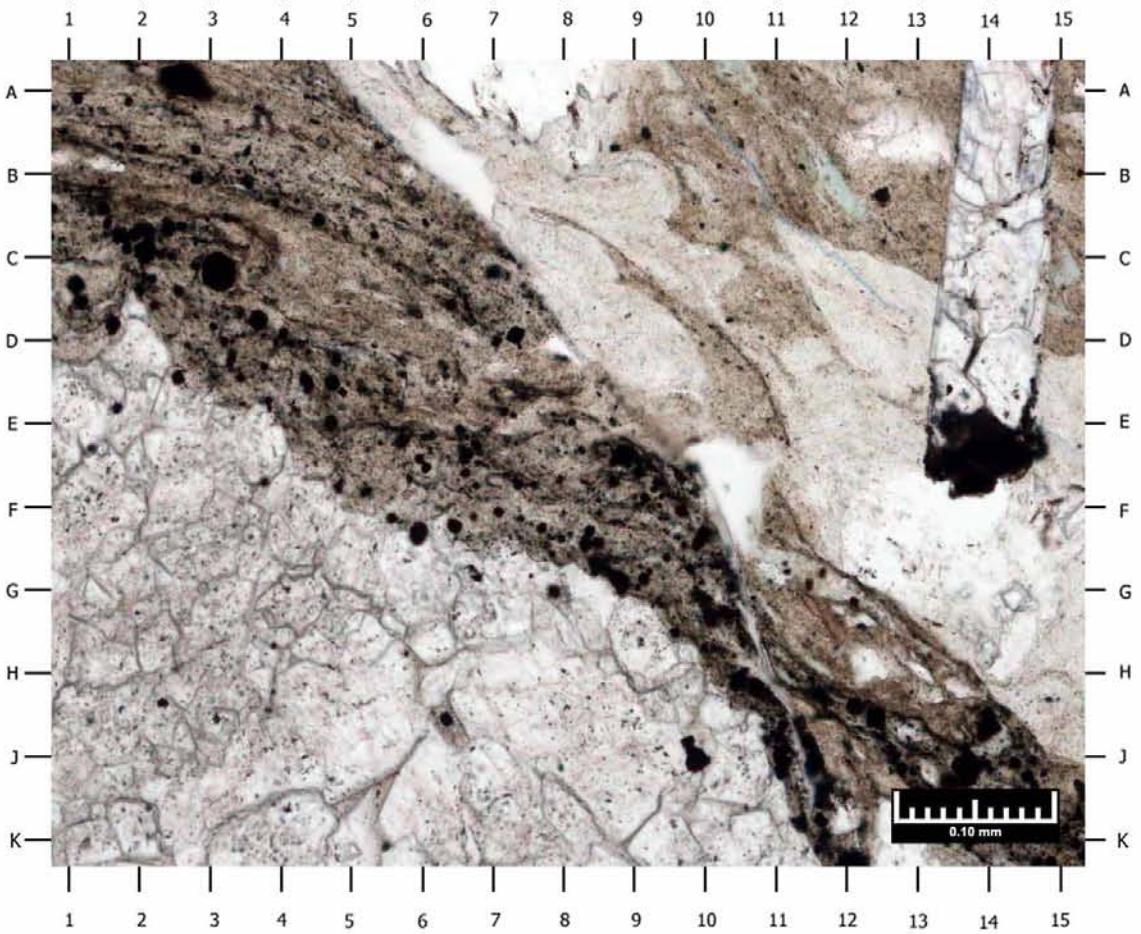

B

200X

Ohio Division of Geological Survey **OMNI File No: HH-38266**
CO_2 No. 1 Well
Tuscarawas County, Ohio
Conasauga group
Rotary Sidewall Core

THIN SECTION PHOTOMICROGRAPHS

SAMPLE DEPTH: 8014.0 FEET
SAMPLE NUMBER: 1-57R

Plate 57

Permeability (Klink.): 0.0029 mD Porosity (NCS): 1.4% Grain Density: 2.82 gm/cc

Sample not selected for petrographic analysis.

Magnification: A: 40X B: 200X

Ohio Division of Geological Survey
CO2 No. 1
Tuscarawas County, Ohio

8014.0'
Plate 57

Weatherford LABORATORIES

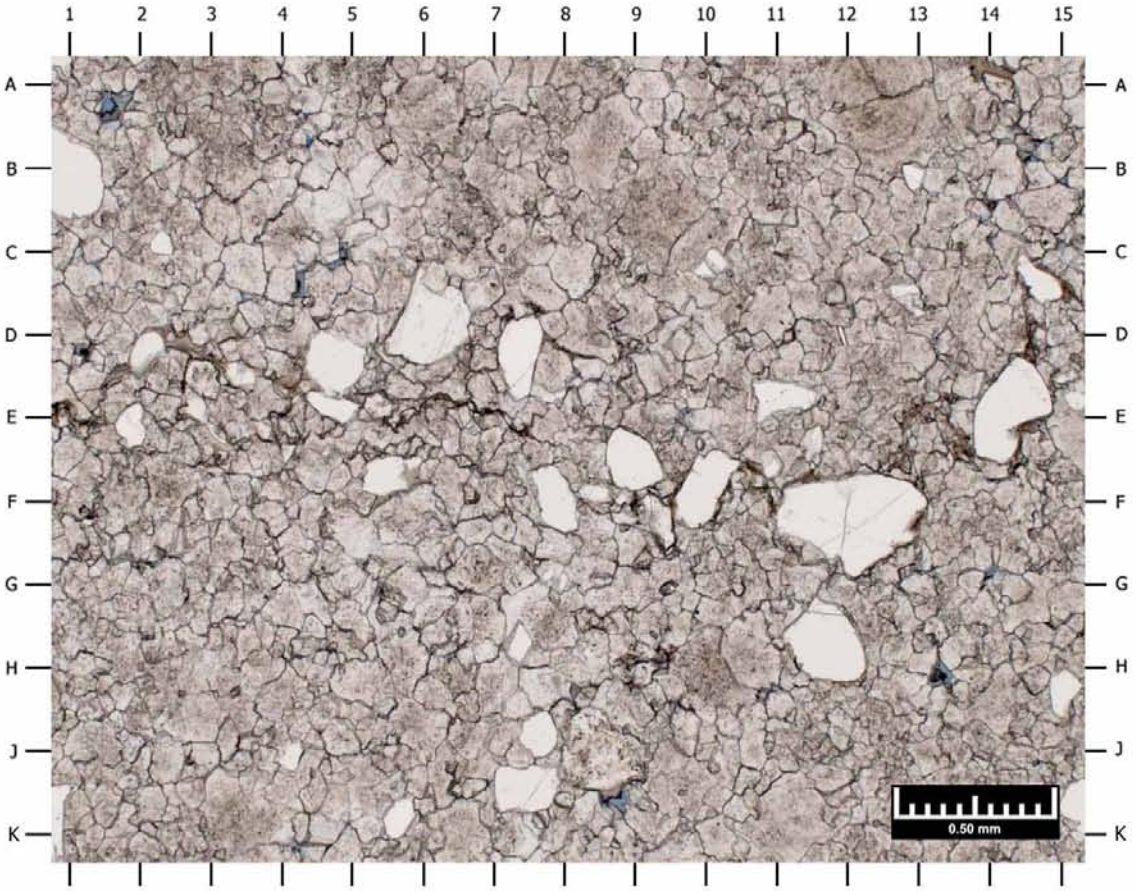

A

40X

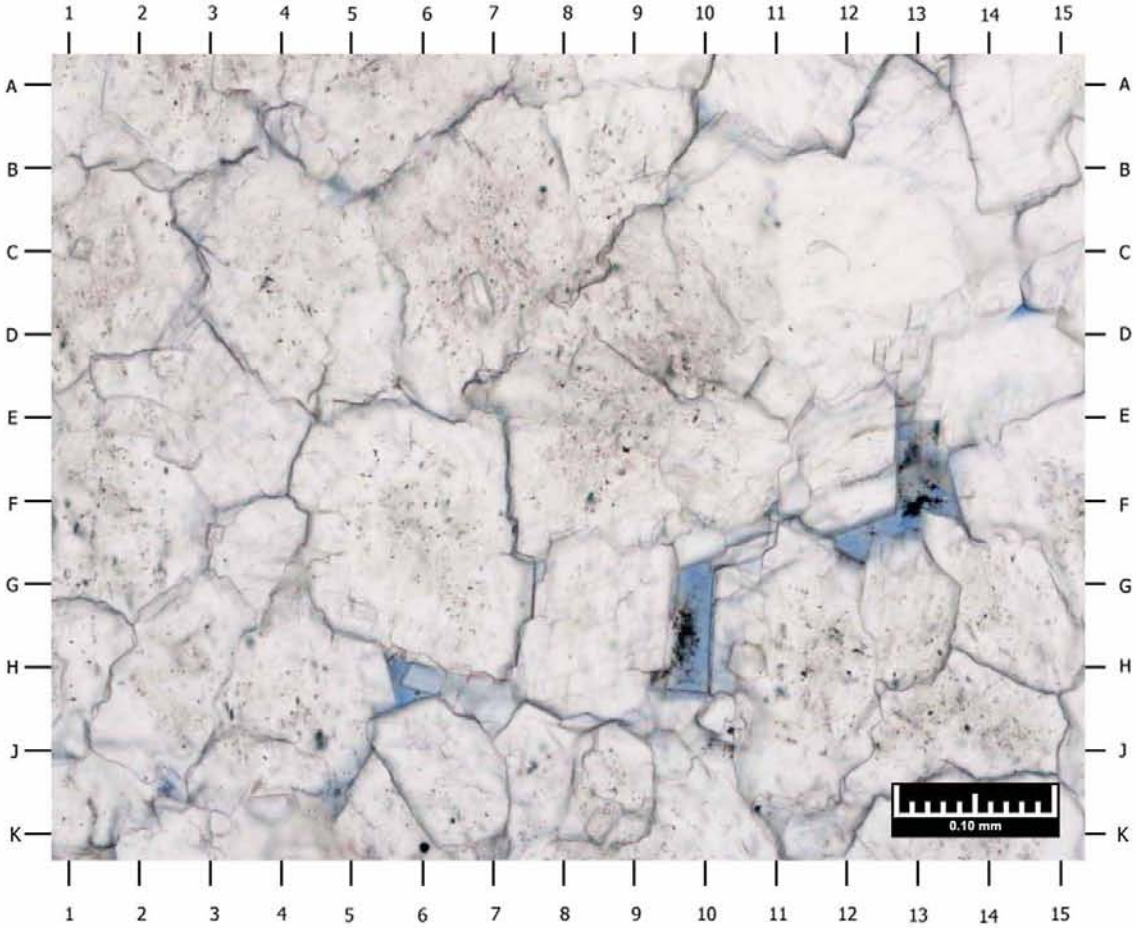

B

200X

Ohio Division of Geological Survey **OMNI File No: HH-38266**
CO_2 No. 1 Well
Tuscarawas County, Ohio
Conasauga group
Rotary Sidewall Core

THIN SECTION PHOTOMICROGRAPHS

SAMPLE DEPTH: 8066.0 FEET
SAMPLE NUMBER: 1-58R

Plate 58

Permeability (Klink.): 0.027 Porosity (ambient): 4.7% Grain Density: 2.84 gm/cc

Sample not selected for petrographic analysis.

Magnification: A: 40X B: 200X

Ohio Division of Geological Survey
CO2 No. 1
Tuscarawas County, Ohio

8066.0'
Plate 58

Weatherford LABORATORIES

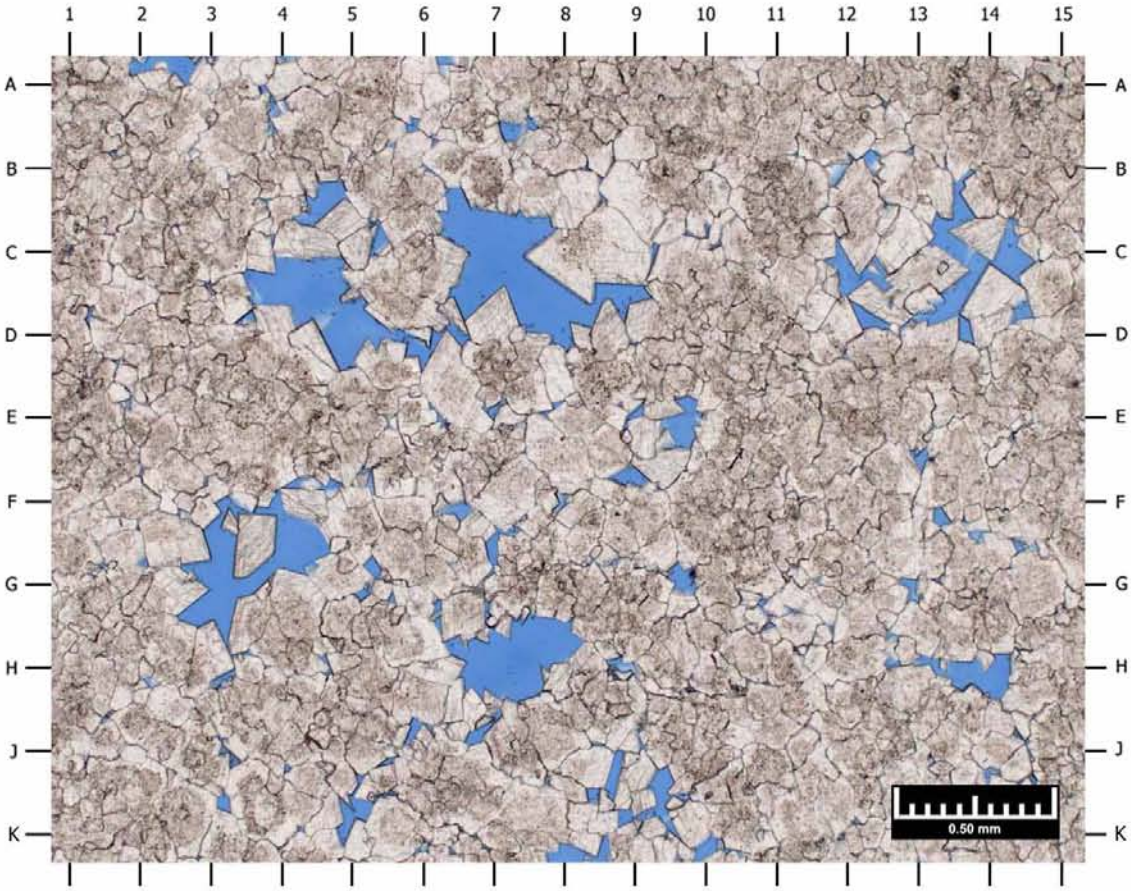

A

40X

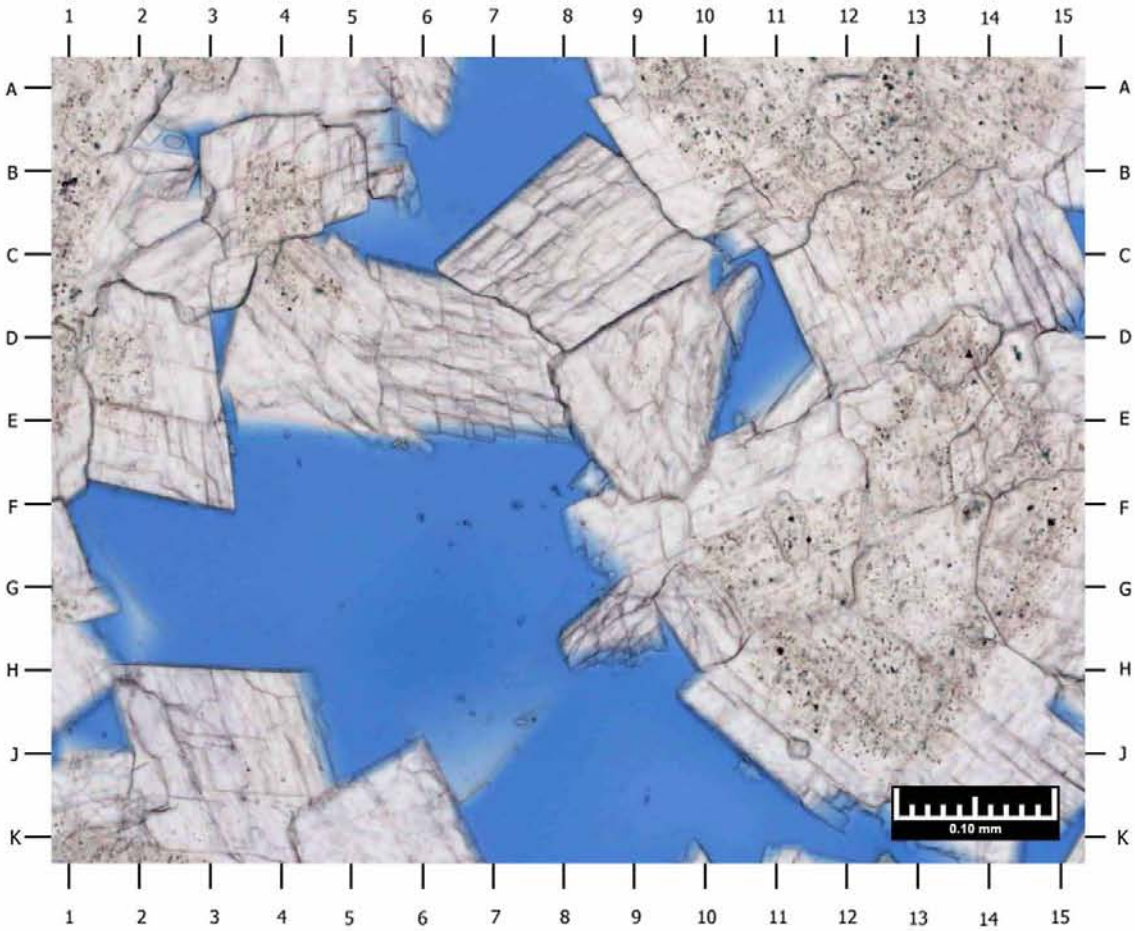

B

200X

Ohio Division of Geological Survey **OMNI File No: HH-38266**
CO_2 No. 1 Well
Tuscarawas County, Ohio
Conasauga group
Rotary Sidewall Core

THIN SECTION PHOTOMICROGRAPHS

SAMPLE DEPTH: 8138.0 FEET
SAMPLE NUMBER: 1-59R

Plate 59

Permeability (Klink.): <0.0001 mD Porosity (NCS): 1.3% Grain Density: 2.84 gm/cc

Sample not selected for petrographic analysis.

Magnification: A: 40X B: 200X

Ohio Division of Geological Survey
CO2 No. 1
Tuscarawas County, Ohio

8138.0'
Plate 59

Weatherford LABORATORIES

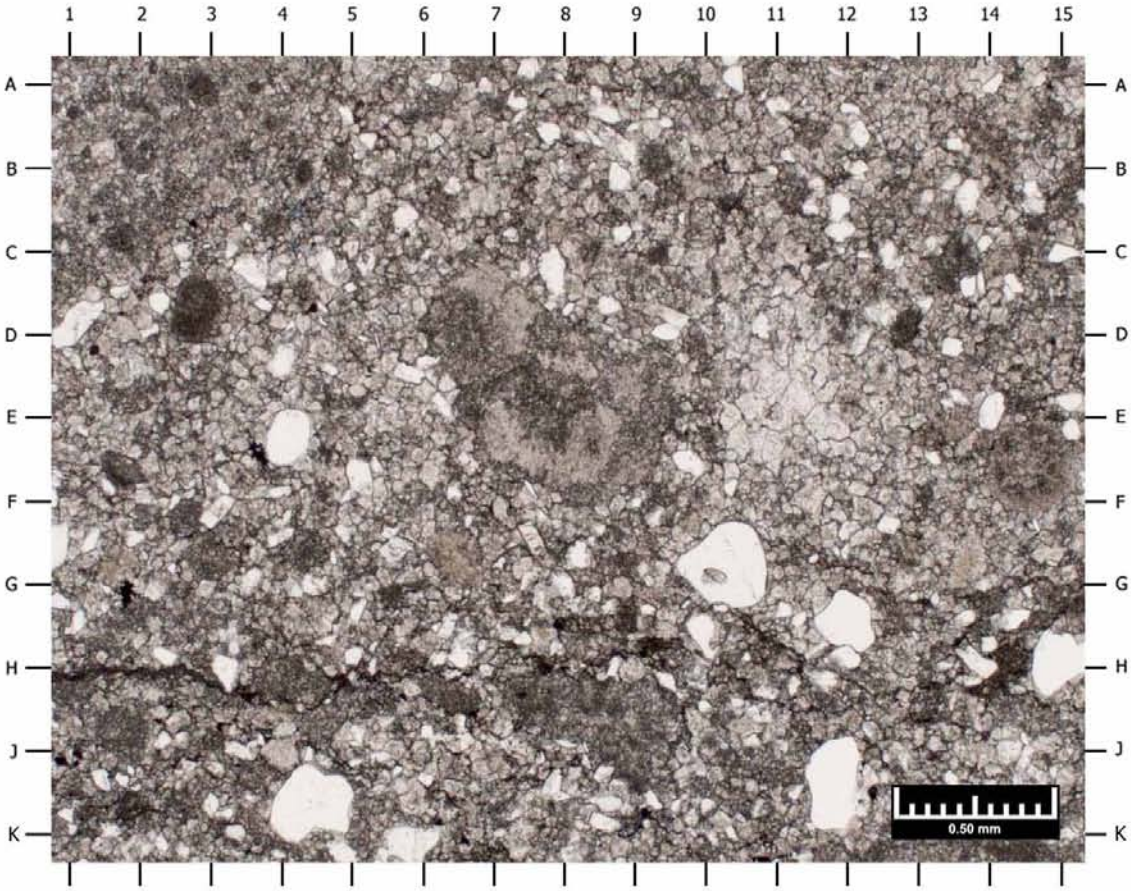

A

40X

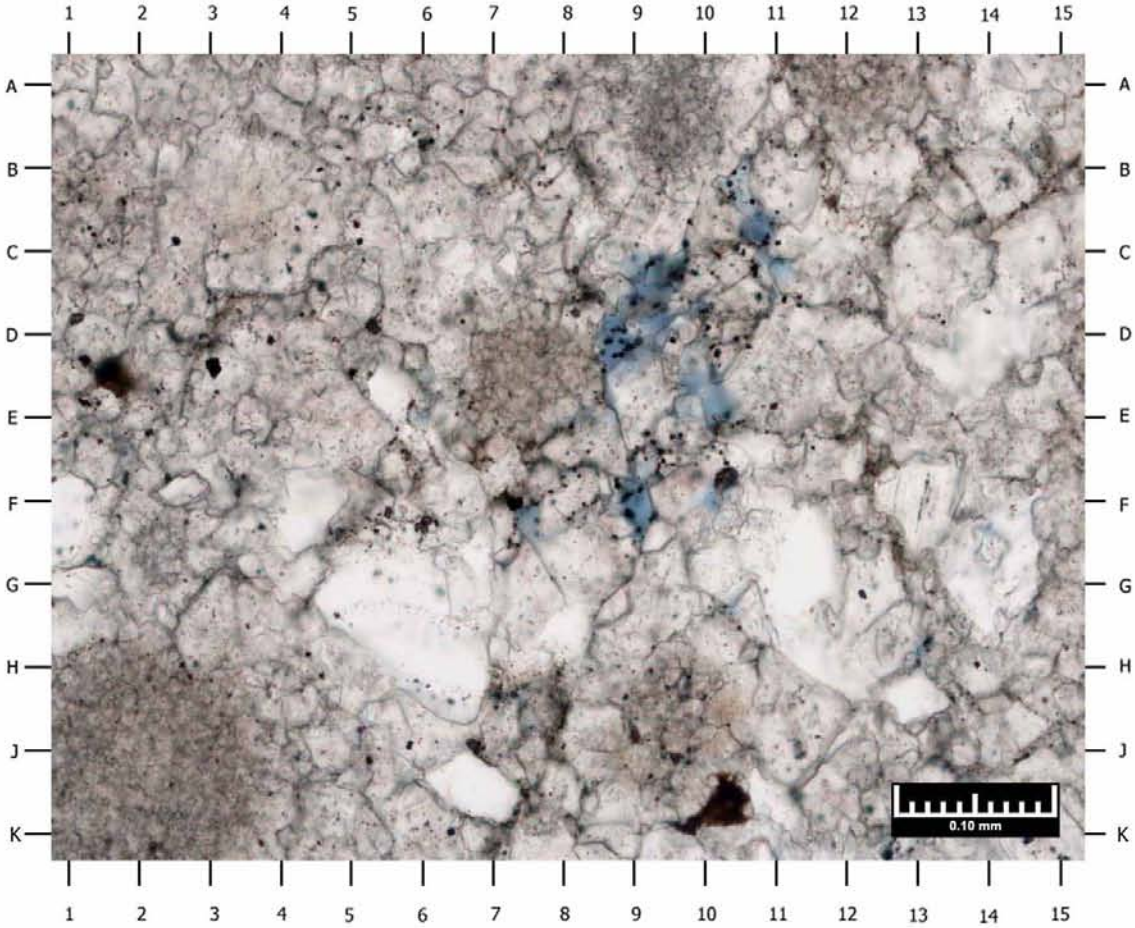

B

200X

Ohio Division of Geological Survey **OMNI File No: HH-38266**
CO_2 No. 1 Well
Tuscarawas County, Ohio
Conasauga group
Rotary Sidewall Core

THIN SECTION PHOTOMICROGRAPHS

SAMPLE DEPTH: 8138.0 FEET
SAMPLE NUMBER: 1-60R

Plate 60

Permeability (Klink.): <0.0001 mD Porosity (NCS): 0.6% Grain Density: 2.85 gm/cc

Sample not selected for petrographic analysis.

Magnification: A: 40X B: 200X

Ohio Division of Geological Survey
CO2 No. 1
Tuscarawas County, Ohio

8176.0'
Plate 60

Weatherford LABORATORIES

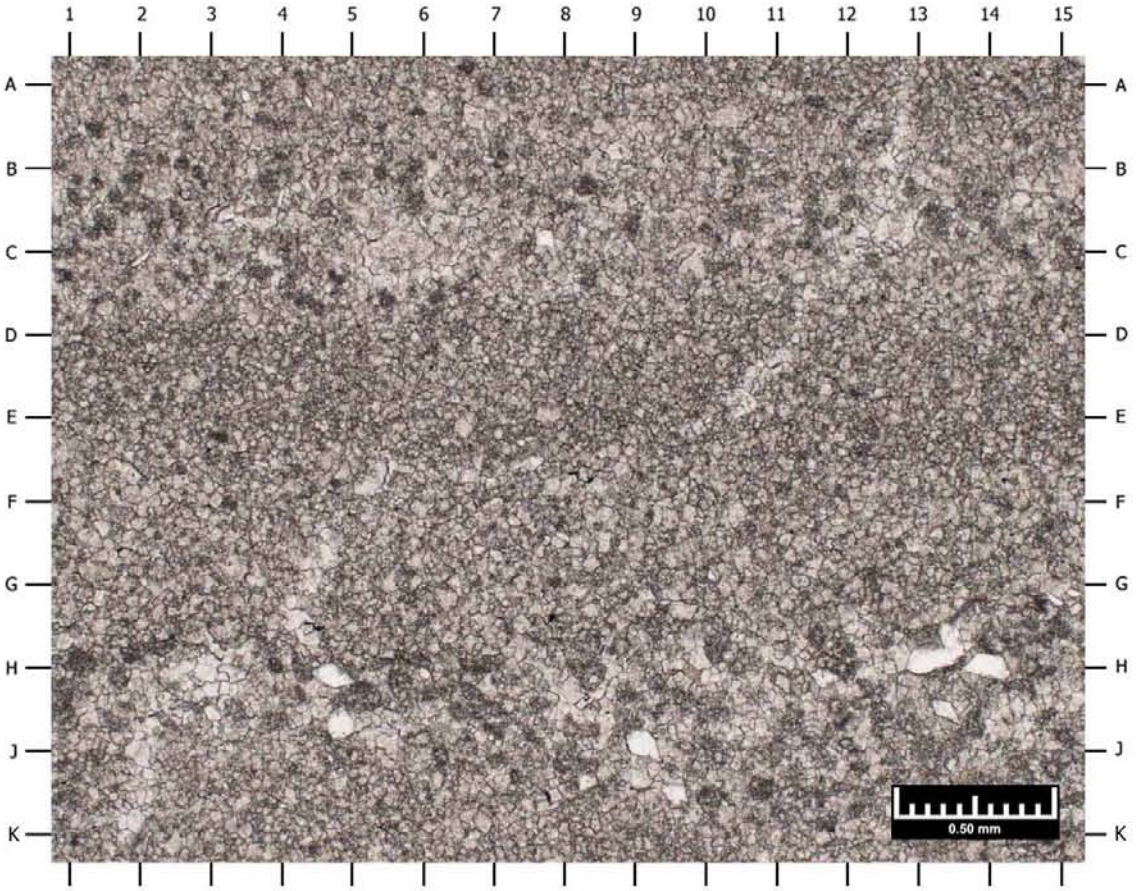

A

40X

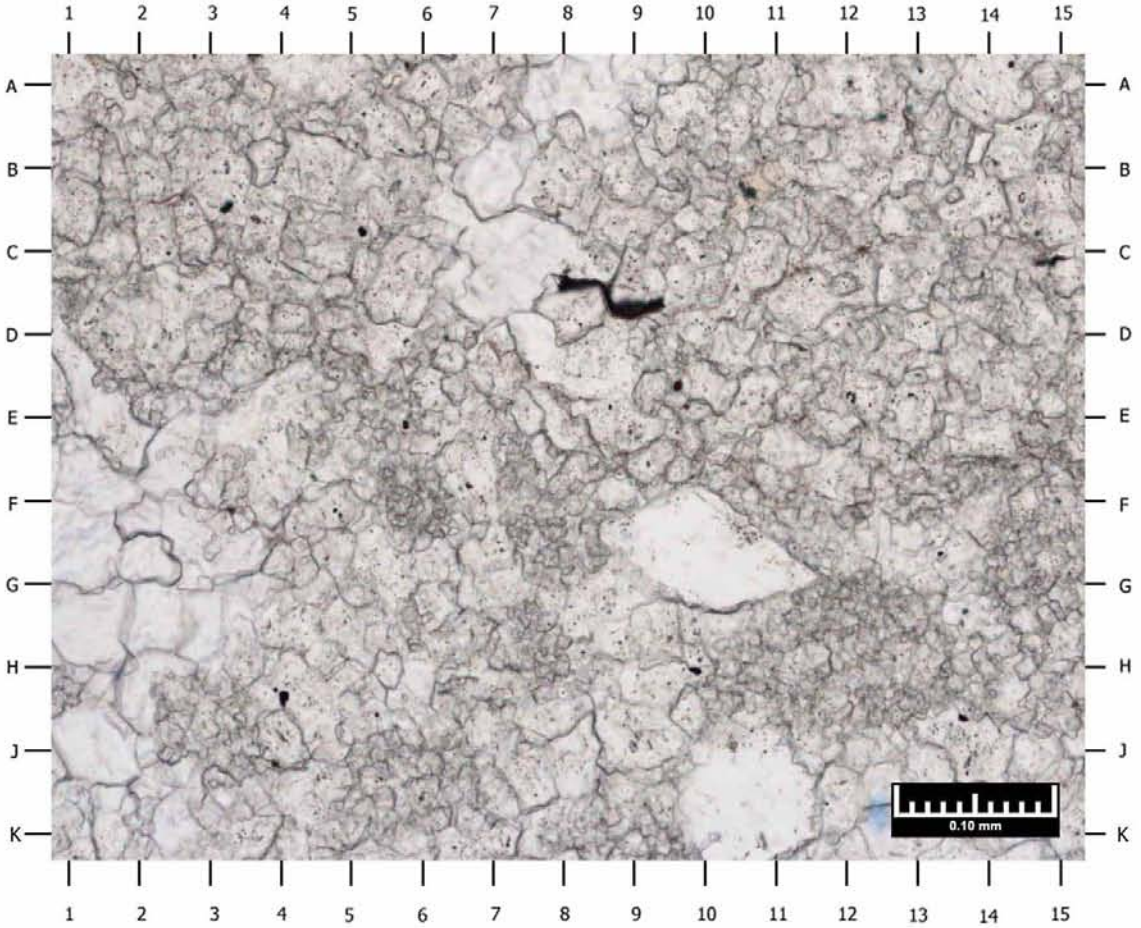

B

200X

Ohio Division of Geological Survey **OMNI File No: HH-38266**
CO_2 No. 1 Well
Tuscarawas County, Ohio
Conasauga group
Rotary Sidewall Core

THIN SECTION DESCRIPTION -- GENERAL

SAMPLE DEPTH: 8274.0 FEET
SAMPLE NUMBER: 1-61R

Plate 61

Permeability (Klink.): <0.0001 mD Porosity (NCS): 0.5% Grain Density: 2.84 gm/cc

Lithology: Dolomite breccia

Texture: Dolomite overprints original fabric (possible packstone / wackestone); vague organic-rich laminations with incipient microstylolites; possible burrow traces in original fabric; post-dolomitization fracturing / brecciation resulted in subangular fragments and fracture voids that were reduced by internal sedimentation, dolomite cement, and very rare, late-stage calcite cement

Framework Grains: Original allochems difficult to recognize due to dolomitization overprint; very rare ghost allochems (undifferentiated); trace amount of fine organic debris and clay, especially concentrated along incipient microstylolites; trace amount of scattered silt-sized and sand-sized quartz

Matrix: Trace matrix clay; original limestone matrix unknown due to dolomitization

Cements and Replacement Minerals: All original fabric and allochems completely replaced by fine crystalline, subhedral to euhedral dolomite; minor amount of microcrystalline pyrite replacement; fracture filling dolomite and rare calcite

Pore System: No visible macropores; minor amount of fracture pores and intercrystalline micropores

Reservoir Quality: Poor

Magnification: A: 40X B: 200X

A) This brecciated dolomite contains healed fractures (A1) and fracture voids filled with internal sediment (H-K 1-3). Post-brecciation stylolites (E1 to D10) have concentrations of insoluble material. Large voids are partially reduced by dolomite (BC14).

B) Late-stage calcite (stained red; D7) and pyrite (AB12) further reduce breccia voids. Note the slightly curved crystals in the last stage of dolomite fill, indicating it is baroque dolomite (B13).

Ohio Division of Geological Survey
CO2 No. 1
Tuscarawas County, Ohio

8274.0'
Plate 61

Weatherford LABORATORIES

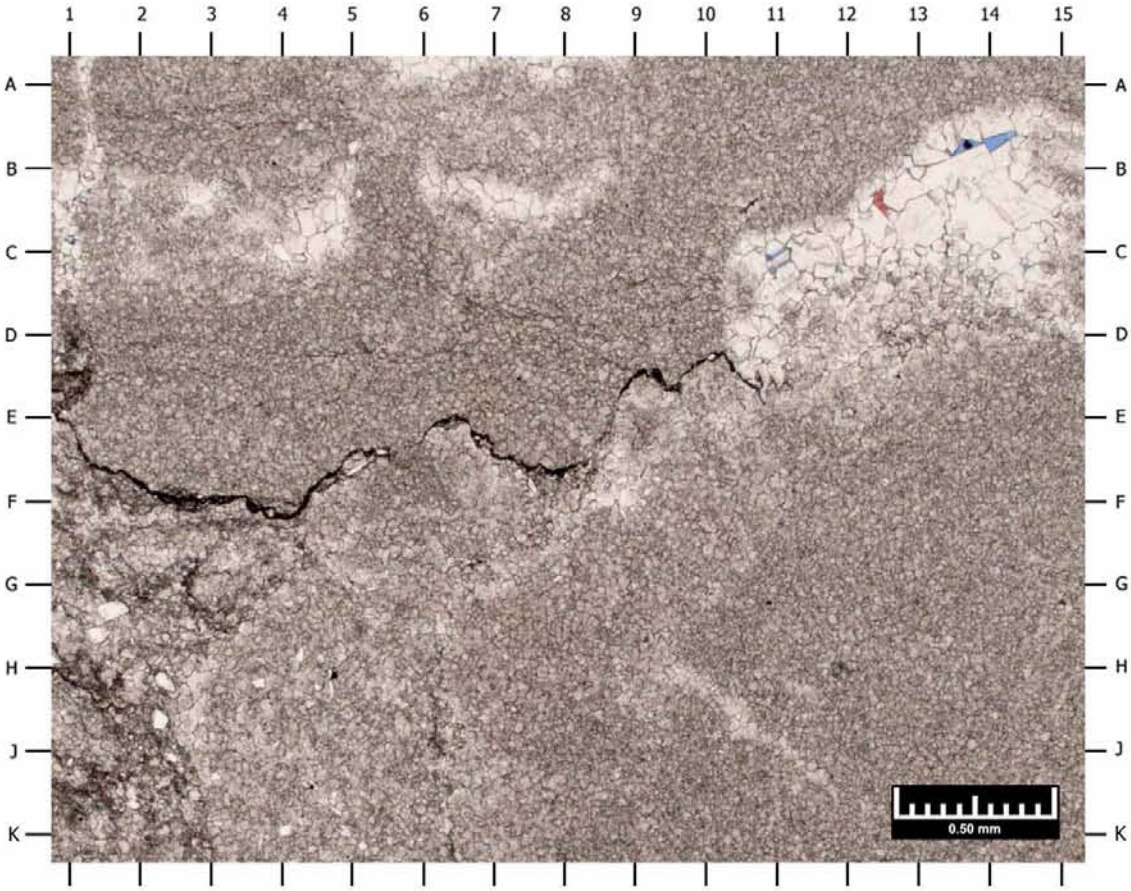

A

40X

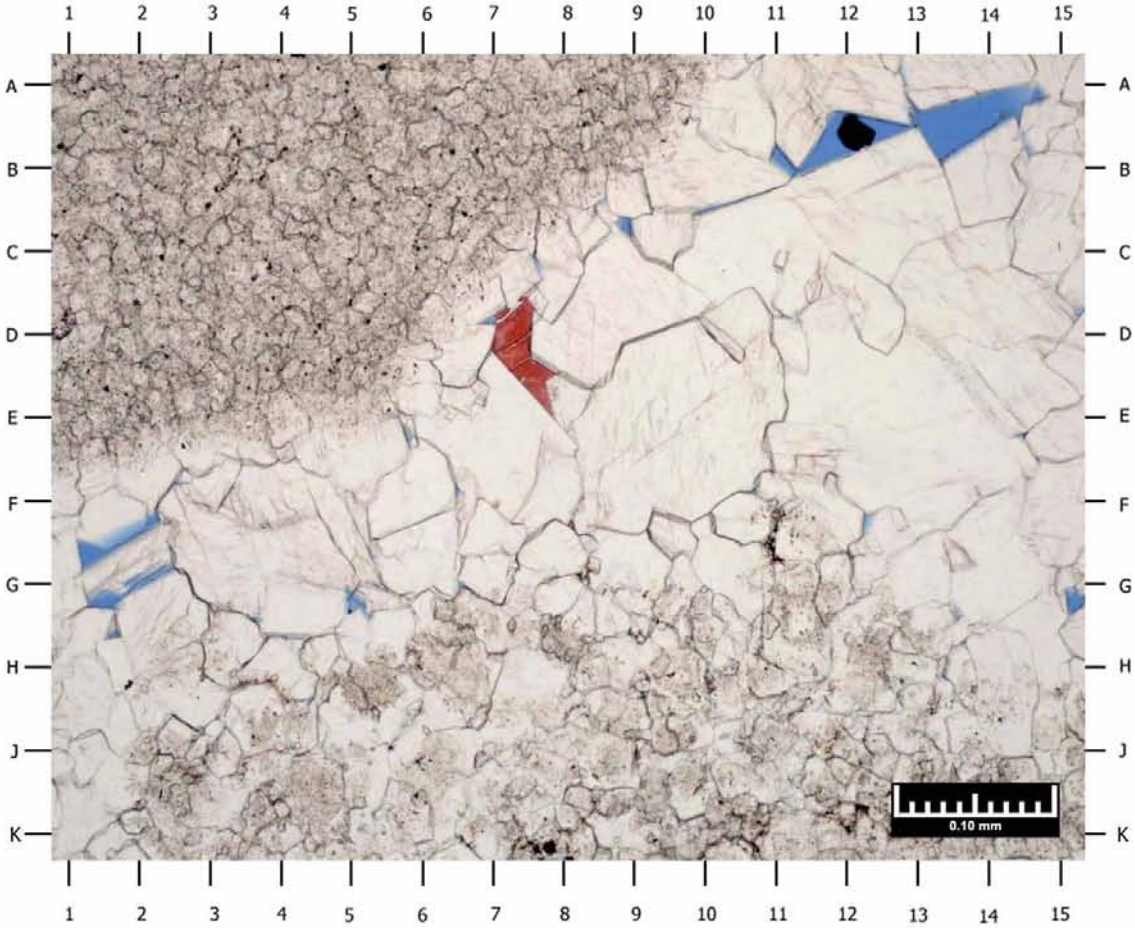

B

200X

Ohio Division of Geological Survey **OMNI File No: HH-38266**
CO_2 No. 1 Well
Tuscarawas County, Ohio
Conasauga group
Rotary Sidewall Core

THIN SECTION PHOTOMICROGRAPHS

SAMPLE DEPTH: 8350.0 FEET
SAMPLE NUMBER: 1-62R

Plate 62

Permeability (Klink.): 0.0001 mD Porosity (NCS): 0.4% Grain Density: 2.85 gm/cc

Sample not selected for petrographic analysis.

Magnification: A: 40X B: 200X

Ohio Division of Geological Survey
CO2 No. 1
Tuscarawas County, Ohio

8350.0'
Plate 62

Weatherford LABORATORIES

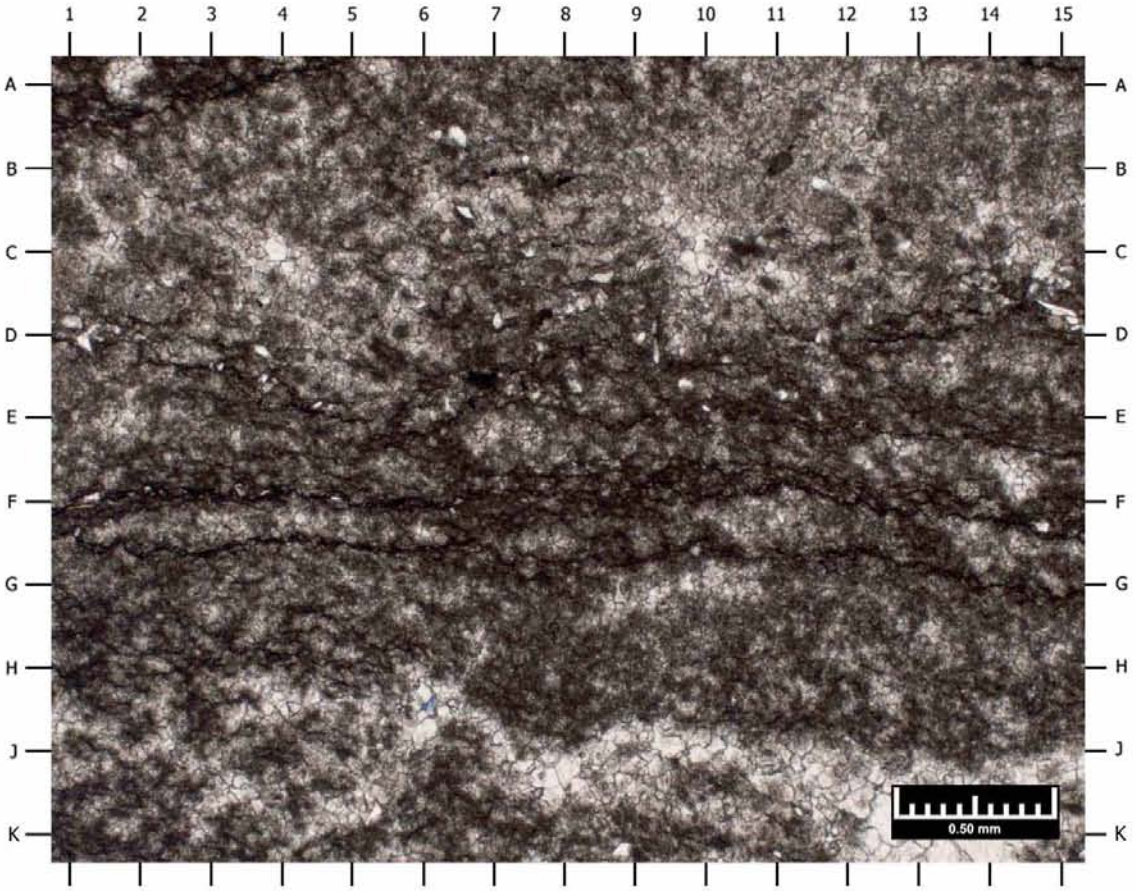

A

40X

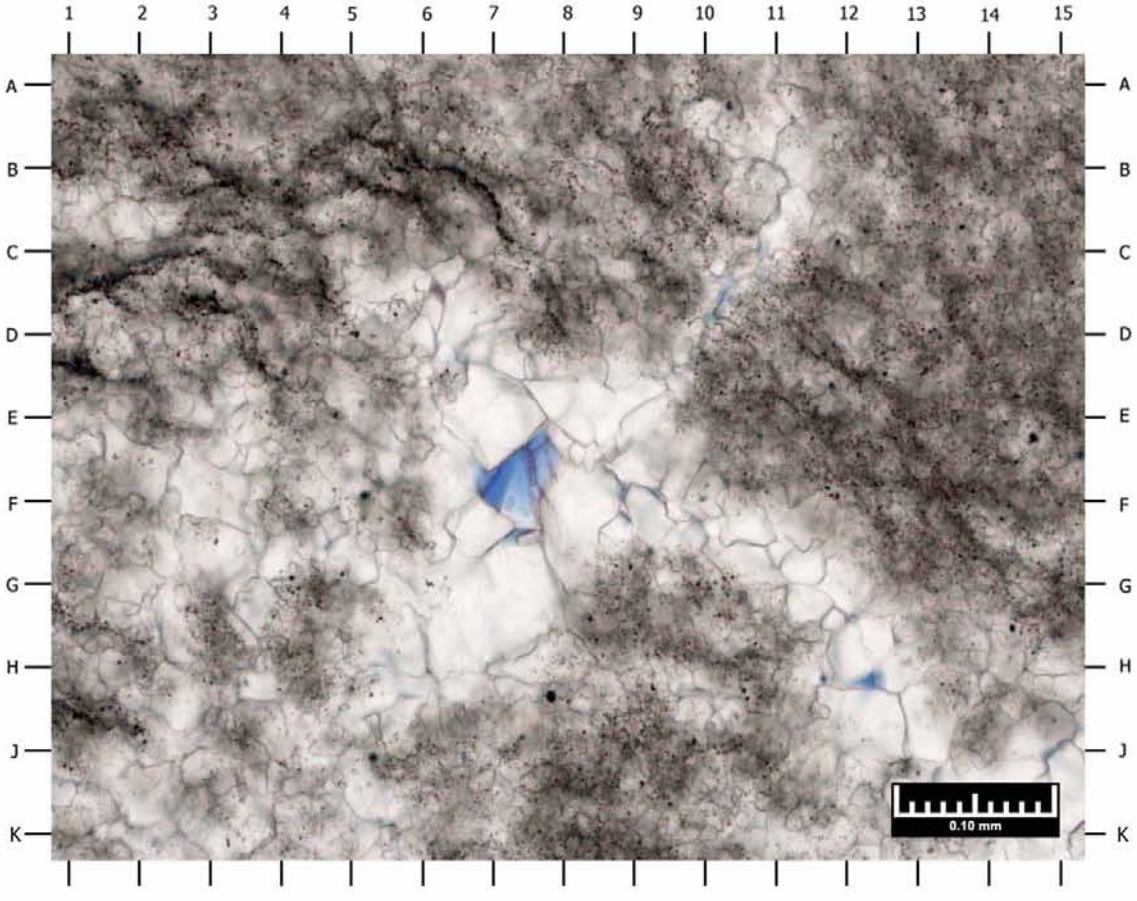

B

200X

Ohio Division of Geological Survey **OMNI File No: HH-38266**
CO_2 No. 1 Well
Tuscarawas County, Ohio
Conasauga group
Rotary Sidewall Core

THIN SECTION PHOTOMICROGRAPHS

SAMPLE DEPTH: 8421.0 FEET
SAMPLE NUMBER: 1-63R

Plate 63

Permeability (Klink.): 0.0085 mD Porosity (NCS): 3.2% Grain Density: 2.69 gm/cc

Sample not selected for petrographic analysis.

Magnification: A: 40X B: 200X

Ohio Division of Geological Survey
CO2 No. 1
Tuscarawas County, Ohio

8421.0'
Plate 63

Weatherford LABORATORIES

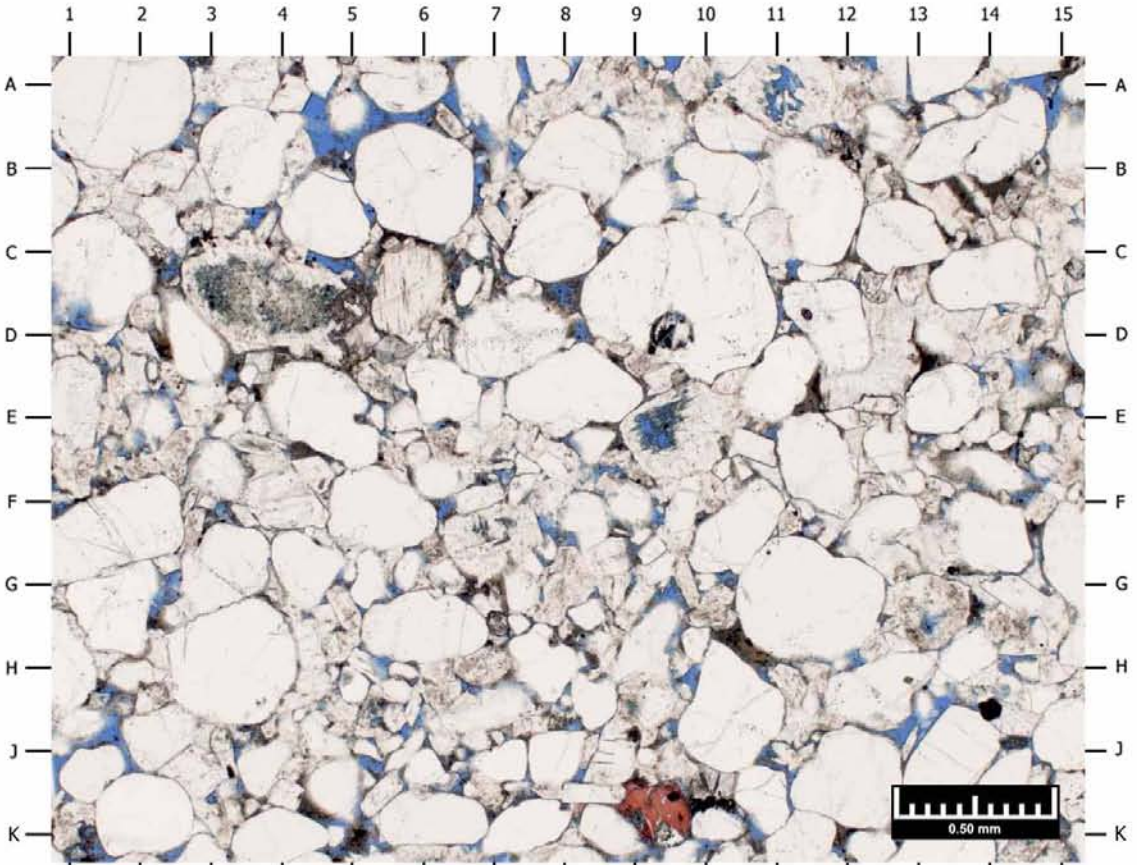

A

40X

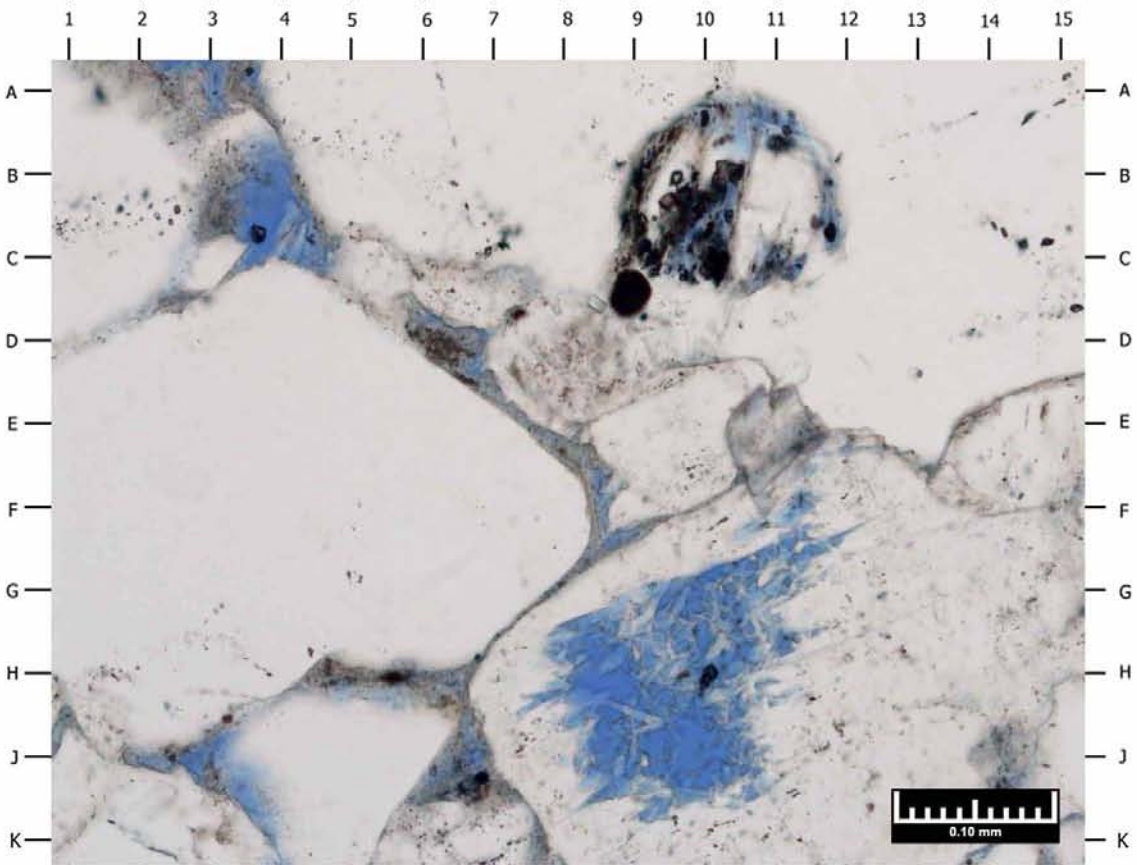

B

200X

Ohio Division of Geological Survey **OMNI File No: HH-38266**
CO_2 No. 1 Well
Tuscarawas County, Ohio
Conasauga group
Rotary Sidewall Core

THIN SECTION PHOTOMICROGRAPHS

SAMPLE DEPTH: 8451.0 FEET
SAMPLE NUMBER: 1-64R

Plate 64

Permeability (Klink.): 0.0084 mD Porosity (NCS): 6.6% Grain Density: 2.63 gm/cc

Sample not selected for petrographic analysis.

Magnification: A: 40X B: 200X

Ohio Division of Geological Survey
CO2 No. 1
Tuscarawas County, Ohio

8451.0'
Plate 64

Weatherford LABORATORIES

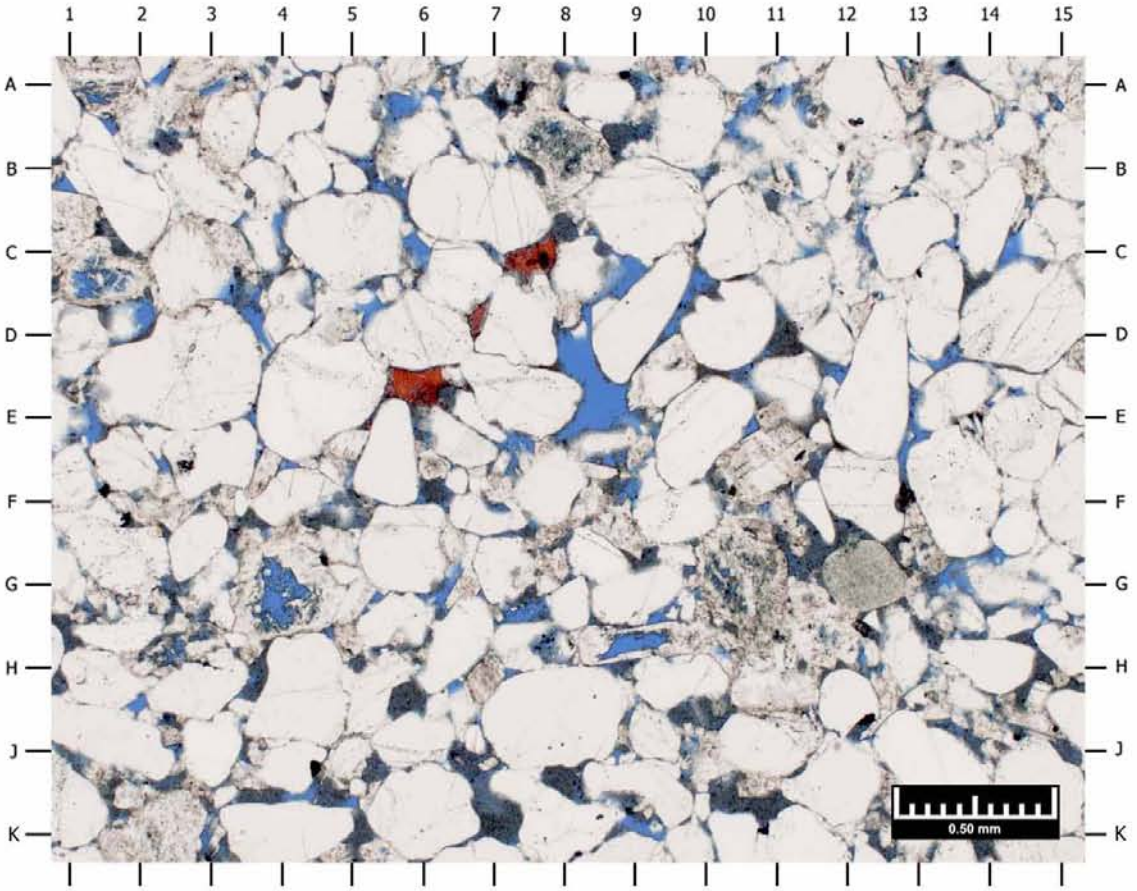

A

40X

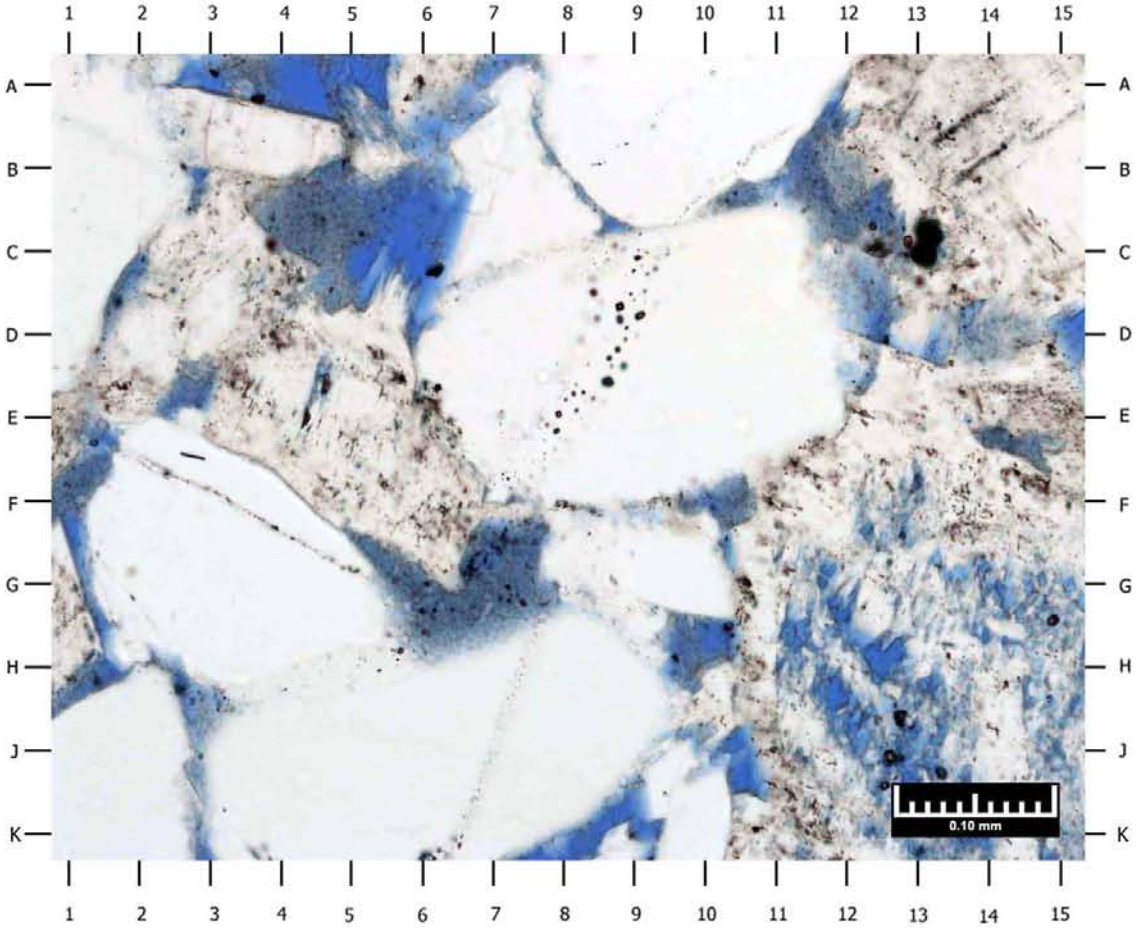

B

200X

Ohio Division of Geological Survey **OMNI File No: HH-38266**
CO_2 No. 1 Well
Tuscarawas County, Ohio
Conasauga group
Rotary Sidewall Core

THIN SECTION PHOTOMICROGRAPHS

SAMPLE DEPTH: 8467.0 FEET
SAMPLE NUMBER: 1-65R

Plate 65

Permeability (Klink.): 0.0028 mD Porosity (NCS): 4.2% Grain Density: 2.62 gm/cc

Sample not selected for petrographic analysis.

Magnification: A: 40X B: 200X

Ohio Division of Geological Survey
CO2 No. 1
Tuscarawas County, Ohio

8467.0'
Plate 65

Weatherford LABORATORIES

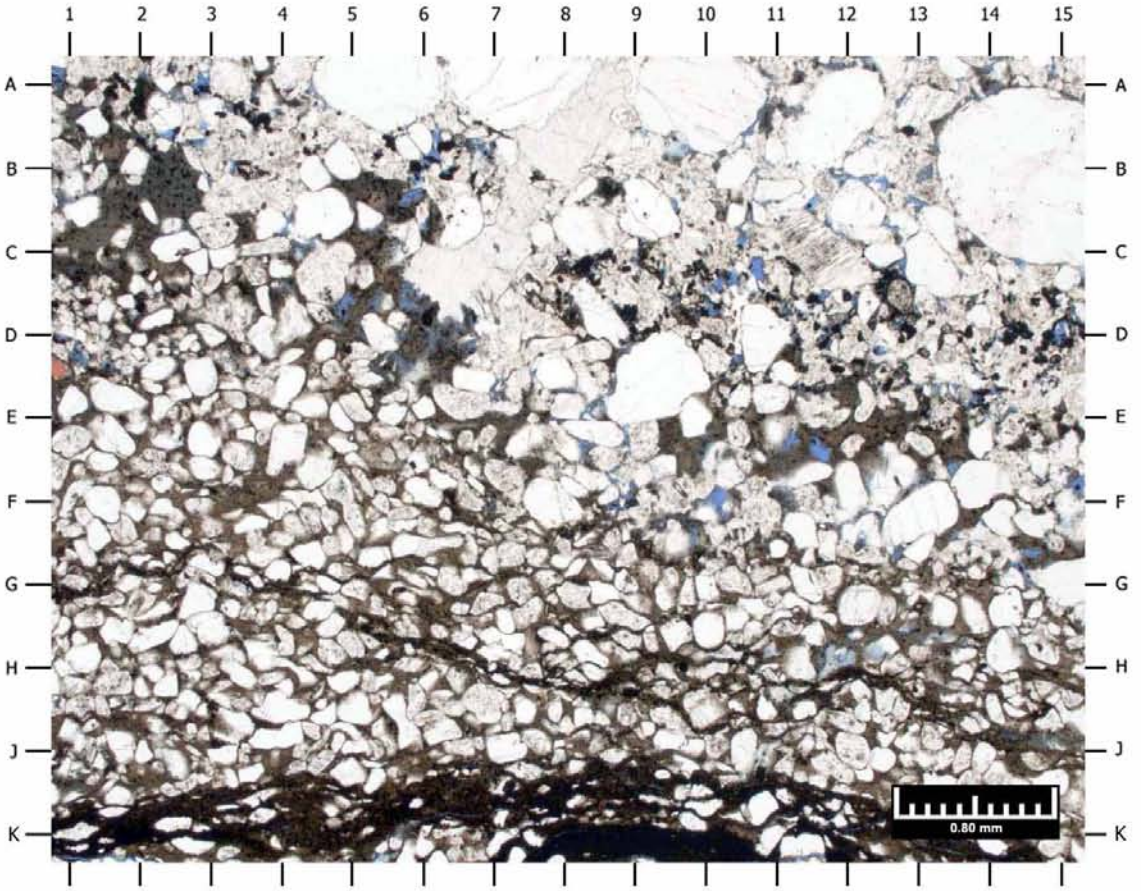

A

25X

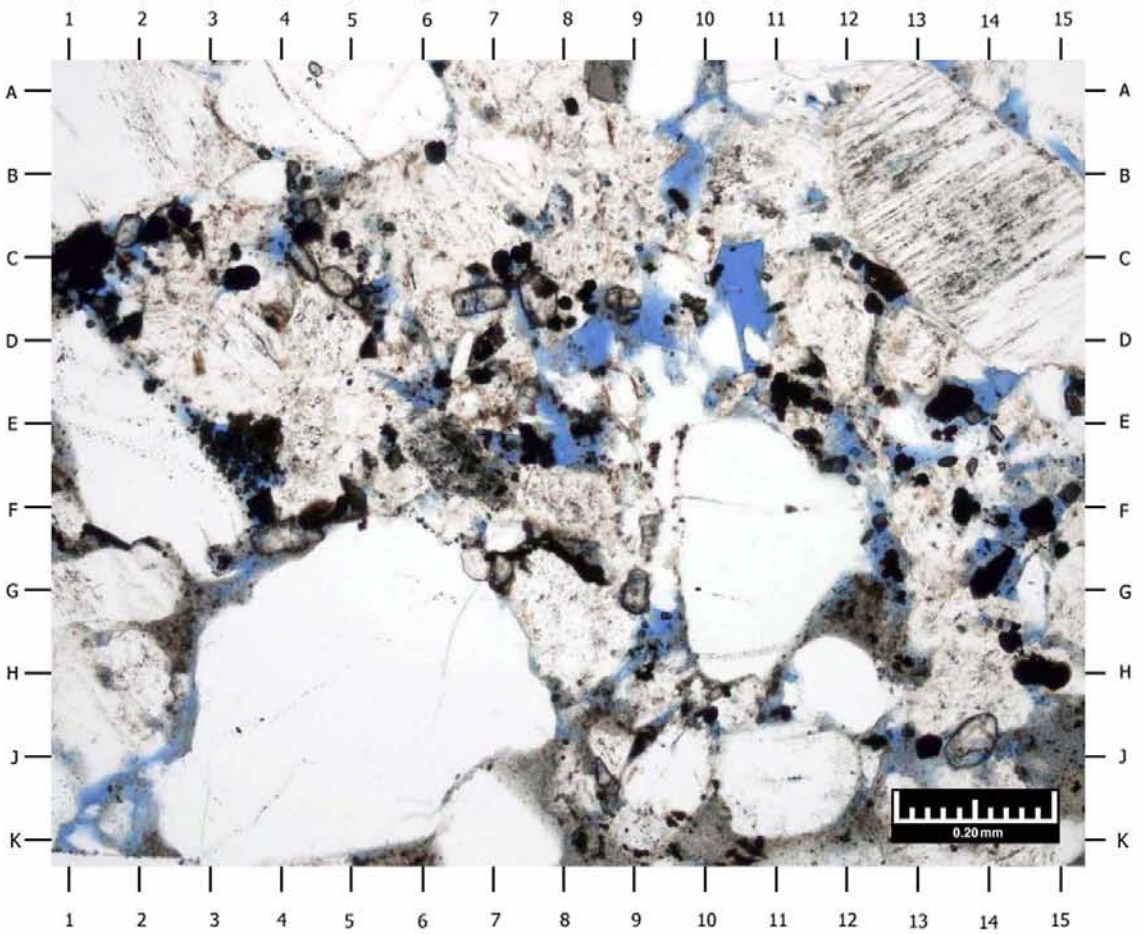

B

100X

Ohio Division of Geological Survey **OMNI File No: HH-38266**
CO_2 No. 1 Well
Tuscarawas County, Ohio
Conasauga group
Rotary Sidewall Core

THIN SECTION PHOTOMICROGRAPHS

SAMPLE DEPTH: 8495.0 FEET
SAMPLE NUMBER: 1-66R

Plate 66

Permeability (Klink.): 0.0001 mD Porosity (NCS): 0.6% Grain Density: 2.81 gm/cc

Sample not selected for petrographic analysis.

Magnification: A: 40X B: 200X

Ohio Division of Geological Survey
CO2 No. 1
Tuscarawas County, Ohio

8495.0'
Plate 66

Weatherford LABORATORIES

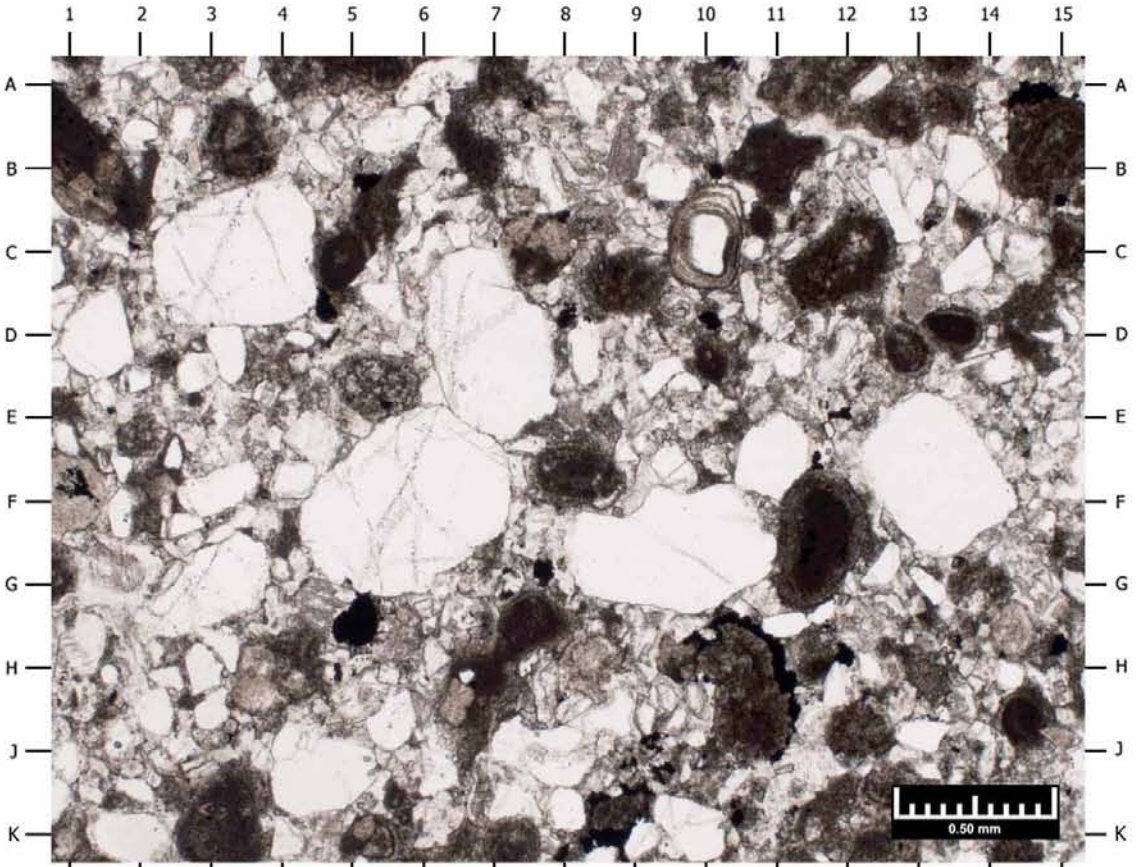

A

40X

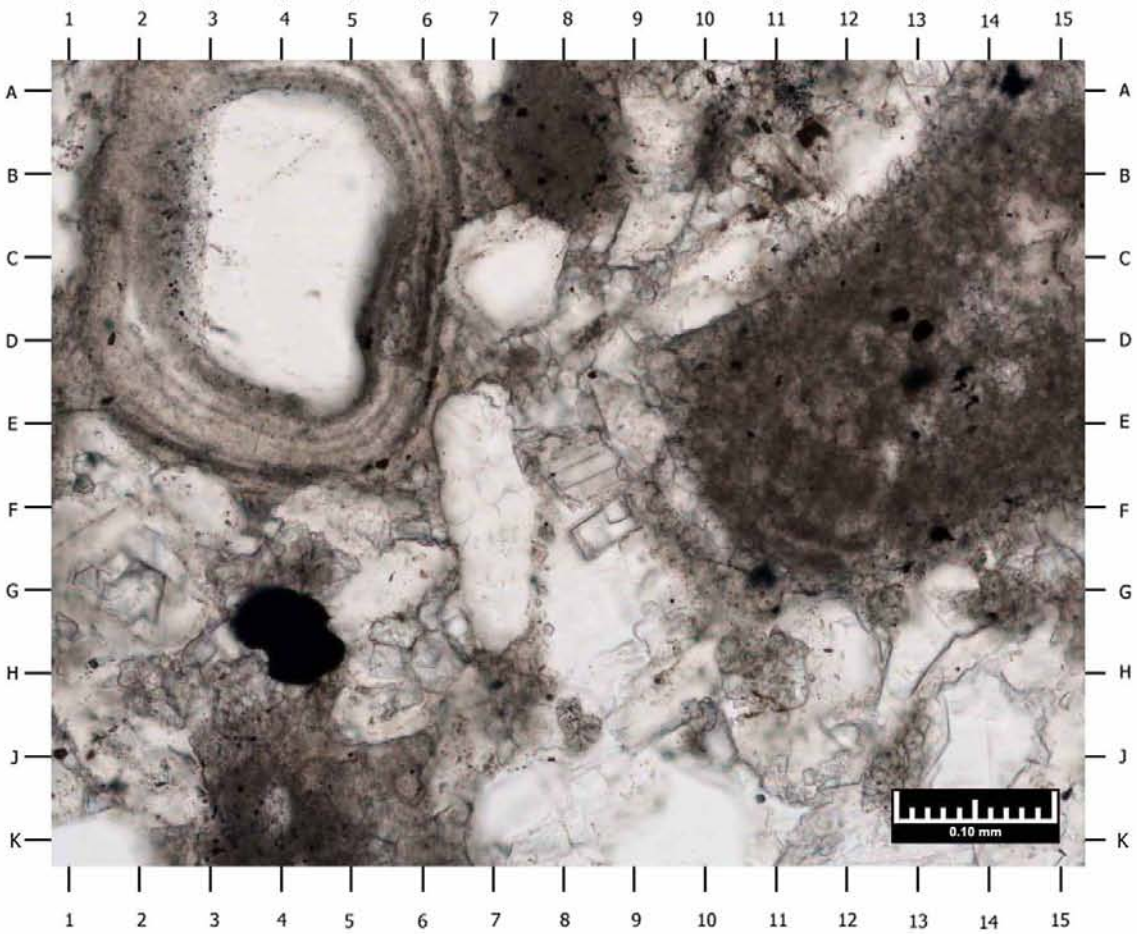

B

200X

Ohio Division of Geological Survey **OMNI File No: HH-38266**
CO_2 No. 1 Well
Tuscarawas County, Ohio
Cambrian Basal Sandstone
Rotary Sidewall Core

THIN SECTION PHOTOMICROGRAPHS

SAMPLE DEPTH: 8528.0 FEET
SAMPLE NUMBER: 1-67R

Plate 67

Permeability (Klink.): N/A Porosity (NCS): 2.7% Grain Density: 2.71 gm/cc

Sample not selected for petrographic analysis.

Magnification: A: 40X B: 200X

Ohio Division of Geological Survey
CO2 No. 1
Tuscarawas County, Ohio

8528.0'
Plate 67

Weatherford LABORATORIES

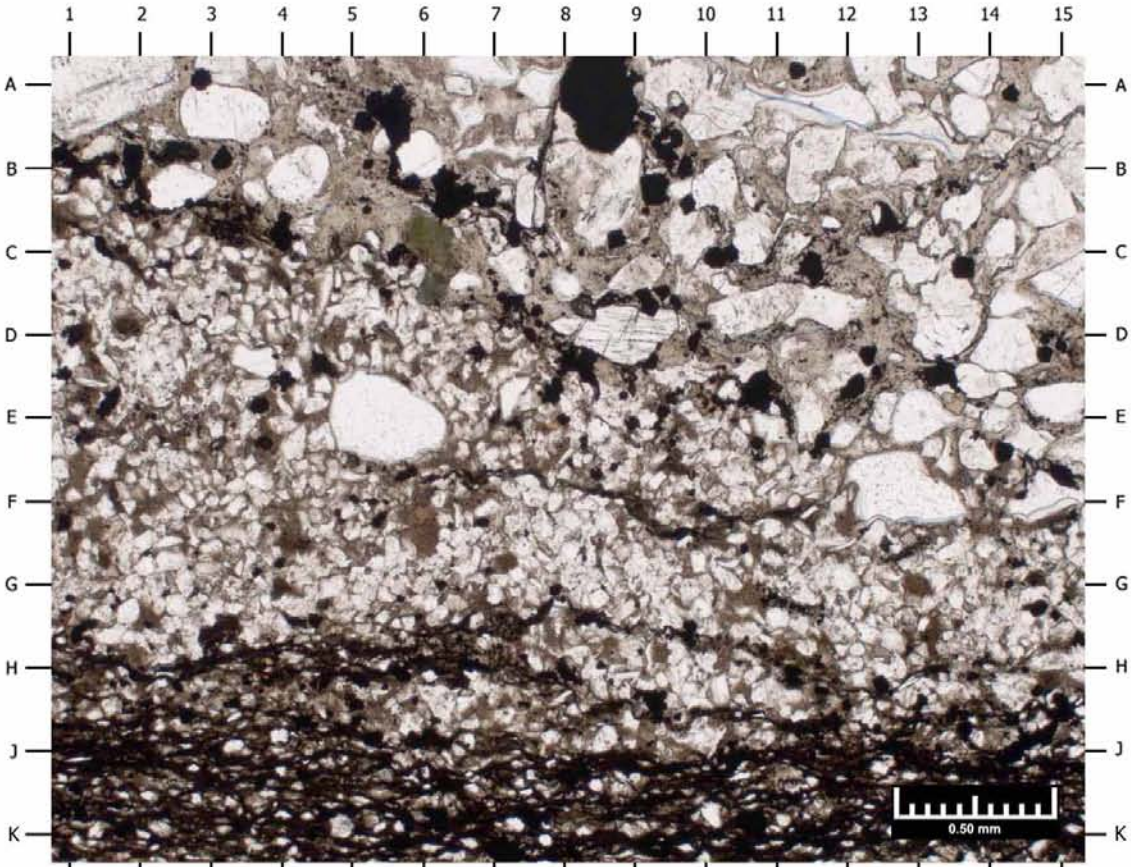

A

40X

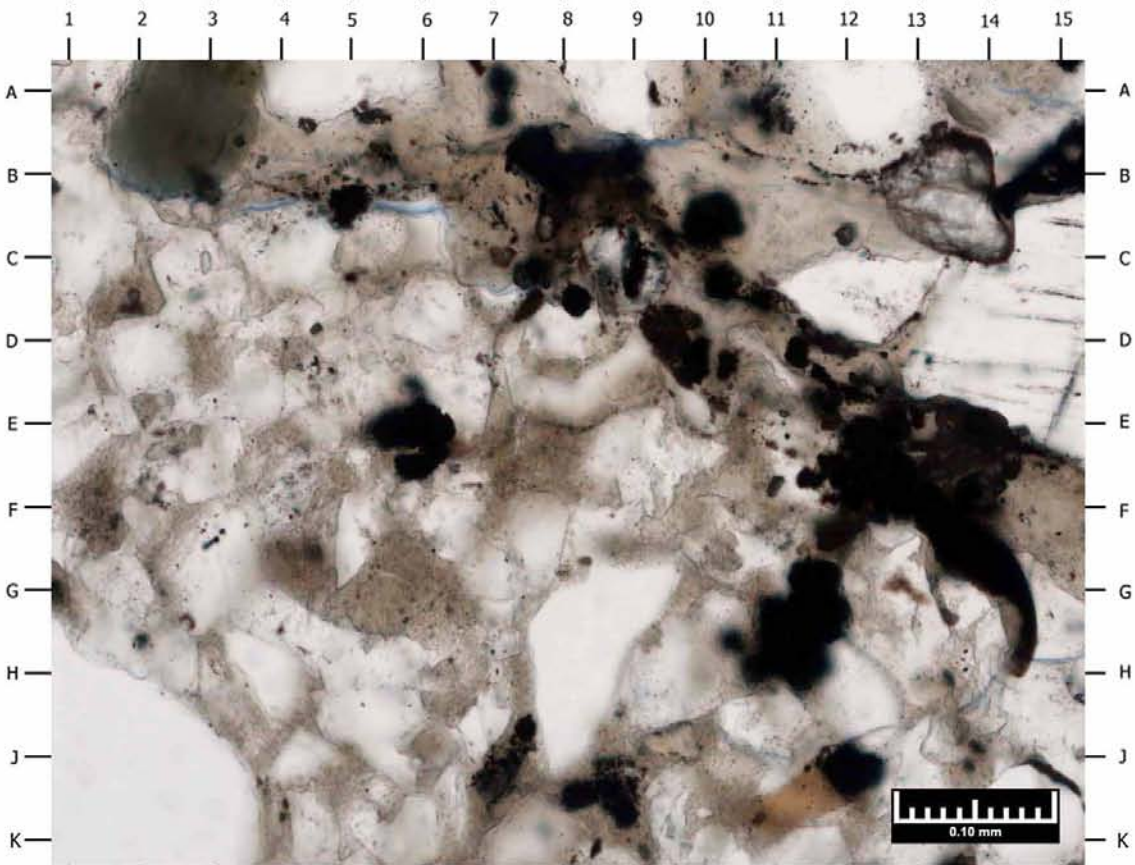

B

200X

Ohio Division of Geological Survey **OMNI File No: HH-38266**
CO_2 No. 1 Well
Tuscarawas County, Ohio
Cambrian Basal Sandstone
Rotary Sidewall Core

THIN SECTION DESCRIPTION - DETAILED

SAMPLE DEPTH: 8538.0 FEET
SAMPLE NUMBER: 1-68R

Plate 68

Permeability (Klink.): 0.0052 mD Porosity (NCS): 4.9% Grain Density: 2.62 gm/cc

Lithology:	Arkose
Sedimentary Fabric:	Grain size-zoning
Grain Size Range:	<0.05mm-1.01mm
Average Grain Size:	0.23mm
Compaction:	Moderate
Sorting:	Poorly sorted
Framework Grains:	
Major:	Monocrystalline quartz, potassium feldspar
Minor:	Polycrystalline quartz, plagioclase feldspar, lithic fragments (chert, mudstone, metamorphic fragments)
Accessory:	Tourmaline, muscovite, biotite, phosphatic grains
Matrix Content:	
Detrital Matrix:	Trace of organic material
Authigenic Clay:	Minor pore-lining clay and pore-filling clay (undifferentiated)
Cement Types:	Common quartz overgrowths and dolomite cement; minor feldspar overgrowths, pyrite, and bitumen; trace amount of Fe/Ti oxides
Porosity Types:	Minor secondary intragranular pores, micropores, and intergranular pores
Reservoir Quality:	Fair to poor

Magnification: A: 40X B: 200X

A) In this poorly sorted arkose, laminations are defined by changes in grain size and size sorting (e.g., CD1 to DE15). Quartz (B4) and metaquartzite (H14) are common. Feldspar grains are altered and partially dissolved (F10.5) and ductile fragments are deformed by compaction (J7.5).

B) The pore system consists of scattered secondary intragranular pores (E5) in partially dissolved feldspar, quartz cement-reduced intergranular pores (H15), and dolomite cement-reduced pores (E7.5). Microcrystalline pyrite (black; E6.5) is a minor cement.

Ohio Division of Geological Survey
CO2 No. 1
Tuscarawas County, Ohio

8538.0'
Plate 68

Weatherford LABORATORIES

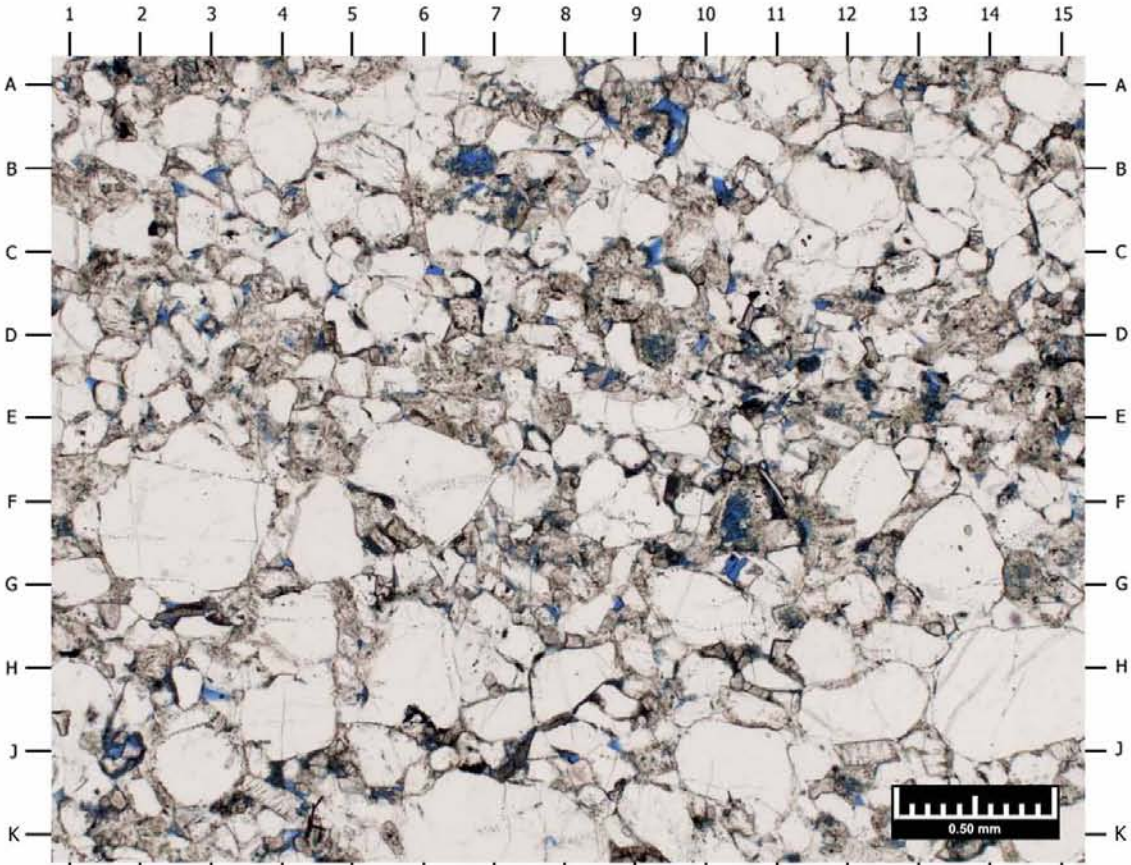

A

40X

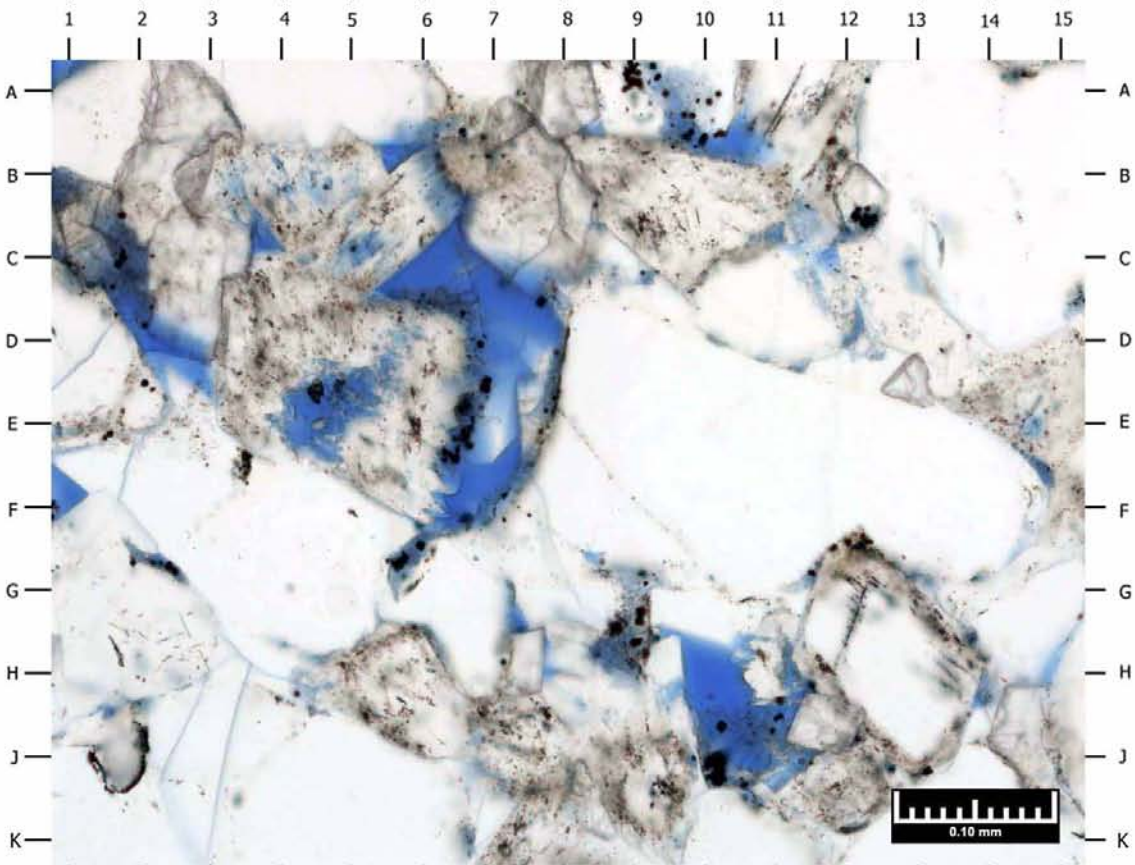

B

200X

Ohio Division of Geological Survey **OMNI File No: HH-38266**
CO_2 No. 1 Well
Tuscarawas County, Ohio
Cambrian Basal Sandstone
Rotary Sidewall Core

THIN SECTION PHOTOMICROGRAPHS

SAMPLE DEPTH: 8544.0 FEET
SAMPLE NUMBER: 1-69R

Plate 69

Permeability (Klink.): 0.0003 mD Porosity (NCS): 3.4% Grain Density: 2.67 gm/cc

Sample not selected for petrographic analysis.

Magnification: A: 40X B: 200X

Ohio Division of Geological Survey
CO2 No. 1
Tuscarawas County, Ohio

8544.0'
Plate 69

Weatherford LABORATORIES

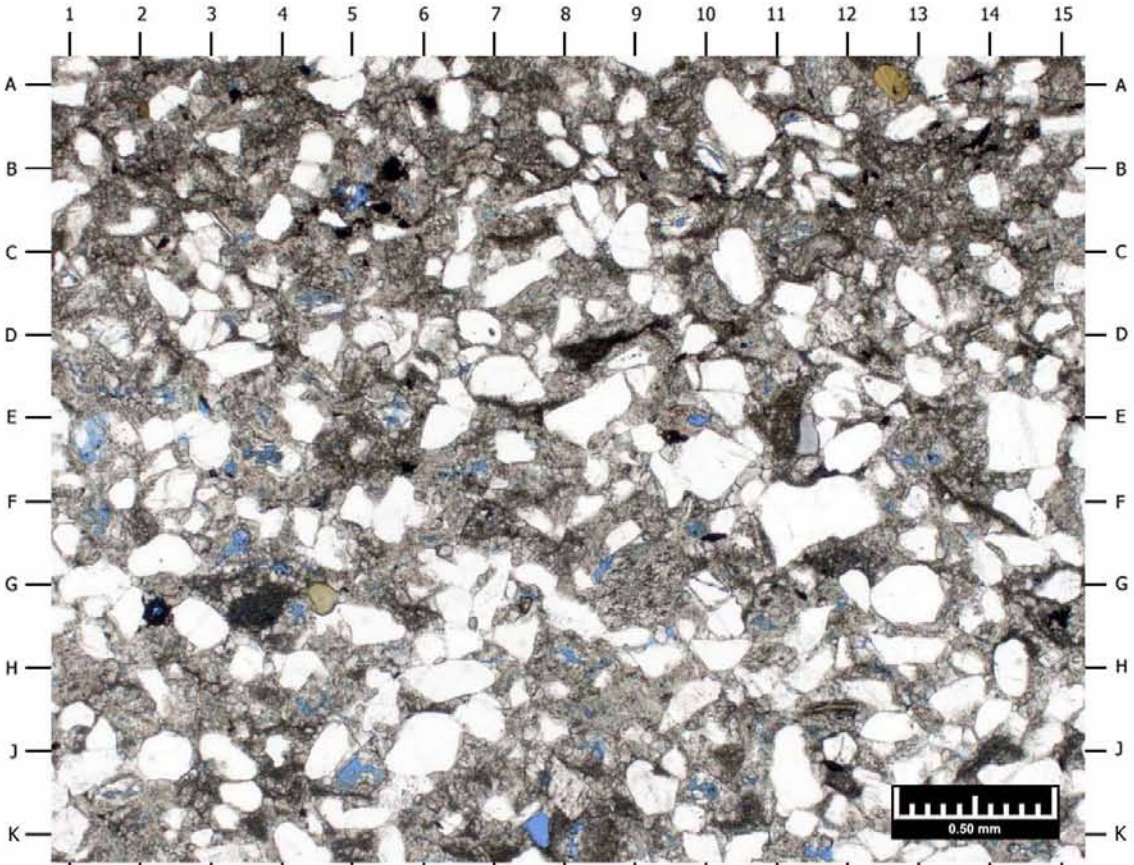

A

40X

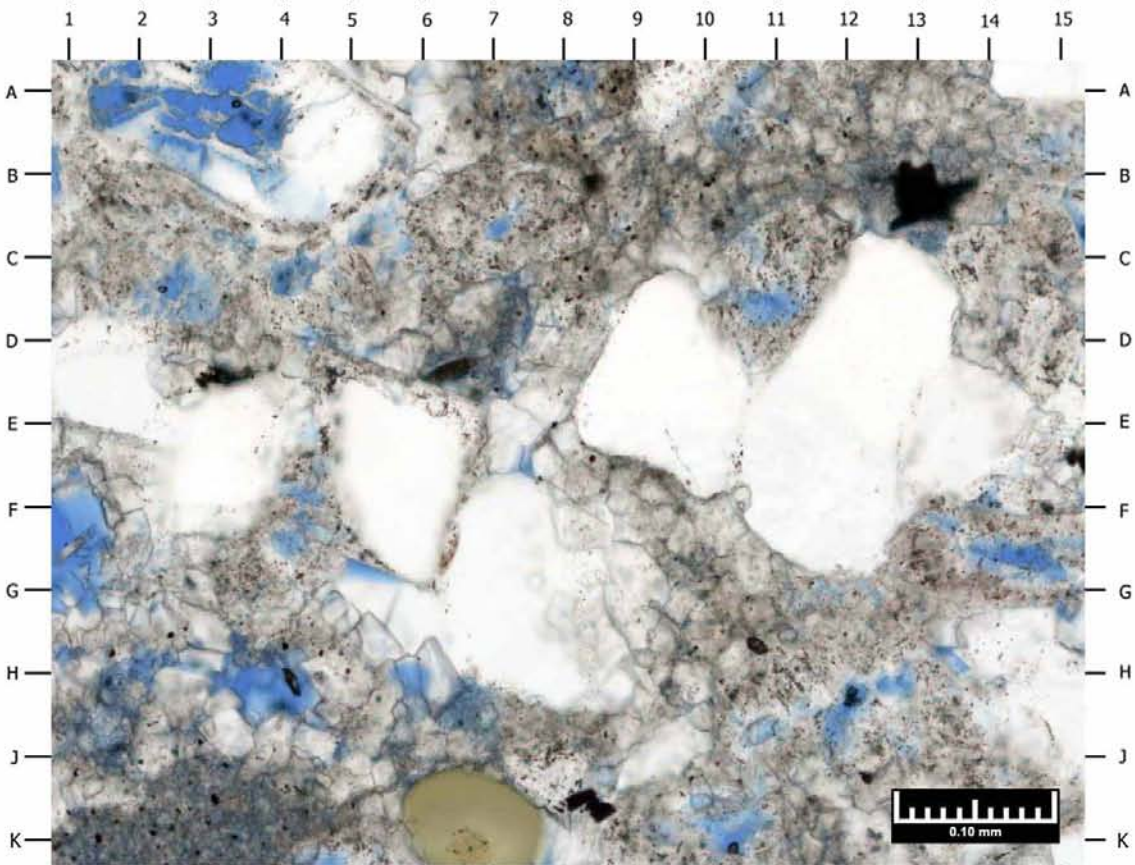

B

200X

Ohio Division of Geological Survey **OMNI File No: HH-38266**
CO_2 No. 1 Well
Tuscarawas County, Ohio
Cambrian Basal Sandstone
Rotary Sidewall Core

THIN SECTION PHOTOMICROGRAPHS

SAMPLE DEPTH: 8549.0 FEET
SAMPLE NUMBER: 1-70R

Plate 70

Permeability (Klink.): 0.0001 mD Porosity (NCS): 1.1% Grain Density: 2.79 gm/cc

Sample not selected for petrographic analysis.

Magnification: A: 40X B: 200X

Ohio Division of Geological Survey
CO2 No. 1
Tuscarawas County, Ohio

8549.0'
Plate 70

Weatherford LABORATORIES

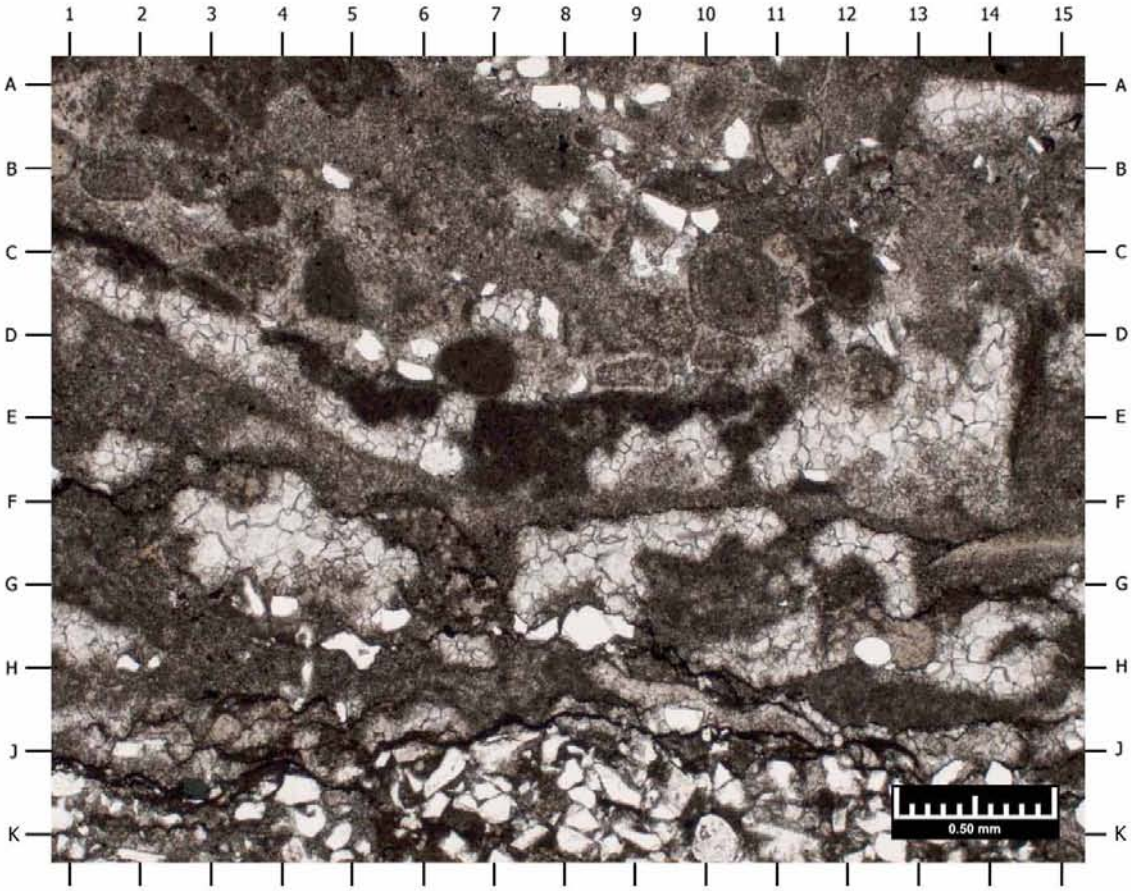

A

40X

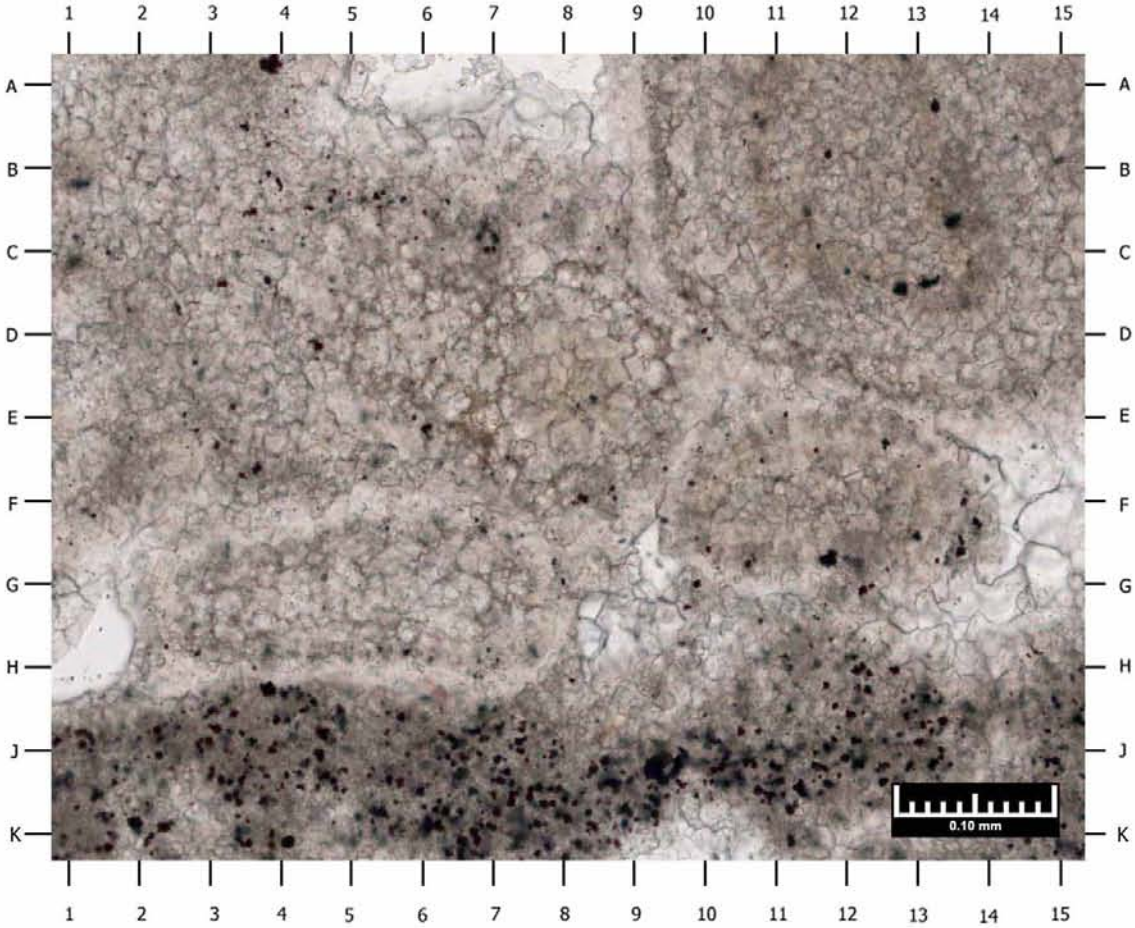

B

200X

Ohio Division of Geological Survey **OMNI File No: HH-38266**
CO_2 No. 1 Well
Tuscarawas County, Ohio
Cambrian Basal Sandstone
Rotary Sidewall Core

THIN SECTION PHOTOMICROGRAPHS

SAMPLE DEPTH: 8555.0 FEET
SAMPLE NUMBER: 1-71R

Plate 71

Permeability (Klink.): 0.044 mD Porosity (NCS): 9.0% Grain Density: 2.63 gm/cc

Sample not selected for petrographic analysis.

Magnification: A: 40X B: 200X

Ohio Division of Geological Survey
CO2 No. 1
Tuscarawas County, Ohio

8555.0'
Plate 71

Weatherford LABORATORIES

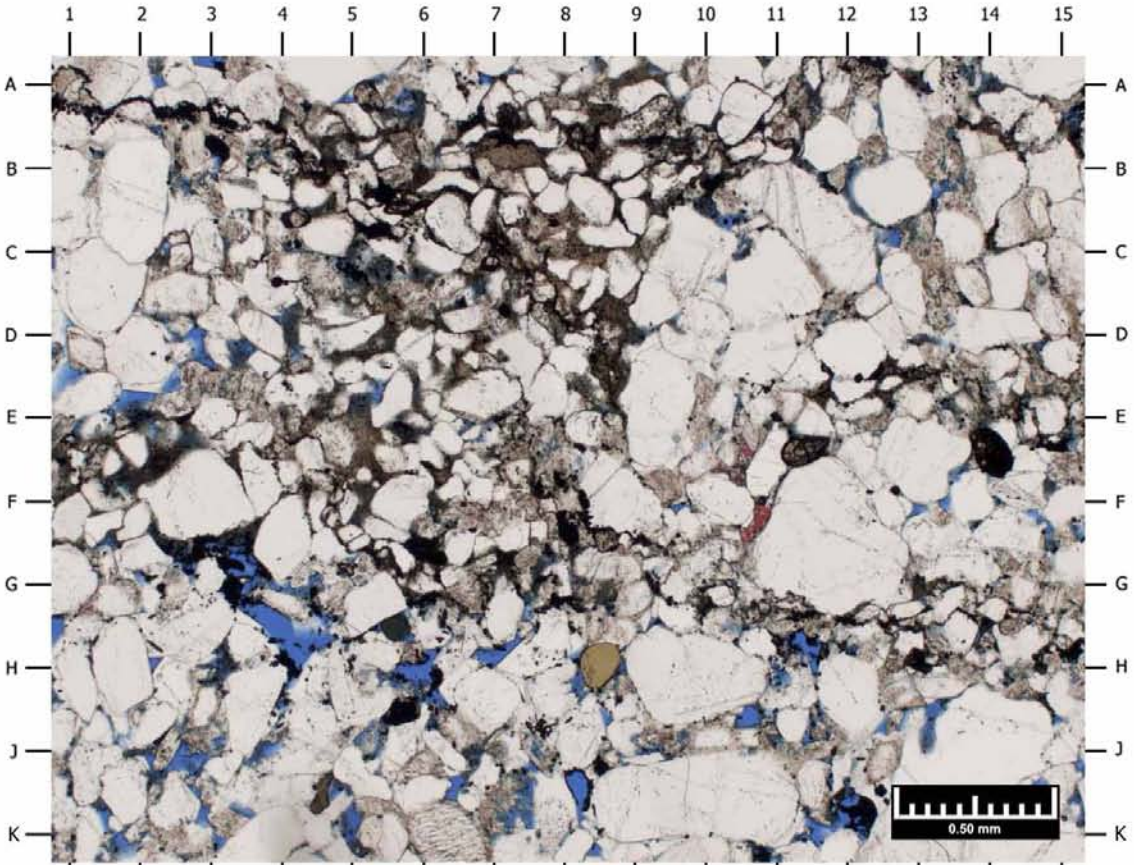

A

40X

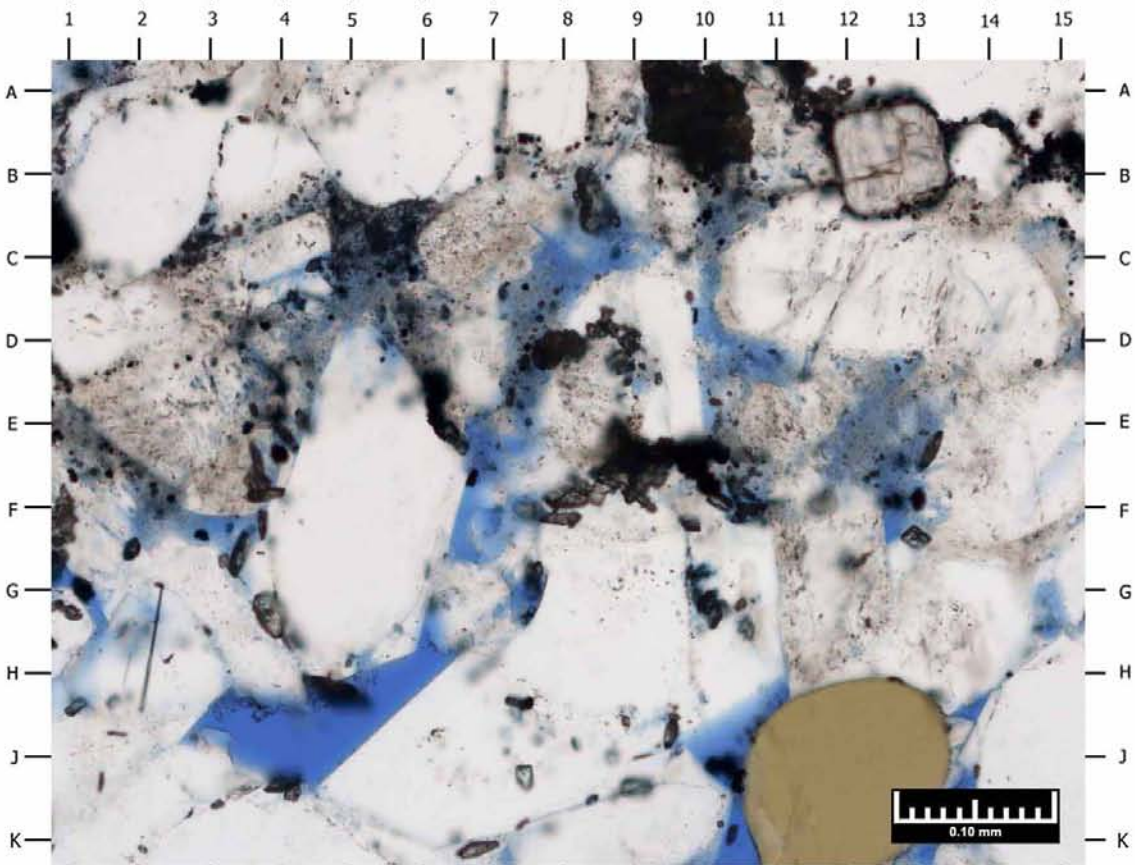

B

200X

Ohio Division of Geological Survey **OMNI File No: HH-38266**
CO_2 No. 1 Well
Tuscarawas County, Ohio
Cambrian Basal Sandstone
Rotary Sidewall Core

THIN SECTION DESCRIPTION - DETAILED

SAMPLE DEPTH: 8561.0 FEET
SAMPLE NUMBER: 1-72R

Plate 72

Permeability (Klink.): 0.836 mD Porosity (NCS): 9.6% Grain Density: 2.60 gm/cc

Lithology:	Arkose
Sedimentary Fabric:	Vaguely laminated /grain size-zoning
Grain Size Range:	<0.01mm-0.99mm
Average Grain Size:	0.26mm
Compaction:	Moderate
Sorting:	Moderately sorted
Framework Grains:	
Major:	Monocrystalline quartz, potassium feldspar
Minor:	Polycrystalline quartz, plagioclase feldspar, lithic fragments (chert, plutonic fragments, and metamorphic fragments)
Accessory:	Tourmaline, muscovite
Matrix Content:	
Detrital Matrix:	Trace of organic material and detrital clay matrix
Authigenic Clay:	Minor pore-lining clay and pore-filling clay (undifferentiated)
Cement Types:	Common quartz overgrowths; minor feldspar overgrowths and pyrite; trace of bitumen, dolomite, and Fe/Ti oxides
Porosity Types:	Common intragranular pores; minor amount of intergranular pores and micropores
Reservoir Quality:	Fair to good

Magnification: A: 40X B: 200X

A) Variably altered feldspar (H4.5, F13) and quartz (B9, F4) are the predominant constituents in this arkose. Although pores are common (blue), most are poorly connected, resulting in low permeability.

B) Constituents include quartz (C3), metaquartzite (B13), compacted argillaceous lithic fragments (B4), altered feldspar (D3), tourmaline (C7), and variably dissolved feldspar (D5.5). Authigenic pyrite partially reduces pores (J1.5, G5.5) and replaces grains (B4, G8.5). Note the poor interconnectivity of the secondary intragranular pores (B8, D5, G11, C1).

Ohio Division of Geological Survey
CO2 No. 1
Tuscarawas County, Ohio

8561.0'
Plate 72

Weatherford LABORATORIES

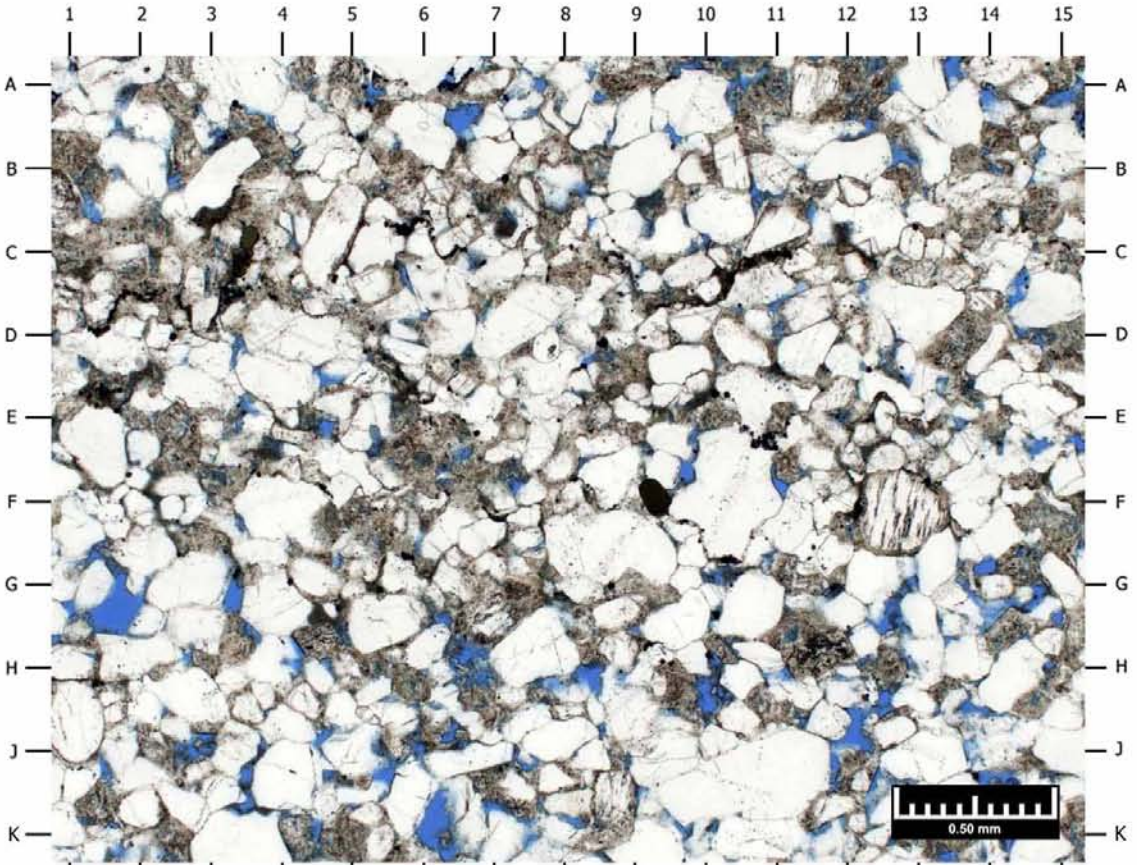

A

40X

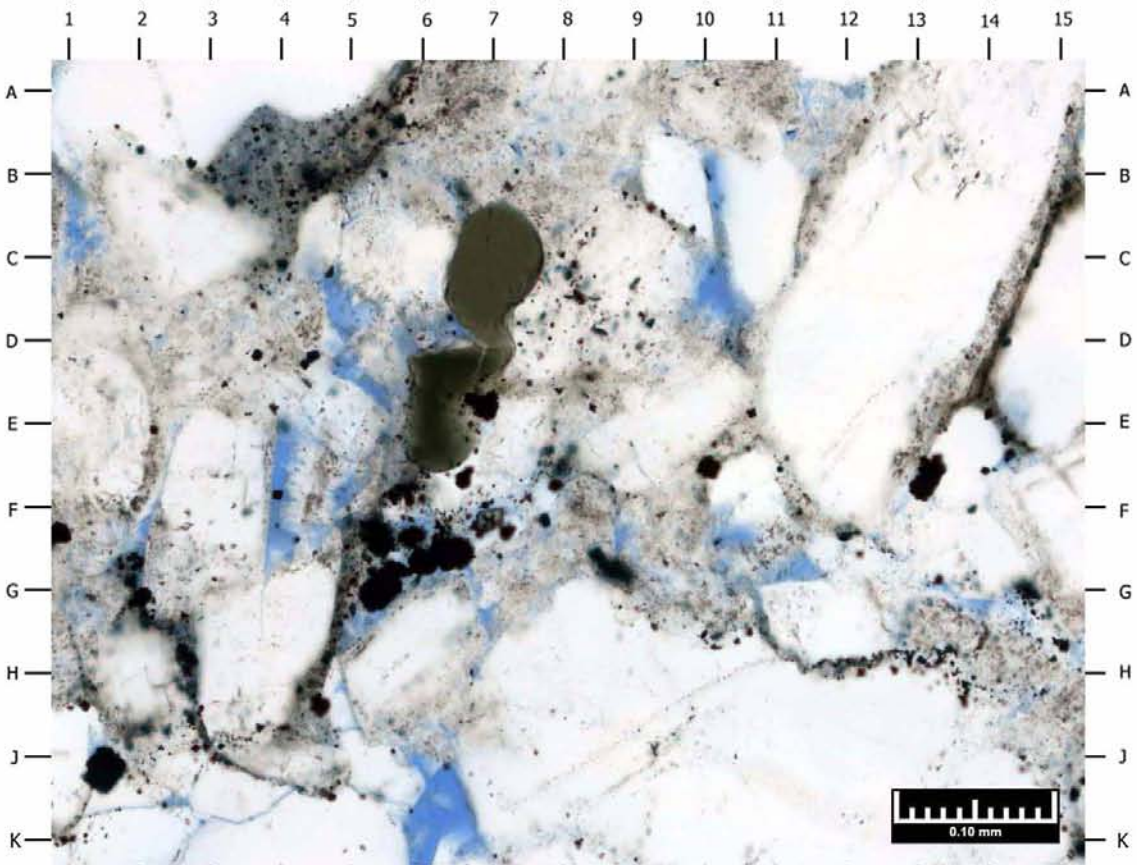

B

200X

Ohio Division of Geological Survey **OMNI File No: HH-38266**
CO_2 No. 1 Well
Tuscarawas County, Ohio
Cambrian Basal Sandstone
Rotary Sidewall Core

THIN SECTION PHOTOMICROGRAPHS

SAMPLE DEPTH: 8570.0 FEET
SAMPLE NUMBER: 1-73R

Plate 73

Permeability (Klink.): 0.0056 mD Porosity (NCS): 5.6% Grain Density: 2.62 gm/cc

Sample not selected for petrographic analysis.

Magnification: A: 40X B: 200X

Ohio Division of Geological Survey
CO2 No. 1
Tuscarawas County, Ohio

8570.0'
Plate 73

Weatherford LABORATORIES

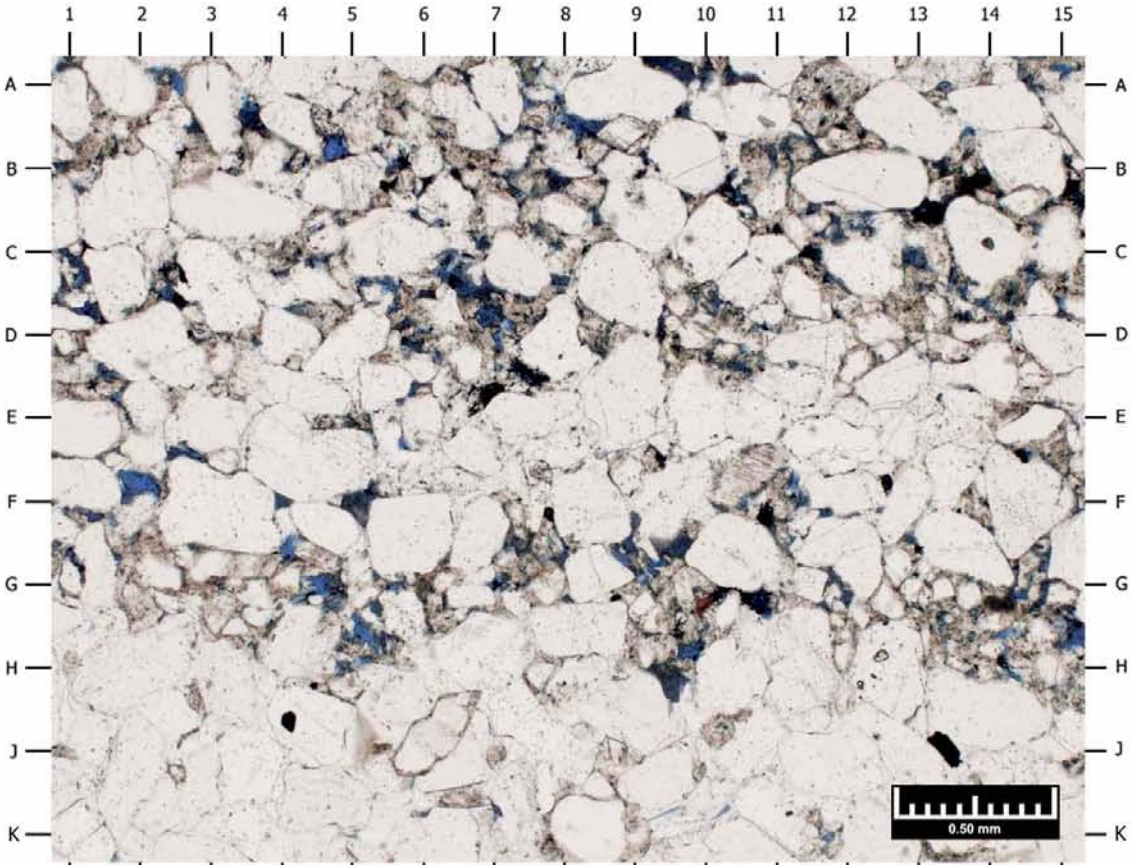

A

40X

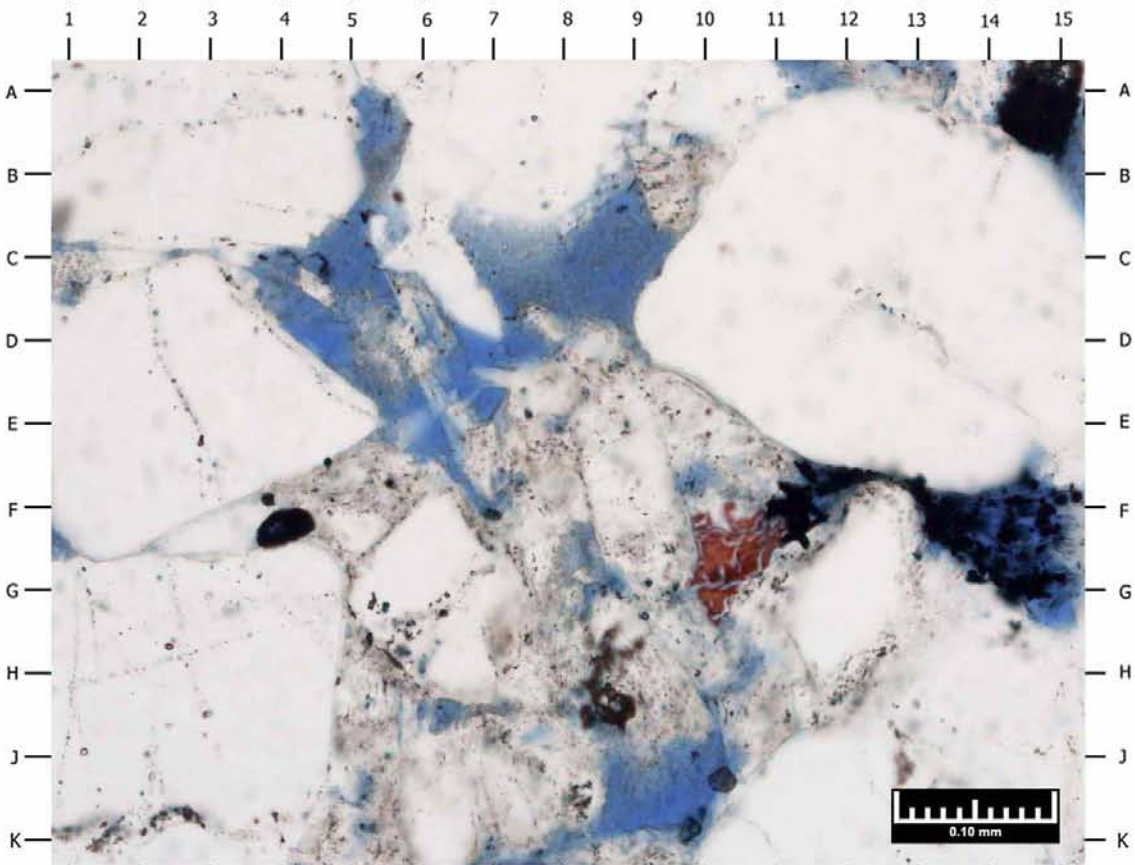

B

200X

Ohio Division of Geological Survey **OMNI File No: HH-38266**
CO_2 No. 1 Well
Tuscarawas County, Ohio
Cambrian Basal Sandstone
Rotary Sidewall Core

THIN SECTION DESCRIPTION - DETAILED

SAMPLE DEPTH: 8583.0 FEET
SAMPLE NUMBER: 1-74R

Plate 74

Permeability (Klink.): 0.013 mD Porosity (NCS): 6.2% Grain Density: 2.62 gm/cc

Lithology:	Arkose
Sedimentary Fabric:	Vaguely laminated /grain size-zoning
Grain Size Range:	0.03mm-0.90mm
Average Grain Size:	0.28mm
Compaction:	Moderate
Sorting:	Moderately poorly sorted
Framework Grains:	
Major:	Monocrystalline quartz, potassium feldspar
Minor:	Polycrystalline quartz, plagioclase feldspar, lithic fragments (plutonic, volcanic, and metamorphic fragments)
Accessory:	Tourmaline, muscovite, biotite/chlorite
Matrix Content:	
Detrital Matrix:	Minor amount of organic material and detrital clay matrix
Authigenic Clay:	Minor pore-lining clay and pore-filling clay (undifferentiated)
Cement Types:	Common dolomite and calcite cement; minor amounts of quartz overgrowths and feldspar overgrowths; minor amount of pyrite and Fe/Ti oxides; trace amount of bitumen
Porosity Types:	Minor amount of intergranular pores, secondary intragranular pores, and micropores
Reservoir Quality:	Fair

Magnification: A: 40X B: 200X

A)

B)

Ohio Division of Geological Survey
CO2 No. 1
Tuscarawas County, Ohio

8583.0'
Plate 74

Weatherford LABORATORIES

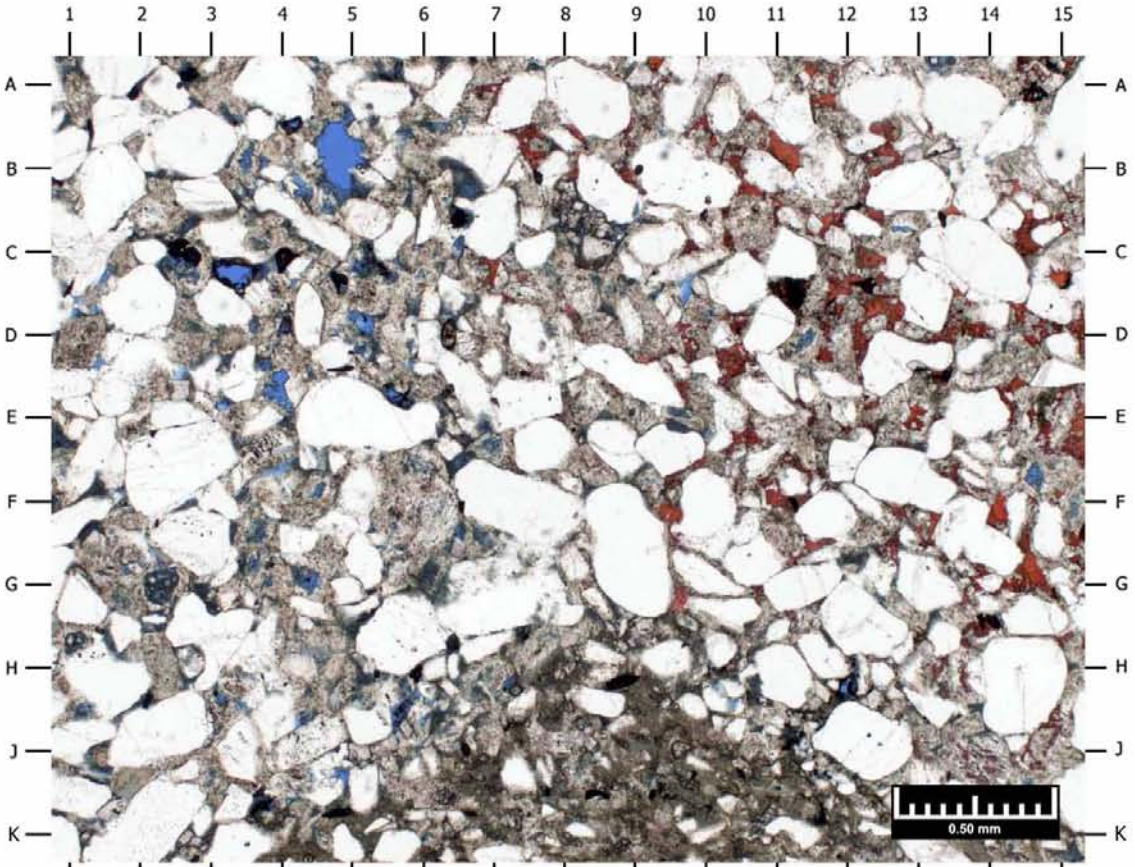

A

40X

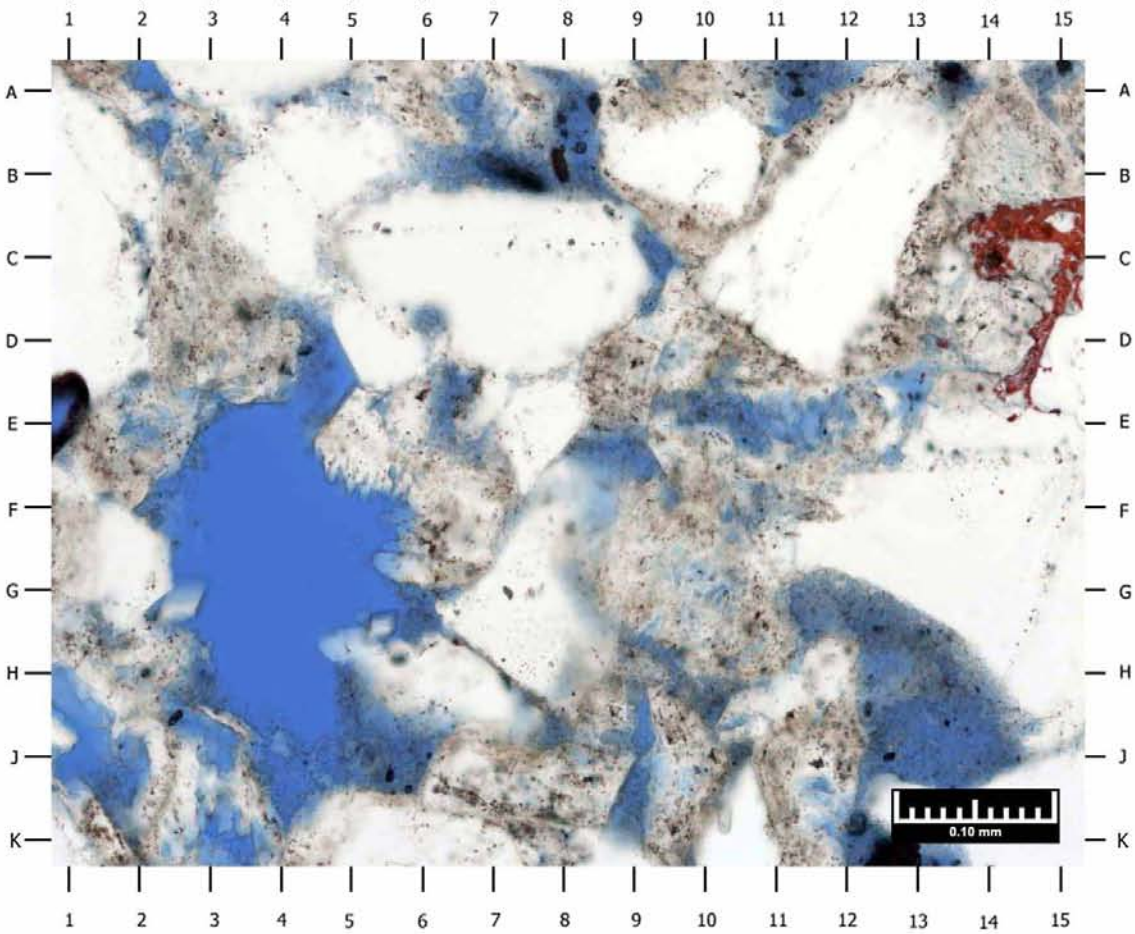

B

200X

Ohio Division of Geological Survey **OMNI File No: HH-38266**
CO_2 No. 1 Well
Tuscarawas County, Ohio
Cambrian Basal Sandstone
Rotary Sidewall Core

THIN SECTION PHOTOMICROGRAPHS

SAMPLE DEPTH: 8585.0 FEET
SAMPLE NUMBER: 1-75R

Plate 75

Permeability (Klink.): 0.033 mD Porosity (NCS): 9.6% Grain Density: 2.57 gm/cc

Sample not selected for petrographic analysis.

Magnification: A: 40X B: 200X

Ohio Division of Geological Survey
CO2 No. 1
Tuscarawas County, Ohio

8585.0'
Plate 75

Weatherford LABORATORIES

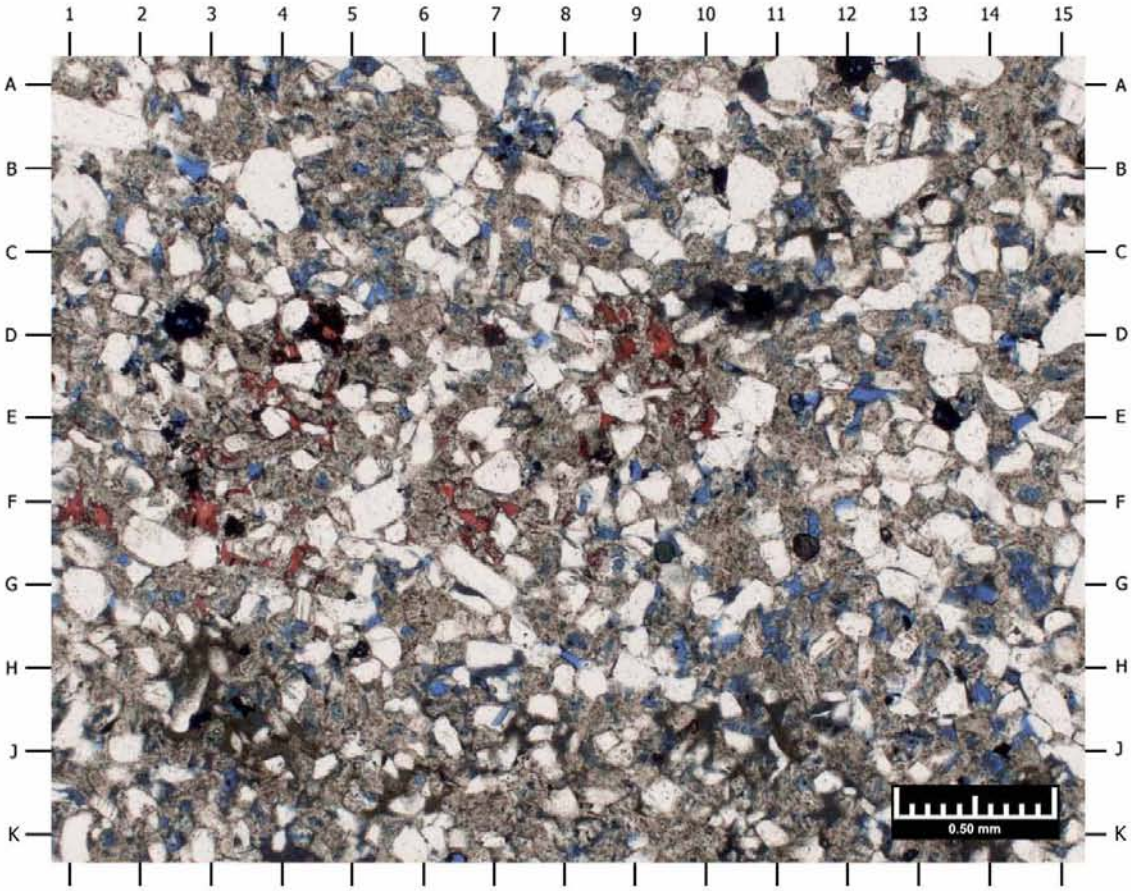

A

40X

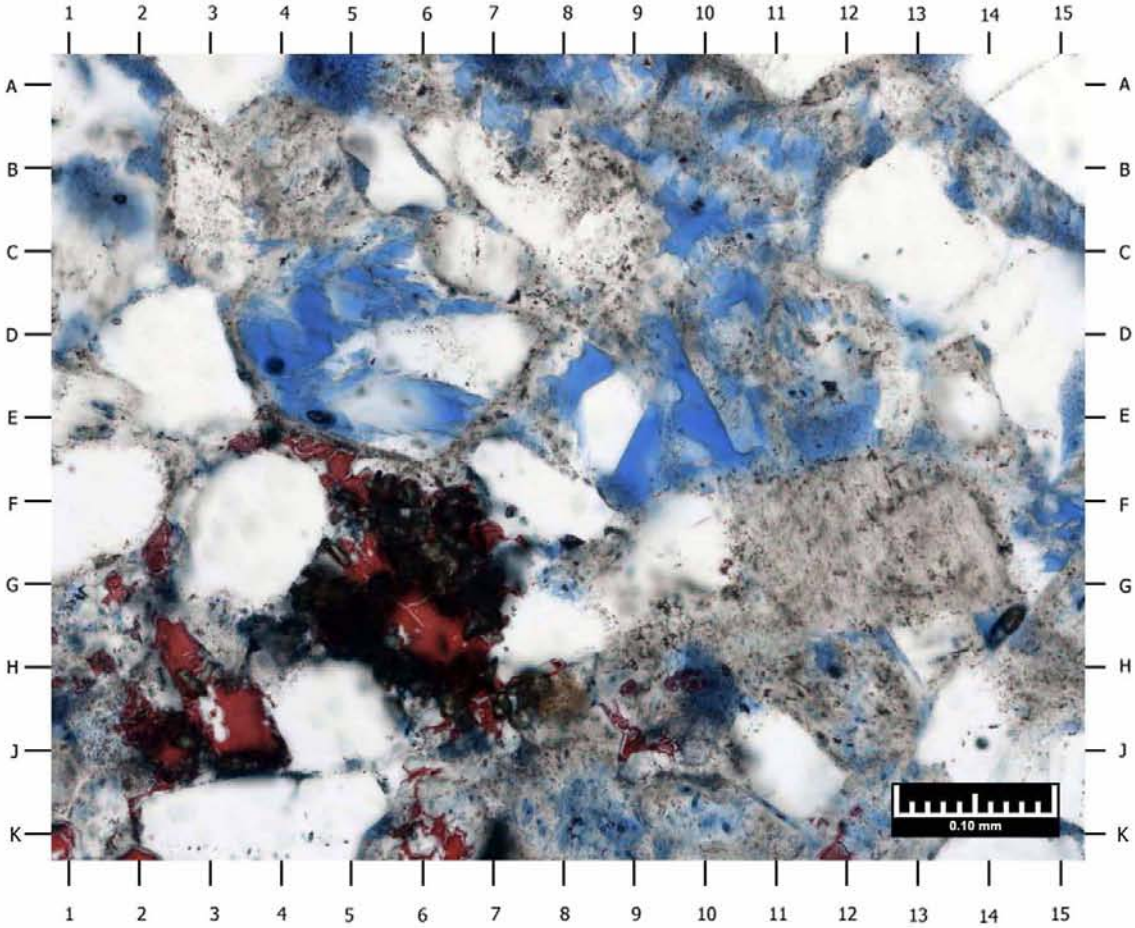

B

200X

Ohio Division of Geological Survey **OMNI File No: HH-38266**
CO_2 No. 1 Well
Tuscarawas County, Ohio
Cambrian Basal Sandstone
Rotary Sidewall Core

THIN SECTION PHOTOMICROGRAPHS

SAMPLE DEPTH: 8590.0 FEET
SAMPLE NUMBER: 1-76R

Plate 76

Permeability (Klink.): 0.118 mD Porosity (NCS): 10.7% Grain Density: 2.62 gm/cc

Sample not selected for petrographic analysis.

Magnification: A: 40X B: 200X

Ohio Division of Geological Survey
CO2 No. 1
Tuscarawas County, Ohio

8590.0'
Plate 76

Weatherford LABORATORIES

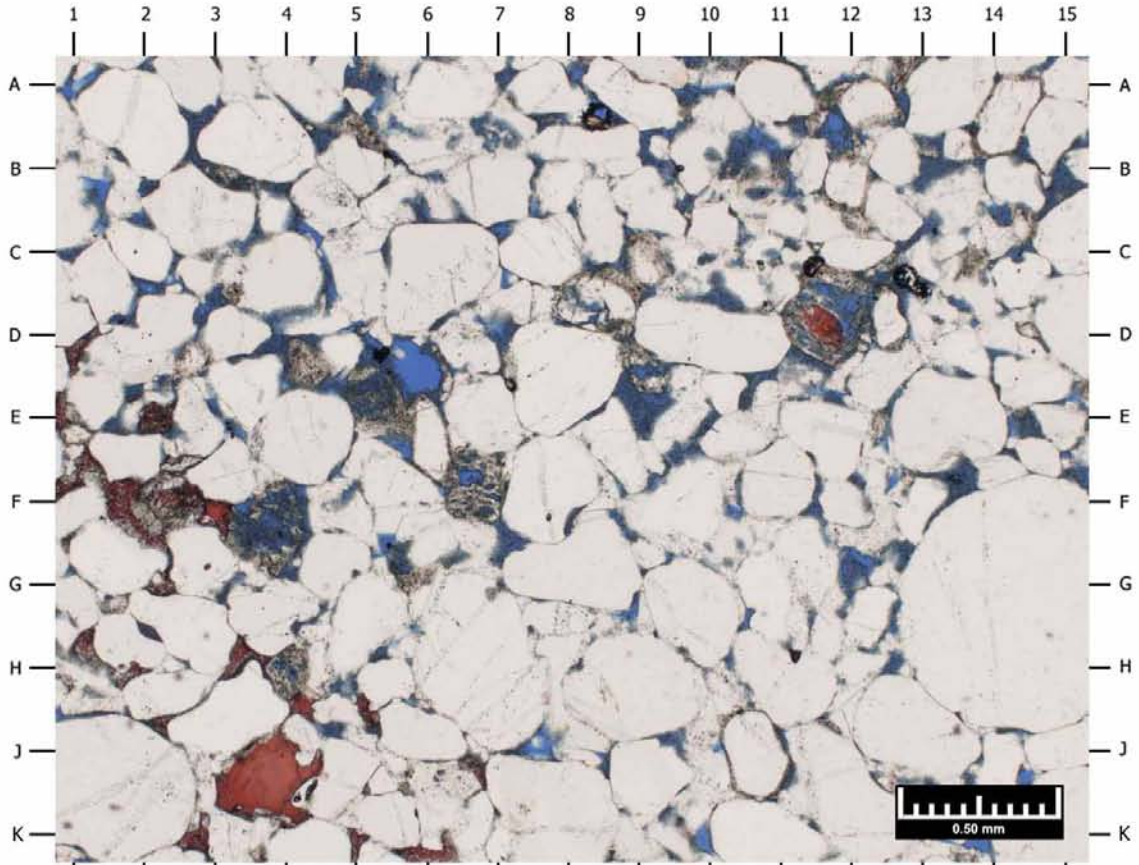

A

40X

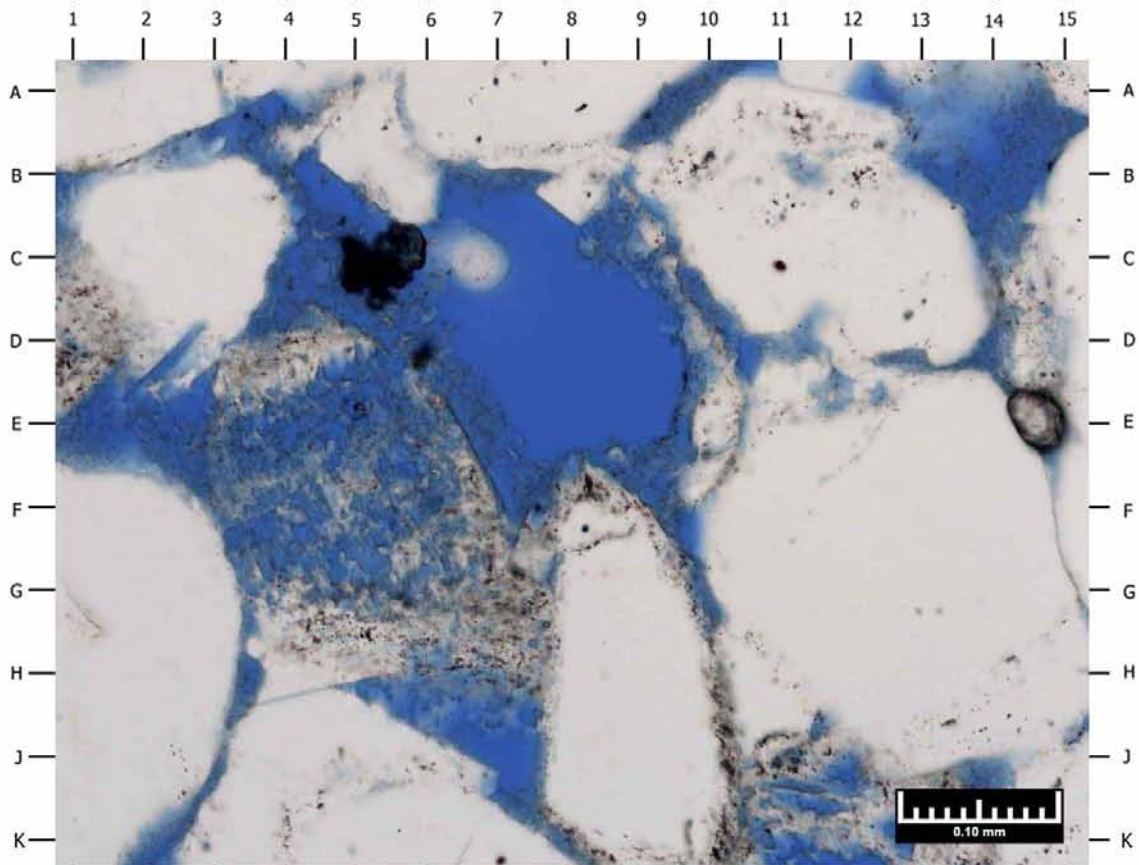

B

200X

Ohio Division of Geological Survey **OMNI File No: HH-38266**
CO_2 No. 1 Well
Tuscarawas County, Ohio
Cambrian Basal Sandstone
Rotary Sidewall Core

THIN SECTION PHOTOMICROGRAPHS

SAMPLE DEPTH: 8603.0 FEET
SAMPLE NUMBER: 1-77R

Plate 77

Permeability (Klink.): 0.120 mD Porosity (NCS): 8.8% Grain Density: 2.62 gm/cc

Sample not selected for petrographic analysis.

Magnification: A: 40X B: 200X

Ohio Division of Geological Survey
CO2 No. 1
Tuscarawas County, Ohio

8603.0'
Plate 77

Weatherford LABORATORIES

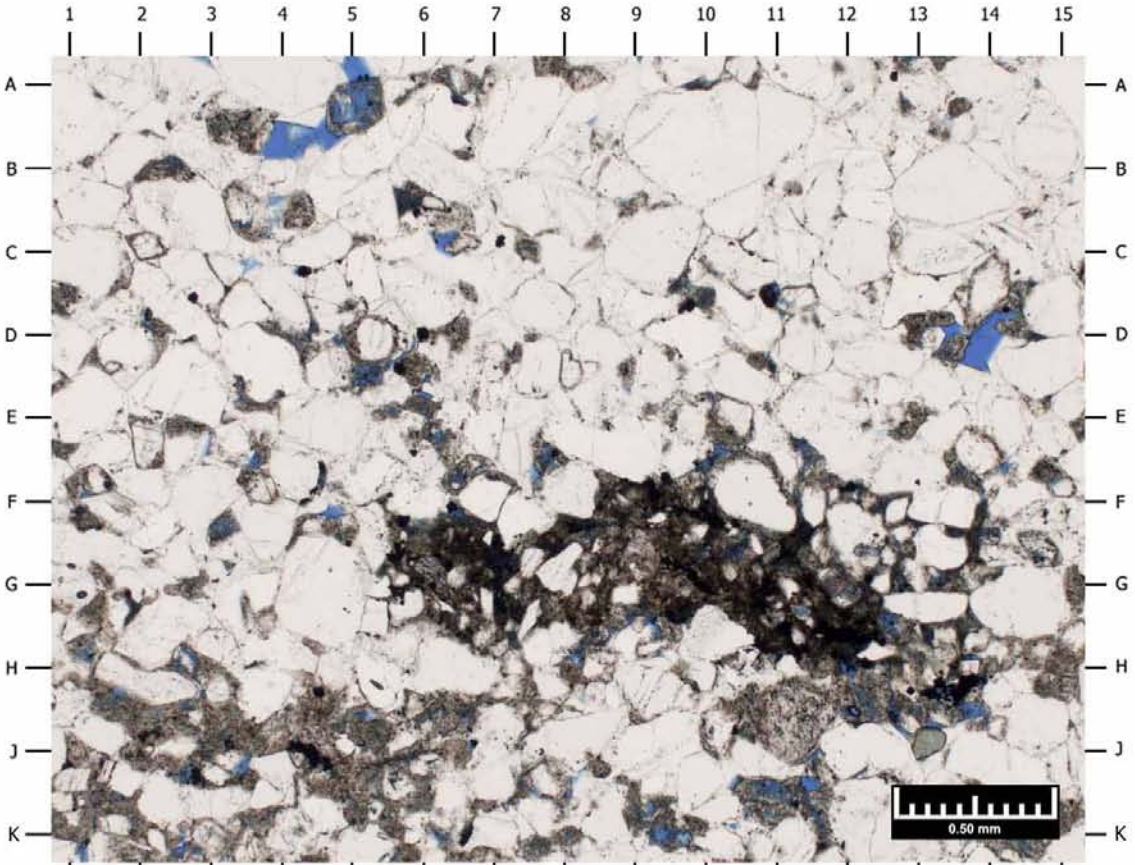

A

40X

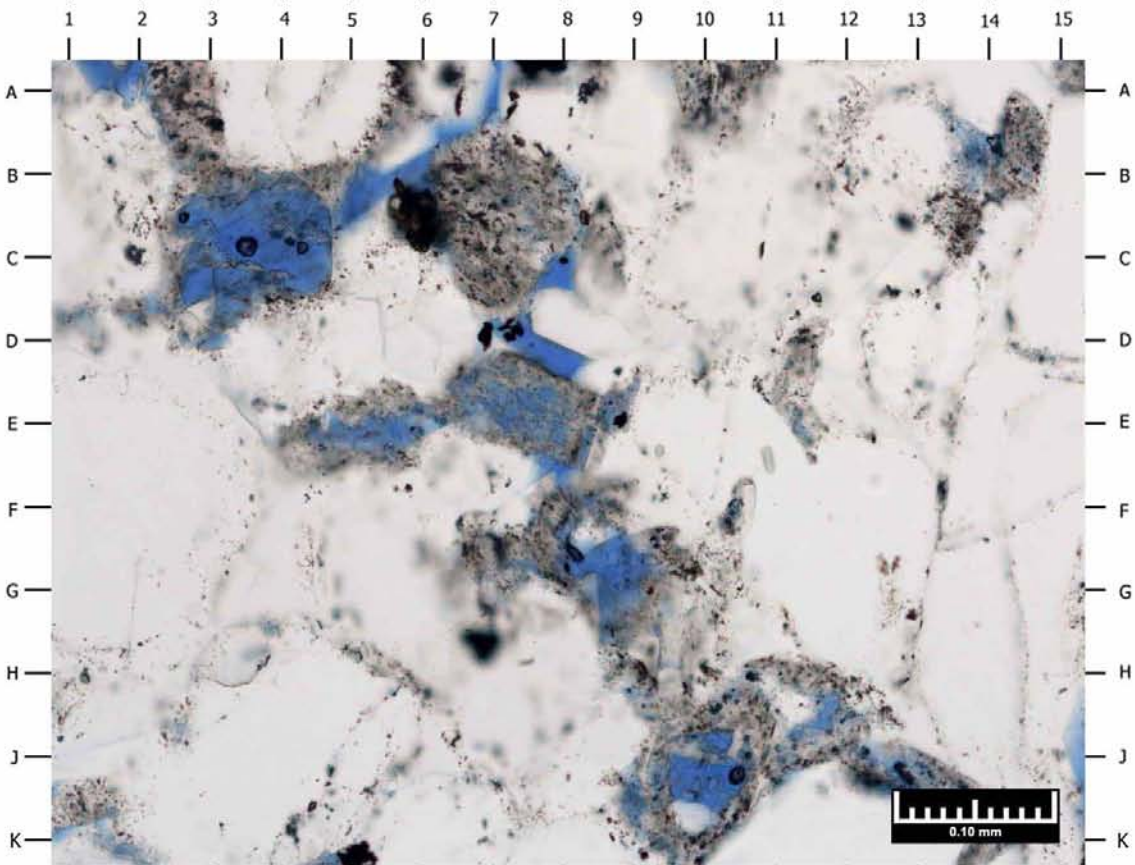

B

200X

Ohio Division of Geological Survey **OMNI File No: HH-38266**
CO_2 No. 1 Well
Tuscarawas County, Ohio
Cambrian Basal Sandstone
Rotary Sidewall Core

THIN SECTION PHOTOMICROGRAPHS

SAMPLE DEPTH: 8610.0 FEET
SAMPLE NUMBER: 1-78R

Plate 78

Permeability (Klink.): 0.044 mD Porosity (NCS): 8.0% Grain Density: 2.60 gm/cc

Sample not selected for petrographic analysis.

Magnification: A: 40X B: 200X

Ohio Division of Geological Survey
CO2 No. 1
Tuscarawas County, Ohio

8610.0'
Plate 78

Weatherford LABORATORIES

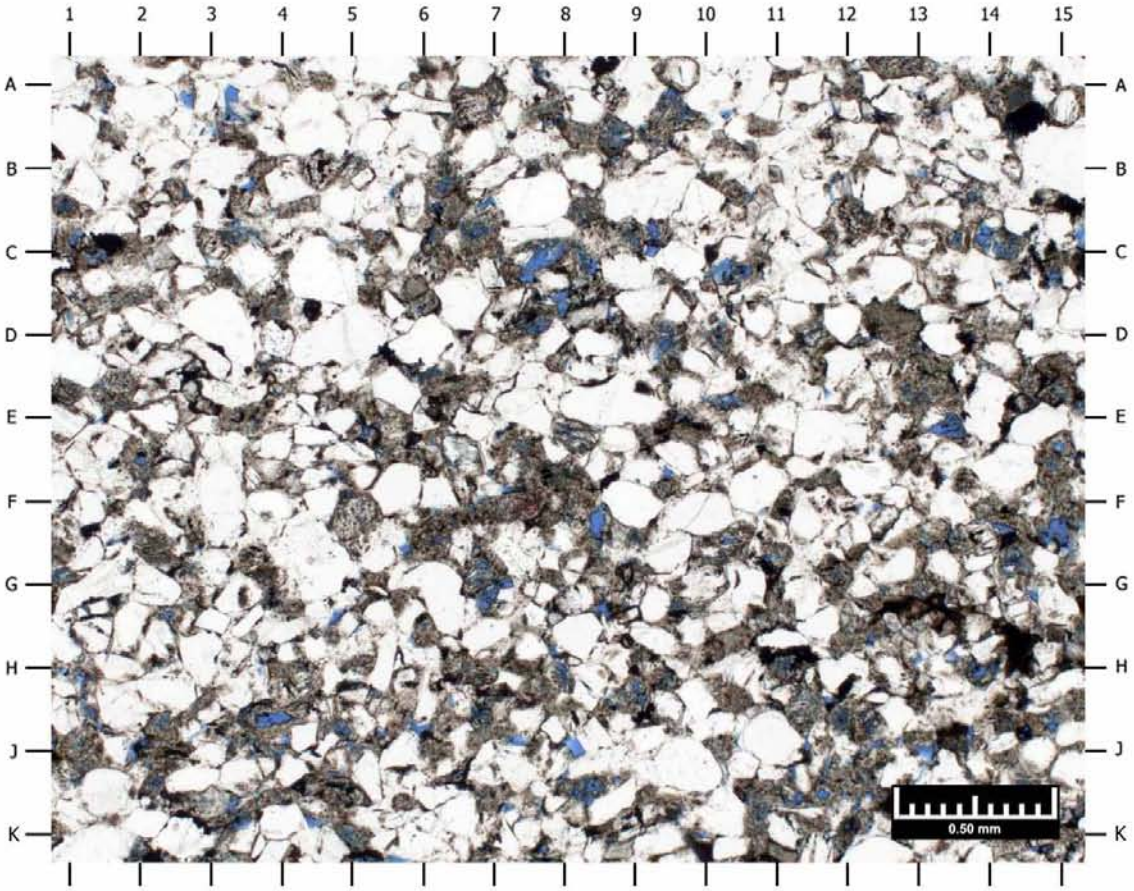

A

40X

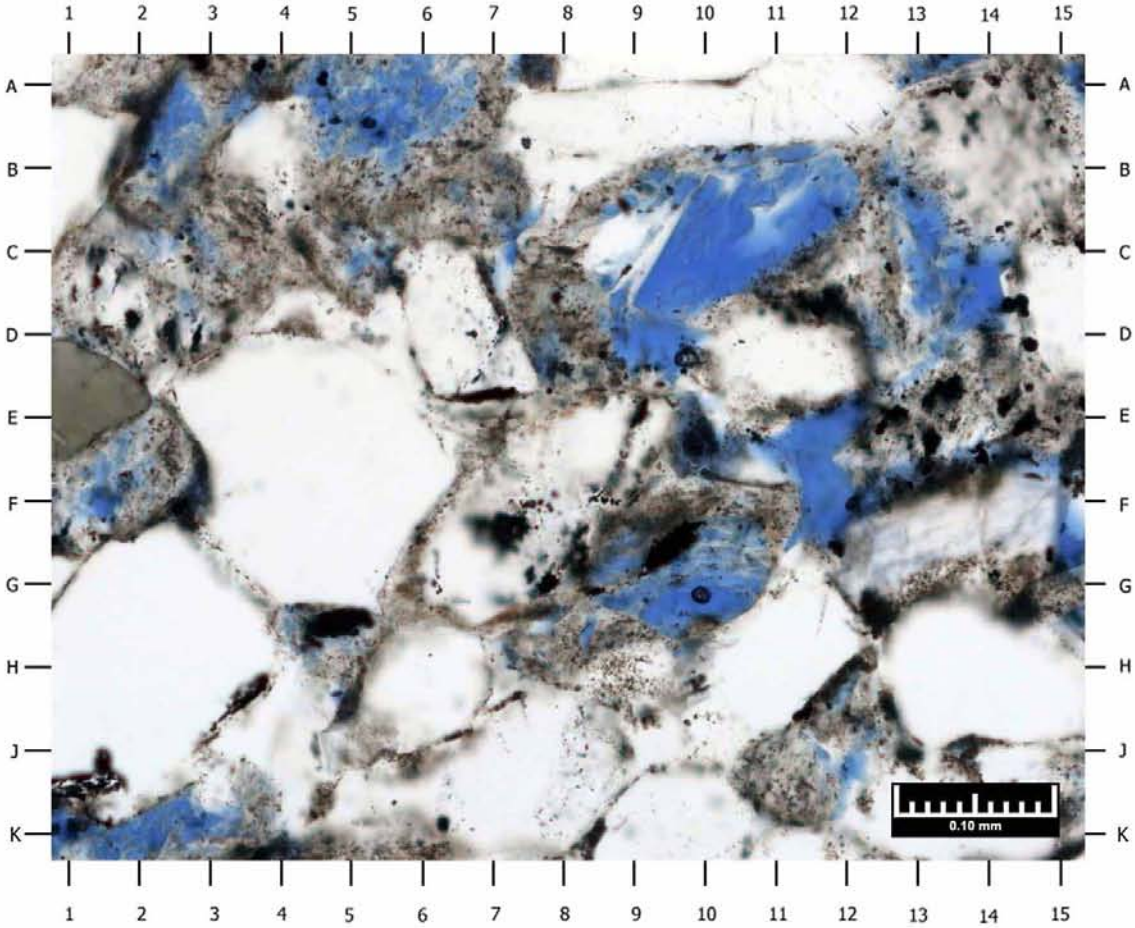

B

200X

Ohio Division of Geological Survey **OMNI File No: HH-38266**
CO_2 No. 1 Well
Tuscarawas County, Ohio
Pre Cambrian Basement
Rotary Sidewall Core

THIN SECTION DESCRIPTION - DETAILED

SAMPLE DEPTH: 8628.0 FEET
SAMPLE NUMBER: 1-79R

Plate 79

Permeability (Klink.): <0.0001 mD Porosity (NCS): 1.6% Grain Density: 2.75 gm/cc

Lithology:	Banded gneiss (slightly weathered); protolith was likely a granite or arkose
Fabric:	Granoblastic in the coarse-crystalline band to foliated/ cataclastic in the chlorite/biotite-rich band
Metamorphic Facies:	High grade regional metamorphism (amphibolite facies?)
Mineral Composition:	
Major:	Quartz (polycrystalline with moderate to intense undulatory extinction; commonly occupies re-entrants or as bleb-like inclusions in feldspar), microcline (commonly crushed / fractured and altered to sericite), and calcic plagioclase feldspar (variably altered to saussurite?), biotite / chlorite
Accessory:	Hematite and magnetite (replacements after biotite); garnet
Replacement Minerals:	Trace amount of replacement calcite; minor amount of pyrite and Fe/Ti oxides; sericite and epidote? sometimes fills microfractures or replaces fractured feldspar grain boundaries
Porosity Types:	No visible macropores
Reservoir Quality:	N/A

Magnification: A: 40X B: 200X

A) The boundary between the granoblastic band and foliated chlorite / biotite-rich band in this banded gneiss extends from F1 to F15. Minerals include quartz (D6), biotite / chlorite (H10.5), altered feldspar (C8), magnetite (K10, and calcite (stained red; F13). Note the late-stage veinlet filled with possible sericite (?) and epidote (?) extending from A5 to K15.

B) Detailed view of the area around F8 shows the extensive alteration of feldspar (B5, H13) and biotite / chlorite (K5 to K15). Late-stage calcite partially replaces feldspar crystals (E6.5, HJ15).

Ohio Division of Geological Survey
CO2 No. 1
Tuscarawas County, Ohio

8628.0'
Plate 79

Weatherford LABORATORIES

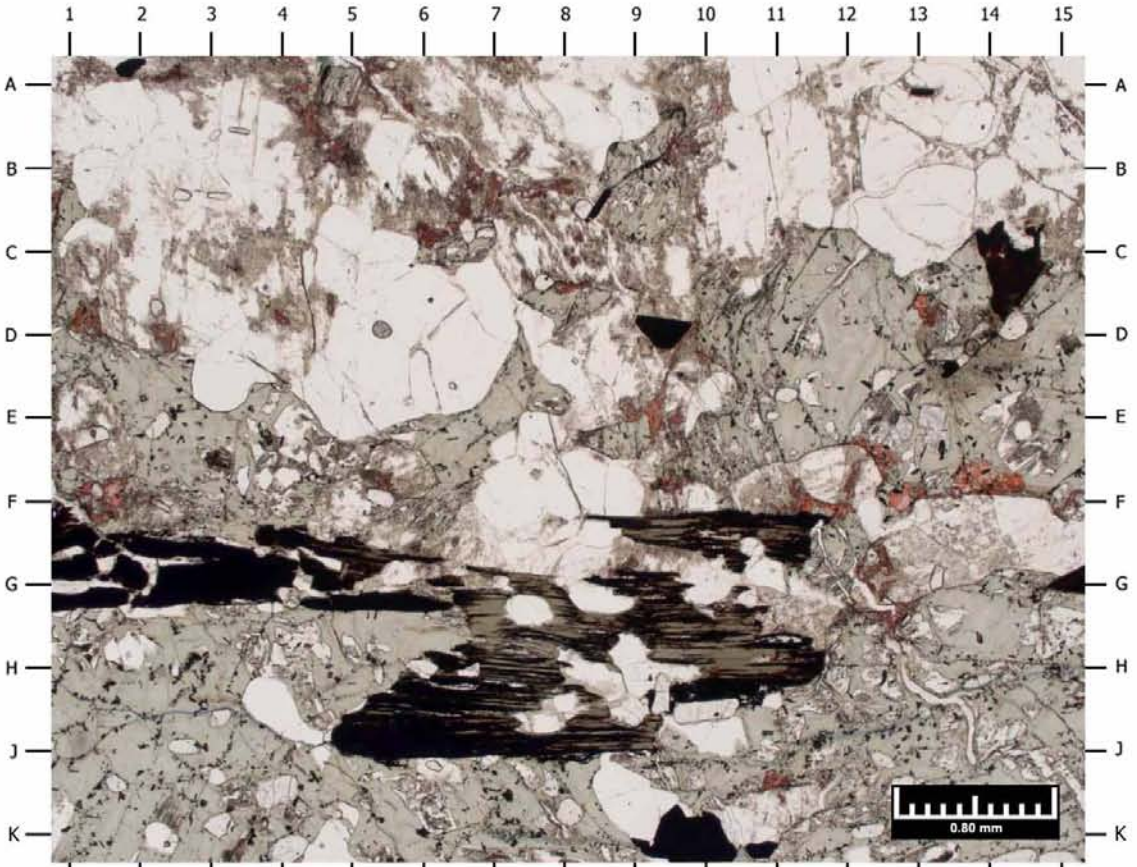

A

25X

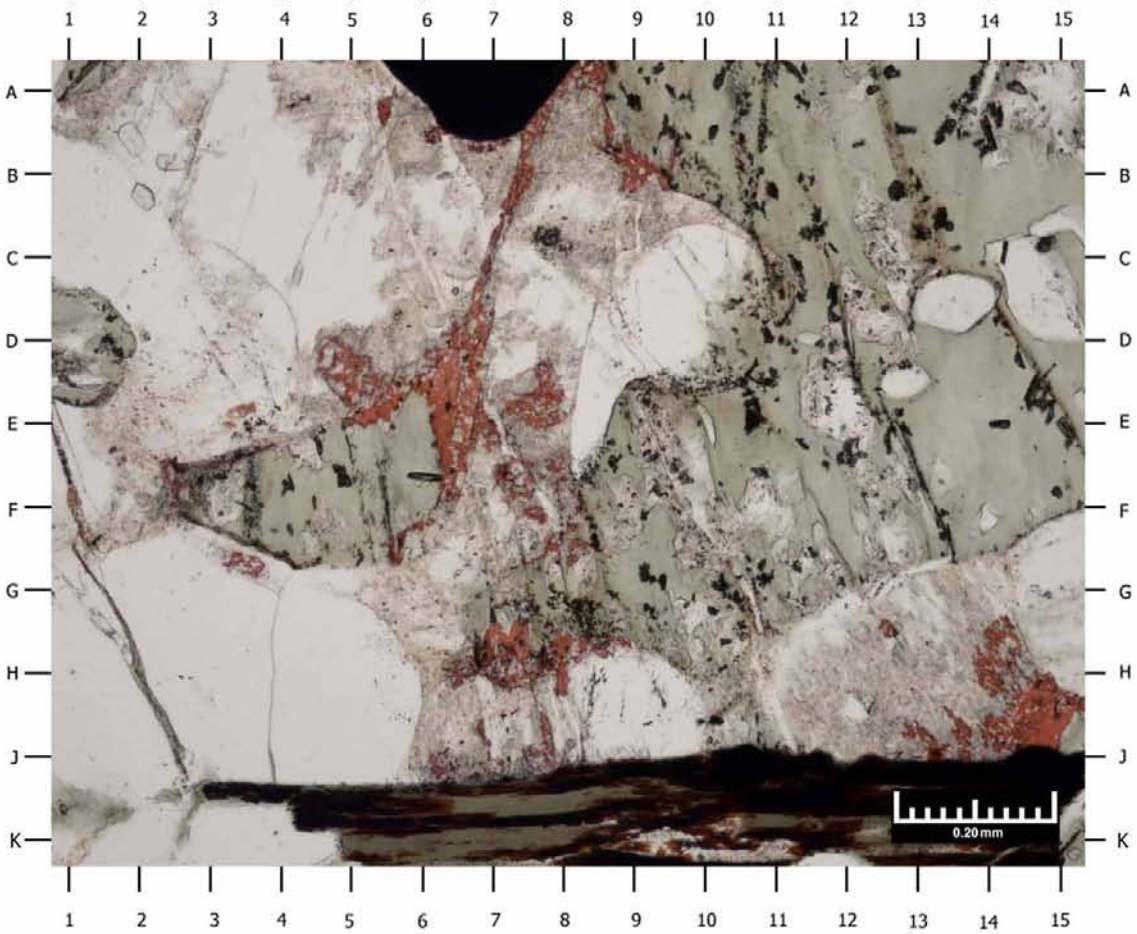

B

100X

Ohio Division of Geological Survey **OMNI File No: HH-38266**
CO_2 No. 1 Well
Tuscarawas County, Ohio
Pre Cambrian Basement
Rotary Sidewall Core

THIN SECTION PHOTOMICROGRAPHS

SAMPLE DEPTH: 8643.0 FEET
SAMPLE NUMBER: 1-80R

Plate 80

Permeability (Klink.): <0.0001 mD Porosity (NCS): 0.2% Grain Density: 3.07 gm/cc

Sample not selected for petrographic analysis.

Magnification: A: 40X B: 200X

Ohio Division of Geological Survey
CO2 No. 1
Tuscarawas County, Ohio

8643.0'
Plate 80

Weatherford LABORATORIES

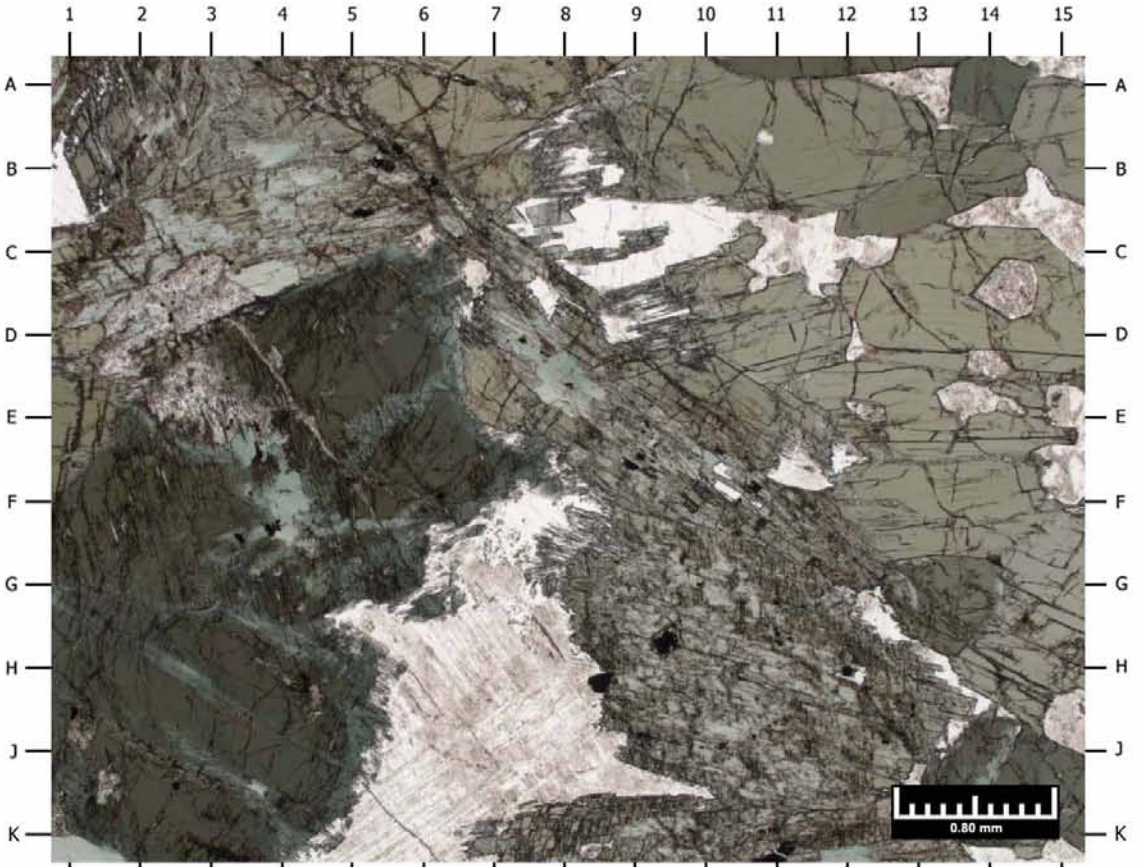

A

25X

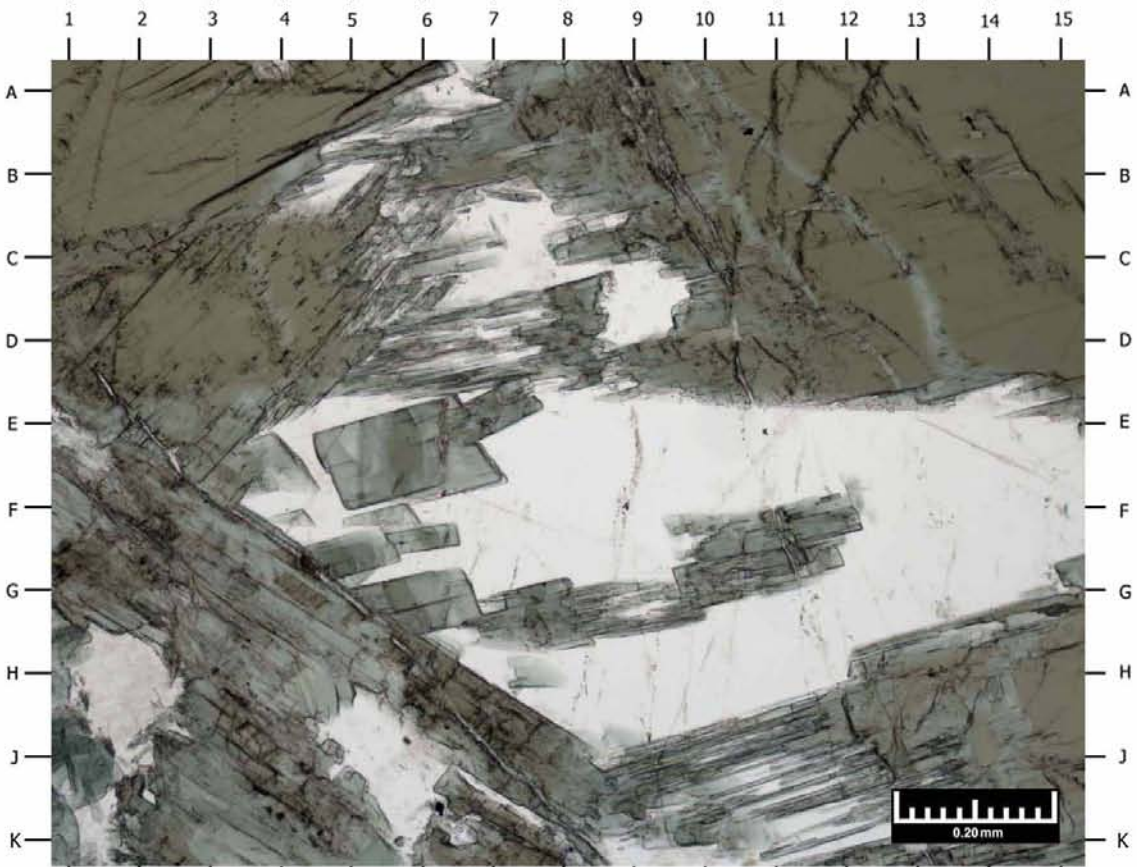

B

100X

Ohio Division of Geological Survey **OMNI File No: HH-38266**
CO_2 No. 1 Well
Tuscarawas County, Ohio
Pre Cambrian Basement
Rotary Sidewall Core

THIN SECTION PHOTOMICROGRAPHS

SAMPLE DEPTH: 8659.0 FEET
SAMPLE NUMBER: 1-81R

Plate 81

Permeability (Klink.): <0.0001 mD Porosity (NCS): 0.5% Grain Density: 2.98 gm/cc

Sample not selected for petrographic analysis.

Magnification: A: 40X B: 200X

Ohio Division of Geological Survey
CO2 No. 1
Tuscarawas County, Ohio

8659.0'
Plate 81

Weatherford LABORATORIES

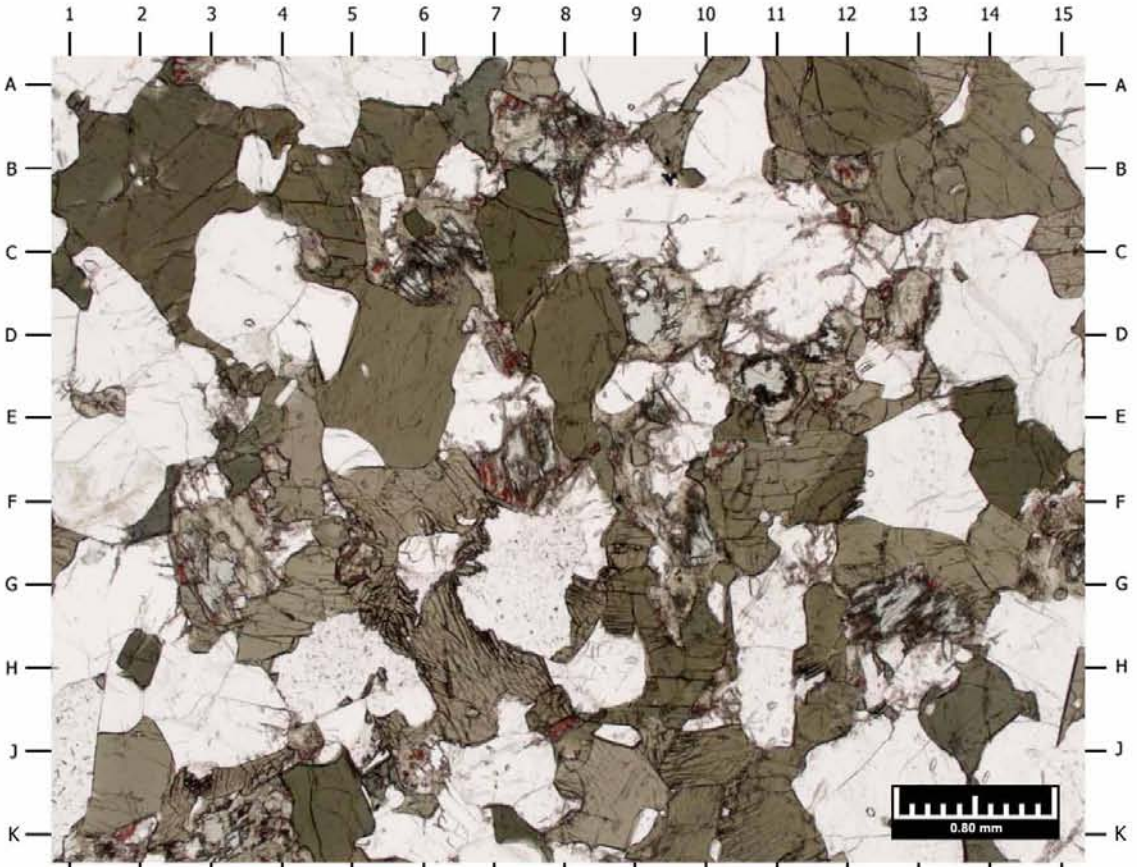

A

25X

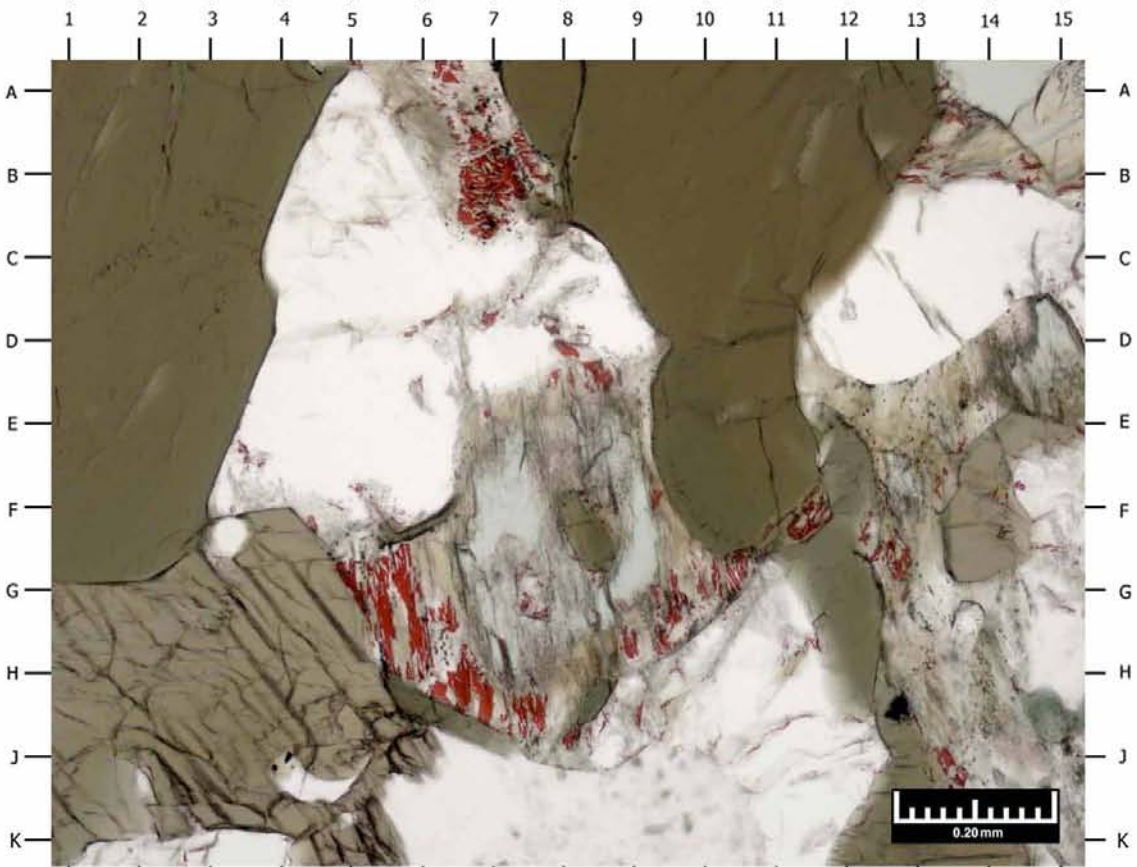

B

100X

Ohio Division of Geological Survey **OMNI File No: HH-38266**
CO_2 No. 1 Well
Tuscarawas County, Ohio
Pre Cambrian Basement
Rotary Sidewall Core

THIN SECTION PHOTOMICROGRAPHS

SAMPLE DEPTH: 8688.0 FEET
SAMPLE NUMBER: 1-82R

Plate 82

Permeability (Klink.): <0.0001 mD Porosity (NCS): 0.3% Grain Density: 2.69 gm/cc

Sample not selected for petrographic analysis.

Magnification: A: 40X B: 200X

Ohio Division of Geological Survey
CO2 No. 1
Tuscarawas County, Ohio

8688.0'
Plate 82

Weatherford LABORATORIES

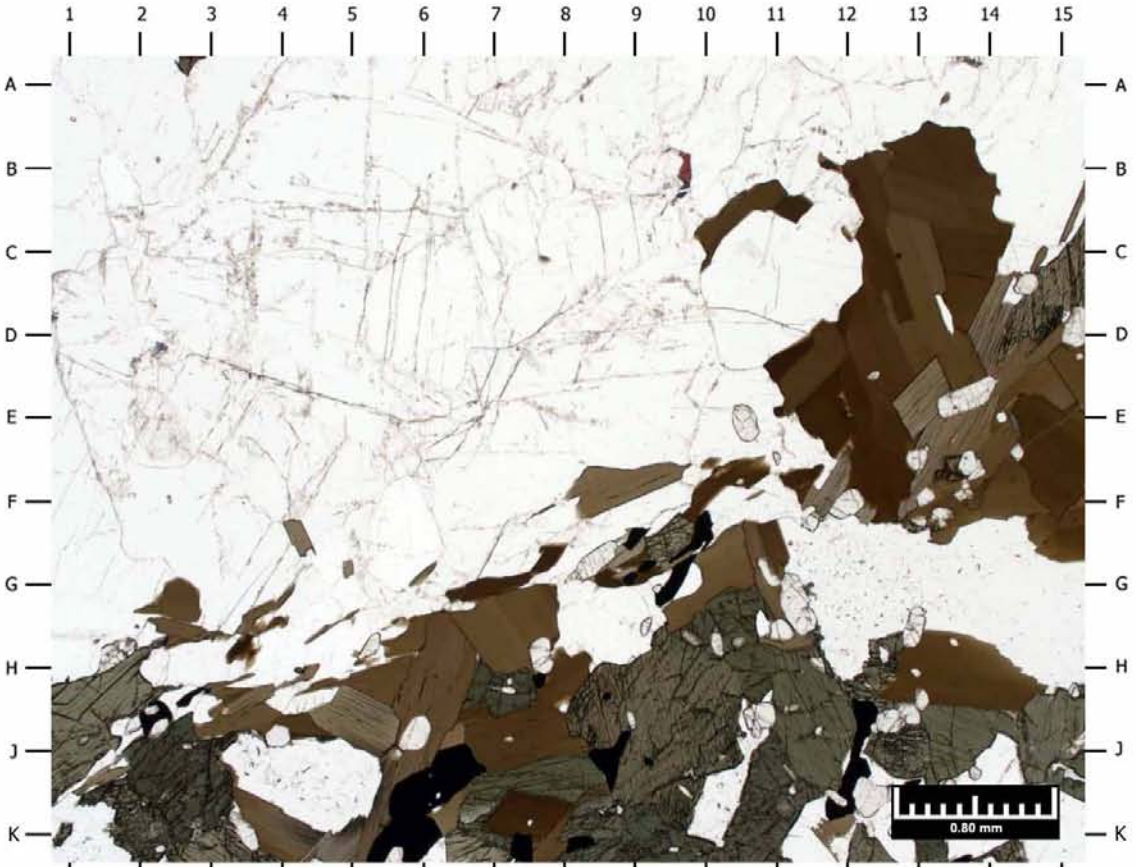

A

25X

B

100X

INTENTIONALLY BLANK

APPENDIX E

SCANNING ELECTRON MICROSCOPY PHOTOMICROGRAPHS AND DESCRIPTIONS

(Note the micron bar at the basal center of each photomicrograph for scale)

Ohio Division of Geological Survey **OMNI File No.: HH-38266**
CO_2 No. 1
Tuscarawas County, Ohio
Clinton Sandstone Formation
Rotary Sidewall Core

SAMPLE DEPTH: 4771.0 FEET
SAMPLE NUMBER: 1-3R

PLATE 83

This quartzarenite is moderately well sorted with an average grain size of 0.10 mm. Quartz (Plate A; C2,E7 / Plate B; B2,B14 / Plate C; E14,K1) is the primary detrital grain type. A rare leached potassium feldspar grain (Plate C; D4-H10), with secondary dissolution pores is visible. Quartz overgrowths (Plate B; G11,L7 / Plate C; F12 / Plate D; L9) are the dominant cement. Intergranular pores (Plate A; B10.8,B-C8,J10 / Plate B; F7 / Plate D; G9) are occluded by chlorite (Plate B; E8,H7 / Plate D; F5,G6) and fibrous illite (Plate B; C9,E-F6 / Plate C; L7,M10 / Plate D; D10,G1) clays.

Magnification: 83A - 100X
Magnification: 83B - 1500X
Magnification: 83C - 1000X
Magnification: 83D - 5000X

Ohio Division of Geological Survey
CO2 No. 1
Tuscarawas County, Ohio

4771.00'
Plate 83

OMNI Laboratories, Inc.

A

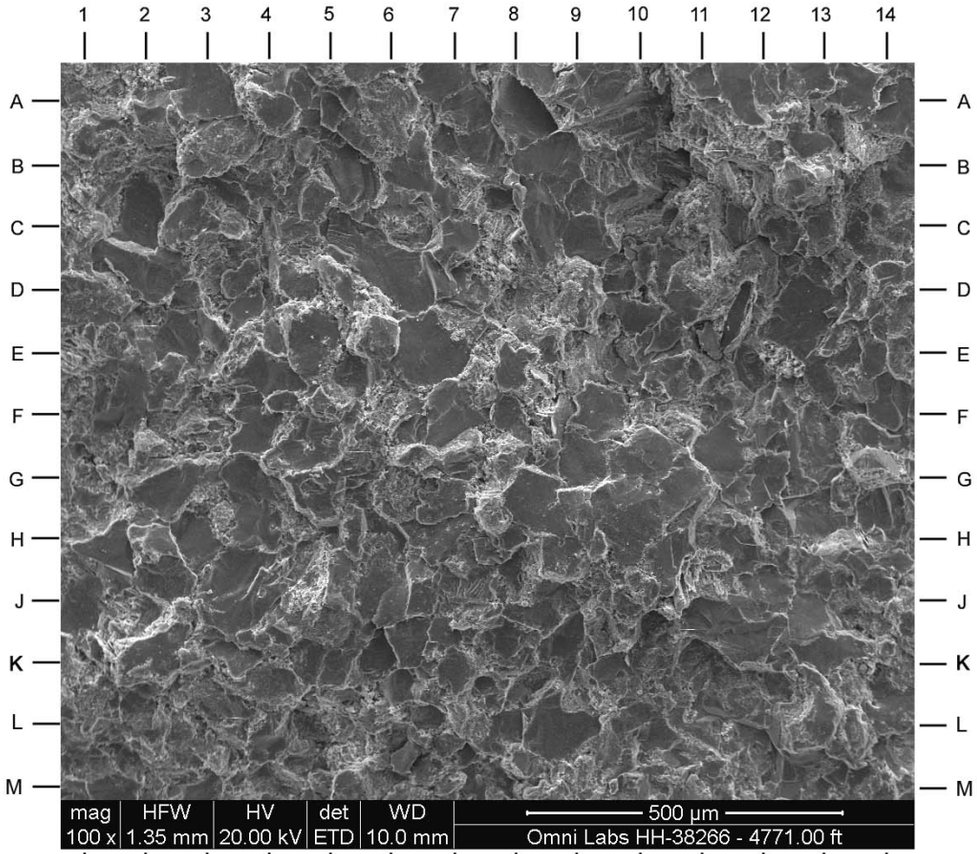

B

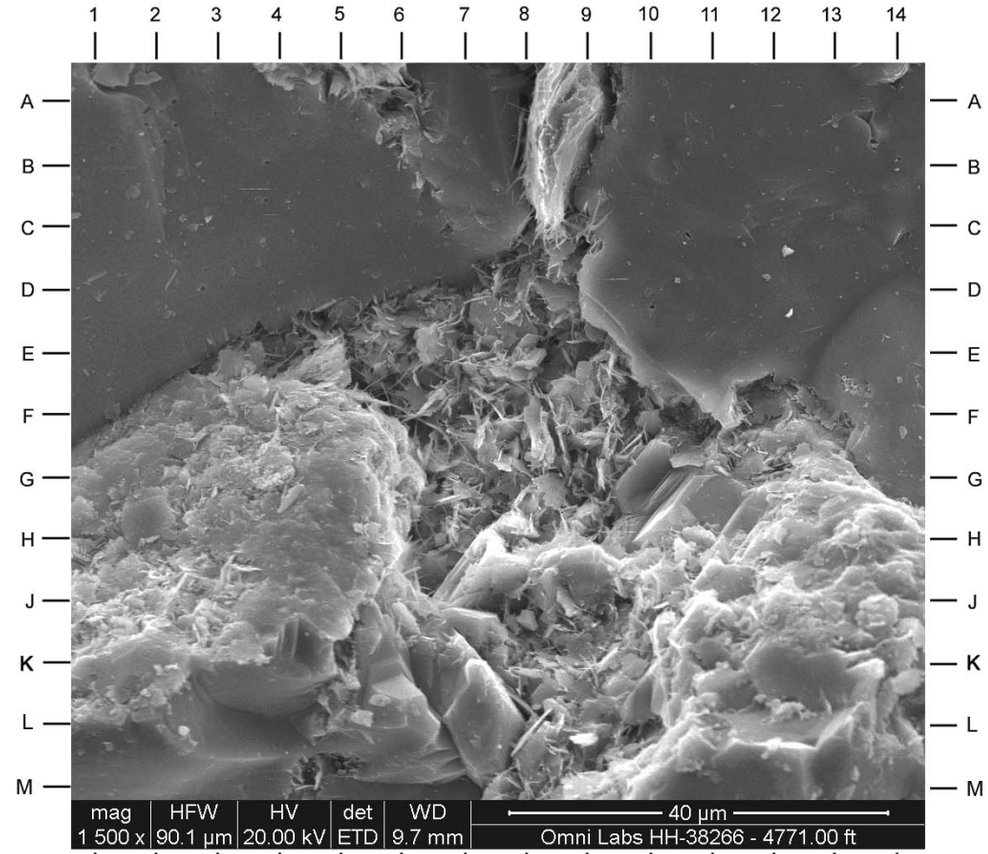

C

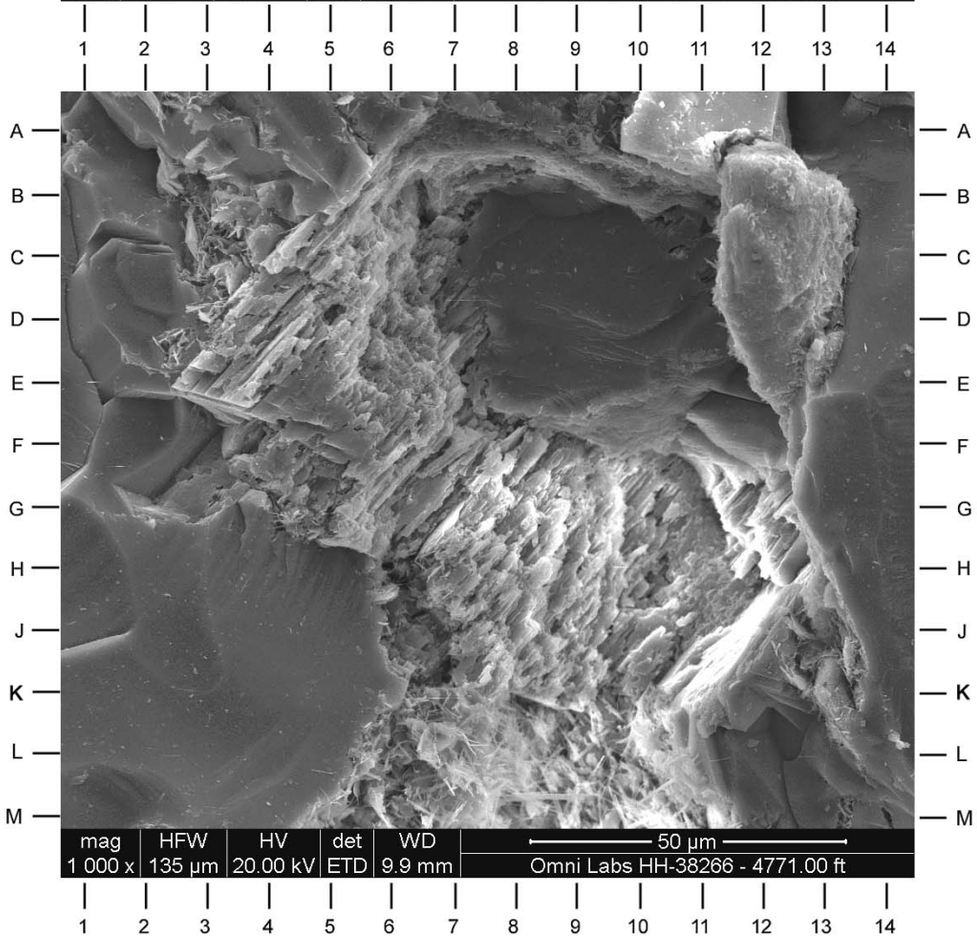

D

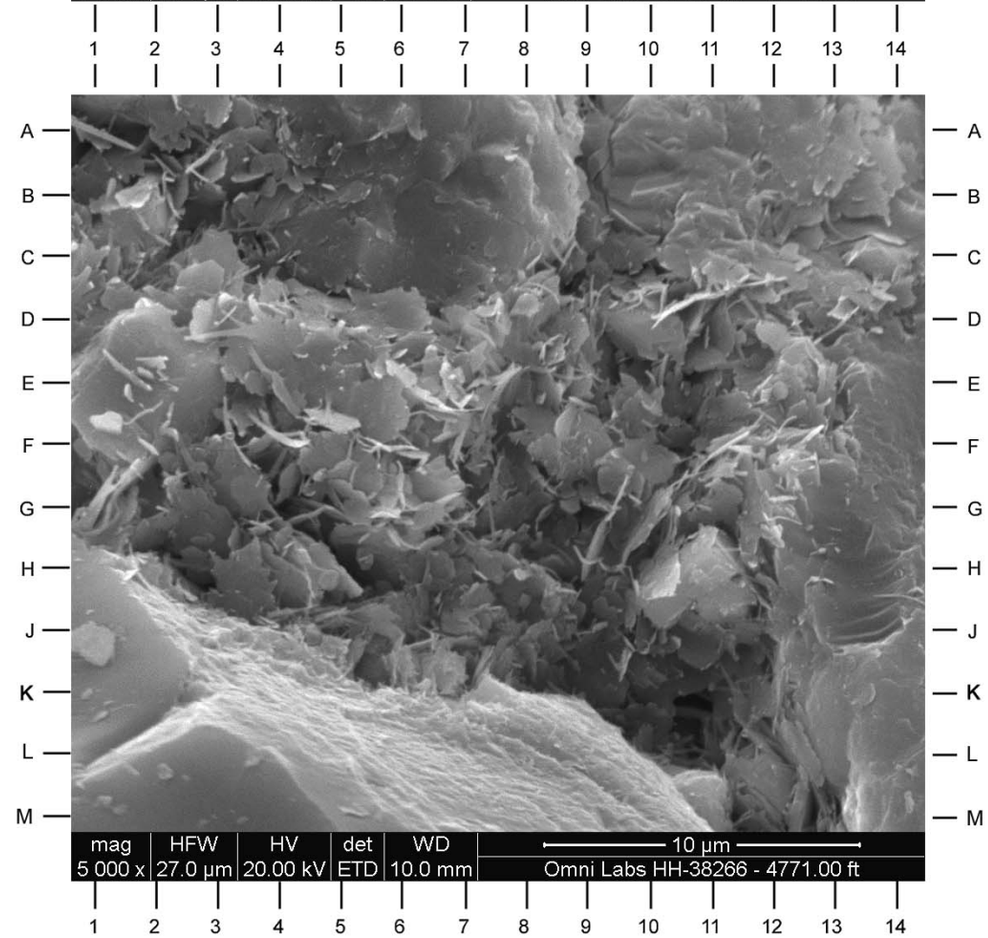

Ohio Division of Geological Survey **OMNI File No.: HH-38266**
CO_2 No. 1
Tuscarawas County, Ohio
Clinton Sandstone Formation
Rotary Sidewall Core

SAMPLE DEPTH: 4790.0 FEET
SAMPLE NUMBER: 1-5R

PLATE 84

This sublitharenite is moderately sorted with an average grain size of 0.11 mm. Primary intergranular pores (Plate A; B0.5,C-D13 / Plate C; G7 / Plate D; D9.5) are typically reduced by quartz overgrowth cement (Plate B; D11,F12,J3 / Plate C; F7,H6,H8 / Plate D; B8,H11.5) and a combination of authigenic illite and chlorite clays (Plate C; B7 / Plate D; E11,G7,J11). Quartz (Plate A; D3,J7,J10 / Plate B; B2,G14 / Plate D; H14) is the primary detrital grain type. A microporous glauconite grain (Plate B; G7) is well cemented by surrounding quartz grains.

Magnification: 84A - 100X
Magnification: 84B - 800X
Magnification: 84C - 1300X
Magnification: 84D - 4000X

Ohio Division of Geological Survey
CO2 No. 1
Tuscarawas County, Ohio

4790.00'
Plate 84

Omni Laboratories, Inc.

A

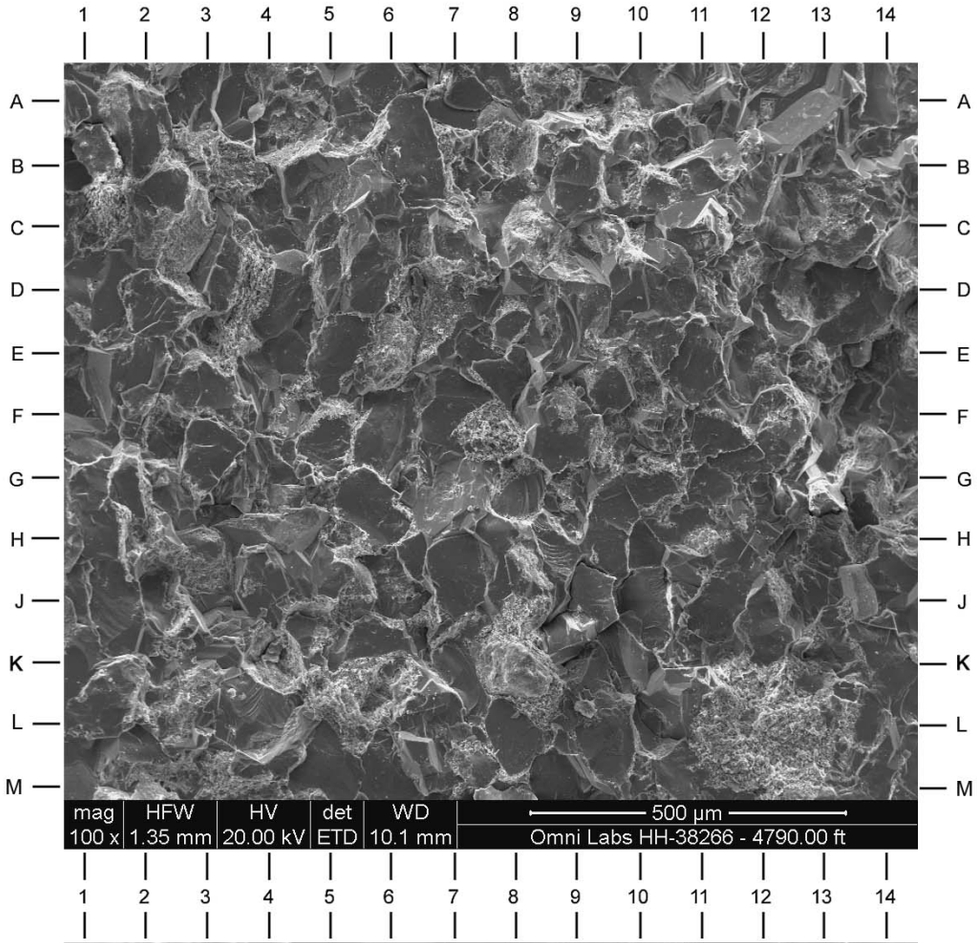

B

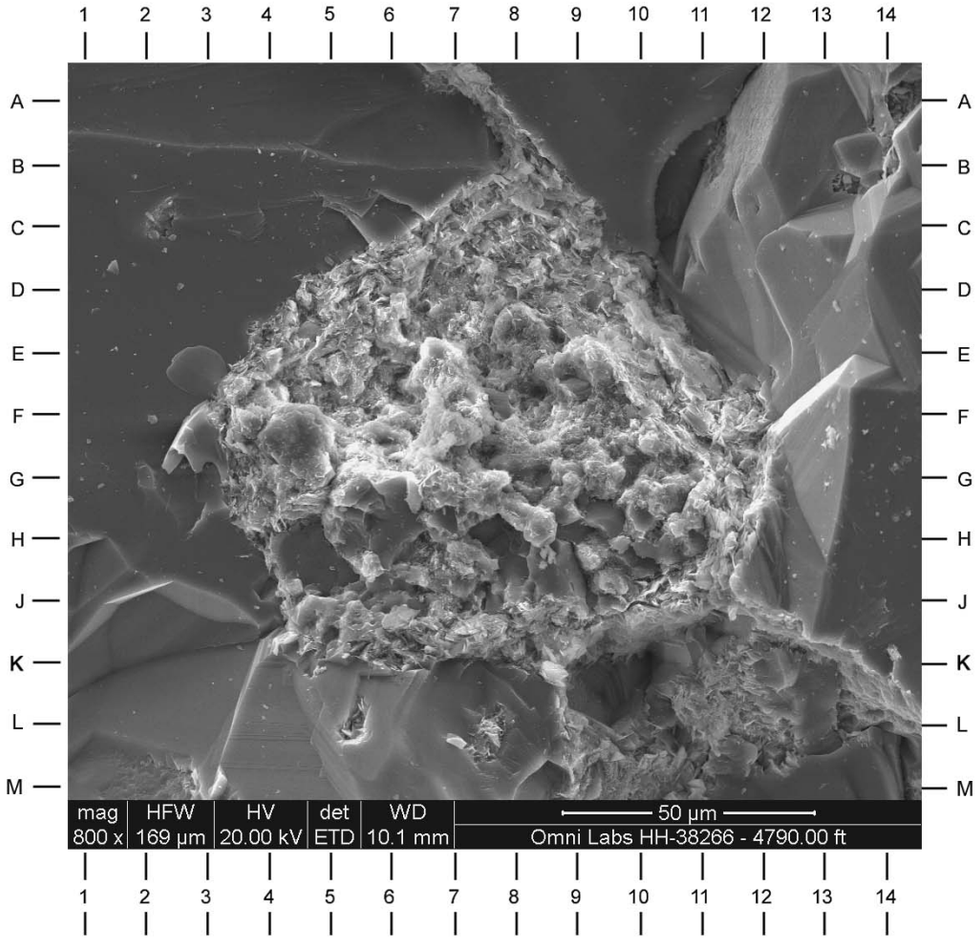

C

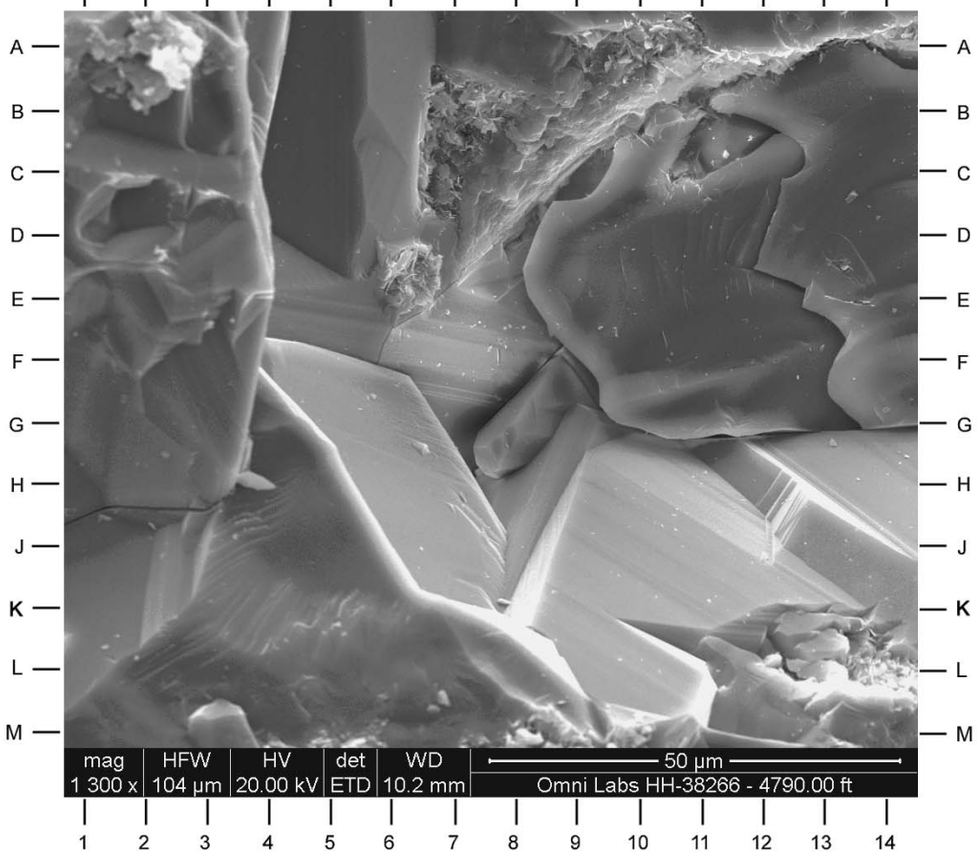

D

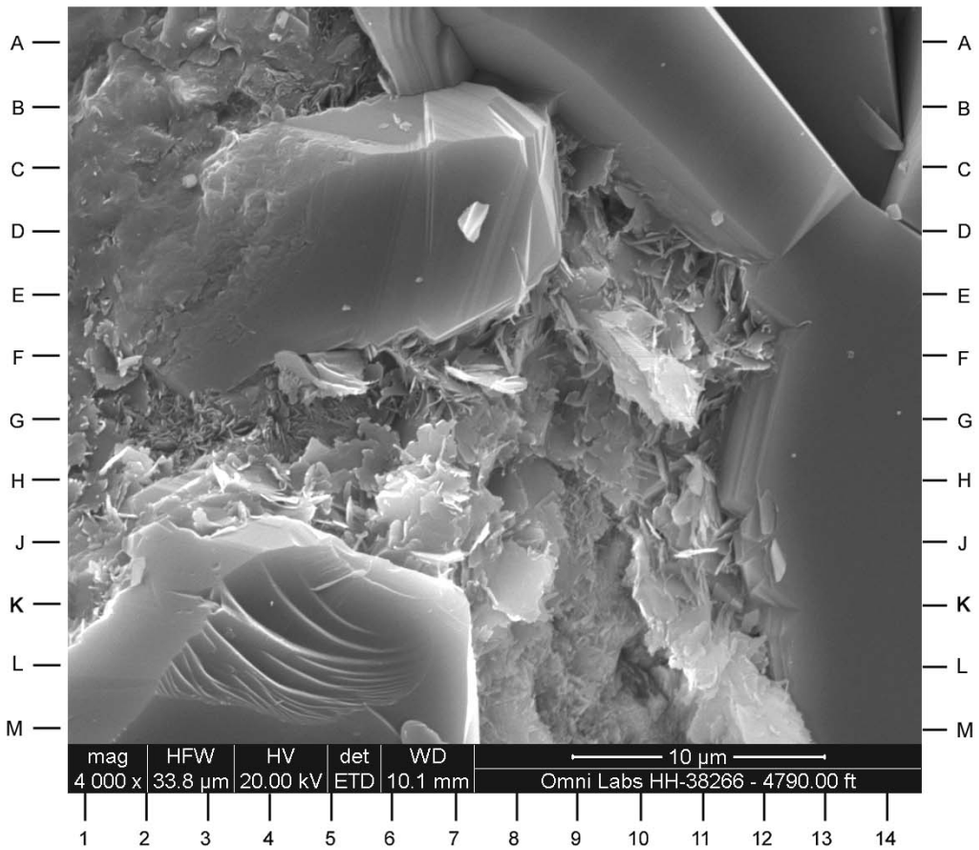

Ohio Division of Geological Survey **OMNI File No.: HH-38266**
CO_2 No. 1
Tuscarawas County, Ohio
Clinton Sandstone Formation
Rotary Sidewall Core

SAMPLE DEPTH: 4840.0 FEET
SAMPLE NUMBER: 1-9R

PLATE 85

This sublitharenite/subarkose is well sorted with an average grain size of 0.15 mm. Quartz (Plate A; C8,E11,H9 / Plate B; L2,K11 / Plate D; A4,A14,L12) is the primary detrital grain type with lesser amounts of altered calcium plagioclase (Plate B; B3,B13) and potassium feldspar (Plate C; G8). Detrital grains are predominantly cemented by quartz overgrowths (Plate B; G6,G8 / Plate C; E12,J5 / Plate D; F9,E7); however, ferroan dolomite (ankerite) cement (Plate D; K1-M6) is also present. Primary intergranular pores (Plate A; B3.3,C8.6,GH12.8 / Plate B; J8 / Plate D; E7.5) dominate the pore system with partially dissolved grains (Plate C; E8) containing secondary intragranular pores also present. Fibrous illite (Plate B; C7.2,K14 / Plate D; B9,H8,K5), inter-mixed with chlorite (Plate B; C7,G12 / Plate D; B10,F12,K6), coats grains and lines pore throats.

Magnification: 85A - 100X
Magnification: 85B - 1000X
Magnification: 85C - 700X
Magnification: 85D - 1800X

Ohio Division of Geological Survey
CO2 No. 1
Tuscarawas County, Ohio

4840.00'
Plate 85

A

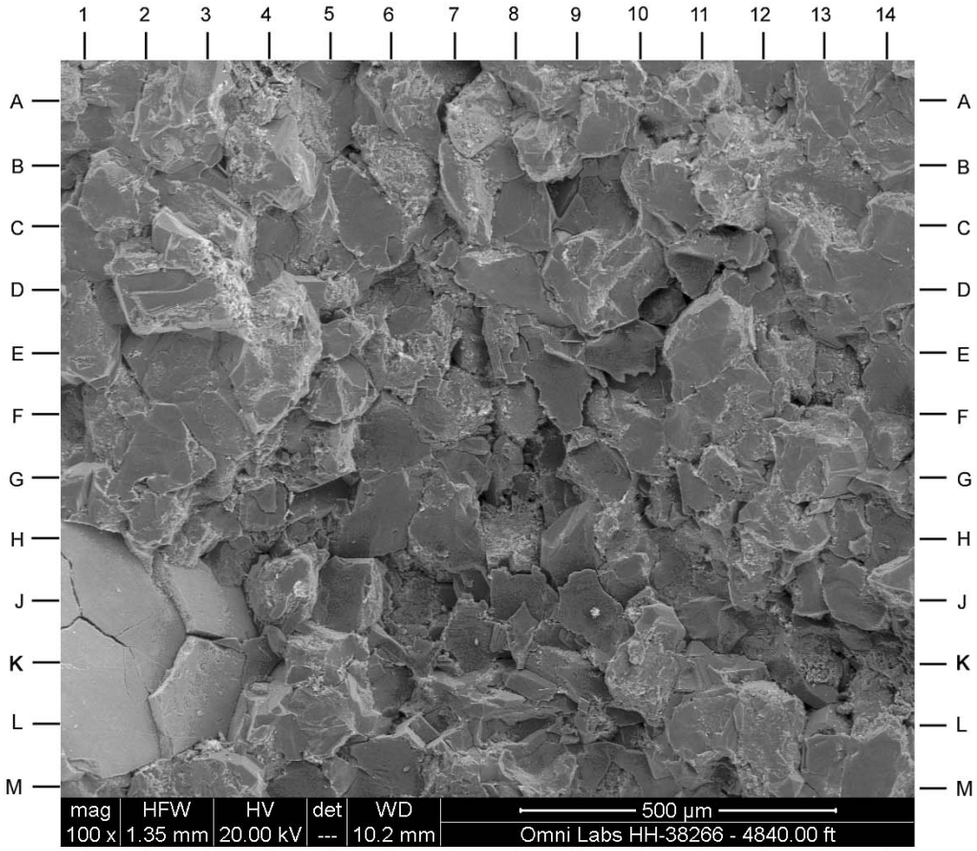

B

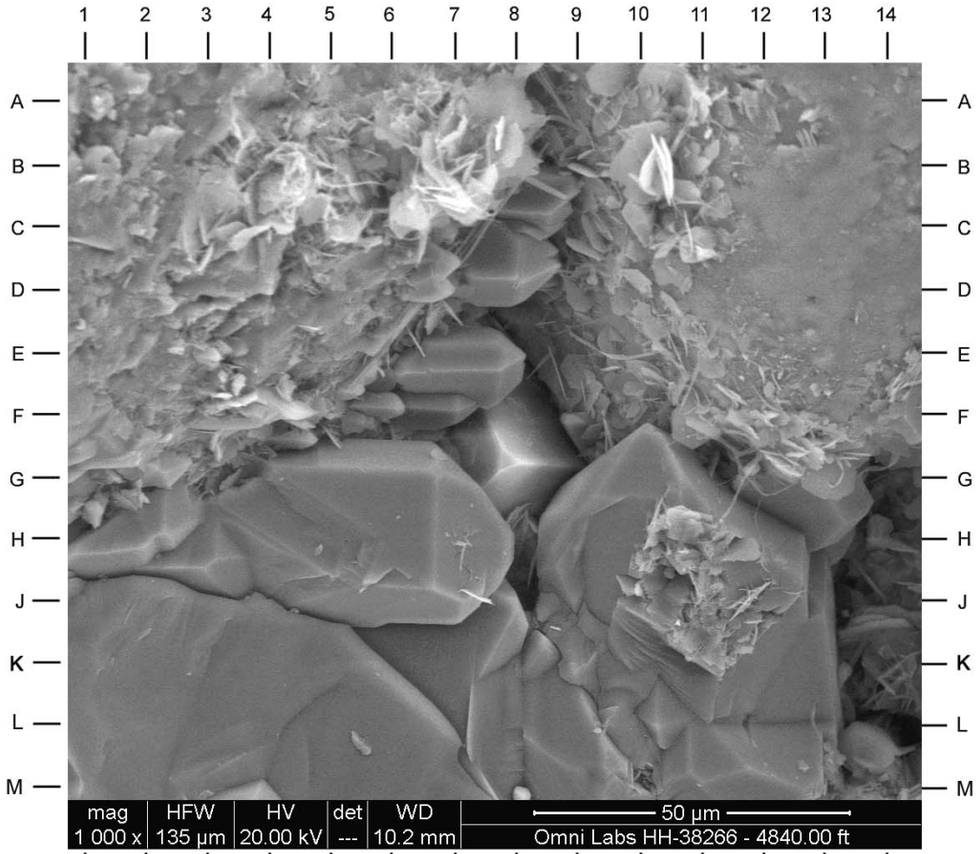

C

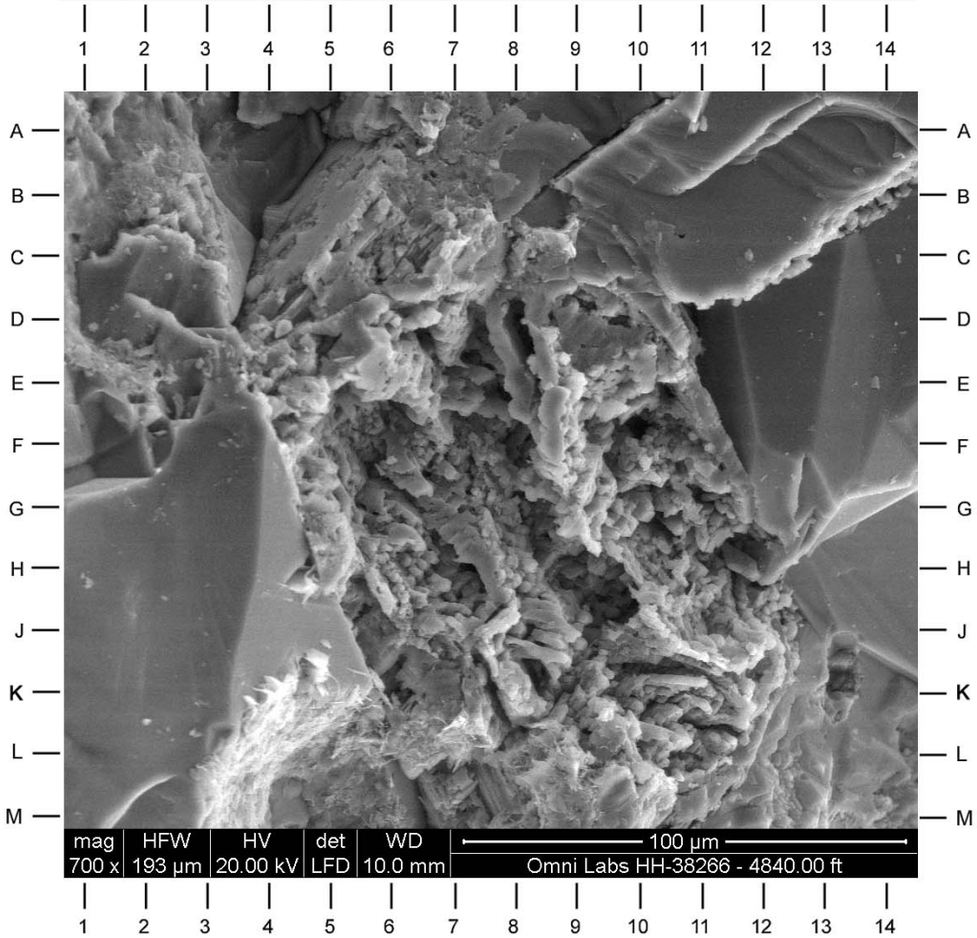

D

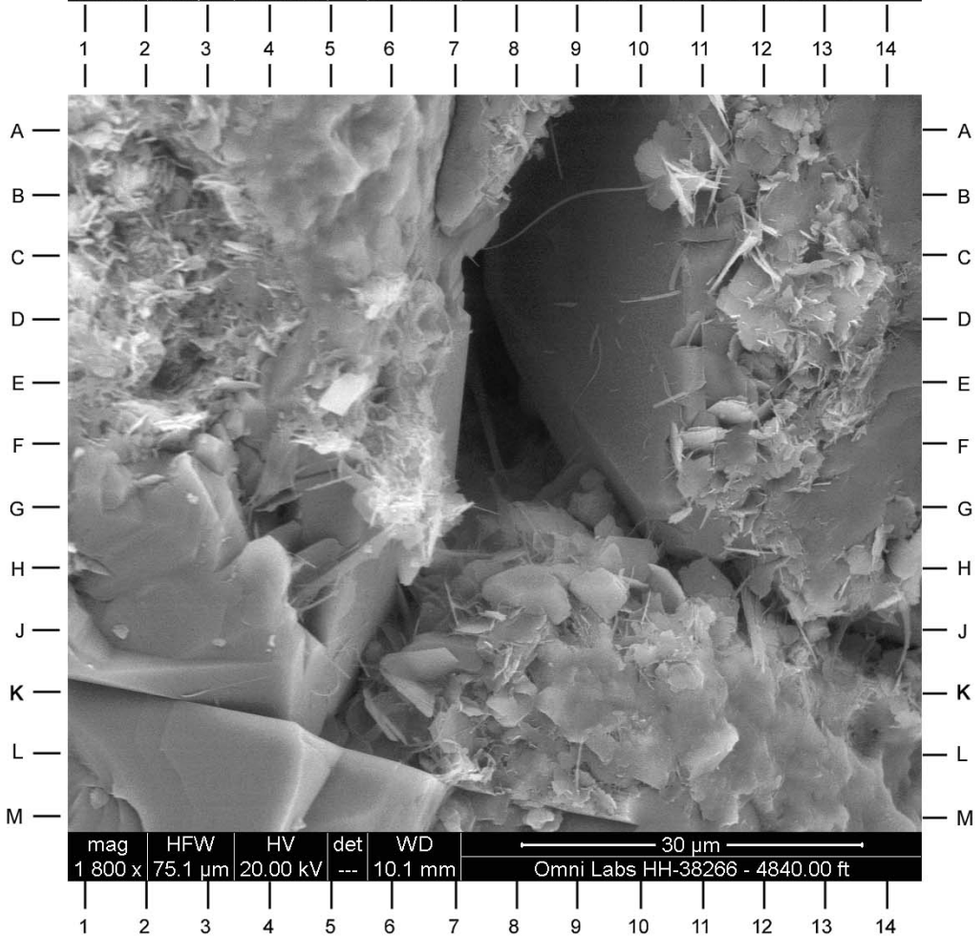

Ohio Division of Geological Survey **OMNI File No.: HH-38266**
CO_2 No. 1
Tuscarawas County, Ohio
Black River Group
Rotary Sidewall Core

SAMPLE DEPTH: 6794.0 FEET
SAMPLE NUMBER: 1-20R

PLATE 86

This skeletal/peloidal lime packstone/grainstone sample contains discontinuous laminations and microstylolites. The pore network is dominated by intercrystalline micropores between calcite crystals (Plate B; C10-K4 / Plate C / Plate D) and intraparticle pores (Plate A; D5.5,J11). Sparry calcite (Plate B; A7-D4,A11-J14,L2,L11) is the primary cement with lesser amounts of dolomite cement (Plate A; H8). A recrystallized skeletal fragment is visible in Plate A at K12.

Magnification: 86A - 200X
Magnification: 86B - 800X
Magnification: 86C - 3000X
Magnification: 86D - 8000X

Ohio Division of Geological Survey
CO2 No. 1
Tuscarawas County, Ohio

6794.00'
Plate 86

Omni Laboratories, Inc.

A

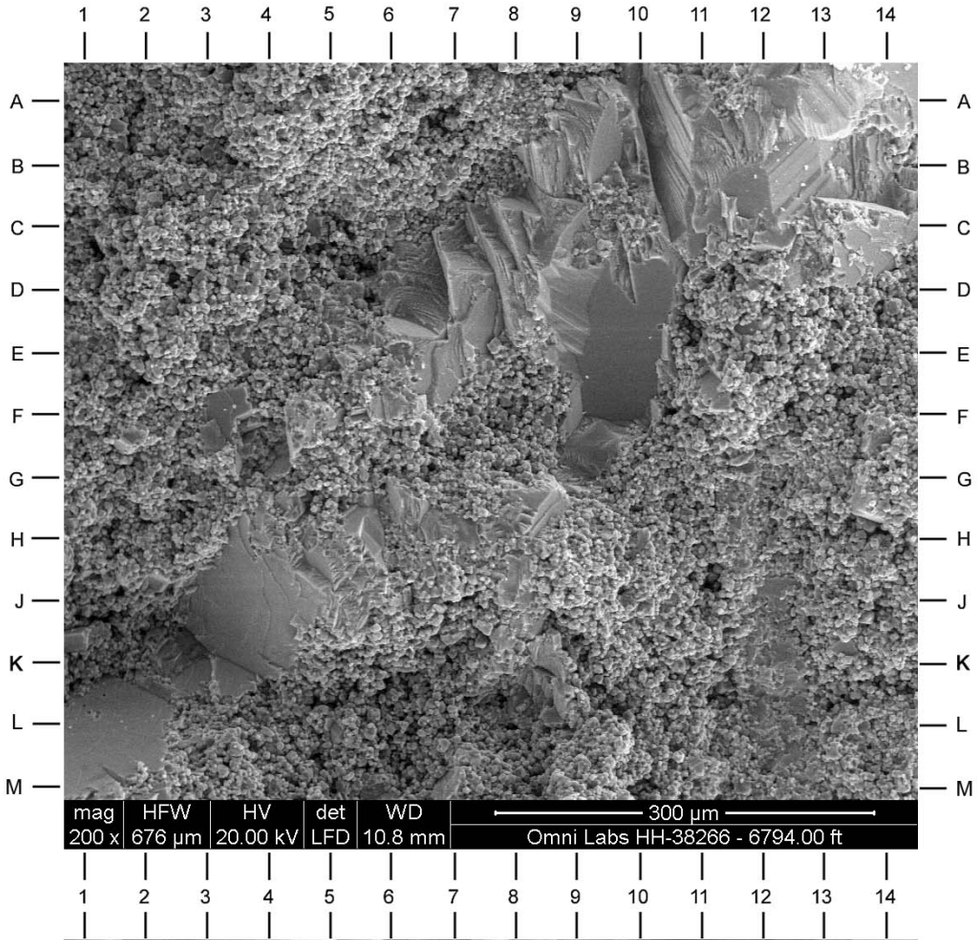

B

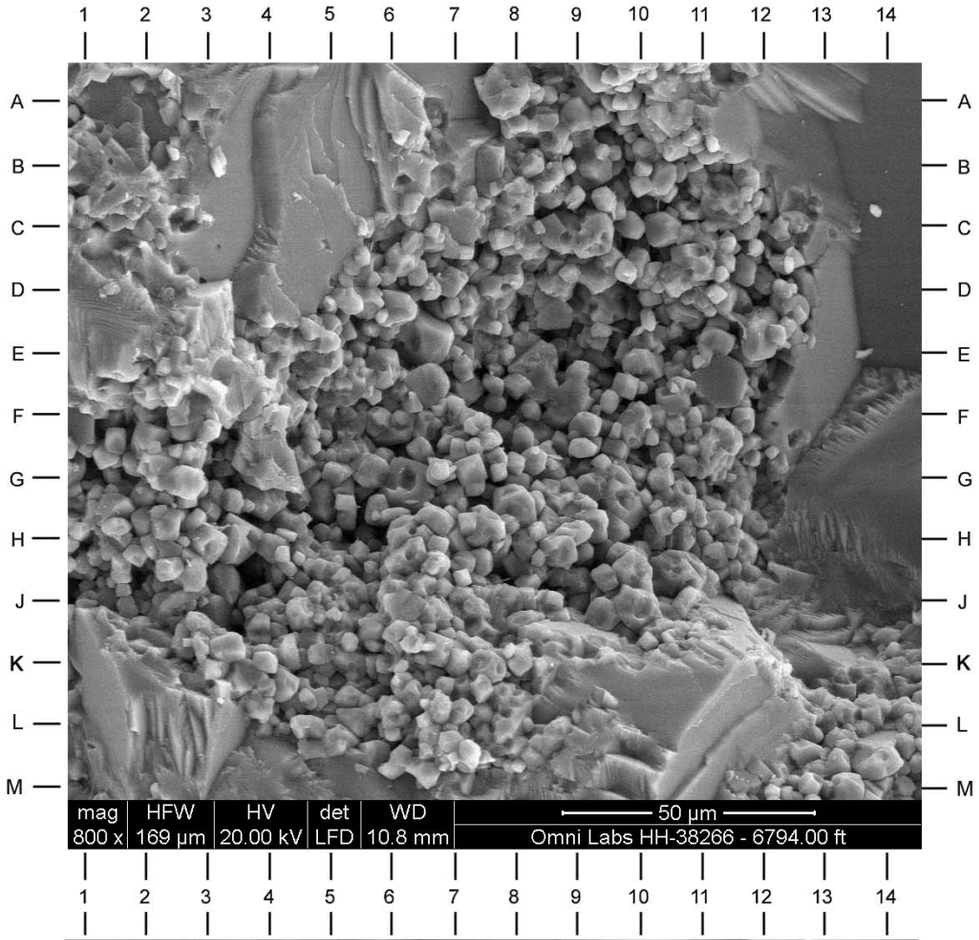

C

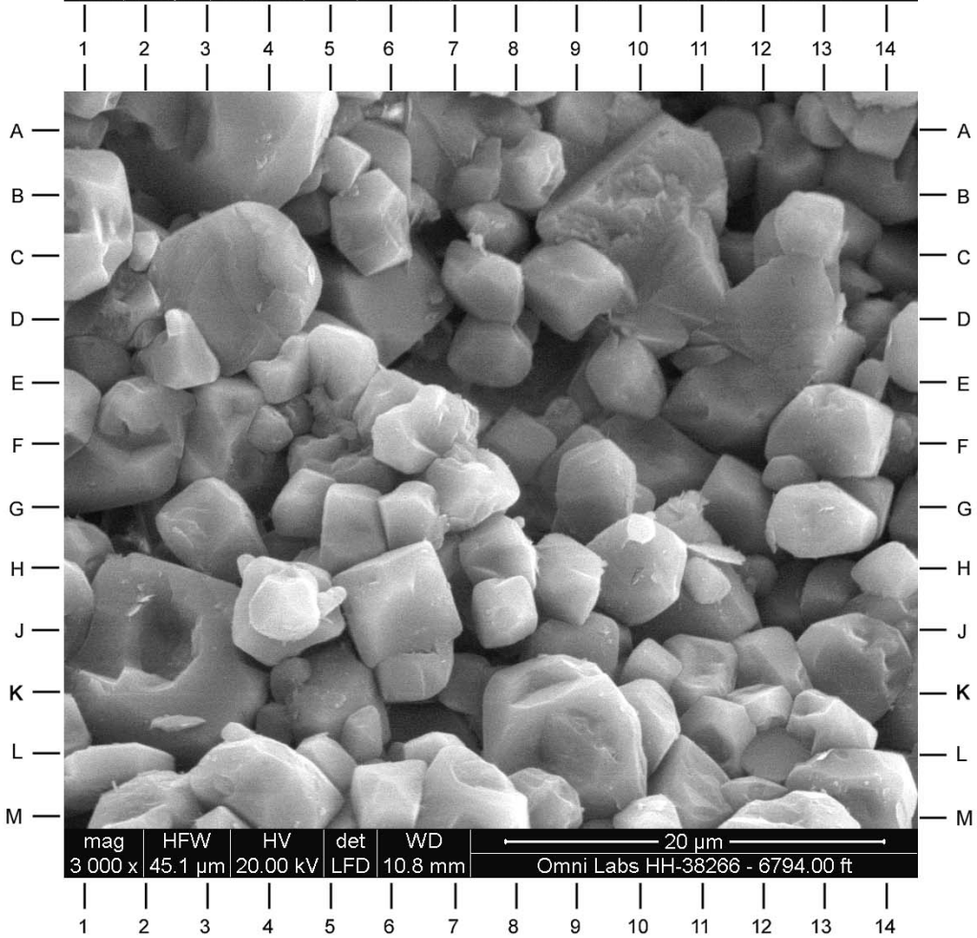

D

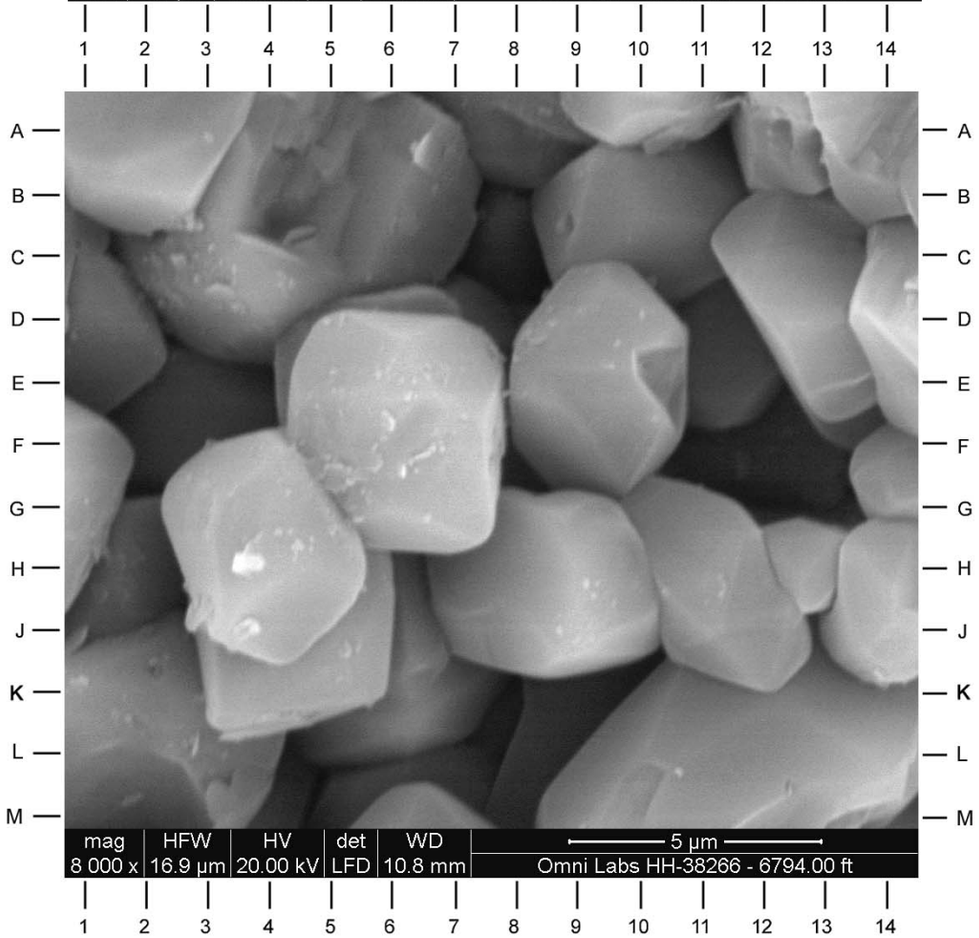

Ohio Division of Geological Survey **OMNI File No.: HH-38266**
CO_2 No. 1
Tuscarawas County, Ohio
Black River Group
Rotary Sidewall Core

SAMPLE DEPTH: 6844.0 FEET
SAMPLE NUMBER: 1-22R

PLATE 87

This skeletal/peloidal lime grainstone/packstone sample has a massive fabric and is possibly borrow-mottled. The sample is predominately cemented by sparry calcite (Plate A; B14,C9,H3 / Plate B; F10) with a minor amount of fine crystalline dolomite cement (Plate B; C7,D3). Micropores associated with microcrystalline calcite (Plate B; B12,H4 / Plate C; D3,G12 / Plate D; C5,K3) dominate the pore system with lesser amounts of secondary dissolution pores (Plate A; D11,F3 / Plate B; K2) in leached grains. An authigenic quartz crystal (Plate C; F8) is surrounded by microcrystalline calcite. Illitic clay bridges micropores (Plate D; F7,F9,J7) between microcrystalline calcite.

Magnification: 87A - 180X
Magnification: 87B - 700X
Magnification: 87C - 1300X
Magnification: 87D - 6000X

Ohio Division of Geological Survey
CO2 No. 1
Tuscarawas County, Ohio

6844.00'
Plate 87

OMNI Laboratories, Inc.

A

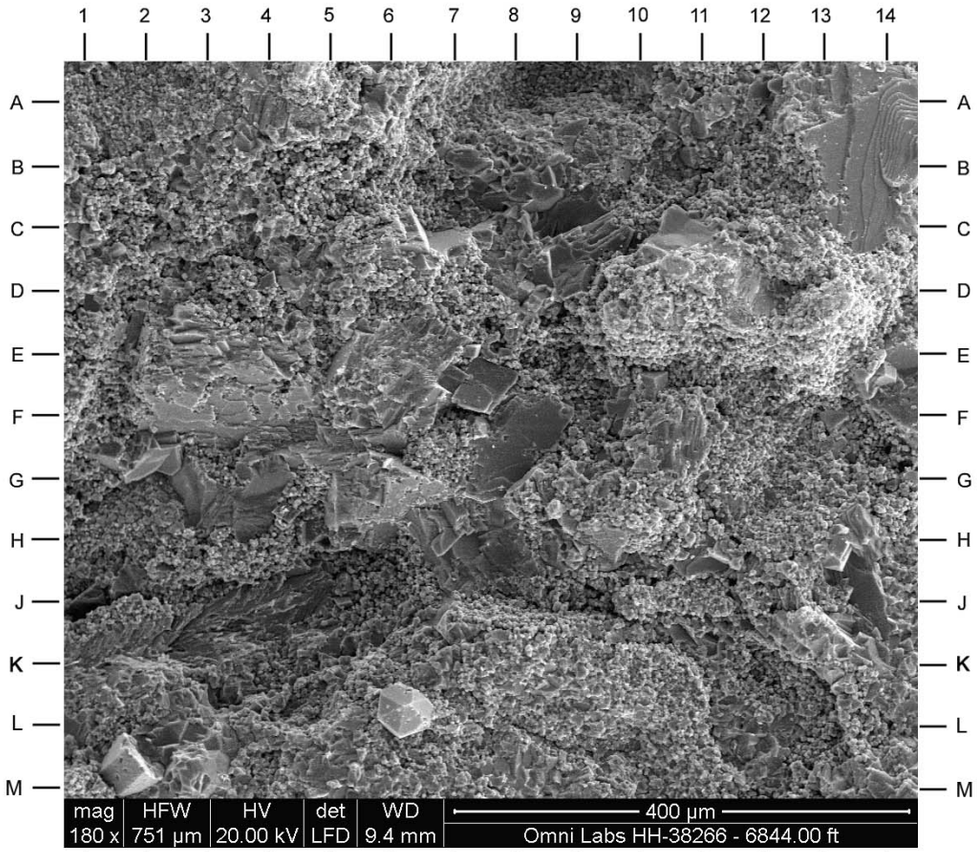

B

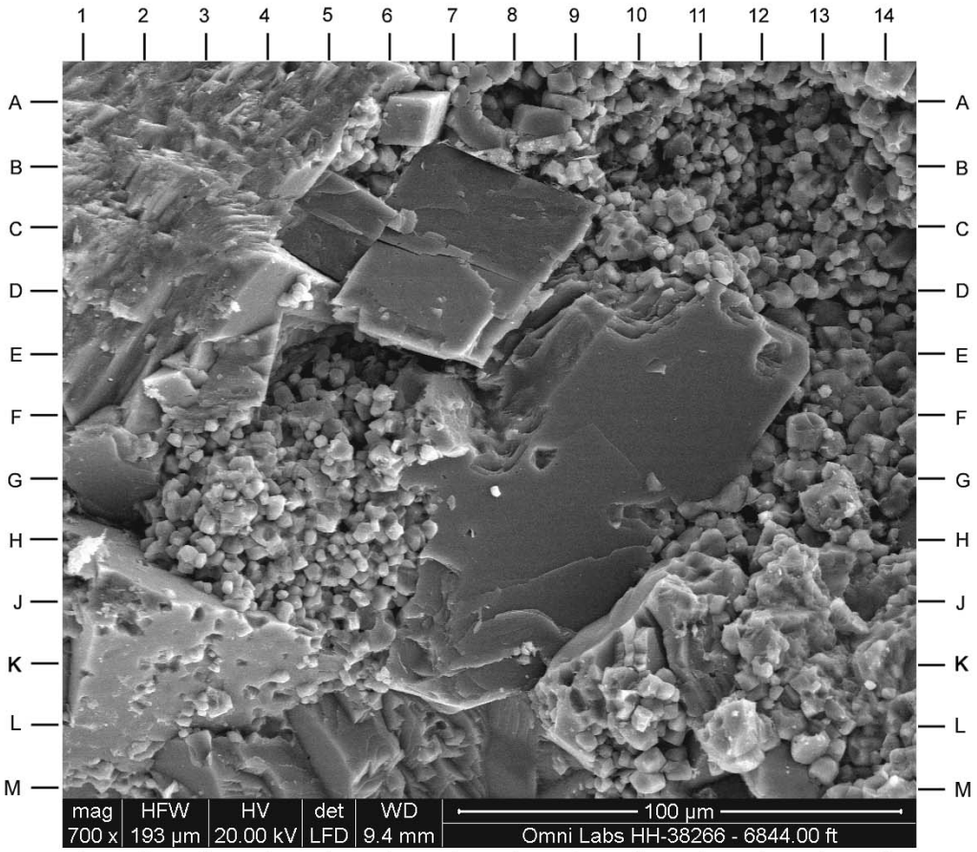

C

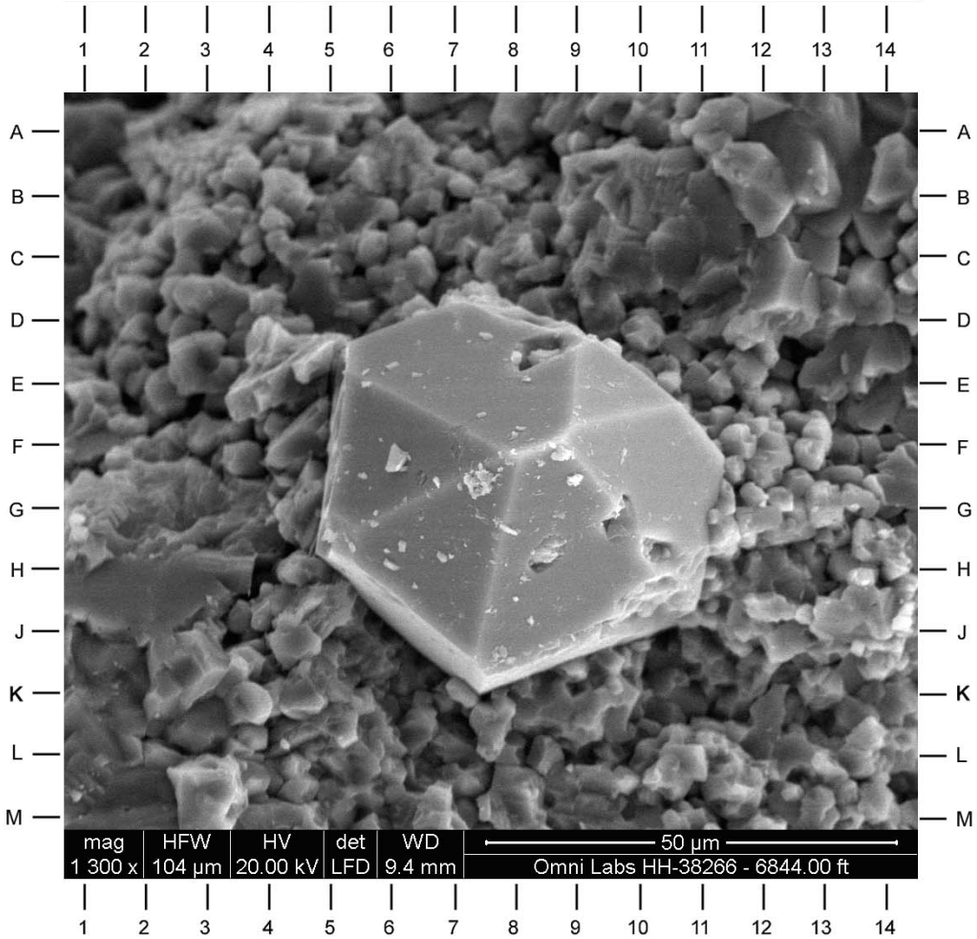

D

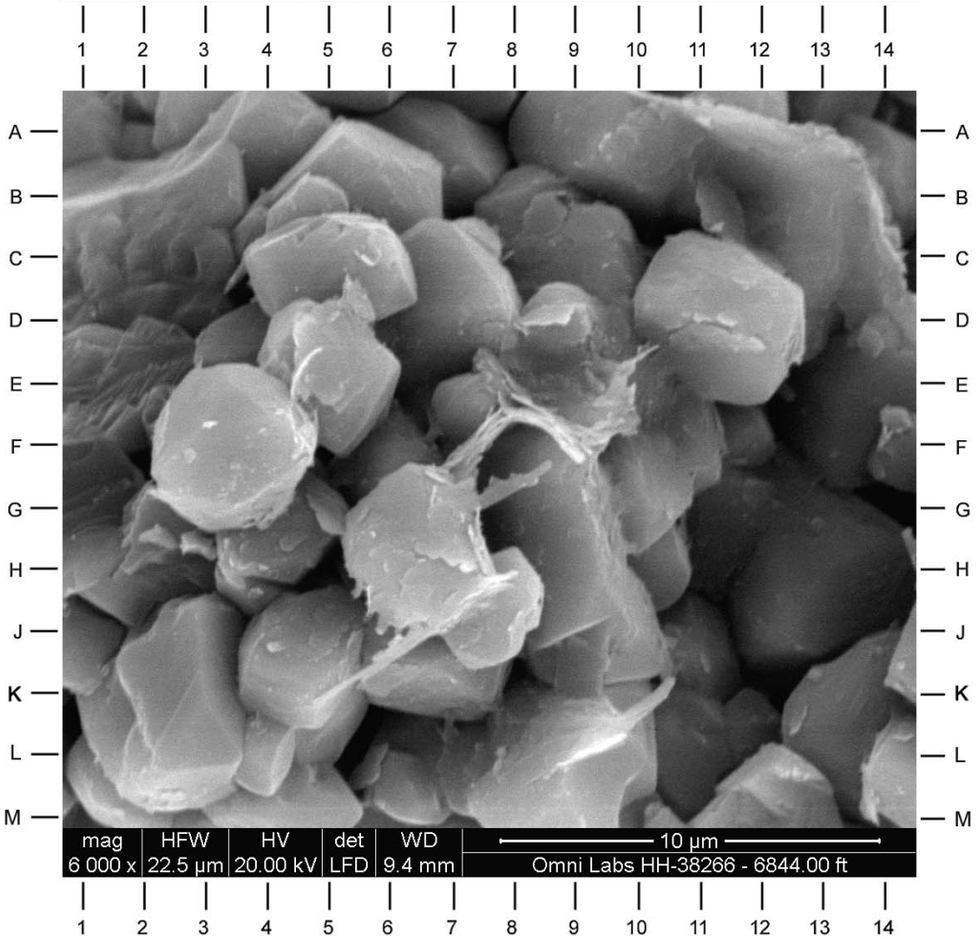

Ohio Division of Geological Survey **OMNI File No.: HH-38266**
CO_2 No. 1
Tuscarawas County, Ohio
Black River Group
Rotary Sidewall Core

SAMPLE DEPTH: 6940.0 FEET
SAMPLE NUMBER: 1-25R

PLATE 88

This skeletal/peloidal lime grainstone/packstone contains irregular bedding and microstylolites. Micropores associated with microcrystalline calcite (Plate B; B3, F4, J-K12 / Plate C; C4, G10, K3 / Plate D; A14, J6) dominate the pore system. Sparry calcite (Plate A; K2, K5, L6 / Plate C; F12,L2) is the predominant cement, with lesser amounts of replacement dolomite cement (Plate B; F8). A few areas contain undifferentiated illitic clay (Plate B; G3,J11, L6 / Plate C; D9,H4 / Plate D; A9.8,J5,J10) mixed with microcrystalline calcite.

Magnification: 88A - 400X
Magnification: 88B - 1600X
Magnification: 88C - 2500X
Magnification: 88D - 10000X

Ohio Division of Geological Survey
CO2 No. 1
Tuscarawas County, Ohio

6940.00'
Plate 88

OMNI Laboratories, Inc.

A

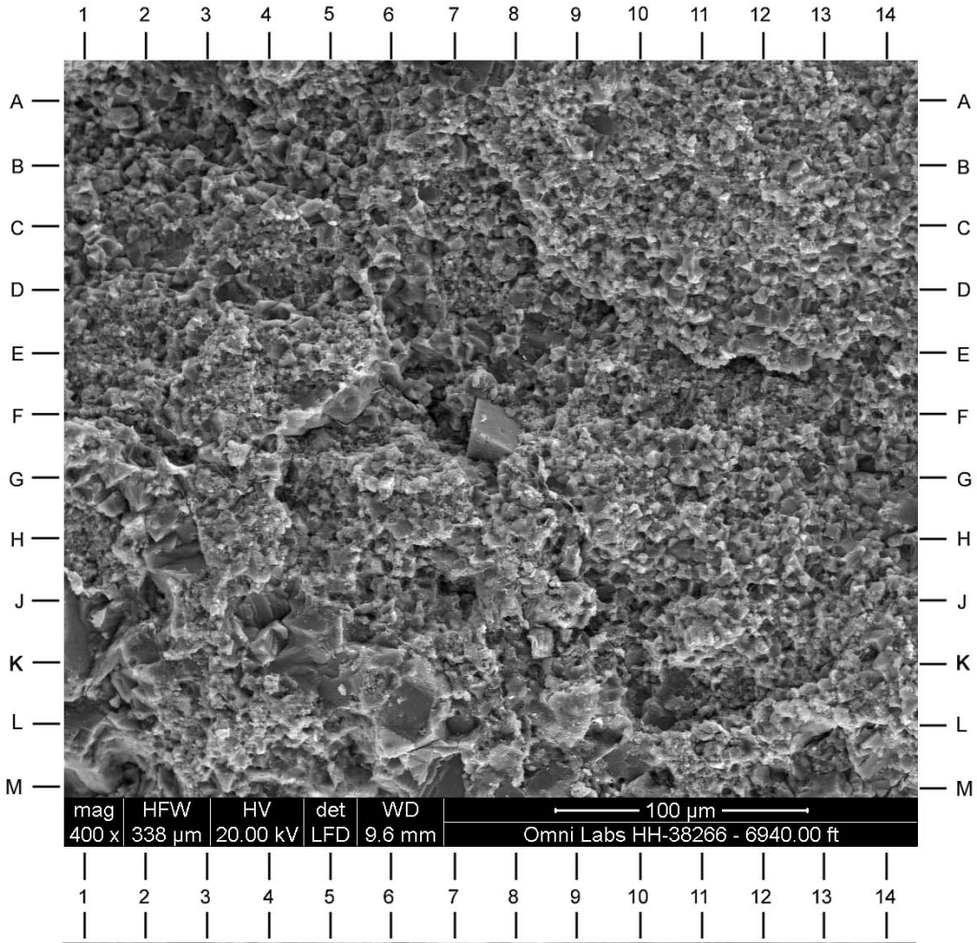

B

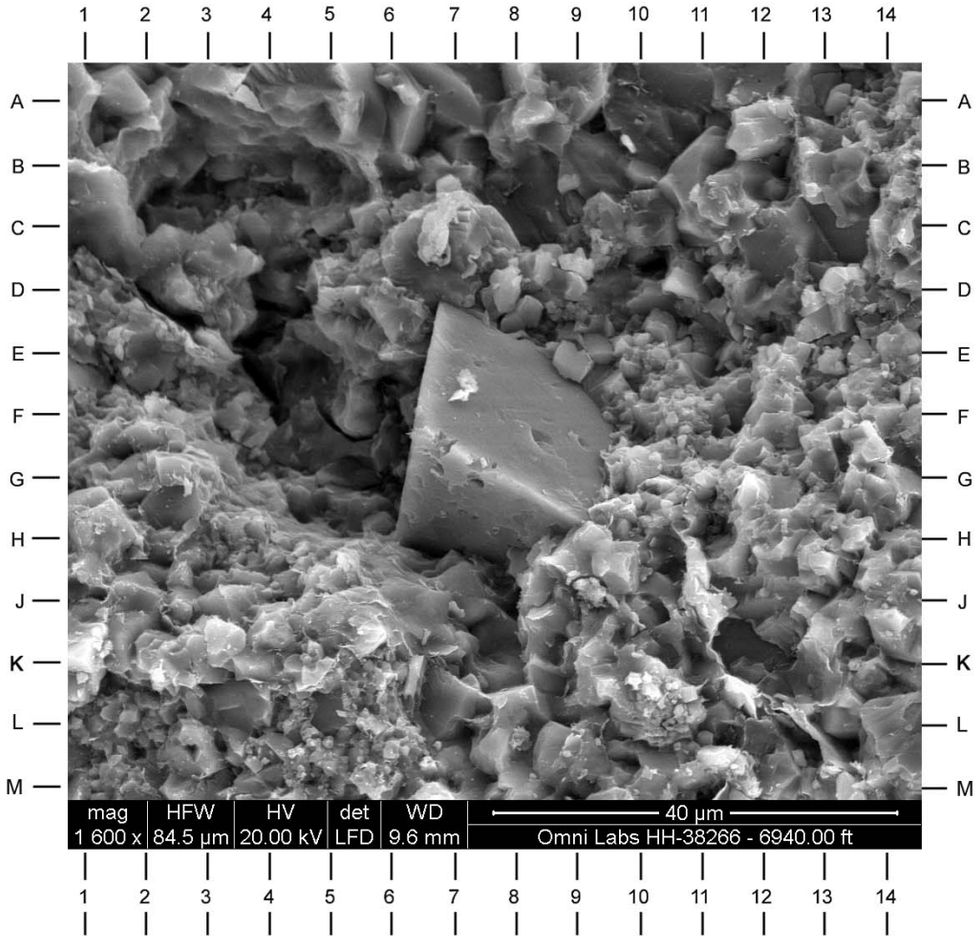

C

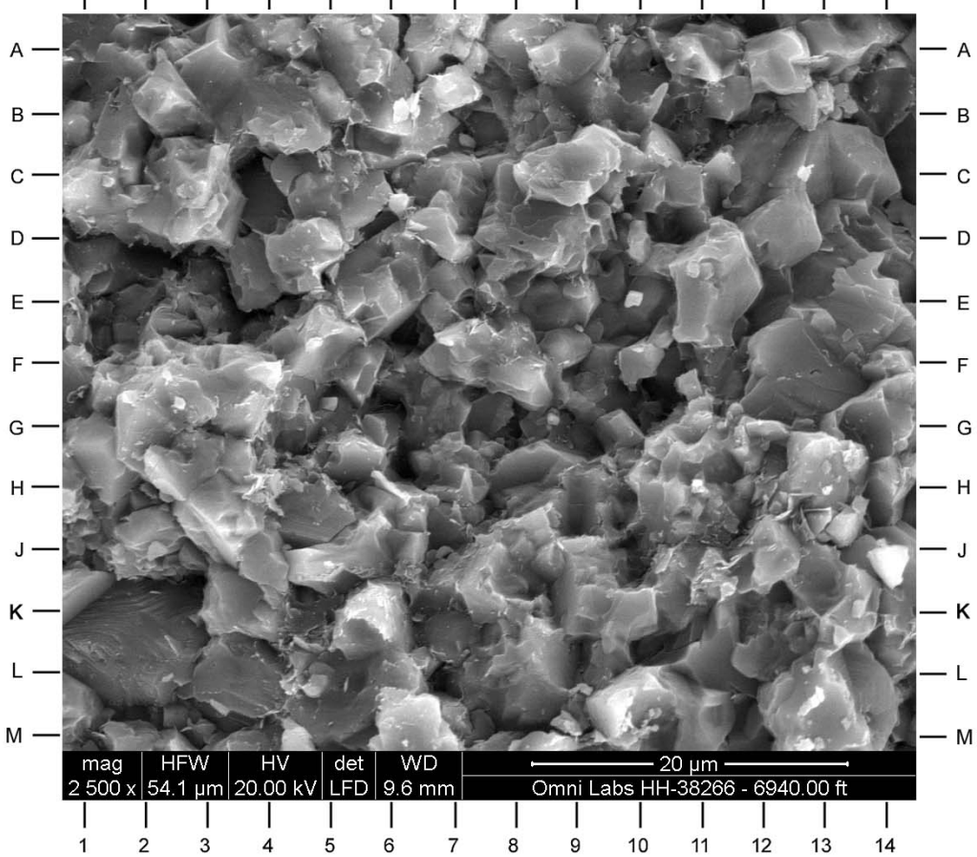

D

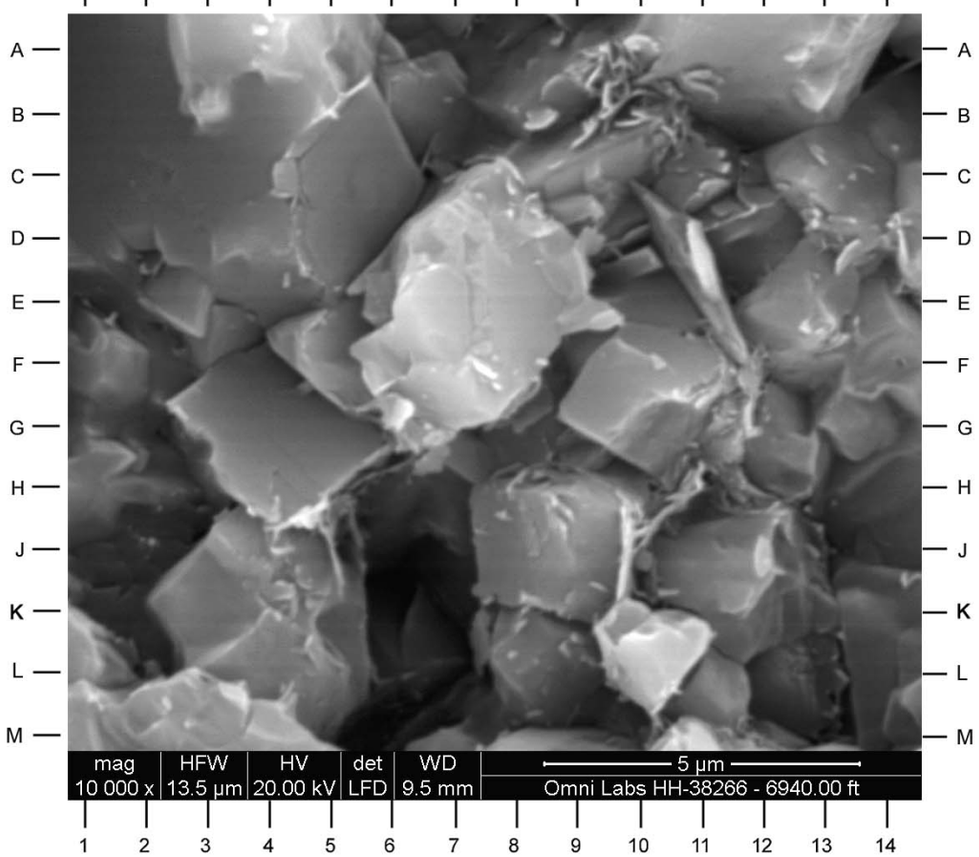

Ohio Division of Geological Survey **OMNI File No.: HH-38266**
CO_2 No. 1
Tuscarawas County, Ohio
Beekmantown Dolomite
Rotary Sidewall Core

SAMPLE DEPTH: 7226.0 FEET
SAMPLE NUMBER: 1-30R

PLATE 89

This medium crystalline dolostone consists predominantly of secondary dolomite (Plate A; A7,D9,L6 / Plate B; E4,H13 / Plate C; A13,B9,H7) cement. Intergranular pores (Plate A; C3,G-H11,J9.5) are the primary pore type with secondary intragranular pores (Plate A; E8,H4.5) and micropores (Plate B; G10,J5 / Plate C; E9,J-K4 / Plate D; E10,J3,I10) also contributing to overall pore volume. Some intergranular voids are partially occluded by a combination of illite and chlorite (Plate B; E8-H5,H10 / Plate C; B13-E6,G12-G3,K3) which reduces pores and pore throats (Plate B; F5.7 / Plate C; B12,B-C9,G2.5-M2) at the grain/pore boundary.

Magnification: 89A - 110X
Magnification: 89B - 1200X
Magnification: 89C - 1500X
Magnification: 89D - 7000X

Ohio Division of Geological Survey
CO2 No. 1
Tuscarawas County, Ohio

7226.00'
Plate 89

OMNI Laboratories, Inc.

A

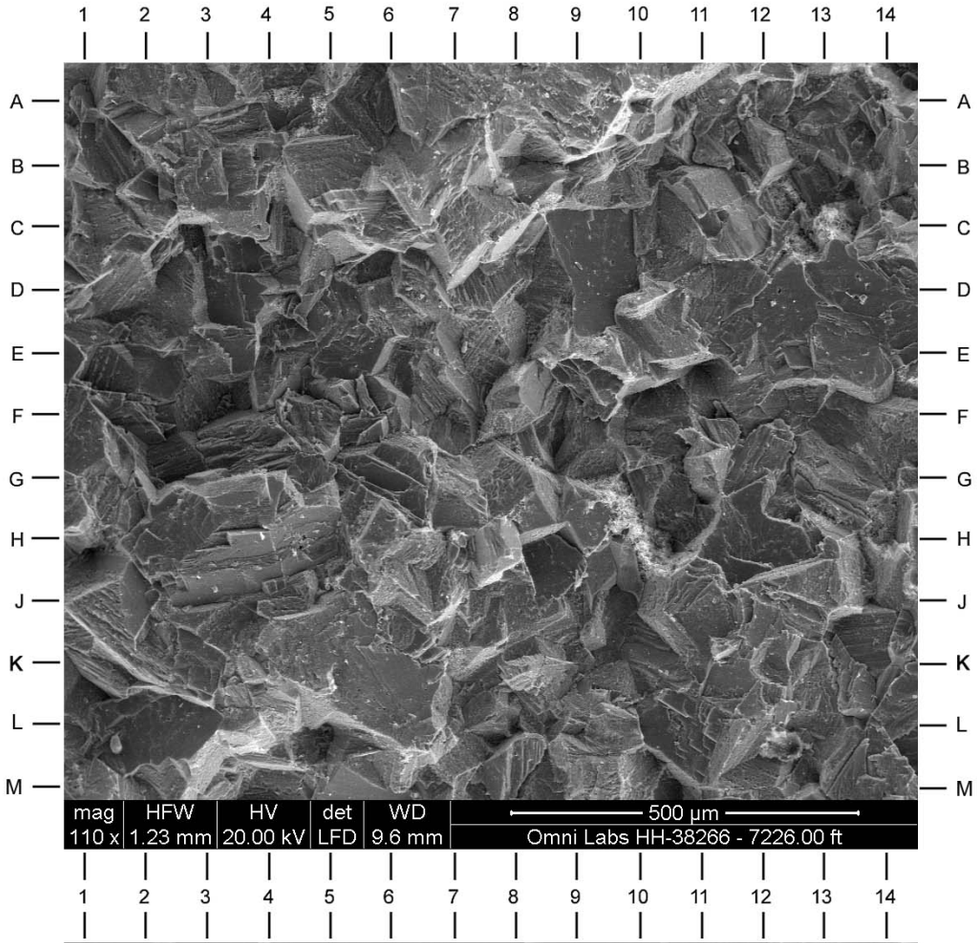

B

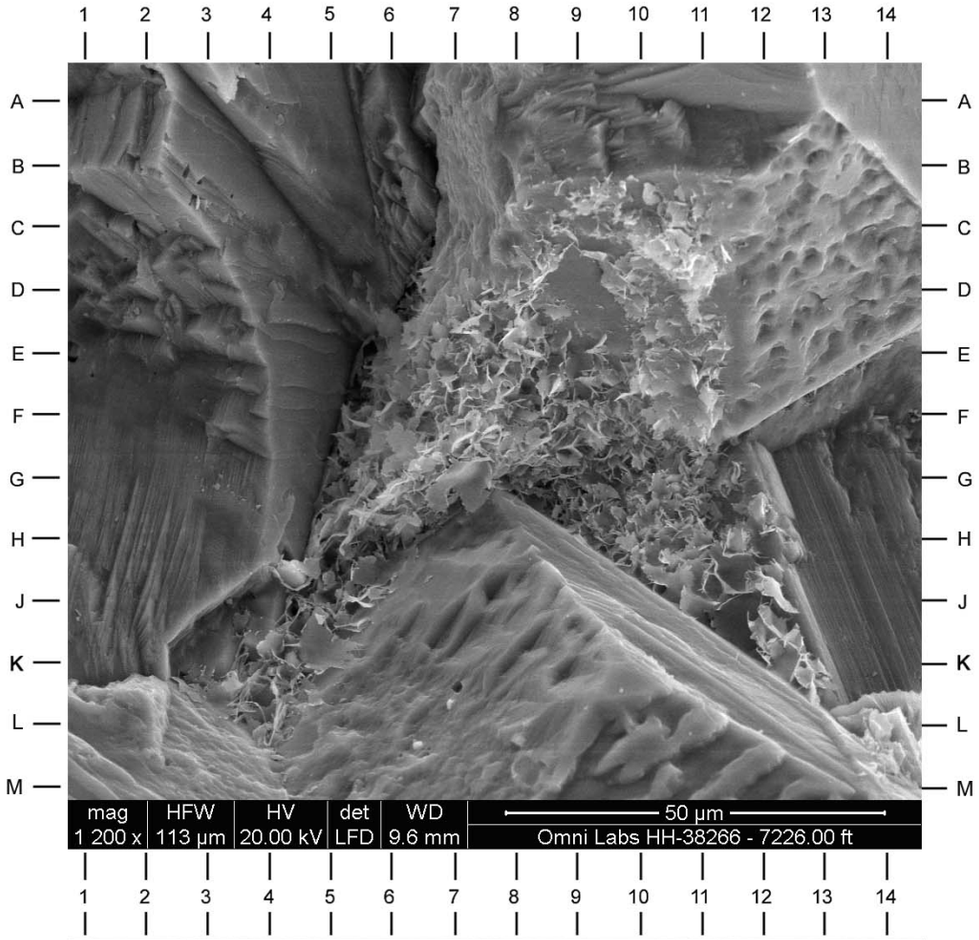

C

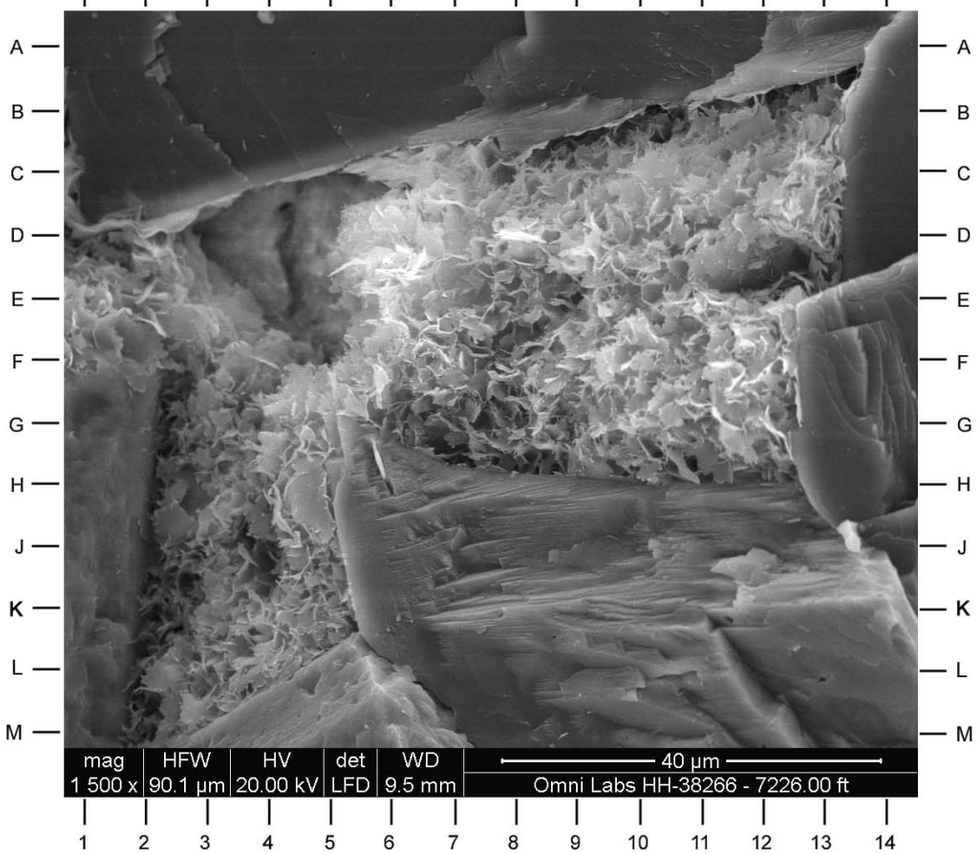

D

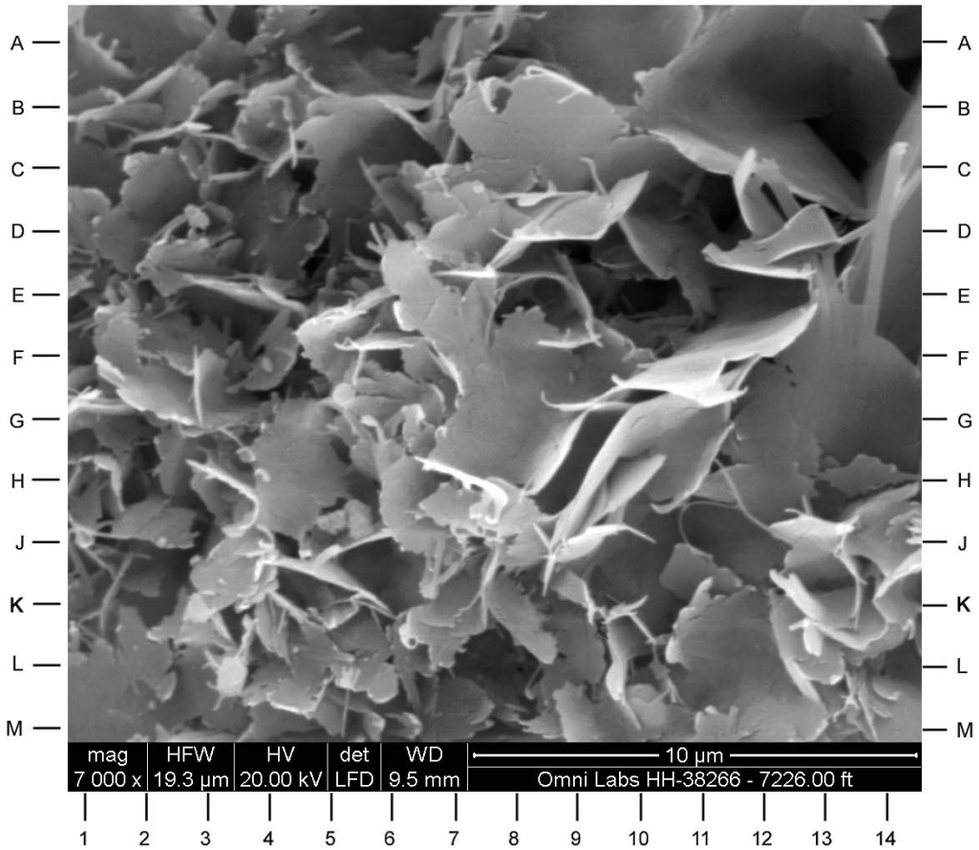

Ohio Division of Geological Survey **OMNI File No.: HH-38266**
CO_2 No. 1
Tuscarawas County, Ohio
Beekmantown Dolomite
Rotary Sidewall Core

SAMPLE DEPTH: 7231.0 FEET
SAMPLE NUMBER: 1-31R

PLATE 90

This fine to medium crystalline dolomite represents a dolomitized overprint of a brecciated limestone. Rare fibrous illitic clay occurs as grain-coatings (Plate B; D-E3,E-F11.5 / Plate C; B-C3,B11,F2,F10) and bridges pore throats (Plate C; D10,J6,K12 / Plate D; C4,E6,F10). A fracture (Plate A; B3-M12) is partially occluded by dolomite crystals (Plate B; B2,H8,K9). The pore system is dominated by fracture pores with lesser amounts of moldic/secondary pores (not visible in SEM) and intercrystalline pores (Plate A; L2,L6.2 / Plate B; E6 / Plate C; H7 / Plate D; G7).

Magnification: 90A - 70X
Magnification: 90B - 250X
Magnification: 90C - 1300X
Magnification: 90D - 1900X

Ohio Division of Geological Survey
CO2 No. 1
Tuscarawas County, Ohio

7231.00'
Plate 90

OMNI Laboratories, Inc.

A

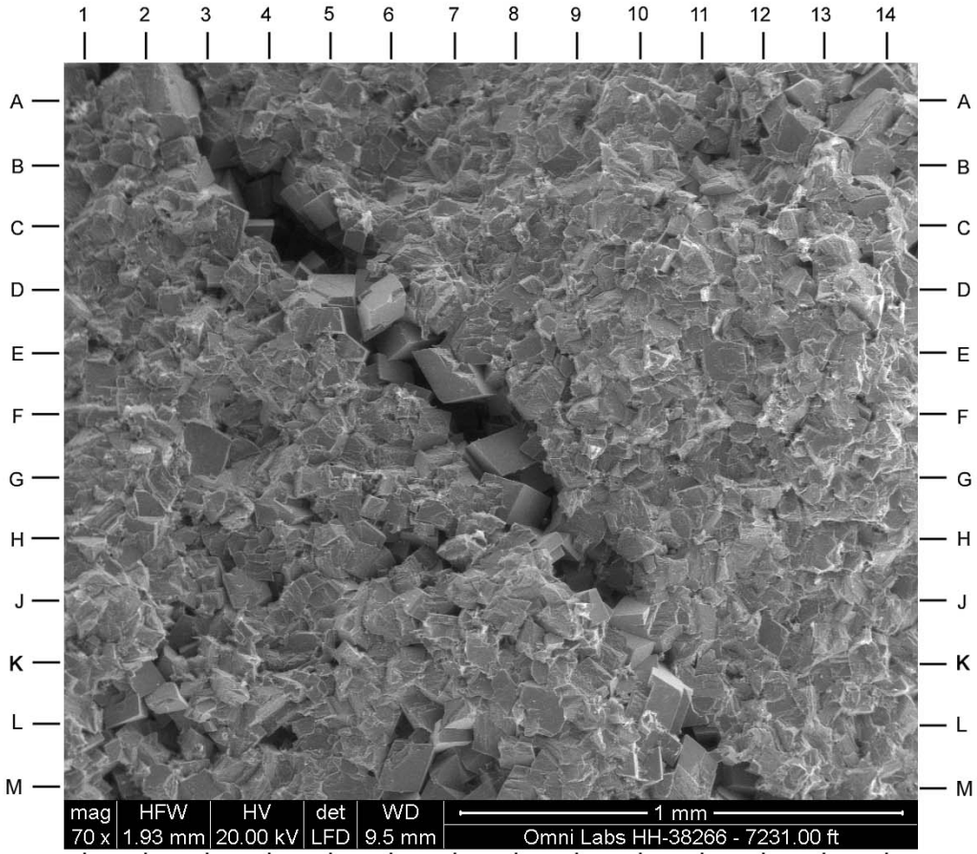

B

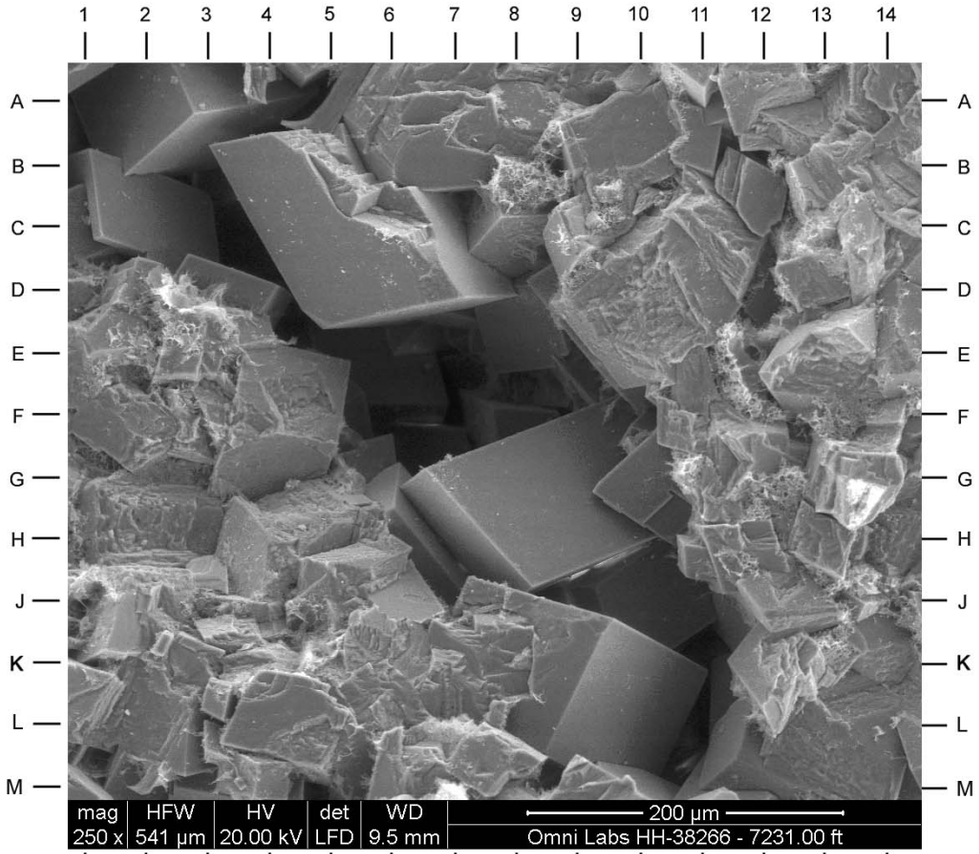

C

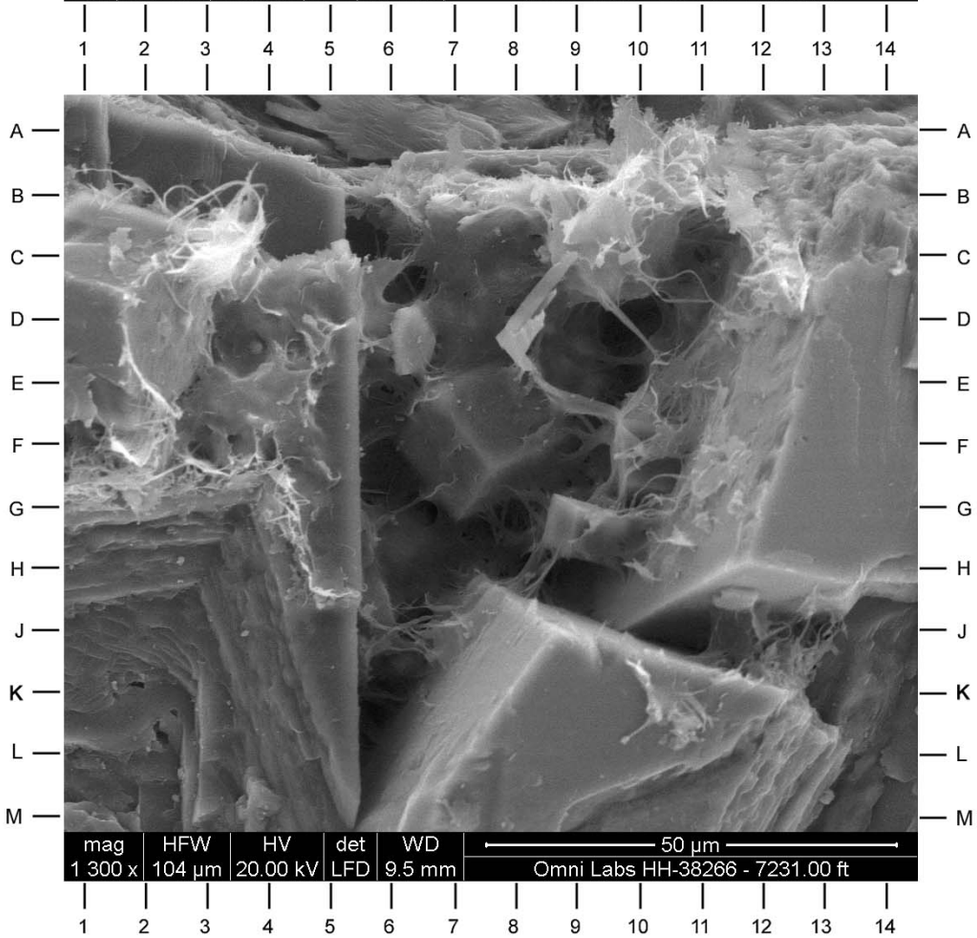

D

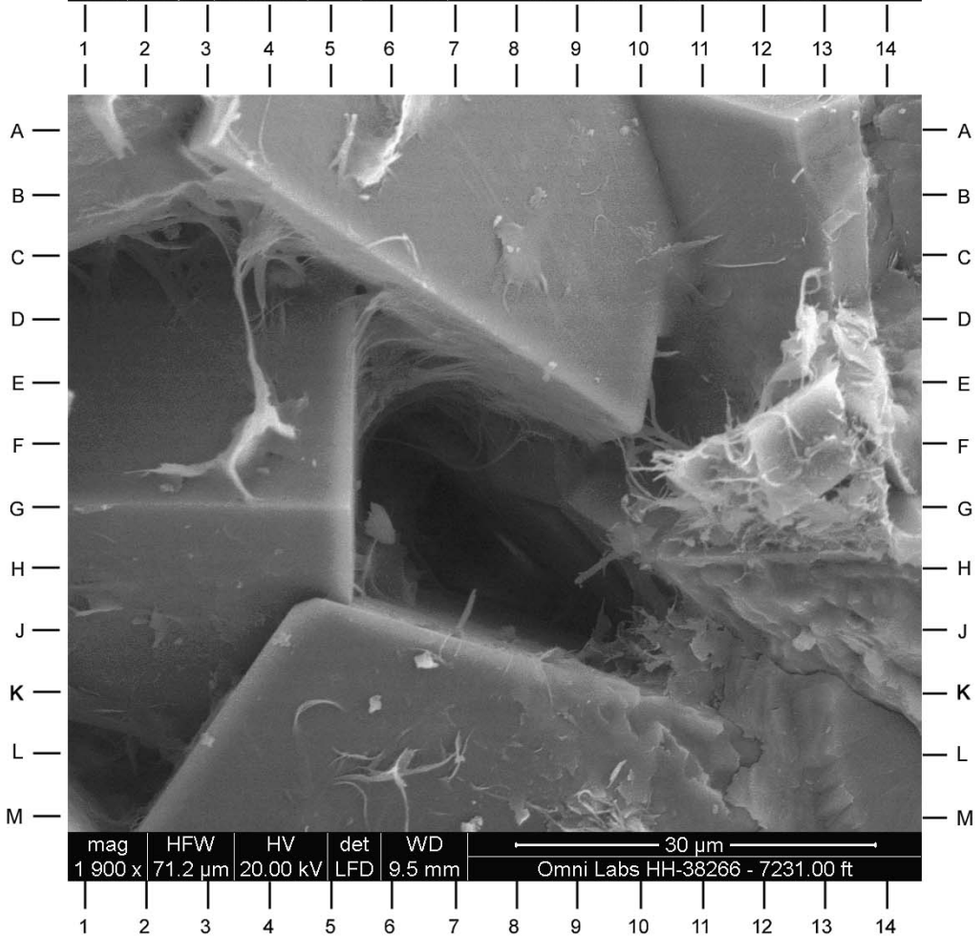

Ohio Division of Geological Survey **OMNI File No.: HH-38266**
CO_2 No. 1
Tuscarawas County, Ohio
Beekmantown Dolomite
Rotary Sidewall Core

SAMPLE DEPTH: 7235.0 FEET
SAMPLE NUMBER: 1-32R

PLATE 91

This very fine crystalline dolostone has a laminated/planar S dolomite fabric. Microscopic pores (Plate B; E8,G7.5, J2 / Plate C; A11,E7,F5 / Plate D; below A4, C9,J2.3,J13) are the primary type of porosity. Illitic clay occludes pores (Plate B; B6,F9 / Plate C; C10,E8,F4,G9 / Plate D; D11,H13) and is intermixed with replacement dolomite cement (Plate B; E6,J11 / Plate C; D9,H8,J12 /Plate D; A3,E12,G9).

Magnification: 91A - 600X
Magnification: 91B - 3100X
Magnification: 91C - 4000X
Magnification: 91D - 4000X

Ohio Division of Geological Survey
CO2 No. 1
Tuscarawas County, Ohio

7235.00'
Plate 91

OMNI Laboratories, Inc.

A

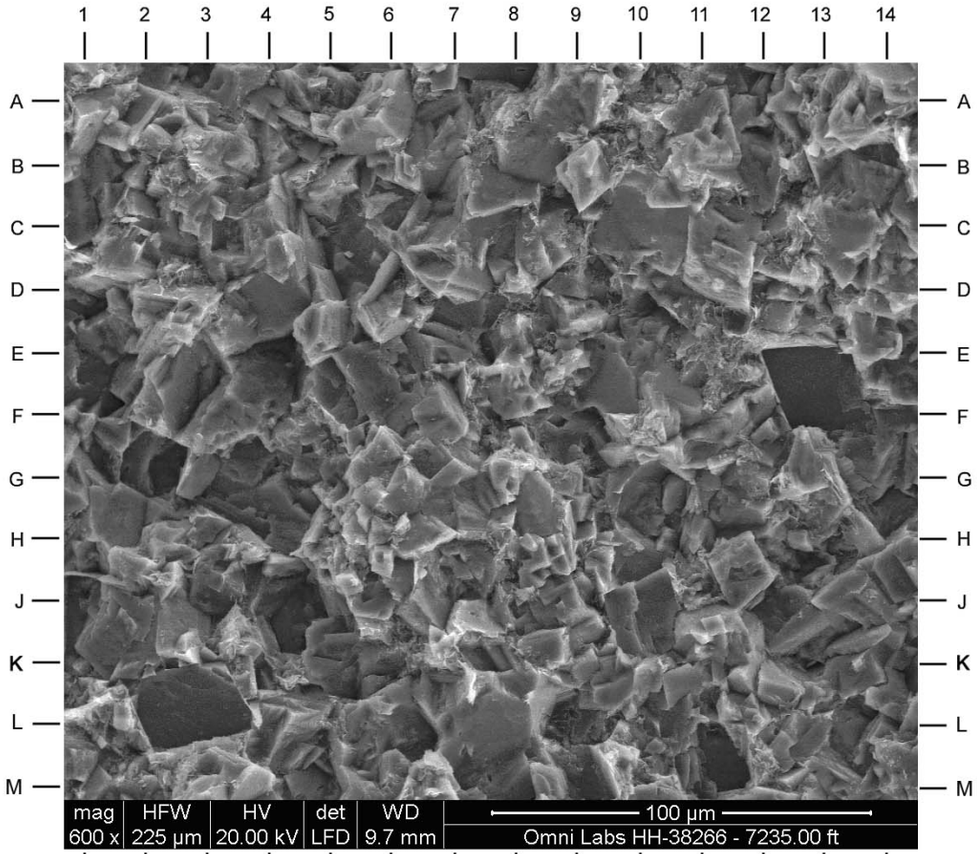

B

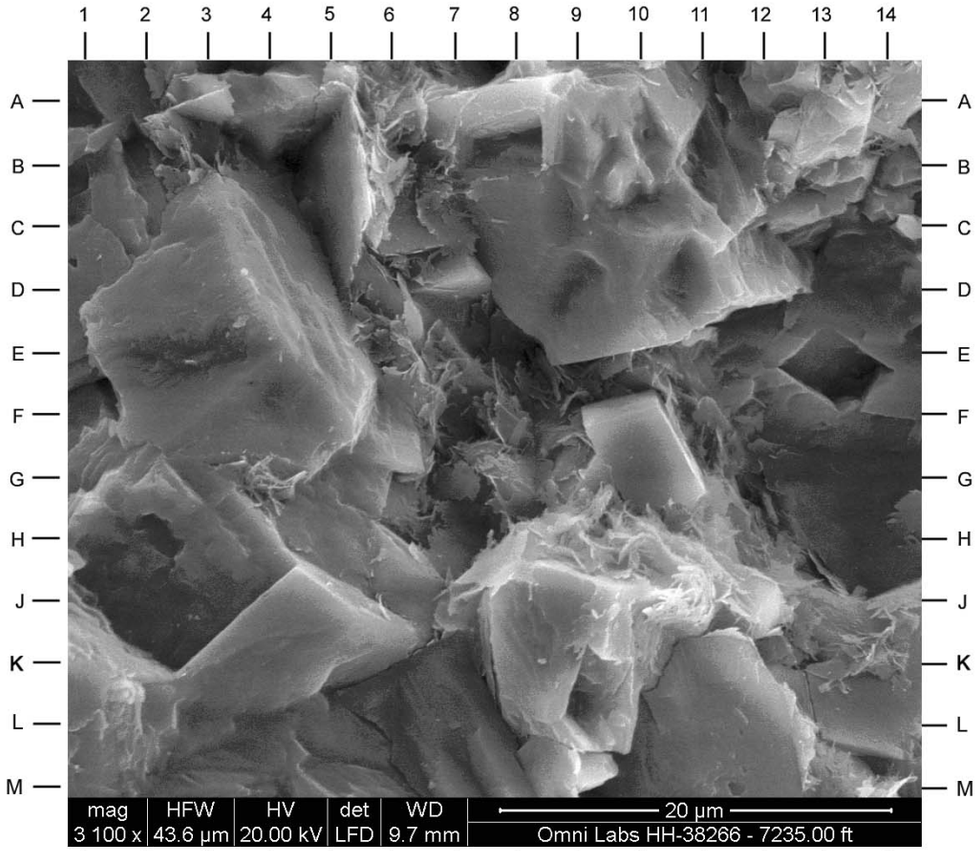

C

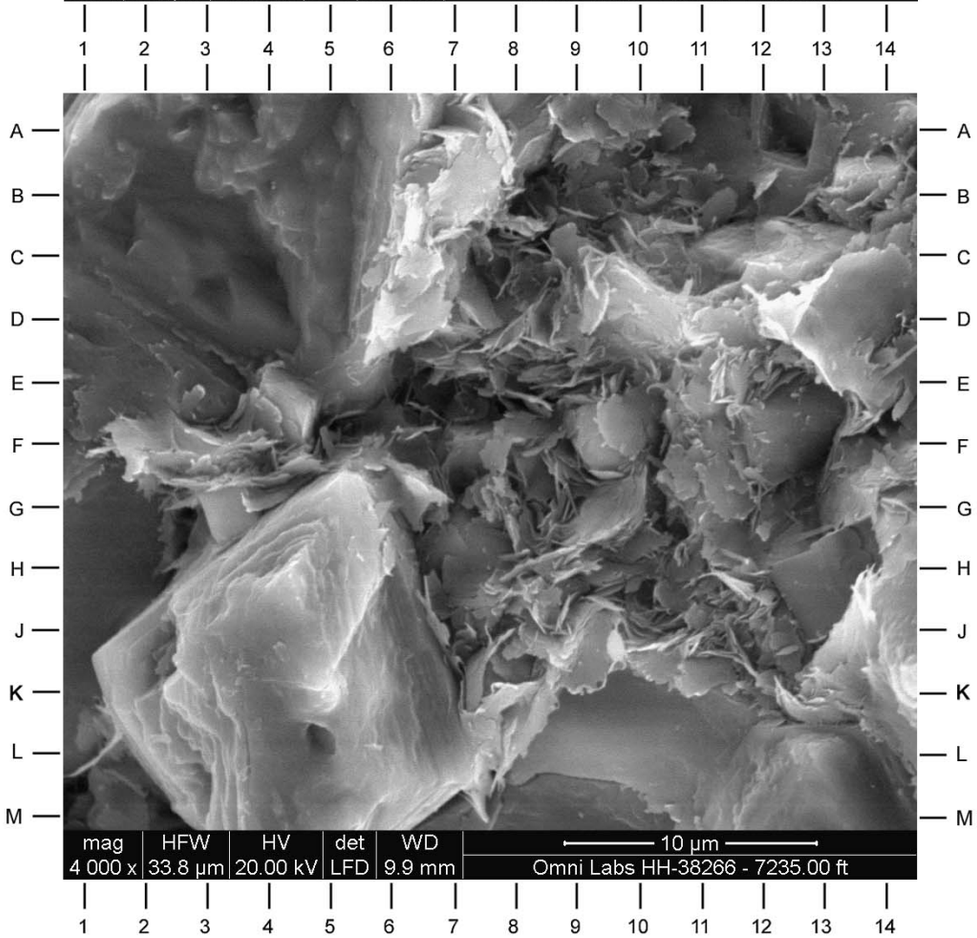

D

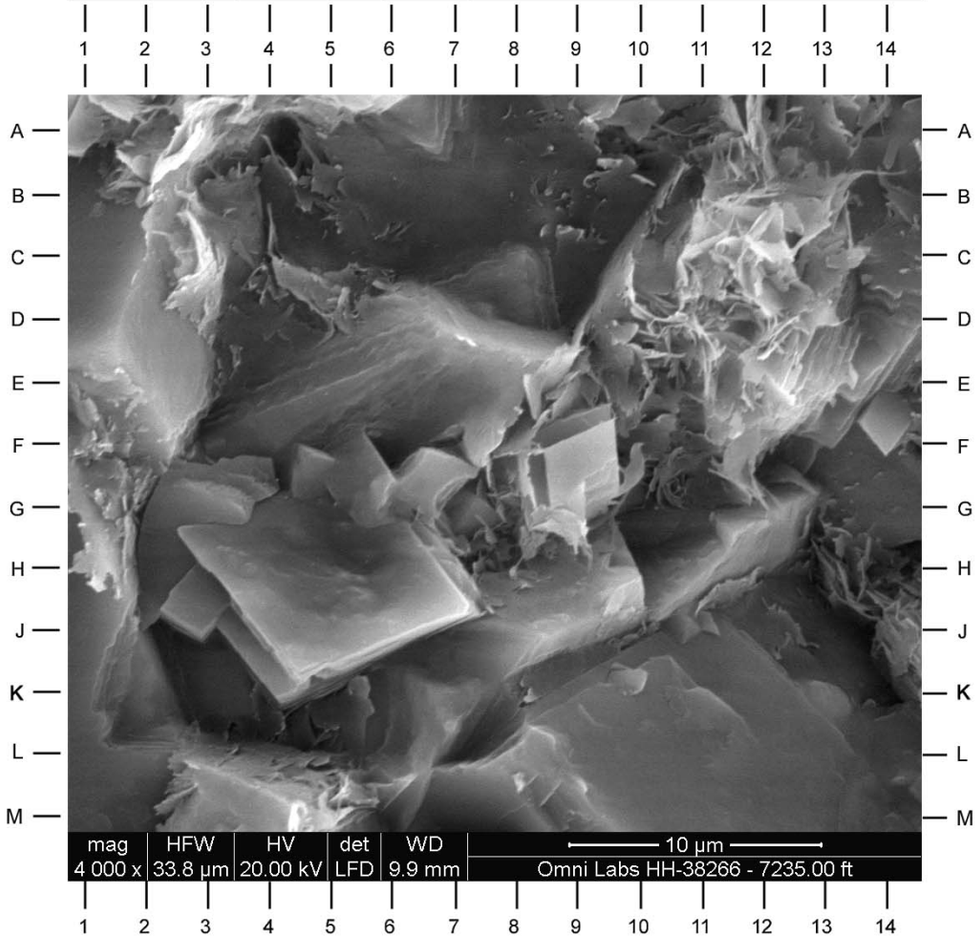

Ohio Division of Geological Survey **OMNI File No.: HH-38266**
CO_2 No. 1
Tuscarawas County, Ohio
Rose Run Sandstone Formation
Rotary Sidewall Core

SAMPLE DEPTH: 7377.0 FEET
SAMPLE NUMBER: 1-37R

PLATE 92

This quartzarenite is moderately well sorted with an average grain size of 0.48mm. Quartz (Plate A; B6,E6,K12 / Plate B; M5 / Plate D; D14) is the primary detrital grain type with a minor amount of feldspars (Plate B; C14) present. Quartz overgrowths (Plate B; F6,G10 / Plate C; D10,F3,H7 / Plate D; D3,J4) are the dominant type of cement. Intergranular pores (Plate A; C3,F-G5,L11 / Plate B; F4.5 Plate D; D6) dominate the pore system with lesser amounts of secondary intragranular pores (Plate A; J9 / Plate C; K13) occurring within partially dissolved grains. Illitic clay coats grain surfaces, inhibiting quartz overgrowths (Plate B; A9,K9 / Plate C; C-D13 / Plate D; C8-K10,M5).

Magnification: 92A - 40X
Magnification: 92B - 500X
Magnification: 92C - 600X
Magnification: 92D - 1300X

Ohio Division of Geological Survey
CO2 No. 1
Tuscarawas County, Ohio

7377.00'
Plate 92

OMNI Laboratories, Inc.

A

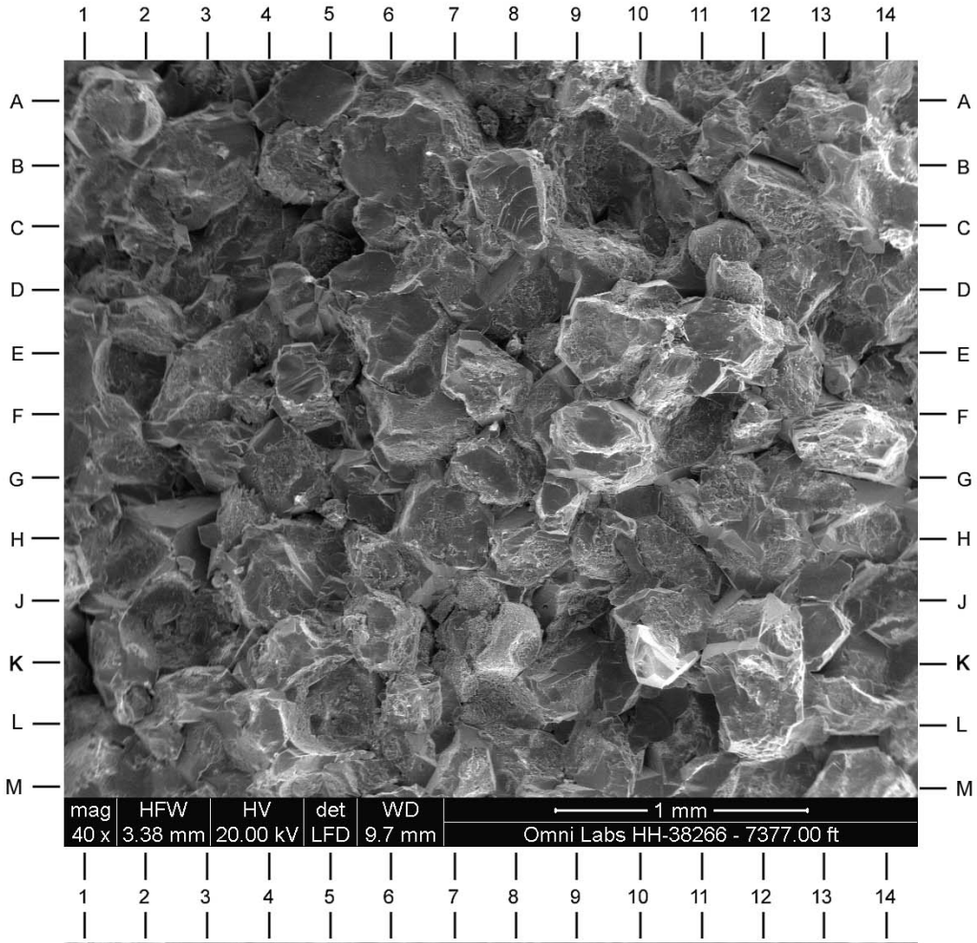

B

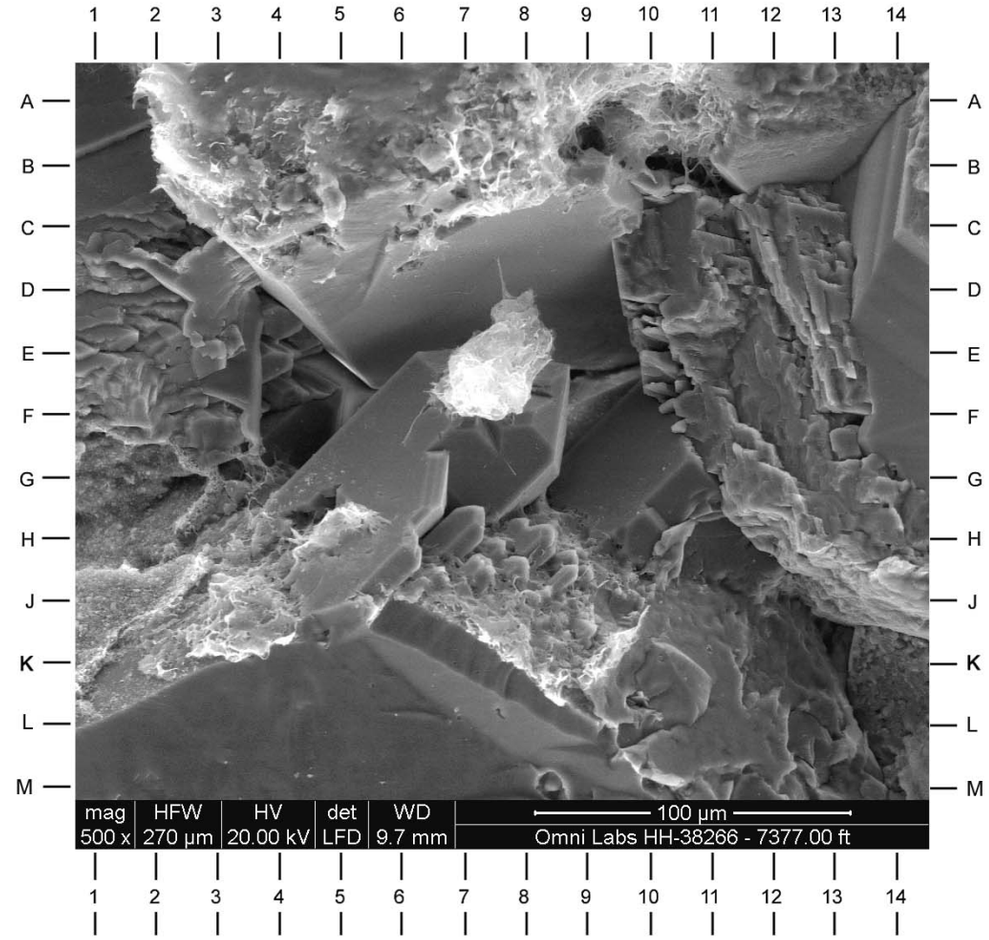

C

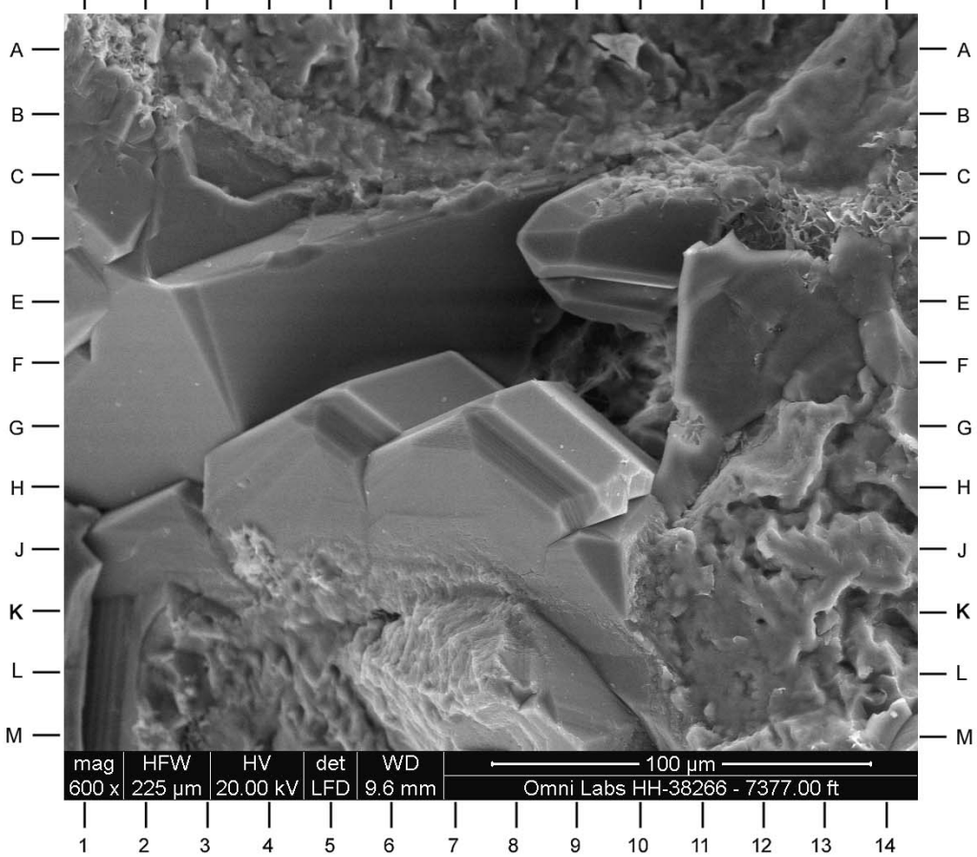

D

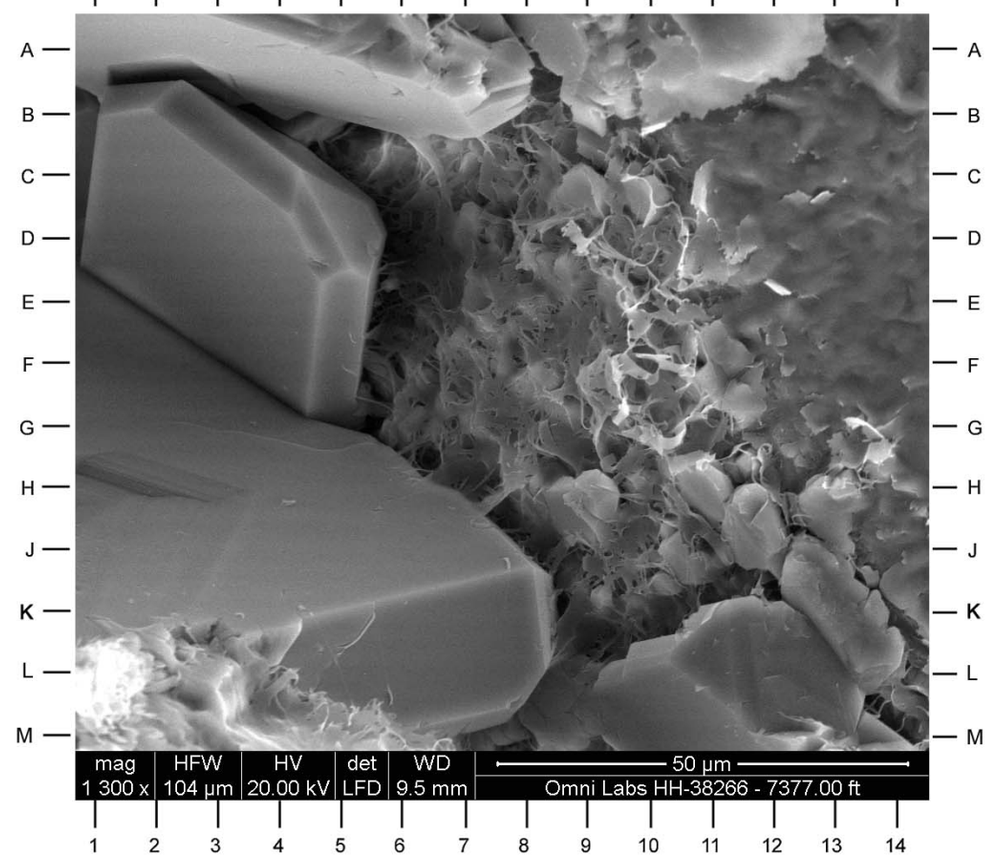

Ohio Division of Geological Survey **OMNI File No.: HH-38266**
CO_2 No. 1
Tuscarawas County, Ohio
Rose Run Sandstone Formation
Rotary Sidewall Core

SAMPLE DEPTH: 7392.0 FEET
SAMPLE NUMBER: 1-39R

PLATE 93

This quartzarenite is moderately sorted with an average grain size of 0.35mm. Intergranular pores (Plate A; B11.5,E6,J7,K1) and secondary intragranular pores in partially dissolved grains (Plate B; D13,L12 / Plate C; A12) are the predominant types of porosity. Illitic clay bridges pore throats (Plate B; E4 / Plate D; H10,J10) and coats grains (Plate B; D9 / Plate C; E13.5,K3 / Plate D; C3,E4,H2,M6). Quartz (Plate A; A12,F7,L11 / Plate B; A6,F1 / Plate C; B4) is the dominant detrital grain type. Quartz overgrowths (Plate B; F5,F9,H7 / Plate C; F1,E8,G10 / Plate D; B3,L10) occlude pores and are the predominant type of cement.

Magnification: 93A - 50X
Magnification: 93B - 700X
Magnification: 93C - 400X
Magnification: 93D - 1500X

Ohio Division of Geological Survey
CO2 No. 1
Tuscarawas County, Ohio

7392.00'
Plate 93

OMNI Laboratories, Inc.

A

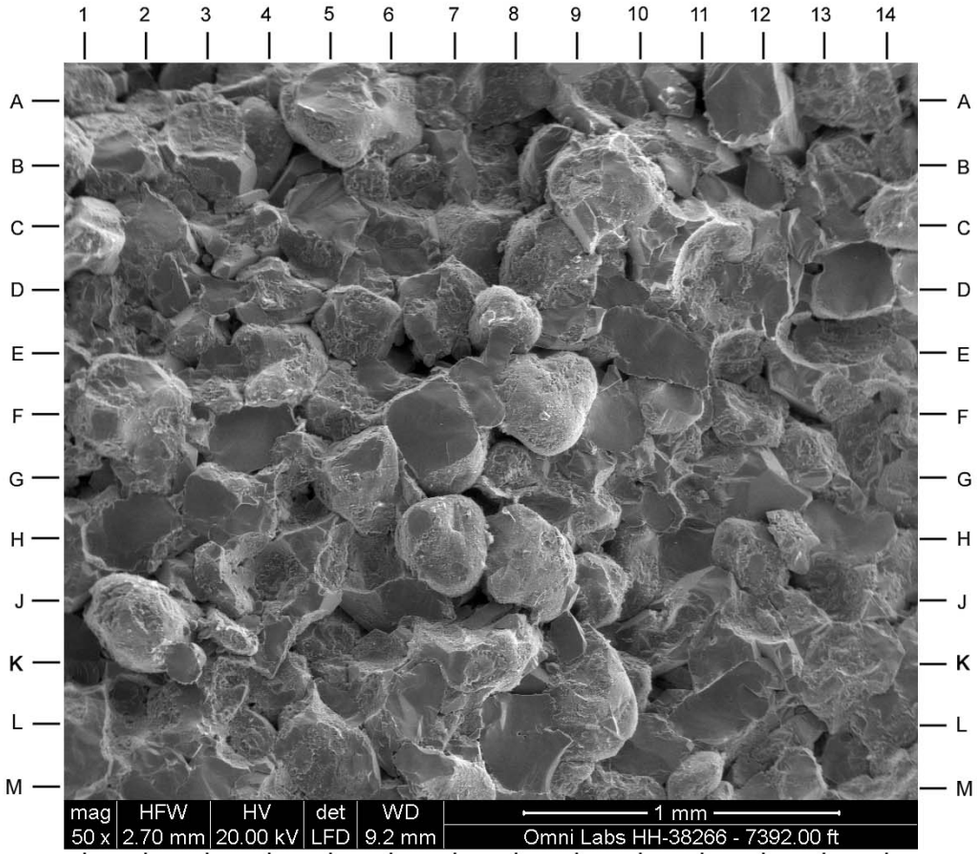

B

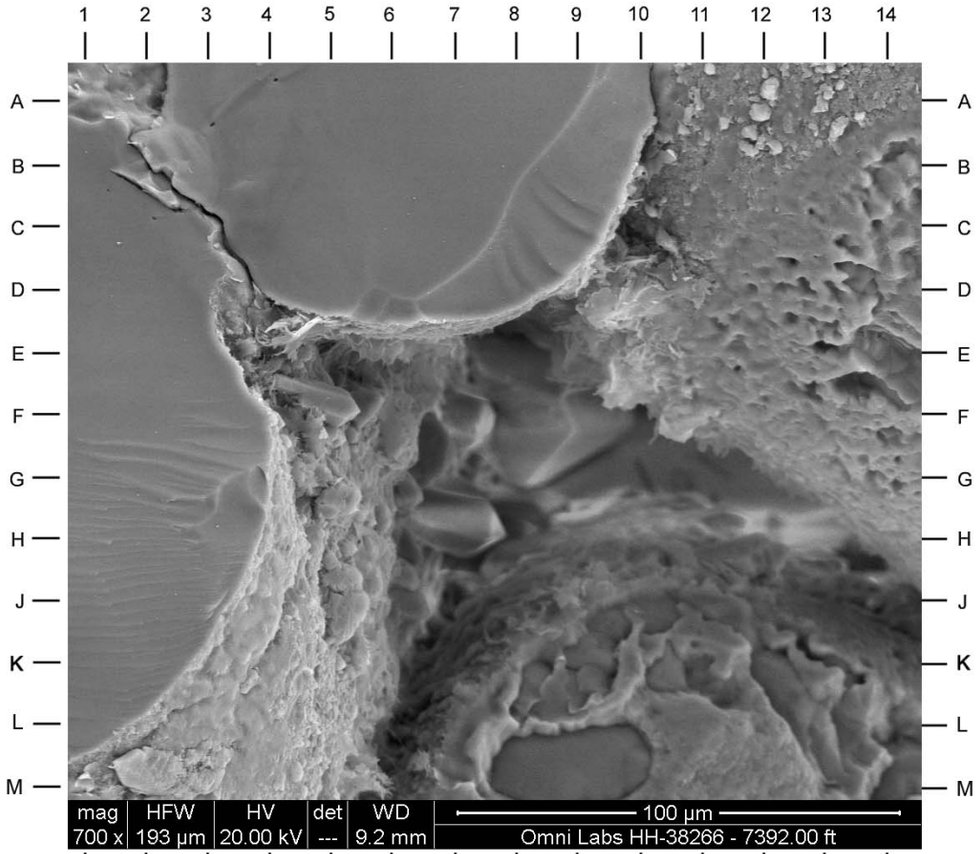

C

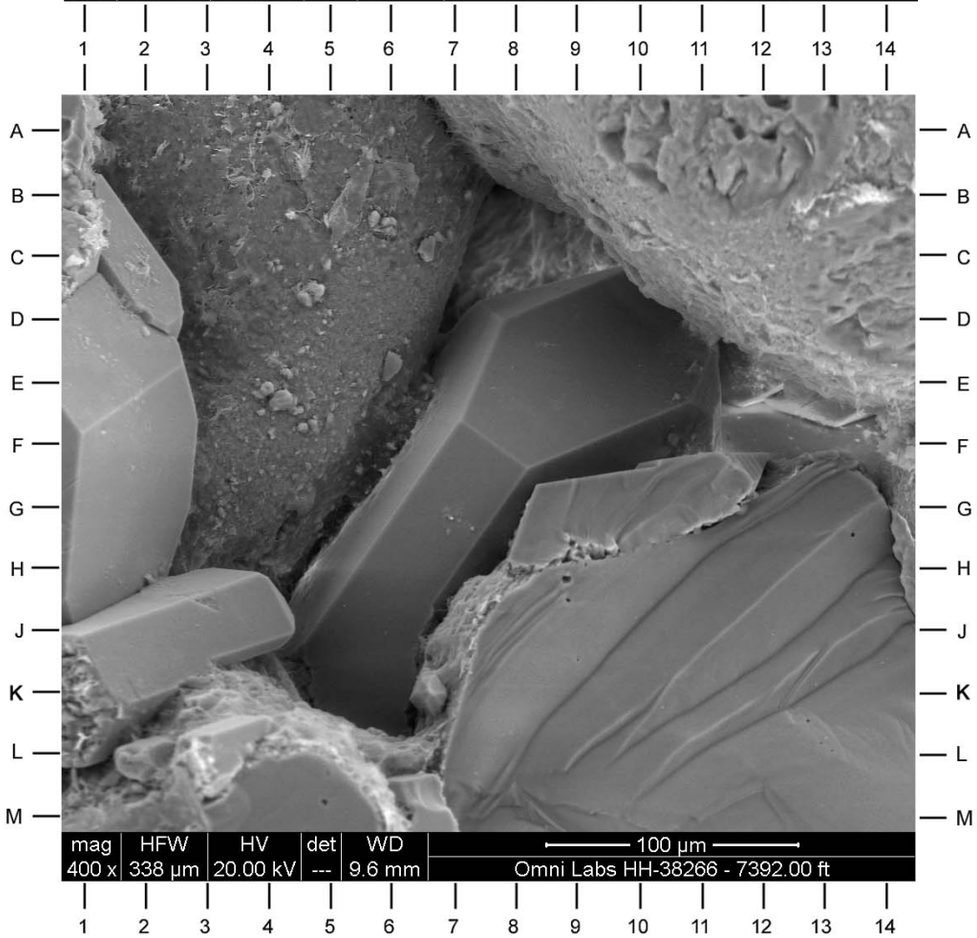

D

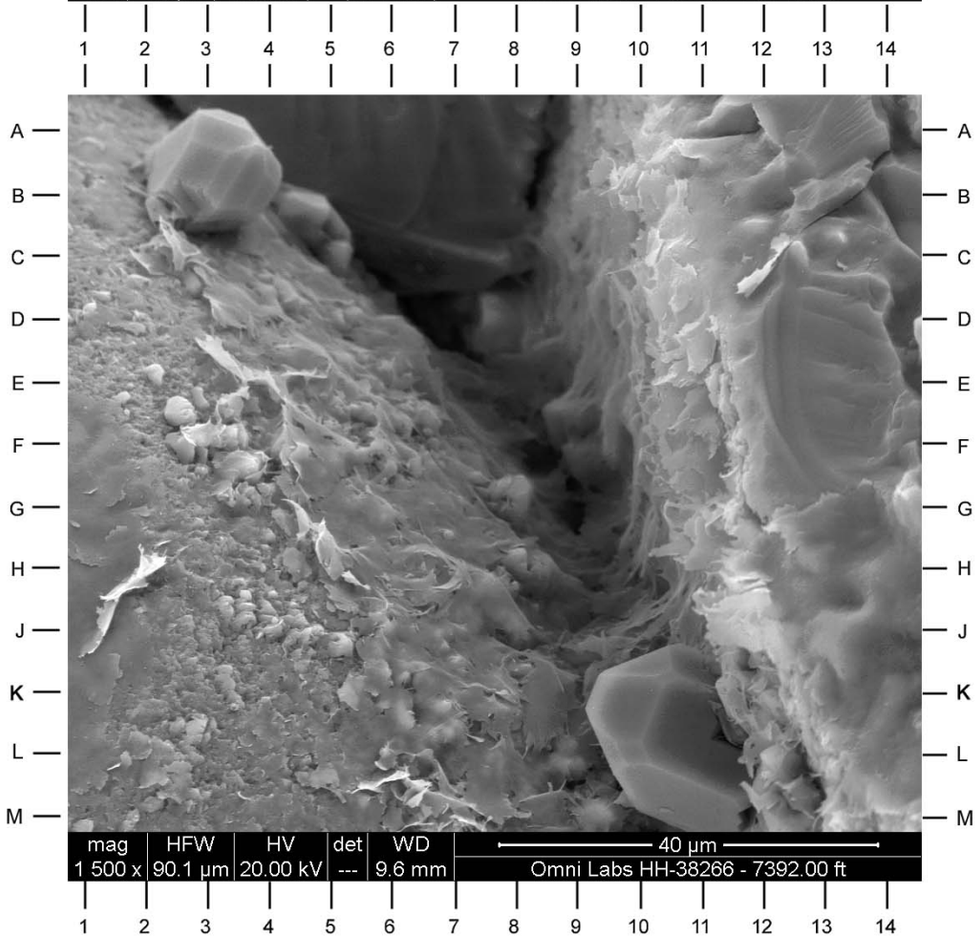

Ohio Division of Geological Survey **OMNI File No.: HH-38266**
CO_2 No. 1
Tuscarawas County, Ohio
Rose Run Sandstone Formation
Rotary Sidewall Core

SAMPLE DEPTH: 7441.0 FEET
SAMPLE NUMBER: 1-43R

PLATE 94

This medium-grained subarkose is moderately sorted with an average grain size of 0.31 mm. Quartz (Plate A; A5,E9,E13 / Plate B; H13 / Plate C; K13,M2) is the primary detrital grain type with abundant feldspar grains (Plate A; B3,D6 / Plate B; F3,K9 / Plate C; B8 / Plate D; L11). Quartz overgrowth cement (Plate B; D11,J4 / Plate C; K3 / Plate D; E2) is the dominant cement with a lesser amount of potassium feldspar overgrowths (Plate C; E5,G5.5,J6 / Plate D; A12,D9.5). Primary intergranular pores (Plate A; D-E10,H2,J5J-K11) are the dominant pore type, with secondary intragranular pores (Plate A; F3.6,L12.5 / Plate B; F2) within partially dissolved grains contributing to overall porosity. Illitic clay coats grains (Plate B; H5,H7-K5 / Plate D; K13) and is intermixed with a partially dissolved potassium feldspar grain (Plate B; G5.5 / Plate C; C12.8,G12,L8 / Plate D; F8.5,H8).

Magnification: 94A - 100X
Magnification: 94B - 700X
Magnification: 94C - 1000X
Magnification: 94D - 1500X

Ohio Division of Geological Survey
CO2 No. 1
Tuscarawas County, Ohio

7441.00'
Plate 94

OMNI Laboratories, Inc.

A

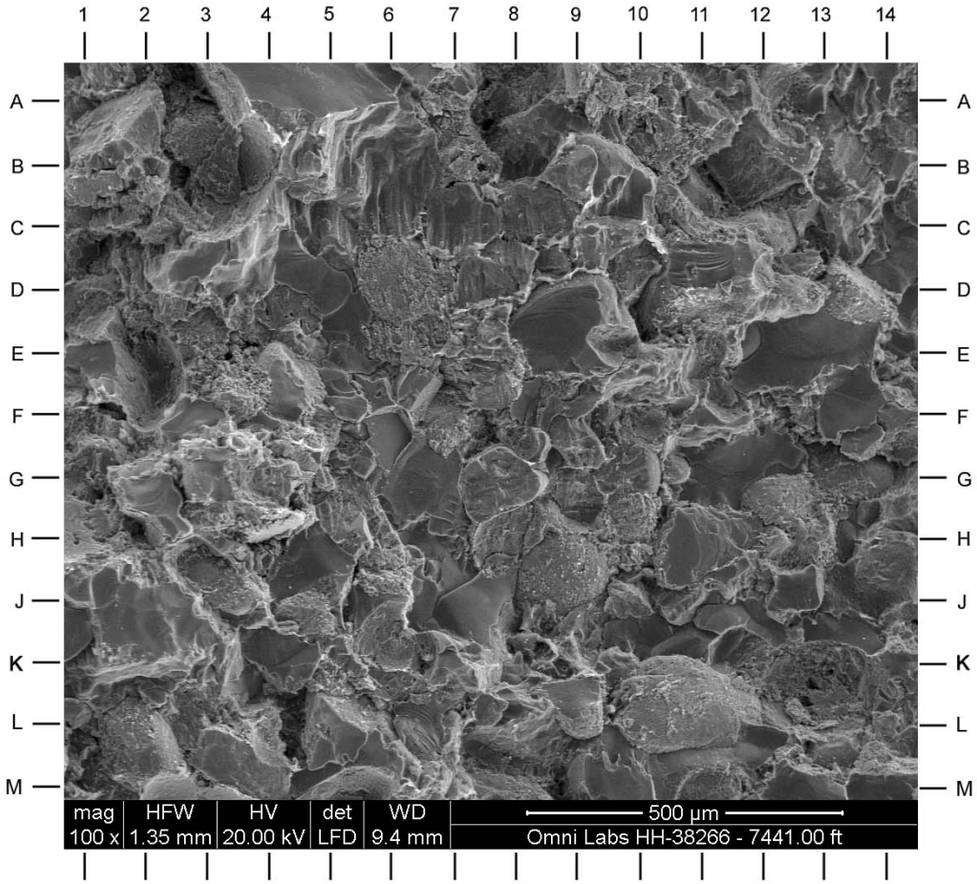

B

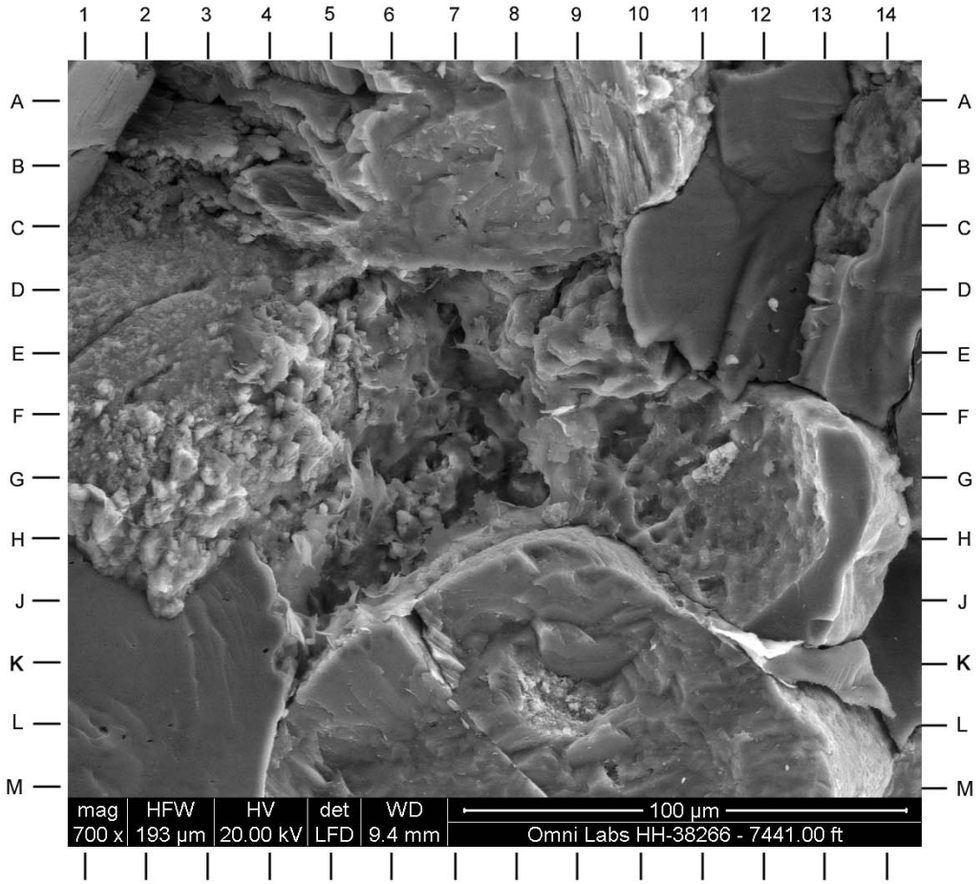

C

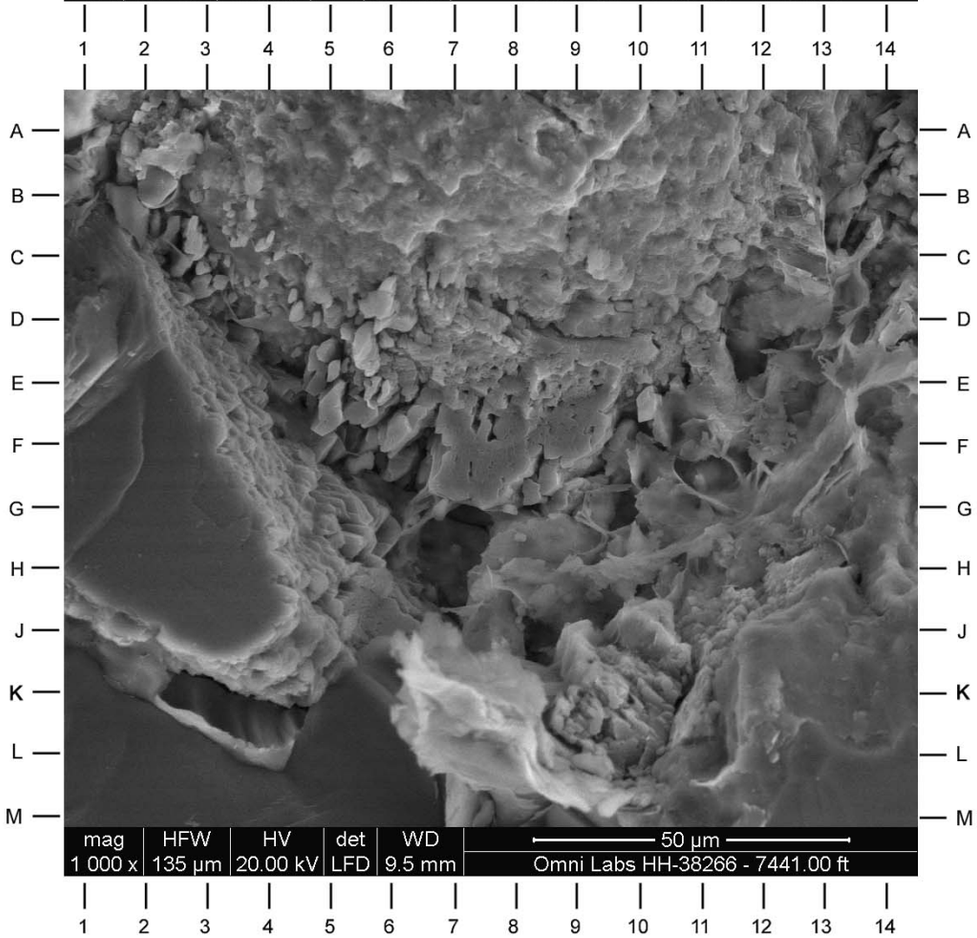

D

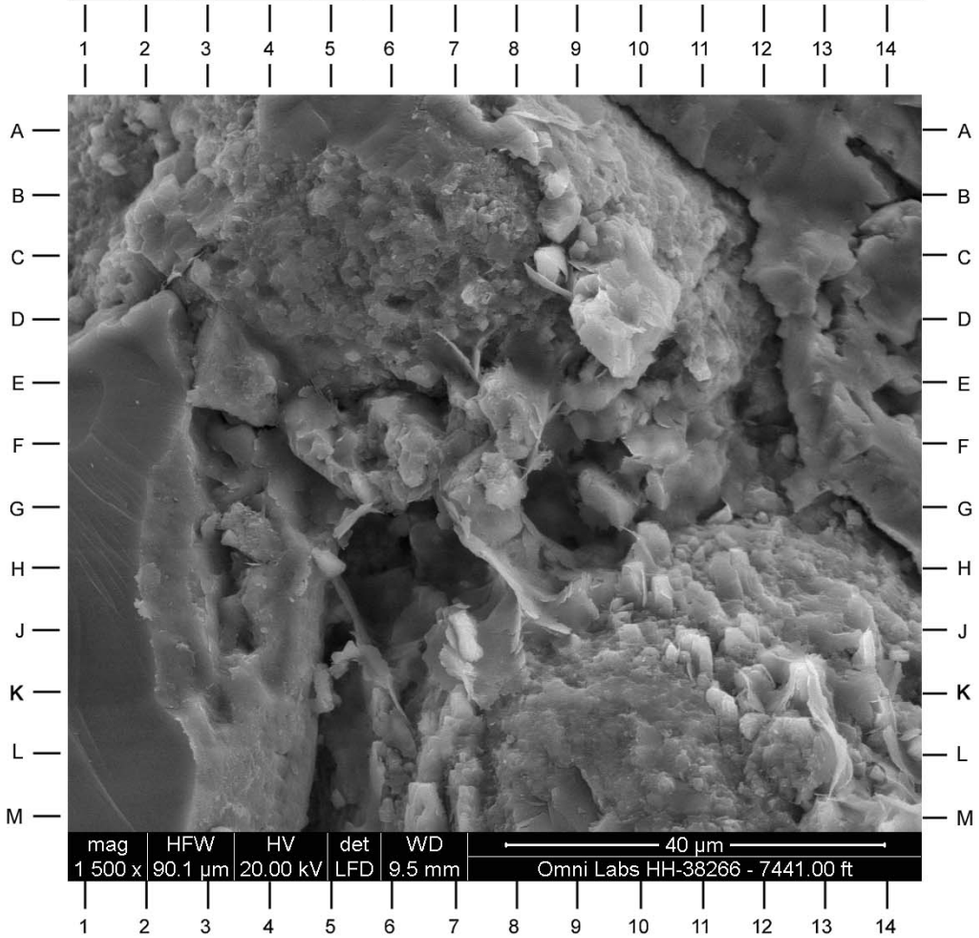

Ohio Division of Geological Survey **OMNI File No.: HH-38266**
CO_2 No. 1
Tuscarawas County, Ohio
Rose Run Sandstone Formation
Rotary Sidewall Core

SAMPLE DEPTH: 7506.0 FEET
SAMPLE NUMBER: 1-47R

PLATE 95

This subarkose has moderately poor sorting with an average grain size of 0.27 mm. Quartz (Plate A; D13.5, J12.5; Plate C; F13; Plate D; D6, J6) is the primary detrital grain type with common potassium feldspar (Plate B; J7 / Plate D; G13). Dolomite cement (Plate B; B8,B11 / Plate C; E4,F6,H8 / Plate D; H5) is the dominant cement type with lesser amounts of quartz overgrowths (Plate B; C4,E11,G5 / Plate C; G5,M3 / Plate D; C8,D4). Partially dissolved grains (Plate A; D3,F-G11,H-J13 / Plate B; J7 / Plate C; G2 / Plate D; G13) containing secondary intragranular pores dominate the pore system with lesser amounts of intergranular pores (Plate A; C-D5.4,G10,J-K11.8 ; Plate D; D8.5).

Magnification: 95A - 70X
Magnification: 95B - 500X
Magnification: 95C - 700X
Magnification: 95D - 1300X

Ohio Division of Geological Survey
CO2 No. 1
Tuscarawas County, Ohio

7506.00'
Plate 95

Omni Laboratories, Inc.

A

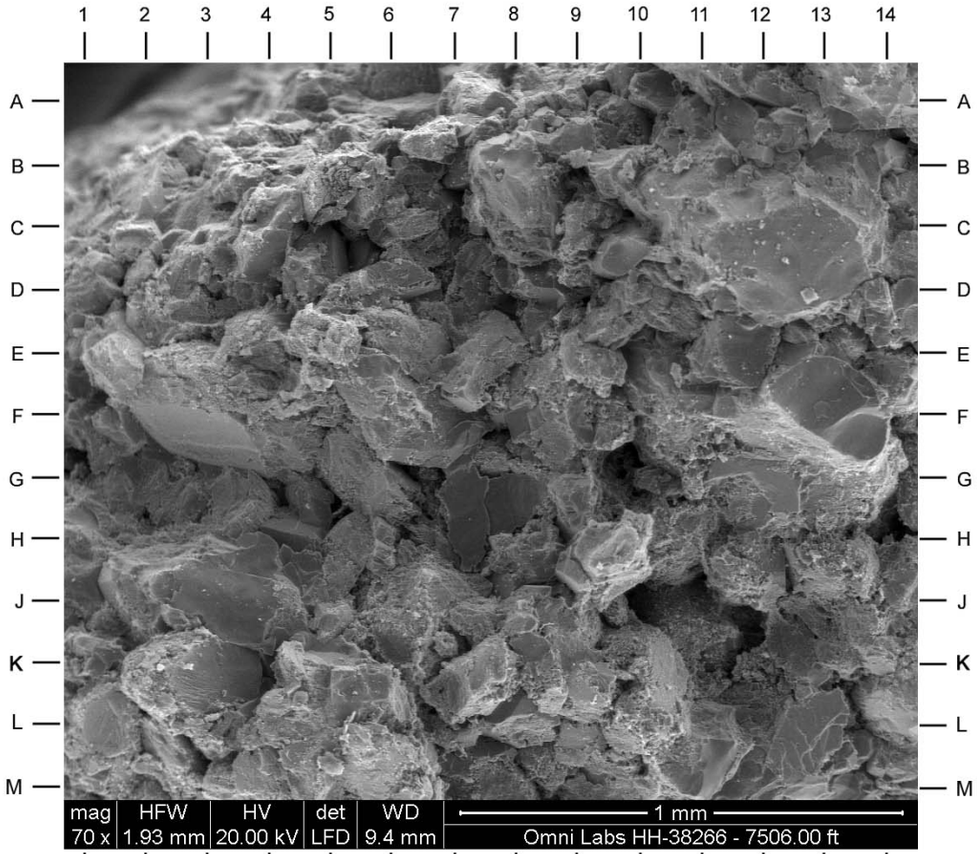

B

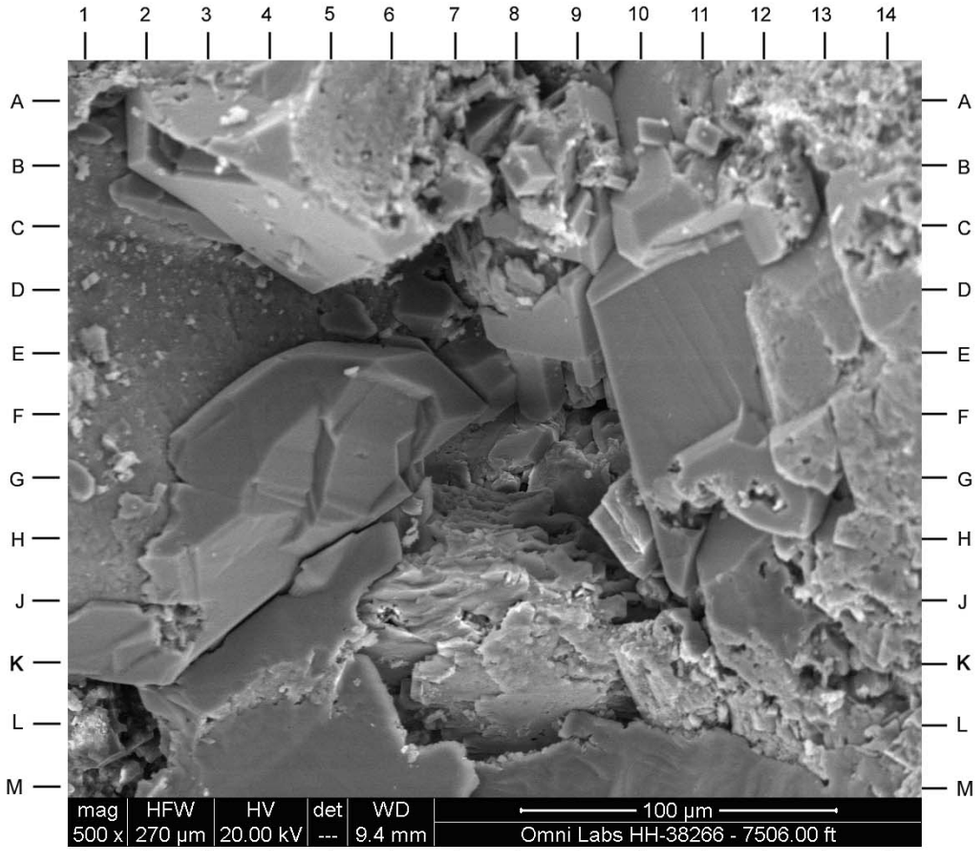

C

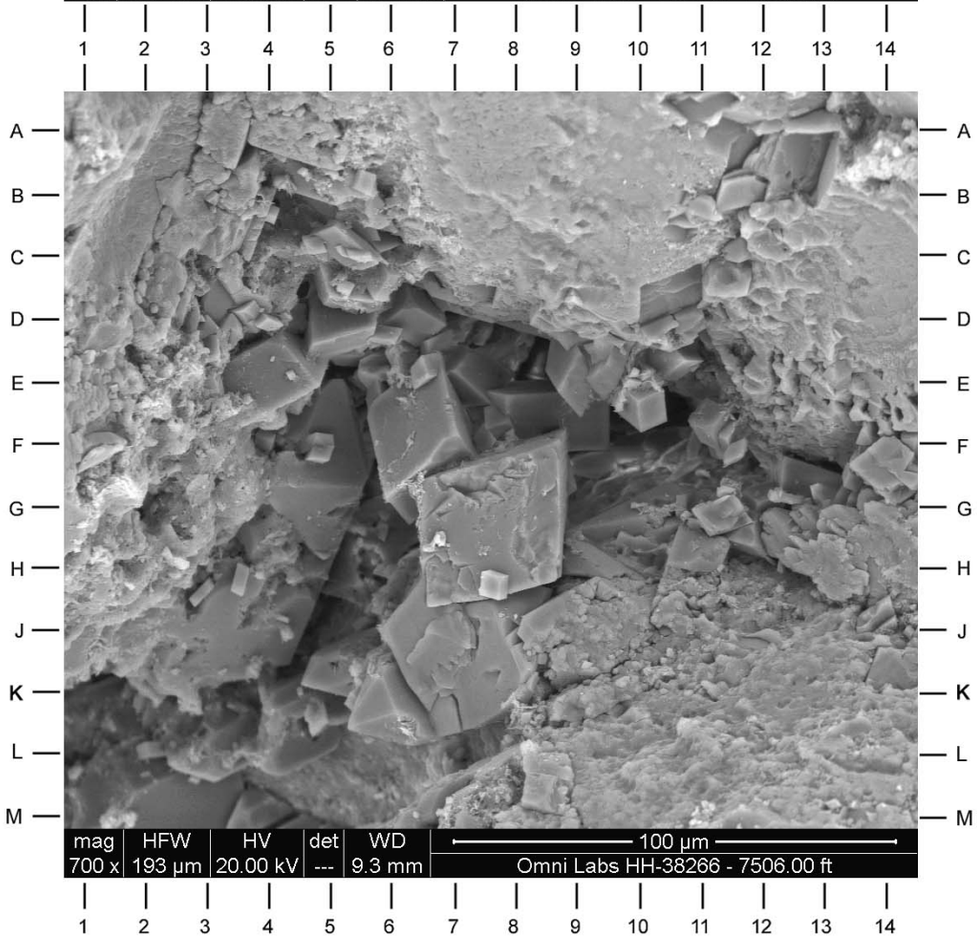

D

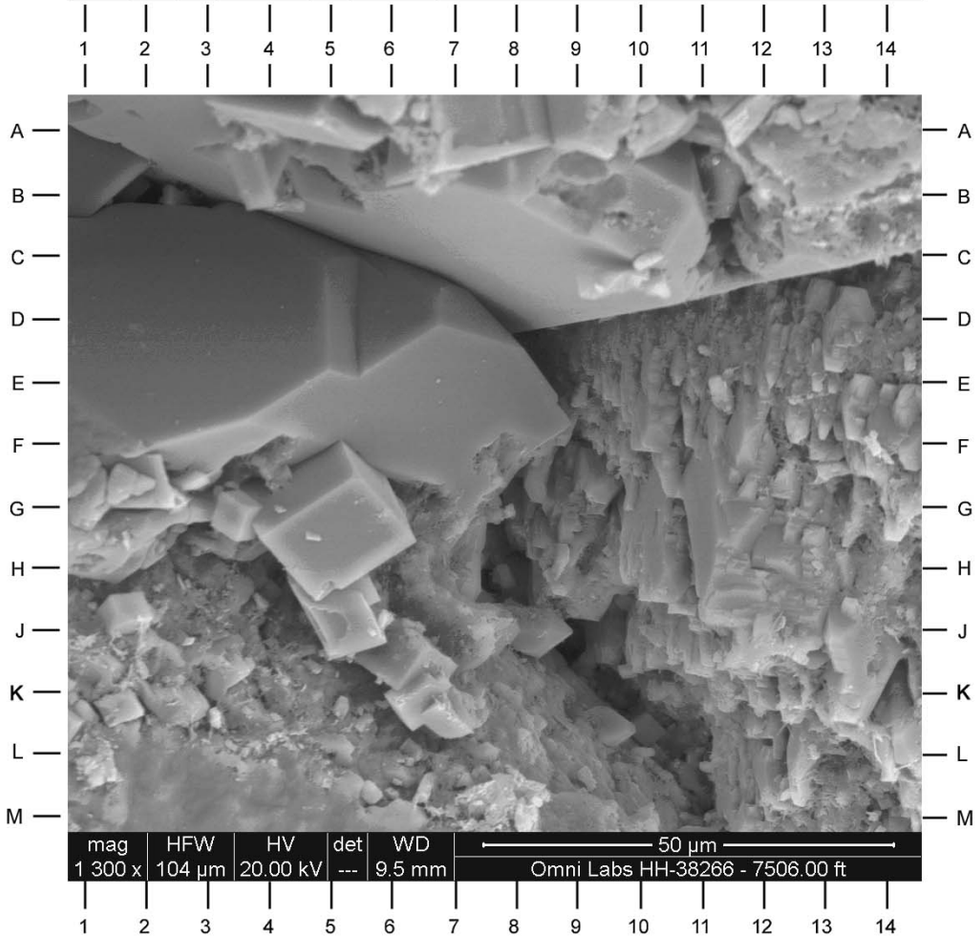

Ohio Division of Geological Survey **OMNI File No.: HH-38266**
CO_2 No. 1
Tuscarawas County, Ohio
Copper Ridge Dolomite Formation
Rotary Sidewall Core

SAMPLE DEPTH: 7692.0 FEET
SAMPLE NUMBER: 1-50R

PLATE 96

This medium crystalline skeletal/peloidal dolostone sample has a massive/non-planar dolomite fabric. Replacement dolomite (Plate A; D3,K4 / Plate B; C6,D8,K12 / Plate D; A12-C1,H14-L4) dominates this rock with a minor amount of detrital quartz (Plate A; D12.3 / Plate B; F4,F11). There are few interparticle pores (Plate A; H11.5,J4.3) with intercrystalline micropores (Plate B; G-H13.8,J7 / Plate C; A6.5 / Plate D; C4,J9) dominating the pore system. Microcrystalline and microporous apatite (Plate D; E14-H1) is visible surrounded by dolomite cement. A trace amount of illitic clay (Plate D; E6,F6,G6) occurs in micropores within a phosphatic shell fragment.

Magnification: 96A - 150X
Magnification: 96B - 700X
Magnification: 96C - 1100X
Magnification: 96D - 1200X

Ohio Division of Geological Survey
CO2 No. 1
Tuscarawas County, Ohio

7692.00'
Plate 96

OMNI Laboratories, Inc.

A

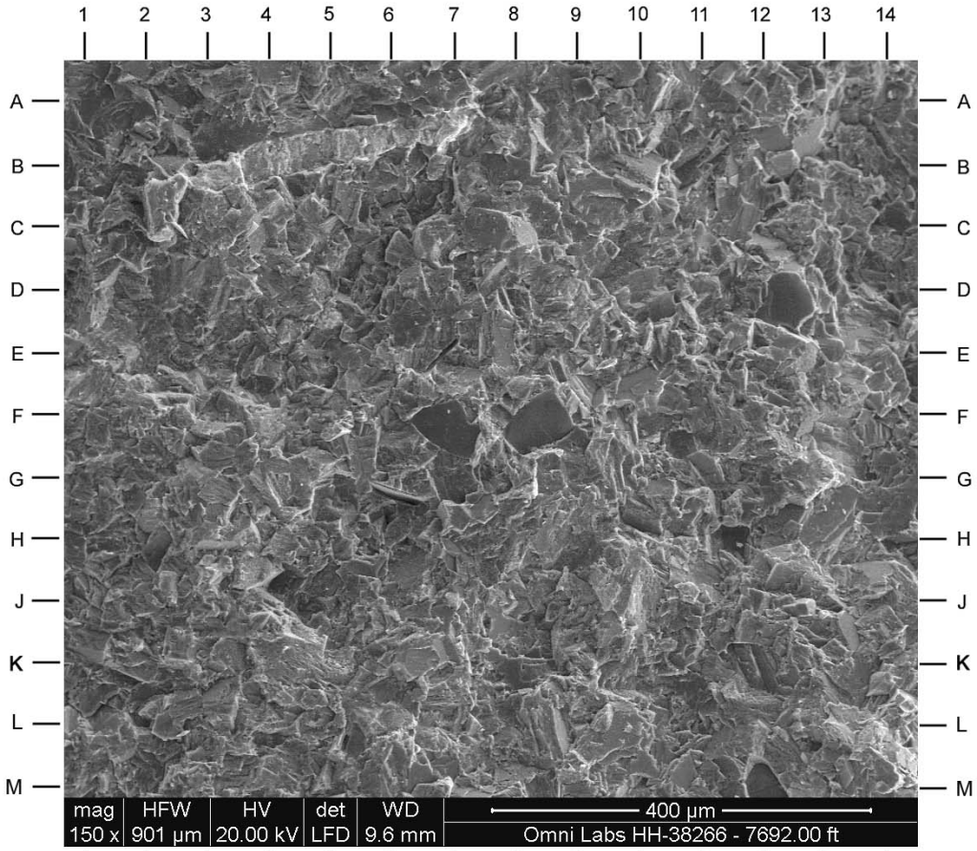

B

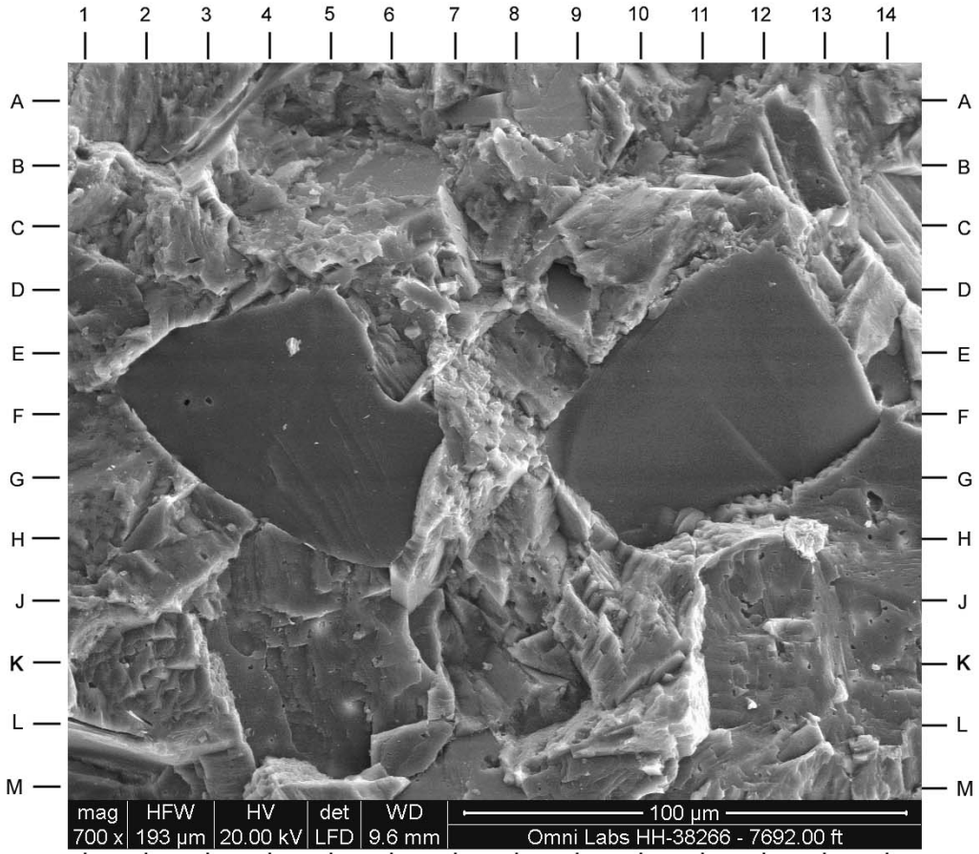

C

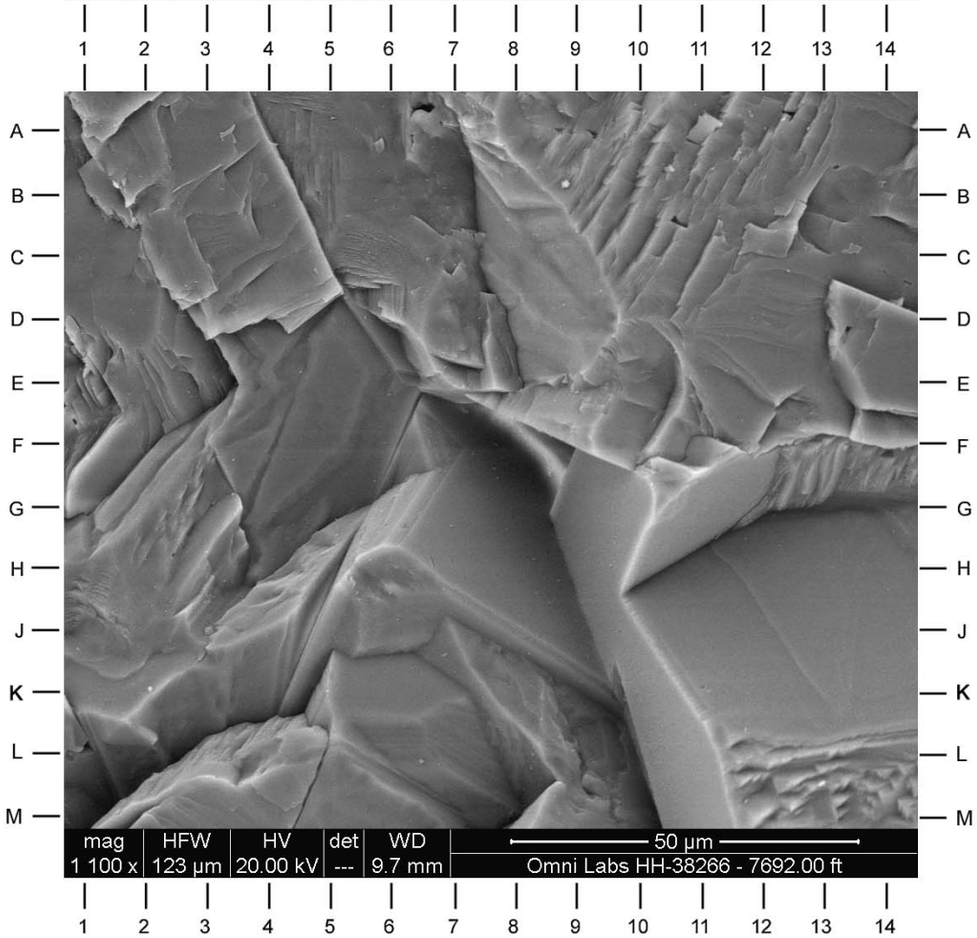

D

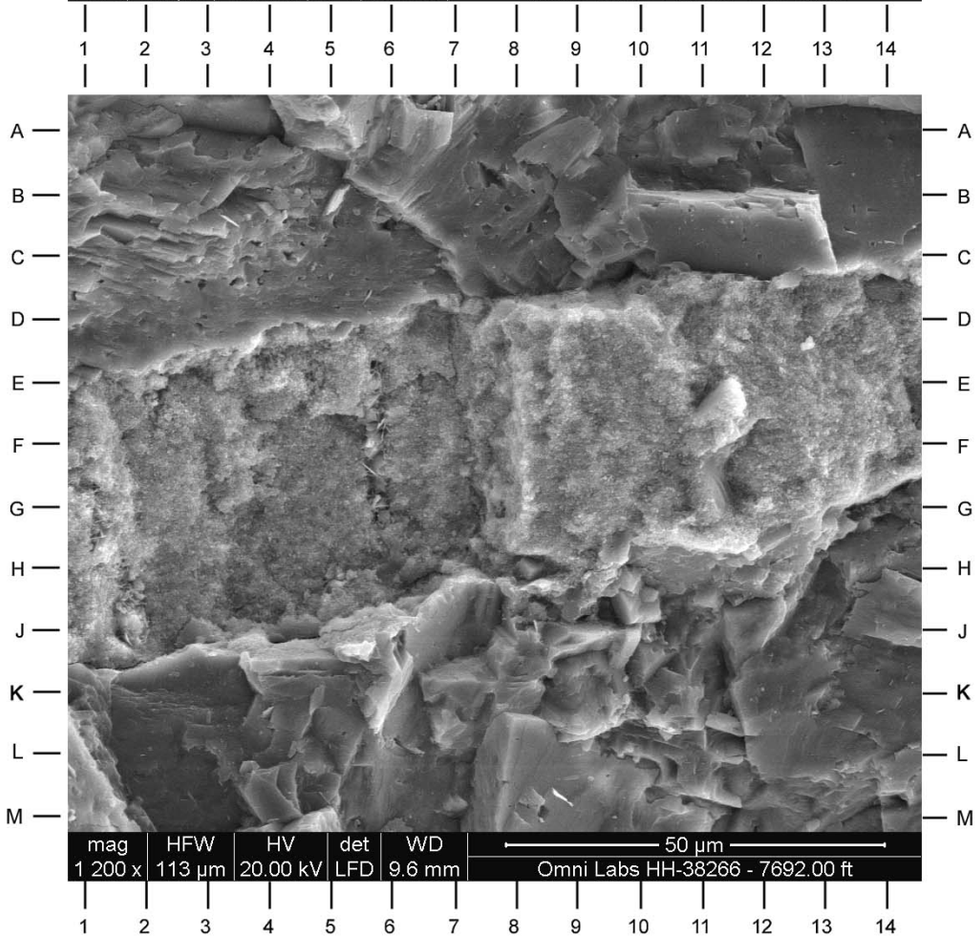

Ohio Division of Geological Survey **OMNI File No.: HH-38266**
CO_2 No. 1
Tuscarawas County, Ohio
Cambrian Basal Sandstone Formation
Rotary Sidewall Core

SAMPLE DEPTH: 8538.0 FEET
SAMPLE NUMBER: 1-68R

PLATE 97

This arkose is poorly sorted with an average grain size of 0.23 mm. The primary cements consist predominantly of dolomite (Plate B; B13,L3 / Plate C; G5) with lesser amounts of quartz overgrowths (Plate B; F9 / Plate C; D9,K11 / Plate D; A3,C4,B11). Secondary intragranular pores in leached grains (Plate A; E7.5,J1.5,L9.5 / Plate B; F2,J12) dominate the pore system with lesser amounts of micropores (Plate B; J7 / Plate C; A6,G2 / Plate D; D8,J6) and intergranular pores (Plate A; F9,H6.3 / Plate B; J5 / Plate C; F8). Detrital chlorite coats grains (Plate B; B8 / Plate C; K13 / Plate D; A9-M8) and occludes intergranular pores (Plate B; F12,G5 / Plate C; H6).

Magnification: 97A - 100X
Magnification: 97B - 800X
Magnification: 97C - 1100X
Magnification: 97D - 1700X

Ohio Division of Geological Survey
CO2 No. 1
Tuscarawas County, Ohio

8538.00'
Plate 97

OMNI Laboratories, Inc.

A

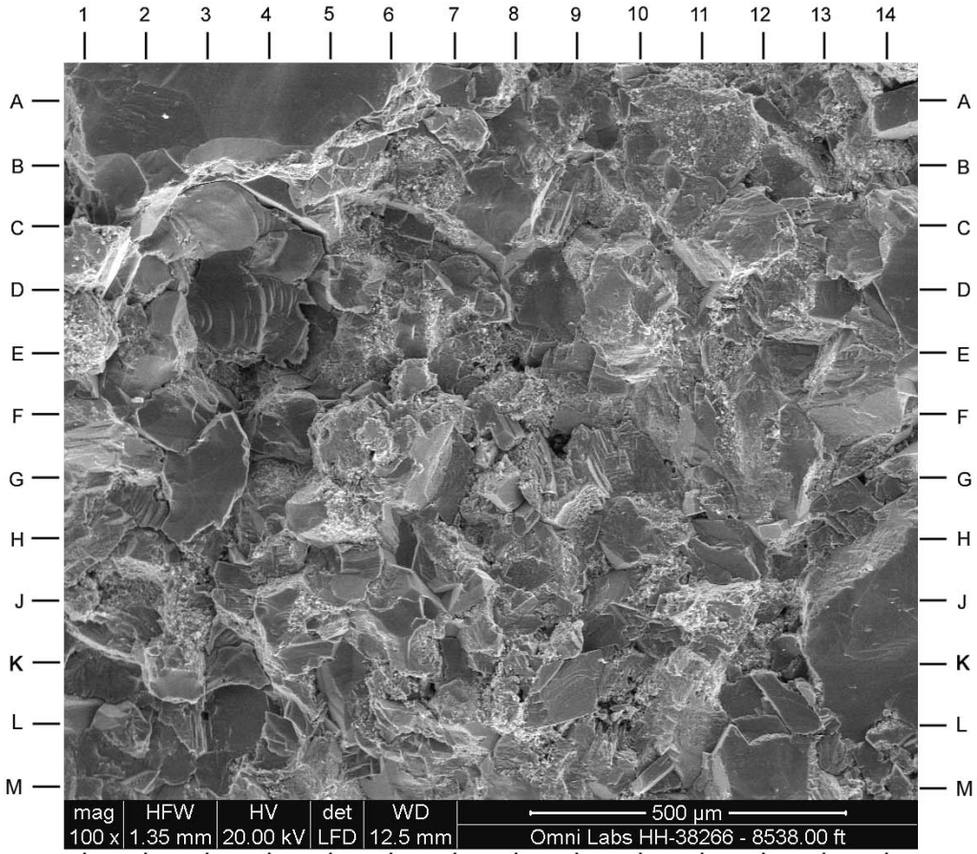

B

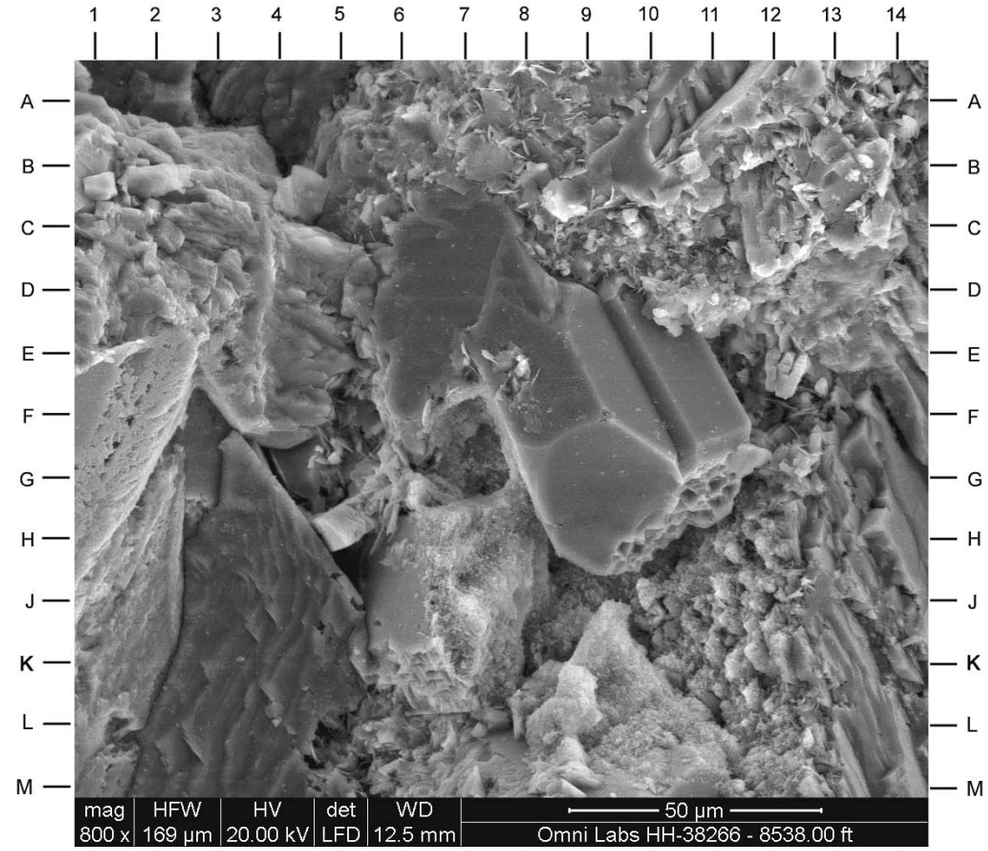

C

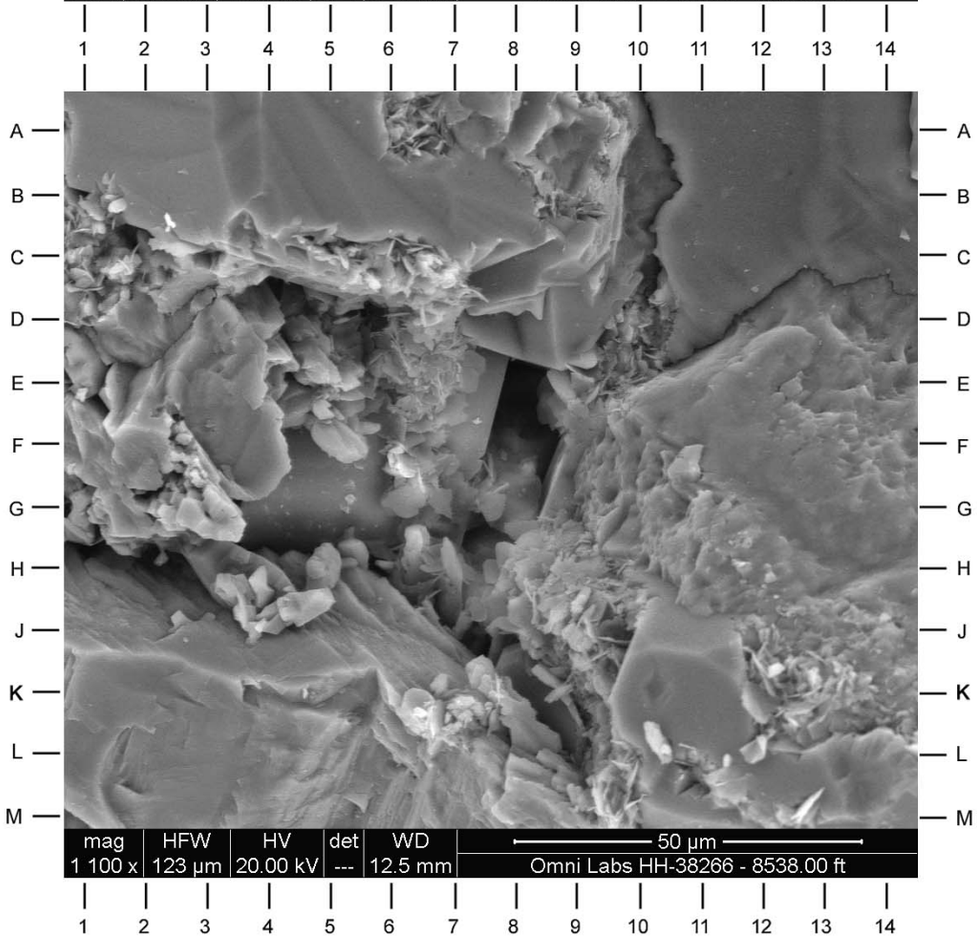

D

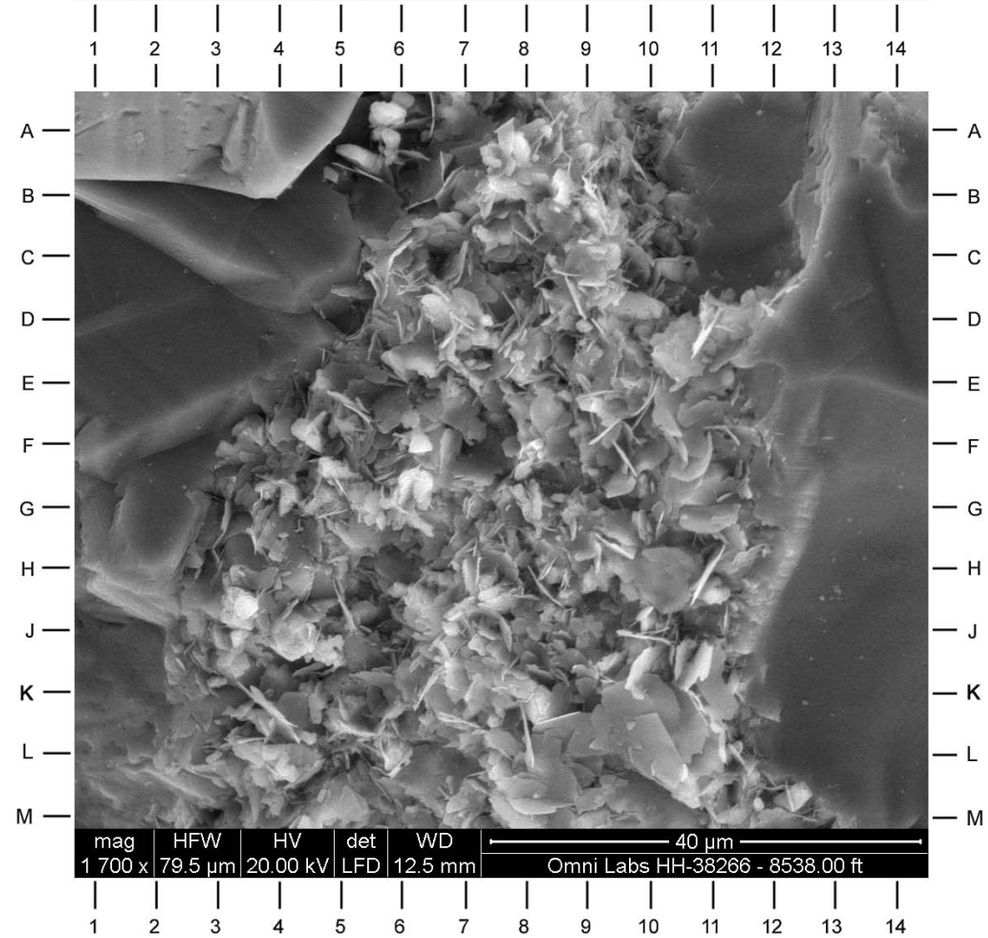

Ohio Division of Geological Survey **OMNI File No.: HH-38266**
CO_2 No. 1
Tuscarawas County, Ohio
Cambrian Basal Sandstone Formation
Rotary Sidewall Core

SAMPLE DEPTH: 8561.0 FEET
SAMPLE NUMBER: 1-72R

PLATE 98

This arkose is moderately well sorted with an average grain size of 0.26 mm (lower to medium sand). The sample has a vaguely laminated fabric. The primary detrital grain type is quartz (Plate A; A-B3,C-D12,J9 / Plate B; F2,H13 / Plate C; H1) with abundant feldspar grains (Plate A; C1,F11 / Plate B; B6 / Plate C; B6,K10). Primary intergranular pores (Plate A; B2,B10.5,D8,K5) are the dominant type of porosity, with partially dissolved grains resulting in secondary intragranular pores (Plate A; C-D4,C9,K3 / Plate C; L10 / Plate D; area centered around G8). Quartz overgrowths (Plate B; D9,H9 / Plate C; D10,K3 / Plate D; B7,E3,H8) are the dominant cement with a lesser amounts of potassium feldspar overgrowths (Plate B; L2). Illitic clay is intermixed with quartz overgrowths (Plate D; C13.5,D10-G5,J11).

Magnification: 98A - 100X
Magnification: 98B - 700X
Magnification: 98C - 1000X
Magnification: 98D - 2000X

Ohio Division of Geological Survey
CO2 No. 1
Tuscarawas County, Ohio

8561.00'
Plate 98

OMNI Laboratories, Inc.

A

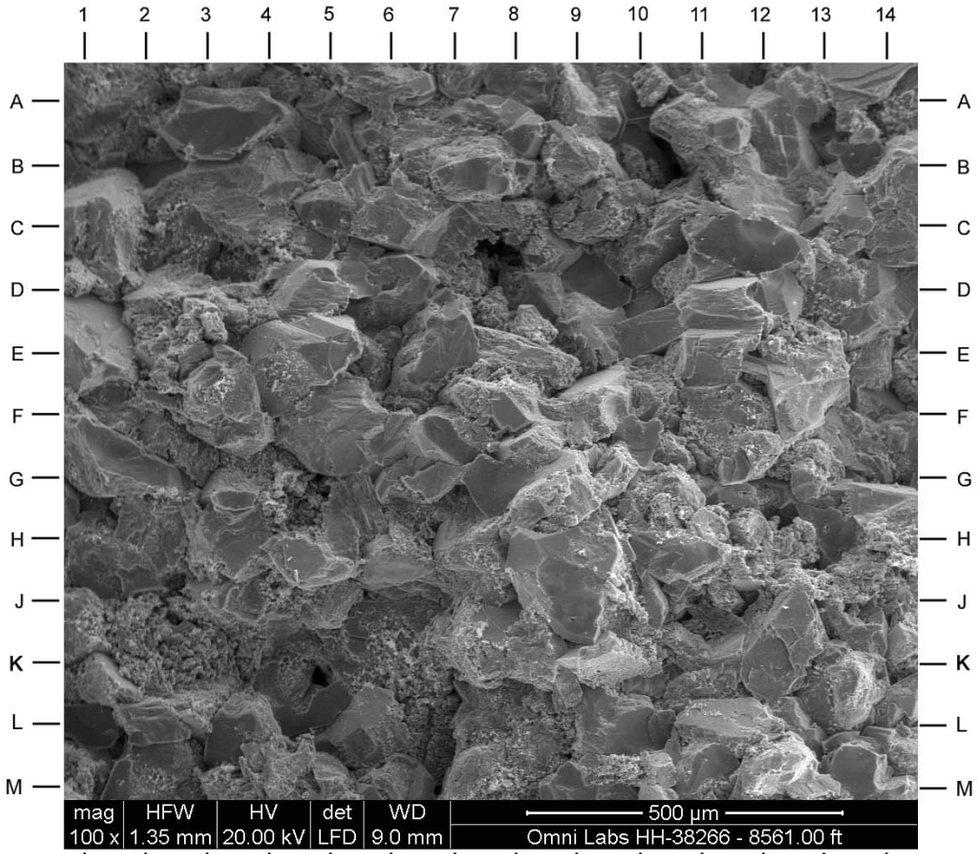

B

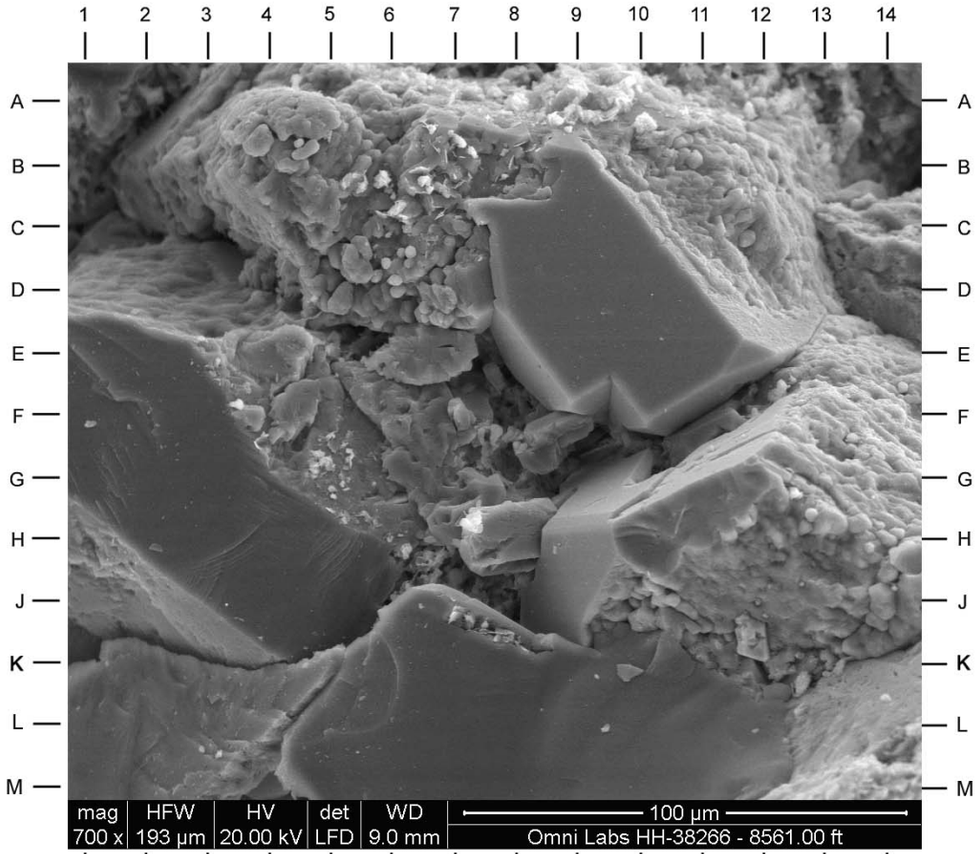

C

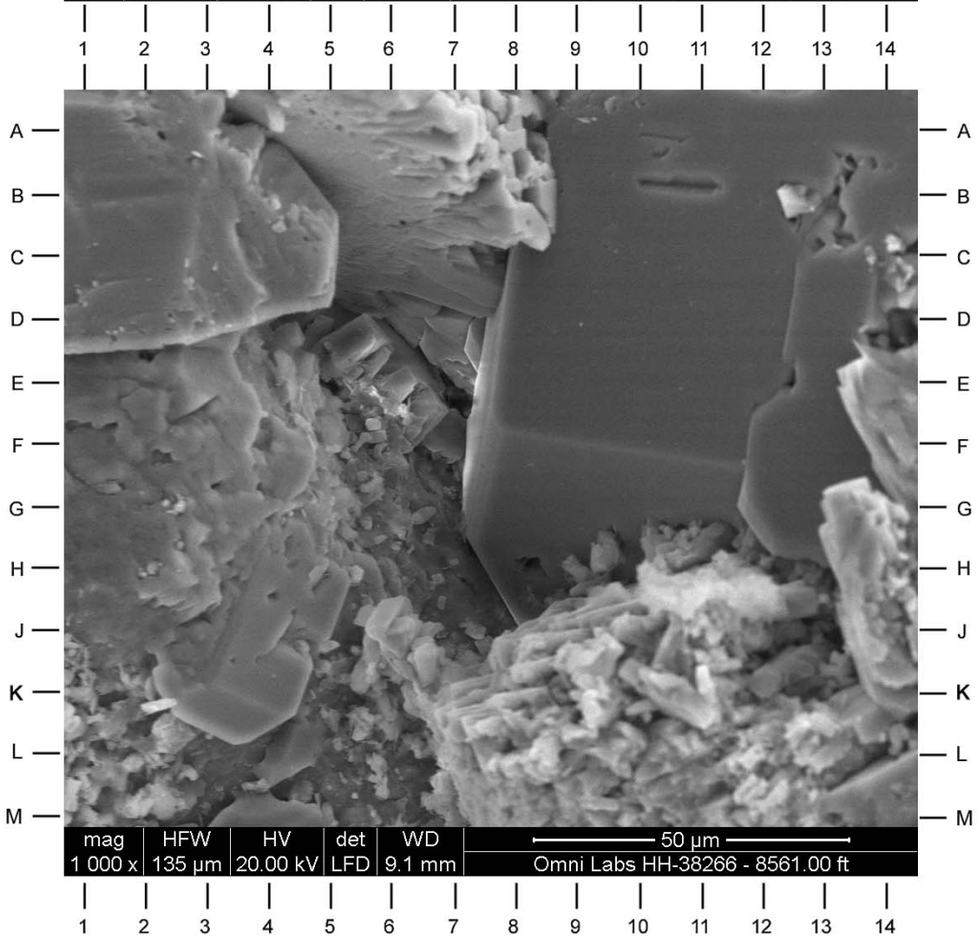

D

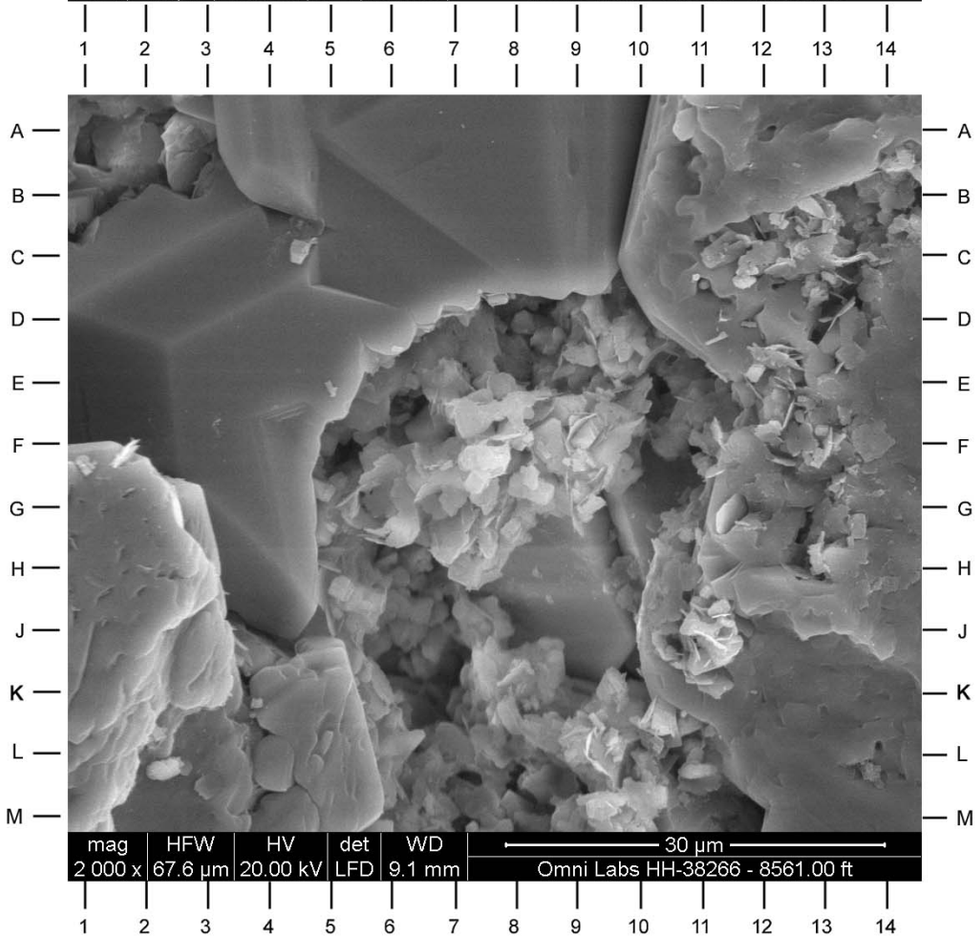

Ohio Division of Geological Survey **OMNI File No.: HH-38266**
CO_2 No. 1
Tuscarawas County, Ohio
Cambrian Basal Sandstone Formation
Rotary Sidewall Core

SAMPLE DEPTH: 8583.0 FEET
SAMPLE NUMBER: 1-74R

PLATE 99

This arkose is moderately poor sorted with an average grain size of 0.28 mm. Quartz (Plate A; F14,H2,J7) is the primary detrital grain type with abundant feldspars (Plate A; E1,J5 / Plate B; C13,L2 / Plate C; E5). Micropores (Plate B; B3,B6,G-H2 / Plate C; A11,E12K9.5) are the dominant pore type with lesser amounts of intergranular pores (Plate A; C3,D6,E-F10.5,G8.5) and secondary intragranular pores (Plate A; C12.8,E-F12.8,E-F2) in leached grains. A combination of illite and chlorite (Plate B; A2-G12 / Plate C; L2,L6.5 / Plate D; B12,H11,L4,L13) is visible replacing leached feldspars. Dolomite cement (Plate D; A3-J4) is the predominant cement with lesser amounts of quartz overgrowths (Plate B; J14) and feldspar overgrowths (Plate C; D11,F2).

Magnification: 99A - 130X
Magnification: 99B - 1500X
Magnification: 99C - 1100X
Magnification: 99D - 2300X

Ohio Division of Geological Survey
CO2 No. 1
Tuscarawas County, Ohio

8583.00'
Plate 99

A

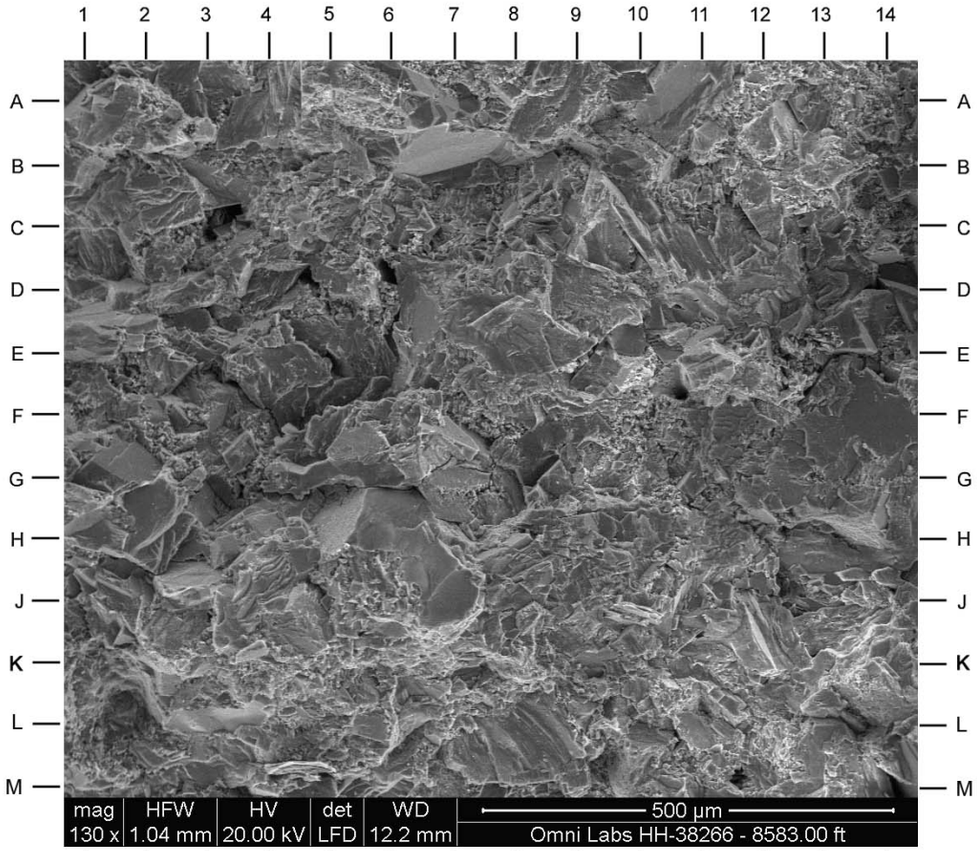

B

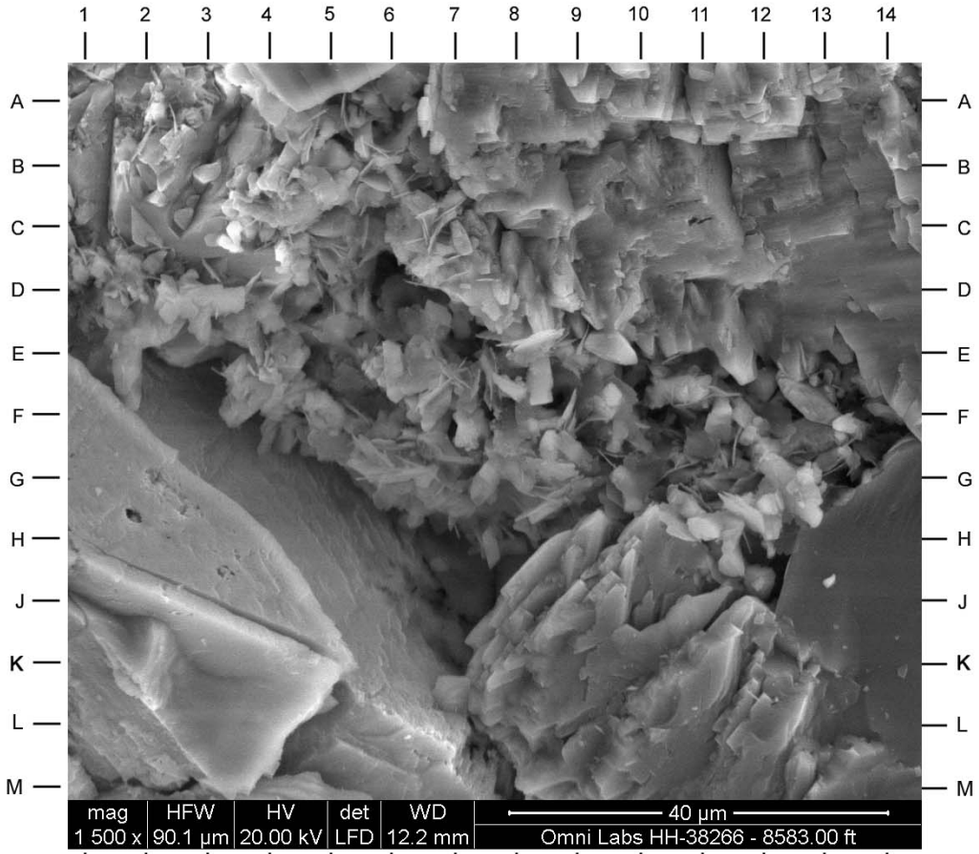

C

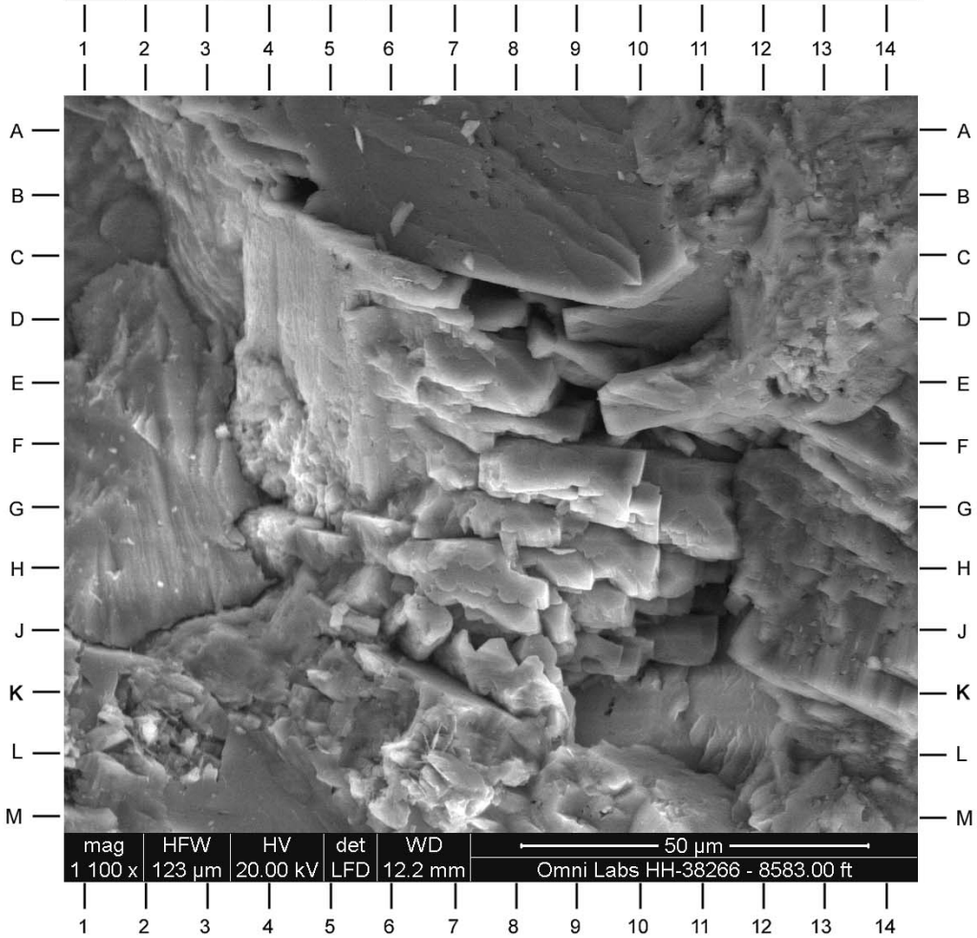

D

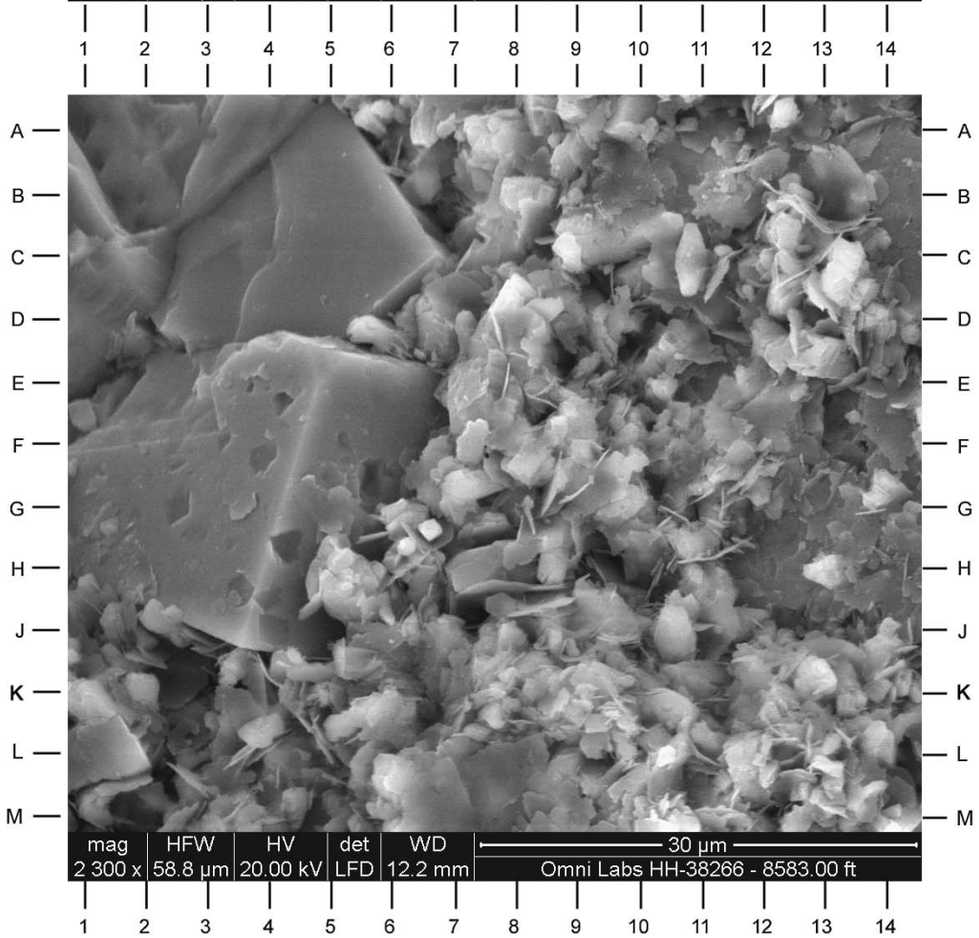

Ohio Division of Geological Survey **OMNI File No.: HH-38266**
CO_2 No. 1
Tuscarawas County, Ohio
Cambrian Basal Sandstone Formation
Rotary Sidewall Core

SAMPLE DEPTH: 8628.0 FEET
SAMPLE NUMBER: 1-79R

PLATE 100

This sample consists of granoblastic quartzo-feldspathic gneiss with banded foliated chlorite/biotite schist that exhibits an aligned and micro-fractured fabric (Plate D). Major minerals consist of quartz (Plate B; B7) and feldspars (Plate B, C12, L5). The sample contains a trace amount of apatite crystals (Plate B; H8 / Plate C; J10) which are surrounded by feldspar with altered / fractured rims (Plate B; H11; F4). Although the sample is well crystallized, micropores to nanopores are visible at high magnification between some crystals and along some fractures (Plat3 D; E4, K11).

Magnification: 100A - 40X
Magnification: 100B - 300X
Magnification: 100C - 500X
Magnification: 100D - 800X

Ohio Division of Geological Survey
CO2 No. 1
Tuscarawas County, Ohio

8628.00'
Plate 100

OMNI Laboratories, Inc.

A

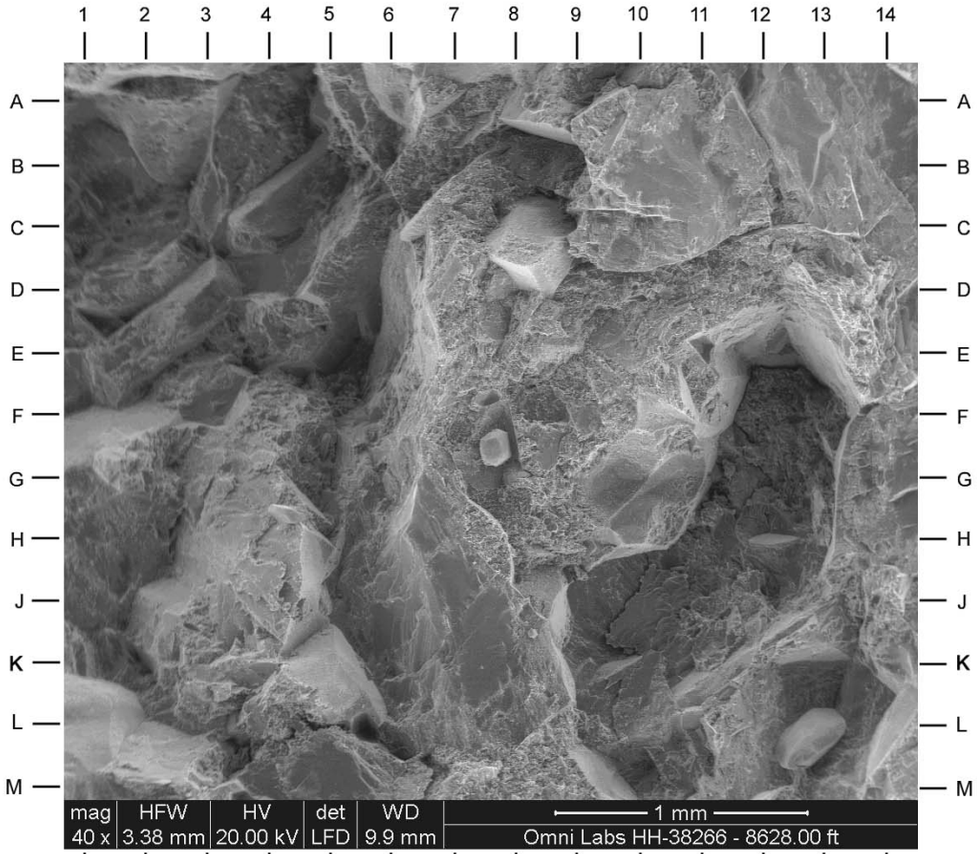

B

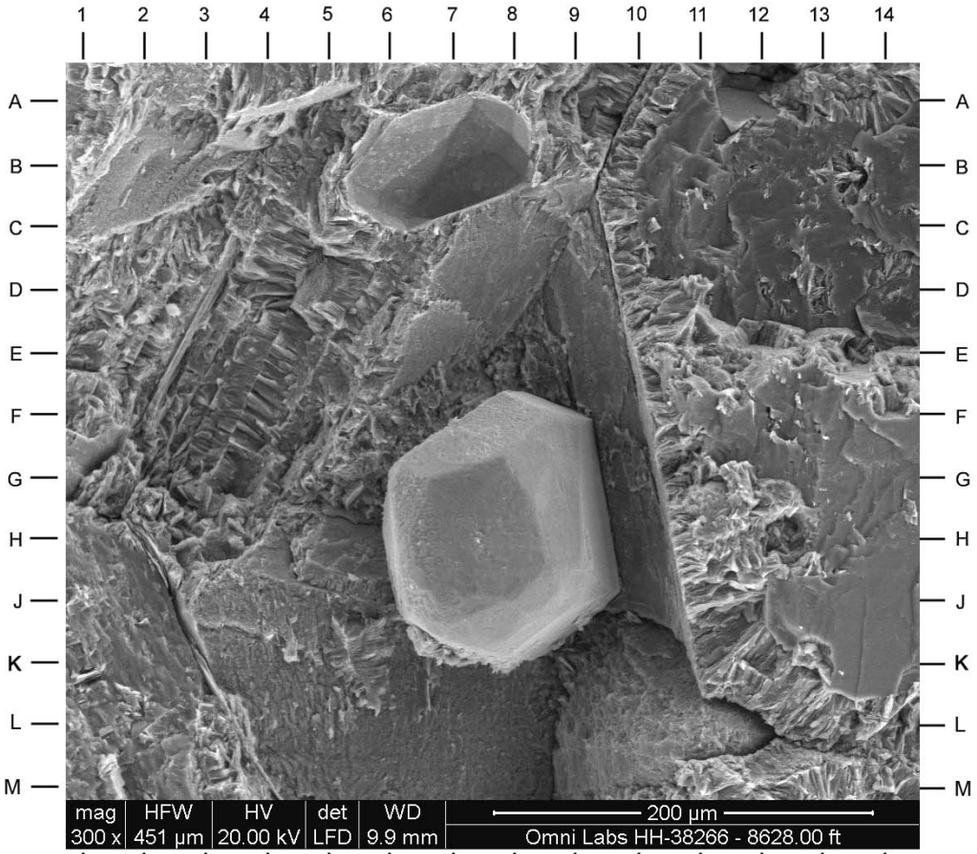

C

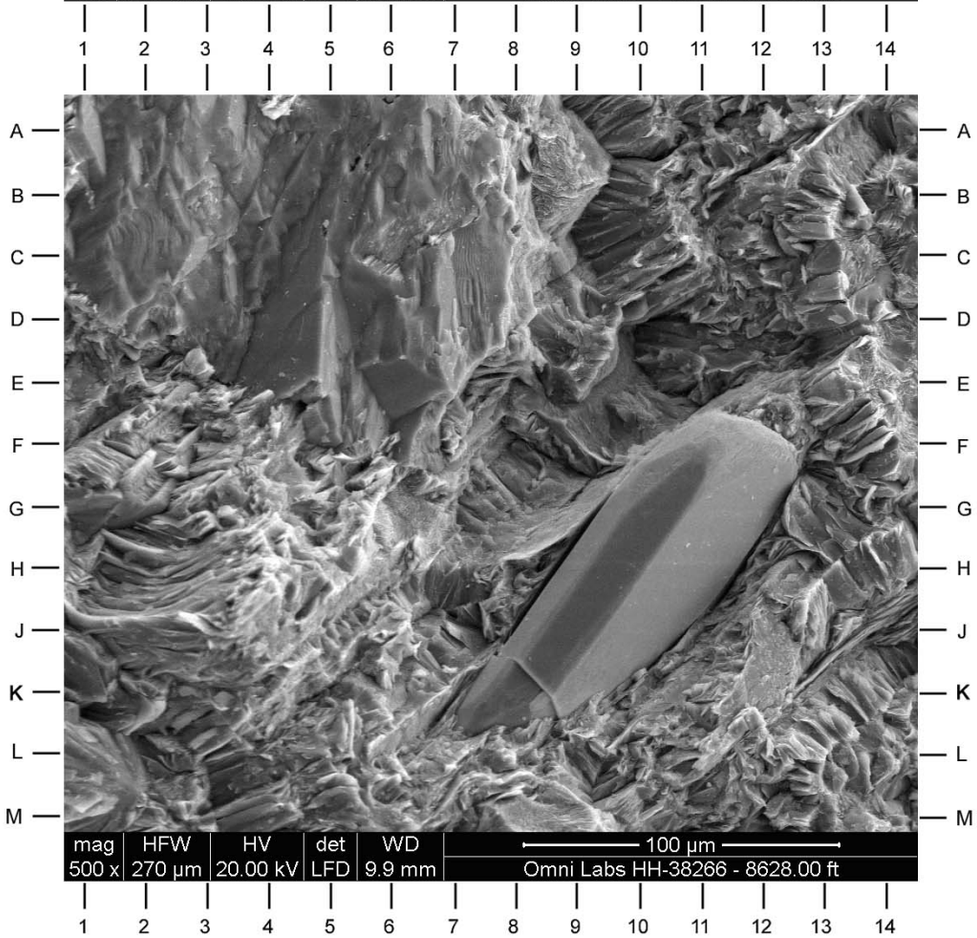

D

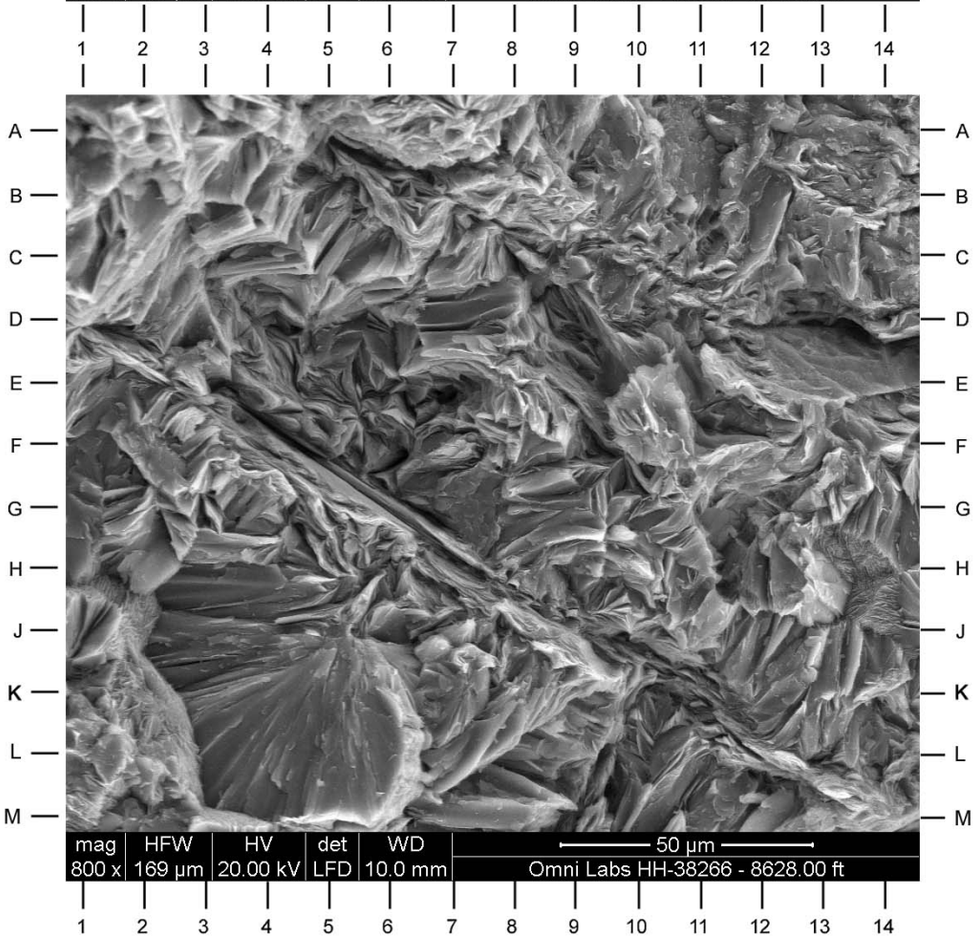

INTENTIONALLY BLANK

APPENDIX F

Rotary Sidewall Core Photography

for

Ohio Division of Geological Survey
CO2 No. 1 Well
Tuscarawas County, Ohio

Omni File No. HH-38266

INTENTIONALLY BLANK

Weatherford LABORATORIES

HH-38266

Ohio Division of Geological Survey
CO2 No. 1 Well
Tuscarawas County, Ohio

Rotary Sidewall Core Photography

Sample No.: 1-1R

Visible Light — Depth: 4605.00 feet — Ultraviolet Light

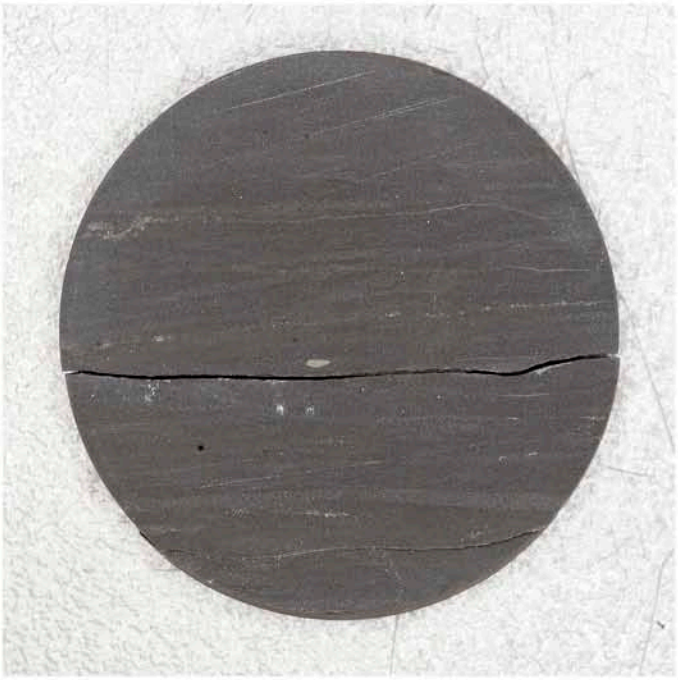

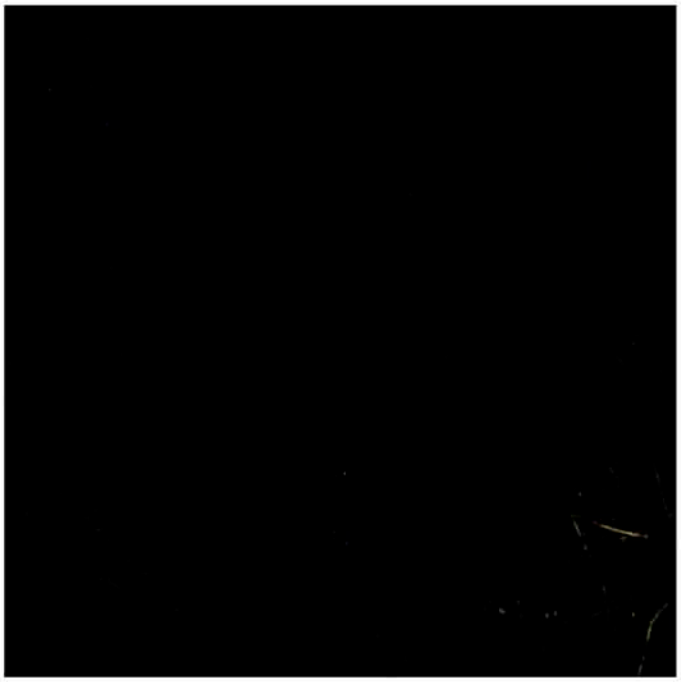

Sample No.: 1-2R

Visible Light — Depth: 4760.00 feet — Ultraviolet Light

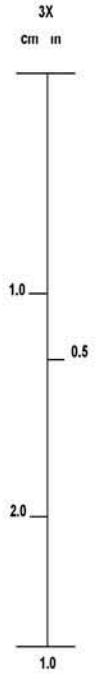

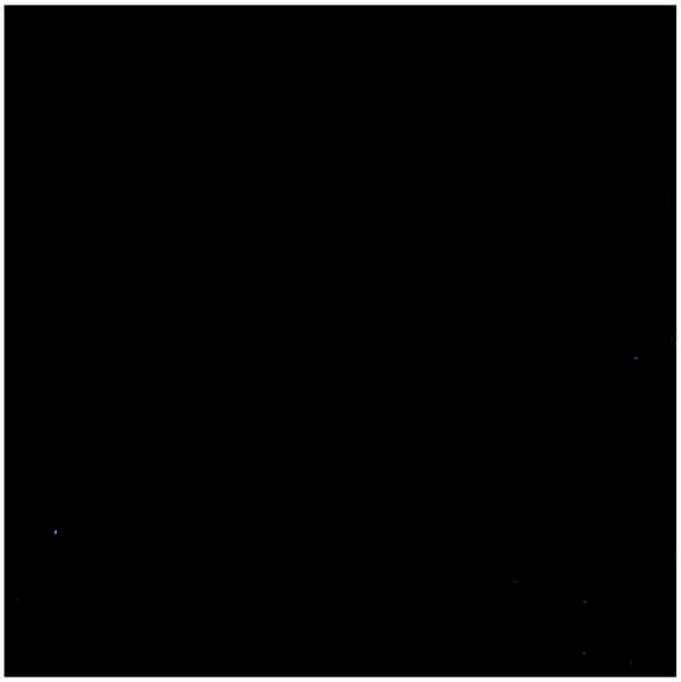

Weatherford LABORATORIES

HH-38266

Ohio Division of Geological Survey
CO2 No. 1 Well
Tuscarawas County, Ohio

Sample No.: 1-1R
Depth: 4605.00 feet

Visible Light

Longitudinal

Ultraviolet Light

Weatherford LABORATORIES

HH-38266

Ohio Division of Geological Survey
CO2 No. 1 Well
Tuscarawas County, Ohio

Sample No.: 1-2R
Depth: 4760.00 feet

Visible Light

Longitudinal

Ultraviolet Light

INTENTIONALLY BLANK

Weatherford LABORATORIES

HH-38266

Ohio Division of Geological Survey
CO2 No. 1 Well
Tuscarawas County, Ohio

Rotary Sidewall Core Photography

Sample No.: 1-3R

Visible Light — Depth: 4771.00 feet — Ultraviolet Light

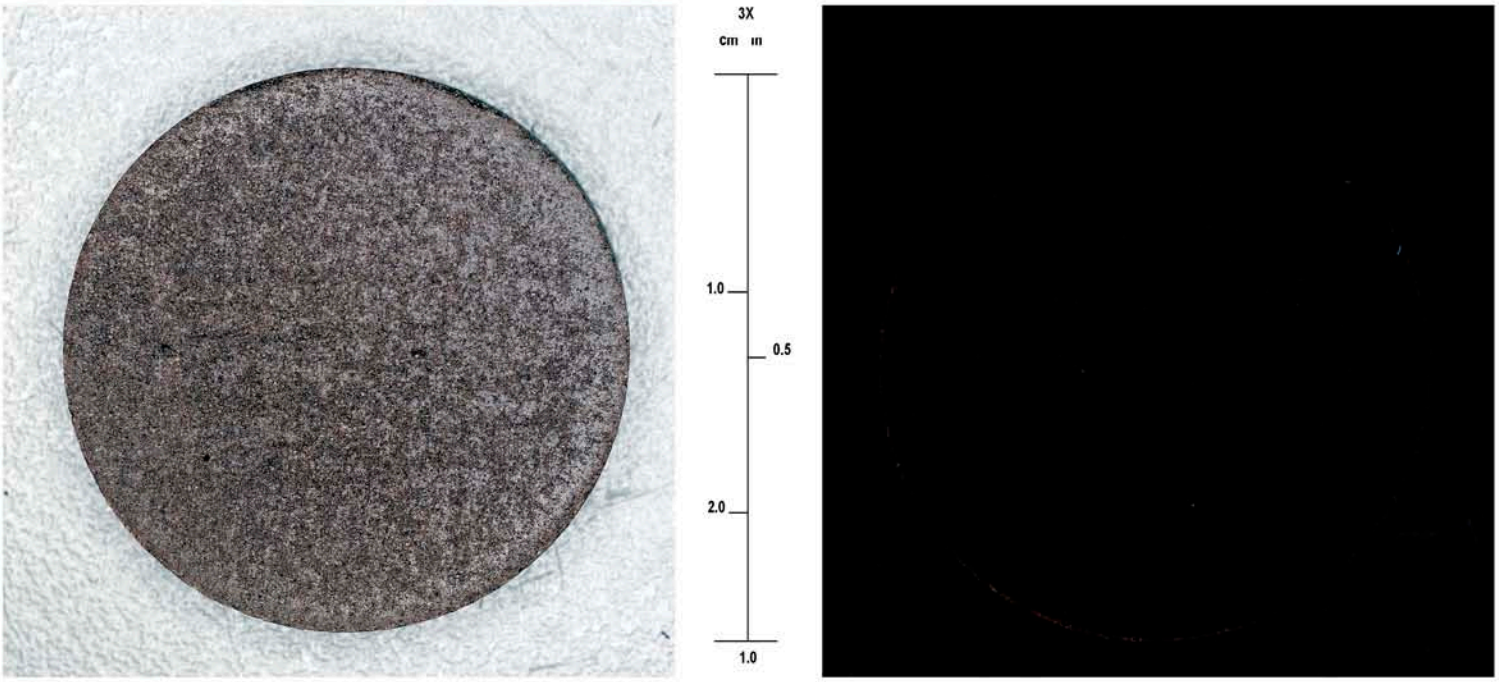

Sample No.: 1-4R

Visible Light — Depth: 4776.00 feet — Ultraviolet Light

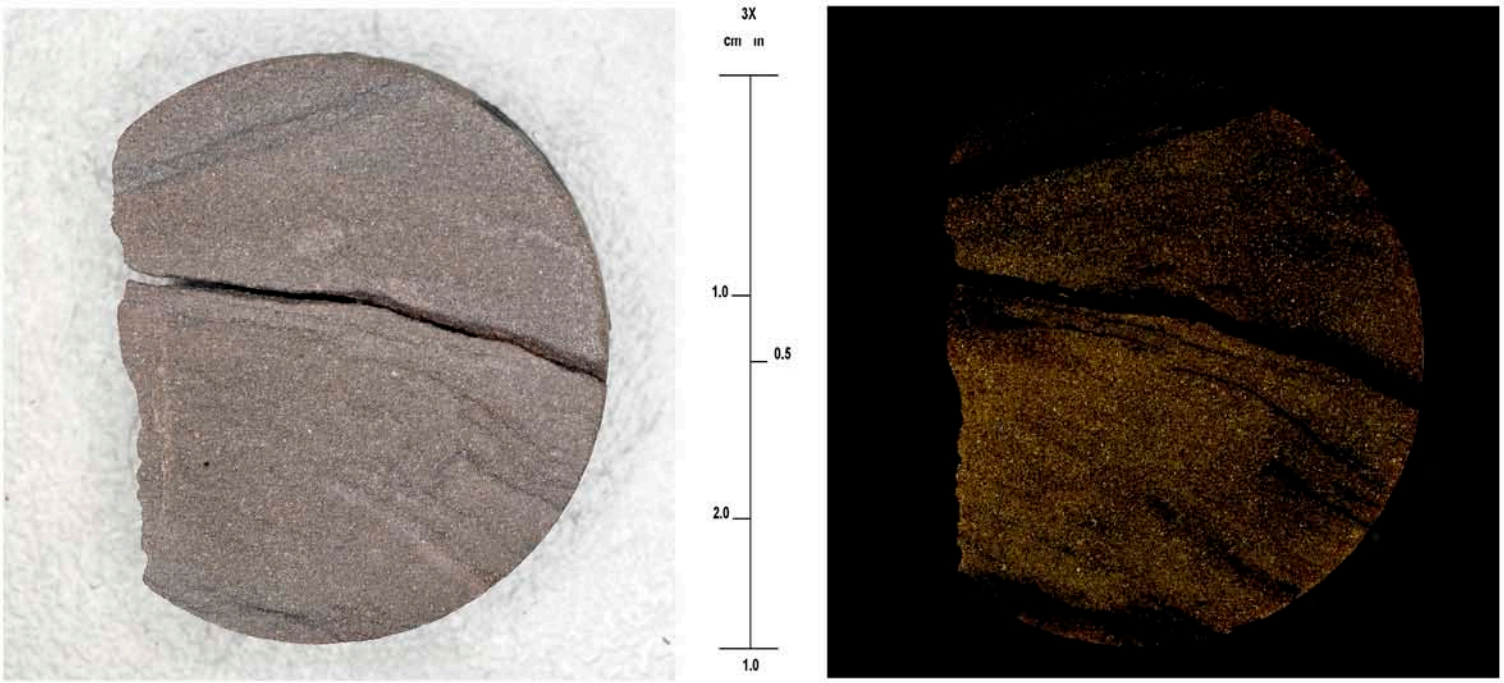

Weatherford LABORATORIES

HH-38266

Ohio Division of Geological Survey
CO2 No. 1 Well
Tuscarawas County, Ohio

Sample No.: 1-3R
Depth: 4771.00 feet

Visible Light

Longitudinal

Ultraviolet Light

Weatherford LABORATORIES

HH-38266

Ohio Division of Geological Survey
CO2 No. 1 Well
Tuscarawas County, Ohio

Sample No.: 1-4R
Depth: 4776.00 feet

Visible Light

Longitudinal

Ultraviolet Light

INTENTIONALLY BLANK

Weatherford LABORATORIES

HH-38266

Ohio Division of Geological Survey
CO2 No. 1 Well
Tuscarawas County, Ohio

Rotary Sidewall Core Photography

Sample No.: 1-5R

Visible Light — Depth: 4790.00 feet — Ultraviolet Light

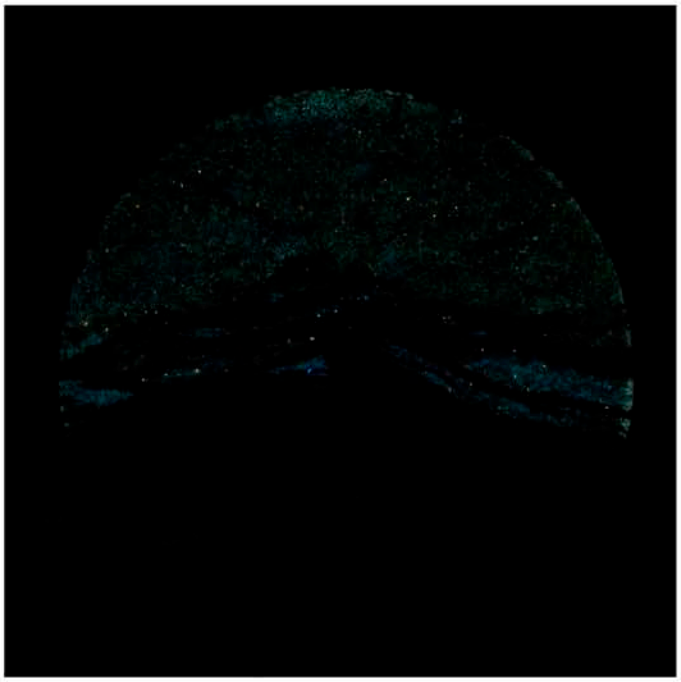

Sample No.: 1-6R

Visible Light — Depth: 4816.00 feet — Ultraviolet Light

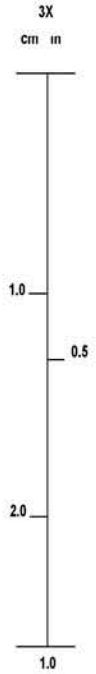

Weatherford LABORATORIES

HH-38266

Ohio Division of Geological Survey
CO2 No. 1 Well
Tuscarawas County, Ohio

Sample No.: 1-5R
Depth: 4790.00 feet

Visible Light

Longitudinal

Ultraviolet Light

Weatherford LABORATORIES

HH-38266

Ohio Division of Geological Survey
CO2 No. 1 Well
Tuscarawas County, Ohio

Sample No.: 1-6R
Depth: 4816.00 feet

Visible Light

Longitudinal

Ultraviolet Light

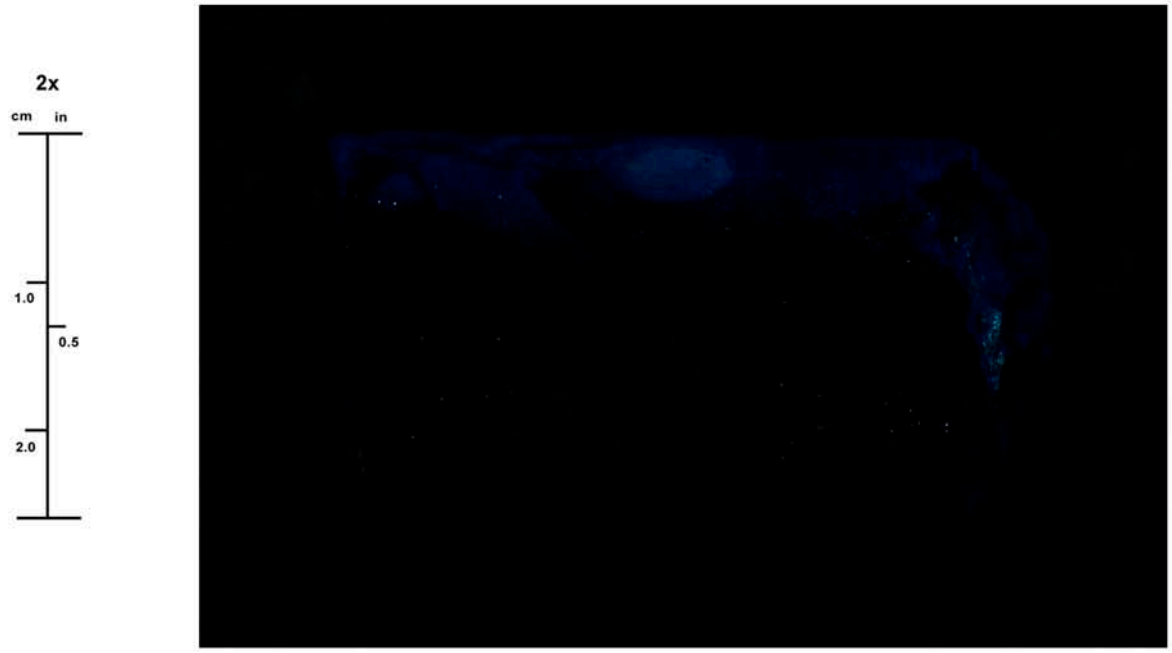

INTENTIONALLY BLANK

Weatherford LABORATORIES

HH-38266

Ohio Division of Geological Survey
CO2 No. 1 Well
Tuscarawas County, Ohio

Rotary Sidewall Core Photography

Sample No.: 1-7R

Visible Light — Depth: 4821.00 feet — Ultraviolet Light

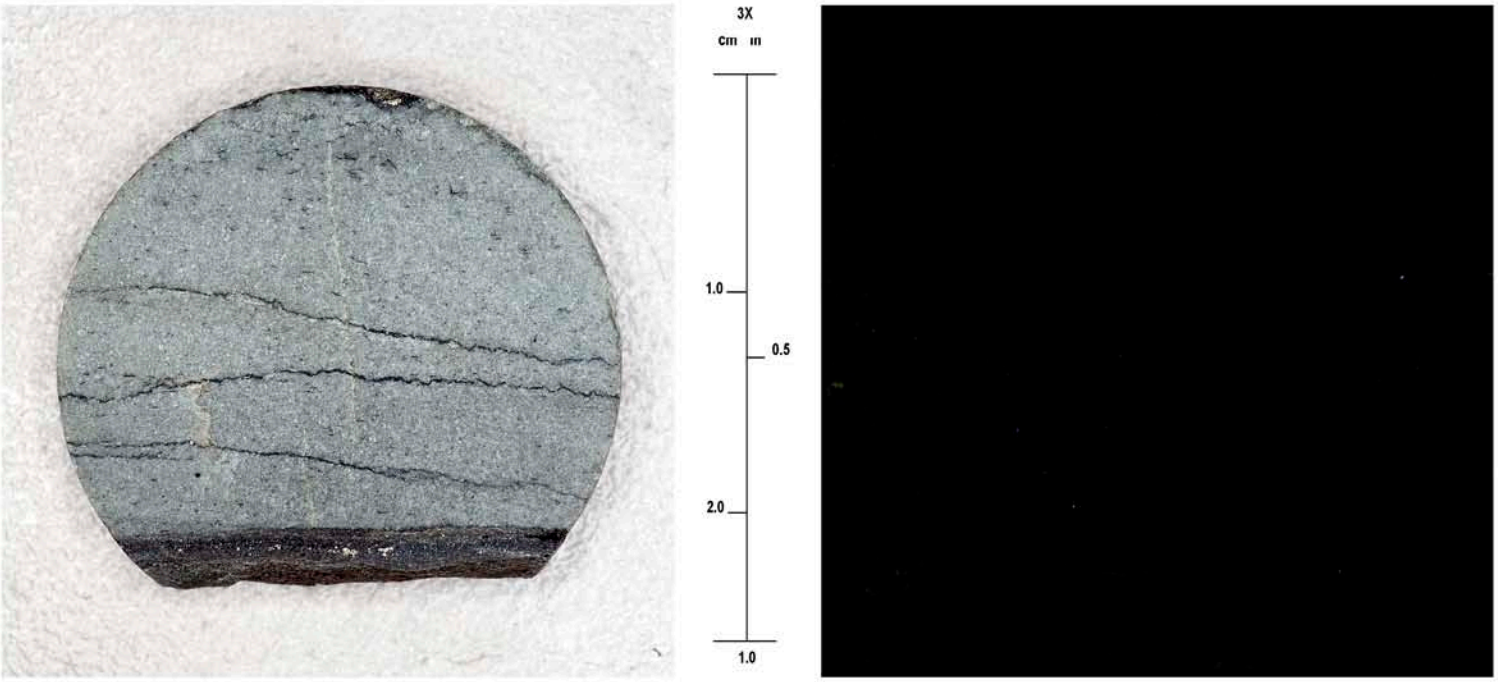

Sample No.: 1-8R

Visible Light — Depth: 4834.00 feet — Ultraviolet Light

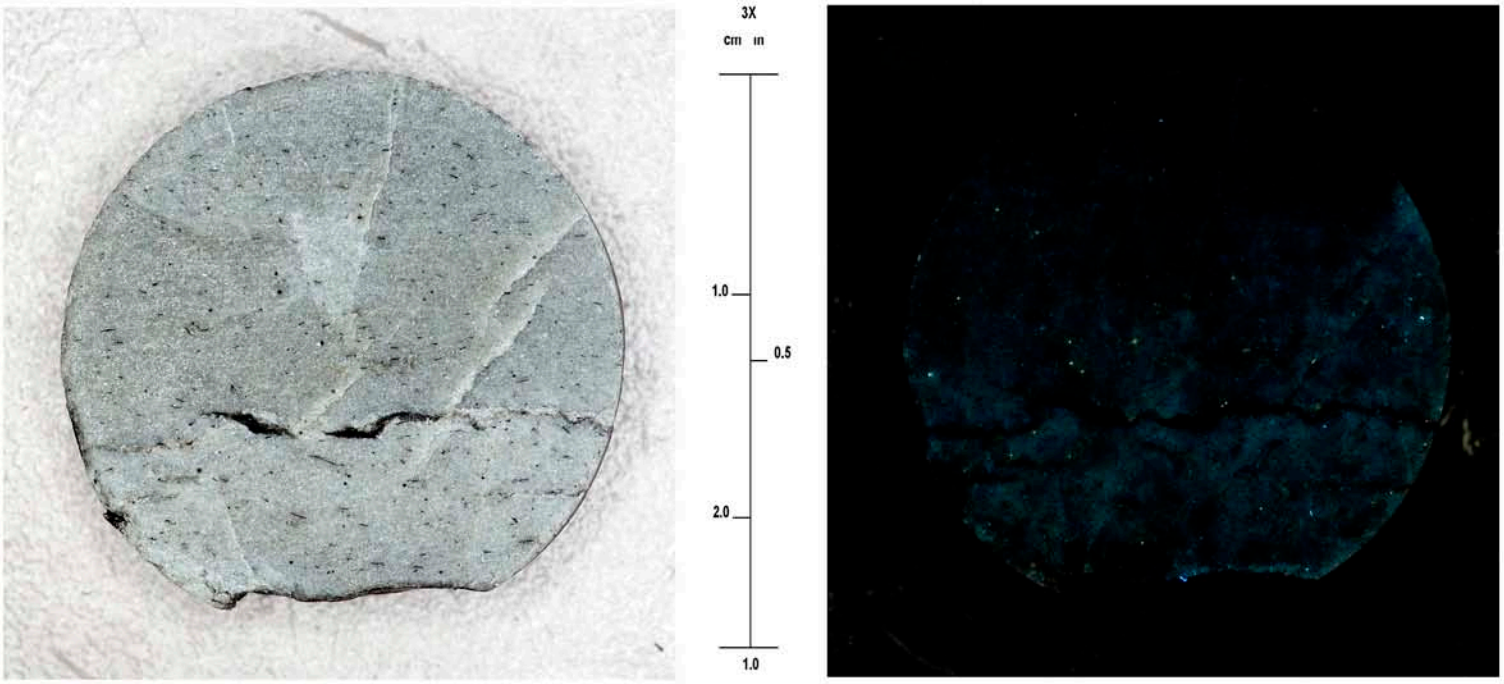

Weatherford LABORATORIES

HH-38266

Ohio Division of Geological Survey
CO2 No. 1 Well
Tuscarawas County, Ohio

Sample No.: 1-7R
Depth: 4821.00 feet

Visible Light

Longitudinal

Ultraviolet Light

Weatherford LABORATORIES

HH-38266

Ohio Division of Geological Survey
CO2 No. 1 Well
Tuscarawas County, Ohio

Sample No.: 1-8R
Depth: 4834.00 feet

Visible Light

Longitudinal

Ultraviolet Light

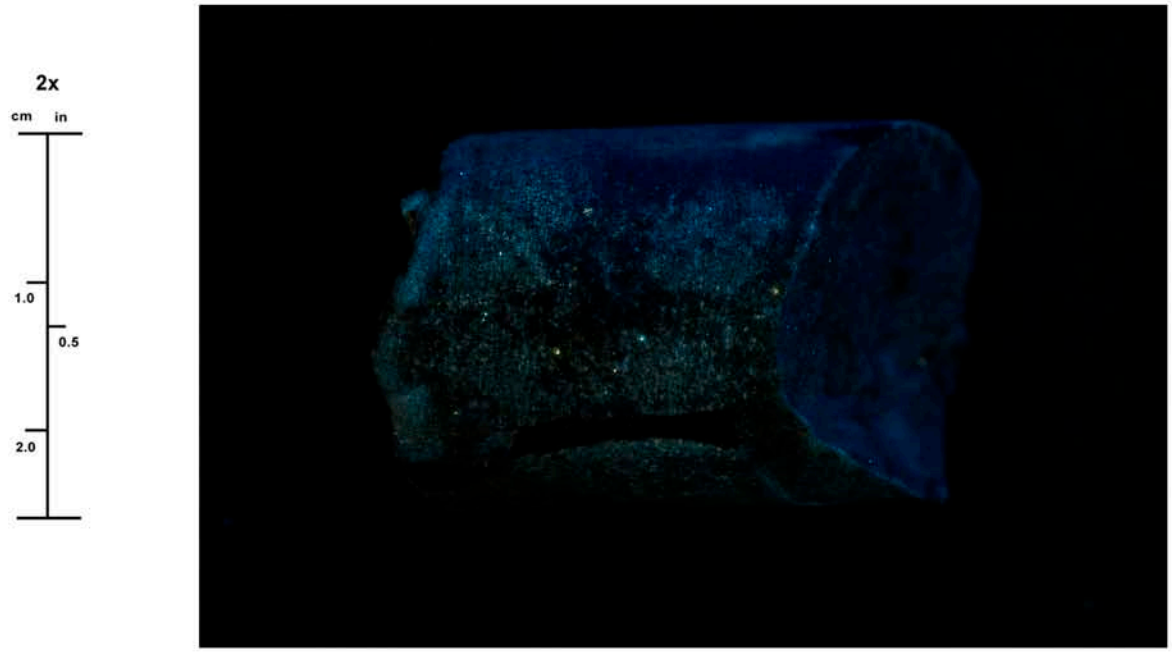

INTENTIONALLY BLANK

Weatherford LABORATORIES

HH-38266

Ohio Division of Geological Survey
CO2 No. 1 Well
Tuscarawas County, Ohio

Rotary Sidewall Core Photography

Sample No.: 1-9R

Visible Light — Depth: 4840.00 feet — Ultraviolet Light

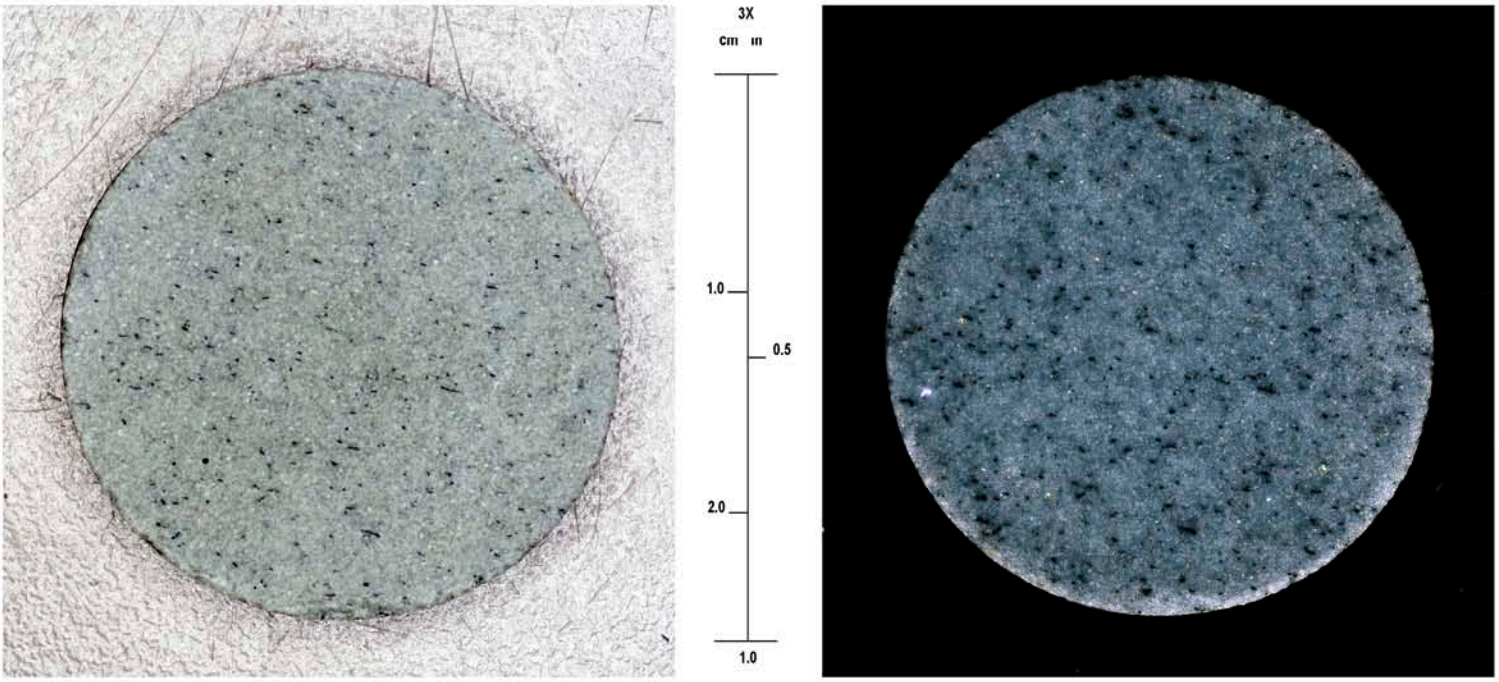

Sample No.: 1-10R

Visible Light — Depth: 6064.00 feet — Ultraviolet Light

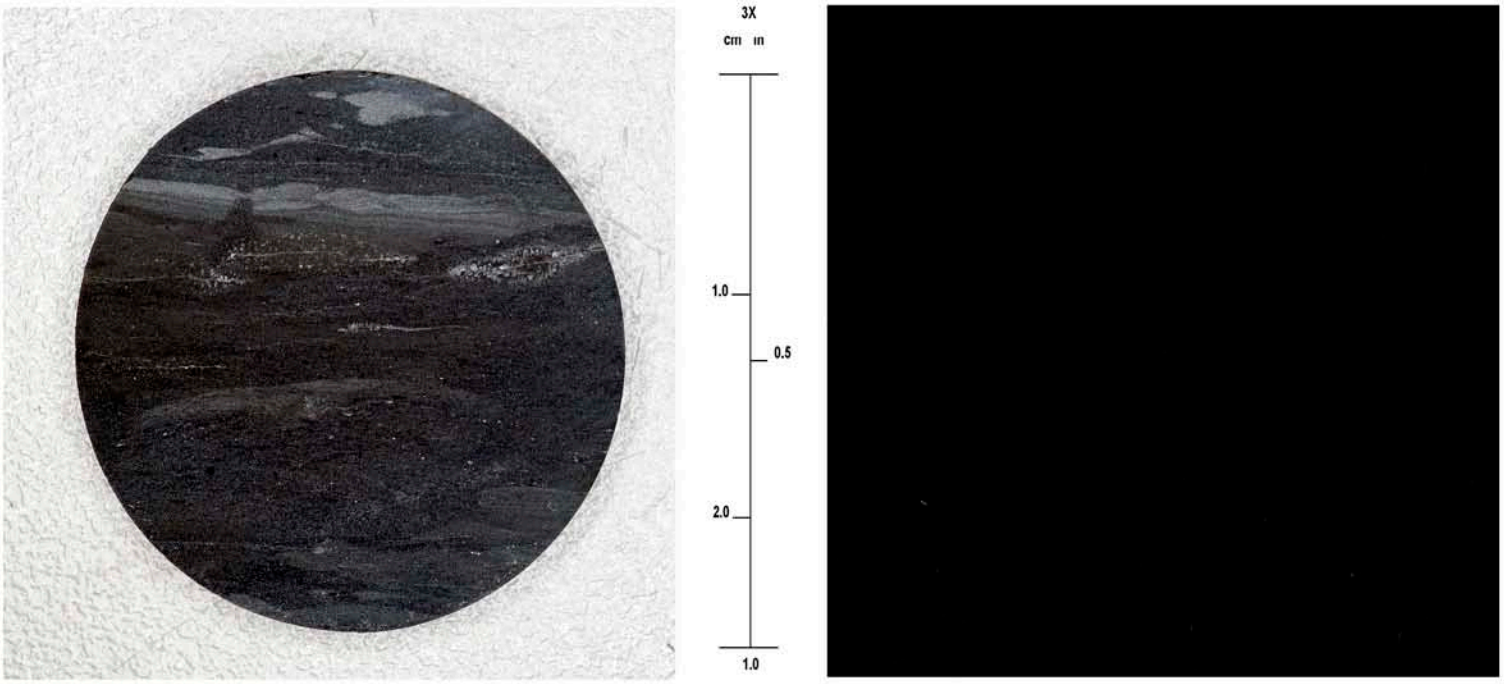

Weatherford LABORATORIES

HH-38266

Ohio Division of Geological Survey
CO2 No. 1 Well
Tuscarawas County, Ohio

Sample No.: 1-9R
Depth: 4840.00 feet

Visible Light

Longitudinal

Ultraviolet Light

Weatherford LABORATORIES

HH-38266

Ohio Division of Geological Survey
CO2 No. 1 Well
Tuscarawas County, Ohio

Sample No.: 1-10R
Depth: 6064.00 feet

Visible Light

Longitudinal

Ultraviolet Light

INTENTIONALLY BLANK

Weatherford LABORATORIES

HH-38266

Ohio Division of Geological Survey
CO2 No. 1 Well
Tuscarawas County, Ohio

Rotary Sidewall Core Photography

Sample No.: 1-11R

Visible Light — Depth: 6141.00 feet — Ultraviolet Light

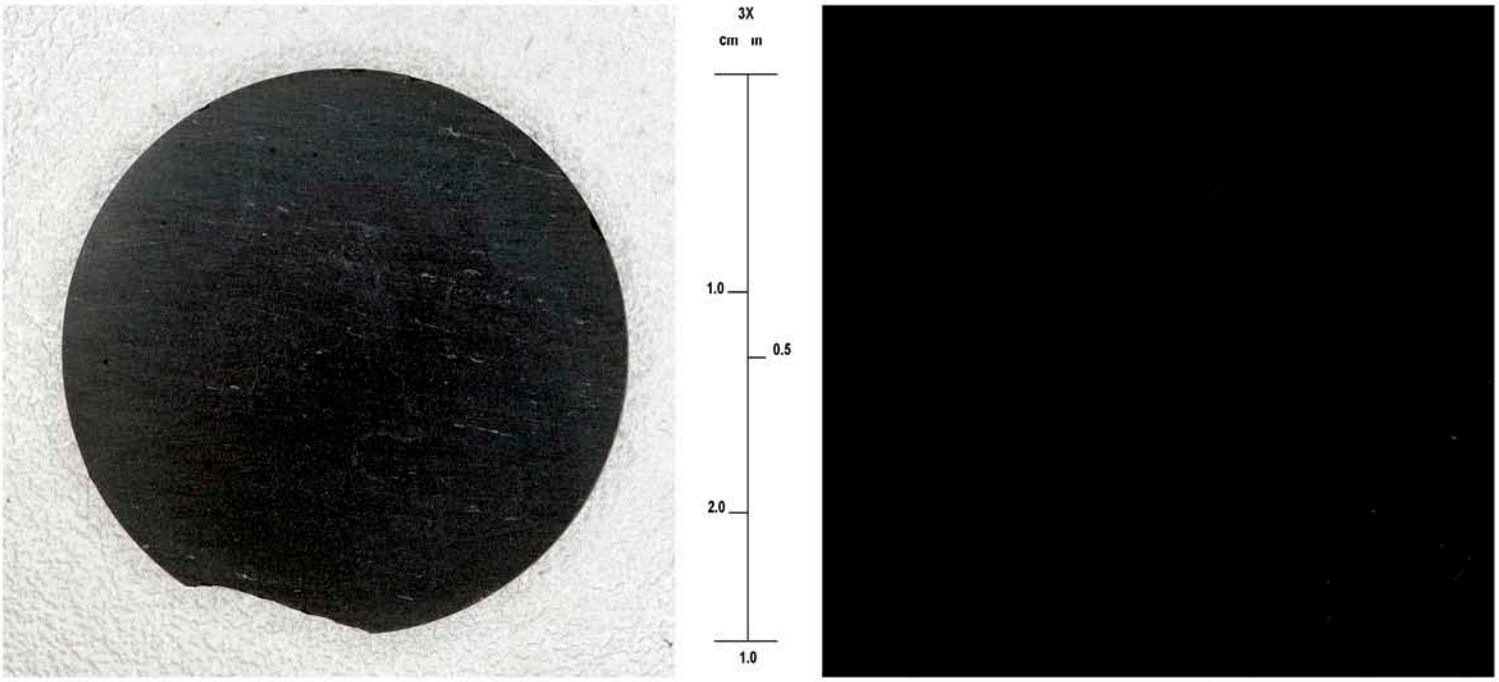

Sample No.: 1-12R

Visible Light — Depth: 6282.00 feet — Ultraviolet Light

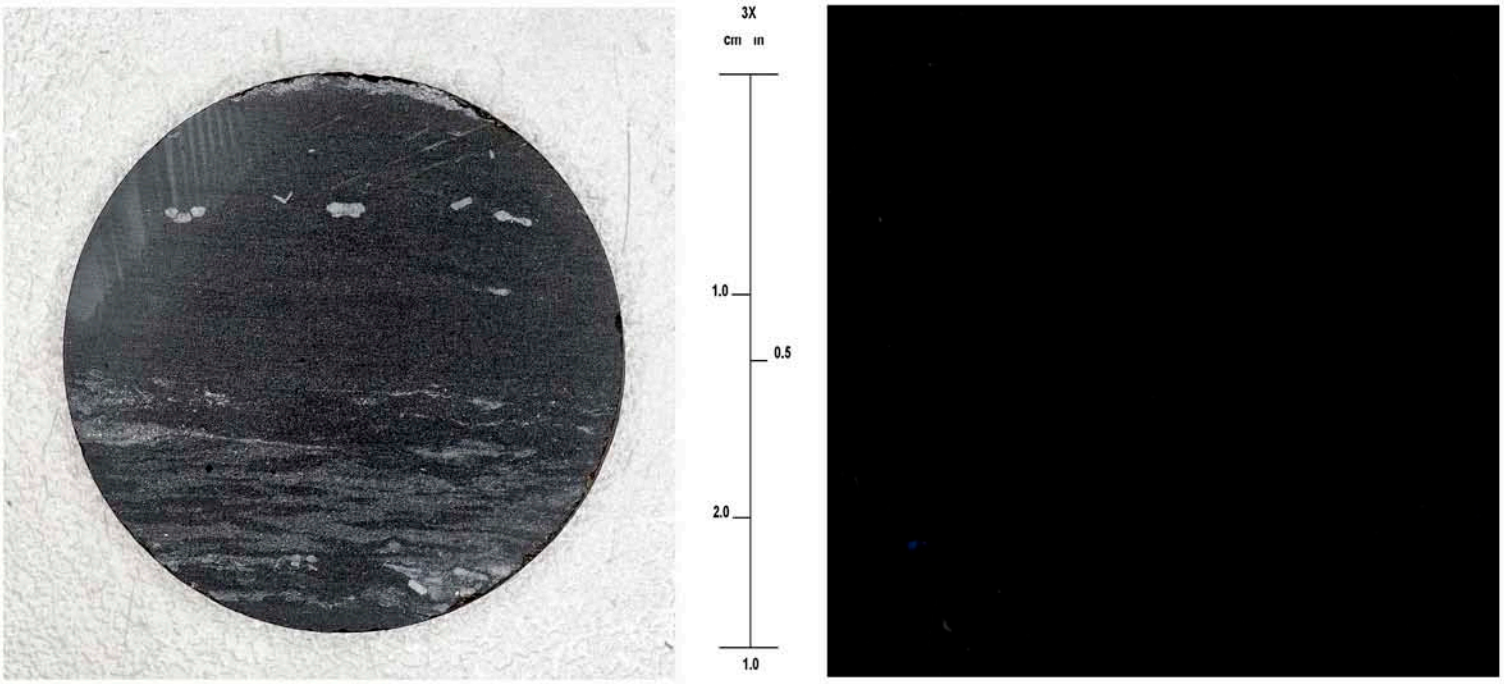

Weatherford LABORATORIES

HH-38266

Ohio Division of Geological Survey
CO2 No. 1 Well
Tuscarawas County, Ohio

Sample No.: 1-11R
Depth: 6141.00 feet

Visible Light

Longitudinal

Ultraviolet Light

Weatherford LABORATORIES

HH-38266

Ohio Division of Geological Survey
CO2 No. 1 Well
Tuscarawas County, Ohio

Sample No.: 1-12R
Depth: 6282.00 feet

Visible Light

Longitudinal

Ultraviolet Light

INTENTIONALLY BLANK

Weatherford LABORATORIES

HH-38266

Ohio Division of Geological Survey
CO2 No. 1 Well
Tuscarawas County, Ohio

Rotary Sidewall Core Photography

Sample No.: 1-13R

Visible Light — Depth: 6336.00 feet — Ultraviolet Light

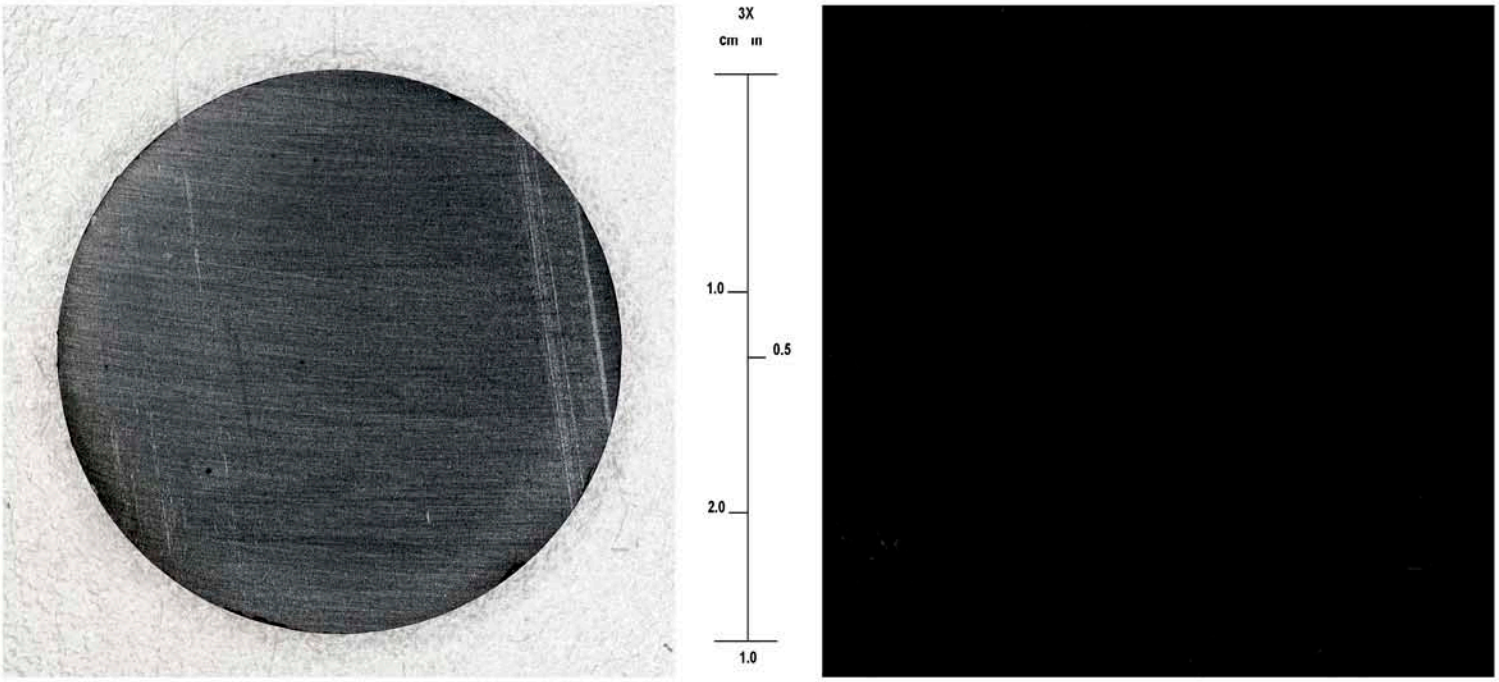

Sample No.: 1-14R

Visible Light — Depth: 6396.00 feet — Ultraviolet Light

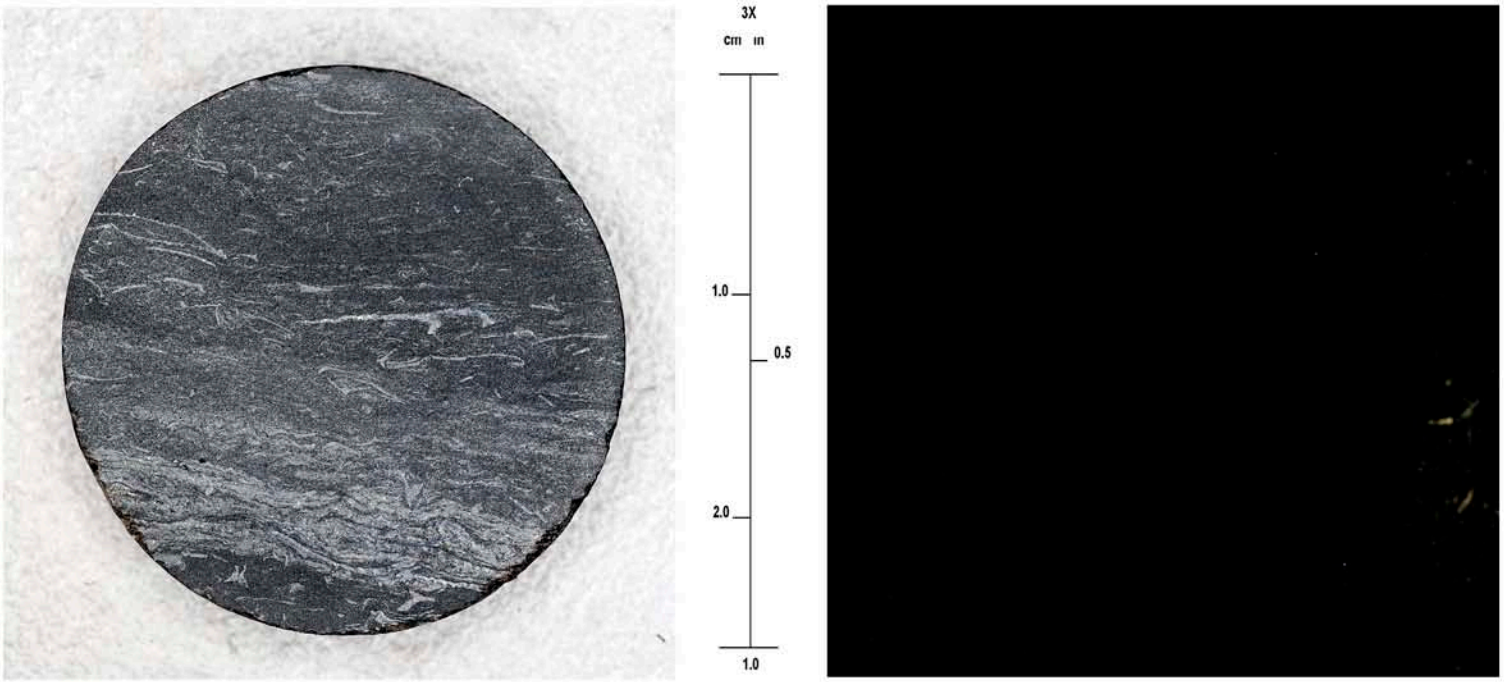

Weatherford LABORATORIES

HH-38266

Ohio Division of Geological Survey
CO2 No. 1 Well
Tuscarawas County, Ohio

Sample No.: 1-13R
Depth: 6336.00 feet

Visible Light

Longitudinal

Ultraviolet Light

Weatherford LABORATORIES

HH-38266

Ohio Division of Geological Survey
CO2 No. 1 Well
Tuscarawas County, Ohio

Sample No.: 1-14R
Depth: 6396.00 feet

Visible Light

Longitudinal

Ultraviolet Light

INTENTIONALLY BLANK

Weatherford LABORATORIES

HH-38266

Ohio Division of Geological Survey
CO2 No. 1 Well
Tuscarawas County, Ohio

Rotary Sidewall Core Photography

Sample No.: 1-15R

Visible Light — Depth: 6490.00 feet — Ultraviolet Light

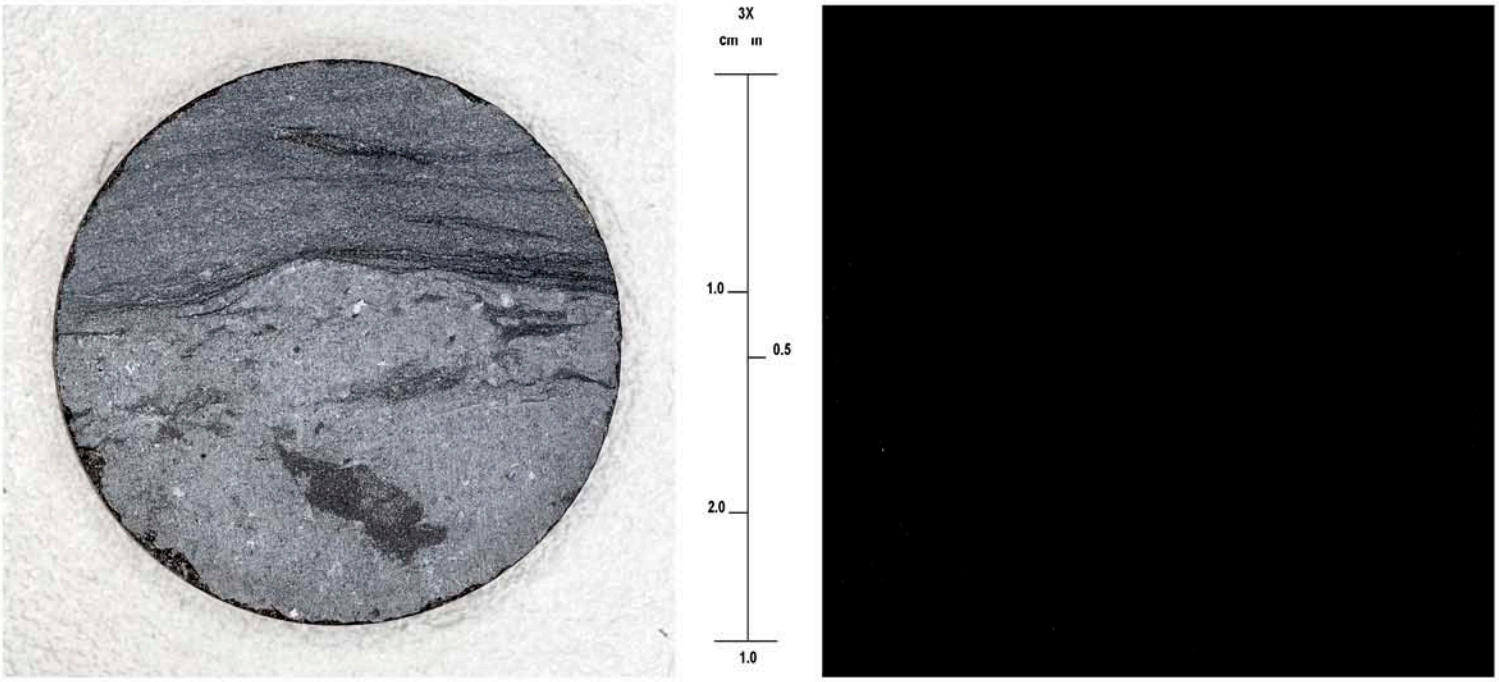

Sample No.: 1-16R

Visible Light — Depth: 6524.00 feet — Ultraviolet Light

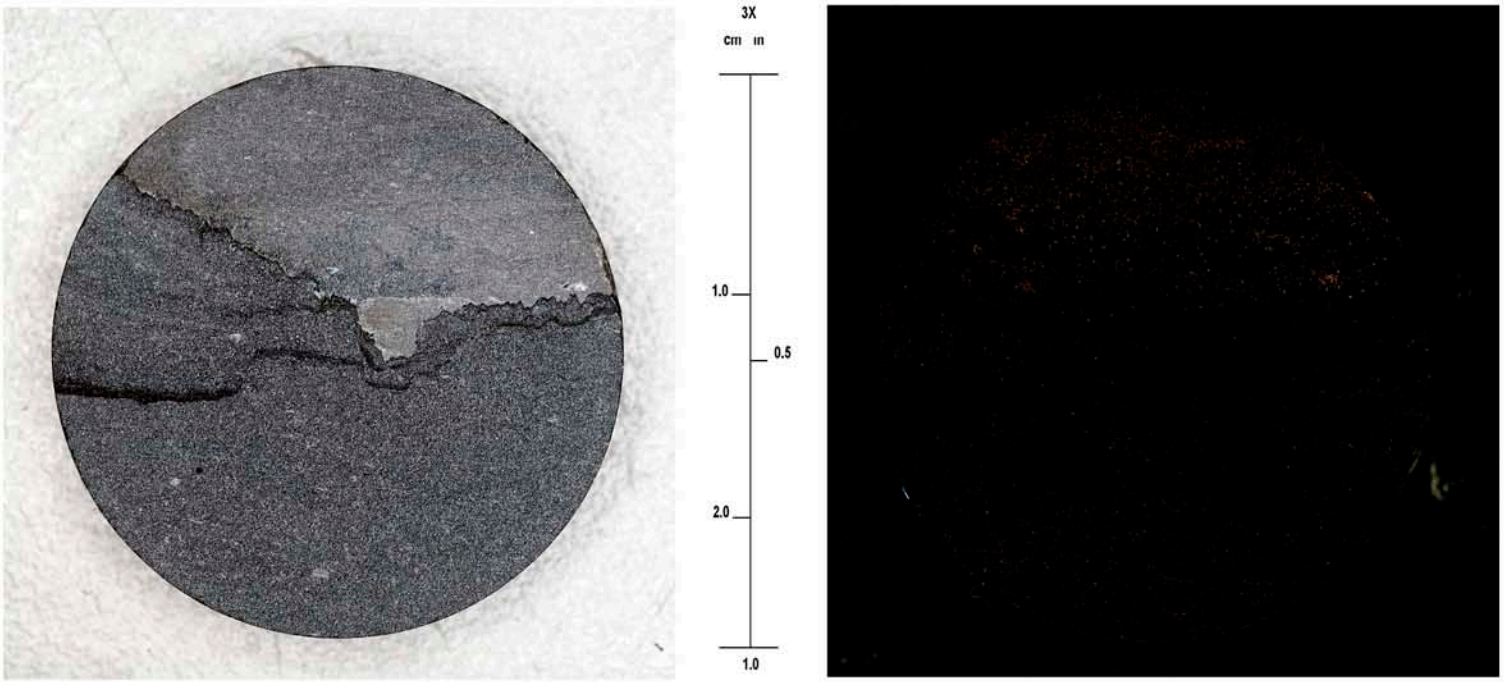

Weatherford LABORATORIES

HH-38266

Ohio Division of Geological Survey
CO2 No. 1 Well
Tuscarawas County, Ohio

Sample No.: 1-15R
Depth: 6490.00 feet

Visible Light

Longitudinal

Ultraviolet Light

Weatherford LABORATORIES

HH-38266

Ohio Division of Geological Survey
CO2 No. 1 Well
Tuscarawas County, Ohio

Sample No.: 1-16R
Depth: 6524.00 feet

Visible Light

Longitudinal

Ultraviolet Light

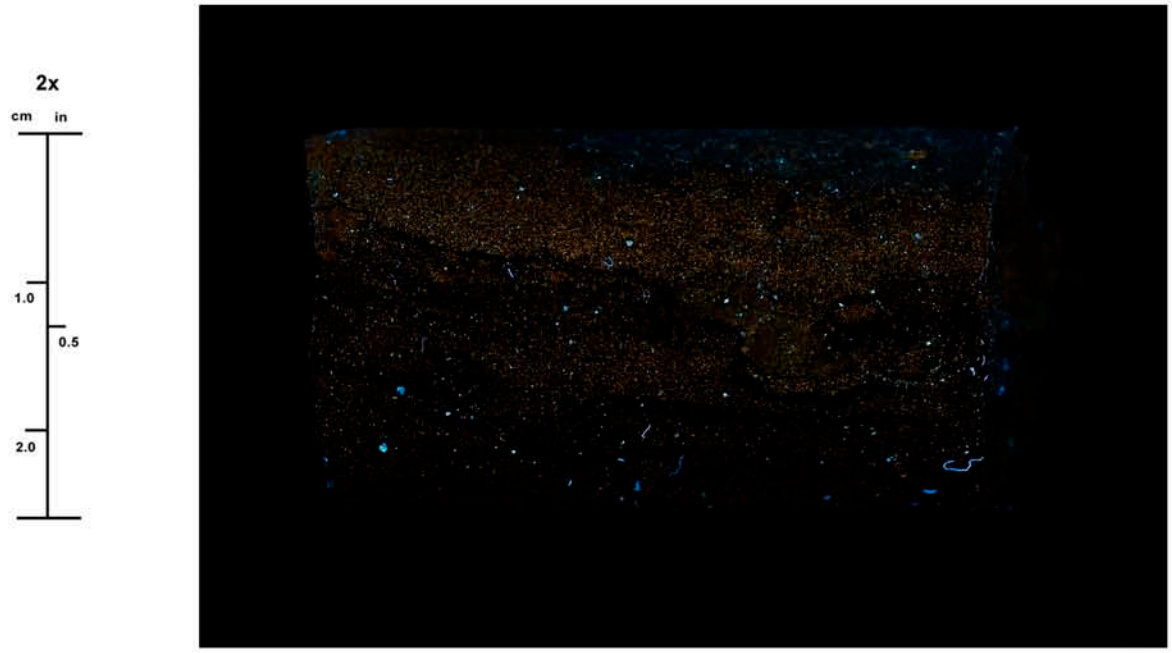

INTENTIONALLY BLANK

Weatherford LABORATORIES

HH-38266

Ohio Division of Geological Survey
CO2 No. 1 Well
Tuscarawas County, Ohio

Rotary Sidewall Core Photography

Sample No.: 1-17R

Visible Light — Depth: 6566.00 feet — Ultraviolet Light

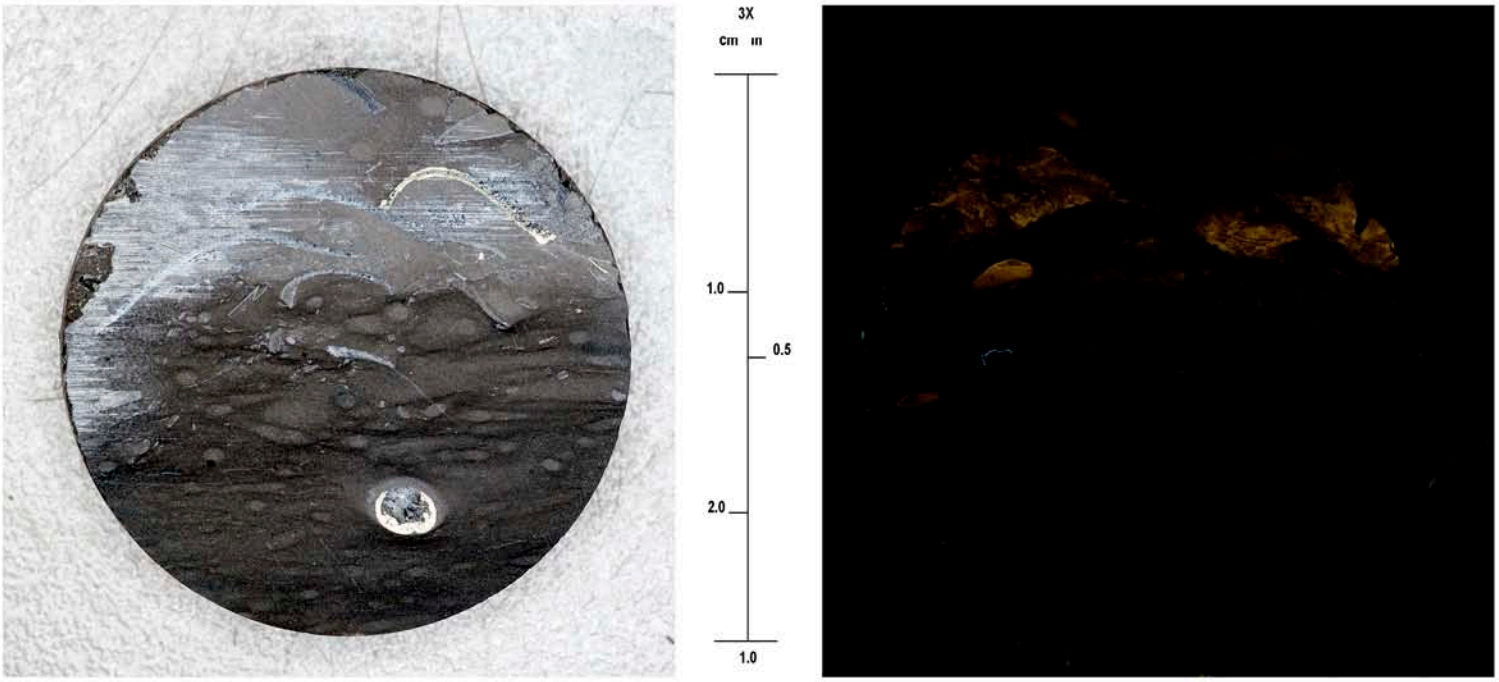

Sample No.: 1-18R

Visible Light — Depth: 6620.00 feet — Ultraviolet Light

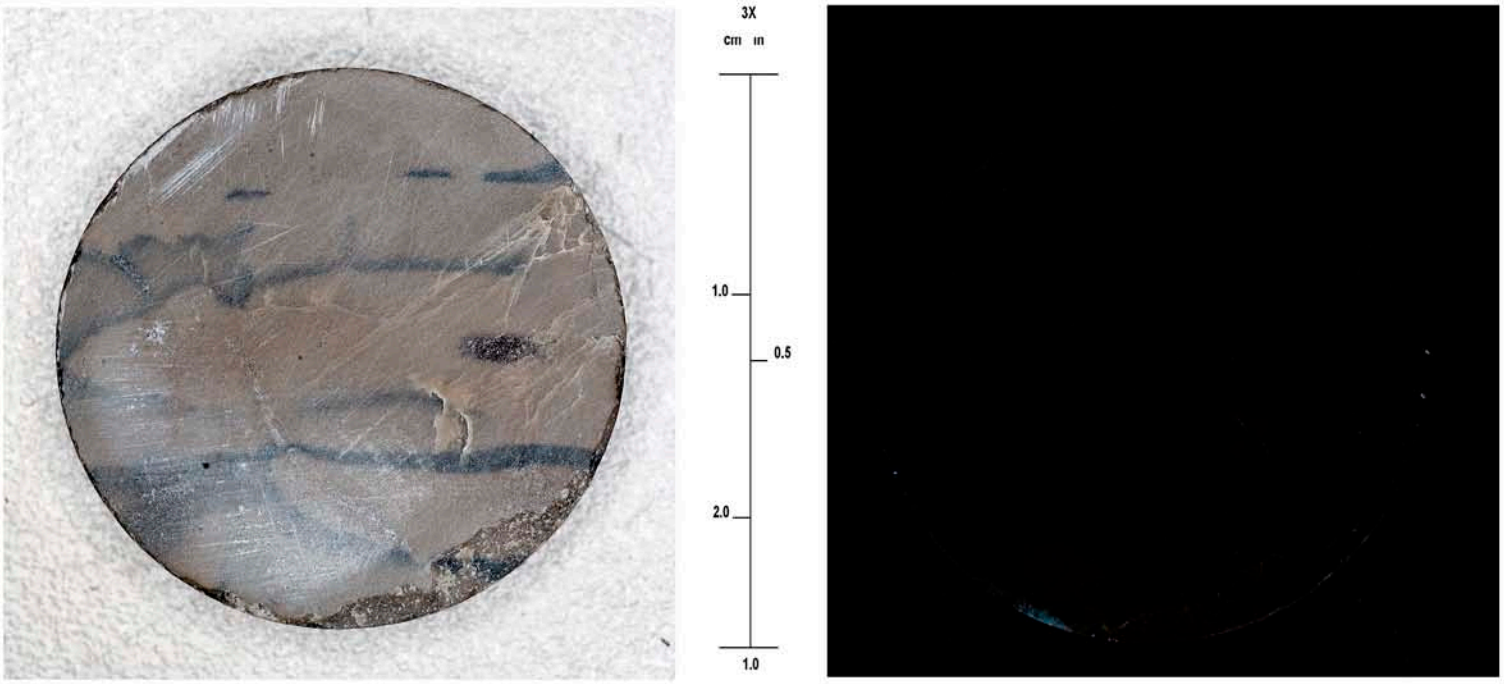

Weatherford LABORATORIES

HH-38266

Ohio Division of Geological Survey
CO2 No. 1 Well
Tuscarawas County, Ohio

Sample No.: 1-17R
Depth: 6566.00 feet

Visible Light

Longitudinal

Ultraviolet Light

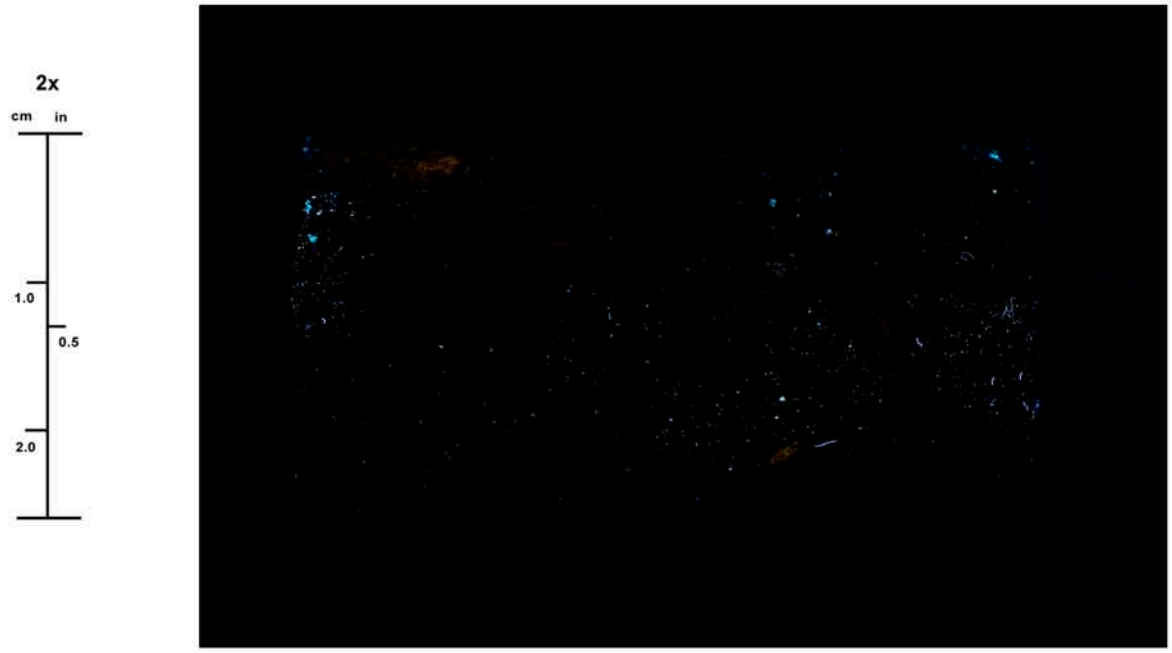

Weatherford LABORATORIES

HH-38266

Ohio Division of Geological Survey
CO2 No. 1 Well
Tuscarawas County, Ohio

Sample No.: 1-18R
Depth: 6620.00 feet

Visible Light

Longitudinal

Ultraviolet Light

INTENTIONALLY BLANK

Weatherford LABORATORIES

HH-38266

Ohio Division of Geological Survey
CO2 No. 1 Well
Tuscarawas County, Ohio

Rotary Sidewall Core Photography

Sample No.: 1-19R

Visible Light — Depth: 6750.00 feet — Ultraviolet Light

Sample No.: 1-20R

Visible Light — Depth: 6794.00 feet — Ultraviolet Light

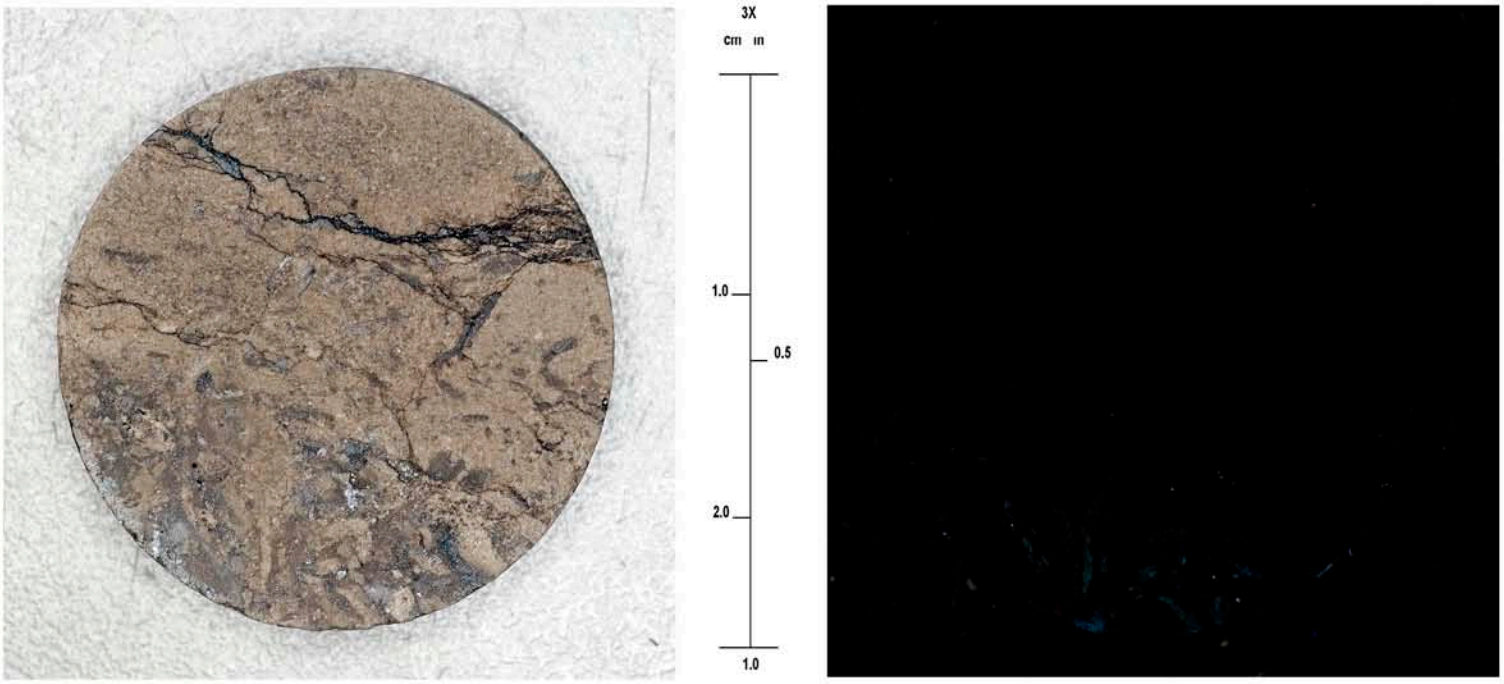

Weatherford LABORATORIES

HH-38266

Ohio Division of Geological Survey
CO2 No. 1 Well
Tuscarawas County, Ohio

Sample No.: 1-19R
Depth: 6750.00 feet

Visible Light

Longitudinal

Ultraviolet Light

Weatherford LABORATORIES

HH-38266

Ohio Division of Geological Survey
CO2 No. 1 Well
Tuscarawas County, Ohio

Sample No.: 1-20R
Depth: 6794.00 feet

Visible Light

Longitudinal

Ultraviolet Light

INTENTIONALLY BLANK

Weatherford LABORATORIES

HH-38266

Ohio Division of Geological Survey
CO2 No. 1 Well
Tuscarawas County, Ohio

Rotary Sidewall Core Photography

Sample No.: 1-21R

Visible Light — Depth: 6808.00 feet — Ultraviolet Light

Sample No.: 1-22R

Visible Light — Depth: 6844.00 feet — Ultraviolet Light

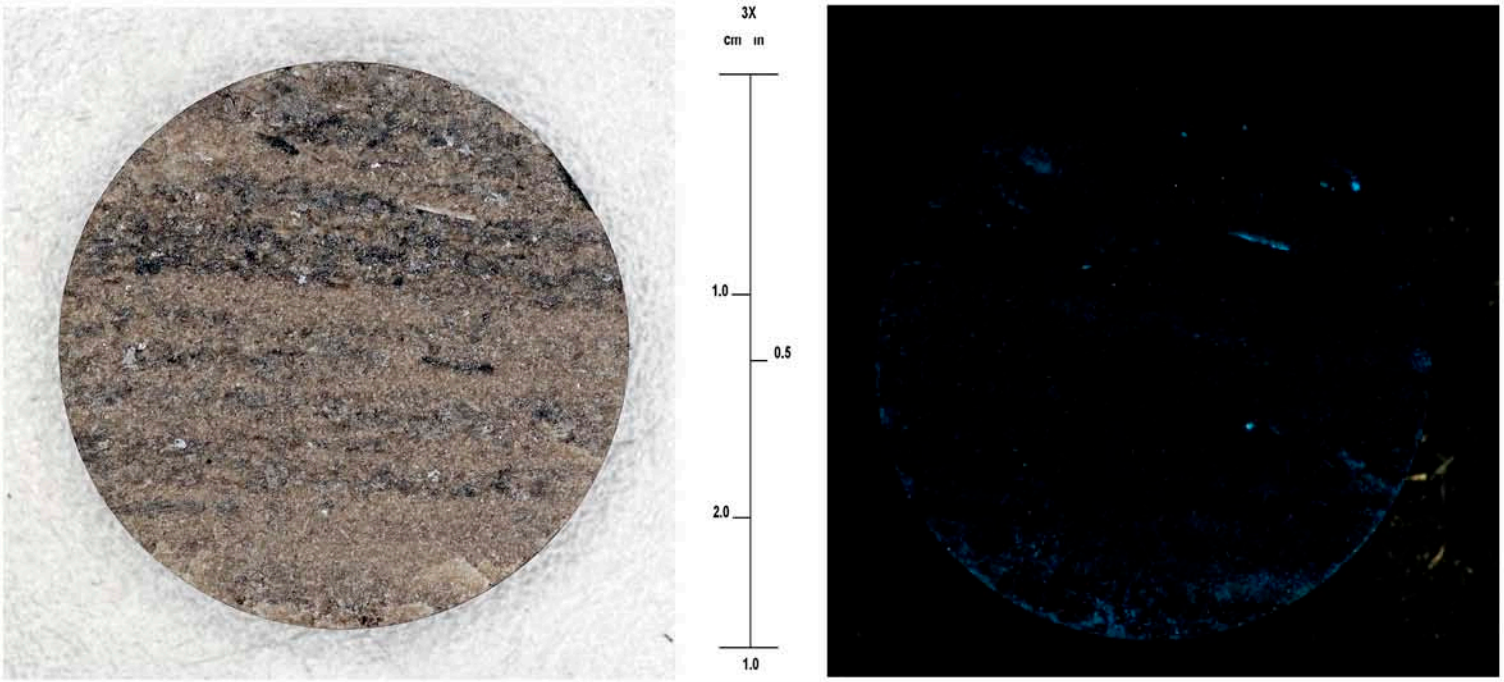

Weatherford LABORATORIES

HH-38266

Ohio Division of Geological Survey
CO2 No. 1 Well
Tuscarawas County, Ohio

Sample No.: 1-21R
Depth: 6808.00 feet

Visible Light

Longitudinal

Ultraviolet Light

Weatherford LABORATORIES

HH-38266

Ohio Division of Geological Survey
CO2 No. 1 Well
Tuscarawas County, Ohio

Sample No.: 1-22R
Depth: 6844.00 feet

Visible Light

Longitudinal

Ultraviolet Light

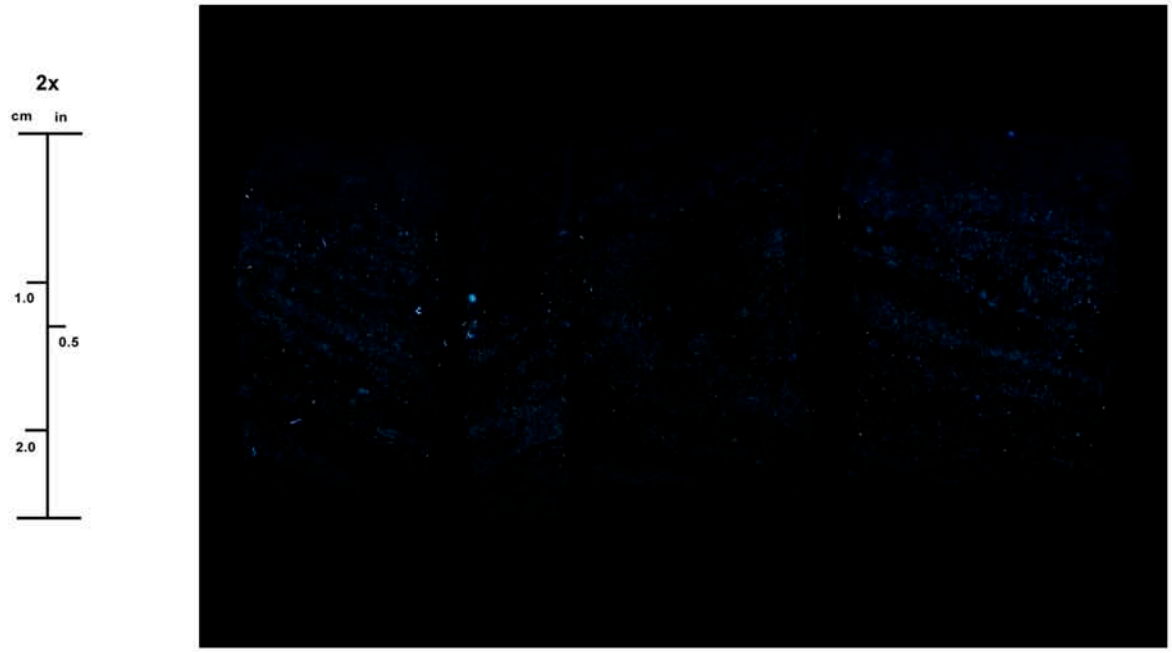

INTENTIONALLY BLANK

Weatherford LABORATORIES

HH-38266

Ohio Division of Geological Survey
CO2 No. 1 Well
Tuscarawas County, Ohio

Rotary Sidewall Core Photography

Sample No.: 1-23R

Visible Light — Depth: 6871.00 feet — Ultraviolet Light

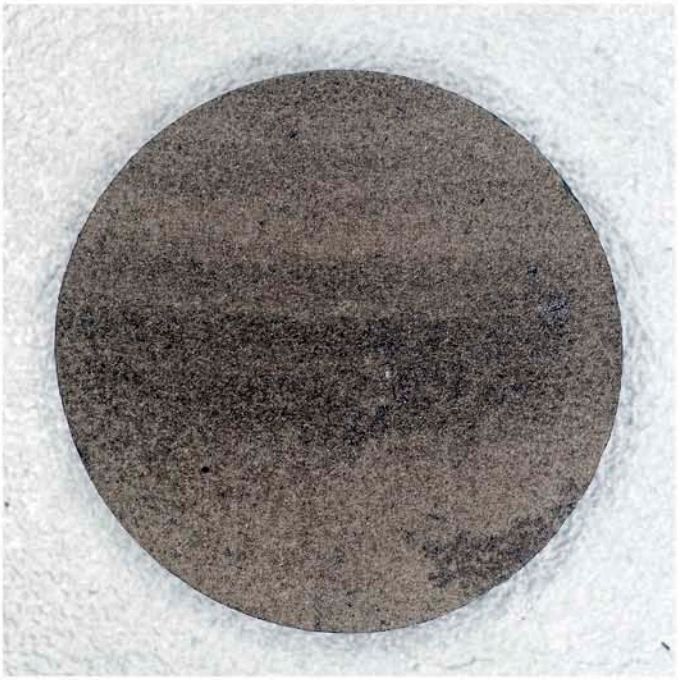

Sample No.: 1-24R

Visible Light — Depth: 6936.00 feet — Ultraviolet Light

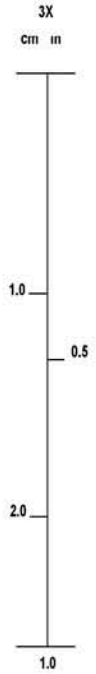

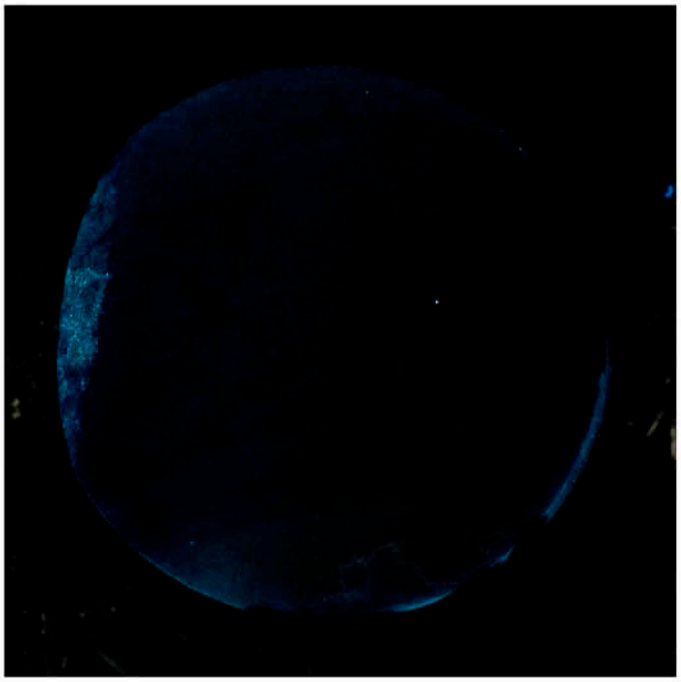

Weatherford LABORATORIES

HH-38266

Ohio Division of Geological Survey
CO2 No. 1 Well
Tuscarawas County, Ohio

Sample No.: 1-23R
Depth: 6871.00 feet

Visible Light

Longitudinal

Ultraviolet Light

Weatherford LABORATORIES

HH-38266

Ohio Division of Geological Survey
CO2 No. 1 Well
Tuscarawas County, Ohio

Sample No.: 1-24R
Depth: 6936.00 feet

Visible Light

Longitudinal

Ultraviolet Light

INTENTIONALLY BLANK

Weatherford LABORATORIES

HH-38266

Ohio Division of Geological Survey
CO2 No. 1 Well
Tuscarawas County, Ohio

Rotary Sidewall Core Photography

Sample No.: 1-25R

Visible Light — Depth: 6940.00 feet — Ultraviolet Light

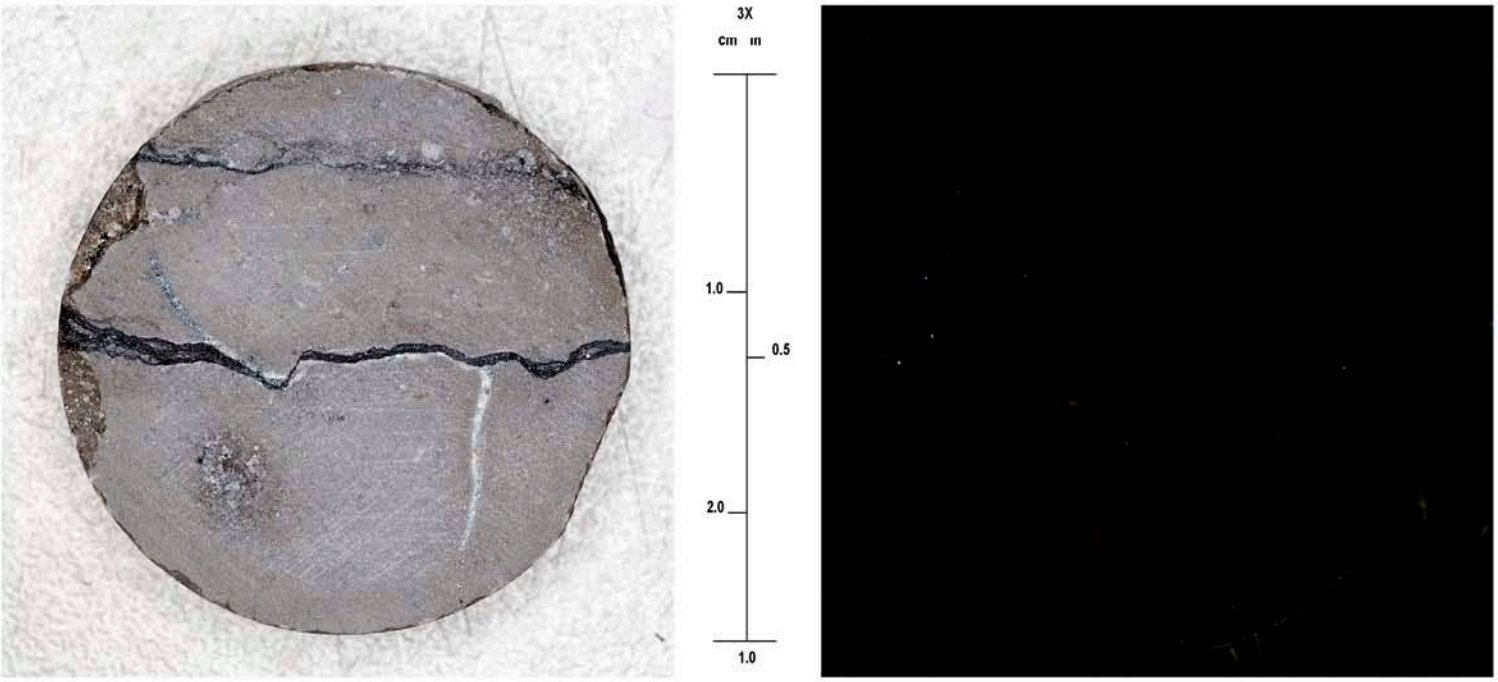

Sample No.: 1-26R

Visible Light — Depth: 7030.00 feet — Ultraviolet Light

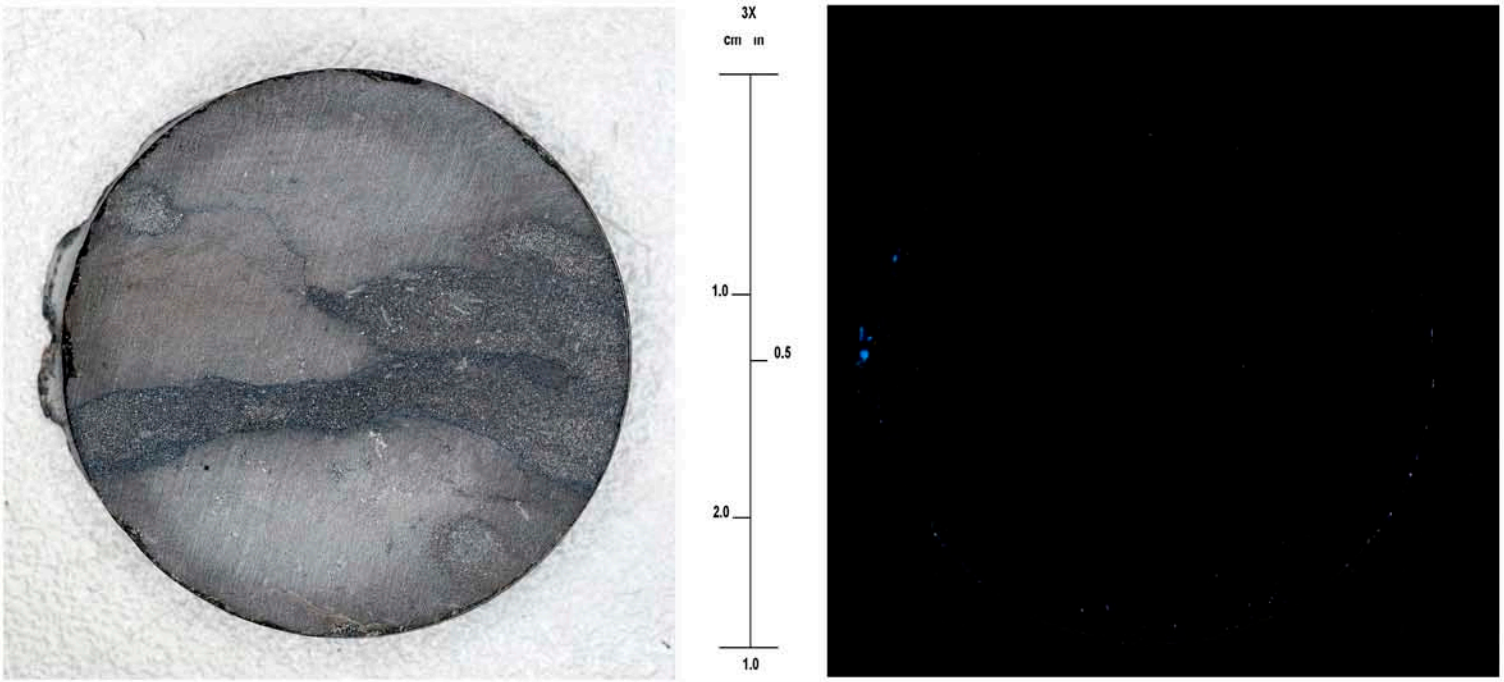

Weatherford LABORATORIES

HH-38266

Ohio Division of Geological Survey
CO2 No. 1 Well
Tuscarawas County, Ohio

Sample No.: 1-25R
Depth: 6940.00 feet

Visible Light

Longitudinal

Ultraviolet Light

Weatherford LABORATORIES

HH-38266

Ohio Division of Geological Survey
CO2 No. 1 Well
Tuscarawas County, Ohio

Sample No.: 1-26R
Depth: 7030.00 feet

Visible Light

Longitudinal

Ultraviolet Light

INTENTIONALLY BLANK

Weatherford LABORATORIES

HH-38266

Ohio Division of Geological Survey
CO2 No. 1 Well
Tuscarawas County, Ohio

Rotary Sidewall Core Photography

Sample No.: 1-27R

Visible Light — Depth: 7128.00 feet — Ultraviolet Light

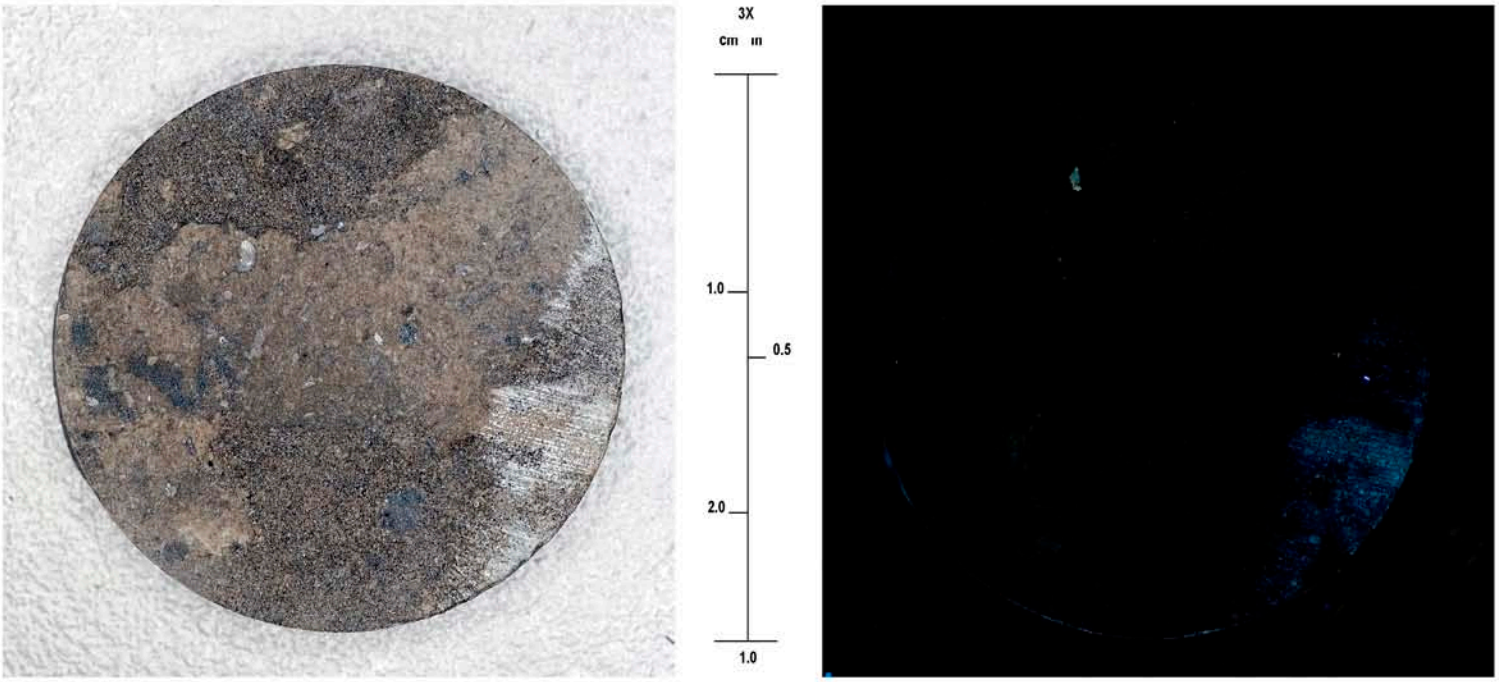

Sample No.: 1-28R

Visible Light — Depth: 7142.00 feet — Ultraviolet Light

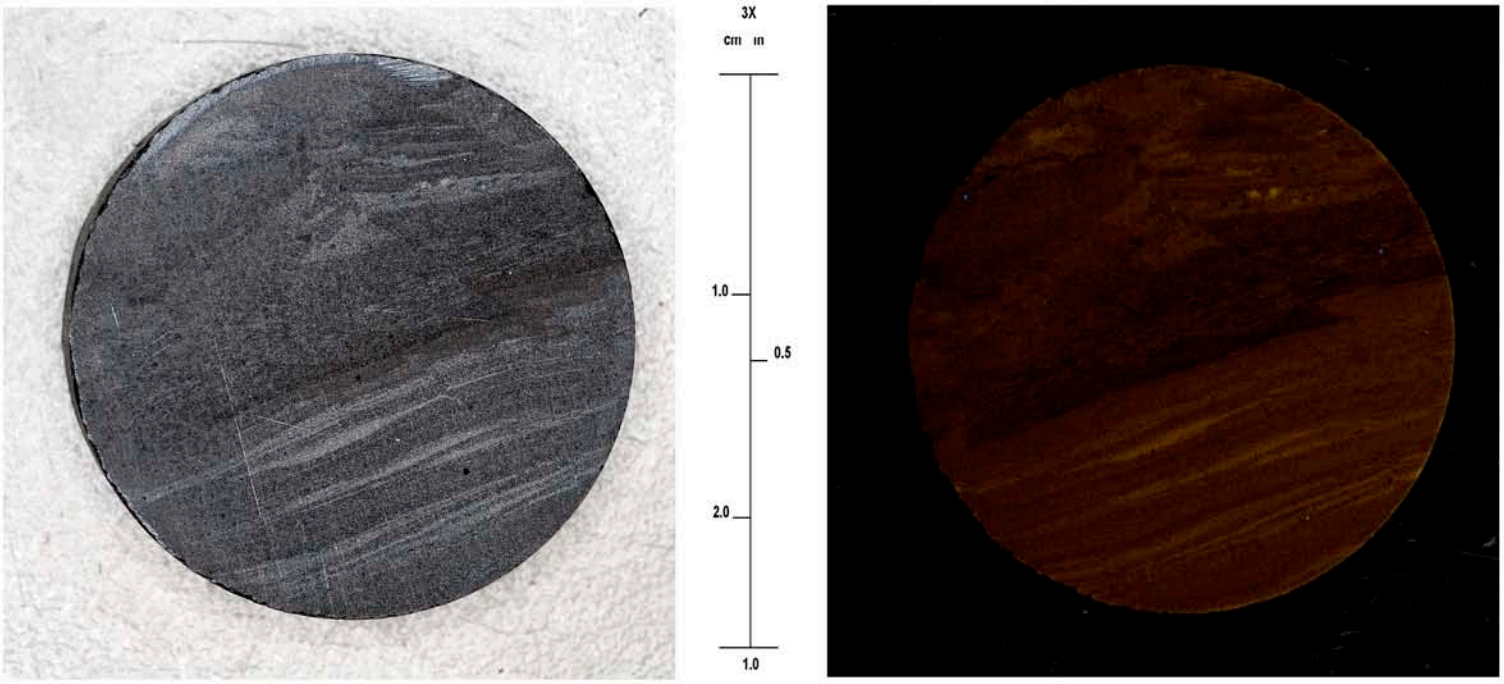

Weatherford LABORATORIES

HH-38266

Ohio Division of Geological Survey
CO2 No. 1 Well
Tuscarawas County, Ohio

Sample No.: 1-27R
Depth: 7128.00 feet

Visible Light

Longitudinal

Ultraviolet Light

Weatherford LABORATORIES

HH-38266

Ohio Division of Geological Survey
CO2 No. 1 Well
Tuscarawas County, Ohio

Sample No.: 1-28R
Depth: 7142.00 feet

Visible Light

Longitudinal

Ultraviolet Light

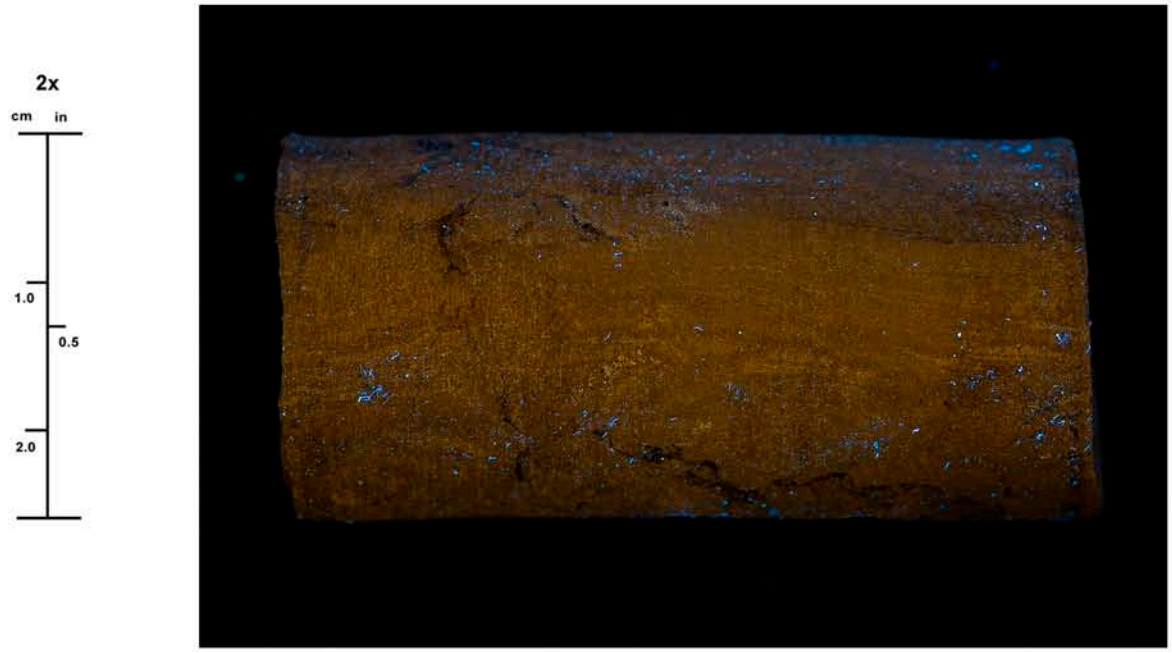

INTENTIONALLY BLANK

Weatherford LABORATORIES

HH-38266

Ohio Division of Geological Survey
CO2 No. 1 Well
Tuscarawas County, Ohio

Rotary Sidewall Core Photography

Sample No.: 1-29R

Visible Light — Depth: 7192.00 feet — Ultraviolet Light

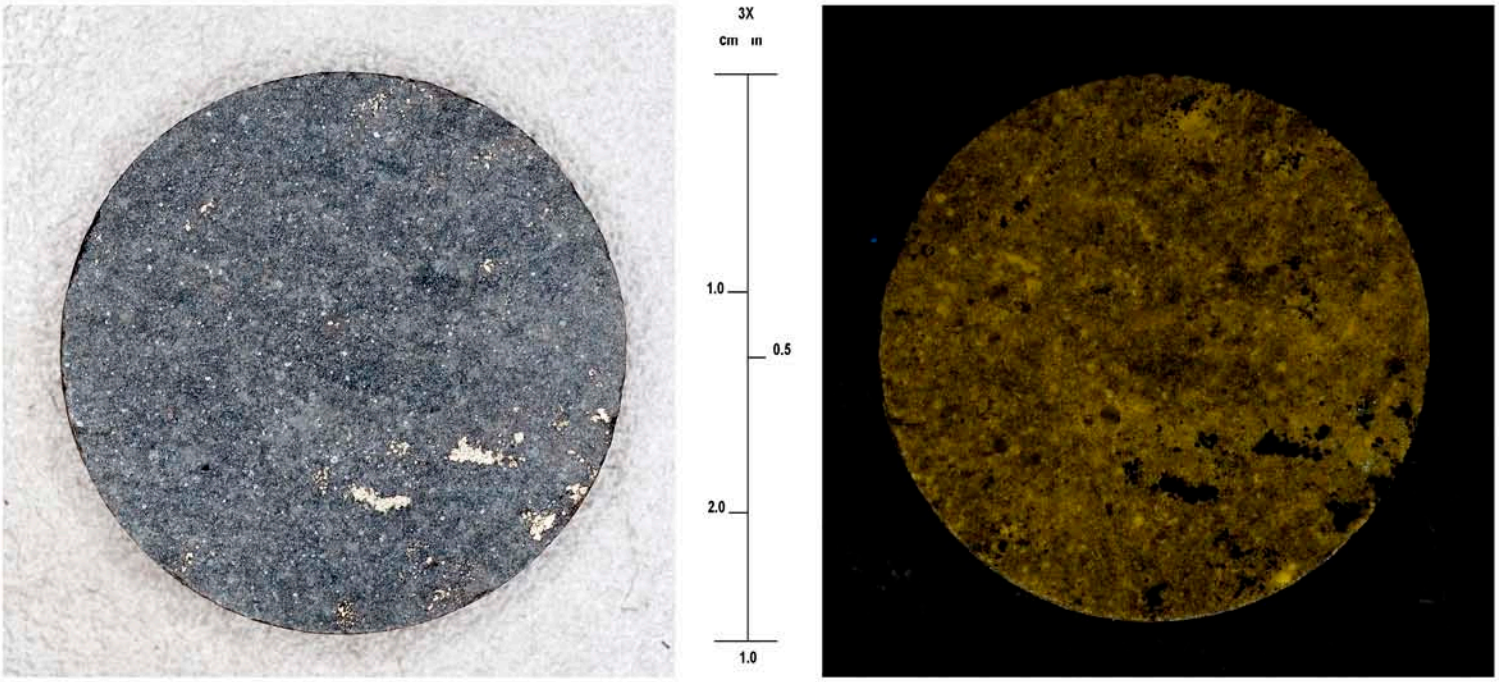

Sample No.: 1-30R

Visible Light — Depth: 7226.00 feet — Ultraviolet Light

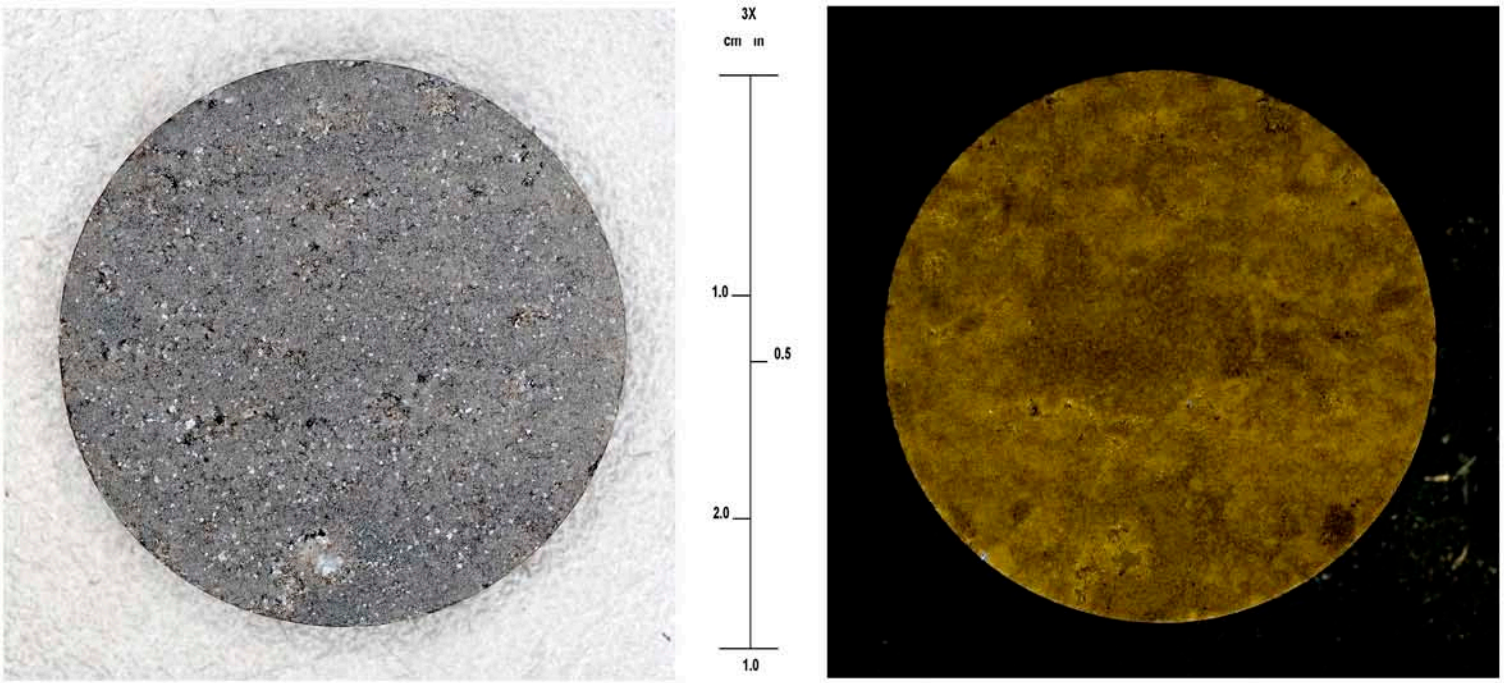

Weatherford LABORATORIES

HH-38266

Ohio Division of Geological Survey
CO2 No. 1 Well
Tuscarawas County, Ohio

Sample No.: 1-29R
Depth: 7192.00 feet

Visible Light

Longitudinal

Ultraviolet Light

Weatherford LABORATORIES

HH-38266

Ohio Division of Geological Survey
CO2 No. 1 Well
Tuscarawas County, Ohio

Sample No.: 1-30R
Depth: 7226.00 feet

Visible Light

Longitudinal

Ultraviolet Light

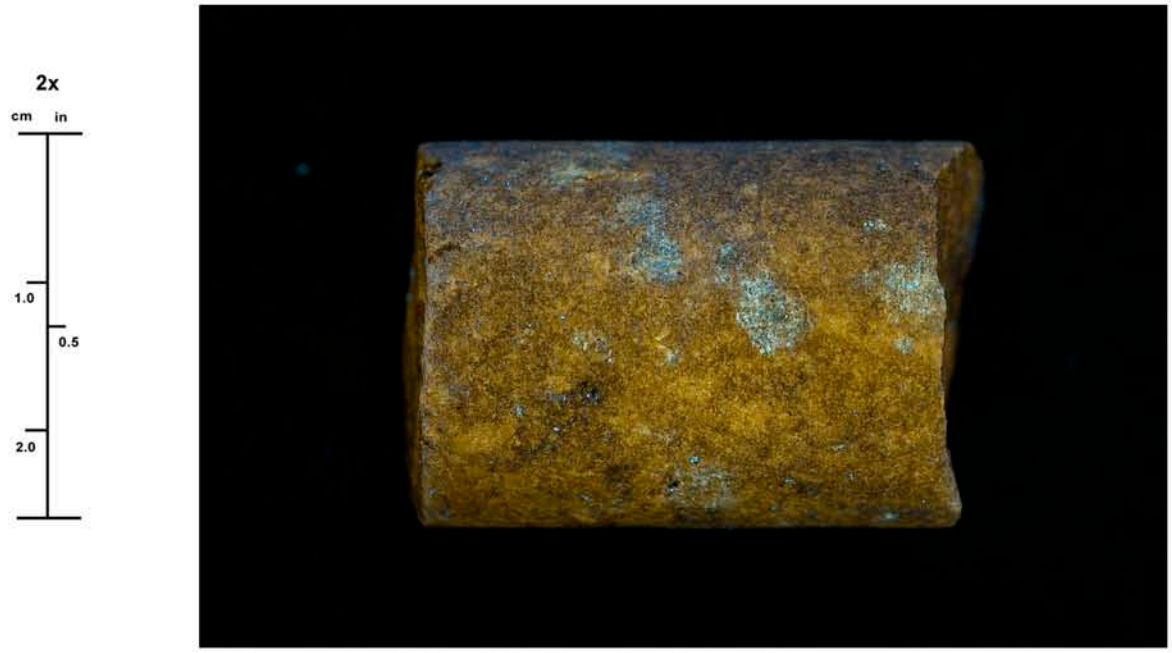

INTENTIONALLY BLANK

Weatherford LABORATORIES

HH-38266

Ohio Division of Geological Survey
CO2 No. 1 Well
Tuscarawas County, Ohio

Rotary Sidewall Core Photography

Sample No.: 1-31R

Visible Light — Depth: 7231.00 feet — Ultraviolet Light

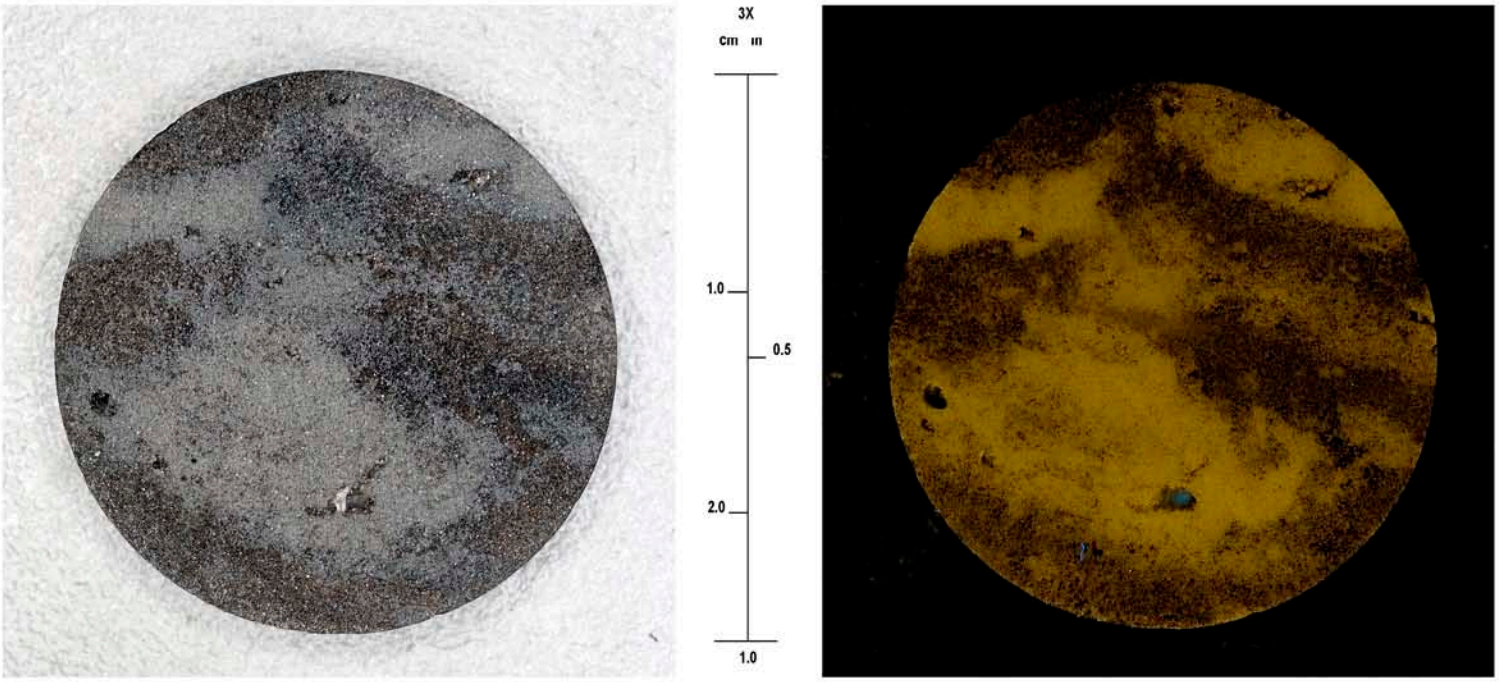

Sample No.: 1-32R

Visible Light — Depth: 7235.00 feet — Ultraviolet Light

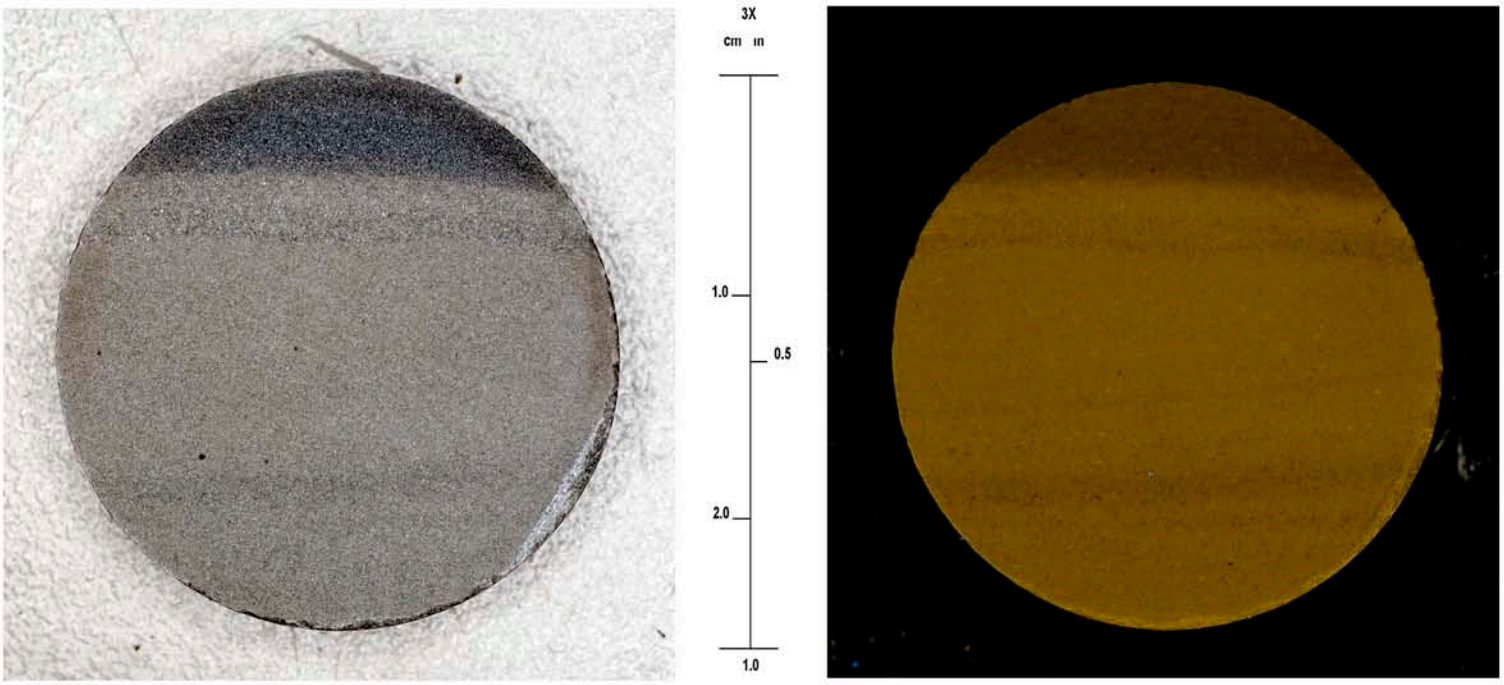

Weatherford LABORATORIES

HH-38266

Ohio Division of Geological Survey
CO2 No. 1 Well
Tuscarawas County, Ohio

Sample No.: 1-31R
Depth: 7231.00 feet

Visible Light

Longitudinal

Ultraviolet Light

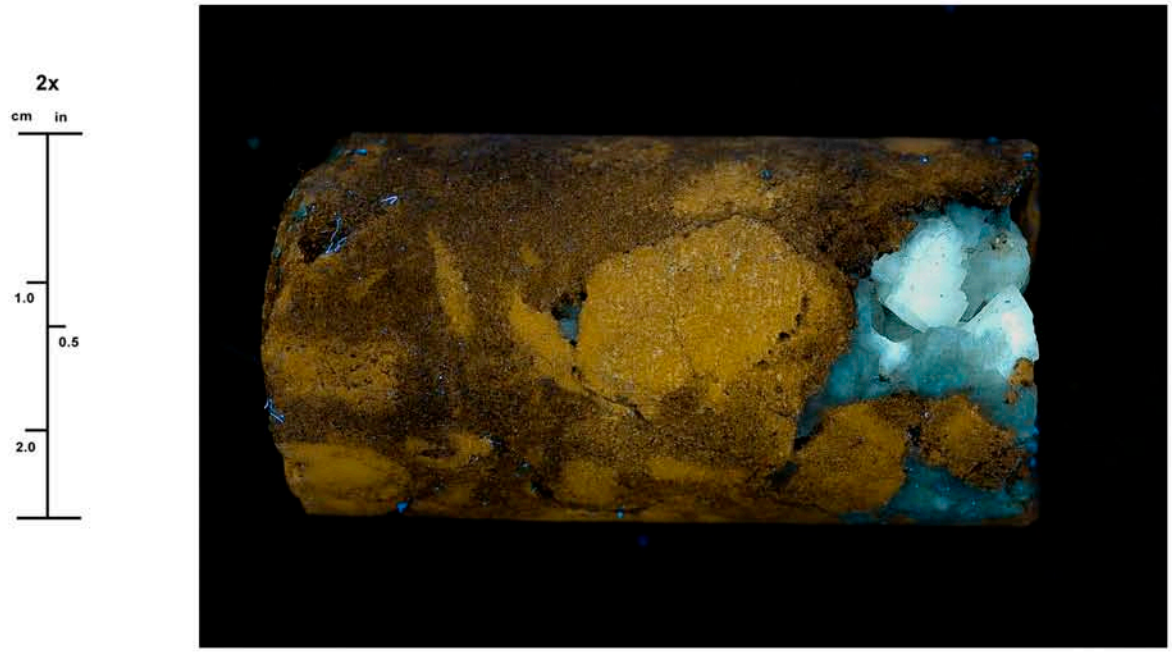

Weatherford LABORATORIES

HH-38266

Ohio Division of Geological Survey
CO2 No. 1 Well
Tuscarawas County, Ohio

Sample No.: 1-32R
Depth: 7235.00 feet

Visible Light

Longitudinal

Ultraviolet Light

INTENTIONALLY BLANK

Weatherford LABORATORIES

HH-38266

Ohio Division of Geological Survey
CO2 No. 1 Well
Tuscarawas County, Ohio

Rotary Sidewall Core Photography

Sample No.: 1-33R

Visible Light — Depth: 7248.00 feet — Ultraviolet Light

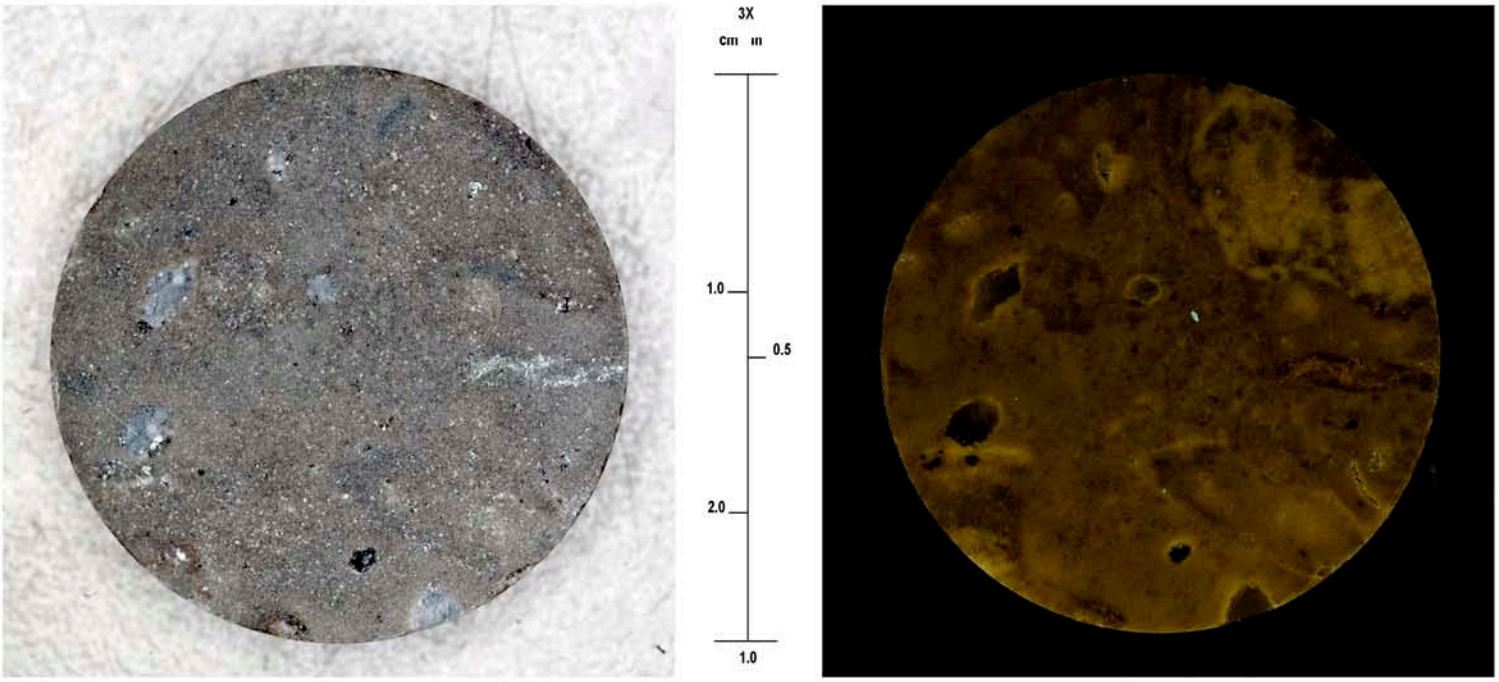

Sample No.: 1-34R

Visible Light — Depth: 7296.00 feet — Ultraviolet Light

Weatherford LABORATORIES

HH-38266

Ohio Division of Geological Survey
CO2 No. 1 Well
Tuscarawas County, Ohio

Sample No.: 1-33R
Depth: 7248.00 feet

Visible Light

Longitudinal

Ultraviolet Light

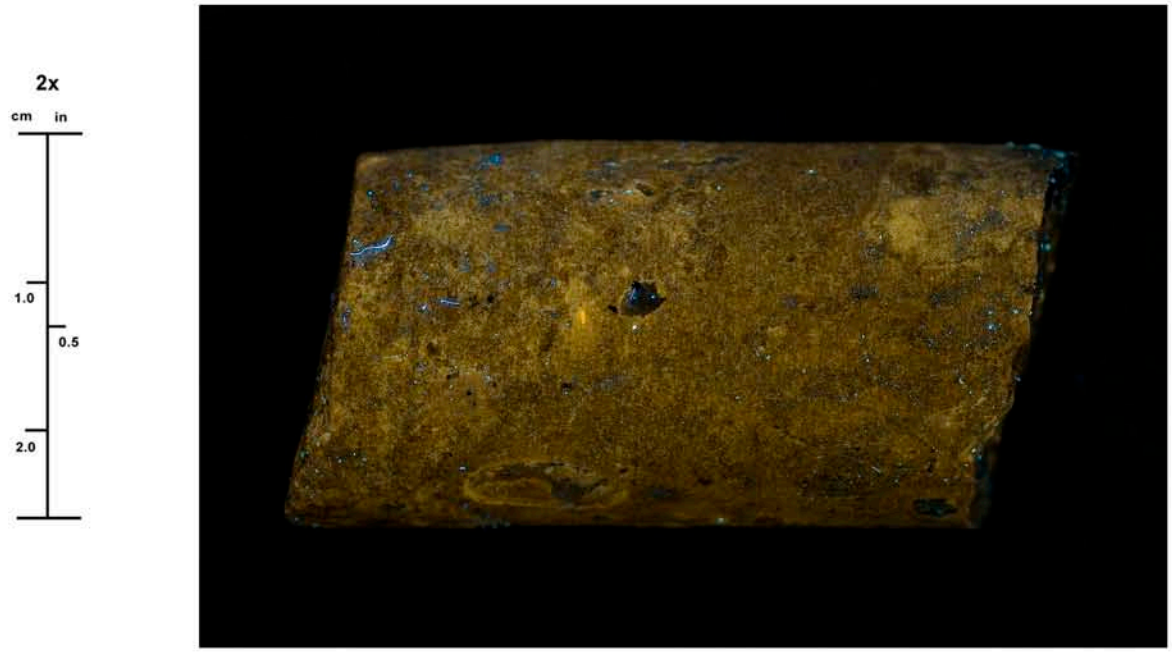

Weatherford LABORATORIES

HH-38266

Ohio Division of Geological Survey
CO2 No. 1 Well
Tuscarawas County, Ohio

Sample No.: 1-34R
Depth: 7296.00 feet

Visible Light

Longitudinal

Ultraviolet Light

INTENTIONALLY BLANK

Weatherford LABORATORIES

HH-38266

Ohio Division of Geological Survey
CO2 No. 1 Well
Tuscarawas County, Ohio

Rotary Sidewall Core Photography

Sample No.: 1-35R

Visible Light — Depth: 7328.00 feet — Ultraviolet Light

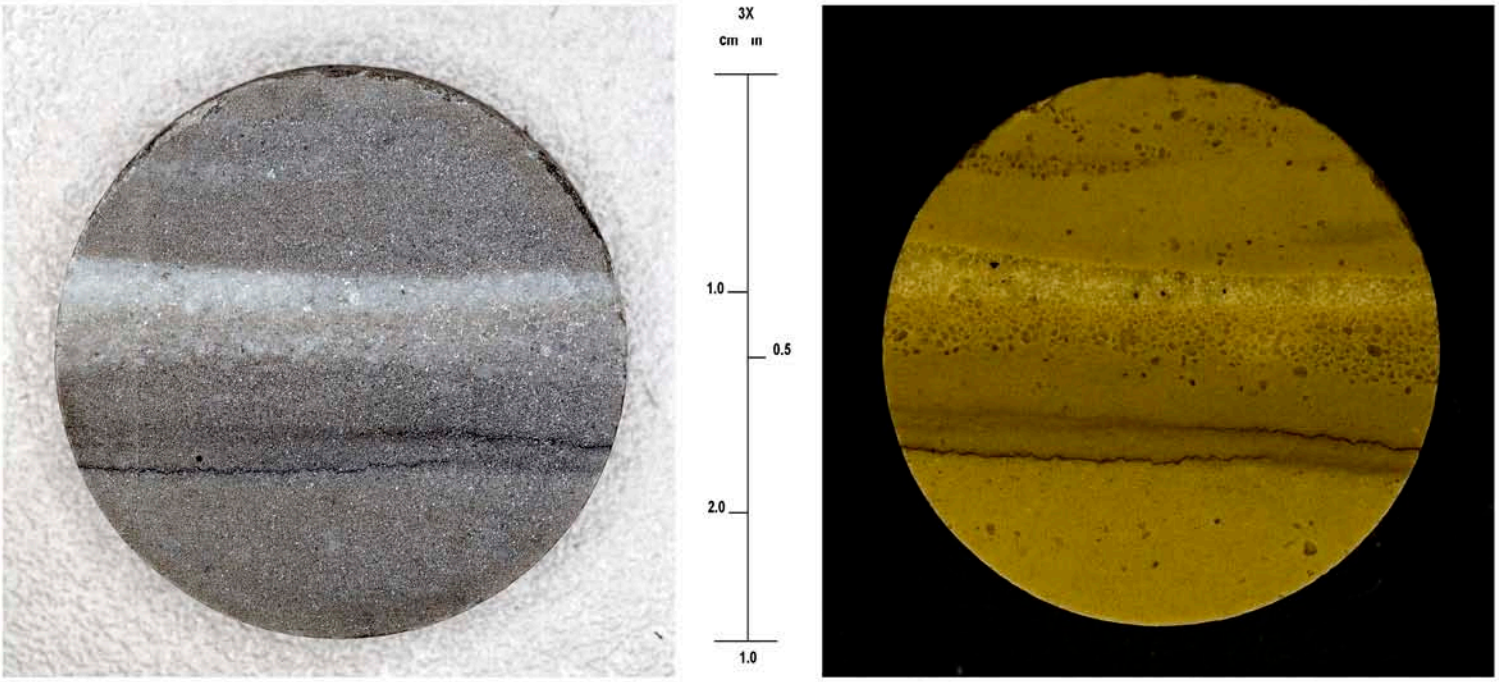

Sample No.: 1-36R

Visible Light — Depth: 7365.00 feet — Ultraviolet Light

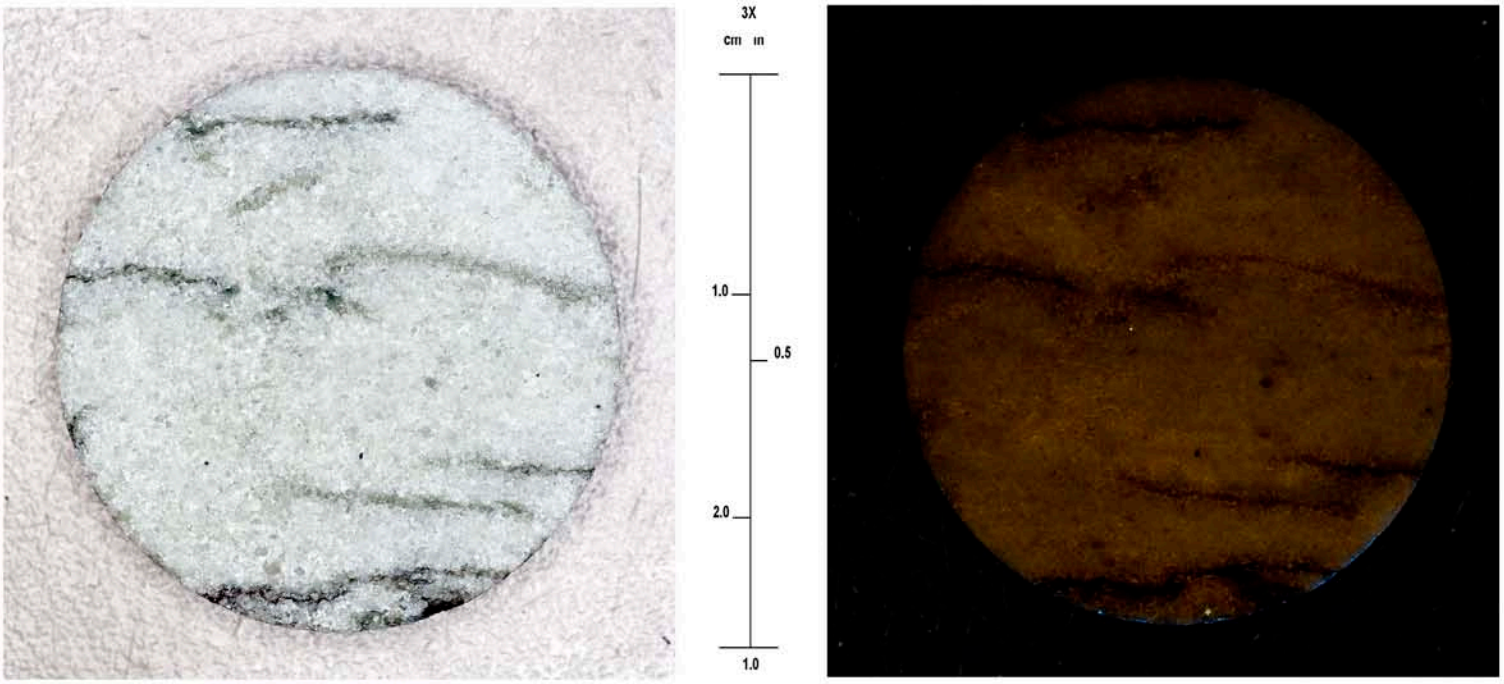

Weatherford LABORATORIES

HH-38266

Ohio Division of Geological Survey
CO2 No. 1 Well
Tuscarawas County, Ohio

Sample No.: 1-35R
Depth: 7328.00 feet

Visible Light

Longitudinal

Ultraviolet Light

Weatherford LABORATORIES

HH-38266

Ohio Division of Geological Survey
CO2 No. 1 Well
Tuscarawas County, Ohio

Sample No.: 1-36R
Depth: 7365.00 feet

Visible Light

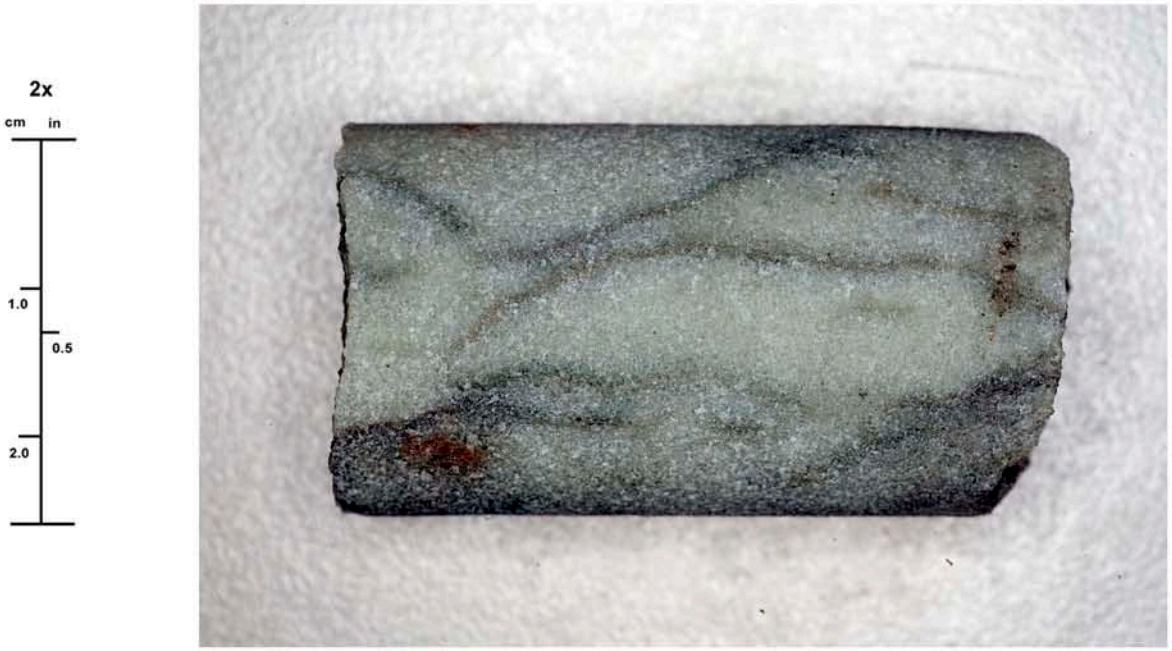

Longitudinal

Ultraviolet Light

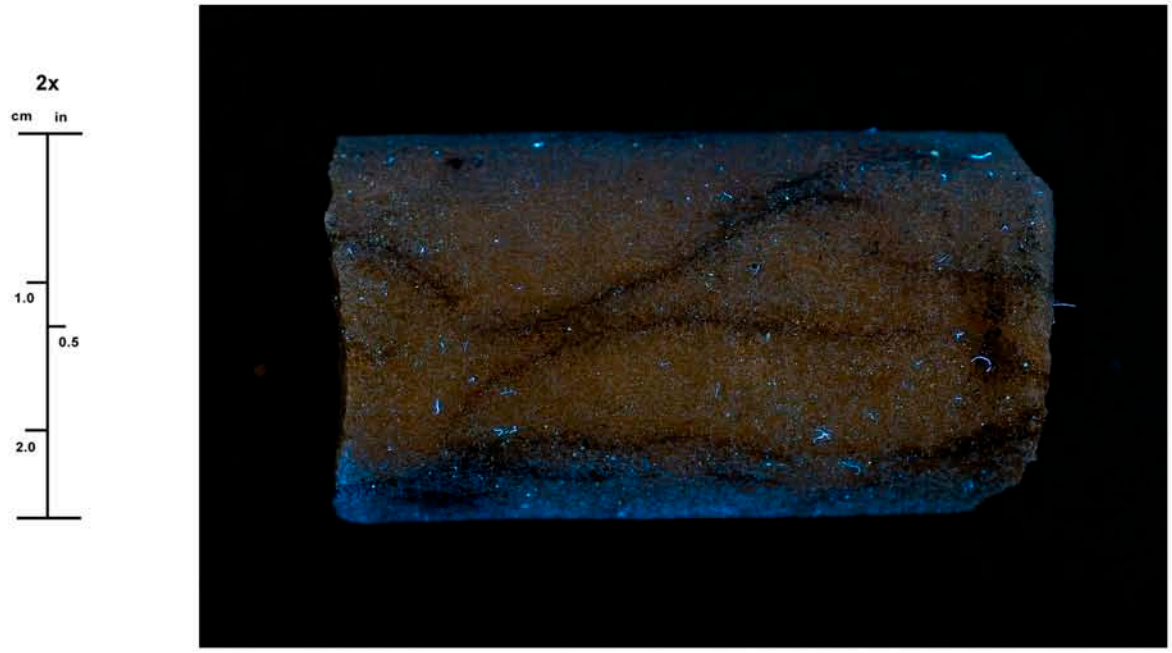

INTENTIONALLY BLANK

Weatherford LABORATORIES

HH-38266

Ohio Division of Geological Survey
CO2 No. 1 Well
Tuscarawas County, Ohio

Rotary Sidewall Core Photography

Sample No.: 1-37R

Visible Light — Depth: 7377.00 feet — Ultraviolet Light

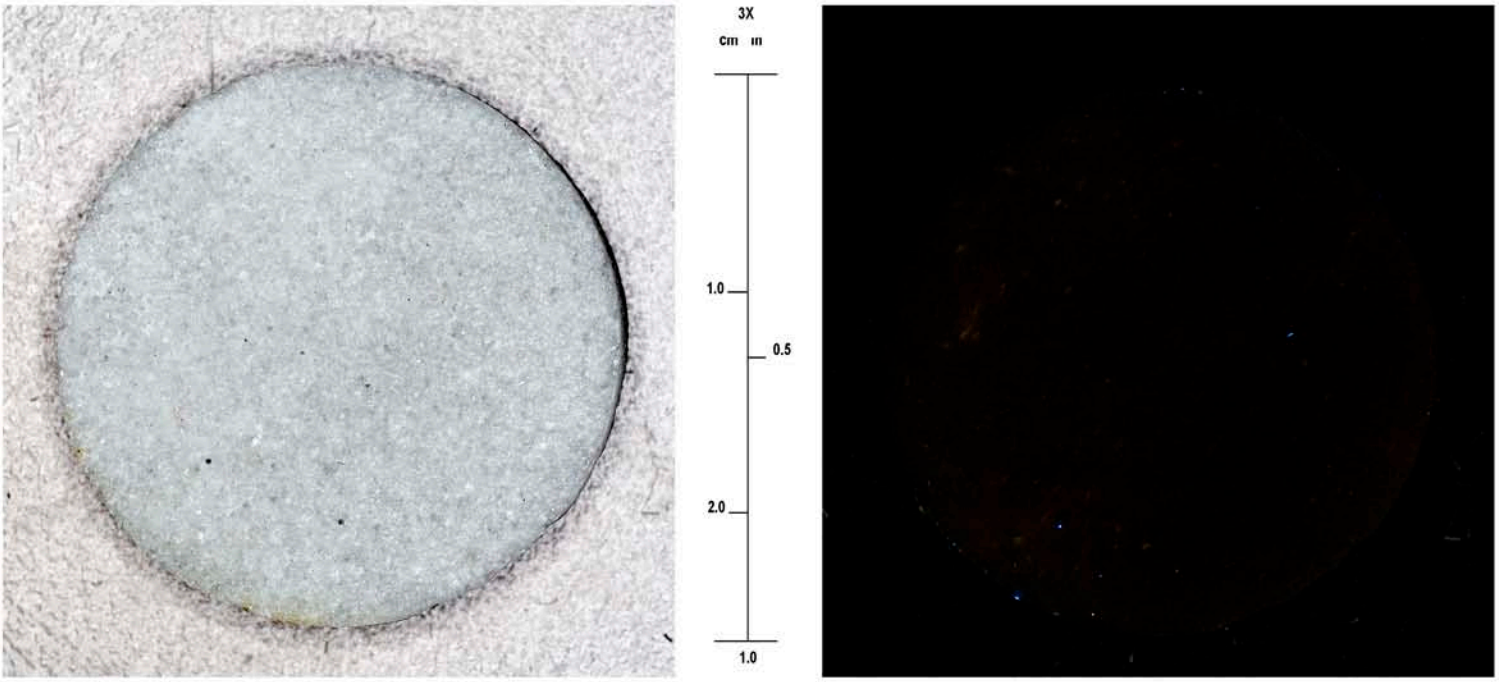

Sample No.: 1-38R

Visible Light — Depth: 7387.00 feet — Ultraviolet Light

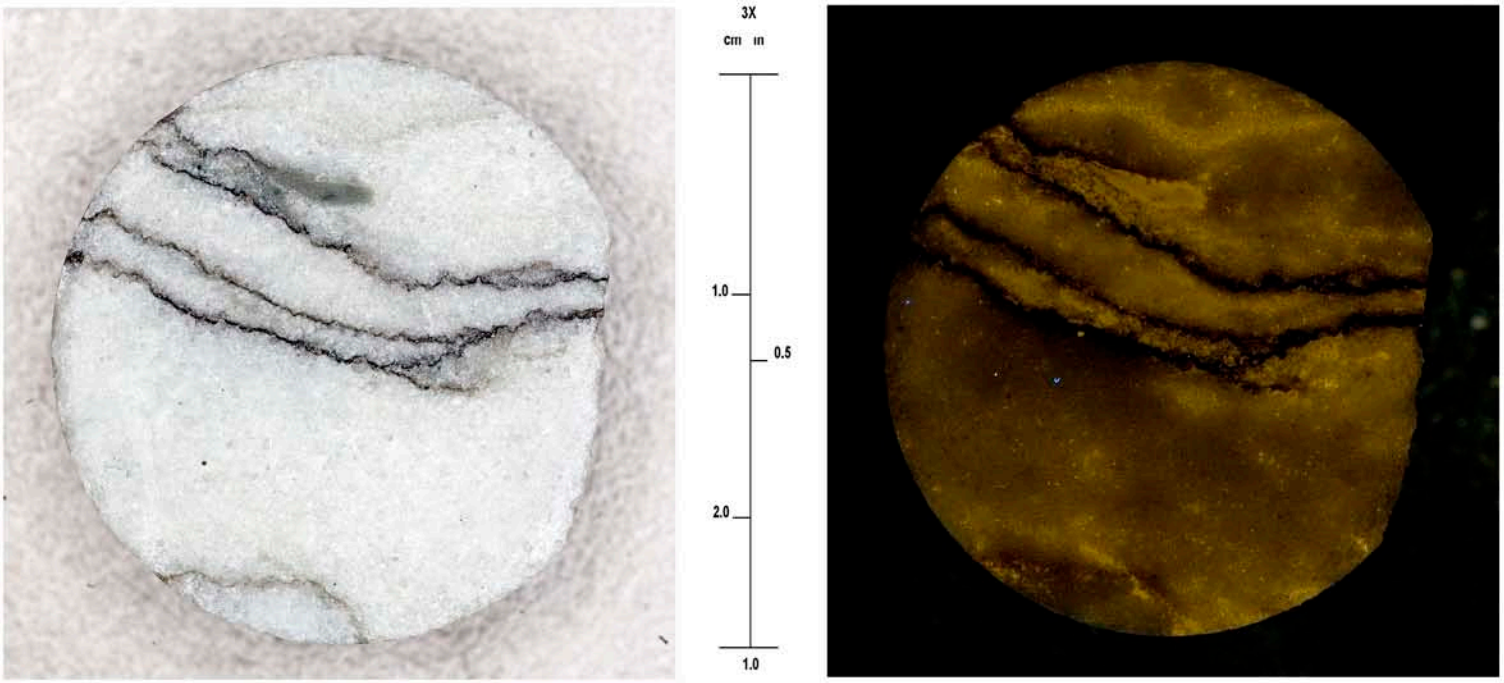

Weatherford LABORATORIES

HH-38266

Ohio Division of Geological Survey
CO2 No. 1 Well
Tuscarawas County, Ohio

Sample No.: 1-37R
Depth: 7377.00 feet

Visible Light

Longitudinal

Ultraviolet Light

Weatherford LABORATORIES

HH-38266

Ohio Division of Geological Survey
CO2 No. 1 Well
Tuscarawas County, Ohio

Sample No.: 1-38R
Depth: 7387.00 feet

Visible Light

Longitudinal

Ultraviolet Light

INTENTIONALLY BLANK

Weatherford LABORATORIES

HH-38266

Ohio Division of Geological Survey
CO2 No. 1 Well
Tuscarawas County, Ohio

Rotary Sidewall Core Photography

Sample No.: 1-39R

Visible Light — Depth: 7392.00 feet — Ultraviolet Light

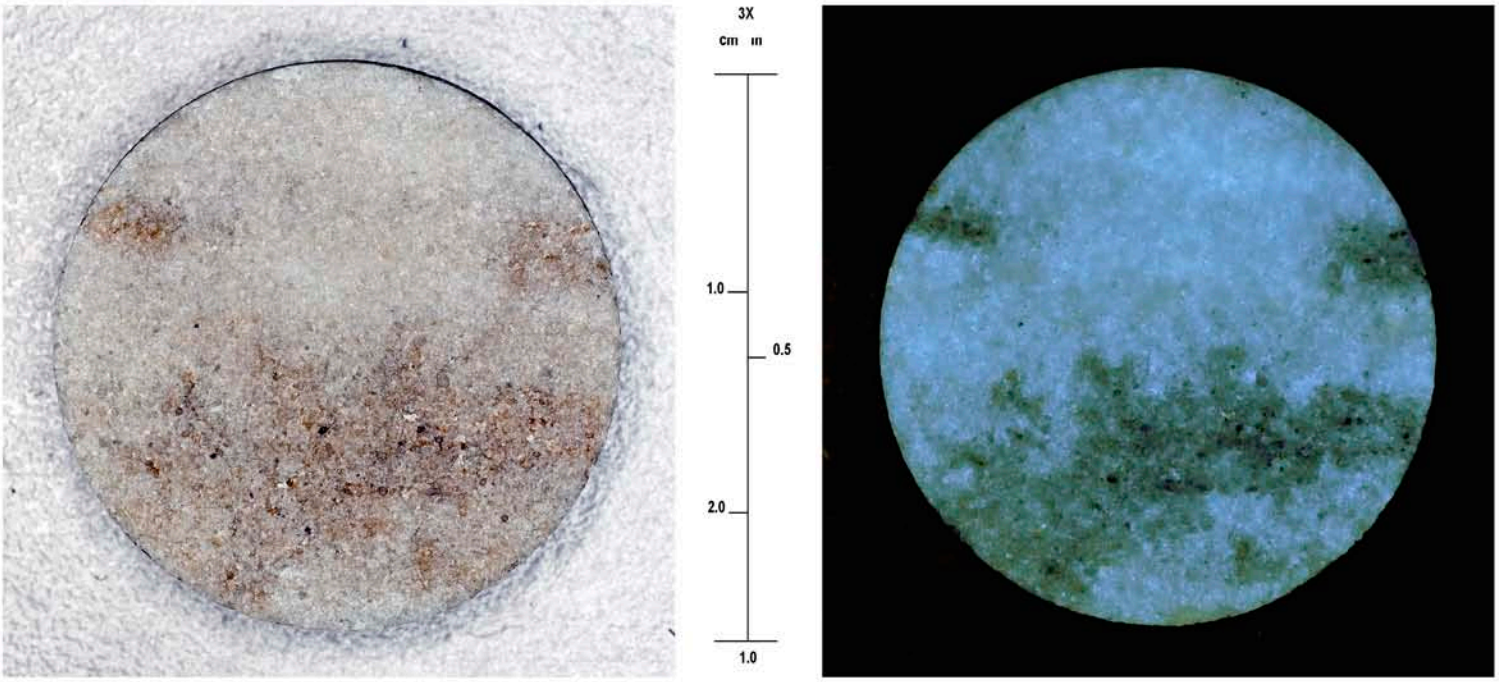

Sample No.: 1-40R

Visible Light — Depth: 7414.00 feet — Ultraviolet Light

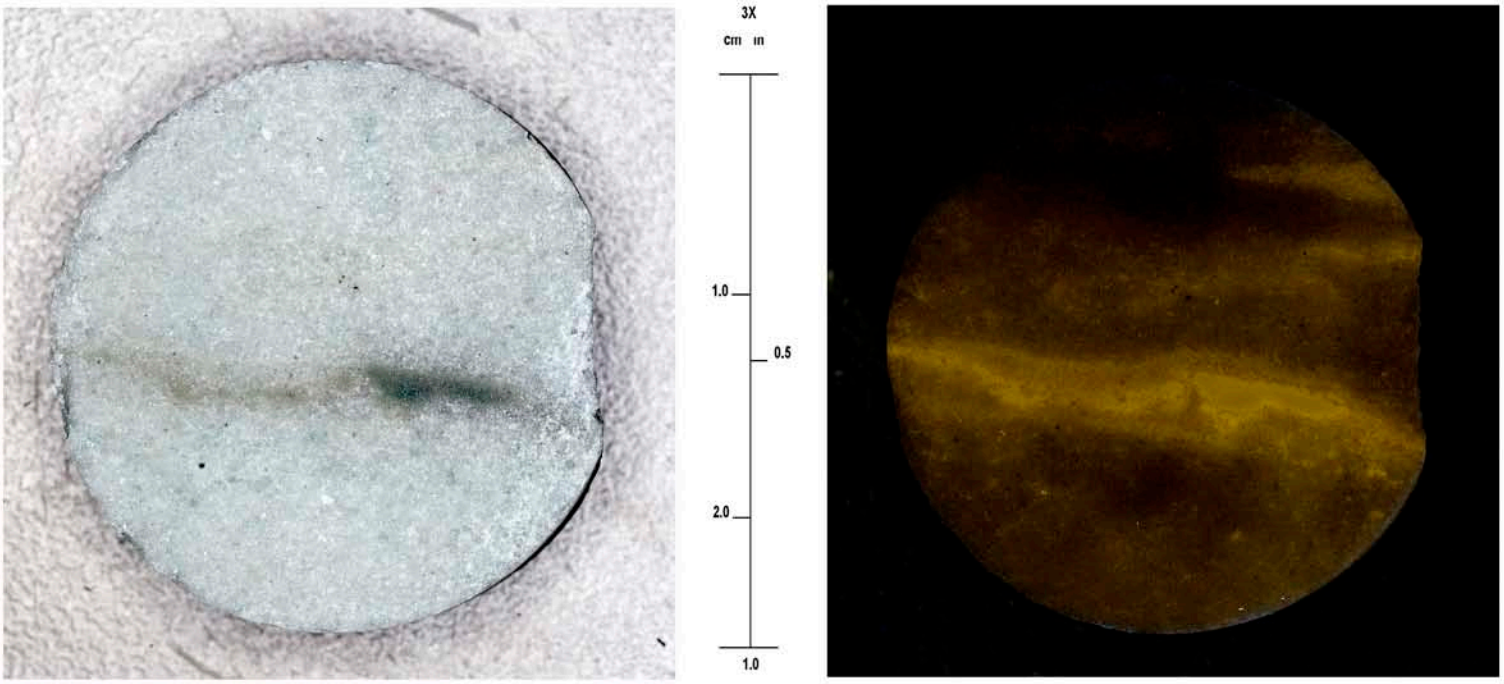

Weatherford LABORATORIES

HH-38266

Ohio Division of Geological Survey
CO2 No. 1 Well
Tuscarawas County, Ohio

Sample No.: 1-39R
Depth: 7392.00 feet

Visible Light

Longitudinal

Ultraviolet Light

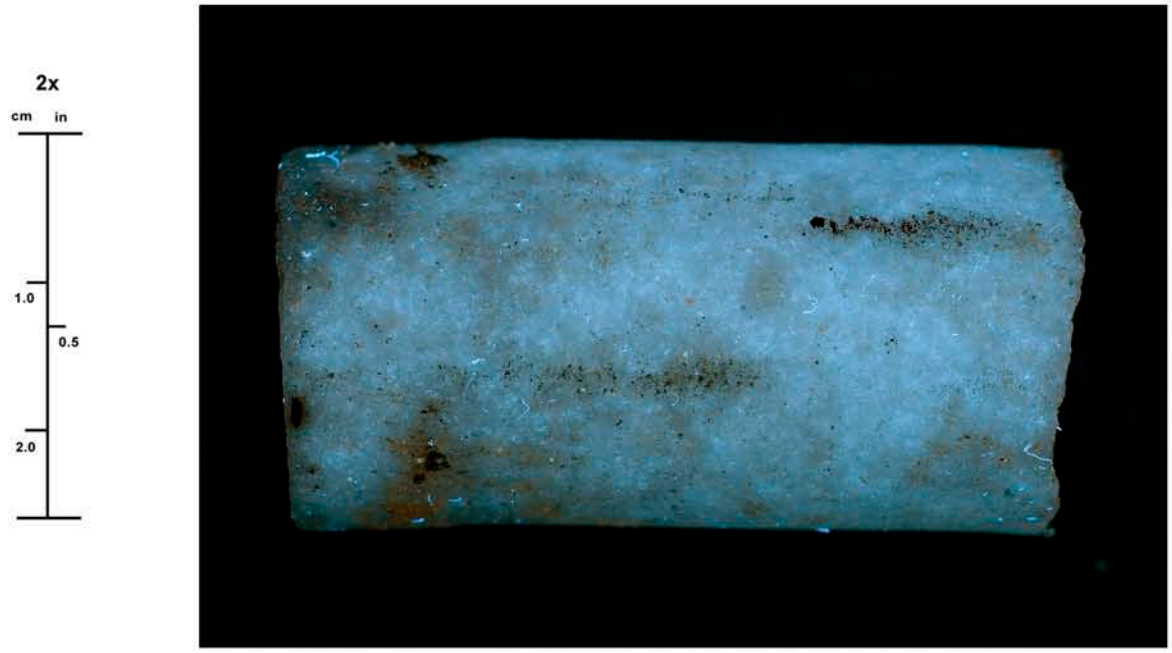

Weatherford LABORATORIES

HH-38266

Ohio Division of Geological Survey
CO2 No. 1 Well
Tuscarawas County, Ohio

Sample No.: 1-40R
Depth: 7414.00 feet

Visible Light

Longitudinal

Ultraviolet Light

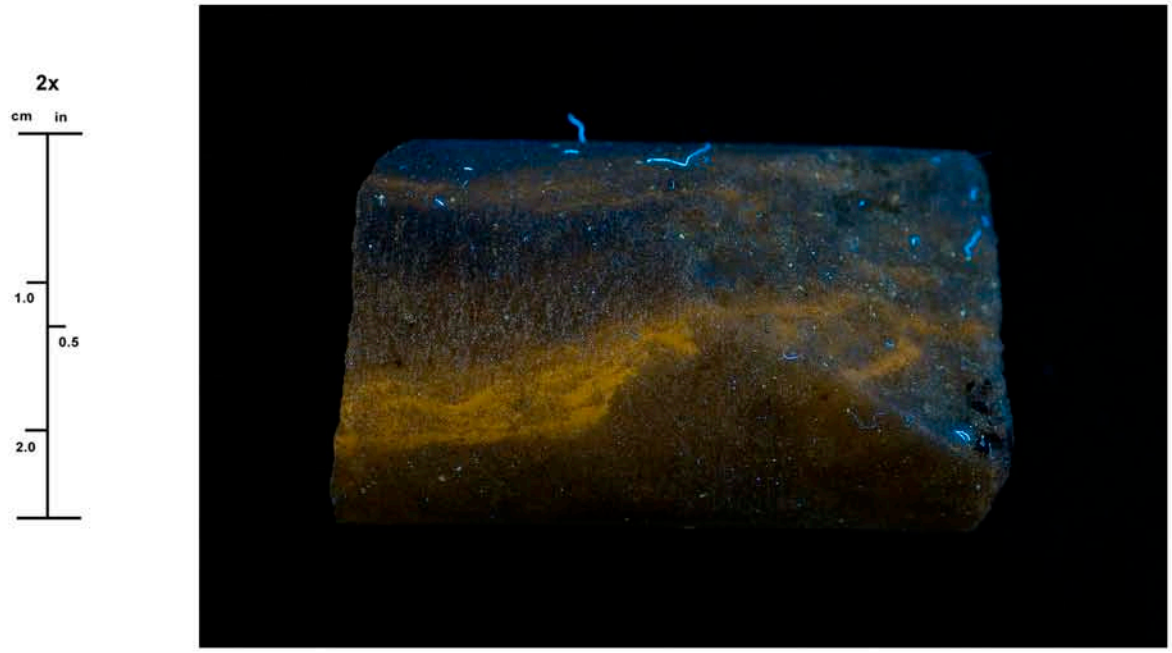

INTENTIONALLY BLANK

Weatherford LABORATORIES

HH-38266

Ohio Division of Geological Survey
CO2 No. 1 Well
Tuscarawas County, Ohio

Rotary Sidewall Core Photography

Sample No.: 1-41R

Visible Light — Depth: 7426.00 feet — Ultraviolet Light

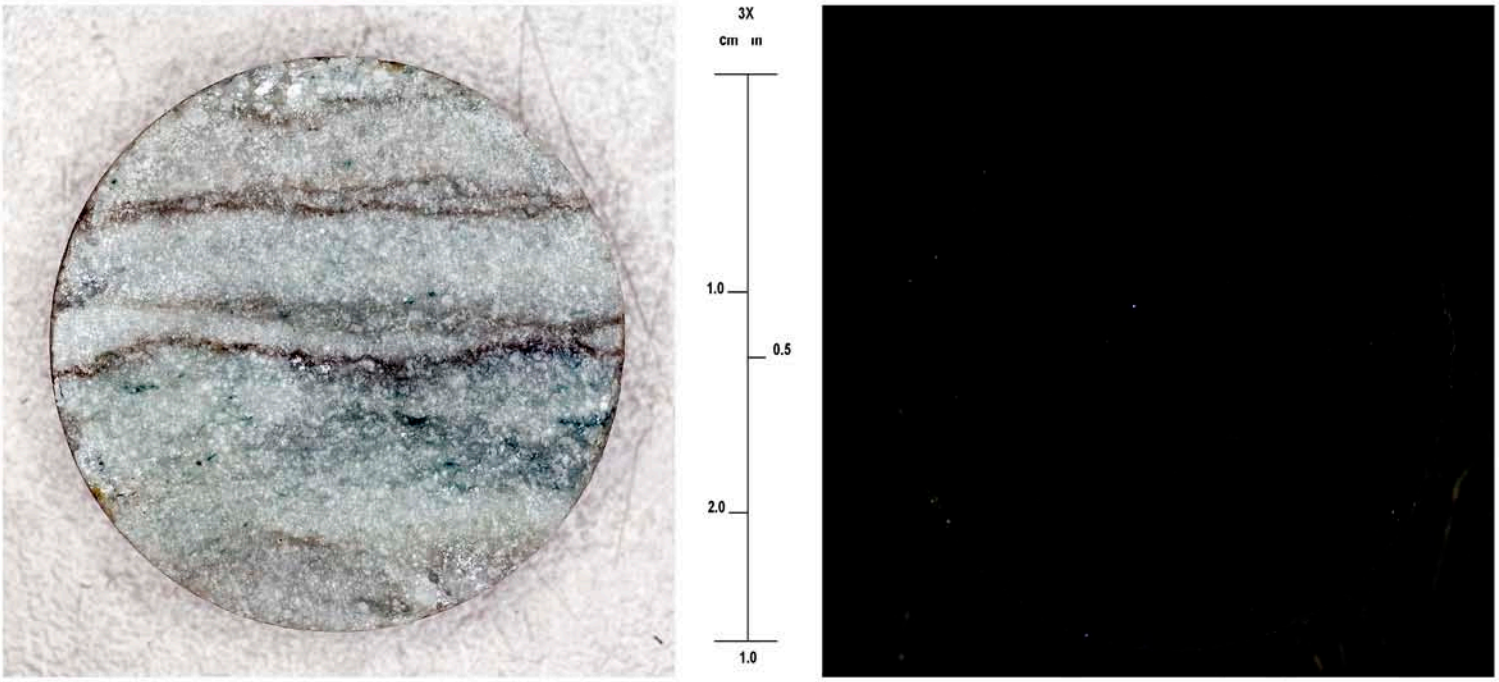

Sample No.: 1-42R

Visible Light — Depth: 7434.00 feet — Ultraviolet Light

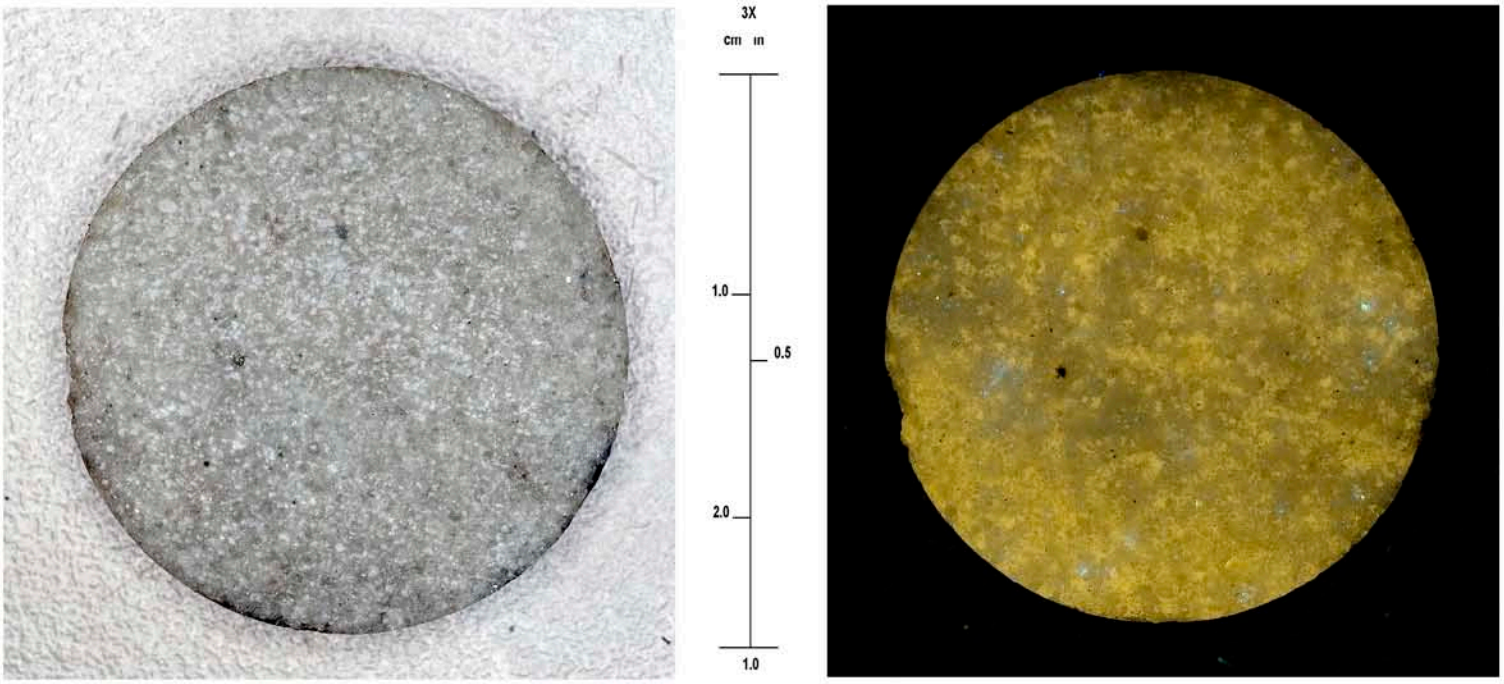

Weatherford LABORATORIES

HH-38266

Ohio Division of Geological Survey
CO2 No. 1 Well
Tuscarawas County, Ohio

Sample No.: 1-41R
Depth: 7426.00 feet

Visible Light

Longitudinal

Ultraviolet Light

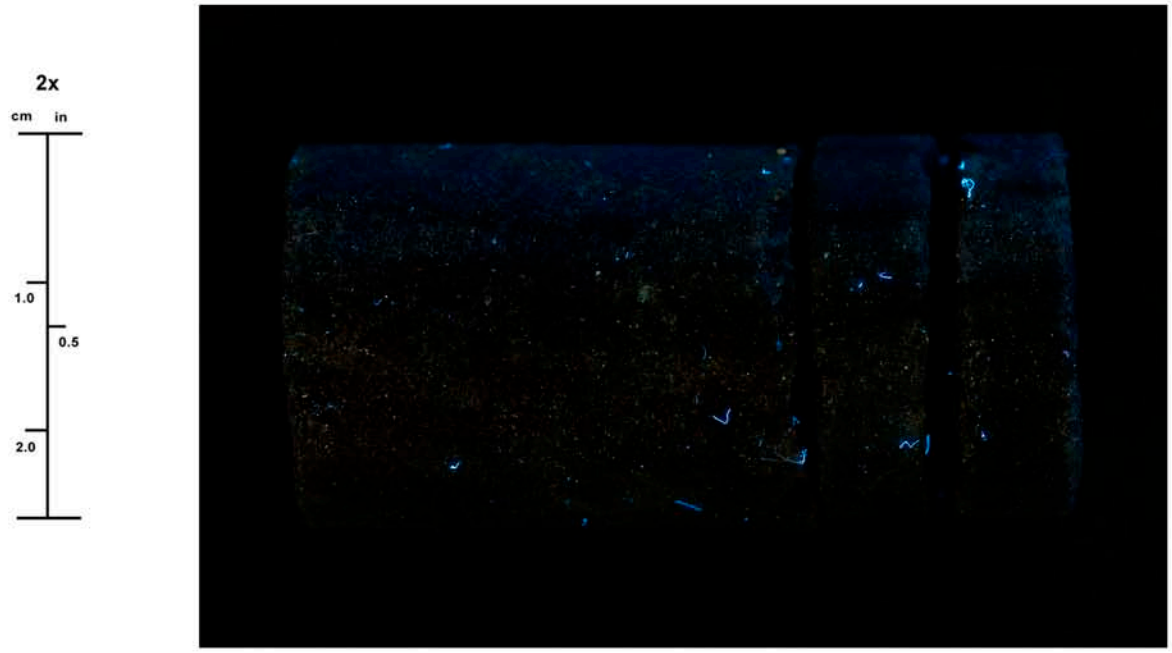

Weatherford LABORATORIES

HH-38266

Ohio Division of Geological Survey
CO2 No. 1 Well
Tuscarawas County, Ohio

Sample No.: 1-42R
Depth: 7434.00 feet

Visible Light

Longitudinal

Ultraviolet Light

INTENTIONALLY BLANK

Weatherford LABORATORIES

HH-38266

Ohio Division of Geological Survey
CO2 No. 1 Well
Tuscarawas County, Ohio

Rotary Sidewall Core Photography

Sample No.: 1-43R

Visible Light — Depth: 7441.00 feet — Ultraviolet Light

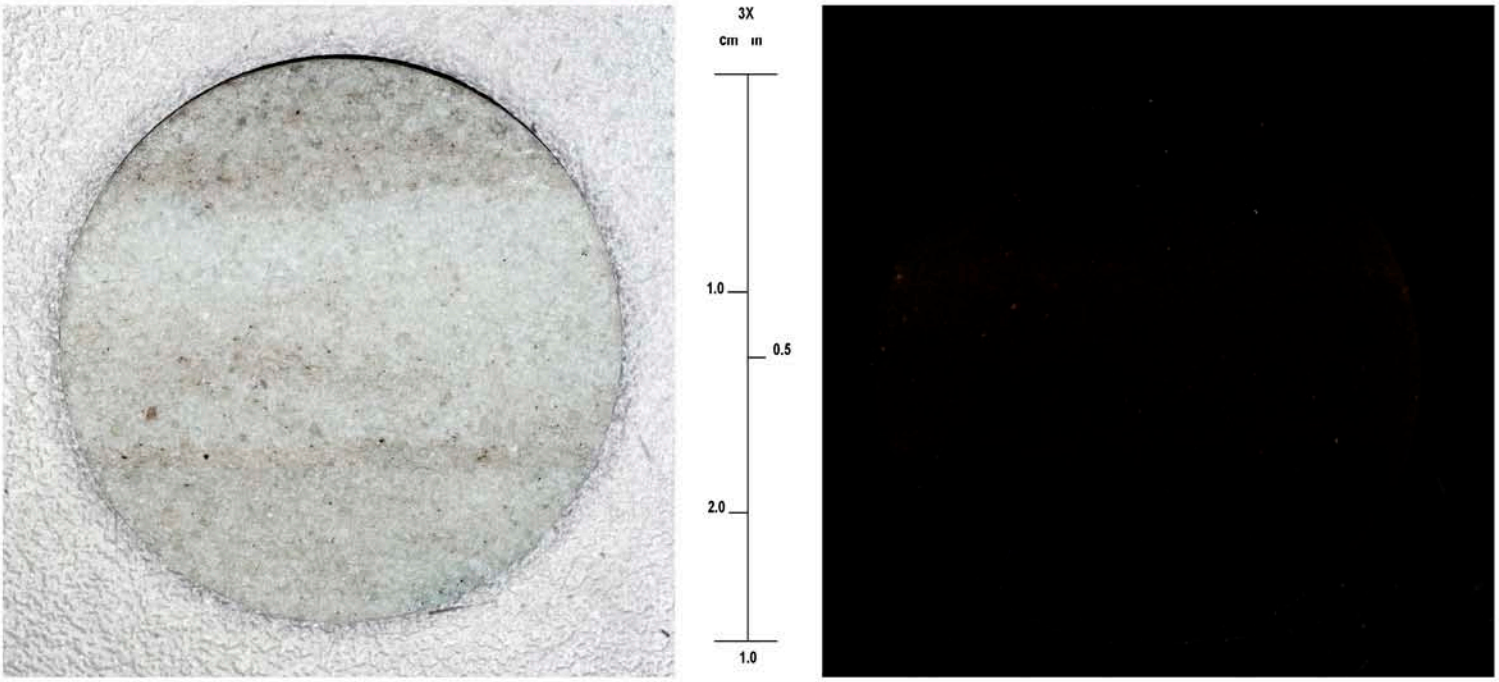

Sample No.: 1-44R

Visible Light — Depth: 7459.00 feet — Ultraviolet Light

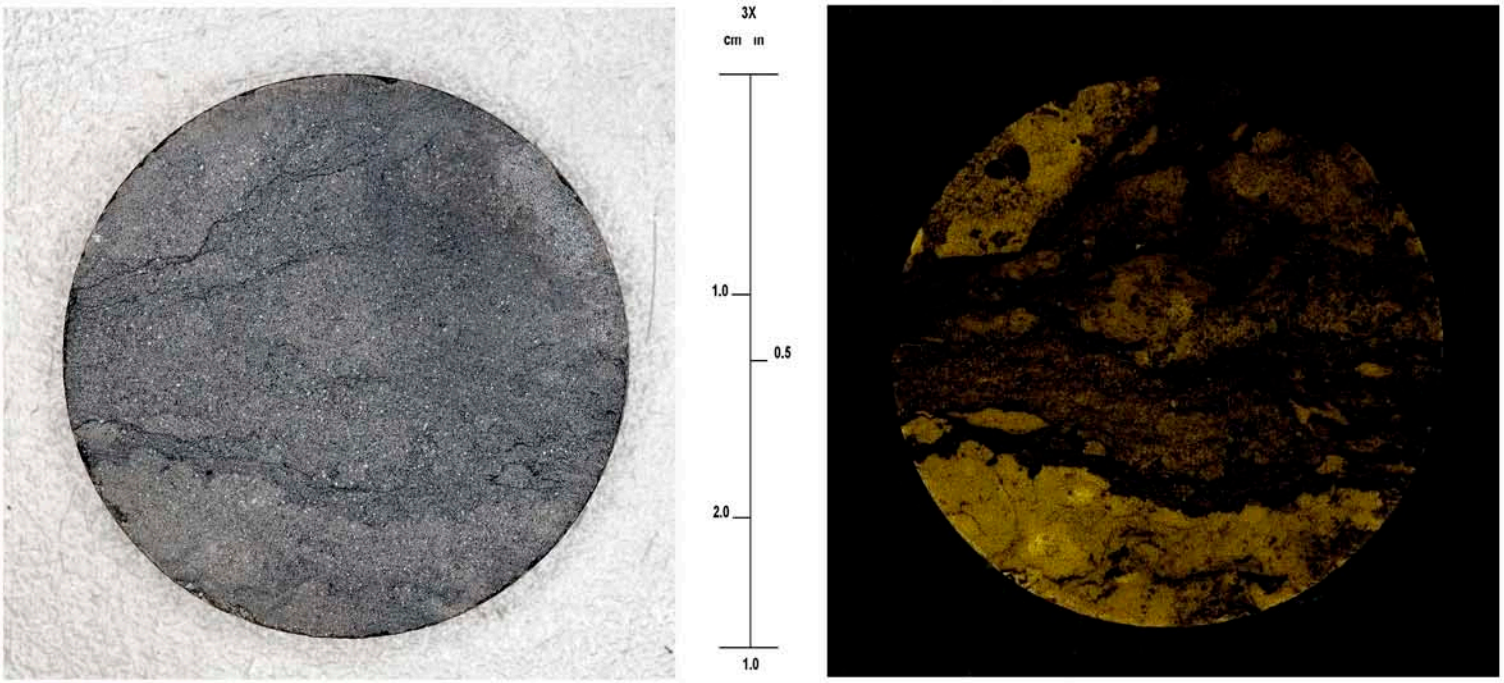

Weatherford LABORATORIES

HH-38266

Ohio Division of Geological Survey
CO2 No. 1 Well
Tuscarawas County, Ohio

Sample No.: 1-43R
Depth: 7441.00 feet

Visible Light

Longitudinal

Ultraviolet Light

Weatherford LABORATORIES

HH-38266

Ohio Division of Geological Survey
CO2 No. 1 Well
Tuscarawas County, Ohio

Sample No.: 1-44R
Depth: 7459.00 feet

Visible Light

Longitudinal

Ultraviolet Light

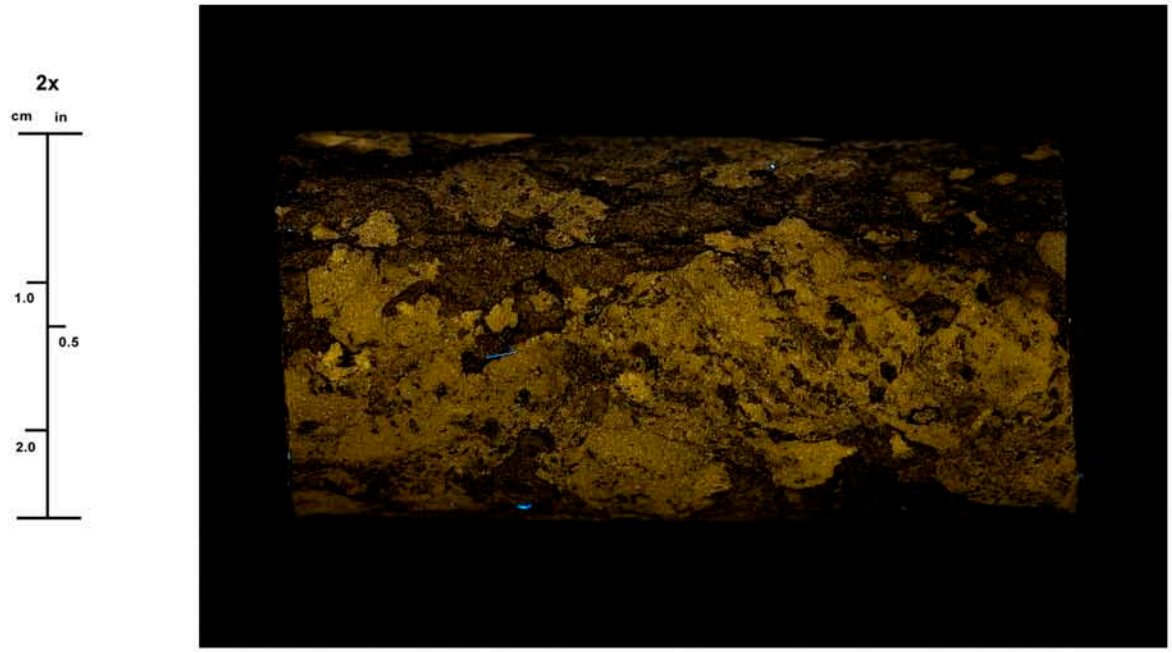

INTENTIONALLY BLANK

Weatherford LABORATORIES

HH-38266

Ohio Division of Geological Survey
CO2 No. 1 Well
Tuscarawas County, Ohio

Rotary Sidewall Core Photography

Sample No.: 1-45R

Visible Light — Depth: 7480.00 feet — Ultraviolet Light

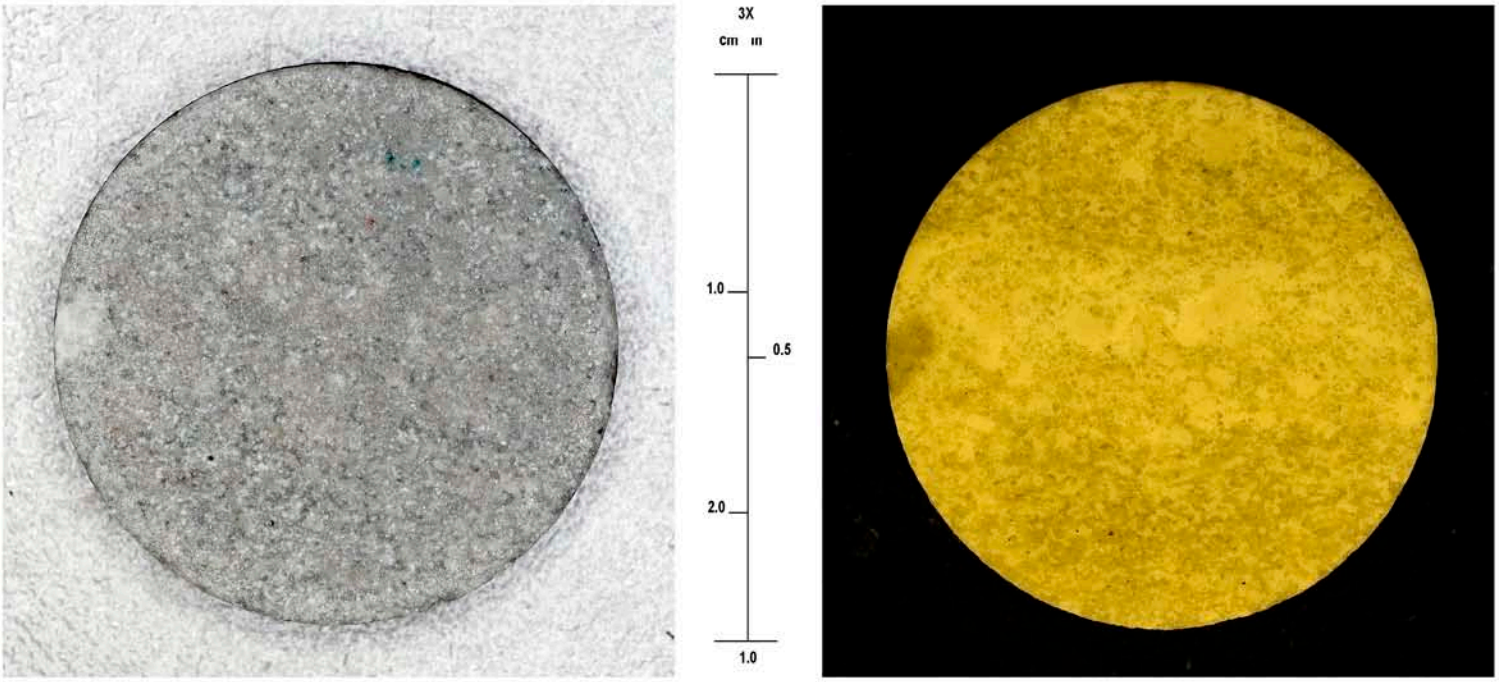

Sample No.: 1-46R

Visible Light — Depth: 7495.00 feet — Ultraviolet Light

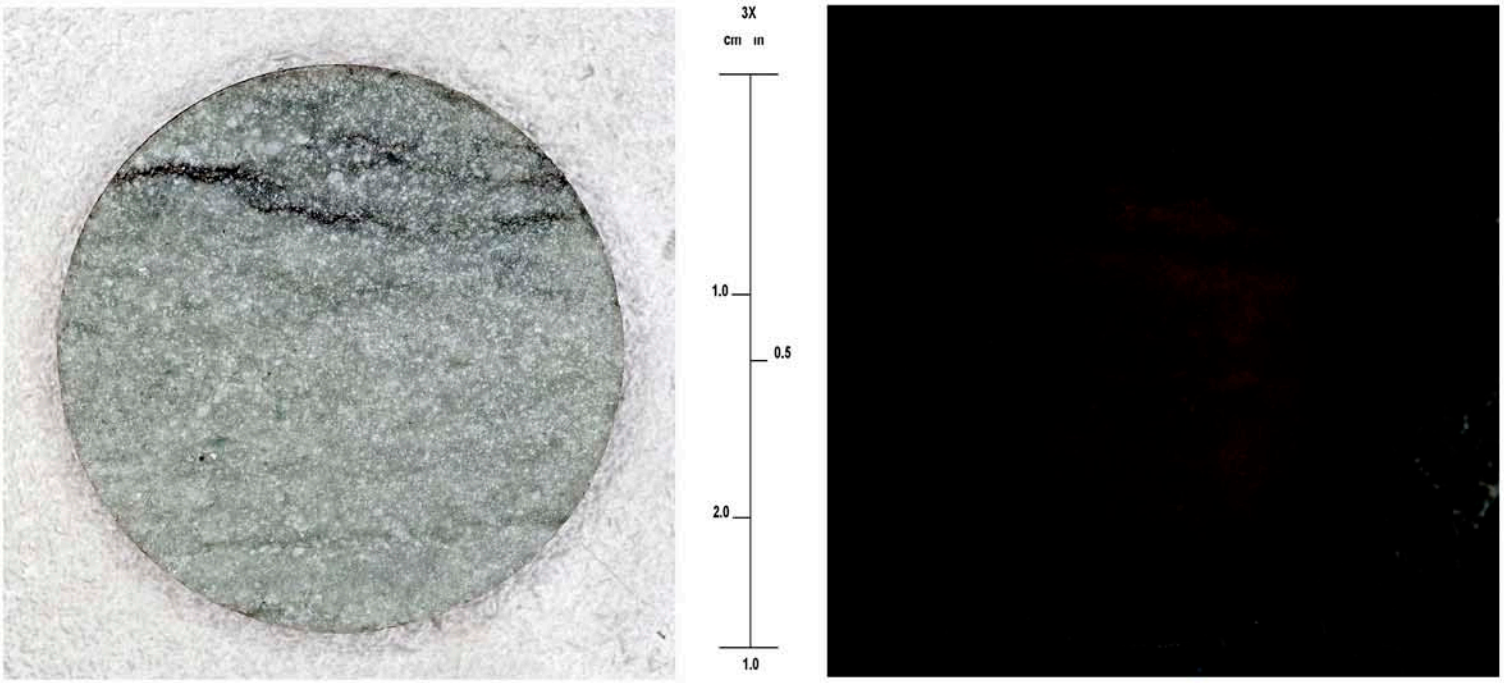

Weatherford LABORATORIES

HH-38266

Ohio Division of Geological Survey
CO2 No. 1 Well
Tuscarawas County, Ohio

Sample No.: 1-45R
Depth: 7480.00 feet

Visible Light

Longitudinal

Ultraviolet Light

Weatherford LABORATORIES

HH-38266

Ohio Division of Geological Survey
CO2 No. 1 Well
Tuscarawas County, Ohio

Sample No.: 1-46R
Depth: 7495.00 feet

Visible Light

Longitudinal

Ultraviolet Light

INTENTIONALLY BLANK

Weatherford LABORATORIES

HH-38266

Ohio Division of Geological Survey
CO2 No. 1 Well
Tuscarawas County, Ohio

Rotary Sidewall Core Photography

Sample No.: 1-47R

Visible Light — Depth: 7506.00 feet — Ultraviolet Light

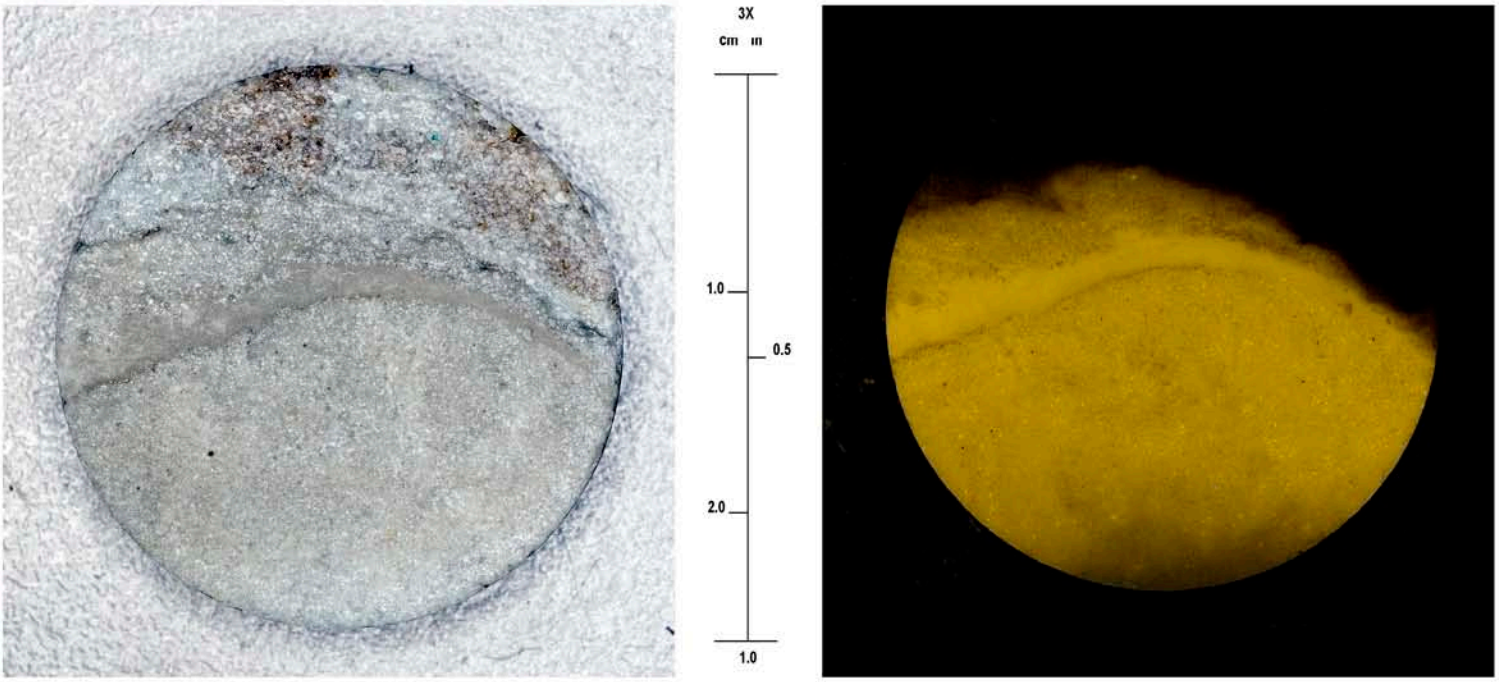

Sample No.: 1-48R

Visible Light — Depth: 7528.00 feet — Ultraviolet Light

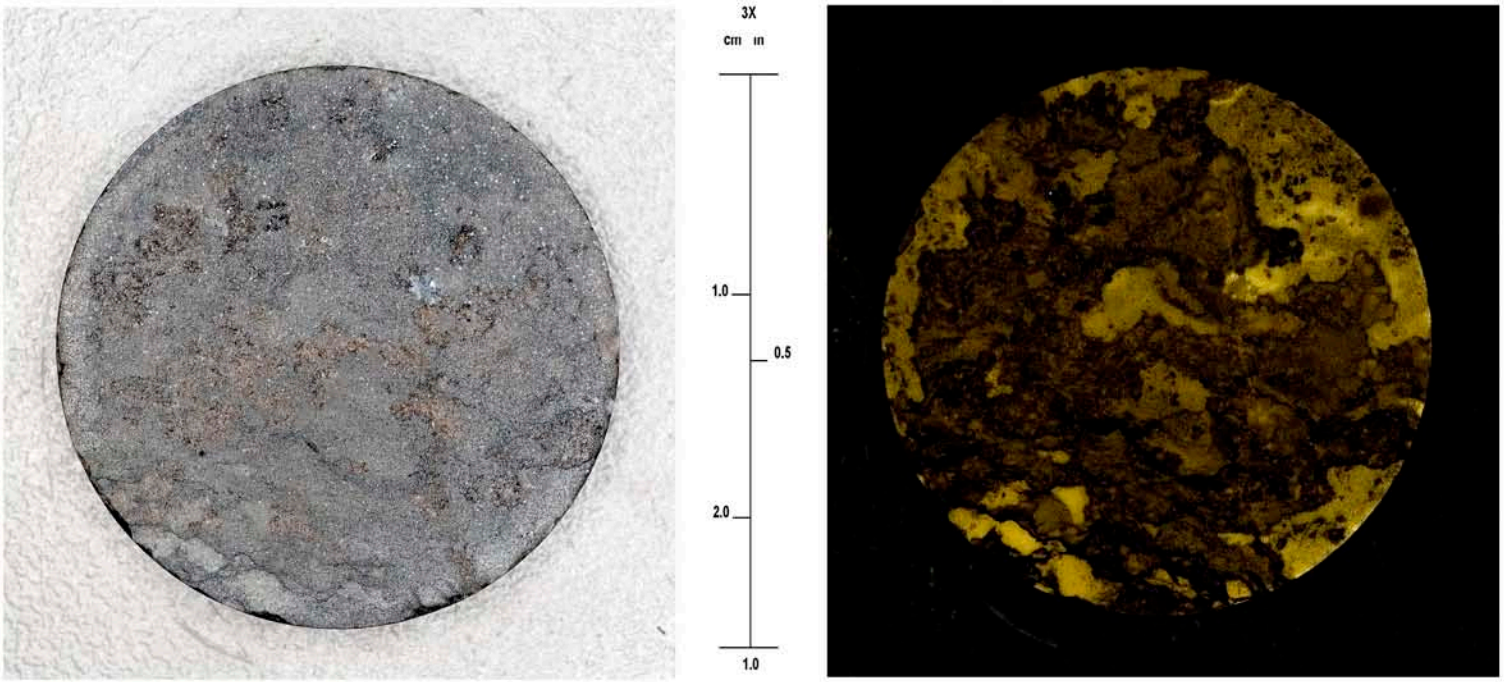

Weatherford LABORATORIES

HH-38266

Ohio Division of Geological Survey
CO2 No. 1 Well
Tuscarawas County, Ohio

Sample No.: 1-47R
Depth: 7506.00 feet

Visible Light

Longitudinal

Ultraviolet Light

Weatherford LABORATORIES

HH-38266

Ohio Division of Geological Survey
CO2 No. 1 Well
Tuscarawas County, Ohio

Sample No.: 1-48R
Depth: 7528.00 feet

Visible Light

Longitudinal

Ultraviolet Light

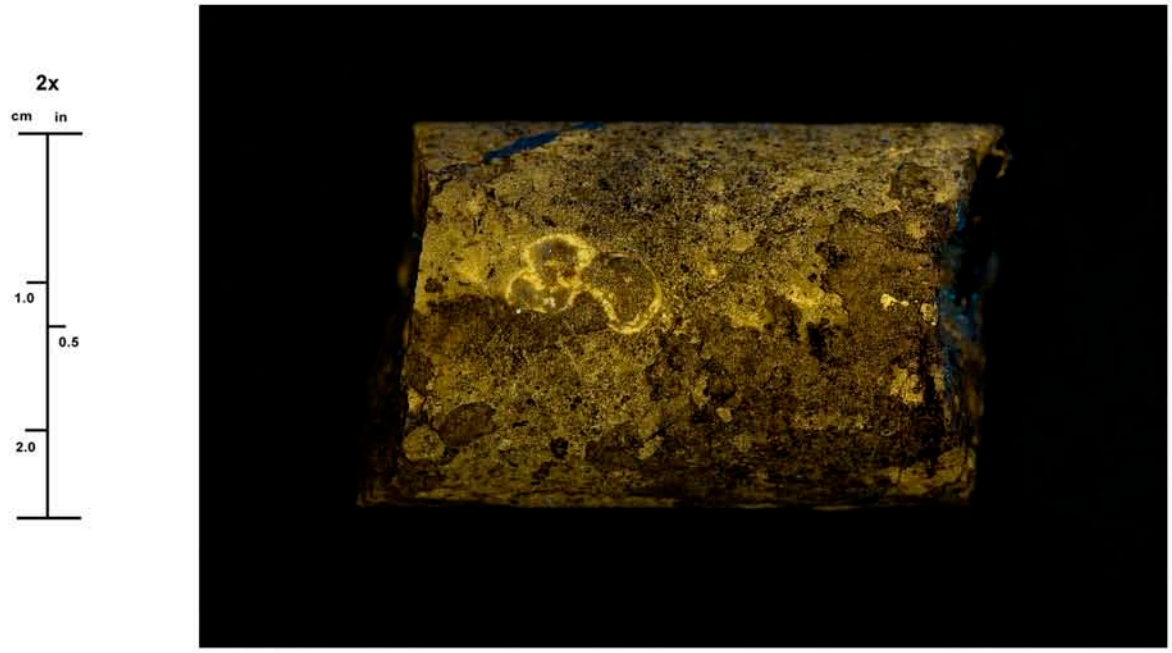

INTENTIONALLY BLANK

Weatherford LABORATORIES

HH-38266

Ohio Division of Geological Survey
CO2 No. 1 Well
Tuscarawas County, Ohio

Rotary Sidewall Core Photography

Sample No.: 1-49R

Visible Light — Depth: 7579.00 feet — Ultraviolet Light

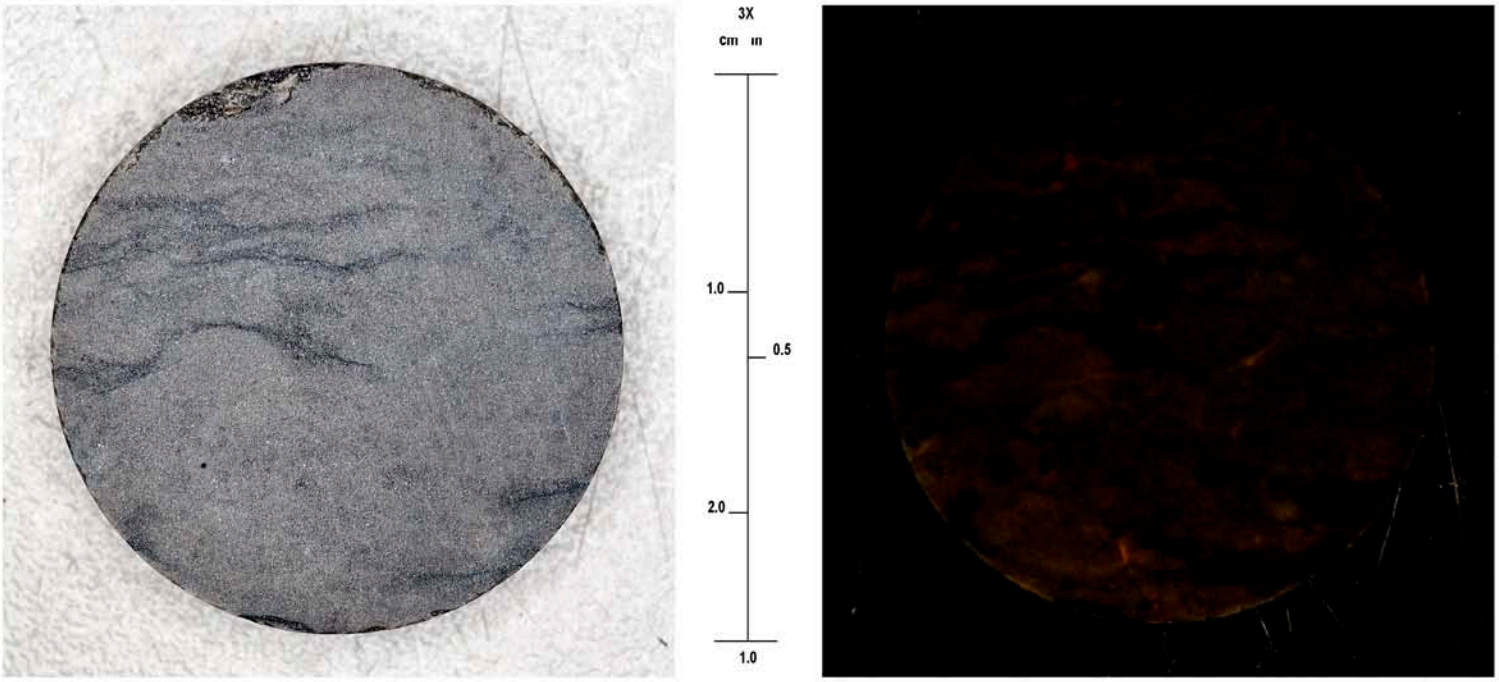

Sample No.: 1-50R

Visible Light — Depth: 7692.00 feet — Ultraviolet Light

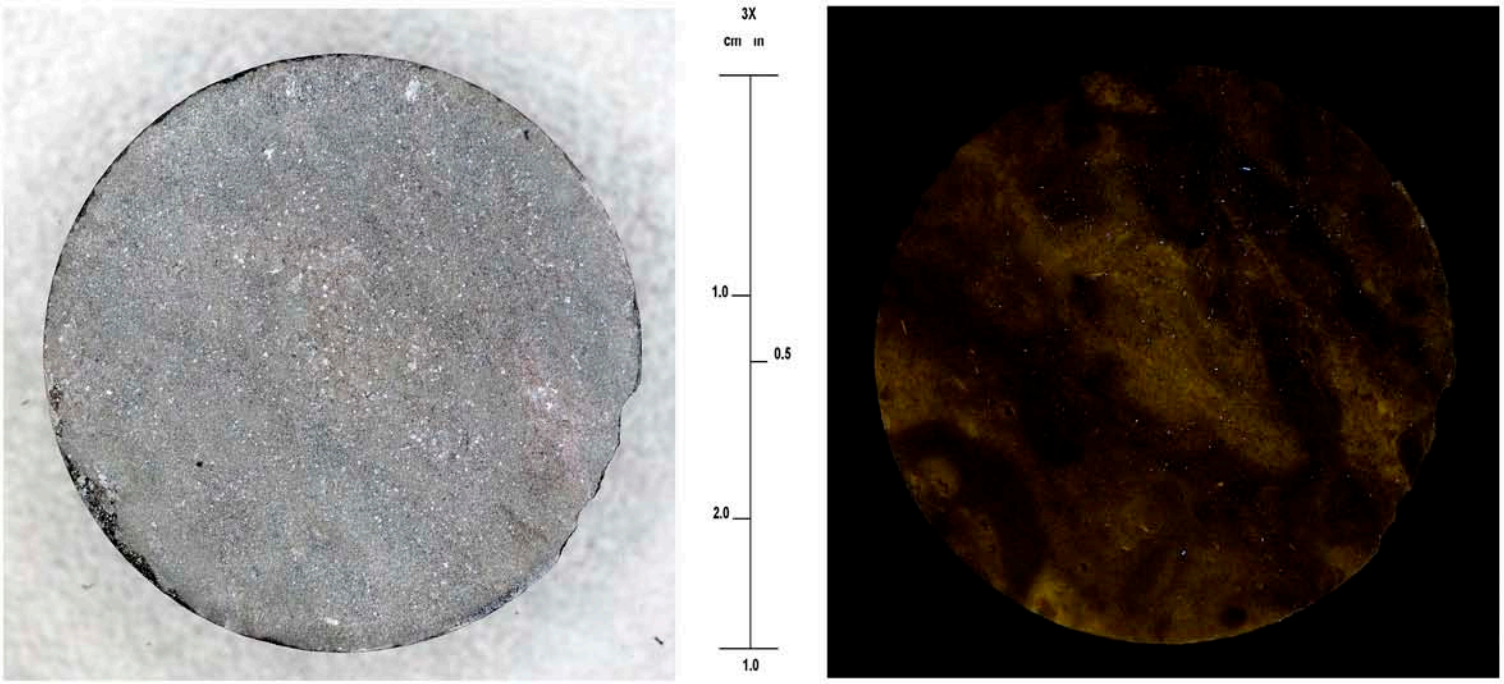

Weatherford LABORATORIES

HH-38266

Ohio Division of Geological Survey
CO2 No. 1 Well
Tuscarawas County, Ohio

Sample No.: 1-49R
Depth: 7579.00 feet

Visible Light

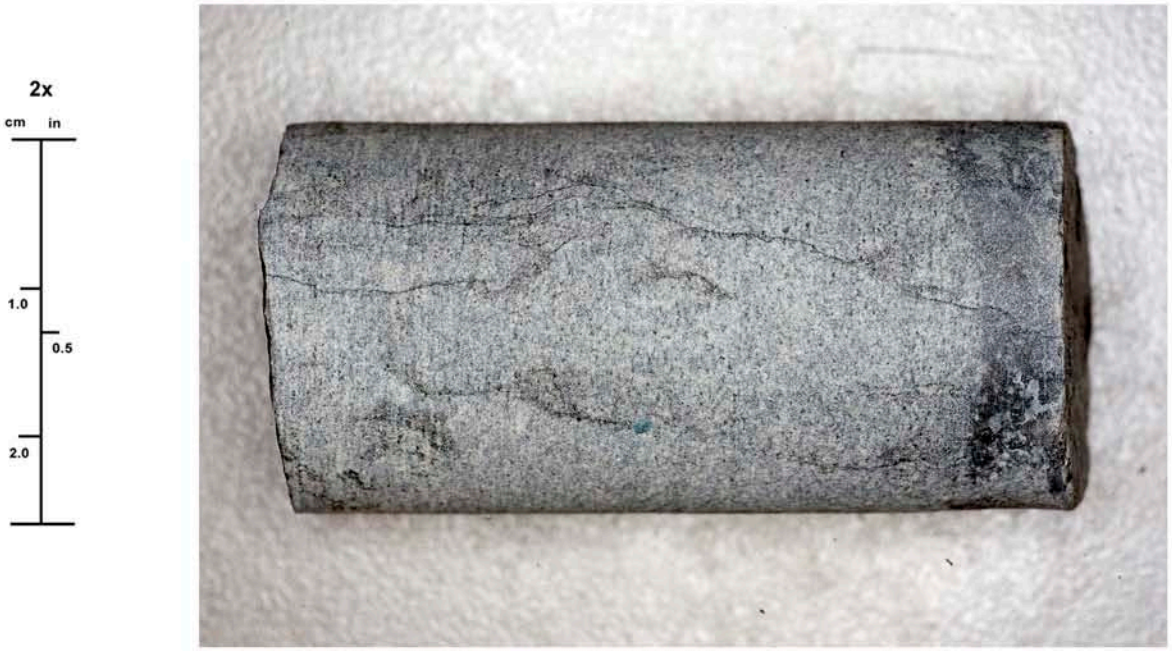

Longitudinal

Ultraviolet Light

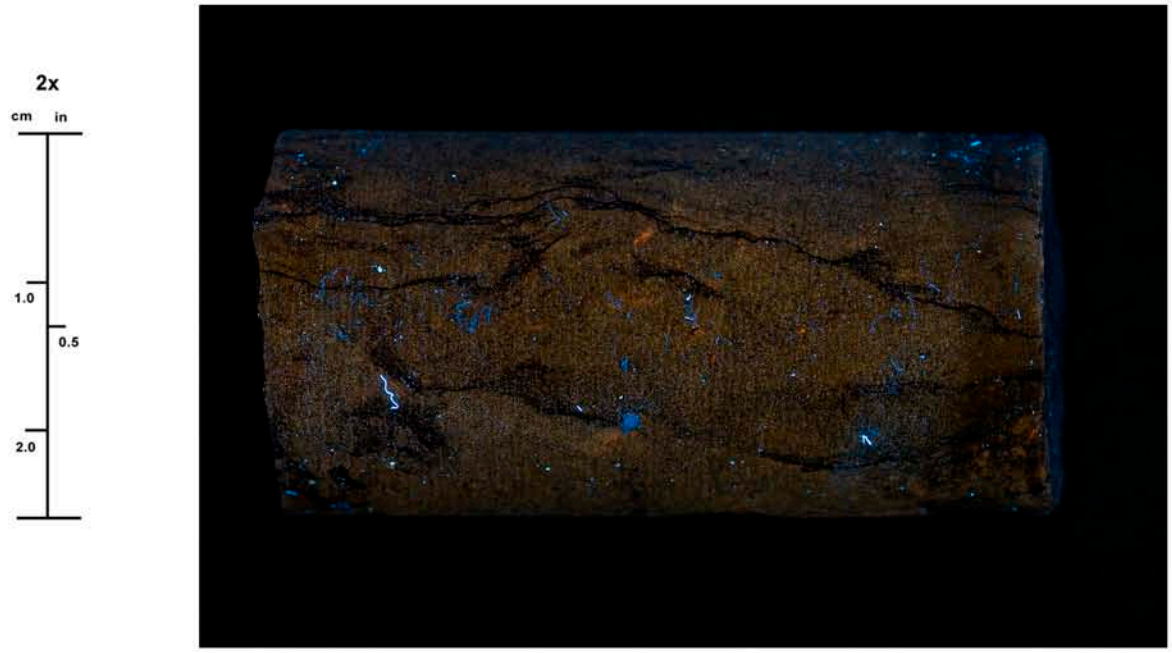

Weatherford LABORATORIES

HH-38266

Ohio Division of Geological Survey
CO2 No. 1 Well
Tuscarawas County, Ohio

Sample No.: 1-50R
Depth: 7692.00 feet

Visible Light

Longitudinal

Ultraviolet Light

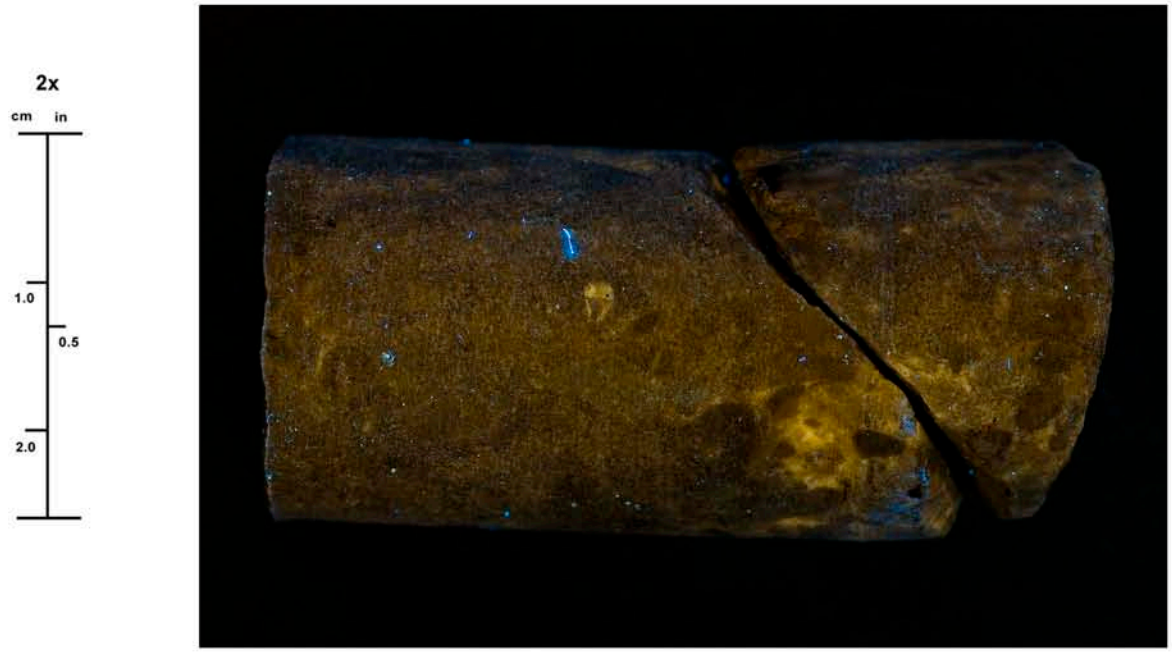

INTENTIONALLY BLANK

Weatherford LABORATORIES

HH-38266

Ohio Division of Geological Survey
CO2 No. 1 Well
Tuscarawas County, Ohio

Rotary Sidewall Core Photography

Sample No.: 1-51R

Visible Light — Depth: 7730.00 feet — Ultraviolet Light

Sample No.: 1-52R

Visible Light — Depth: 7742.00 feet — Ultraviolet Light

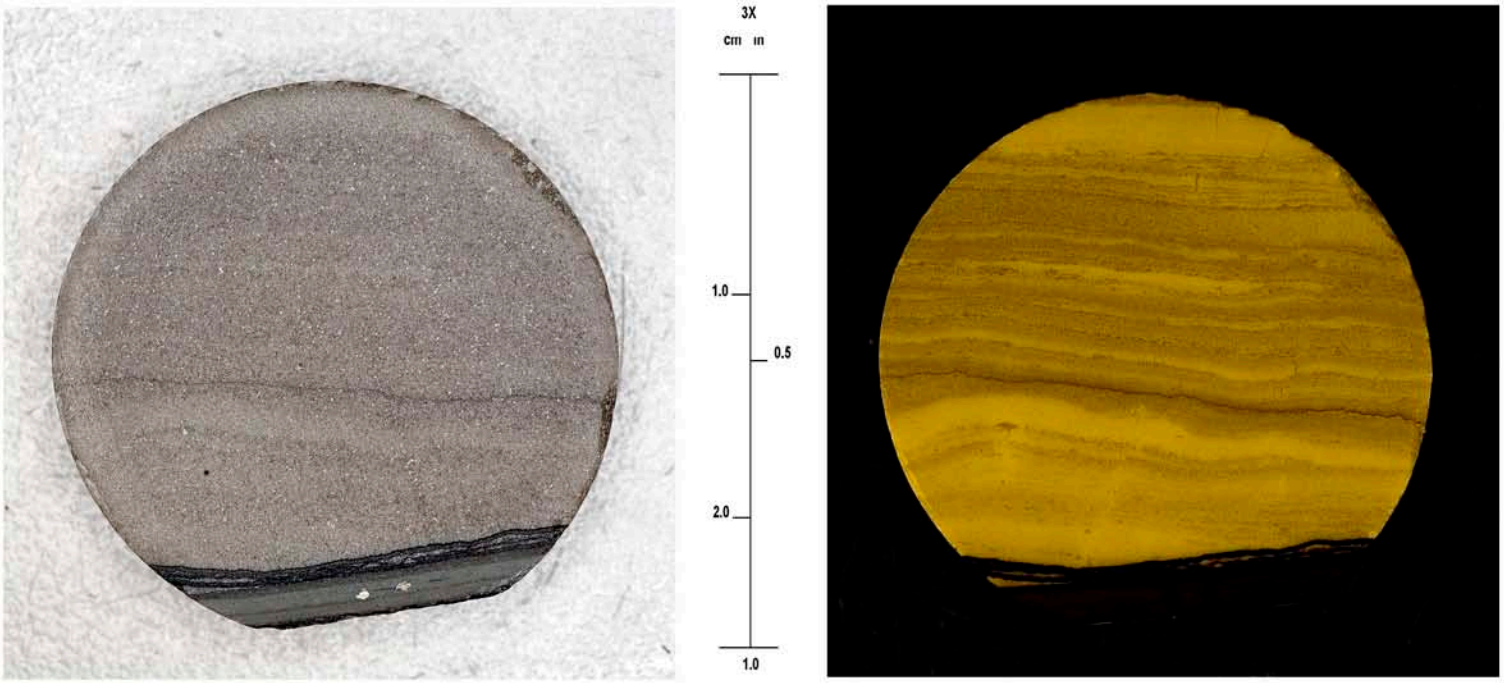

Weatherford LABORATORIES

HH-38266

Ohio Division of Geological Survey
CO2 No. 1 Well
Tuscarawas County, Ohio

Sample No.: 1-51R
Depth: 7730.00 feet

Visible Light

Longitudinal

Ultraviolet Light

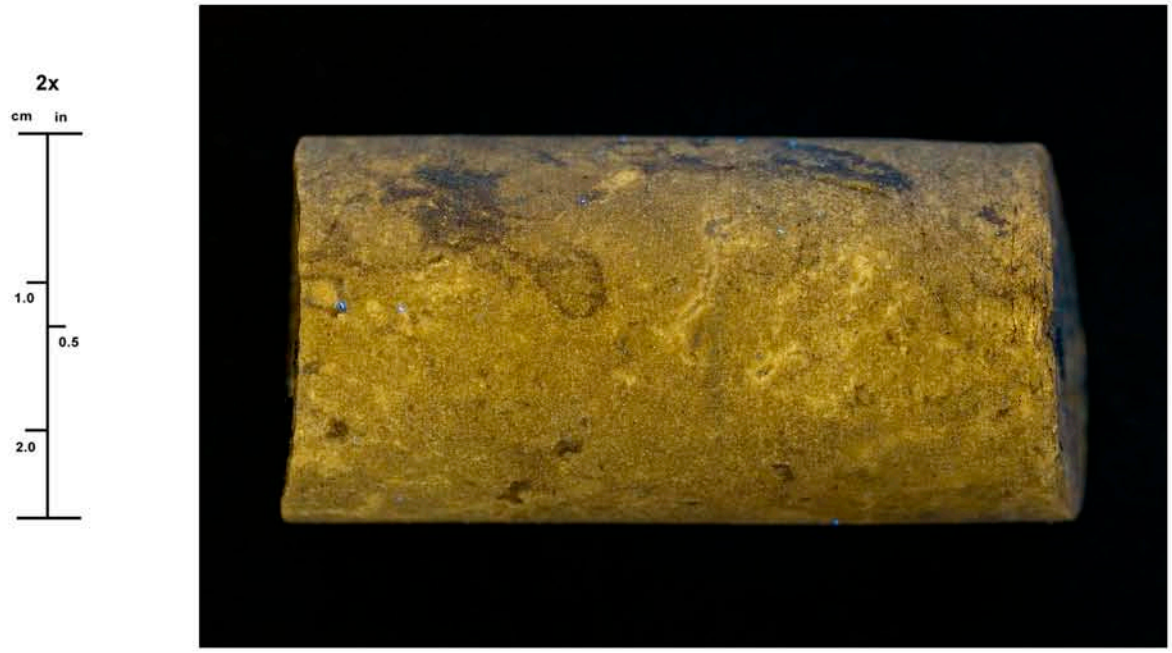

Weatherford LABORATORIES

HH-38266

Ohio Division of Geological Survey
CO2 No. 1 Well
Tuscarawas County, Ohio

Sample No.: 1-52R
Depth: 7742.00 feet

Visible Light

Longitudinal

Ultraviolet Light

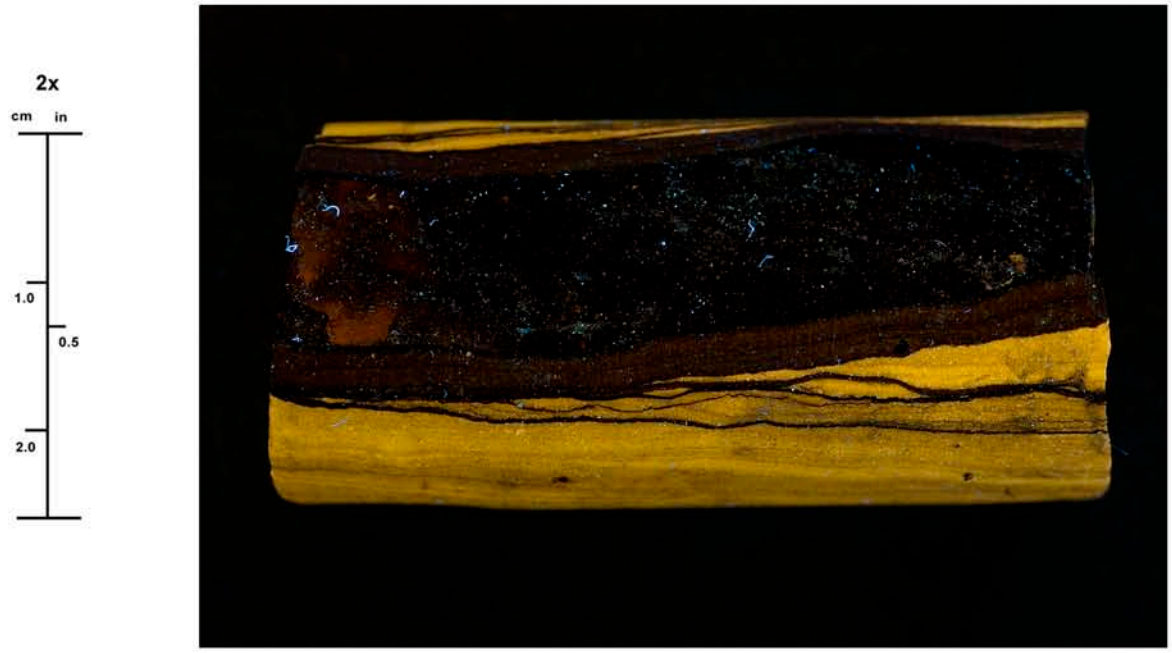

INTENTIONALLY BLANK

Weatherford LABORATORIES

HH-38266

Ohio Division of Geological Survey
CO2 No. 1 Well
Tuscarawas County, Ohio

Rotary Sidewall Core Photography

Sample No.: 1-53R

Visible Light | Depth: 7818.00 feet | Ultraviolet Light

Sample No.: 1-54R

Visible Light | Depth: 7868.00 feet | Ultraviolet Light

Weatherford LABORATORIES

HH-38266

Ohio Division of Geological Survey
CO2 No. 1 Well
Tuscarawas County, Ohio

Sample No.: 1-53R
Depth: 7818.00 feet

Visible Light

Longitudinal

Ultraviolet Light

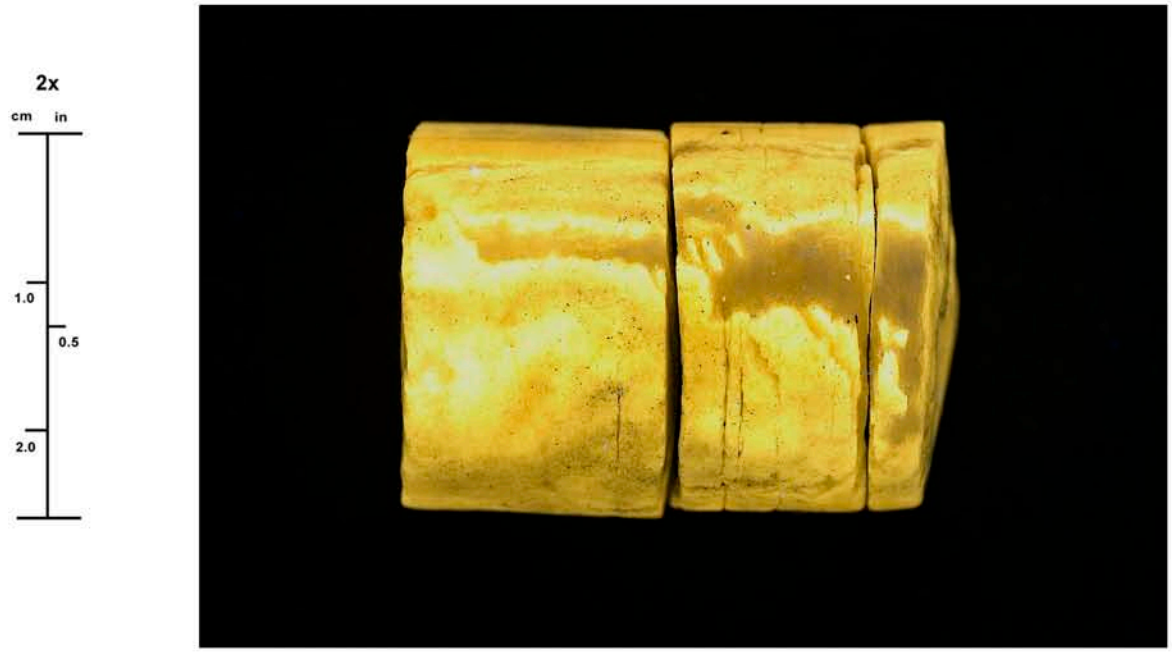

Weatherford LABORATORIES

HH-38266

Ohio Division of Geological Survey
CO2 No. 1 Well
Tuscarawas County, Ohio

Sample No.: 1-54R
Depth: 7868.00 feet

Visible Light

Longitudinal

Ultraviolet Light

INTENTIONALLY BLANK

Weatherford LABORATORIES

HH-38266

Ohio Division of Geological Survey
CO2 No. 1 Well
Tuscarawas County, Ohio

Rotary Sidewall Core Photography

Sample No.: 1-55R

Visible Light — Depth: 7931.00 feet — Ultraviolet Light

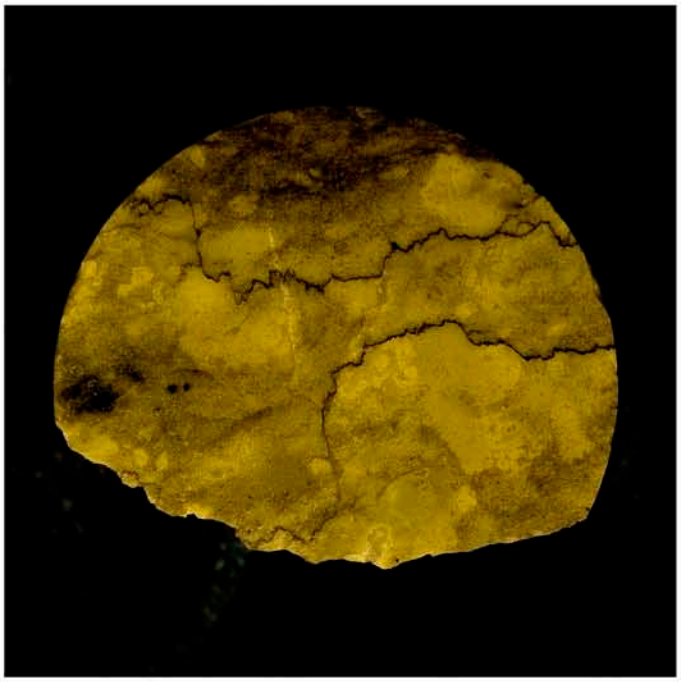

Sample No.: 1-56R

Visible Light — Depth: 7991.00 feet — Ultraviolet Light

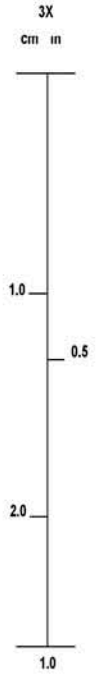

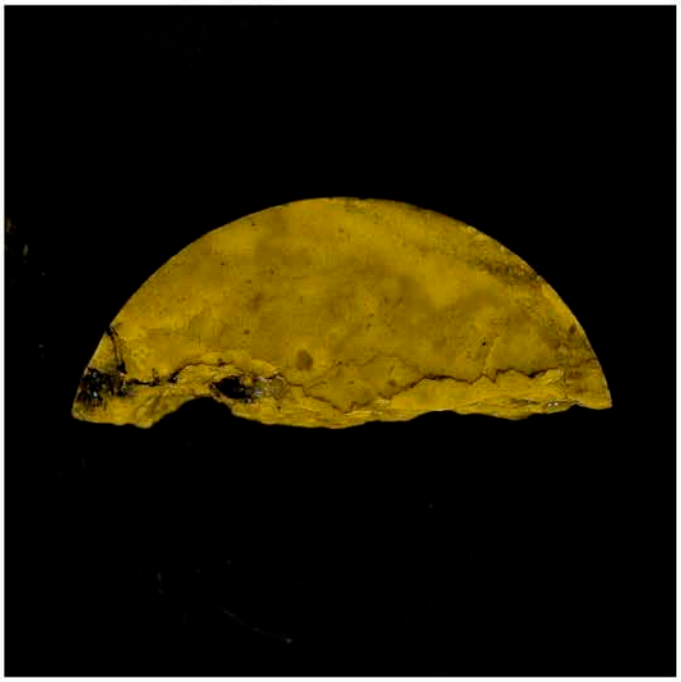

Weatherford LABORATORIES

HH-38266

Ohio Division of Geological Survey
CO2 No. 1 Well
Tuscarawas County, Ohio

Sample No.: 1-55R
Depth: 7931.00 feet

Visible Light

Longitudinal

Ultraviolet Light

Weatherford LABORATORIES

HH-38266

Ohio Division of Geological Survey
CO2 No. 1 Well
Tuscarawas County, Ohio

Sample No.: 1-56R
Depth: 7991.00 feet

Visible Light

Longitudinal

Ultraviolet Light

INTENTIONALLY BLANK

Weatherford LABORATORIES

HH-38266

Ohio Division of Geological Survey
CO2 No. 1 Well
Tuscarawas County, Ohio

Rotary Sidewall Core Photography

Sample No.: 1-57R

Visible Light — Depth: 8014.00 feet — Ultraviolet Light

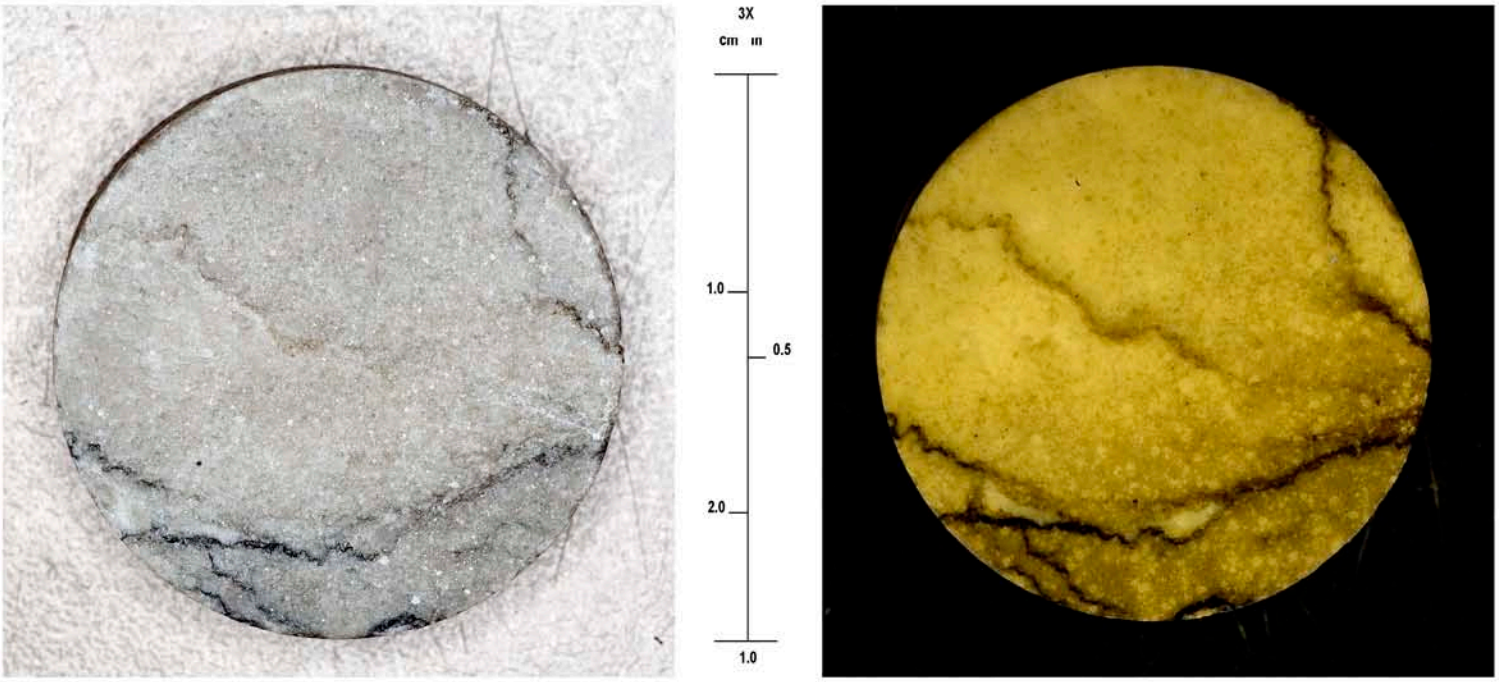

Sample No.: 1-58R

Visible Light — Depth: 8066.00 feet — Ultraviolet Light

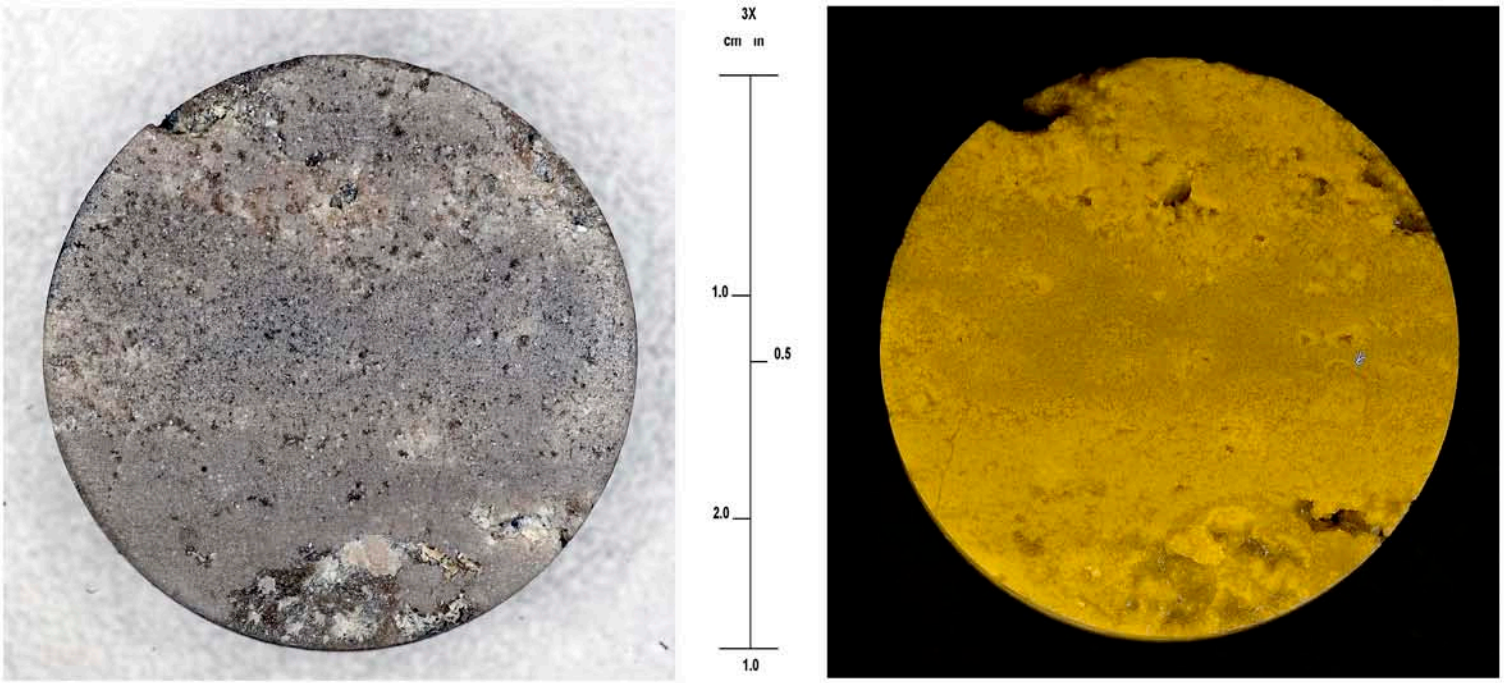

Weatherford LABORATORIES

HH-38266

Ohio Division of Geological Survey
CO2 No. 1 Well
Tuscarawas County, Ohio

Sample No.: 1-57R
Depth: 8014.00 feet

Visible Light

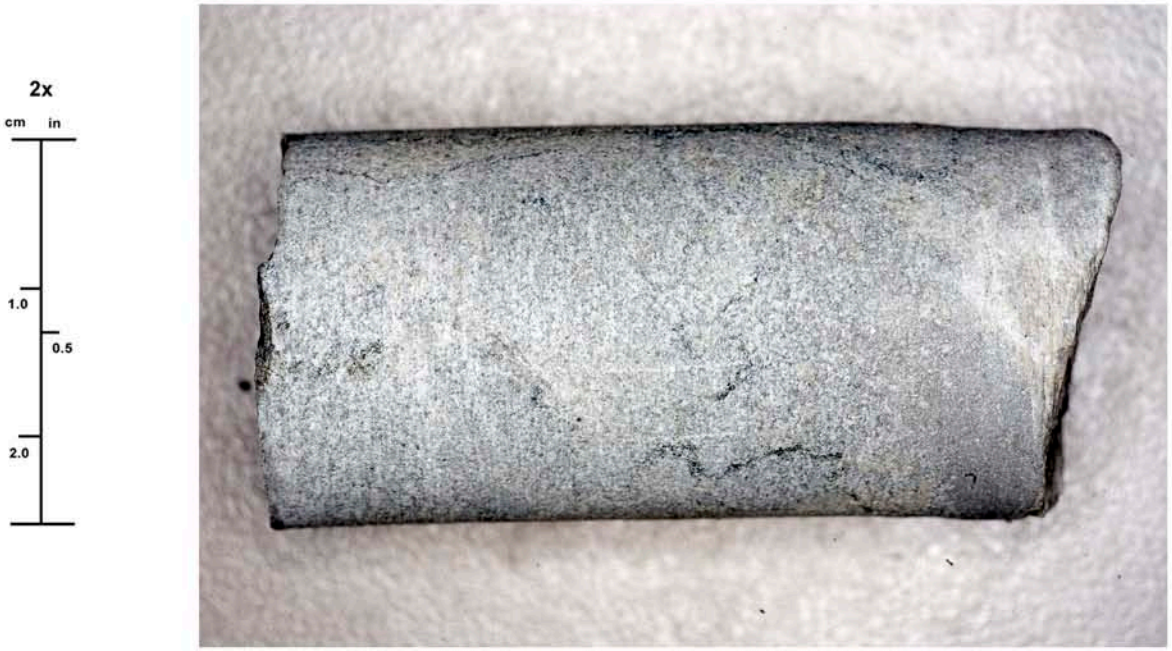

Longitudinal

Ultraviolet Light

Weatherford LABORATORIES

HH-38266

Ohio Division of Geological Survey
CO2 No. 1 Well
Tuscarawas County, Ohio

Sample No.: 1-58R
Depth: 8066.00 feet

Visible Light

Longitudinal

Ultraviolet Light

INTENTIONALLY BLANK

Weatherford LABORATORIES

HH-38266

Ohio Division of Geological Survey
CO2 No. 1 Well
Tuscarawas County, Ohio

Rotary Sidewall Core Photography

Sample No.: 1-59R

Visible Light — Depth: 8138.00 feet — Ultraviolet Light

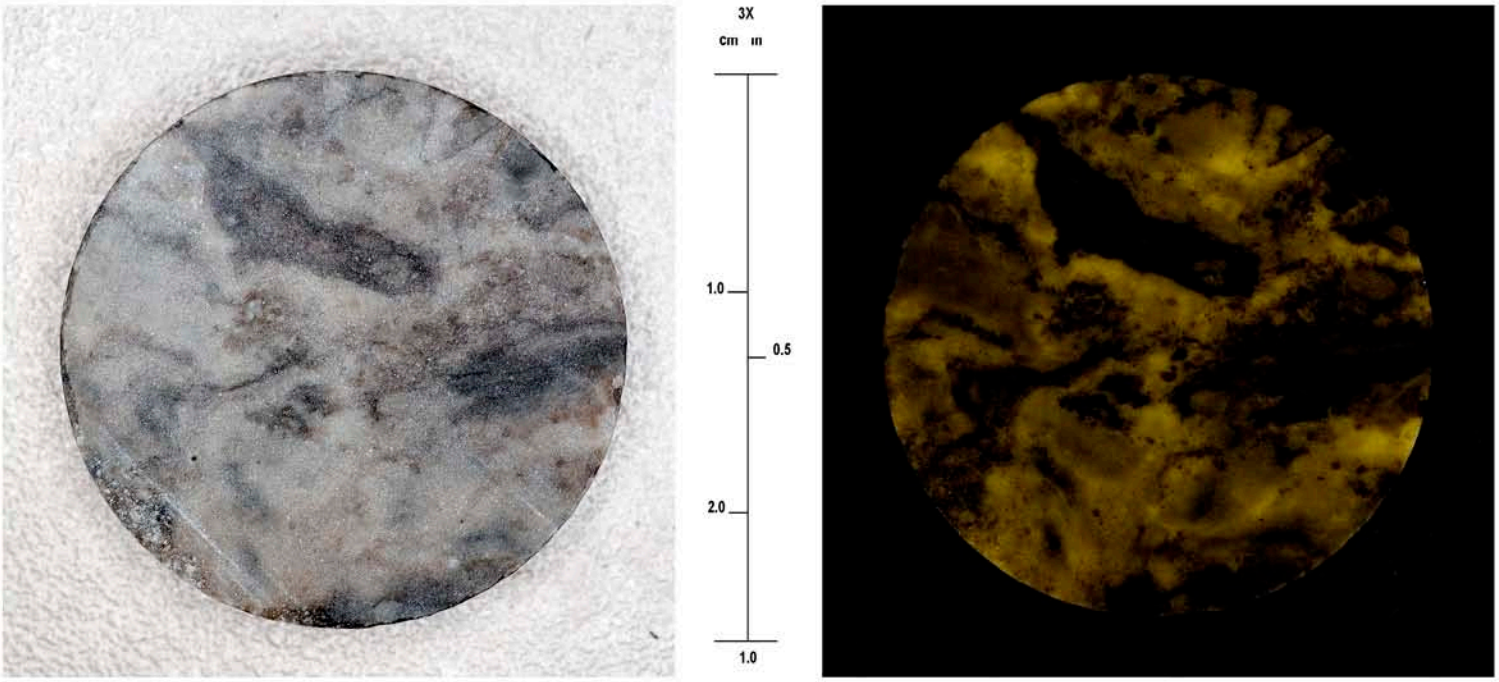

Sample No.: 1-60R

Visible Light — Depth: 8176.00 feet — Ultraviolet Light

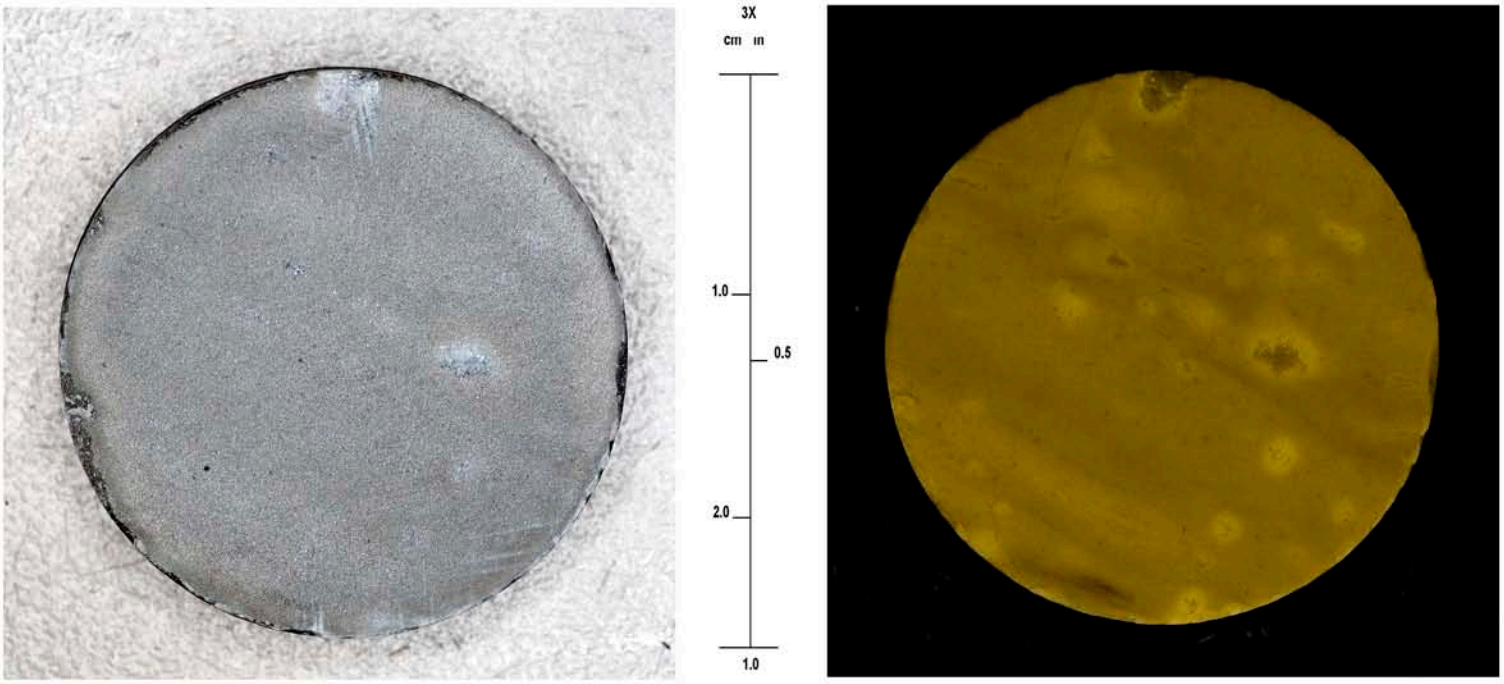

Weatherford LABORATORIES

HH-38266

Ohio Division of Geological Survey
CO2 No. 1 Well
Tuscarawas County, Ohio

Sample No.: 1-59R
Depth: 8138.00 feet

Visible Light

Longitudinal

Ultraviolet Light

Weatherford LABORATORIES

HH-38266

Ohio Division of Geological Survey
CO2 No. 1 Well
Tuscarawas County, Ohio

Sample No.: 1-60R
Depth: 8176.00 feet

Visible Light

Longitudinal

Ultraviolet Light

INTENTIONALLY BLANK

Weatherford LABORATORIES

HH-38266

Ohio Division of Geological Survey
CO2 No. 1 Well
Tuscarawas County, Ohio

Rotary Sidewall Core Photography

Sample No.: 1-61R

Visible Light — Depth: 8274.00 feet — Ultraviolet Light

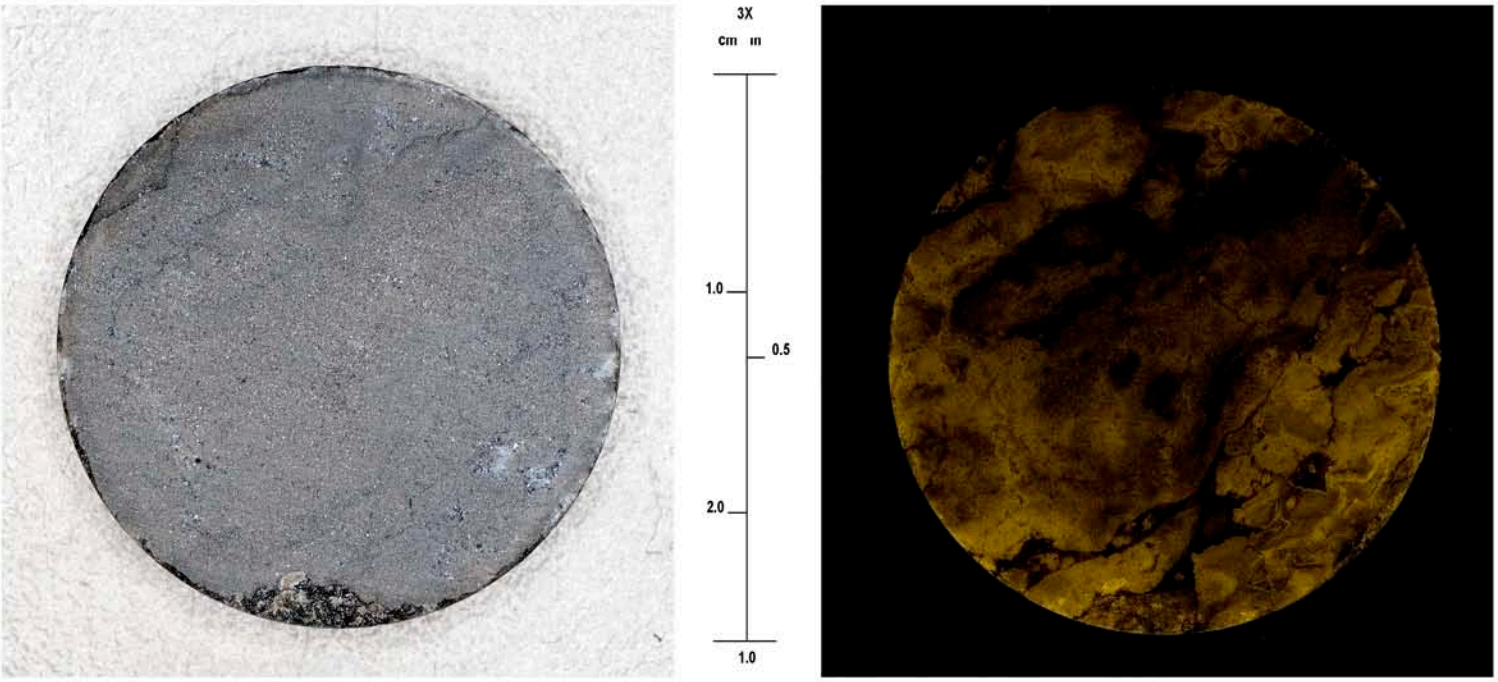

Sample No.: 1-62R

Visible Light — Depth: 8350.00 feet — Ultraviolet Light

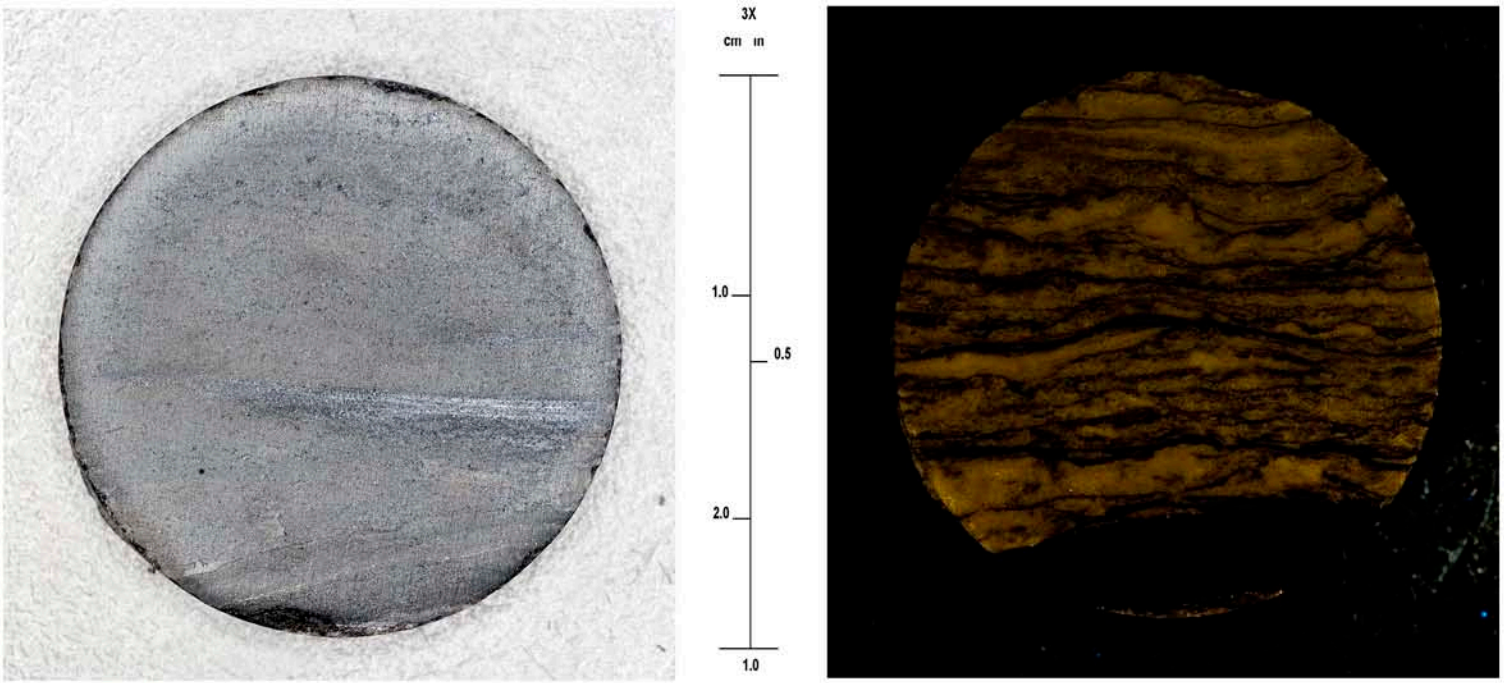

Weatherford LABORATORIES

HH-38266

Ohio Division of Geological Survey
CO2 No. 1 Well
Tuscarawas County, Ohio

Sample No.: 1-61R
Depth: 8274.00 feet

Visible Light

Longitudinal

Ultraviolet Light

Weatherford LABORATORIES

HH-38266

Ohio Division of Geological Survey
CO2 No. 1 Well
Tuscarawas County, Ohio

Sample No.: 1-62R
Depth: 8350.00 feet

Visible Light

Longitudinal

Ultraviolet Light

INTENTIONALLY BLANK

Weatherford LABORATORIES

HH-38266

Ohio Division of Geological Survey
CO2 No. 1 Well
Tuscarawas County, Ohio

Rotary Sidewall Core Photography

Sample No.: 1-63R

Visible Light — Depth: 8421.00 feet — Ultraviolet Light

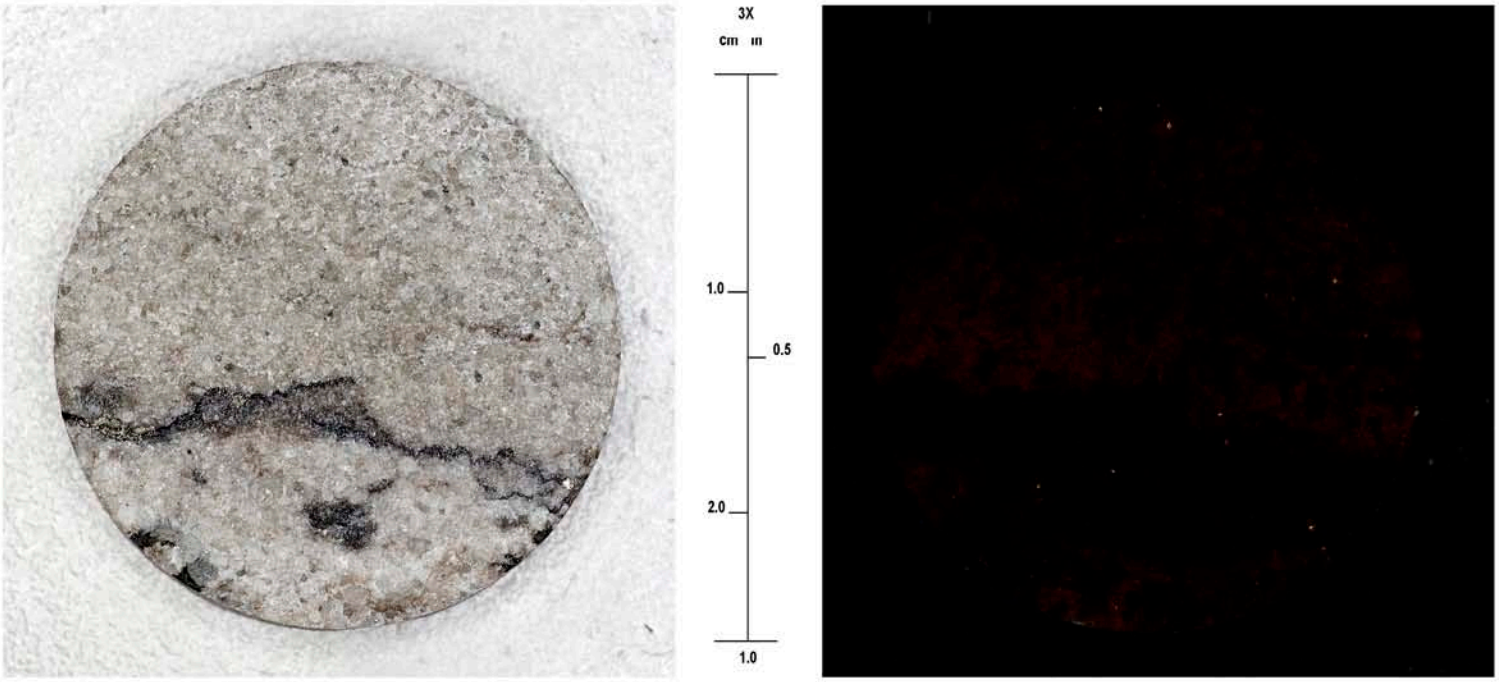

Sample No.: 1-64R

Visible Light — Depth: 8451.00 feet — Ultraviolet Light

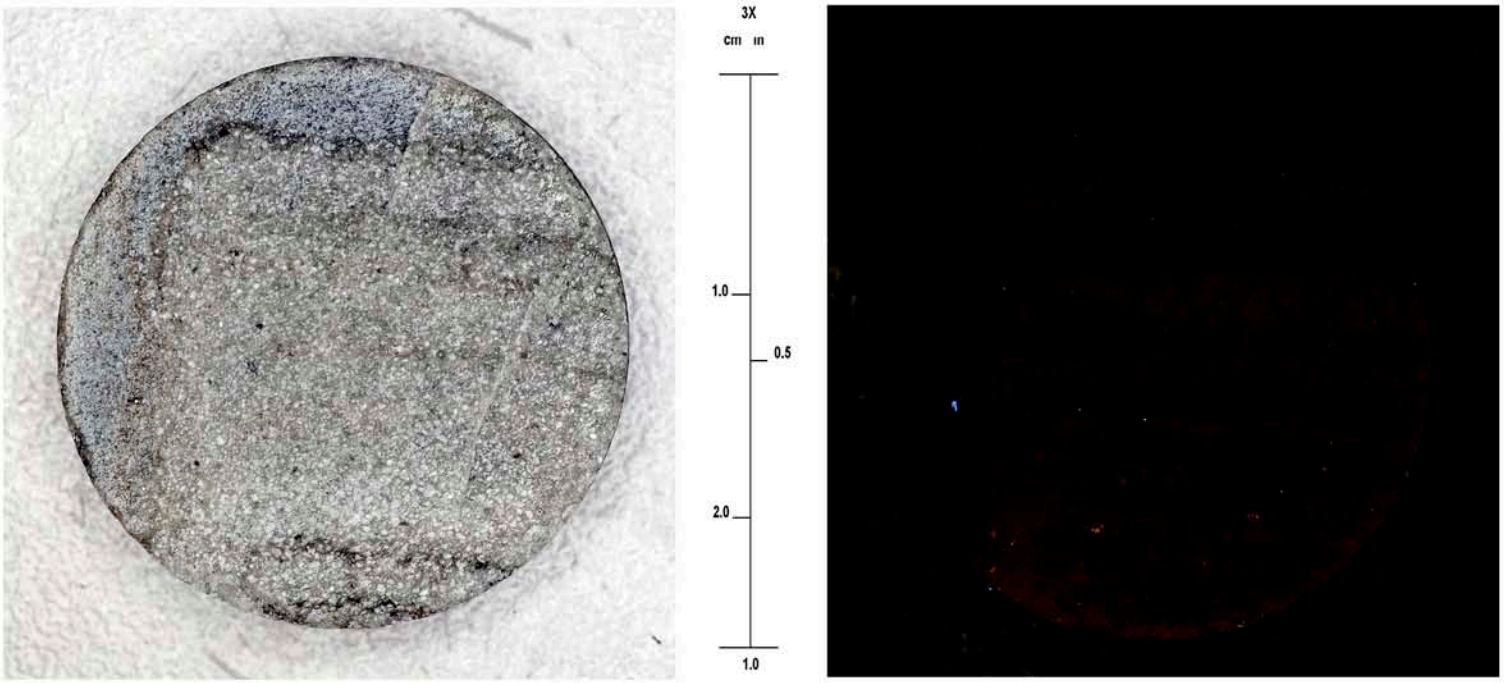

Weatherford LABORATORIES

HH-38266

Ohio Division of Geological Survey
CO2 No. 1 Well
Tuscarawas County, Ohio

Sample No.: 1-63R
Depth: 8421.00 feet

Visible Light

Longitudinal

Ultraviolet Light

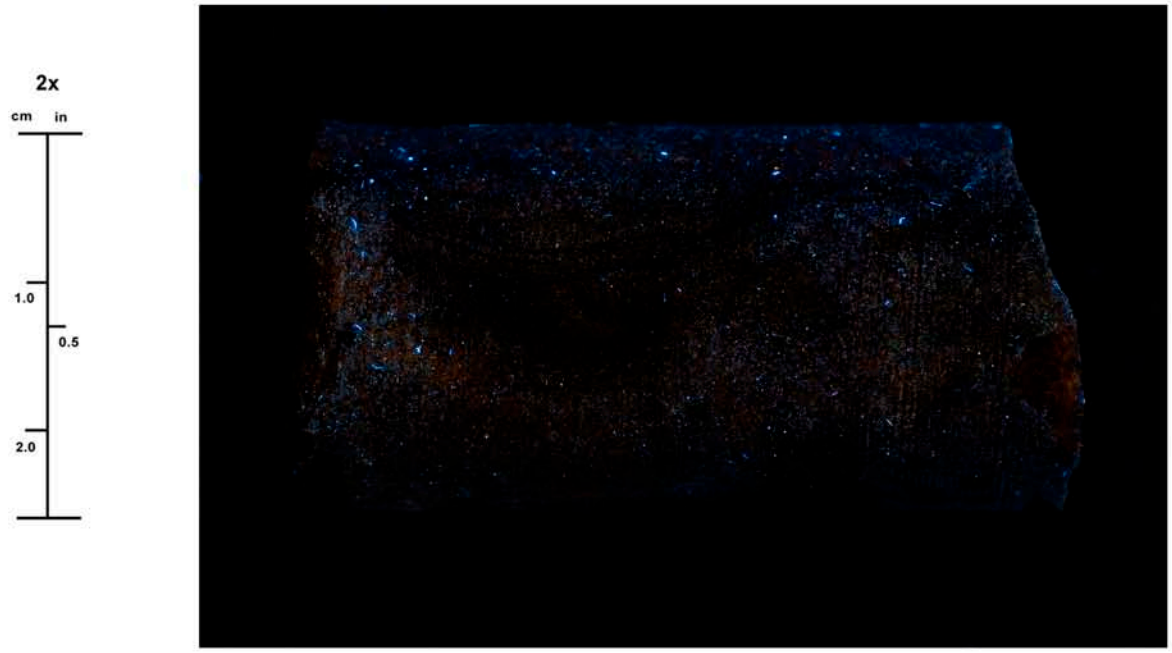

Weatherford LABORATORIES

HH-38266

Ohio Division of Geological Survey
CO2 No. 1 Well
Tuscarawas County, Ohio

Sample No.: 1-64R
Depth: 8451.00 feet

Visible Light

Longitudinal

Ultraviolet Light

INTENTIONALLY BLANK

Weatherford LABORATORIES

HH-38266

Ohio Division of Geological Survey
CO2 No. 1 Well
Tuscarawas County, Ohio

Rotary Sidewall Core Photography

Sample No.: 1-65R

Visible Light — Depth: 8467.00 feet — Ultraviolet Light

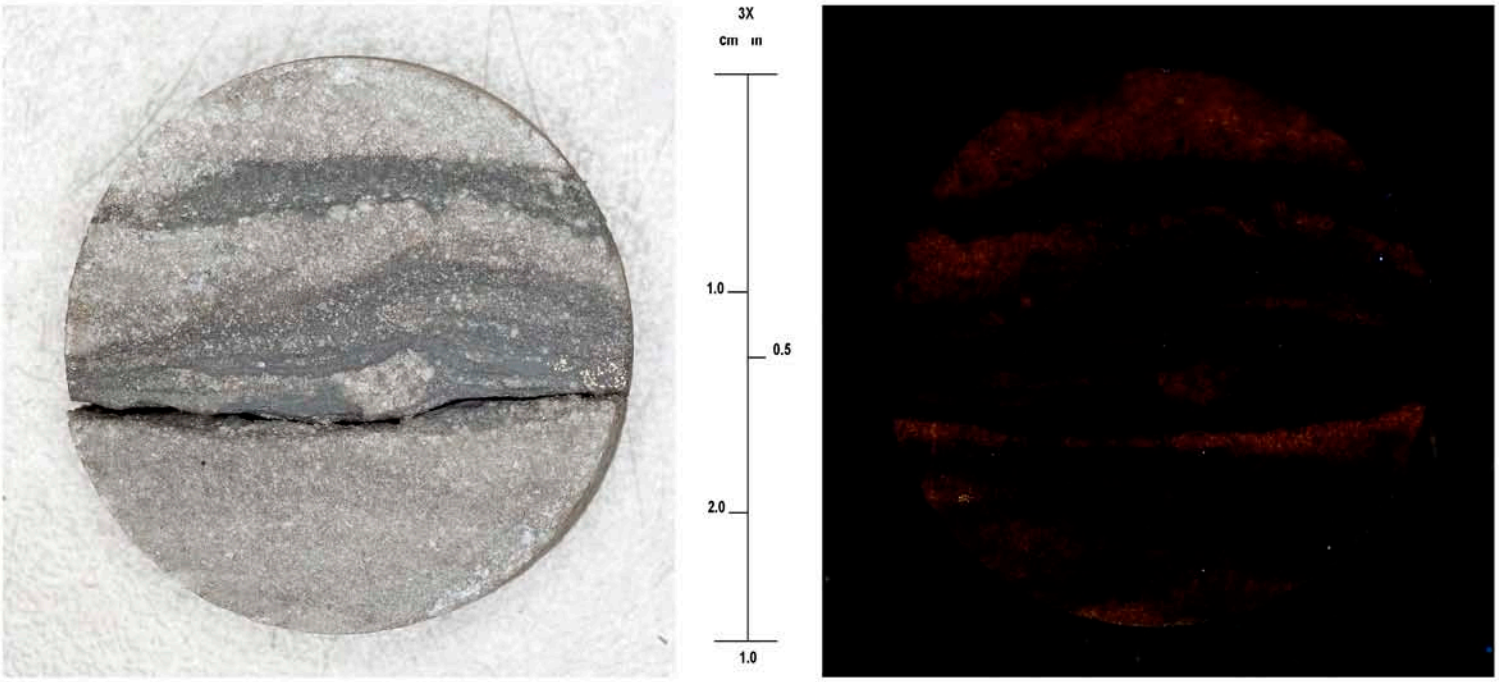

Sample No.: 1-66R

Visible Light — Depth: 8495.00 feet — Ultraviolet Light

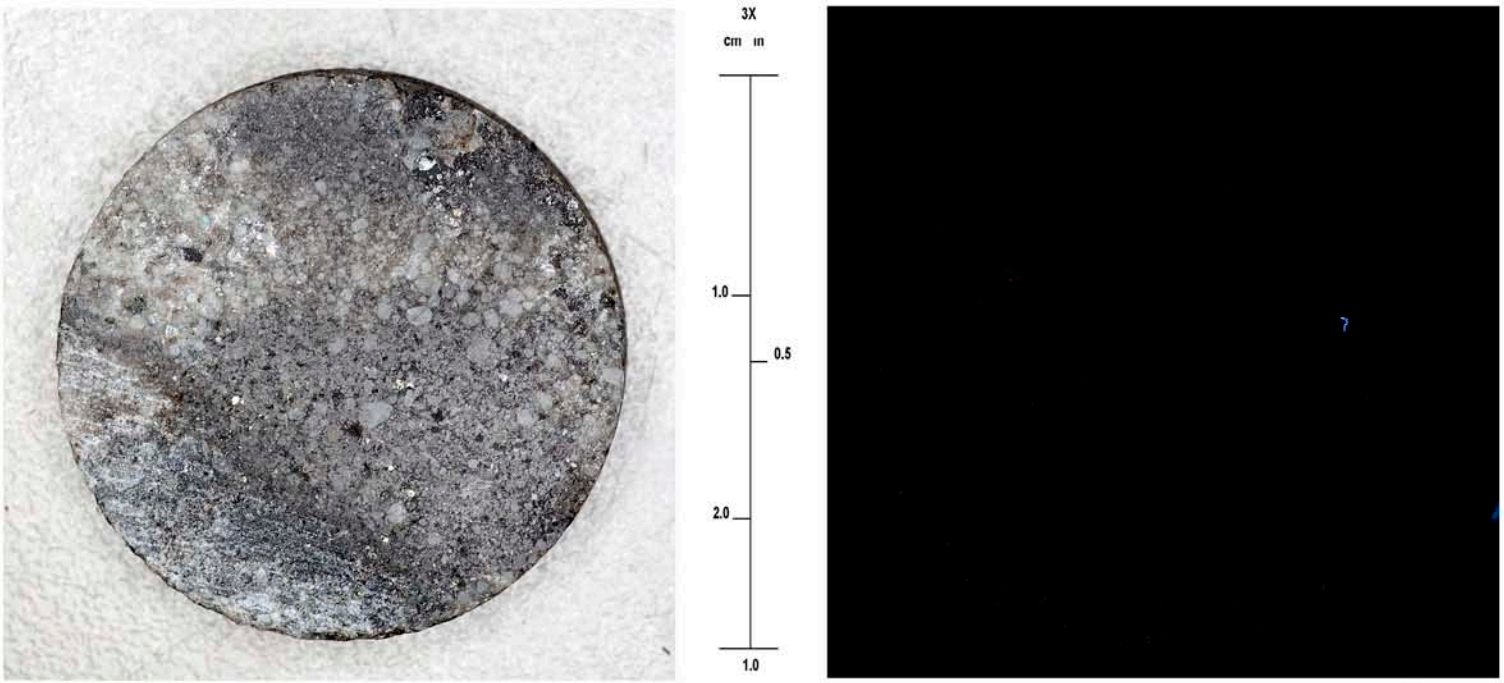

Weatherford LABORATORIES

HH-38266

Ohio Division of Geological Survey
CO2 No. 1 Well
Tuscarawas County, Ohio

Sample No.: 1-65R
Depth: 8467.00 feet

Visible Light

Longitudinal

Ultraviolet Light

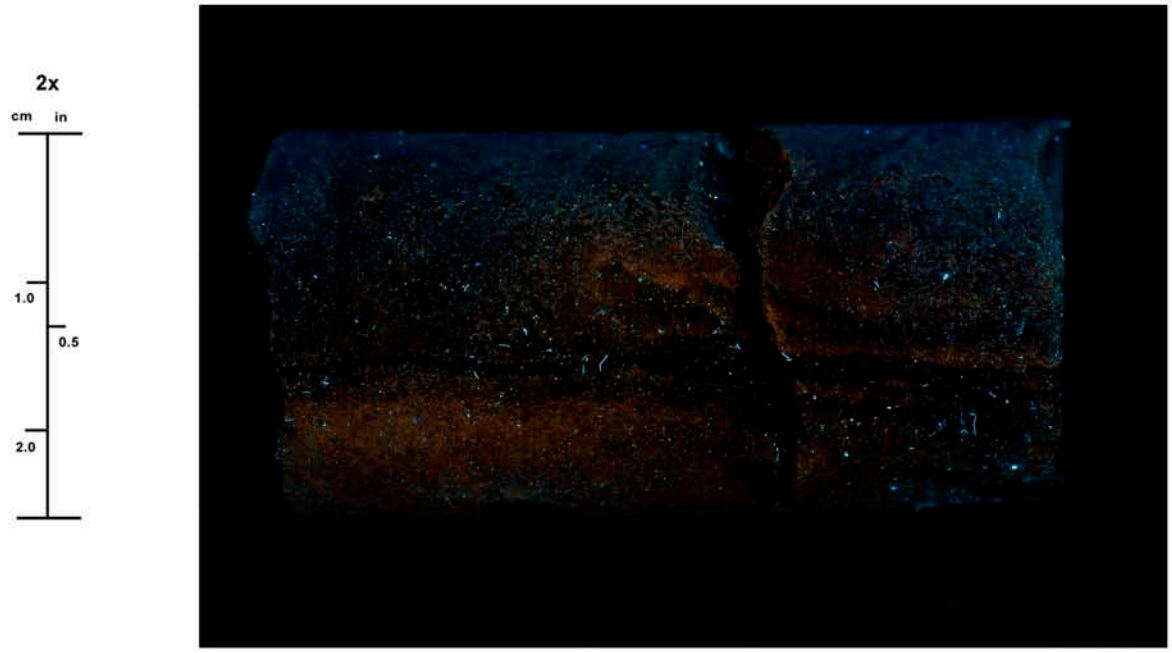

Weatherford LABORATORIES

HH-38266

Ohio Division of Geological Survey
CO2 No. 1 Well
Tuscarawas County, Ohio

Sample No.: 1-66R
Depth: 8495.00 feet

Visible Light

Longitudinal

Ultraviolet Light

INTENTIONALLY BLANK

Weatherford LABORATORIES

HH-38266

Ohio Division of Geological Survey
CO2 No. 1 Well
Tuscarawas County, Ohio

Rotary Sidewall Core Photography

Sample No.: 1-67R

Visible Light — Depth: 8528.00 feet — Ultraviolet Light

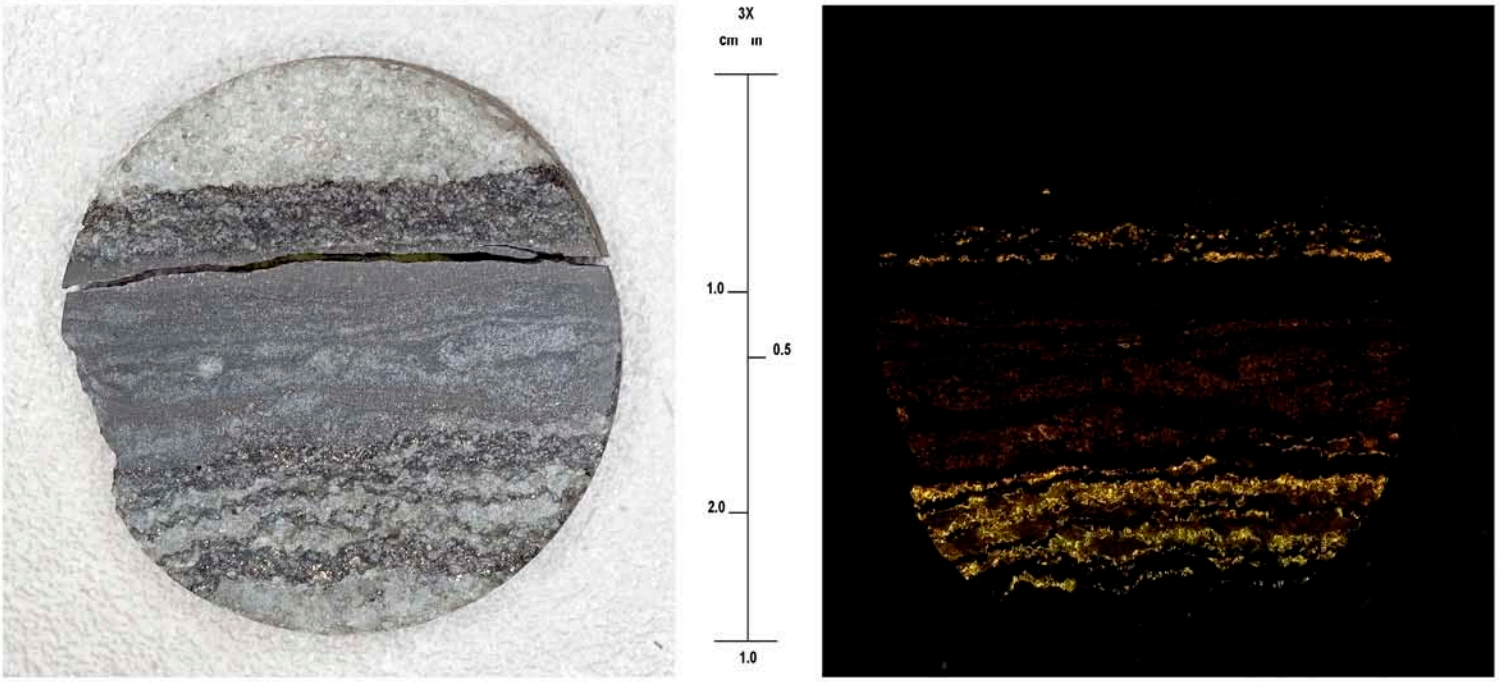

Sample No.: 1-68R

Visible Light — Depth: 8538.00 feet — Ultraviolet Light

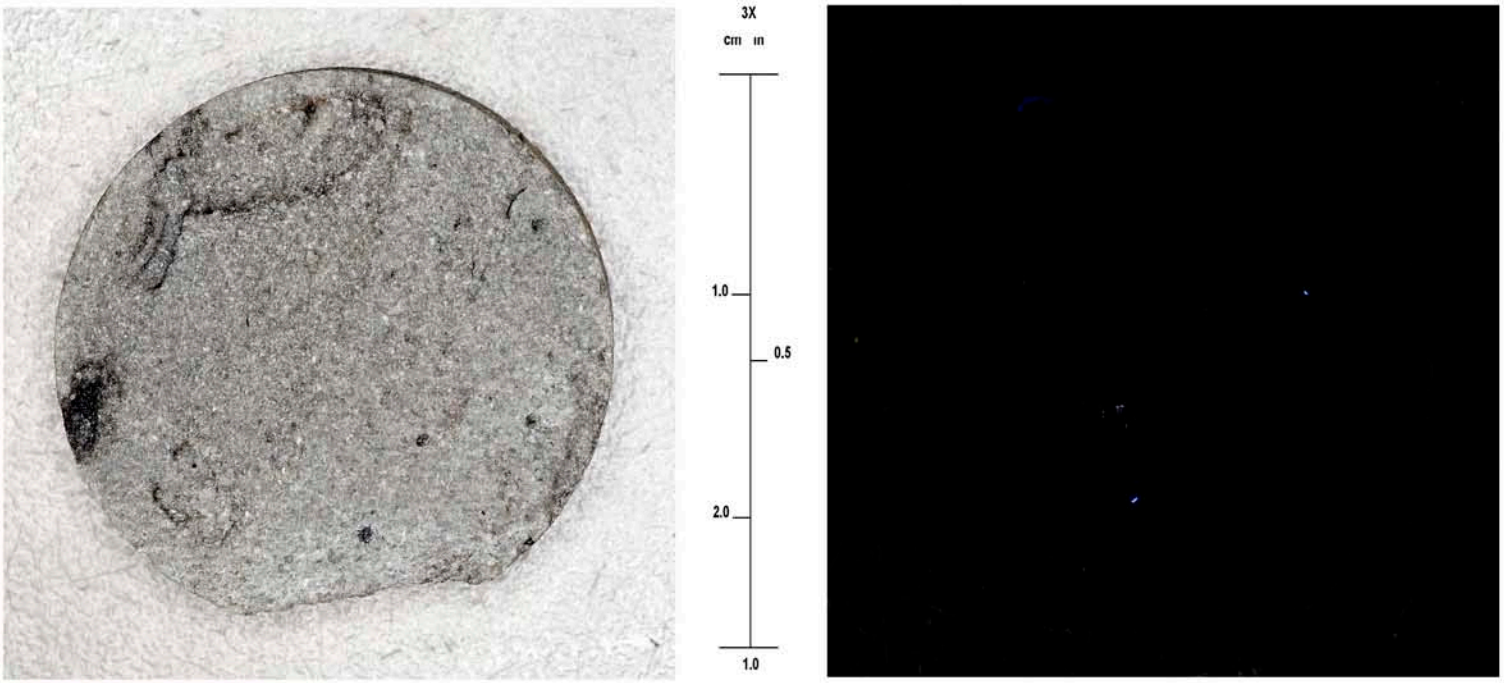

Weatherford LABORATORIES

HH-38266

Ohio Division of Geological Survey
CO2 No. 1 Well
Tuscarawas County, Ohio

Sample No.: 1-67R
Depth: 8528.00 feet

Visible Light

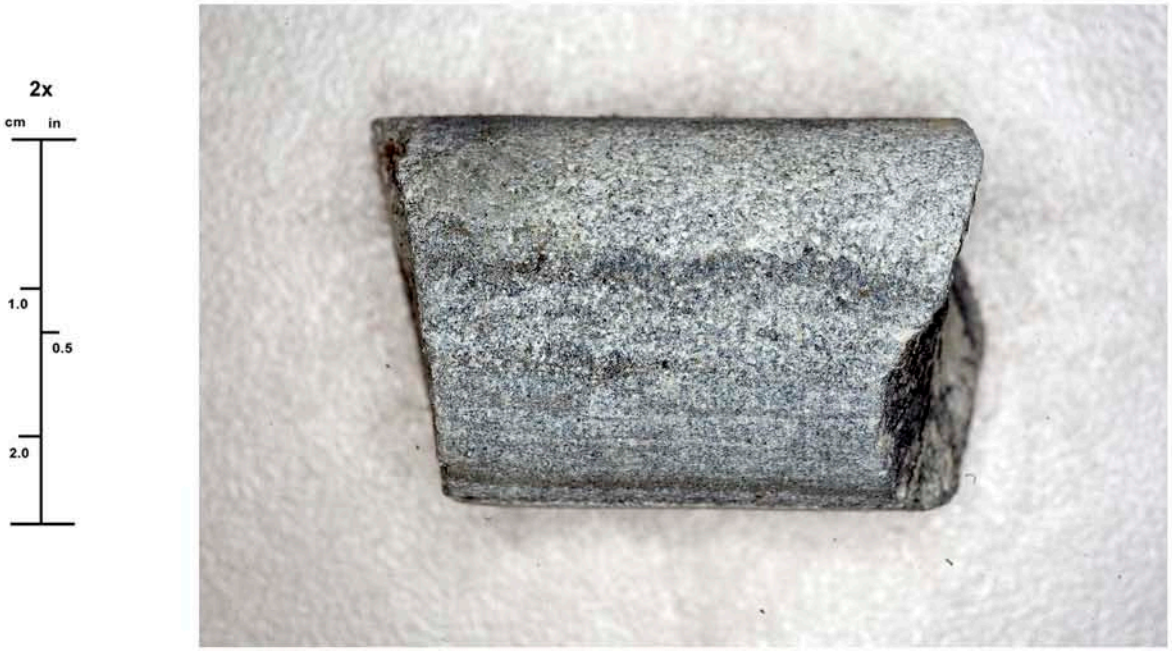

Longitudinal

Ultraviolet Light

Weatherford LABORATORIES

HH-38266

Ohio Division of Geological Survey
CO2 No. 1 Well
Tuscarawas County, Ohio

Sample No.: 1-68R
Depth: 8538.00 feet

Visible Light

Longitudinal

Ultraviolet Light

INTENTIONALLY BLANK

Weatherford LABORATORIES

HH-38266

Ohio Division of Geological Survey
CO2 No. 1 Well
Tuscarawas County, Ohio

Rotary Sidewall Core Photography

Sample No.: 1-69R

Visible Light — Depth: 8544.00 feet — Ultraviolet Light

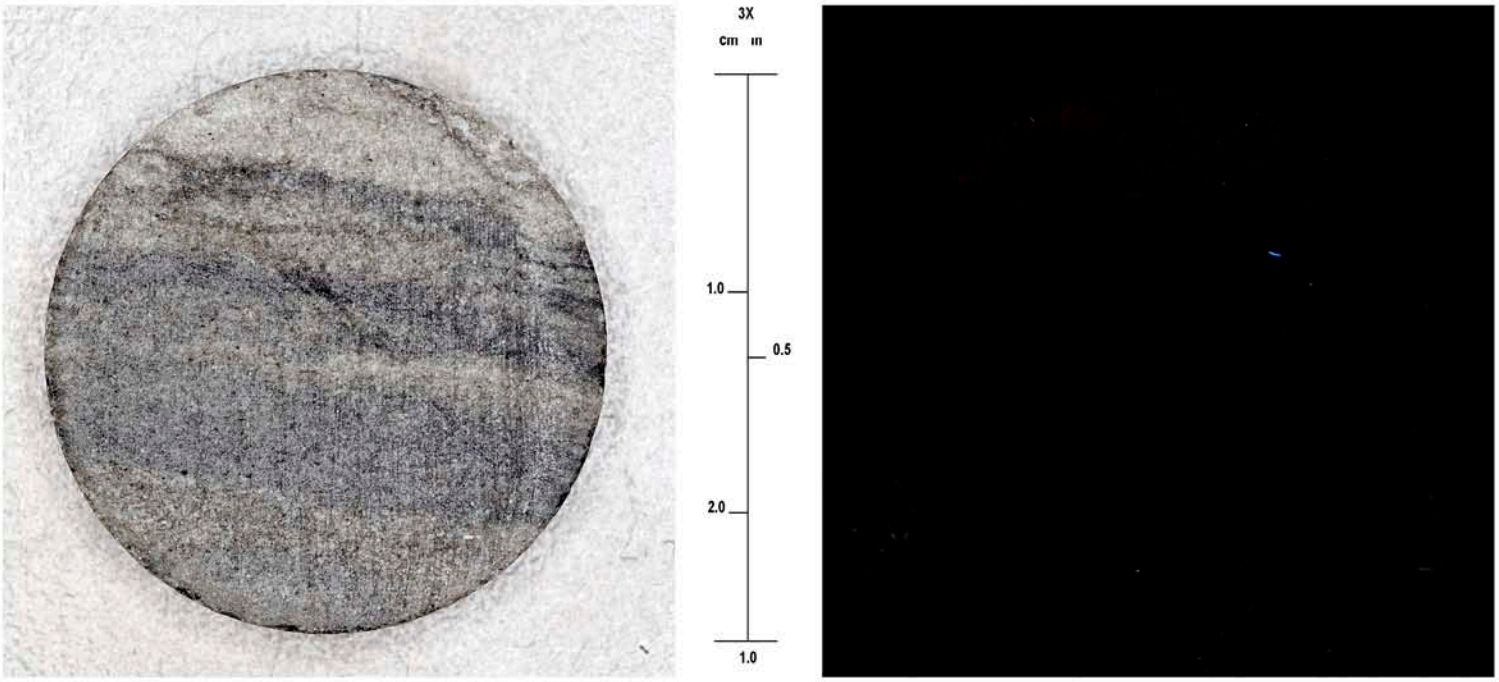

Sample No.: 1-70R

Visible Light — Depth: 8549.00 feet — Ultraviolet Light

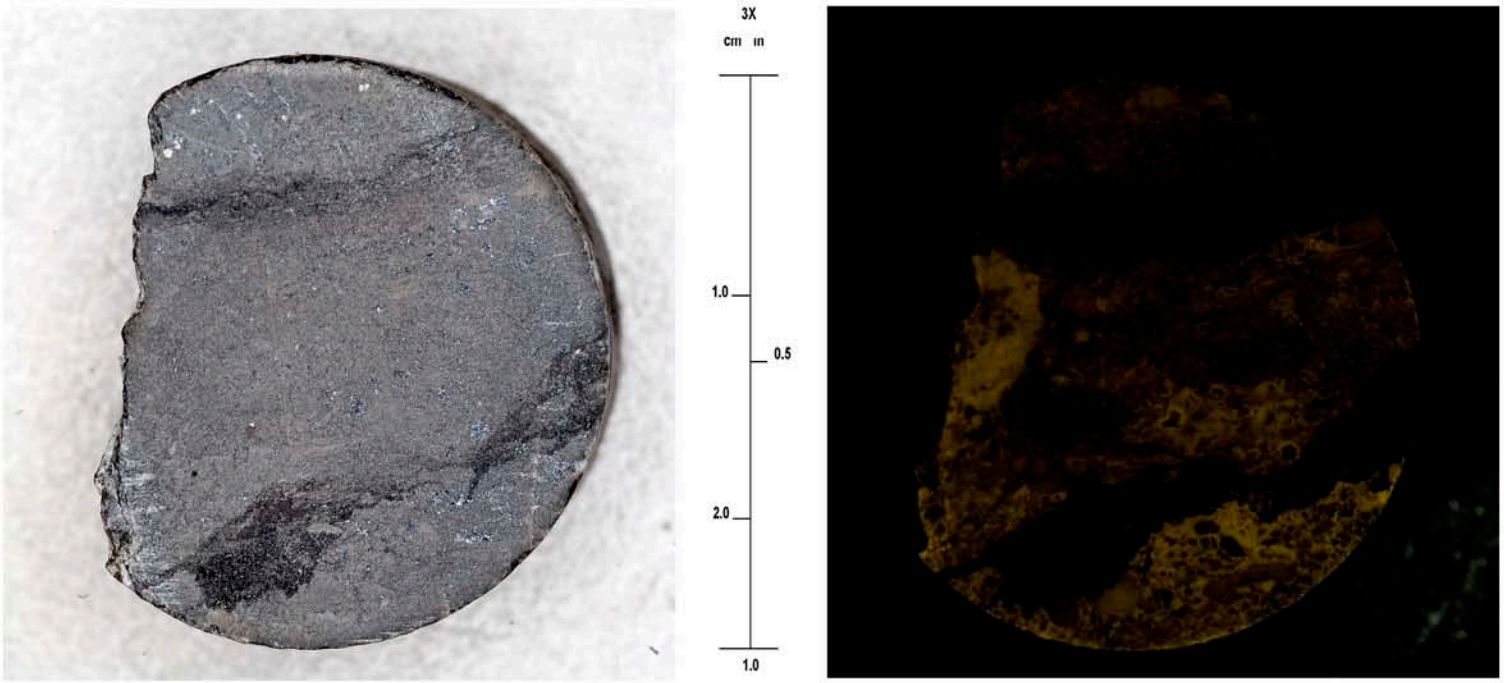

Weatherford LABORATORIES

HH-38266

Ohio Division of Geological Survey
CO2 No. 1 Well
Tuscarawas County, Ohio

Sample No.: 1-69R
Depth: 8544.00 feet

Visible Light

Longitudinal

Ultraviolet Light

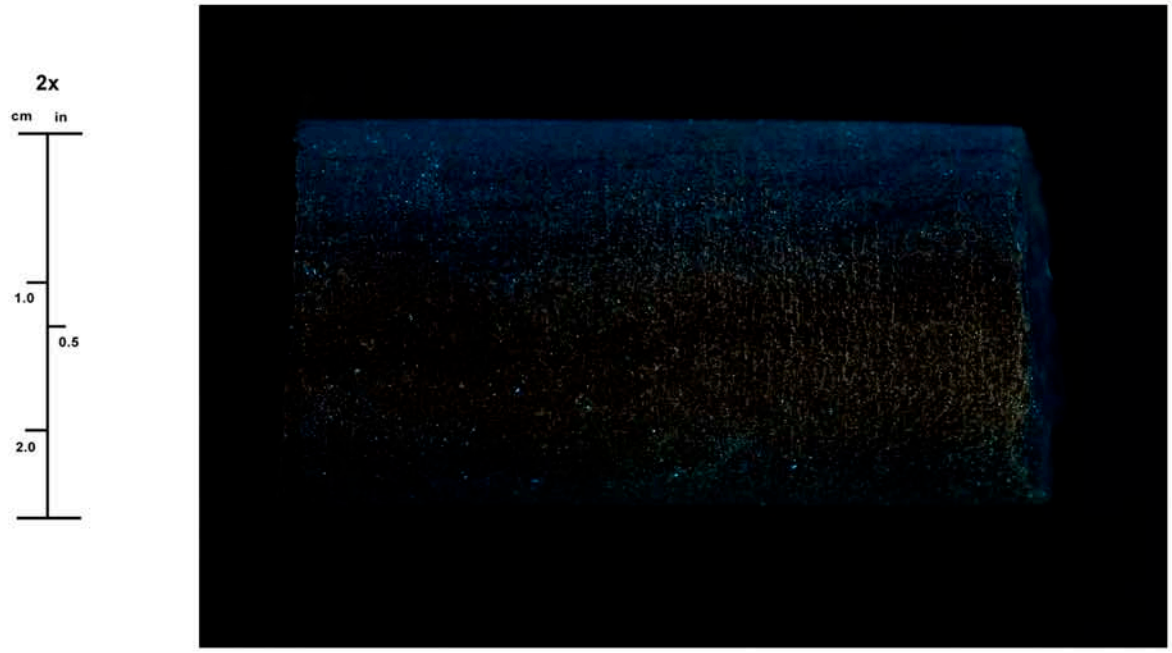

Weatherford LABORATORIES

HH-38266

Ohio Division of Geological Survey
CO2 No. 1 Well
Tuscarawas County, Ohio

Sample No.: 1-70R
Depth: 8549.00 feet

Visible Light

Longitudinal

Ultraviolet Light

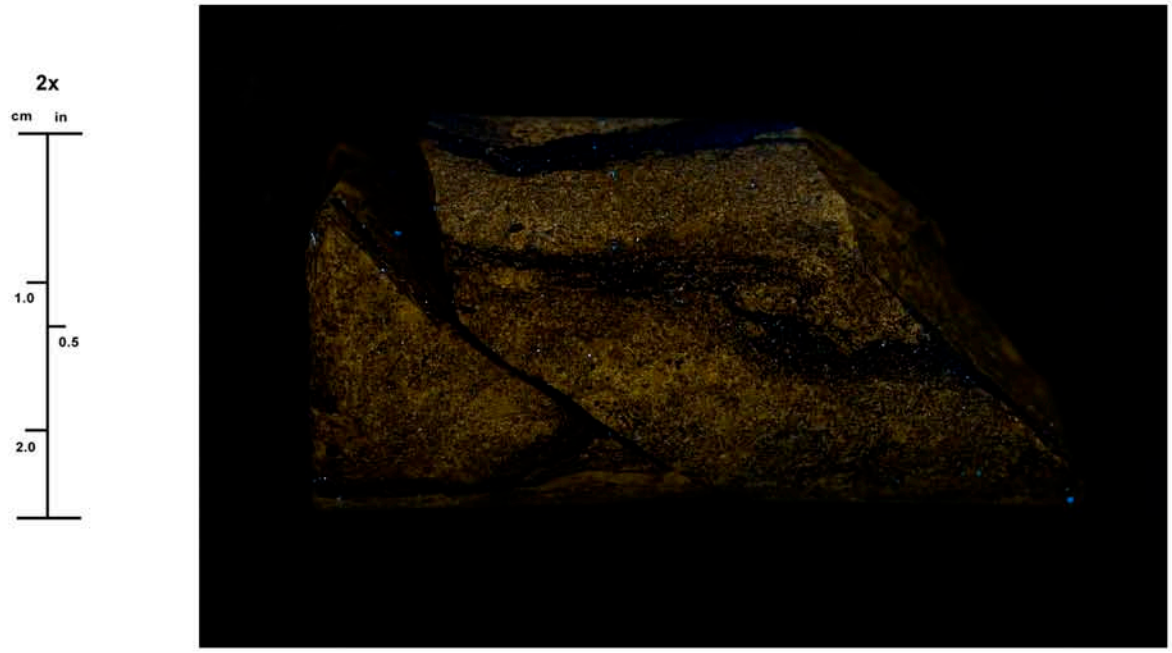

INTENTIONALLY BLANK

Weatherford LABORATORIES

HH-38266

Ohio Division of Geological Survey
CO2 No. 1 Well
Tuscarawas County, Ohio

Rotary Sidewall Core Photography

Sample No.: 1-71R

Visible Light — Depth: 8555.00 feet — Ultraviolet Light

Sample No.: 1-72R

Visible Light — Depth: 8561.00 feet — Ultraviolet Light

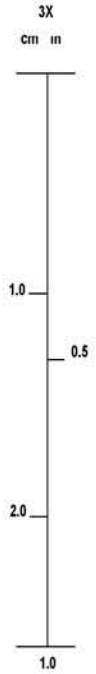

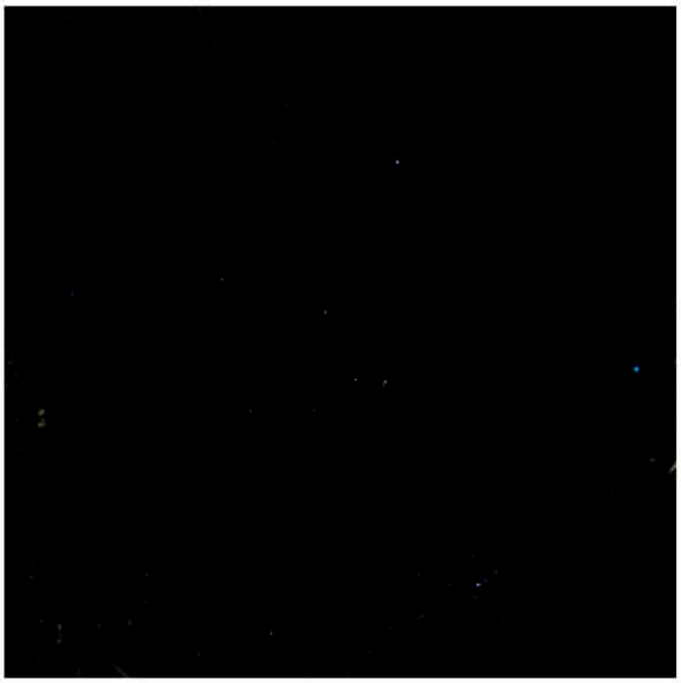

Weatherford LABORATORIES

HH-38266

Ohio Division of Geological Survey
CO2 No. 1 Well
Tuscarawas County, Ohio

Sample No.: 1-71R
Depth: 8555.00 feet

Visible Light

Longitudinal

Ultraviolet Light

Weatherford LABORATORIES

HH-38266

Ohio Division of Geological Survey
CO2 No. 1 Well
Tuscarawas County, Ohio

Sample No.: 1-72R
Depth: 8561.00 feet

Visible Light

Longitudinal

Ultraviolet Light

INTENTIONALLY BLANK

Weatherford LABORATORIES

HH-38266

Ohio Division of Geological Survey
CO2 No. 1 Well
Tuscarawas County, Ohio

Rotary Sidewall Core Photography

Sample No.: 1-73R

Visible Light — Depth: 8570.00 feet — Ultraviolet Light

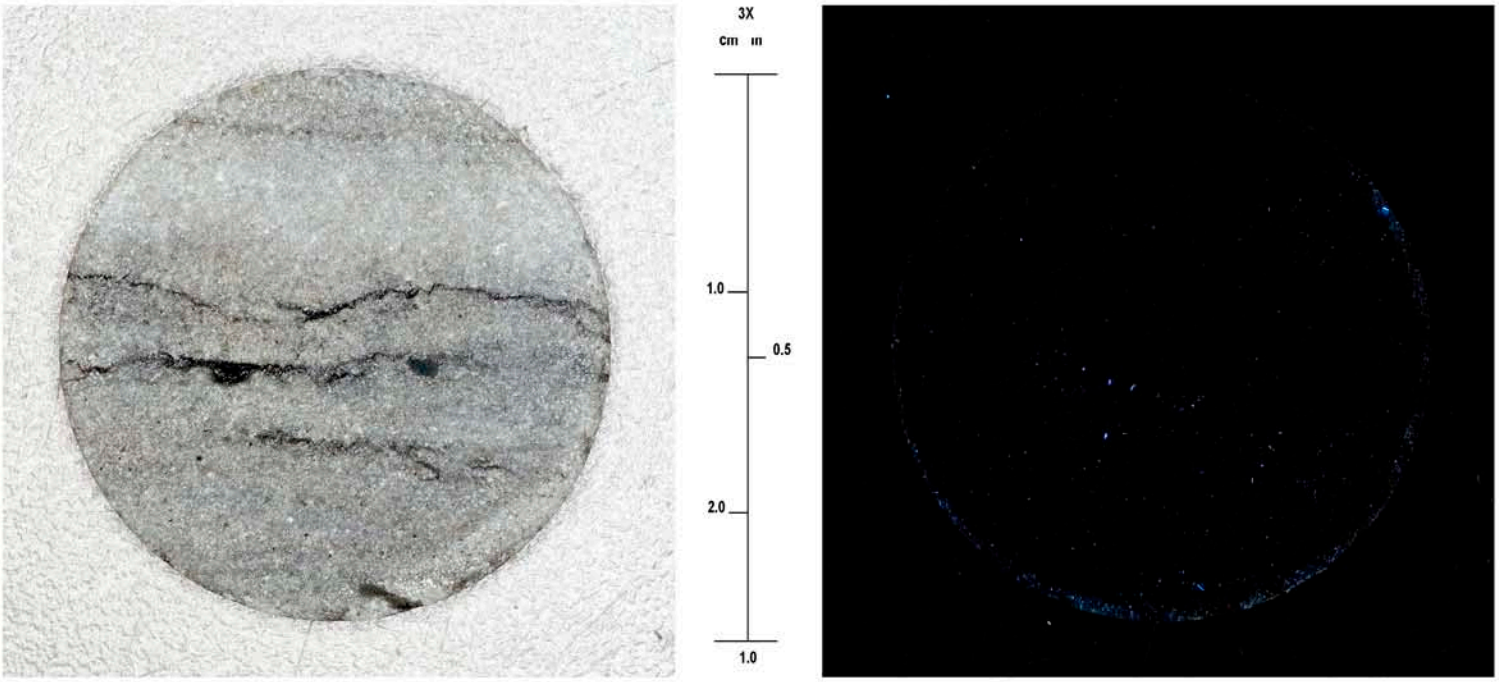

Sample No.: 1-74R

Visible Light — Depth: 8583.00 feet — Ultraviolet Light

Weatherford LABORATORIES

HH-38266

Ohio Division of Geological Survey
CO2 No. 1 Well
Tuscarawas County, Ohio

Sample No.: 1-73R
Depth: 8570.00 feet

Visible Light

Longitudinal

Ultraviolet Light

Weatherford LABORATORIES

HH-38266

Ohio Division of Geological Survey
CO2 No. 1 Well
Tuscarawas County, Ohio

Sample No.: 1-74R
Depth: 8583.00 feet

Visible Light

Longitudinal

Ultraviolet Light

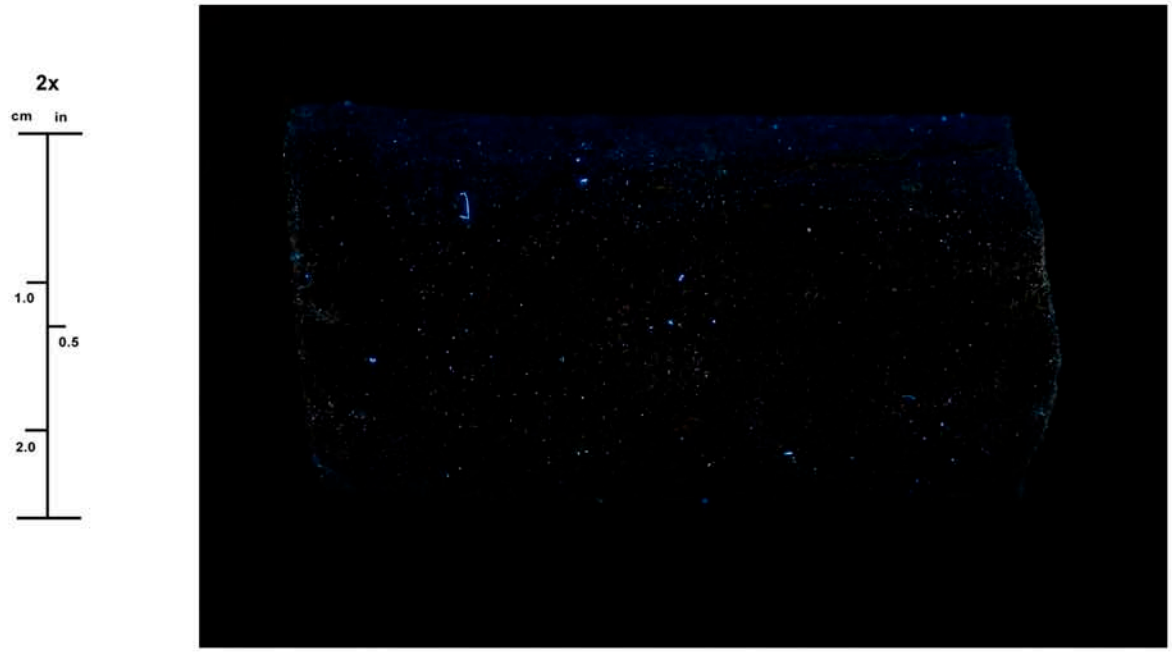

INTENTIONALLY BLANK

Weatherford LABORATORIES

HH-38266

Ohio Division of Geological Survey
CO2 No. 1 Well
Tuscarawas County, Ohio

Rotary Sidewall Core Photography

Sample No.: 1-75R

Visible Light — Depth: 8585.00 feet — Ultraviolet Light

Sample No.: 1-76R

Visible Light — Depth: 8590.00 feet — Ultraviolet Light

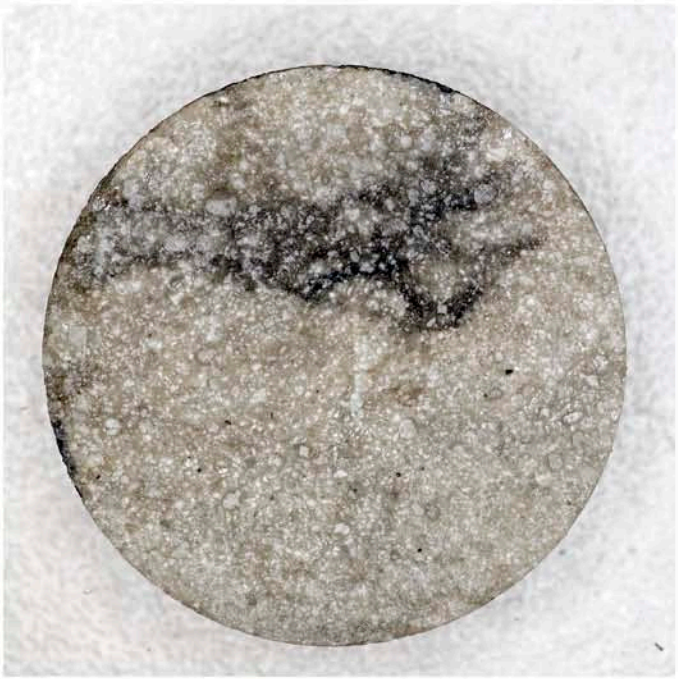

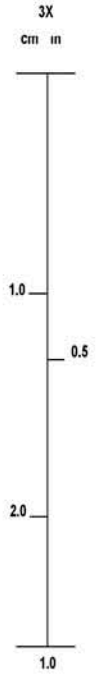

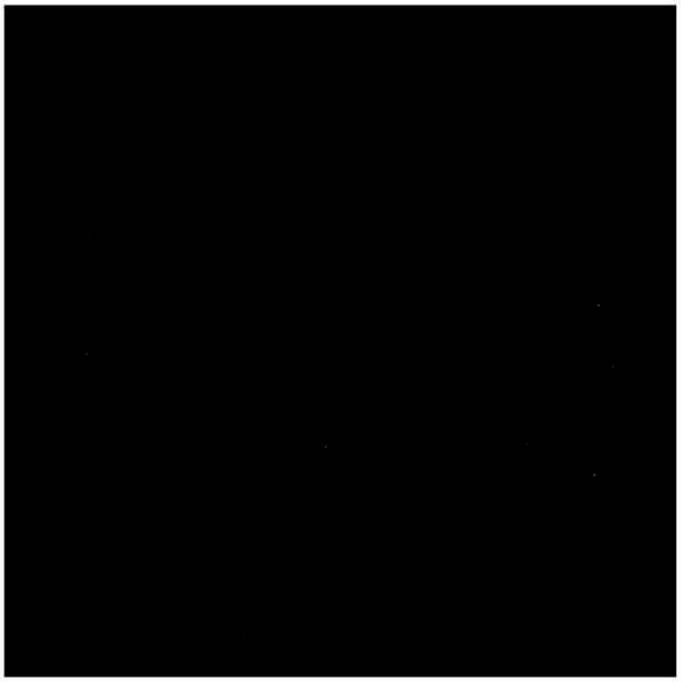

Weatherford LABORATORIES

HH-38266

Ohio Division of Geological Survey
CO2 No. 1 Well
Tuscarawas County, Ohio

Sample No.: 1-75R
Depth: 8585.00 feet

Visible Light

Longitudinal

Ultraviolet Light

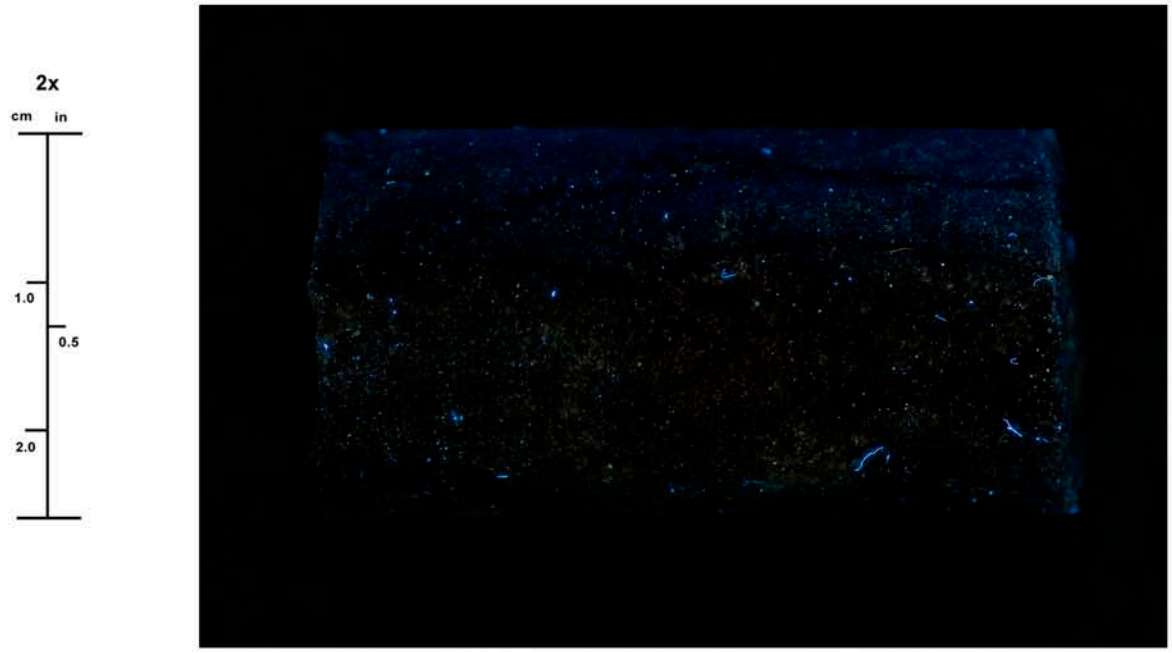

Weatherford LABORATORIES

HH-38266

Ohio Division of Geological Survey
CO2 No. 1 Well
Tuscarawas County, Ohio

Sample No.: 1-76R
Depth: 8590.00 feet

Visible Light

Longitudinal

Ultraviolet Light

INTENTIONALLY BLANK

Weatherford LABORATORIES

HH-38266

Ohio Division of Geological Survey
CO2 No. 1 Well
Tuscarawas County, Ohio

Rotary Sidewall Core Photography

Sample No.: 1-77R

Visible Light — Depth: 8603.00 feet — Ultraviolet Light

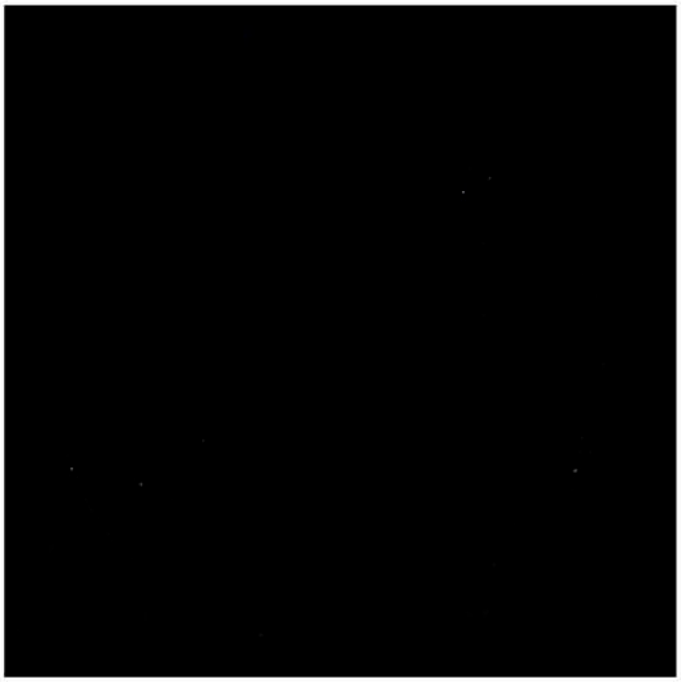

Sample No.: 1-78R

Visible Light — Depth: 8610.00 feet — Ultraviolet Light

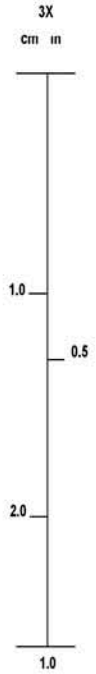

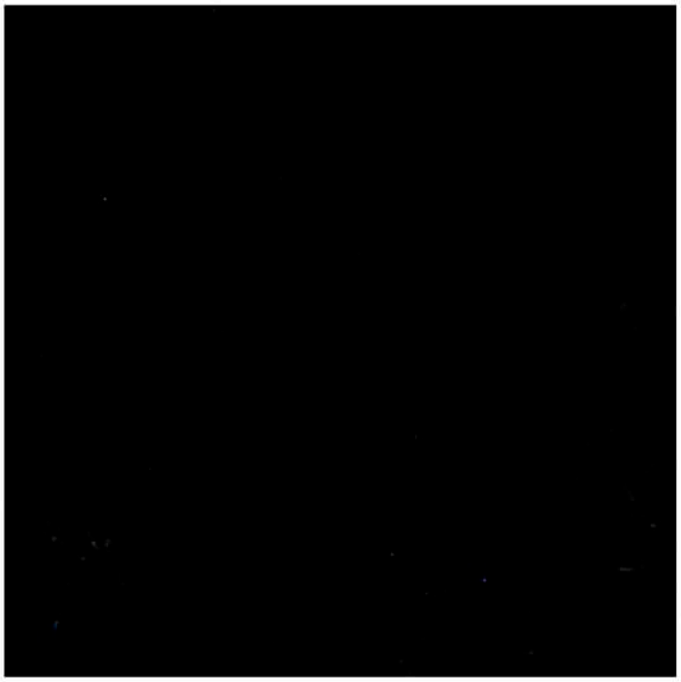

Weatherford LABORATORIES

HH-38266

Ohio Division of Geological Survey
CO2 No. 1 Well
Tuscarawas County, Ohio

Sample No.: 1-77R
Depth: 8603.00 feet

Visible Light

Longitudinal

Ultraviolet Light

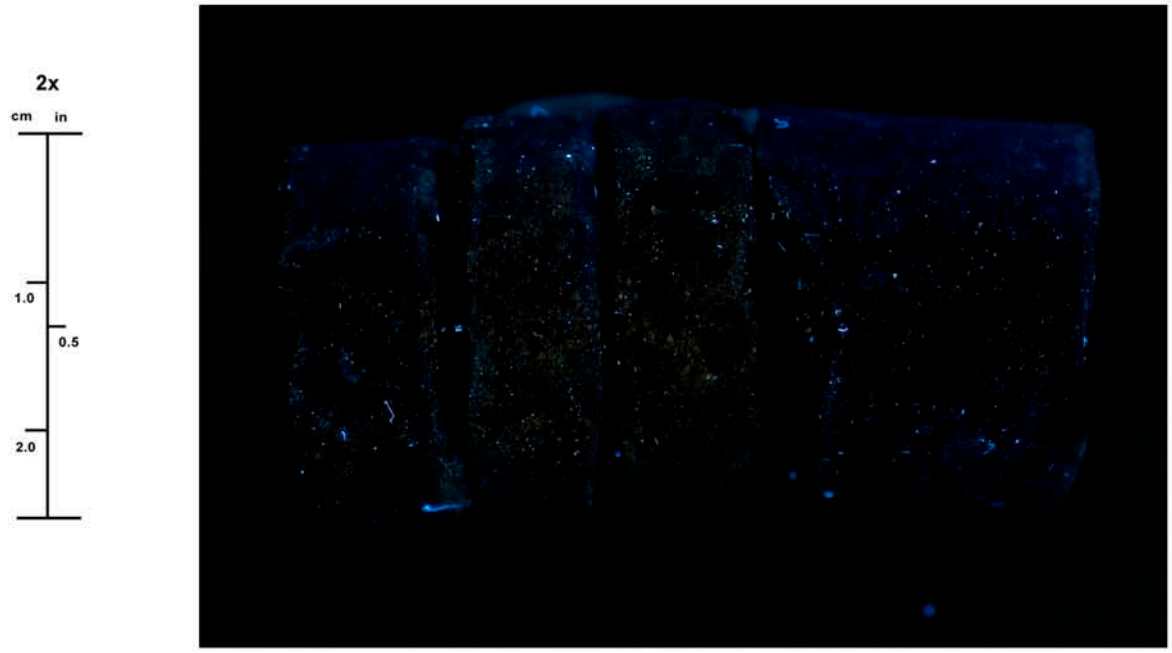

Weatherford LABORATORIES

HH-38266

Ohio Division of Geological Survey
CO2 No. 1 Well
Tuscarawas County, Ohio

Sample No.: 1-78R
Depth: 8610.00 feet

Visible Light

Longitudinal

Ultraviolet Light

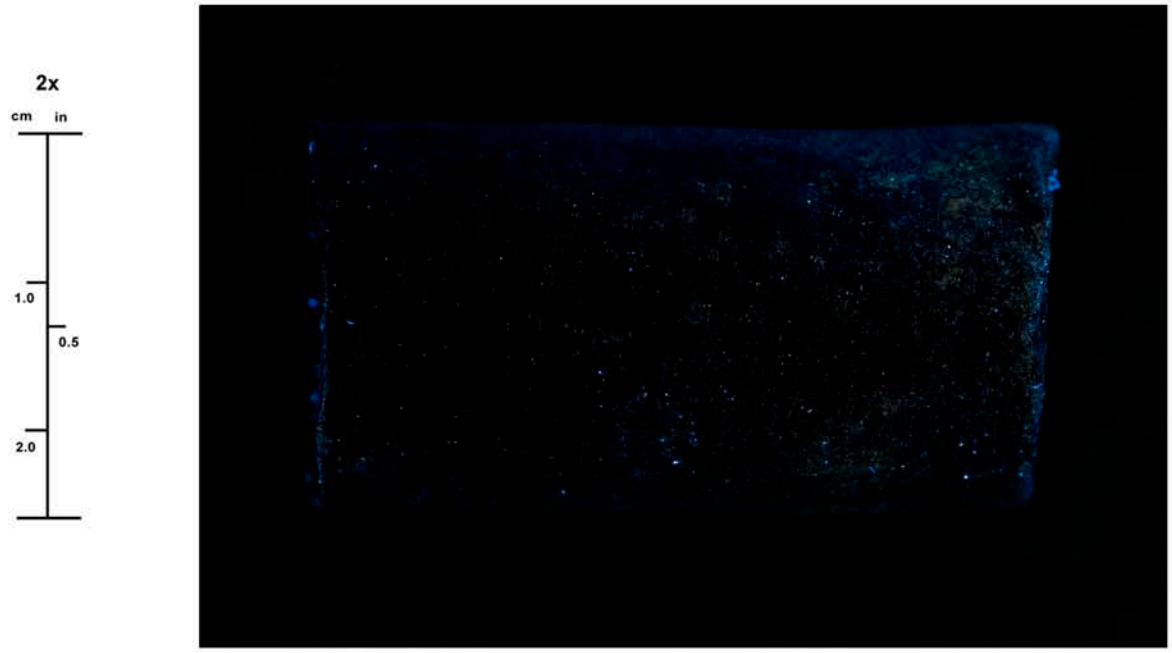

INTENTIONALLY BLANK

Weatherford LABORATORIES

HH-38266

Ohio Division of Geological Survey
CO2 No. 1 Well
Tuscarawas County, Ohio

Rotary Sidewall Core Photography

Sample No.: 1-79R

Visible Light — Depth: 8628.00 feet — Ultraviolet Light

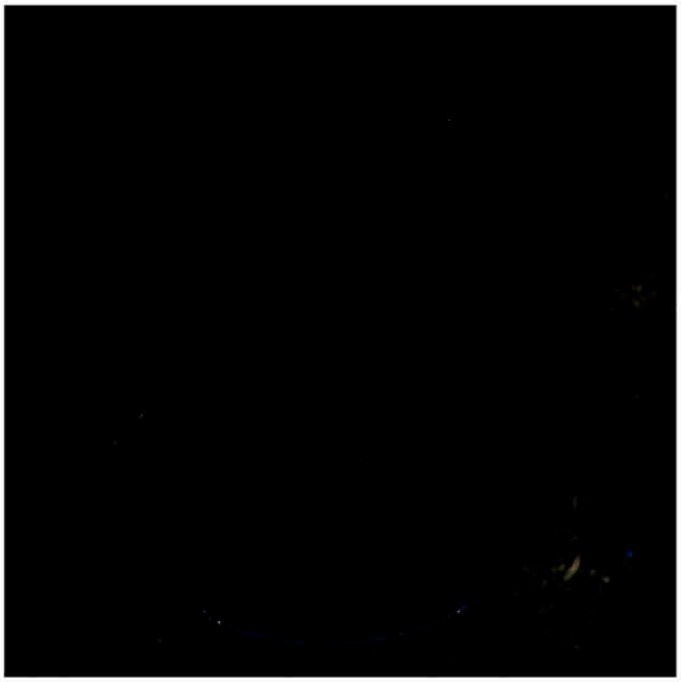

Sample No.: 1-80R

Visible Light — Depth: 8643.00 feet — Ultraviolet Light

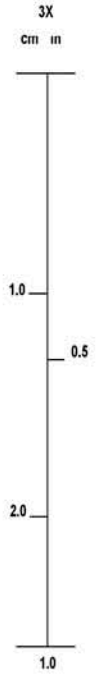

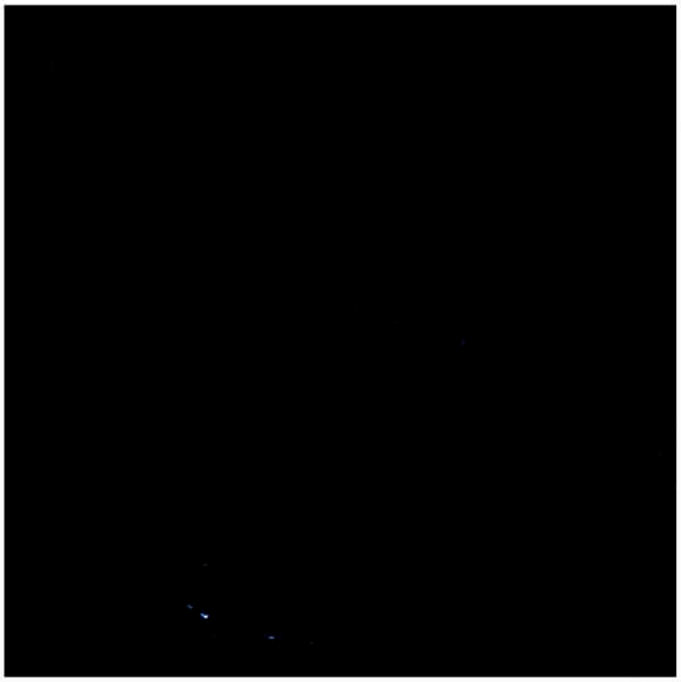

Weatherford LABORATORIES

HH-38266

Ohio Division of Geological Survey
CO2 No. 1 Well
Tuscarawas County, Ohio

Sample No.: 1-79R
Depth: 8628.00 feet

Visible Light

Longitudinal

Ultraviolet Light

Weatherford LABORATORIES

HH-38266

Ohio Division of Geological Survey
CO2 No. 1 Well
Tuscarawas County, Ohio

Sample No.: 1-80R
Depth: 8643.00 feet

Visible Light

Longitudinal

Ultraviolet Light

INTENTIONALLY BLANK

Weatherford LABORATORIES

HH-38266

Ohio Division of Geological Survey
CO2 No. 1 Well
Tuscarawas County, Ohio

Rotary Sidewall Core Photography

Sample No.: 1-81R

Visible Light — Depth: 8659.00 feet — Ultraviolet Light

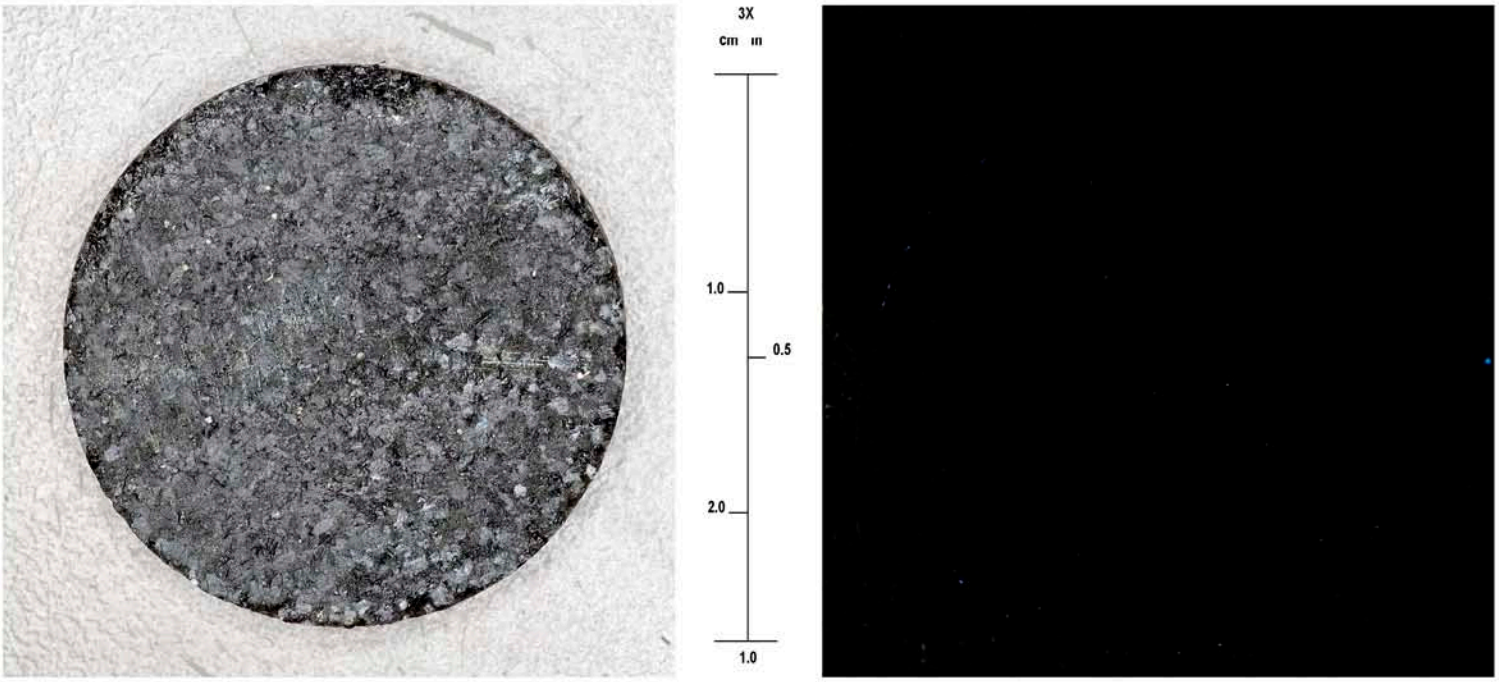

Sample No.: 1-82R

Visible Light — Depth: 8688.00 feet — Ultraviolet Light

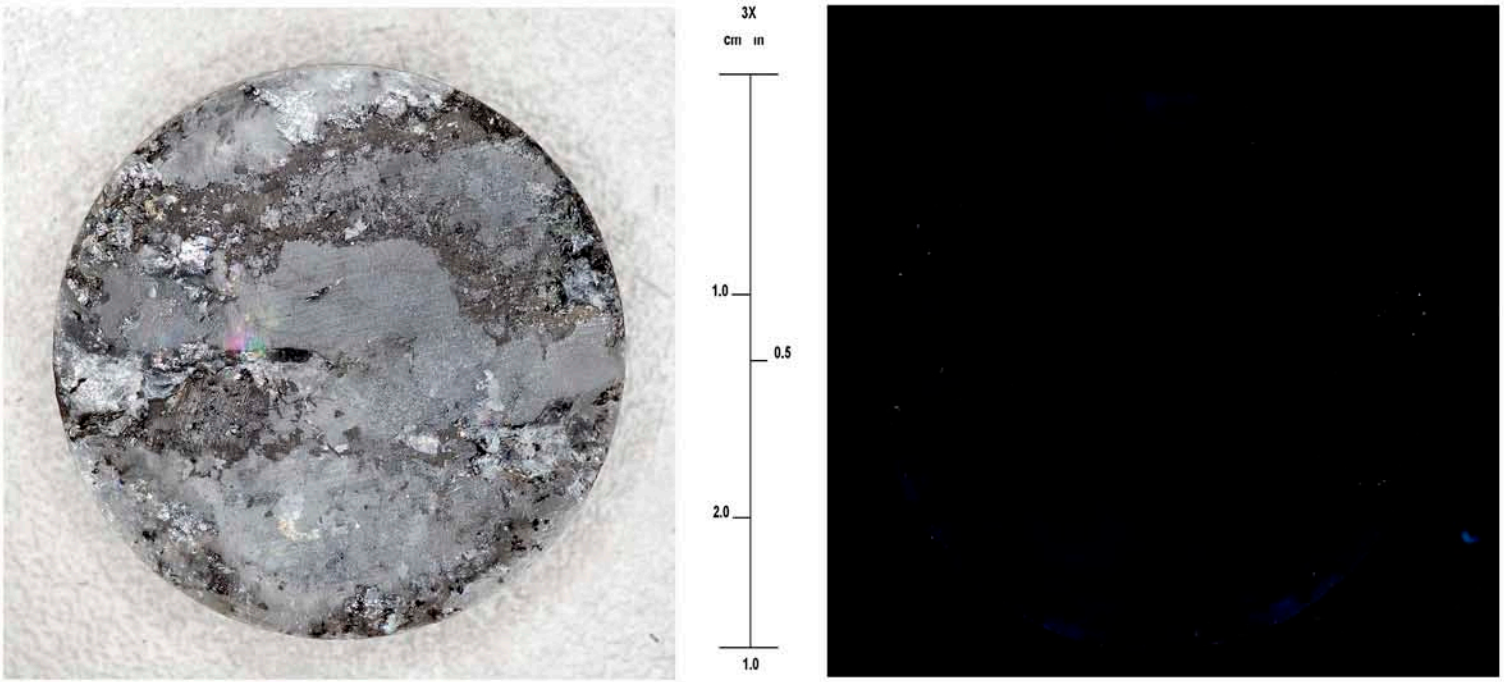

Weatherford LABORATORIES

HH-38266

Ohio Division of Geological Survey
CO2 No. 1 Well
Tuscarawas County, Ohio

Sample No.: 1-81R
Depth: 8659.00 feet

Visible Light

Longitudinal

Ultraviolet Light

Weatherford LABORATORIES

HH-38266

Ohio Division of Geological Survey
CO2 No. 1 Well
Tuscarawas County, Ohio

Sample No.: 1-82R
Depth: 8688.00 feet

Visible Light

Longitudinal

Ultraviolet Light

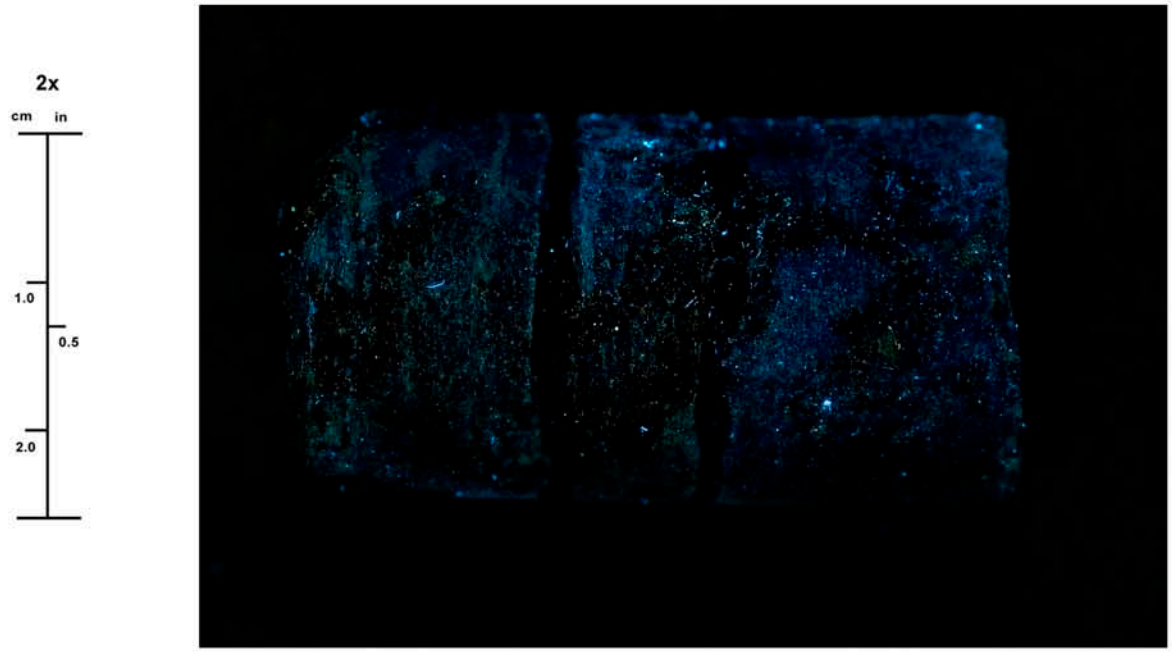

INTENTIONALLY BLANK

APPENDIX G

SUMMARY OF ROUTINE ROTARY CORE ANALYSES

INTENTIONALLY BLANK

3-14-08

PERMEABILITY AND FLUID SATURATIONS VERSUS POROSITY

Vacuum Dried at 180°F

Ohio Divison Of Geological Survey
CO2 No. 1 Well

Tuscarawas County, Ohio
File: HH-38266

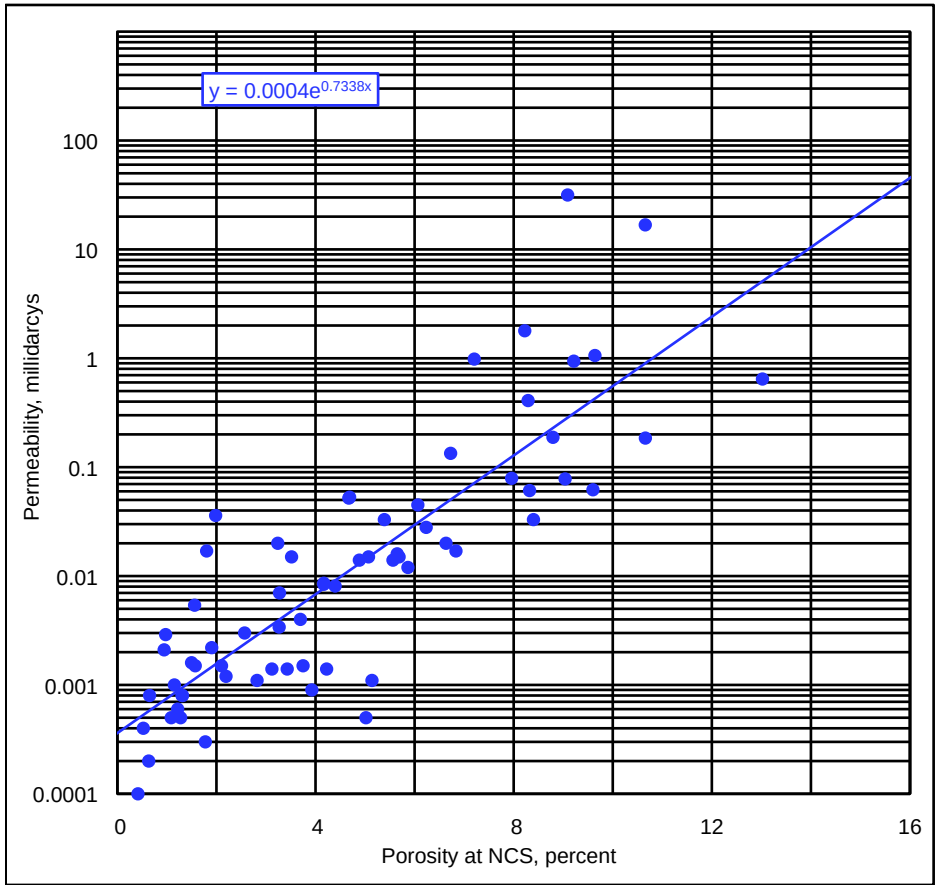

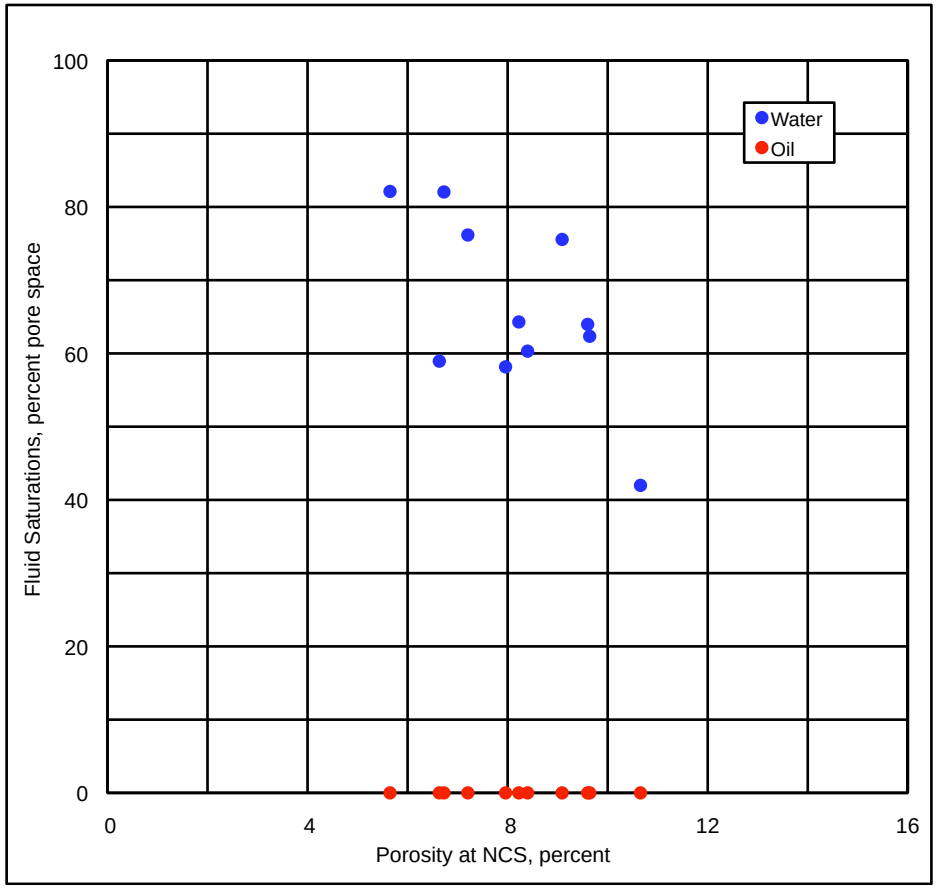

OMNI Laboratories, Inc.

SUMMARY OF ROTARY CORE ANALYSES RESULTS

Vacuum Dried at 180°F

Ohio Divison Of Geological Survey
CO2 No. 1 Well

Tuscarawas County, Ohio
File: HH-38266

Run Number	Sample Number	Sample Depth, feet	Net Confining Stress, psi	Permeability, millidarcys to Air	Permeability, millidarcys Klinkenberg	Porosity, percent Ambient	Porosity, percent NCS	Grain Density, gm/cc	Fluid Saturations, percent Water	Fluid Saturations, percent Oil	Fluid Saturations, percent Total	Lithological Descriptions
1	1-1R	4605.0	1350		+	6.4		2.78	58.0	0.0	58.0	Dol shly slty frac
1	1-2R	4760.0	1400		+	5.8	5.7	2.67			**	Ss vfg-fg frac
1	1-3R	4771.0	1400	0.017	0.0069	6.9	6.8	2.65			**	Ss vfg-fg
1	1-4R	4776.0	1400		+	8.6		2.67			**	Ss vfg-fg frac
1	1-5R	4790.0	1400		+	7.8	7.7	2.70			**	Ss fg w/shly lams frac
1	1-6R	4816.0	1400		+	4.1		2.80			**	Silt shly vpyr frac
1	1-7R	4821.0	1400		+	4.3	4.2	2.72			**	Ss vfg-fg scalc pyr sorg w/shly lam frac
1	1-8R	4834.0	1400		+	3.6	3.5	2.66			**	Ss fg w/shly inclusion frac
1	1-9R	4840.0	1400	0.015	0.0061	5.8	5.7	2.66			**	Ss fg scalc
1	1-10R	6064.0	1750		+	4.9	4.8	2.78			**	Sh slty dol spyr frac
1	1-11R	6141.0	1800	0.0011	0.0002	5.2	5.1	2.70			**	Sh calc
1	1-12R	6282.0	1800	0.0014	0.0003	4.3	4.2	2.70			**	Ls shly spyr sfoss
1	1-13R	6336.0	1850	0.0005	0.0001	5.1	5.0	2.61			**	Sh calc spyr
1	1-14R	6396.0	1850	0.0011	0.0002	2.9	2.8	2.69			**	Ls shly sfoss spyr
1	1-15R	6490.0	1900	0.0014	0.0003	3.2	3.1	2.69			**	Ls shly
1	1-16R	6524.0	1900	0.015	0.0058	3.6	3.5	2.75			**	Ls sfoss spyr
1	1-17R	6566.0	1900	0.0016	0.0003	1.6	1.5	2.73			**	Ls sfoss spyr
1	1-18R	6620.0	1900	0.0015	0.0003	1.7	1.6	2.71			**	Ls spyr
1	1-19R	6750.0	2000	0.015	0.0057	5.2	5.1	2.71			**	Ls foss
1	1-20R	6794.0	2000	0.409	0.286	8.4	8.3	2.70			**	Ls sfoss shly streaks
1	1-21R	6808.0	2000	0.052	0.027	4.8	4.7	2.71			**	Ls sfoss styolites
1	1-22R	6844.0	2000	0.0081	0.0027	4.6	4.4	2.71			**	Ls sfoss
1	1-23R	6871.0	2000	0.645	0.482	13.2	13.0	2.73			*	Ls fn xln
1	1-24R	6936.0	2000	0.061	0.032	8.5	8.3	2.73			**	Ls xln
1	1-25R	6940.0	2000	0.0008	0.0001	1.4	1.3	2.71			**	Ls sfoss spyr w/shly lam
1	1-26R	7030.0	2050	0.0006	0.0001	1.3	1.2	2.73			**	Ls sdol
1	1-27R	7128.0	2100	0.033	0.016	5.5	5.4	2.74			**	Ls sfoss w/calcite inclusions
1	1-28R	7142.0	2100	0.0012	0.0002	2.3	2.2	2.76			**	Ls dol spyr
1	1-29R	7192.0	2100	0.0015	0.0003	3.8	3.7	2.82			**	Dol pyr
1	1-30R	7226.0	2100	0.0015	0.0003	2.2	2.1	2.83			**	Dol svug
1	1-31R	7231.0	2100	0.941	0.726	9.4	9.2	2.84			*	Dol vug
1	1-32R	7235.0	2100	0.0009	0.0002	4.0	3.9	2.85			**	Dol
1	1-33R	7248.0	2100		<0.0001	1.5	1.4	2.80			**	Dol svug
1	1-34R	7296.0	2100	0.007	0.0022	3.5	3.3	2.84			**	Dol spyr
1	1-35R	7328.0	2100	0.017	0.0067	2.0	1.8	2.83			**	Dol
1	1-36R	7365.0	2150	0.016	0.0065	5.8	5.6	2.66	82.1	0.0	82.1	Ss mg-crs scalc w/shly streaks
1	1-37R	7377.0	2150	0.045	0.023	6.2	6.1	2.64			**	Ss mg
1	1-38R	7387.0	2150	0.012	0.0044	6.0	5.9	2.66			**	Ss mg-crs calc
1	1-39R	7392.0	2150	16.8	13.8	10.8	10.7	2.64	42.0	0.0	42.0	Ss mg
1	1-40R	7414.0	2150	0.0034	0.0009	3.4	3.3	2.67			**	Ss fg-mg scalc
1	1-41R	7426.0	2150	0.134	0.081	6.8	6.7	2.62	82.0	0.0	82.0	Ss fg-mg
1	1-42R	7434.0	2150	31.6	26.6	9.2	9.1	2.68	75.6	0.0	75.6	Ss mg-crs scalc
1	1-43R	7441.0	2150	0.983	0.766	7.3	7.2	2.61	76.2	0.0	76.2	Ss fg-mg
1	1-44R	7459.0	2150	0.001	0.0002	1.3	1.2	2.82			**	Dol sshly spyr
1	1-45R	7480.0	2200	0.0086	0.0029	4.3	4.2	2.74			**	Ss fg-mg sdol
1	1-46R	7495.0	2200	0.033	0.015	8.5	8.4	2.62	60.3	0.0	60.3	Ss fg-mg
1	1-47R	7506.0	2200	1.79	1.40	8.3	8.2	2.71	64.3	0.0	64.3	Ss mg sdol
1	1-48R	7528.0	2200	0.036	0.017	2.1	2.0	2.83			**	Dol
1	1-49R	7579.0	2200	0.0022	0.0005	2.0	1.9	2.83			**	Dol
1	1-50R	7692.0	2250	0.0005	0.0001	1.4	1.3	2.81			**	Dol
1	1-51R	7730.0	2250	0.0008	0.0001	1.4	1.3	2.83			**	Dol
1	1-52R	7742.0	2250	0.0021	0.0004	1.0	0.9	2.81			**	Dol w/shly lams frac
1	1-53R	7818.0	2300	0.0040	0.0011	3.8	3.7	2.86			**	Dol svug
1	1-54R	7868.0	2300	0.0003	<0.0001	1.9	1.8	2.84			**	Dol
1	1-55R	7931.0	2300	0.0030	0.0007	2.7	2.6	2.82			**	Dol spyr
1	1-56R	7991.0	2300	0.0054	0.0016	1.7	1.6	2.84			**	Dol w/ shly lam
1	1-57R	8014.0	2300	0.0029	0.0007	1.1	1.0	2.82			**	Dol
1	1-58R	8066.0	2350	0.053	0.027	4.8	4.7	2.84			**	Dol vug
1	1-59R	8138.0	2350		+	1.3		2.84			**	Dol partial frac
1	1-60R	8176.0	2400	0.0002	<0.0001	0.7	0.6	2.85			**	Dol
1	1-61R	8274.0	2400	0.0004	<0.0001	0.6	0.5	2.84			**	Dol w/shlystreaks
1	1-62R	8350.0	2400	0.0001	<0.0001	0.5	0.4	2.85			**	Dol spyr

OMNI Laboratories, Inc.

SUMMARY OF ROTARY CORE ANALYSES RESULTS

Vacuum Dried at 180°F

Ohio Divison Of Geological Survey
CO2 No. 1 Well

Tuscarawas County, Ohio
File: HH-38266

Run Number	Sample Number	Sample Depth, feet	Net Confining Stress, psi	Permeability, millidarcys to Air	Permeability, millidarcys Klinkenberg	Porosity, percent Ambient	Porosity, percent NCS	Grain Density, gm/cc	Fluid Saturations, percent Water	Fluid Saturations, percent Oil	Fluid Saturations, percent Total	Lithological Descriptions
1	1-63R	8421.0	2450	0.020	0.0085	3.4	3.2	2.69			**	Ss mg-crs spyr scalc
1	1-64R	8451.0	2450	0.020	0.0084	6.7	6.6	2.63	58.9	0.0	58.9	Ss fg-mg
1	1-65R	8467.0	2450	0.0084	0.0028	4.3	4.2	2.62			**	Ss mg-crs spyr w/shly lam
1	1-66R	8495.0	2450	0.0008	0.0001	0.7	0.6	2.81			**	Ss fg pyr sdol
1	1-67R	8528.0	2450		+	2.8	2.7	2.71			**	Ss fg-mg spyr w/shly lam frac
1	1-68R	8538.0	2500	0.014	0.0052	5.1	4.9	2.62			**	Ss fg-mg scalc
1	1-69R	8544.0	2500	0.0014	0.0003	3.5	3.4	2.67			**	Ss fg sdol w/shly lams
1	1-70R	8549.0	2500	0.0005	0.0001	1.2	1.1	2.79			**	Dol spyr
1	1-71R	8555.0	2500	0.078	0.044	10.7	9.0	2.63			**	Ss vfg-fg w/shy lam spyr
1	1-72R	8561.0	2500	1.06	0.836	9.8	9.6	2.60	62.3	0.0	62.3	Ss fg-mg
1	1-73R	8570.0	2500	0.014	0.0056	5.7	5.6	2.62			**	Ss vfg-fg spyr
1	1-74R	8583.0	2500	0.028	0.013	6.3	6.2	2.62			**	Ss fg-mg scalc
1	1-75R	8585.0	2500	0.062	0.033	9.7	9.6	2.57	64.0	0.0	64.0	Ss fg-mg w/shly streaks
1	1-76R	8590.0	2500	0.185	0.118	10.9	10.7	2.62			**	Ss fg-mg
1	1-77R	8603.0	2500	0.188	0.120	9.0	8.8	2.62			**	Ss fg-mg spyr
1	1-78R	8610.0	2500	0.079	0.044	8.2	8.0	2.60	58.2	0.0	58.2	Ss vfg-fg scalc spyr w/shly streaks
1	1-79R	8628.0	2500		<0.0001	1.7	1.6	2.75			**	Metamorphic/crystalline
1	1-80R	8643.0	2500		<0.0001	0.3	0.2	3.07			**	Metamorphic/crystalline pyr
1	1-81R	8659.0	2500		<0.0001	0.6	0.5	2.98			**	Metamorphic/crystalline pyr
1	1-82R	8688.0	2500		<0.0001	0.4	0.3	2.69			**	Metamorphic/crystalline/quartz inclusions pyr
			Average values:	0.829	0.724	4.6	4.4	2.73	65.3	0.0	65.3	

+ Indicates sample is unsuitable for this type of measurement
* Water captured from DS and weight loss other than water were below detectable limits
** Unable to report saturation levels due to insufficient pore volume

INTENTIONALLY BLANK

APPENDIX H

ROCK EVALUATION AND TOC (TOTAL ORGANIC CONTENT) ANALYSIS

INTENTIONALLY BLANK

TOC and ROCK-EVAL DATA REPORT

Ohio Division of Geological Survey, Tuscarawas, OH

Omni File #: HH-38266

HGS No.	Well Name	Top Depth (ft)	Bottom Depth (ft)	Median Depth (ft)	Sample Type	Leco TOC	**	S1	S2	S3	Tmax (°C)		Calc. %Ro	Meas. %Ro	HI	OI	S2/S3	S1/TOC	PI	Notes Checks	Notes Pyrogram
07-5156-220088	CO2 No. 1	6064		6064	core	0.48		0.23	0.51	0.18	442		0.80		106	38	3	48	0.31	c, lc	n
07-5156-220089	CO2 No. 1	6141		6141	core	2.72		3.22	4.42	0.35	442		0.80		163	13	13	118	0.42	lc	n
07-5156-220090	CO2 No. 1	6282		6282	core	2.41		3.73	3.09	0.52	447		0.89		128	22	6	155	0.55	lc	n
07-5156-220091	CO2 No. 1	6336		6336	core	3.73		5.35	5.63	0.43	451		0.96		151	12	13	143	0.49	lc	n
07-5156-220092	CO2 No. 1	6396		6396	core	1.61		2.04	1.54	0.31	443		0.81		96	19	5	127	0.57	lc	n;ltS2sh
07-5156-220093	CO2 No. 1	7192		7192	core	0.11		0.05	0.09	0.12	460	*	1.12		82	109	1	45	0.36	lc	f
07-5156-220094	CO2 No. 1	7579		7579	core	0.14		0.04	0.12	0.20	505	*	1.93		86	143	1	29	0.25	lc	f
07-5156-220095	CO2 No. 1	8274		8274	core	0.23		0.02	0.08	0.12	450	*	0.94		35	52	1	9	0.20	c, lc	f

Note: "-1" indicates not measured or meaningless ratio

* Tmax data not reliable due to poor S2 peak

TOC = weight percent organic carbon in rock
S1, S2 = mg hydrocarbons per gram of rock
S3 = mg carbon dioxide per gram of rock
Tmax = ºC

HI = hydrogen index = S2 x 100 / TOC
OI = oxygen index = S3 x 100 / TOC
S1/TOC = normalized oil content = S1 x 100 / TOC
PI = production index = S1 / (S1+S2)
Calculcated%VRo = 0.0180 x Tmax - 7.16 (Jarvie et al., 2001)
Measured %Ro = measured vitrinite reflectance

Notes:
c = Rock-Eval analysis checked and confirmed
lc = Leco TOC analysis checked and confirmed

Pyrogram:
n=normal
ltS2sh = low temperature S2 shoulder
ltS2p = low temperature S2 peak
htS2p = high temperature S2 peak
f = flat S2 peak
na = printer malfunction pyrogram not available

Geochemical Log

Ohio Division of Geological Survey, Tuscarawas, OH

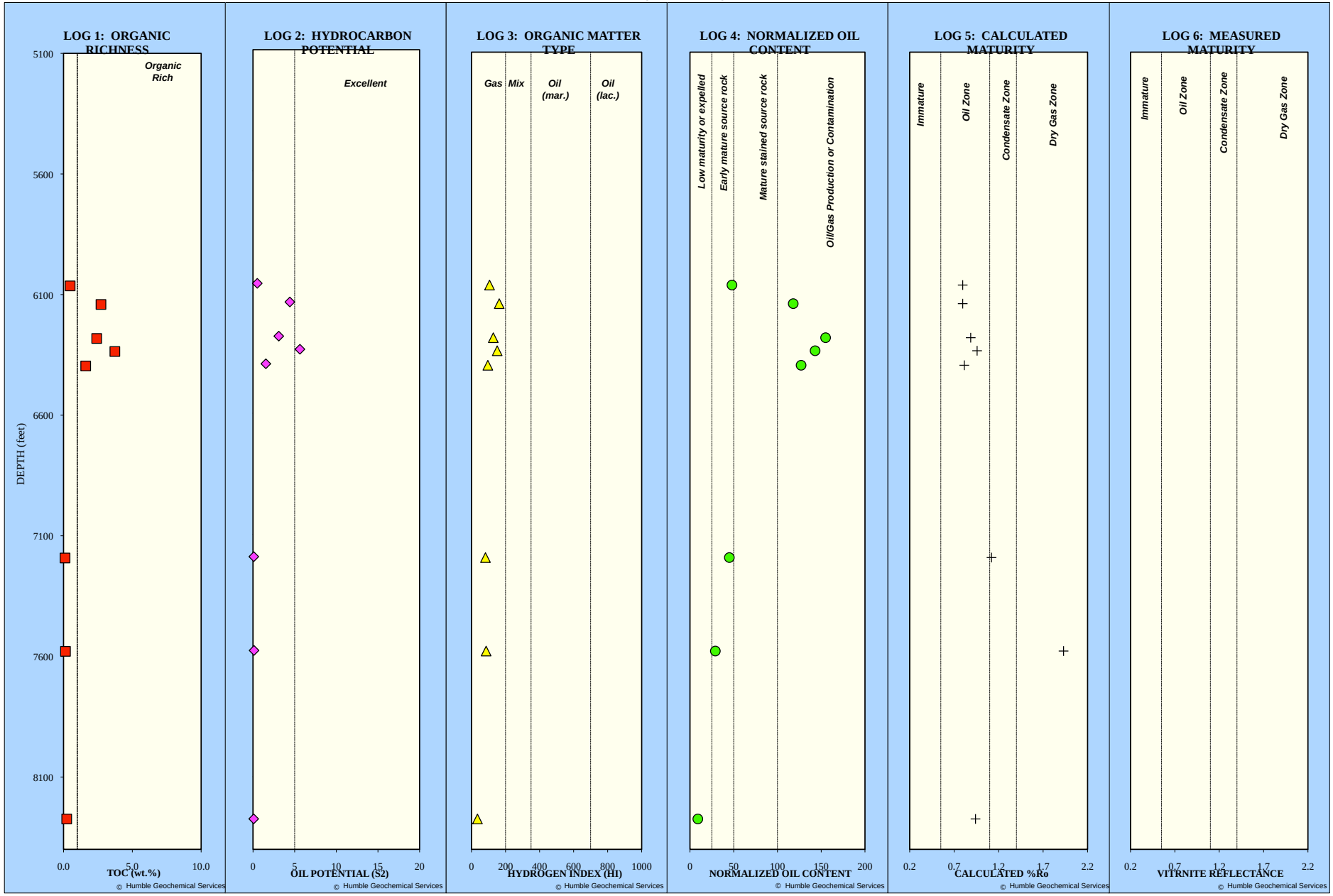

Figure 1. Geochemical log of TOC, remaining potential (S2), kerogen type (HI), normalized oil content, and calculated and measured vitrinite reflectance.

Humble Geochemical Services Division

KEROGEN QUALITY

Ohio Division of Geological Survey, Tuscarawas, OH

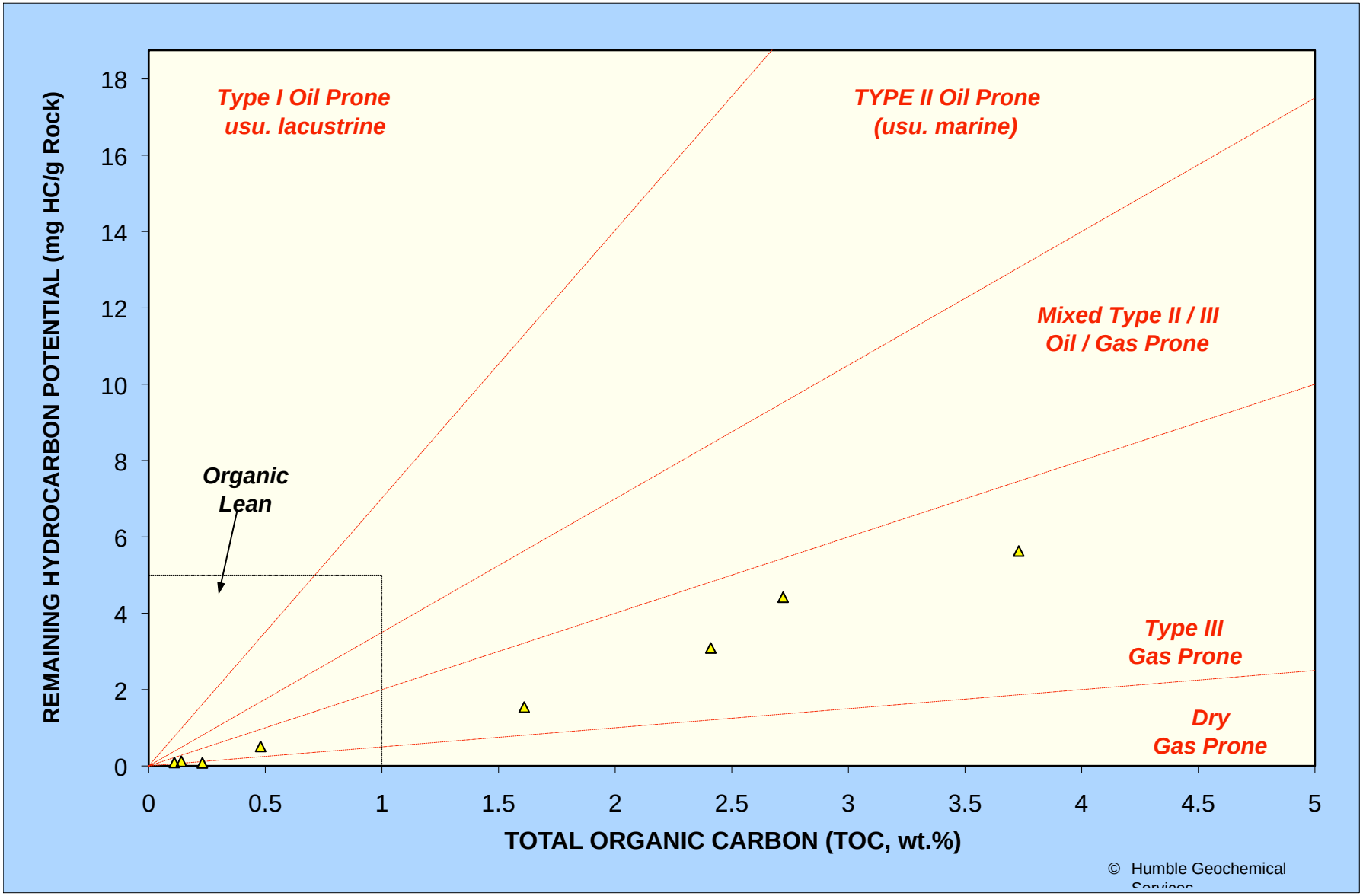

Figure 2. Kerogen Quality

Humble Geochemical Services Division

KEROGEN QUALITY

Ohio Division of Geological Survey, Tuscarawas, OH

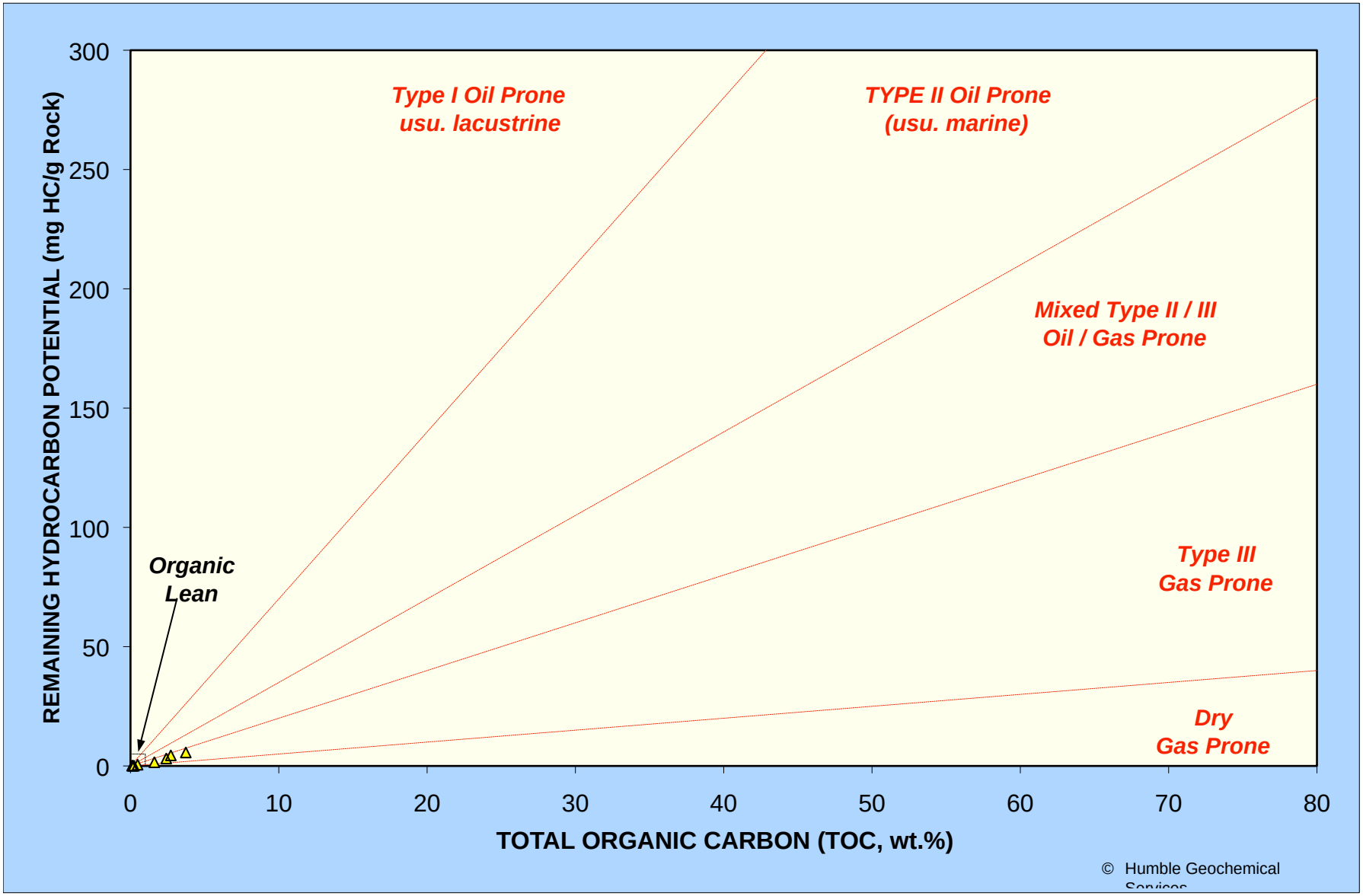

Figure 2. Kerogen Quality

Humble Geochemical Services Division

KEROGEN TYPE
Ohio Division of Geological Survey, Tuscarawas, OH

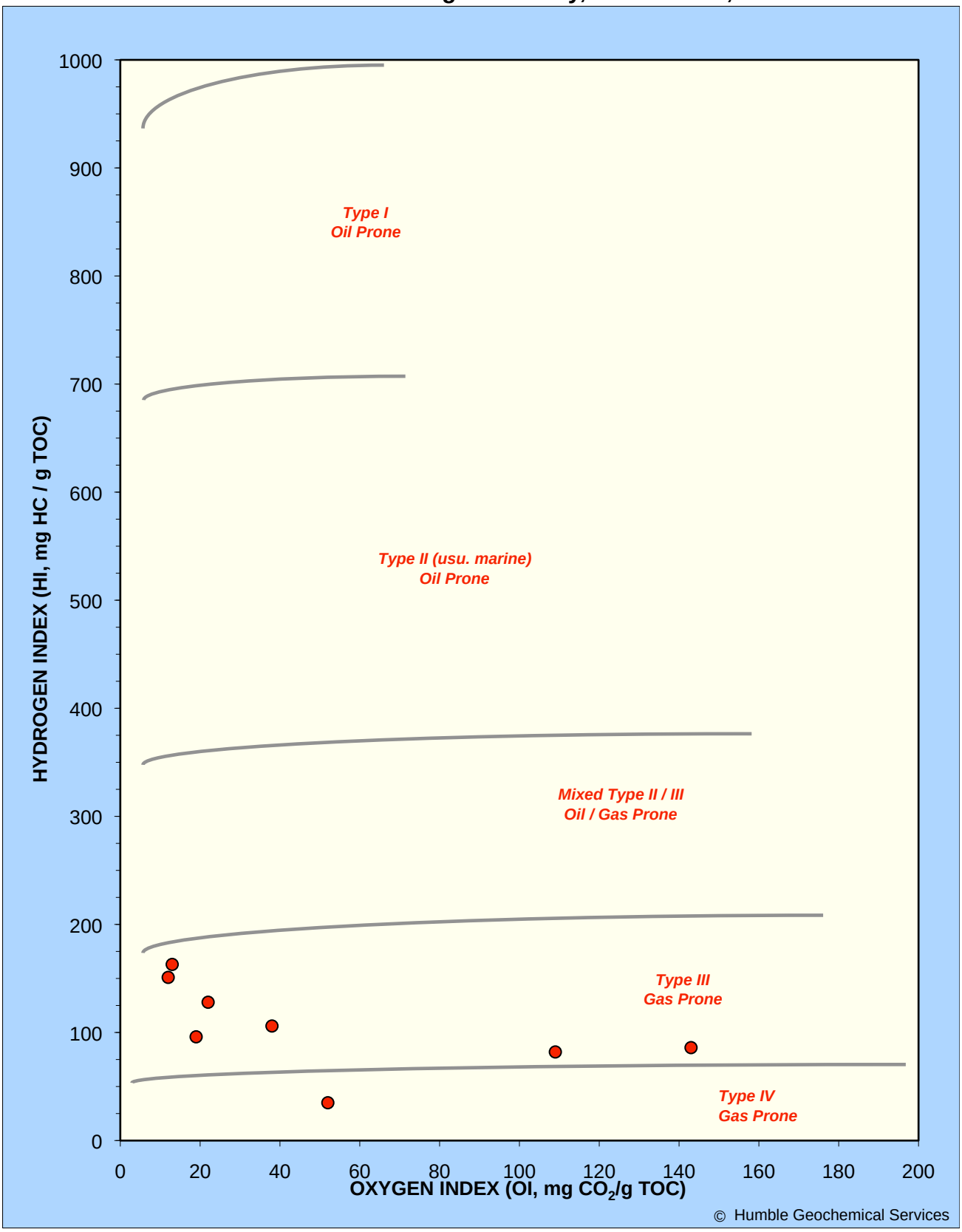

Figure 3. Kerogen type

KEROGEN TYPE and MATURITY

Ohio Division of Geological Survey, Tuscarawas, OH

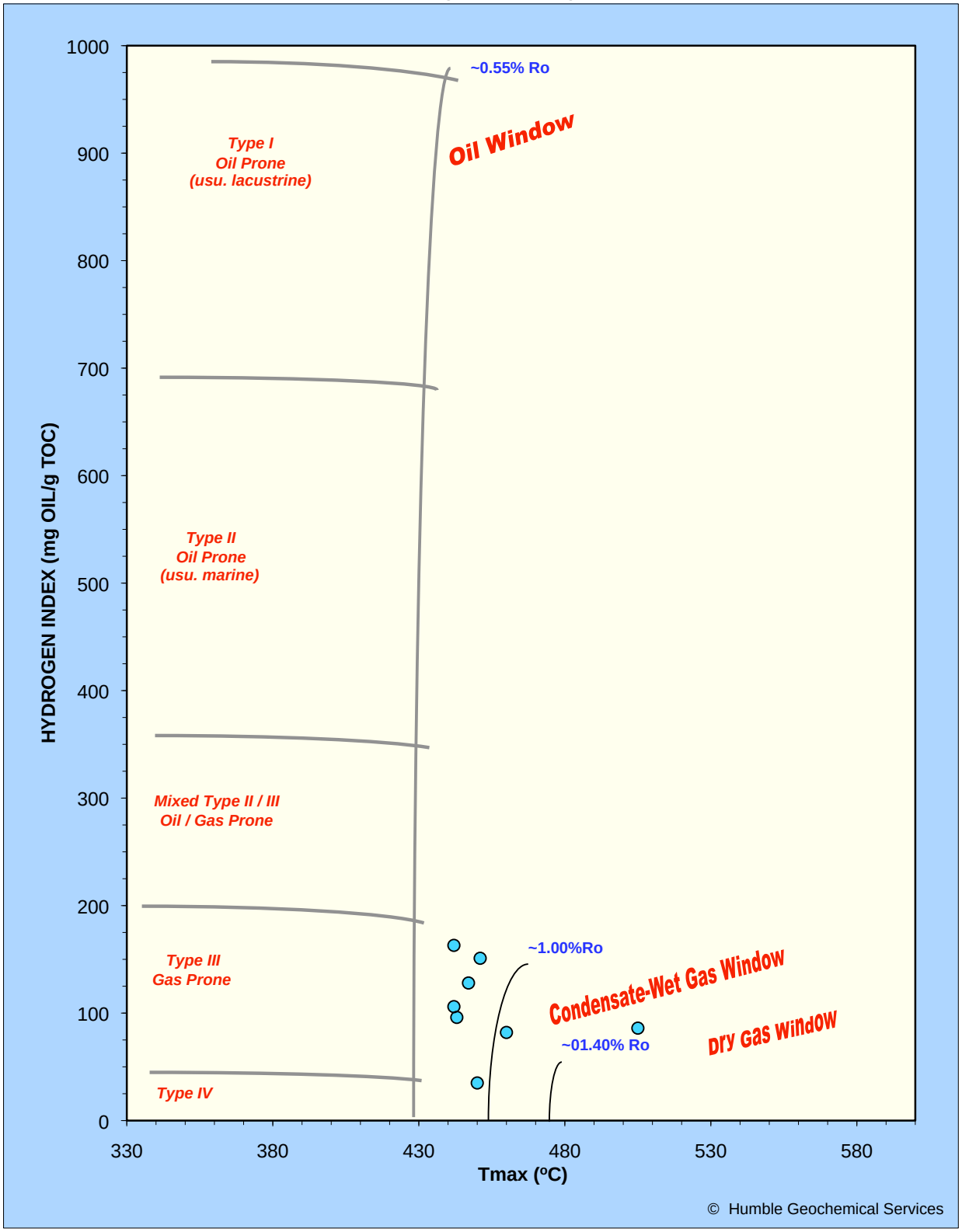

Figure 4a. Kerogen Type and Maturity (Tmax)

KEROGEN TYPE and MATURITY

Ohio Division of Geological Survey, Tuscarawas, OH

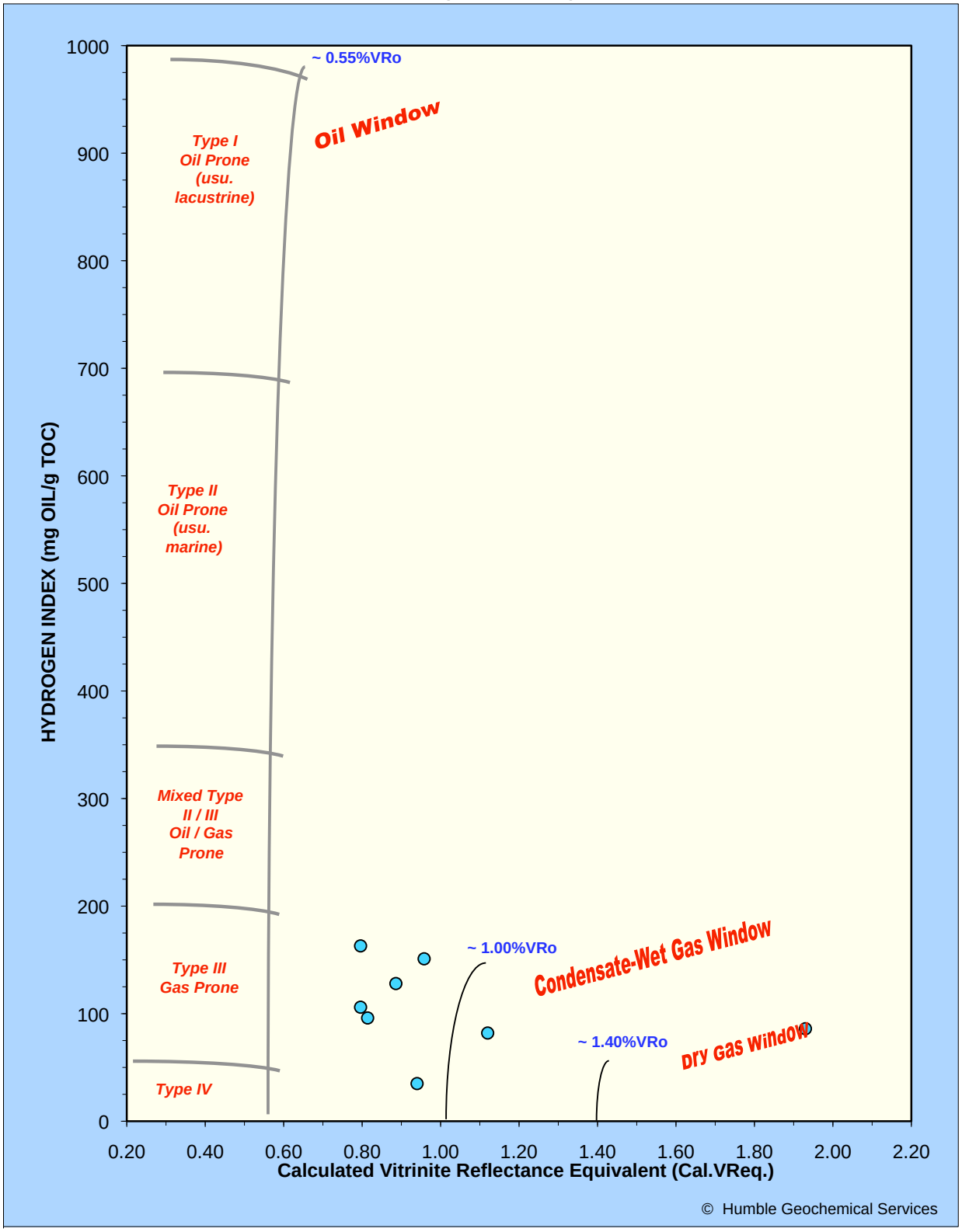

Figure 4b. Kerogen Type and Maturity (Tmax calculated %VRo)

KEROGEN TYPE and MATURITY

Ohio Division of Geological Survey, Tuscarawas, OH

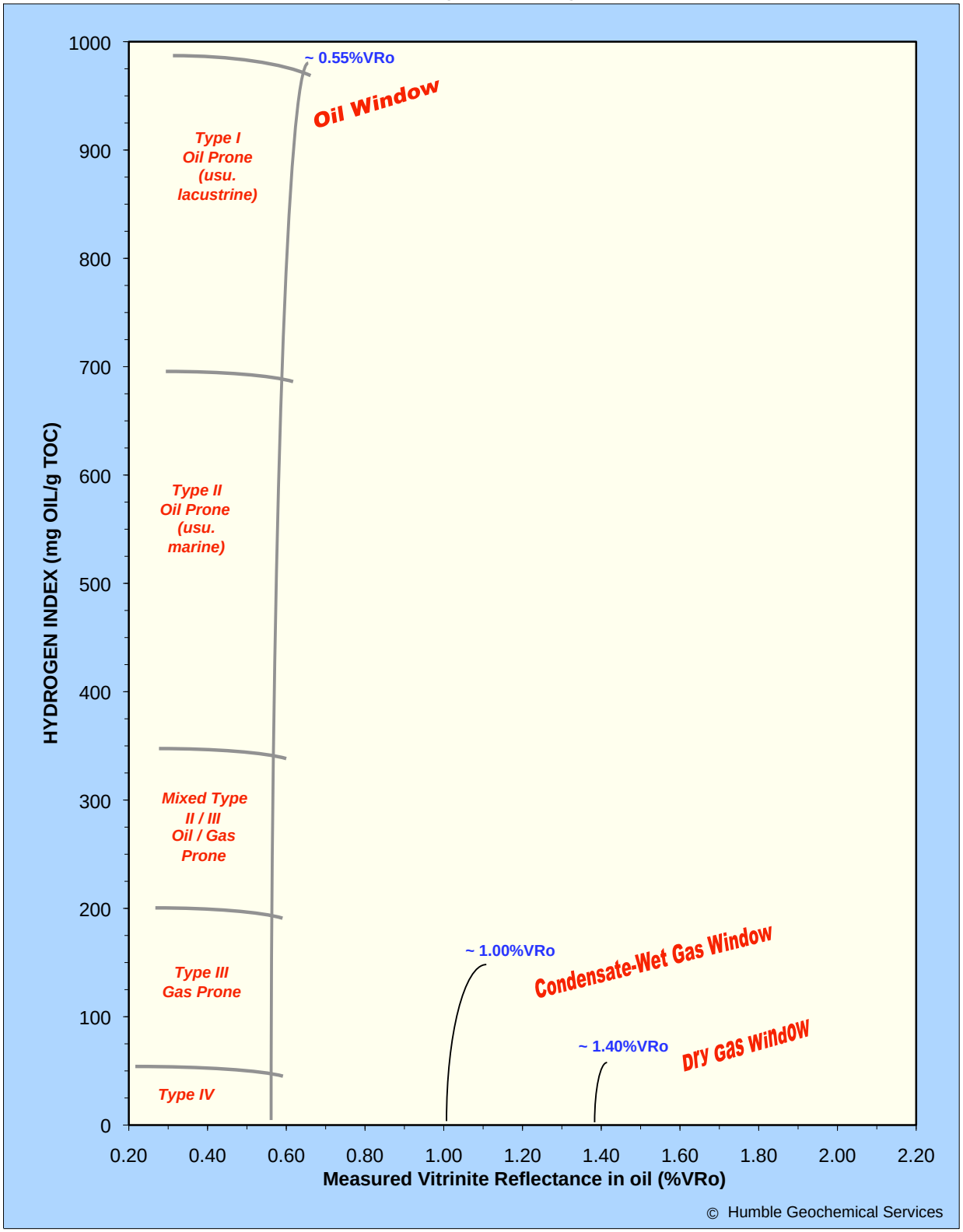

Figure 4c. Kerogen Type and Maturity (Measured vitrinite reflectance)

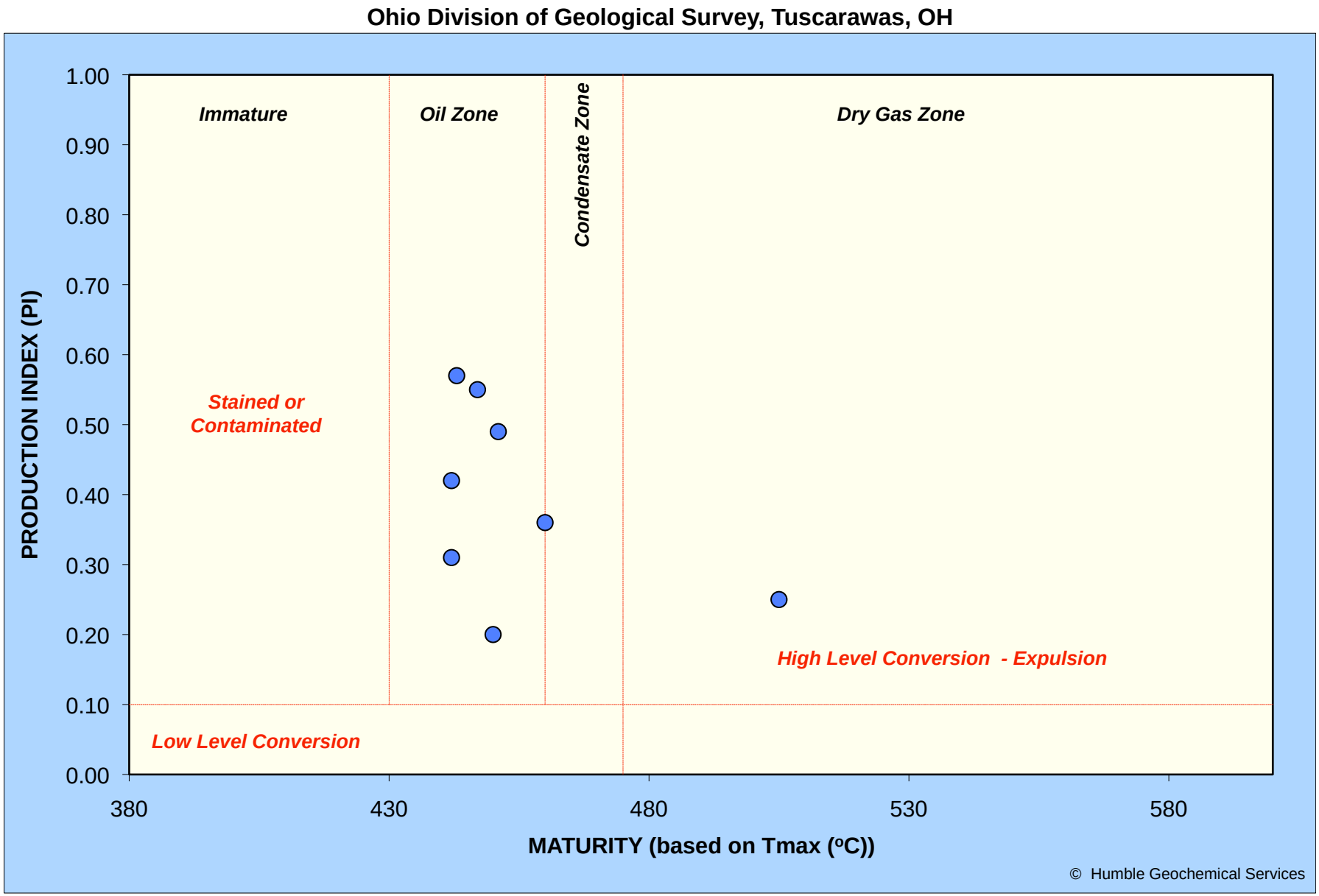

Figure 5a. Kerogen conversion and maturity (based on Tmax).

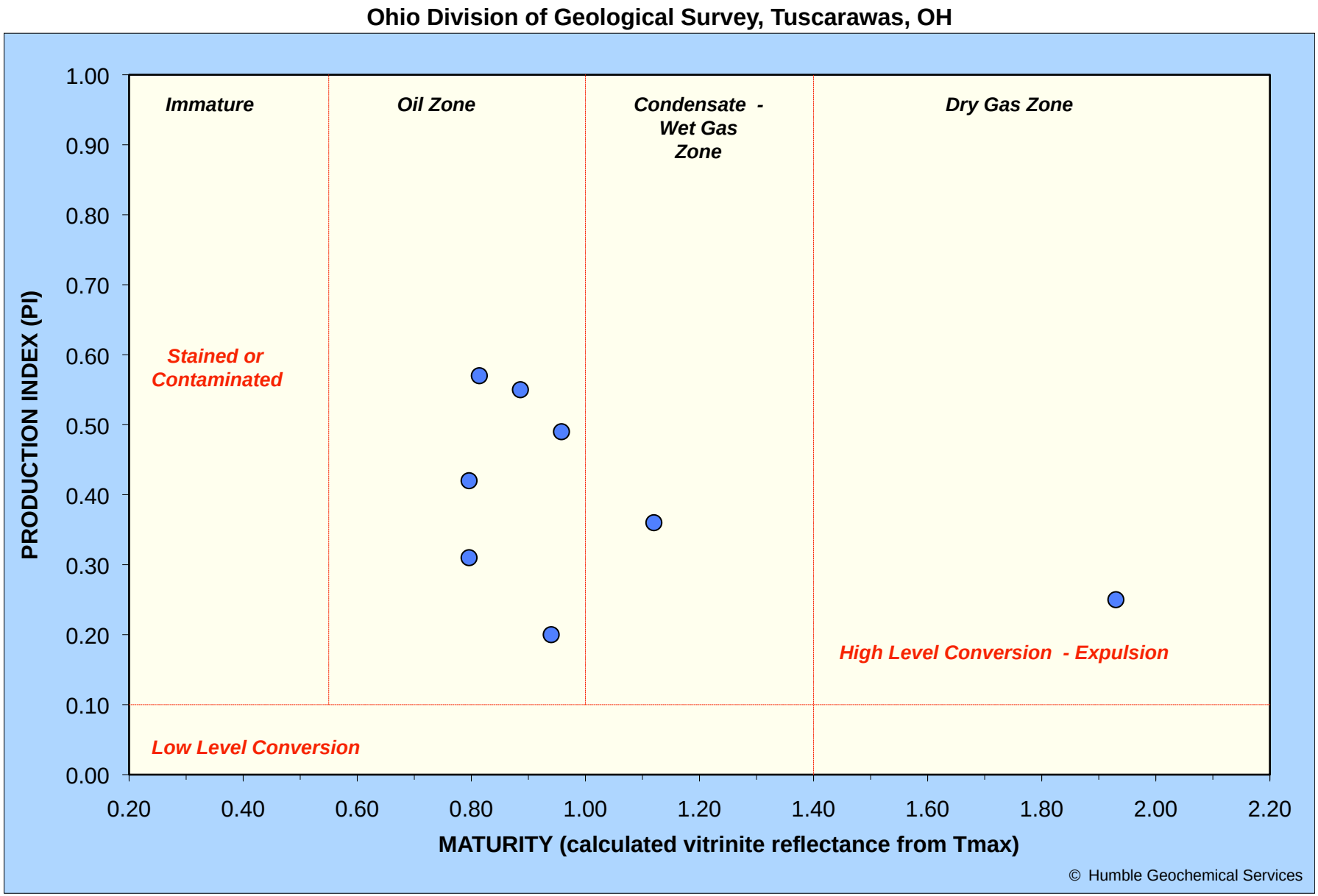

Figure 5b. Kerogen conversion and maturity (calculated %VRo from Tmax).

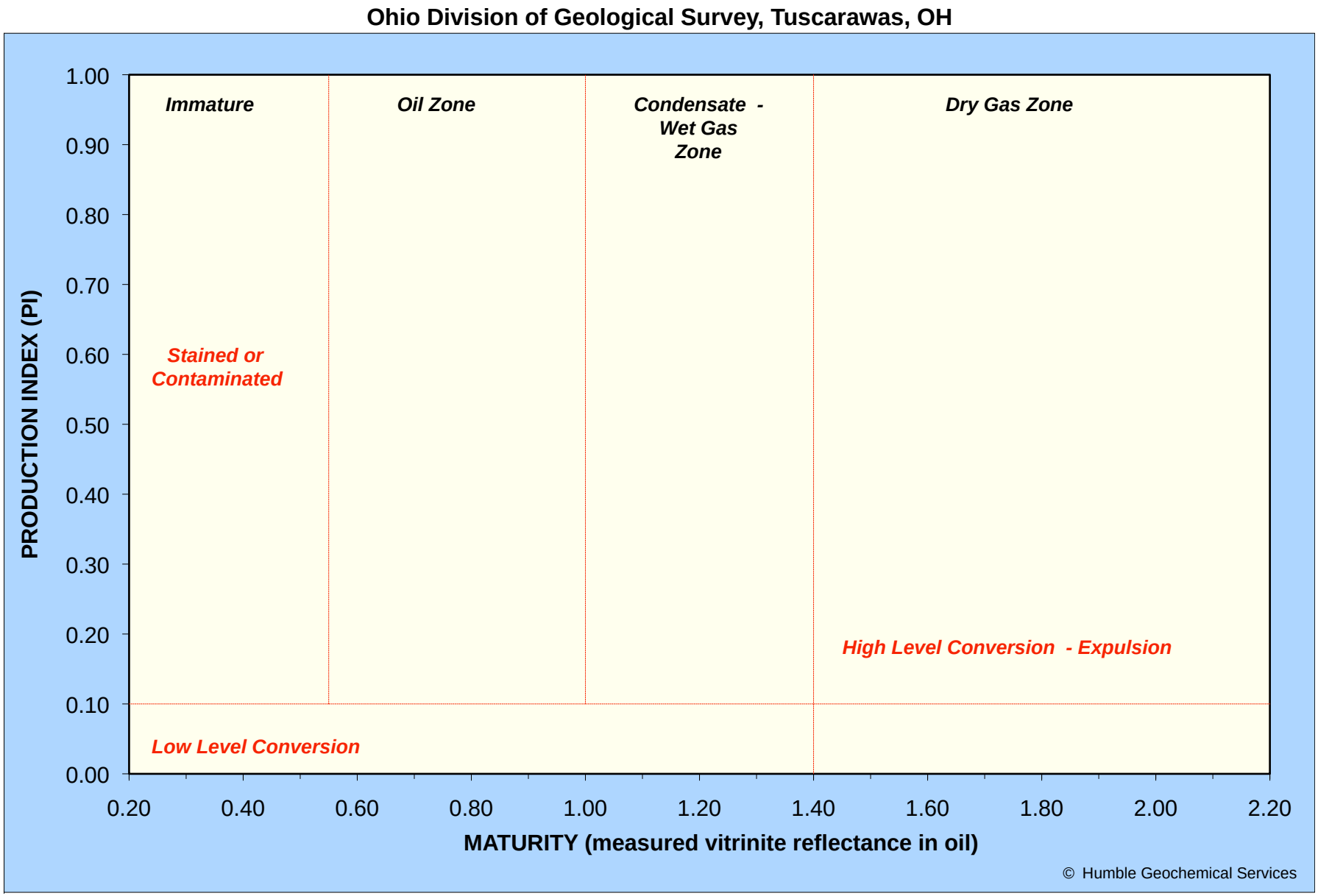

Figure 5c. Kerogen conversion and maturity (measured vitrinite reflectance).

INTENTIONALLY BLANK

APPENDIX I

ROCK MECHANICS FINAL REPORT
(TRIAXIAL COMPRESSIVE TESTS AND ULTRASONIC VELOCITIES)

INTENTIONALLY BLANK

ROCK MECHANICS TESTING & ANALYSES
CO2 NO. 1
OHIO DIVISION OF GEOLOGICAL SURVEY

ROCK MECHANICS FINAL REPORT

(Triaxial Compressive Tests)

(Ultrasonic Velocities)

OMNI HH-38266

Performed by:

OMNI Laboratories
Weatherford Intl. Integrated Laboratory Services
8845 Fallbrook Drive
Houston, TX 77064

Ohmyoung Kwon, Ph.D.

Report Issued:

March, 2008

The interpretations or opinions expressed represent the best judgment of OMNI Laboratories and assumes no responsibility and makes no warranty or representations, as to the productivity, proper operation, or profitableness of any oil, gas or any other mineral well. These analyses, opinions or interpretations are based on observations and materials supplied by the client for whom this report is made.

Procedures for Triaxial Compressive Strength Test

The general procedures for triaxial compressive test are summarized in the following:

1) A right cylindrical plug is cut from the sample core and their ends ground parallel according to International Society for Rock Mechanics (ISRM) and American Society for Testing and Materials (ASTM) standards. A length to diameter ratio of 2:1 is recommended to obtain representative mechanical properties of the sample, which is also recommended by ASTM and ISRM. Physical dimensions of the specimen are recorded and the specimen is saturated with simulated formation brine.

2) The specimen is then placed between two endcaps and a heat-shrink jacket is placed over the specimen.

3) Axial strain and radial strain devices are mounted in the endcaps and on the lateral surface of the specimen, respectively.

4) The specimen assembly is placed into the pressure vessel and brought into the contact with a loading piston that allows application of axial load.

5) Confining pressure is increased to the desired hydrostatic testing pressure.

6) Measure ultrasonic velocities at the hydrostatic confining pressure.

7) Increase axial load at a constant rate until the specimen fails or axial strain reaches a desired amount of strain while confining pressure is held constant.

8) Reduce axial stress to the initial hydrostatic condition after sample fails or reaches a desired axial strain.

9) Reduce confining pressure to zero and disassemble sample.

SUMMARY OF TRIAXIAL COMPRESSIVE TESTS

saturated with 2% KCl

Ohio Division of Geological Survey
CO2 No. 1

Sample No.	Depth (ft)	Confining Pressure (psi)	Compressive Strength (psi)	Static Young's Modulus ($x10^6$ psi)	Static Poisson's Ratio
1-43R	7441.00	2600	41110	4.82	0.38
1-72R	8561.00	2950	45360	5.65	0.25

SUMMARY OF ULTRASONIC VELOCITIES AND DYNAMIC ELASTIC PARAMETERS

saturated with 2% KCl

Ohio Division of Geological Survey
CO2 No. 1

Sample No.	Depth (ft)	Confining Pressure (psi)	Bulk Density (g/cc)	Ultrasonic Wave Velocity				Dynamic Elastic Parameter			
				Compressional		Shear		Young's Modulus ($x10^6$ psi)	Poisson's Ratio	Bulk Modulus ($x10^6$ psi)	Shear Modulus ($x10^6$ psi)
				ft/sec	µsec/ft	ft/sec	µsec/ft				
1-43R	7441.00	2600	2.50	15282	65.44	9261	107.98	7.00	0.21	4.02	2.89
1-72R	8561.00	2950	2.45	14839	67.39	9176	108.98	6.62	0.19	3.56	2.78

Result of Triaxial Compressive Test

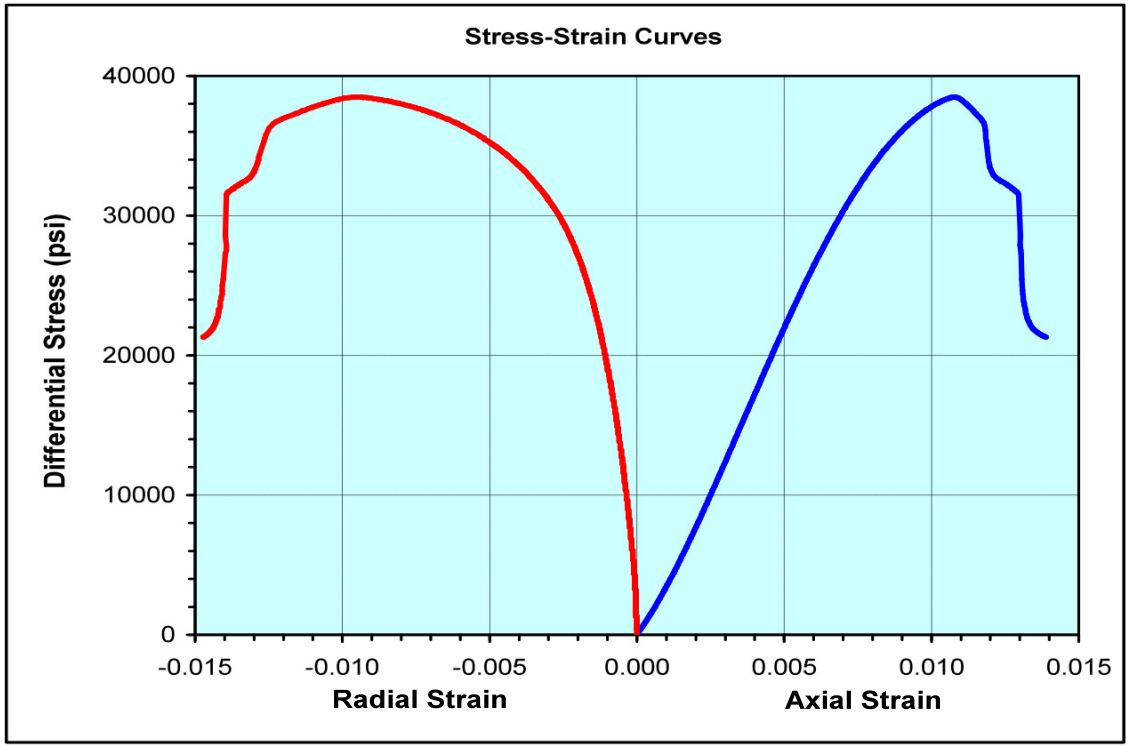

Company	Ohio GS
Project Title	CO2 No. 1
OMNI Project No.	HH-38266
Date	Mar., 2008

Sample No.	1-43R
Depth (ft)	7441.00
Saturation State	2% KCl
Confining Pressure (psi)	2600
Bulk Density* (g/cc)	2.50
Compressive Strength (psi)	41110
Young's Modulus ($x10^6$ psi)	4.82
Poisson's Ratio	0.38

* saturated

OMNI Laboratories

Result of Triaxial Compressive Test

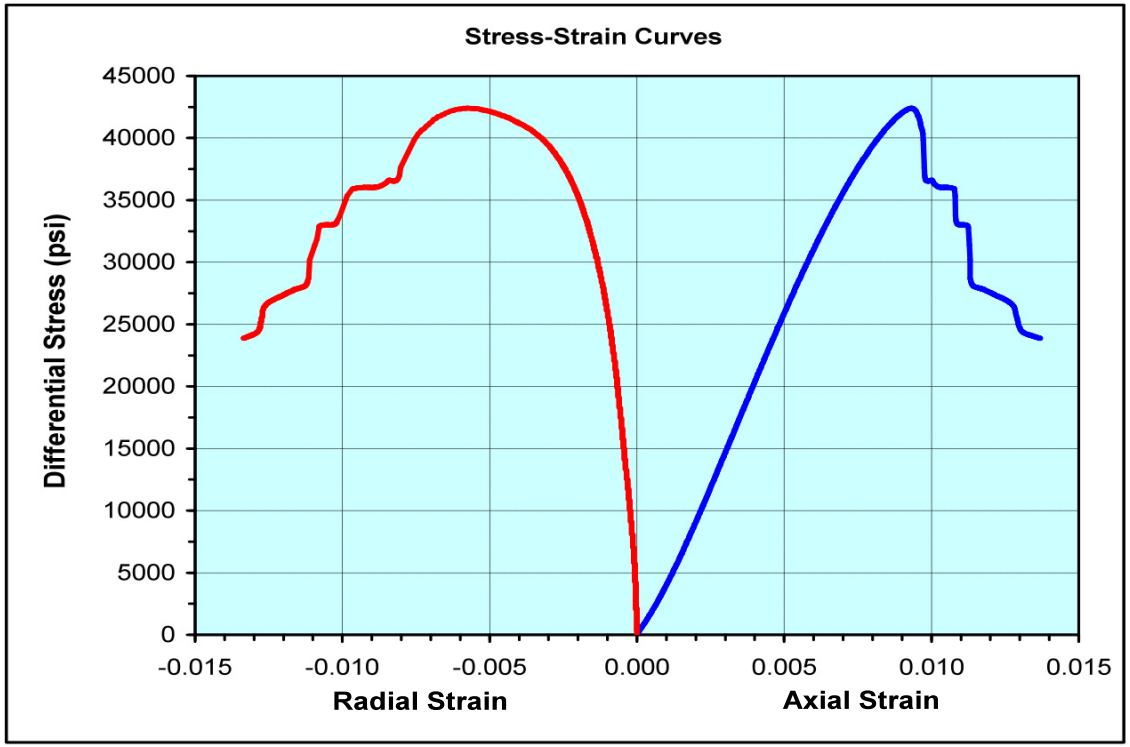

Company	Ohio GS
Project Title	CO2 No. 1
OMNI Project No.	HH-38266
Date	Mar., 2008

Sample No.	1-72R
Depth (ft)	8561.00
Saturation State	2% KCl
Confining Pressure (psi)	2950
Bulk Density* (g/cc)	2.45
Compressive Strength (psi)	45360
Young's Modulus ($x10^6$ psi)	5.65
Poisson's Ratio	0.25

* saturated

OMNI Laboratories

APPENDIX 3

PETROPHYSICAL ANALYSIS—CROSS PLOTS

Erica Howat—Battelle Memorial Institute, Columbus, Ohio

Geophysical wireline tools are often used in geologic explorations, whether it is for petroleum or carbon storage potential. However, these tools have limitations that must be accounted for when making a geologic assessment. For example, all three of the most common porosity logs, neutron, density and sonic, can be effected by natural gas in the formation. In addition, complex lithologies, such as shaley sands or carbonate sequences, can distort tool responses.

By using a technique called cross plotting some of the common log interpretation problems can be avoided. Cross plots simply take two separate measurements at a given depth and plot them versus each other. Placed on a specific grid, patterns can emerge which gives more detailed information about the lithology. These grids typically have lithology and porosity indicators which help to assess the geologic potential of the formations of interest.

Although numerous wireline logs were collected for the well, the most common and one of the more useful cross plots is taken from the traditional, density-neutron-resistivity log. This log was collected across the entire lower section of the well and the information was initially used for formation top identifications. Data was collected typically every six inches. Once formations of interest were identified, the neutron-density cross plot was employed. The results of these plots as well as brief analyses of each are below. More detailed analysis of the geology of each formation can be found in the body of this report.

Oriskany Sandstone:

The neutron-density cross plot indicates a low porosity (1-2%) sandstone with carbonate cement (fig. 1). The data cloud of 47 samples is tightly clustered, indicating high confidence in the data.

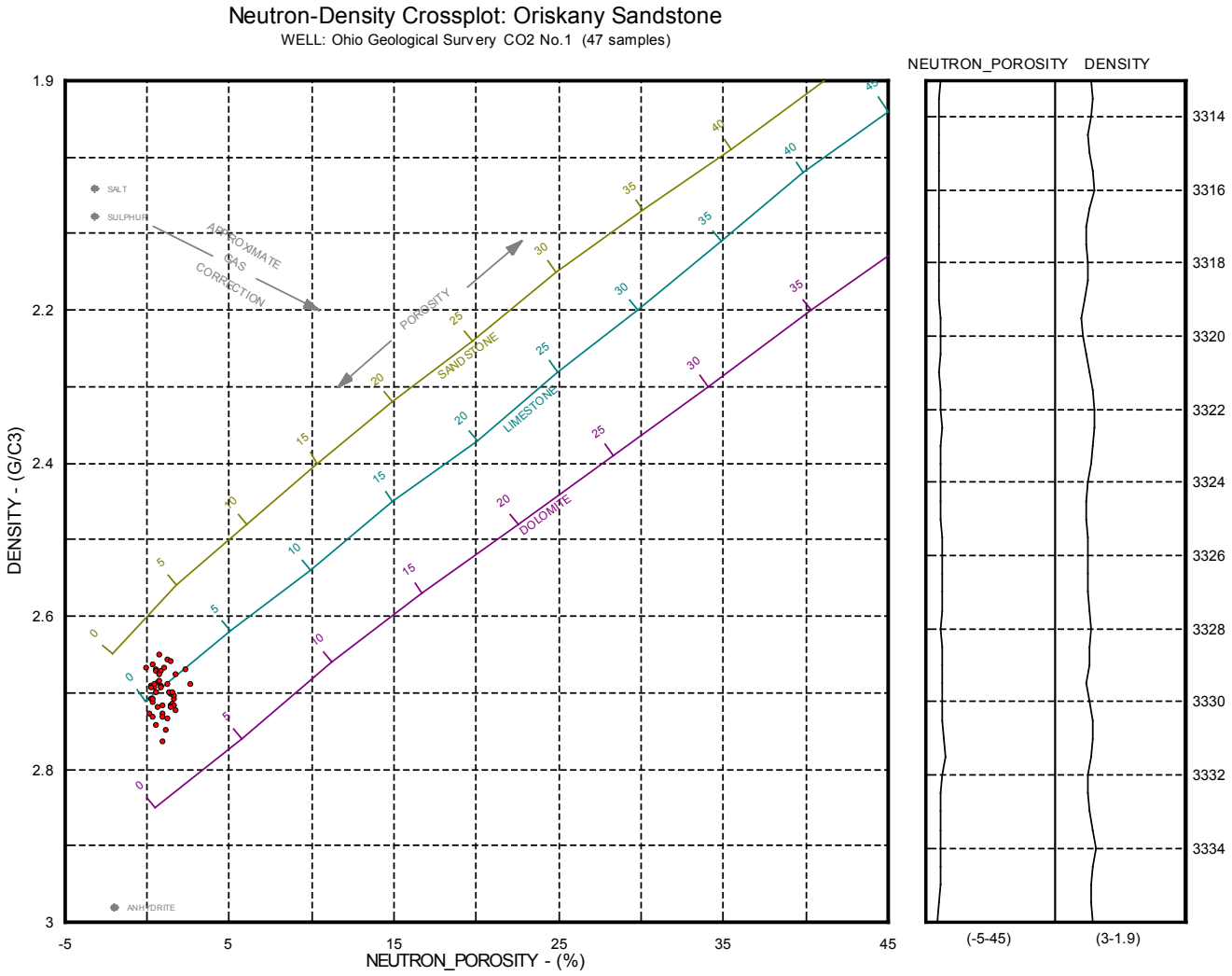

Figure 1

Lockport Dolomite:

The neutron-density cross plot indicates dolomite with low porosity, between 0 and 5% (fig. 2). The data cloud is well behaved with little scatter and includes 553 samples, again indicating high confidence in the data.

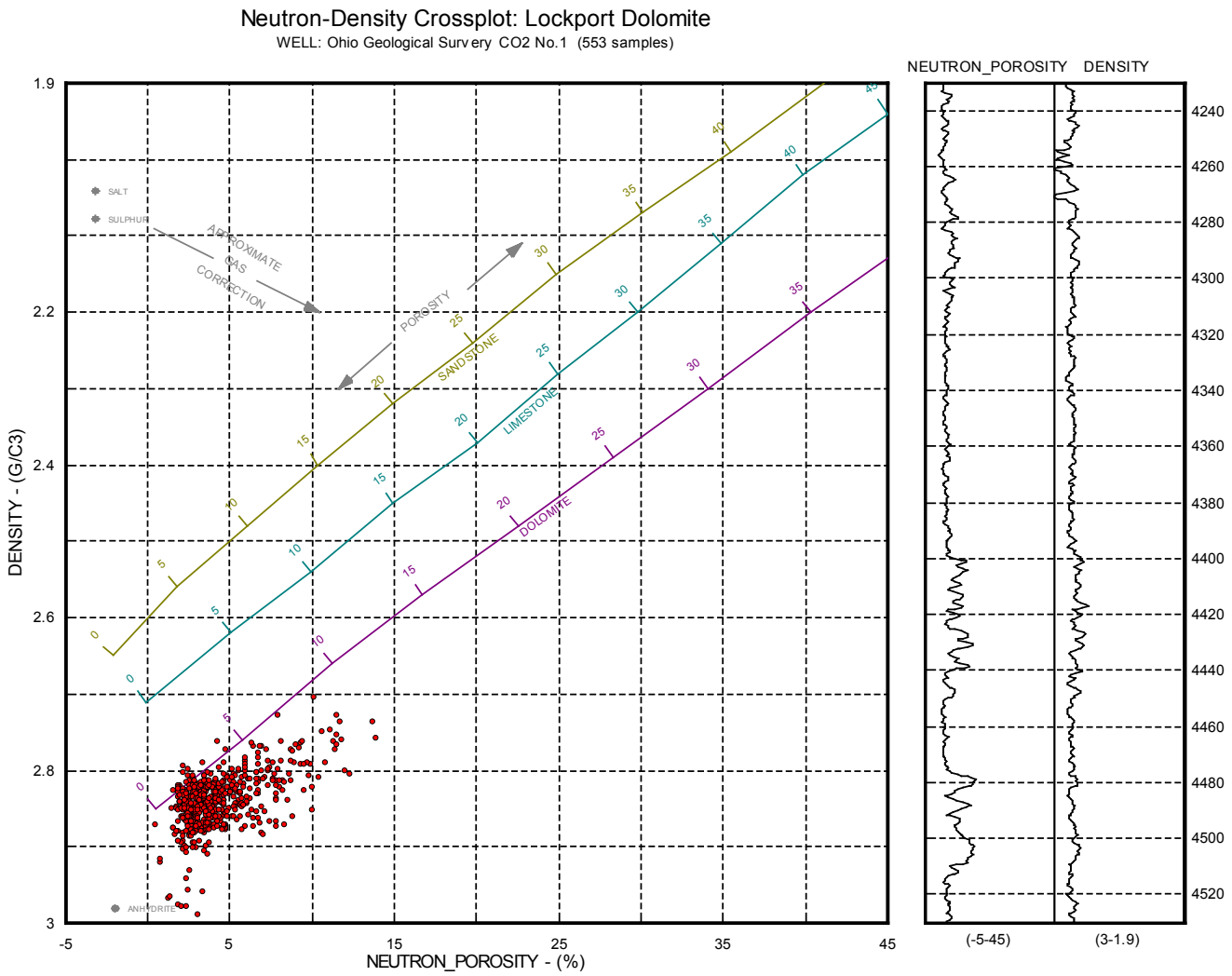

Figure 2

Bass Islands Dolomite:

The neutron-density cross plot composed of 74 samples is poorly defined and largely scattered (fig. 3). Further analysis is not recommended due to the high level of scatter and uncertainty in the data.

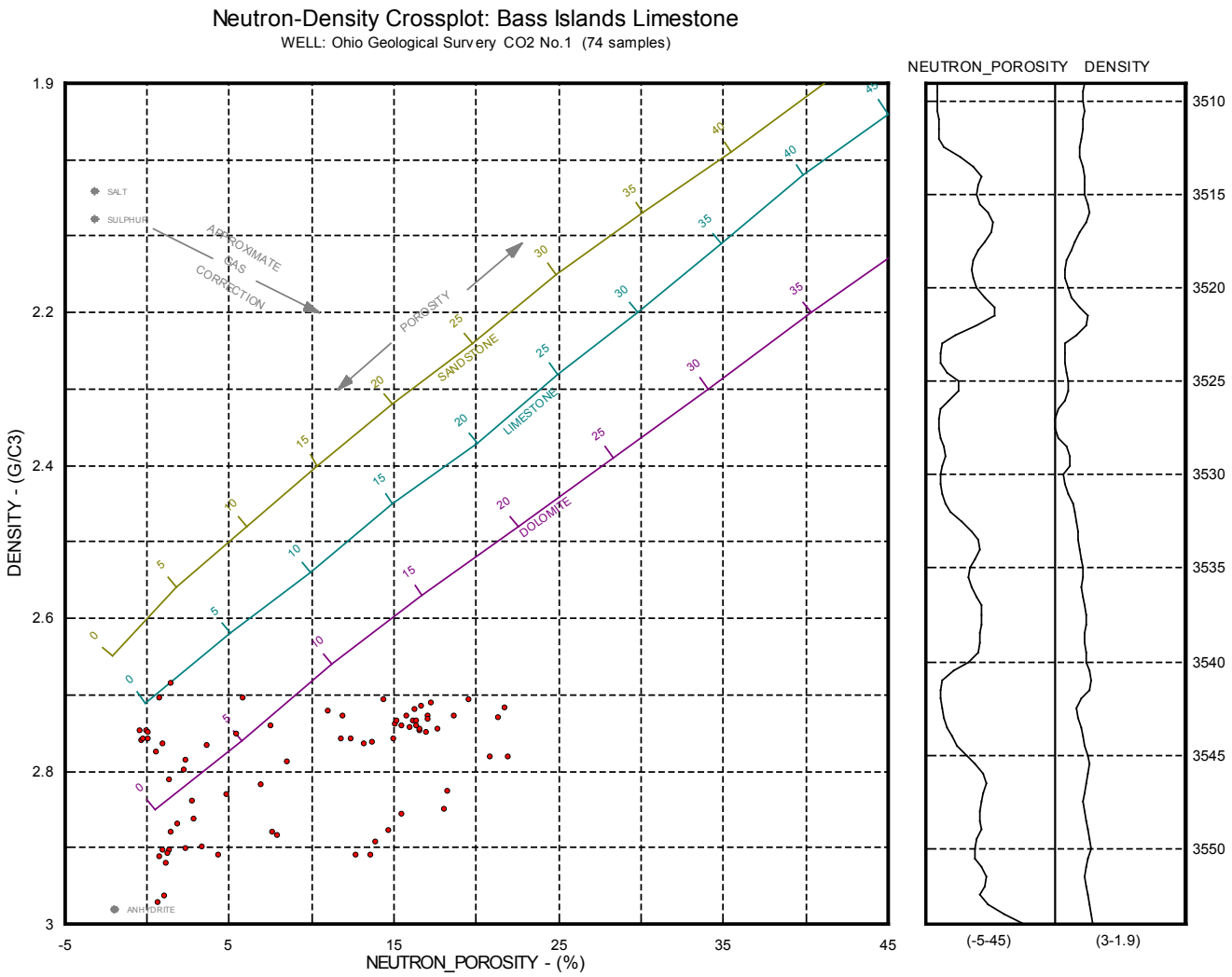

Figure 3

Beekmantown "A" dolomite:

The 209 samples plotted for the neutron-density cross plot indicate a dolomite with porosity ranging from about 2% up to about 8% (fig. 4). The data is fairly well behaved with a minimal amount of scatter.

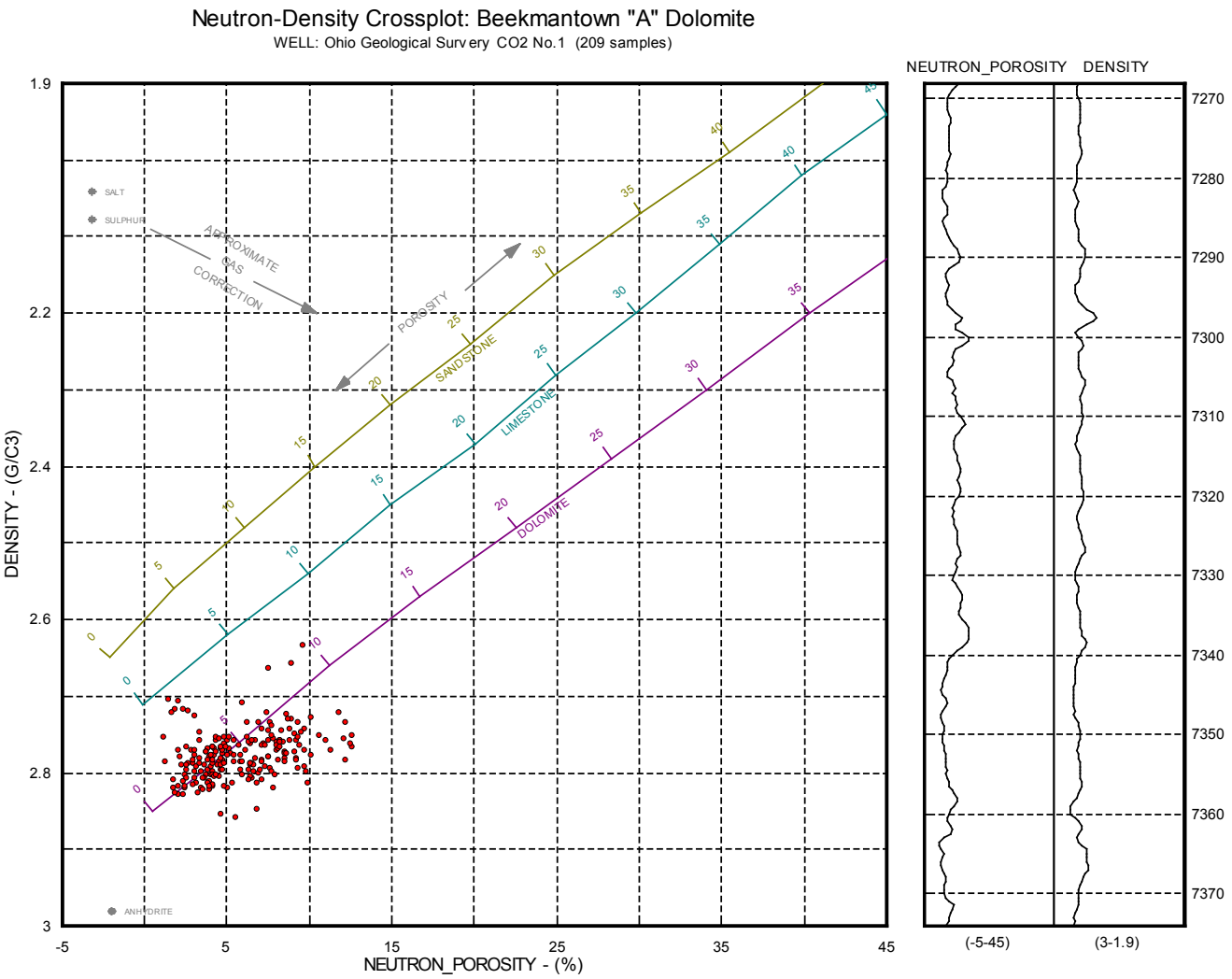

Figure 4

Beekmantown "B" dolomite:

Although there are fewer data points for the Beekmantown "B" dolomite (85 samples), the neutron-density cross plot behaves similarly to the "A" dolomite, likely indicative of similar lithology (fig. 5). The cross plot does indicate slightly higher porosity ranging from about 3% to about 10%.

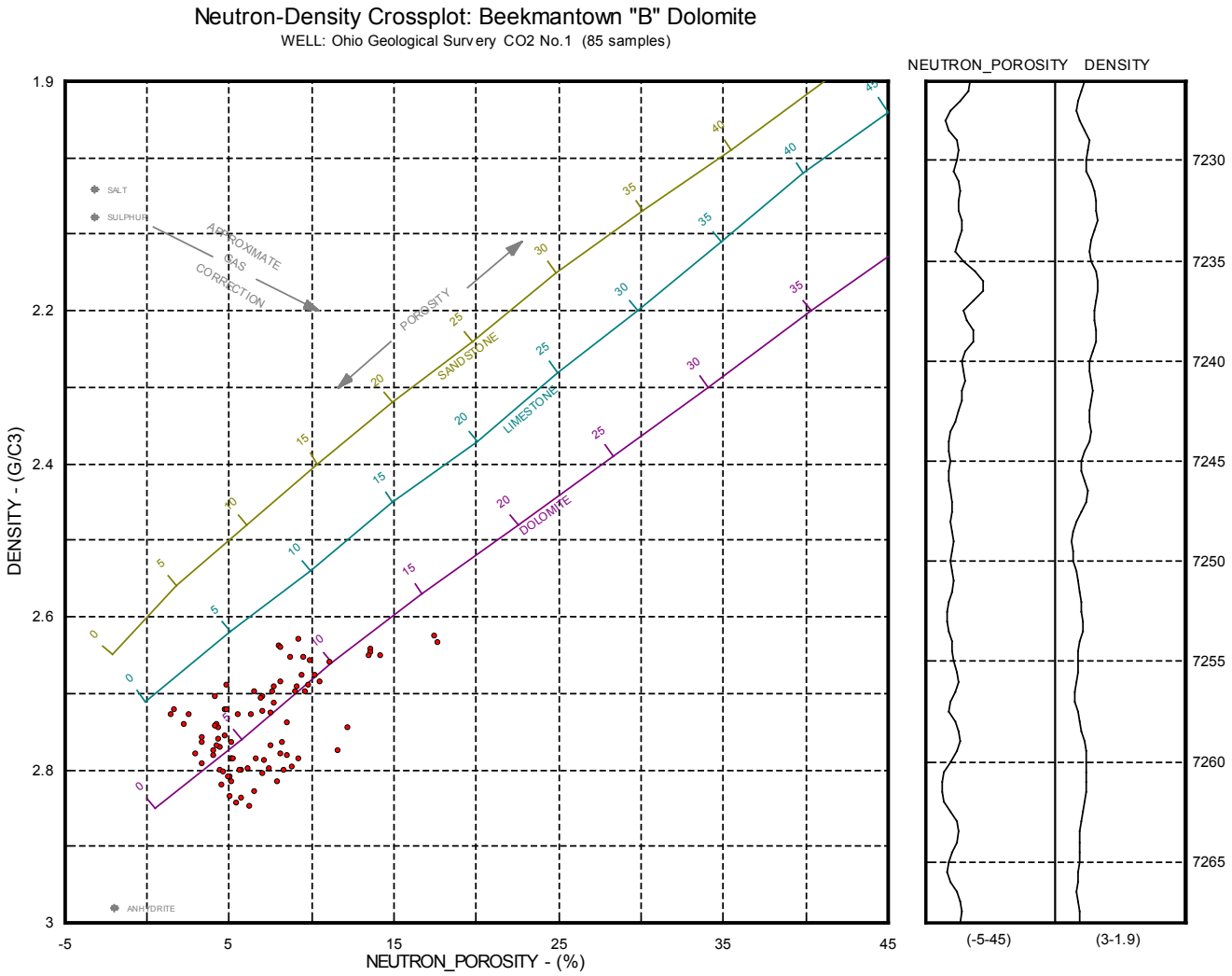

Figure 5

Rose Run sandstone:

The neutron-density cross plot for the Rose Run sandstone of 209 samples is scattered between the sandstone, limestone and dolomite lithology lines (fig. 6). Such scatter between lithology lines indicates either a high degree of carbonate cementation or the presence of carbonate interbeds. Porosity mainly scatters around 5% with some points higher up to 10%. Higher porosity data points lie in the area of the graph with very little carbonate influence.

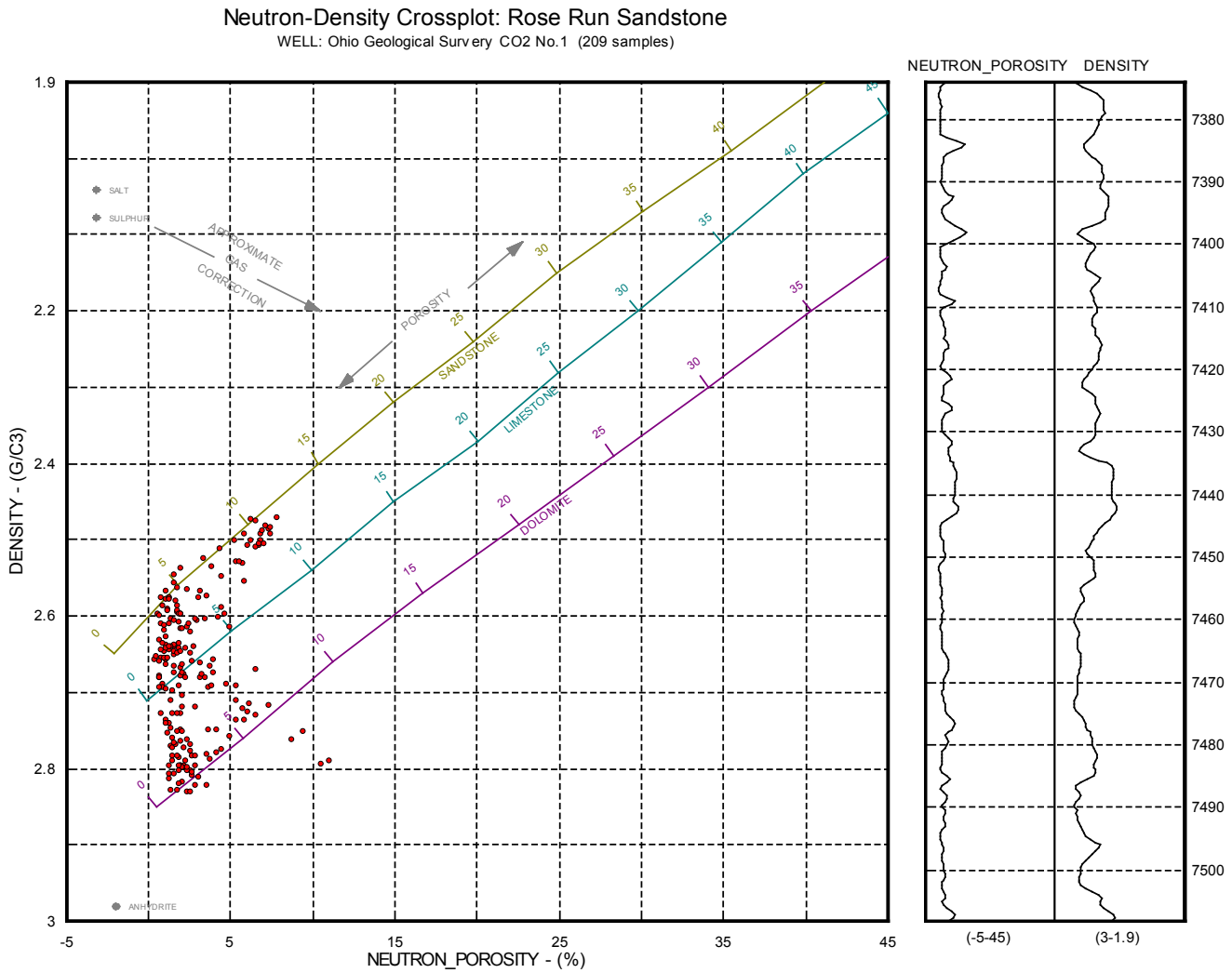

Figure 6

Cambrian basal sandstone:

There are relatively few data points (20 samples) in the neutron-density cross plot for the basal sandstone (fig. 7). Those data appear to cluster around 5% and scatter up to 10% porosity just below the sandstone line. This indicates fairly clean sandstone with the presence of either minor carbonate cement or very thin carbonate laminations.

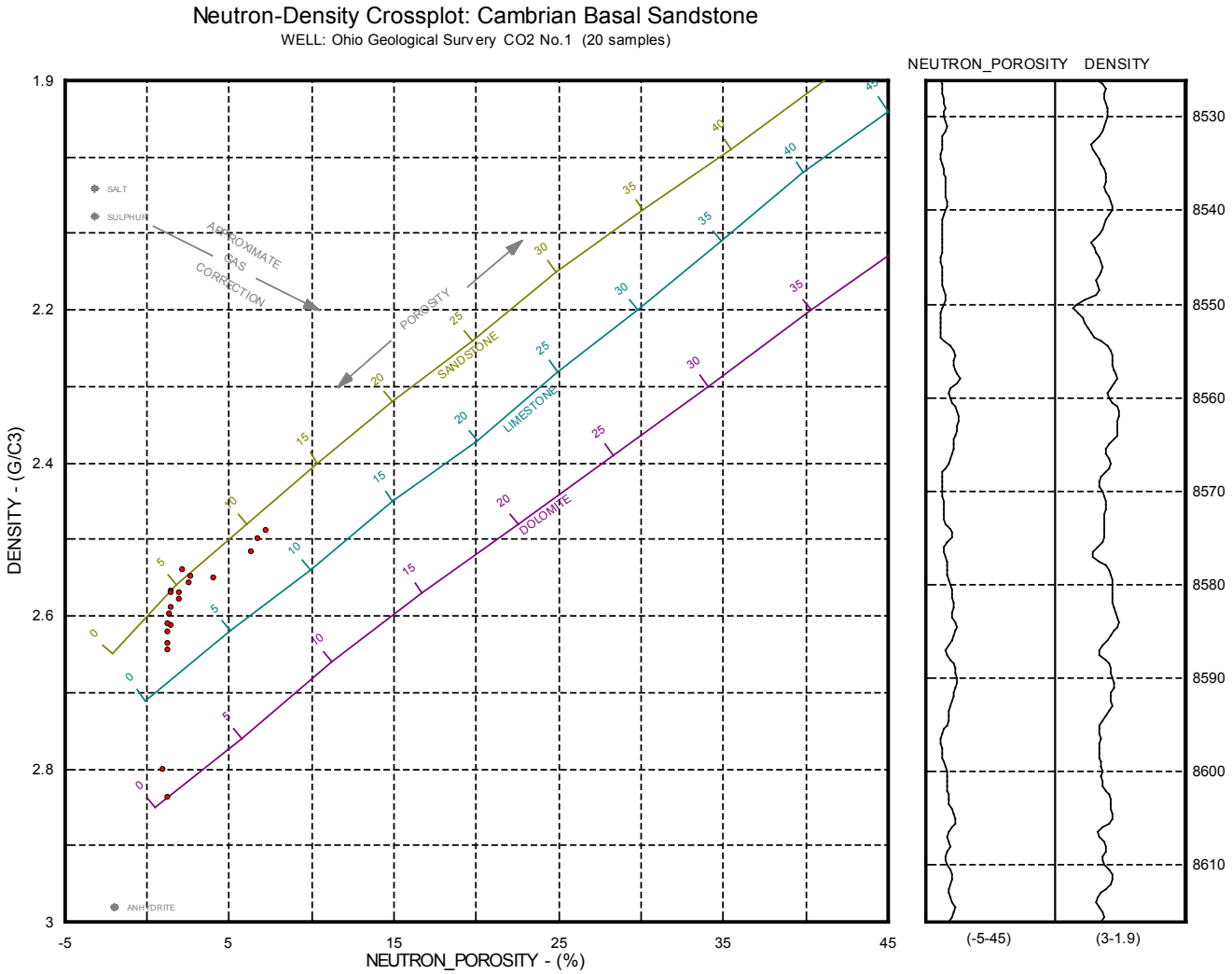

Figure 7

INTENTIONALLY BLANK

Battelle
The Business of Innovation

PNWD-4000

APPENDIX 4

Results of Detailed Hydrologic Characterization Tests Conducted within Ohio Geological Survey CO_2 No. 1 Well

F. A. Spane

Battelle
Pacific Northwest Division
Richland, Washington 99352

Prepared for
The Ohio Coal Development Office
Columbus, Ohio 43229
under Contract No. 53864A

October 2008

LEGAL NOTICE

This report was prepared by Battelle Memorial Institute (Battelle) as an account of sponsored research activities. Neither Client nor Battelle nor any person acting on behalf of either:

MAKES ANY WARRANTY OR REPRESENTATION, EXPRESS OR IMPLIED, with respect to the accuracy, completeness, or usefulness of the information contained in this report, or that the use of any information, apparatus, process, or composition disclosed in this report may not infringe privately owned rights; or

Assumes any liabilities with respect to the use of, or for damages resulting from the use of, any information, apparatus, process, or composition disclosed in this report.

Reference herein to any specific commercial product, process, or service by trade name, trademark, manufacturer, or otherwise, does not necessarily constitute or imply its endorsement, recommendation, or favoring by Battelle. The views and opinions of authors expressed herein do not necessarily state or reflect those of Battelle.

Abstract

This report provides the results of detailed hydrologic characterization tests conducted within selected perforated test intervals of the Ohio Geological Survey CO_2 No. 1 Well during July and August 2007. Detailed characterization tests performed included slug/drill-stem tests and constant-rate and constant-pressure injection and recovery tests. The objectives of the hydrologic test program were to provide detailed hydraulic and storage property information for regionally recognized sedimentary formations (Cambrian Basal sandstone and Rose Run formations) that are currently being examined for potential as candidate injection reservoirs for carbon sequestration applications. Characterization information obtained from this borehole testing program adds to the hydrogeologic understanding of the tested reservoirs from both a local and regional perspective.

Summary

Field-test characterization activities conducted within the Ohio Geological Survey CO_2 No. 1 Well[(a)] between July 19 and August 6, 2007, provided significant site specific characterization information concerning the sequestration potential of CO_2 fluids in selected, regionally recognized reservoir horizons. The characterization information obtained from the field-test program includes hydraulic and storage property information for selected test horizons within the Cambrian Basal sandstone and Rose Run formations. The principal hydraulic/storage parameters characterized during testing include transmissivity, hydraulic conductivity, permeability (intrinsic), and storativity. The field-test characterization was completed using a hydrologic test sequence approach that included short-duration, slug-injection/drill-stem (DST) recovery tests, used in conjunction with longer duration injection tests and test recoveries. Hydrologic tests were analyzed individually using standard analytical methods and collectively employing a test-history matching approach. The combination of both individual and test-sequence analyses provides a better means for flow model identification and determining best-estimate property values for the respective test intervals. Specific intervals tested include:

Test Unit	Stratigraphic Position	Test Depth, ft
Basal Sandstone	Total	8,526 to 8,613
Rose Run #1	Bottom	7,506 to 7,509
Rose Run #2	Middle	7,416 to 7,446
Rose Run #3	Upper	7,377 to 7,396
Composite Rose Run	Total	7,377 to 7,509

Testing complexities identified for some of the zones tested during the characterization phase include 1) high test system/formation fluid compressibility, due to the presence of gas (Basal sandstone, Rose Run #3), 2) moderate well-skin effects (Rose Run #2), 3) multi-layer, commingled reservoir conditions (composite Rose Run), and 4) transitional, non-radial flow conditions, possibly imposed by the partial penetration/perforation well completion (Rose Run #1 and #2). All test zones, except for the composite Rose Run, were successfully characterized with standard analytical methods. Average hydraulic-property estimates obtained from field testing are generally comparable and within the range of small-scale values obtained from wireline Combinable Magnetic Resonance (CMR) survey results and discrete sidewall cores obtained within the perforated intervals tested. The hydraulic property values obtained from the small-scale wireline PressureXpress test results consistently provided lower estimates in comparison to the other test characterization methods. The field-test-derived composite transmissivity summation value for the 28-ft perforated Rose Run test intervals of 0.93 ft^2/day (K = 0.033 ft/day; k = 10.7 milli-darcies) is very similar to the transmissivity estimate of 0.78 ft^2/day reported for the Rose Run at a deep characterization borehole located ~100 miles south of CO_2 No. 1 Well (Spane et al. 2006). This well

(a) The Ohio Geological Survey CO_2 No. 1 Well will be referred to as the CO_2 No. 1 Well hereafter.

(Mountaineer AEP #1) was also characterized with similar hydrologic test methods as employed at CO_2 No. 1 Well. No successful test results for the Basal sandstone were completed within this borehole for comparison with current test results obtained from CO_2 No. 1 Well. Qualitative open borehole tests for this stratigraphic horizon at AEP #1, however, suggest relatively low permeability conditions for this stratigraphic unit.

The radius of investigation of the hydrologic tests conducted at CO_2 No. 1 Well for boundary detection is variable and a function of the 1) duration and magnitude of the stress applied, 2) formation hydraulic and storage properties, and 3) test system/formation fluid compressibility. Of these parameters, the presence of gas and its large influence on total fluid compressibility greatly limits the radius of investigation of the imposed hydrologic test. For the individual test zone injection tests conducted at CO_2 No. 1 Well that were not impacted by the presence of high-compressibility fluid (gas) conditions, the radii of investigations are estimated to have ranged from ~25 ft (Rose Run #1) to ~90 ft (Rose Run #2). Test zones exhibiting high fluid-compressibility conditions of test systems/formations (i.e., Basal sandstone and Rose Run #3) are assumed of have radii of investigations of 10 ft or less. The radius of investigation for the shorter duration slug-injection/DST recovery tests would be considerably less than for the longer duration injection tests. The relative correspondence of hydraulic properties obtained from the smaller scale slug-injection/DST recovery tests with the larger scale, longer duration injection tests; however, suggest a degree of formational uniformity for the test intervals in the immediate vicinity of CO_2 No. 1 Well.

Pertinent test zone characterization results of importance include:

1) Well damage (well-skin effects) was evident in the well test analyses for two of the intervals tested and ranged from minor (Rose Run #1; $s_K = +0.4$) to moderate (Rose Run #2; $s_K = +13.7$) well-skin damage conditions.

2) Only one test interval (Rose Run #3) indicated hydraulic communication with the underlying perforated test interval (Rose Run #2).

3) Approximately 95 percent of the composite Rose Run zones tested is contained within the middle Rose Run section (i.e., Rose Run #2).

4) High formation compressibility was indicated for two of the test zones (Basal sandstone and Rose Run #3) and is indicative of the presence of multi-phase conditions within the test interval.

5) Test zones exhibiting high formation compressibility and the presence of gas are situated within the upper sections of their respective stratigraphic units.

Transient injection rates were calculated for both the Basal sandstone and Rose Run formations at CO_2 No. 1 Well, based on selected constant surface injection pressures and best-estimate hydraulic/storage properties obtained from the field-test-derived results. For the Basal sandstone, the predicted injection rates are extremely low, ranging from 0.60 to 2.16 gpm, after 100 days of continuous injection for the surface injection pressure range of 250 to 1,960 psi examined, respectively. The low predicted injection rates are primarily a function of the low transmissivity value calculated for the Basal

sandstone at CO_2 Well No. 1. Because of the higher estimated transmissivity for the composite Rose Run, predicted injection rates are higher and range from 6.01 to 19.19 gpm after 100 days of continuous injection for the surface-injection pressure range of 250 to 1,700 psi examined, respectively.

Acknowledgments

Several Pacific Northwest National Laboratory staff members contributed to the hydrologic tests presented in this report. In particular, Paul Thorne provided field support during the initial phase of testing and technical peer review. Wayne Cosby and Bruce Bjornstad also provided editorial comments and graphics support for the technical report preparation, respectively.

In addition, Battelle Columbus staff members contributed significantly to performance of the field-testing program. Danielle Meggyesy implemented and managed the daily coordination of subcontractors and participants involved in the field-testing program. Thanks are also extended to Phil Jagucki for providing financial and project management support during the course of the test program. The field contributions of Artur Kraszewski, of Universal/Eastern Reservoir Services, who was responsible for the maintenance of the surface and downhole test equipment used during the field-testing program, are also recognized. Background well construction and subsurface geologic information presented in this report were provided by Ron Riley, and technical peer review comments were also provided by Larry Wickstrom, both of the Ohio Geological Survey.

Acronyms

CMR	Combinable Magnetic Resonance
DOE	U.S. Department of Energy
EDT	Eastern Daylight Time
I.D.	Inside diameter
KB	Kelley Bushing datum
KGS	Kansas Geological Survey
MSL	mean sea level
OGS	Ohio Geological Survey
O.D.	outside diameter
PNNL	Pacific Northwest National Laboratory

Nomenclature

A_i = area of test investigation; L^2
b = aquifer thickness; L
C_D = dimensionless wellbore storage constant
C_f = rock matrix compressibility; L^2/F
C_{fw} = formation fluid compressibility; L^2/F
C_{ts} = total compressibility of the shut-in, well test system; L^2/F
g = acceleration due to gravity; L/T^2
k = intrinsic permeability; L^2
K = hydraulic conductivity; L/T
K_h = hydraulic conductivity in the horizontal direction; L/T
L = leakage response; dimensionless
n = formation porosity; dimensionless
P_{sf} = static formation pressure; F/L^2
psi = pounds per square inch
Q = injection rate; L^3/T
r_c = well casing radius; L
r_{eq} = equivalent well casing radius; L
r_i = radius of test investigation; L
r_w = radius of well/borehole; L
S = storativity; dimensionless
S_i = storativity of layer i within a mult-layer reservoir; dimensionless
s_K = well skin; dimensionless
S_s = specific storage; 1/L
t = elapsed injection time; T
t' = elapsed recovery time ; T
T = transmissivity; L^2/T
T_i = transmissivity of layer i within a multi-layer reservoir; L^2/T
V_{ts} = volume of closed, in-well test system
α_i = proportional storativity contribution of layer i within multi-layer reservoir; dimensionless
β_i = proportional transmissivity contribution of layer i within multi-layer reservoir; dimensionless
γ_{fw} = formation fluid specific-weight density; F/L^3
ΔP = constant-head injection pressure; FT/L^2
μ_{fw} = formation fluid dynamic viscosity; FT/L^2
ρ_w = formation fluid density; F/L^3

Contents

Abstract iii

Summary v

Acknowledgments ix

Acronyms xi

Nomenclature xiii

1.0 Introduction 1.1

1.1 Borehole Drilling and Completion History 1.1

1.2 Test Zone Preparation 1.2

2.0 Background 2.1

2.1 Characterization Design 2.1

2.2 Borehole Hydrologic Test Equipment 2.2

2.3 Reservoir Zone Test Methods 2.5

2.3.1 Slug/DST Methods 2.5

2.3.2 Constant-Rate Injection Test 2.6

2.3.3 Constant-Head (Pressure) Injection Test 2.7

2.3.4 Test History Matching 2.9

2.3.5 Property Conversions/Calculations/Assumptions 2.9

3.0 Hydrologic Test Results 3.1

3.1 Basal Sandstone 3.1

3.1.1 Constant-Head Injection Test 3.3

3.1.2 Slug-Injection Test 3.5

3.1.3 Test History Match 3.6

3.2 Rose Run #1 ..... 3.8

3.2.1 Constant-Head Injection 3.8

3.2.2 Slug-Injection/DST 3.12

3.2.3 Test History Match 3.13

3.3 Rose Run #2 ..... 3.15

3.3.1 Constant-Head Injection 3.15

3.3.2 Slug-Injection/DST 3.21

3.3.3 Test History Match 3.22

3.4 Rose Run #3 ..... 3.24

3.4.1 Constant-Head Injection 3.24

3.4.2 Slug-Injection/DST 3.27
3.4.3 Test History Match 3.28

3.5 Composite Rose Run 3.30
3.5.1 Constant-Head Injection 3.31
3.5.2 Slug-Injection/DST 3.33

4.0 Predicted Injection Rates 4.1

4.1 Basal Sandstone 4.2

4.2 Rose Run 4.2

5.0 Conclusions 5.1

5.1 Basal Sandstone 5.2

5.2 Rose Run 5.2

6.0 References 6.1

Appendix A: Detailed Test Summary/Activity Tables for the CO_2 No. 1 Well A.1

Appendix B: Selected Pictures of Test Equipment Used at the CO_2 No. 1 Well B.1

Appendix C: Selected Analysis Figures for CO_2 No. 1 Well C.1

Appendix D: Lower Bridge Plug Pressure Plots for CO_2 **No.** 1 Well D.1

Figures

1.1. Location Map for the Ohio Geological Survey CO_2 No. 1 Well 1.3

1.2. General Stratigraphy and Well As-Built for CO_2 No. 1 Well 1.4

2.1. Simulated Pressure Response for a Test Characterization Sequence 2.2

2.2. Drawing of Downhole Pressure Probe Assembly Deployment During Injection (a) Shut-in Tool Open, and During Recovery (b) Shut-In Tool Closed 2.4

2.3. Characteristic Log-Log Drawdown and Drawdown Derivative Plots for Various Hydrogeologic Formation and Boundary Conditions 2.8

3.1. CO_2 No. 1 Well Test Event Pressure History Plot: Basal Sandstone 3.3

3.2. CO_2 No. 1 Well Test History Analysis Match: Basal Sandstone 3.7

3.3. CO_2 No. 1 Well Test History Sensitivity Analysis: Basal Sandstone 3.7

3.4. CO_2 No. 1 Well Test Event Pressure History Plot: Rose Run #1 ..... 3.9

3.5. CO_2 No. 1 Well Test History Analysis Match: Rose Run #1 ..... 3.14

3.6. CO_2 No. 1 Well Test History Sensitivity Analysis: Rose Run #1 ..... 3.14

3.7. CO_2 No. 1 Well Test Event Pressure History Plot: Rose Run #2 ..... 3.16

3.8. CO_2 No. 1 Well Test History Analysis Match: Rose Run #2 ..... 3.23

3.9. CO_2 No. 1 Well Test History Sensitivity Analysis: Rose Run #2 ..... 3.23

3.10. CO_2 No. 1 Well Test Event Pressure History Plot: Rose Run #3 ..... 3.25

3.11. CO_2 No. 1 Well Test History Analysis Match: Rose Run #3 ..... 3.29

3.12. CO_2 No. 1 Well Test History Sensitivity Analysis: Rose Run #3 ..... 3.30

3.13. CO_2 No. 1 Well Test Event Pressure History Plot: Composite Rose Run 3.31

4.1. Comparison of Predicted Transient Injection Rates for the Basal Sandstone at CO_2 No. 1 Well at Selected Surface Injection Pressures 4.5

4.2. Comparison of Predicted Transient Injection Rates for the Composite Rose Run at CO_2 No. 1 Well at Selected Surface Injection Pressures 4.6

5.1. Permeability Comparison Plot: Field Testing, CMR and PressureXpress Surveys, and Sidewall-Core Sample Results: Basal Sandstone 5.4

5.2. Permeability Comparison Plot: Field Testing, CMR and PressureXpress Surveys, and Sidewall-Core Sample Results: Rose Run Sandstone 5.5

Tables

2.1. Summary of Single-Well, Hydrologic Test Methods Used for Reservoir Zone Characterization (modified from Reidel et al. 2002) 2.3

3.1. CO_2 No. 1 Well: Hydrologic Testing/Analysis Summary: Basal Sandstone (Perforated Zone: 8,526 to 8,613 ft bKB[(a)]) 3.2

3.2. CO_2 No. 1 Well: Hydrologic Testing/Analysis Summary: Rose Run #1 (Perforated Zone: 7,506 to 7,509 ft bKB) 3.10

3.3. CO_2 No. 1 Well: Hydrologic Testing/Analysis Summary: Rose Run #2 (Perforated Zone: 7,416 to 7,446 ft bKB) 3.17

3.4. CO_2 No. 1 Well: Hydrologic Testing/Analysis Summary: Rose Run #3 (Perforated Zone: 7,377 to 7,396 ft bKB) 3.26

4.1. Predicted Transient Injection Rates for the Basal Sandstone at CO_2 No. 1 Well, at Selected Surface Injection Pressures 4.3

4.2. Predicted Transient Injection Rates for the Composite Rose Run at CO_2 No. 1 Well, at Selected Surface Injection Pressures 4.4

5.1. Intrinsic Permeability Test Zone Comparison by Characterization Method 5.3

1.0 Introduction

This report provides the description and results of hydrologic tests conducted within a deep characterization borehole (i.e., the Ohio Geological Survey [OGS] CO_2 No. 1 Well[(a)]) drilled in eastern Ohio by the Ohio Department of Natural Resources, Division of Geological Survey (DGS), and Battelle (Columbus, Ohio). The primary objective of the characterization borehole was to provide initial hydraulic (injectivity) and storage property information for several regionally recognized saline water formations for assessing their potential as candidate injection reservoirs for CO_2 sequestration applications. This characterization is in response to national initiatives sponsored by the U.S. Department of Energy (e.g. FutureGen and Regional Partnership programs), which focus on the reduction of CO_2 emissions from carbon-based electrical power generation plants through the capture and subsurface sequestration of CO_2 within deep geologic formations.

The Ohio Geological Survey test well (CO_2 No. 1 Well) is located in southern Tuscarawas County in eastern Ohio (Figure 1.1). As noted by Riley,[(b)] the borehole site location was selected for a number of technical and cost-related reasons, including:

- The subsurface geology is representative of the large portion of eastern Ohio, with no known wells drilled into the Precambrian basement complex within the county.
- A thick, complete stratigraphic section exists (2,500 to 9,000 ft) with multiple, potential candidate sequestration injection horizons available.
- The site is located within a stable aseismic area with no known geologic faults.
- There is good transportation and accessibility to the site for supporting drilling and testing activities.
- Only limited, quantitative well injection/storage capacity information is available, prompting the need for a detailed characterization borehole.

1.1 Borehole Drilling and Completion History

Drilling of the Ohio Geological Survey CO_2 No. 1 Well (American Petroleum Identification # 3415725334) began on May 10, 2007, and continued until reaching the Precambrian crystalline rock basement complex at a depth of 8,695 feet on June 9, 2007. Upon cessation of drilling activities, a suite of wireline geophysical surveys was performed by Schlumberger, Inc. within the open-borehole section of the well (i.e., 4,941 to 8,695 ft). Based on the results of the wireline surveys, 82 sidewall cores were subsequently drilled within selected prospective injection reservoirs and caprock horizons as part of the general borehole characterization assessment. The sidewall cores were submitted for detailed laboratory analyses, including quantitative measurements of porosity and permeability, total organic content (TOC), thermal maturity, and rock mechanics. The results of the laboratory analyses and wireline geophysical

---

(a) The Ohio Geological Survey CO_2 No. 1 Well will be referred to as the CO_2 No. 1 Well in the remainder of this report.

(b) Ron Riley. 2008. "Background Information Concerning the Ohio Geological Survey CO_2 No. 1 Well." Personal communication, May 1, 2008.

survey results are not provided in this report, but will be presented in other subcontractor or Ohio Geological Survey technical reports.

Following completion of the sidewall coring operations, a 4.5-in. outside diameter (O.D.) casing was installed within the borehole from ground surface to the total depth, and the casing annulus was cemented from the borehole bottom to a depth of approximately 6,600 ft below ground surface (note: depth to top of cement calculated based on the volume of cement used). Figure 1.2 shows the stratigraphy, associated locations of the sidewall cores, and well as-built completion conditions for the CO_2 No. 1 Well, at the onset of the hydraulic test characterization program. Following cementing of the 4.5-in. casing, sections within the Cambrian Basal sandstone and overlying Rose Run sandstone were perforated, acid-wash developed, and tested for detailed hydraulic-property characterization. Details pertaining to the test zone preparation and results for the hydraulic test characterization are contained in report Sections 1.2 and 3.0, respectively. Following completion of the hydraulic test characterization on August 6, 2007, the well was turned over to Artex, the independent well operator and owner of the oil and gas mineral rights.

1.2 Test Zone Preparation

After cementing the 4.5-in. casing string, selected depth sections within two sandstone formations (i.e., the Cambrian Basal sandstone and Rose Run formations) were perforated based on inferred permeability conditions obtained from wireline geophysical survey results. The sandstone sections were perforated, acid-washed developed, and hydraulically tested sequentially. Pertinent information concerning test zone perforation and development for the Basal and Rose Run sandstones is presented in Appendix A Tables A.1 and A.5, respectively. Briefly stated, six depth intervals were perforated on July 18, 2007, within the Basal sandstone: 8,526 to 8,531 ft, 8,536 to 8,542 ft, 8,554 to 8,566 ft, 8,566 to 8,576 ft, 8,578 to 8,587 ft, 8,602 to 8,604 ft, and 8,608 to 8,613 ft. The zones were perforated with a Schlumberger perforation tool (shown in Appendix B Figure B.1) that produced two shot perforations per foot within the designated depth intervals. A packer tubing string was used for perforated zone isolation, and 850 gallons of HCL acid were subsequently injected into the composite Basal sandstone perforated intervals for test zone development on July 19, 2007. Fluid was swabbed from the composite perforated zone after acid injection and continued to July 20, 2007. Fluid weight density, pH, and chloride concentration were monitored within the discharge water removed during swabbing as a qualitative indicator of test zone development. A total of 3,970 gallons (94.5 barrels) of test system fluid were removed during the swabbing activity.

Following the development and subsequent hydraulic testing of the Basal sandstone, a bridge plug packer was set above the Basal sandstone at a depth of 7,530 ft, and the Rose Run sandstone was perforated. In all, five Rose Run depth intervals were perforated on July 23, 2007: 7,377 to 7,380 ft, 7,387 to 7,396 ft, 7,416 to 7,418 ft, 7,435 to 7,446 ft, and 7,506 to 7,509 ft. The zones were perforated following the same procedure, and the Schlumberger perforation tool was used as it was previously during the Basal sandstone perforation. The bridge plug packer and a packer tubing string were used for perforated zone isolation, and 800 gallons of HCL acid were subsequently injected into the composite Rose Run perforated intervals for test zone development on July 24, 2007. Swabbing of fluid from the composite perforated zone was initiated after acid injection and continued to July 25, 2007. Fluid weight density, pH, and chloride concentration were monitored within the discharge water removed during

swabbing as a qualitative indicator of test zone development. A total of 10,330 gallons (246 barrels) of test system fluid were removed during the swabbing activity.

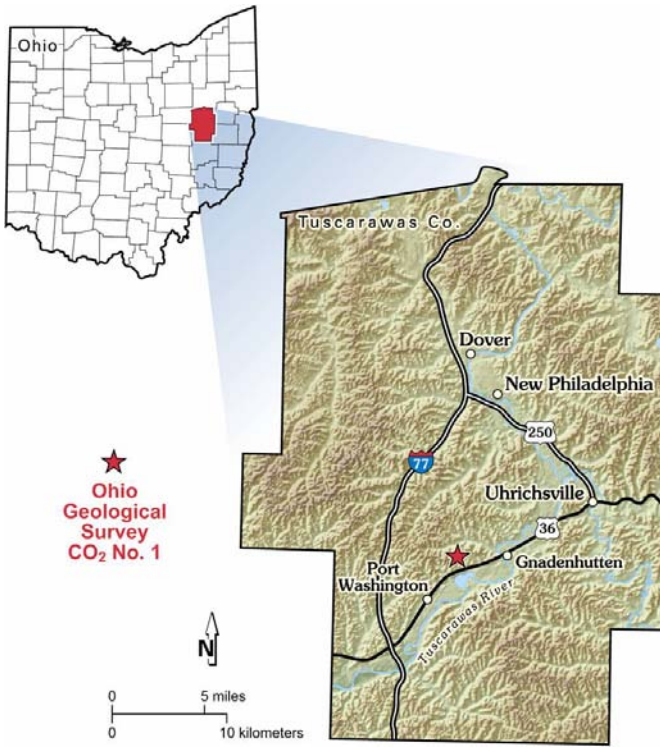

Figure 1.1. Location Map for the Ohio Geological Survey CO_2 No. 1 Well

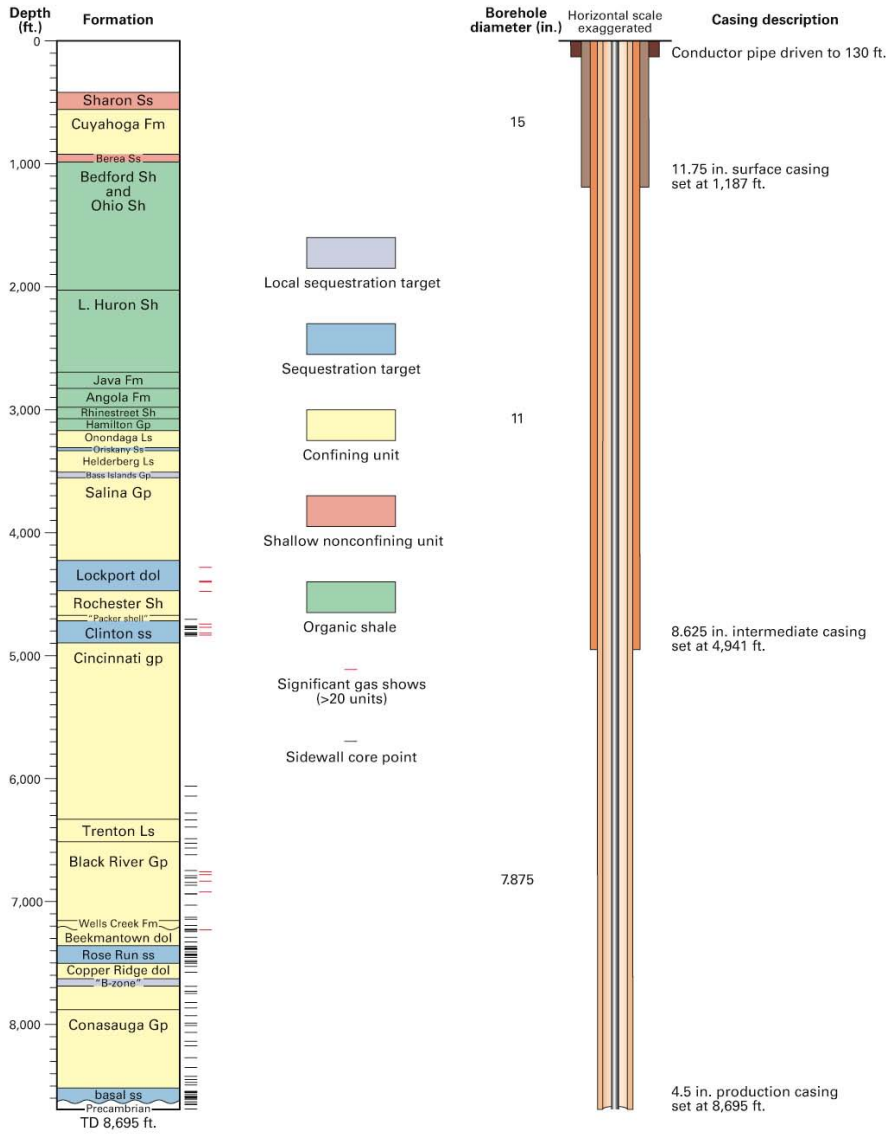

Figure 1.2. General Stratigraphy and Well As-Built for CO_2 No. 1 Well

2.0 Background

This section describes the detailed hydrologic field-testing program conducted at CO_2 No.1 Well. The field-testing program follows the guidance and rationale originally presented in the field-testing work plan by Gupta (2003), which was designed for similarly completed deep reconnaissance boreholes within the Ohio Valley region. The primary objective of the field-testing program was for quantitative determination of *in situ* hydraulic and storage properties of candidate reservoir horizons (i.e., Cambrian Basal and Rose Run sandstones) that have been identified within the region for potential CO_2 sequestration. The principal hydraulic/storage parameters to be characterized during testing include transmissivity, hydraulic conductivity, intrinsic permeability, and storativity (porosity/storage volume). Additionally, the composite and individual testing of separate perforated test intervals provided the opportunity to assess the hydraulic connectedness of several of the more pervious sandstone units within the encompassing sandstone formation.

2.1 Characterization Design

Initially, the characterization program at CO_2 No. 1 Well was design based on the assumption of using a real-time downhole pressure monitoring system, which can be used to monitor and re-direct the progress of characterization tests. Figure 2.1 shows an initial simulation of a proposed test characterization program, including an initial slug withdrawal test, which would be analyzed in the field for test design of the subsequent, more areally investigative, multi-stage constant-rate, injections test and recovery (fall-off test). The figure is based on hydraulic and storage characteristics estimated for similar formations and test horizons characterized at the Mountaineer AEP #1 borehole in West Virginia as reported in Spane.[(a)] Using a characterization program that includes field hydrologic test methods having different scales-of-investigation (i.e., "radius of influence") and varying degrees of hydraulic-property sensitivity provides a means for assessing local vs. intermediate-scale conditions surrounding the borehole location (see Table 2.1).

As will be discussed in Section 3.2, a reliable real-time downhole pressure monitoring system could not be secured, and only a test system equipped with downhole memory gauges could be obtained for the hydraulic test characterization program at CO_2 No. 1 Well. Because downhole pressure responses can only be observed after the tests are completed and the memory gauges are removed from the borehole, a fixed hydraulic test characterization sequence was designed for the test intervals at CO_2 No. 1 Well. The test sequence included the following elements: 1) an initial, short-duration test-interval equilibration, 2) a single-step, 8- to 24-hr constant-rate injection test and recovery test, and 3) slug-injection/DST (drill-stem test) recovery test. This characterization program was designed to provide near-well to intermediate-scale hydraulic-property information within the scheduled time for borehole test characterization. Based on the unanticipated low injection rates for the initial test interval (Basal sandstone), the constant-rate injection phase (step 2) was further modified to a constant-head (pressure) injection test, which afforded more quantitative, observable surface control of the imposed hydrologic test.

(a) FA Spane. 2004. "The Ohio River Valley CO_2 Storage Project -Results of the Mountaineer AEP#1 Borehole Field Testing Characterization Program FY-2004." Letter Report to Neeraj Gupta, Battelle, August 24, 2004.

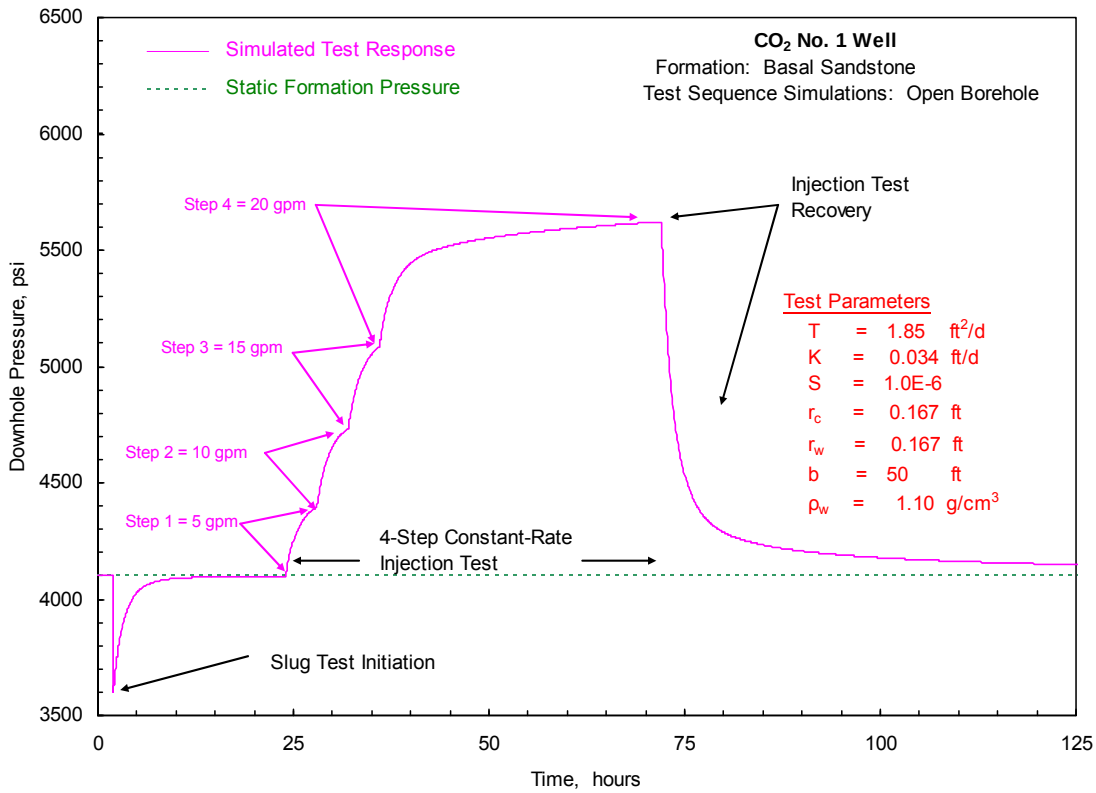

Figure 2.1. Simulated Pressure Response for a Test Characterization Sequence

2.2 Borehole Hydrologic Test Equipment

All hydrologic field tests were performed with a service rig placed over the CO_2 No. 1 Well. Test zone isolation for perforated intervals within the cemented 4.5-in. O.D. well casing was accomplished using a detached Baker Oil Tools bridge plug and overlying Baker Oil Tools tubing packer system. The test tubing string used with the tubing packer test system was 2 $^3/_8$-in. O.D. (1.995-in. nominal inside diameter [I.D.]), 4.7 lb, J-55 tubing. Two 15,000 psi Cal-Scan Services, LTD pressure memory gauges were suspended below the bridge plug for detecting possible cross-formational responses during testing. Two additional pressure memory gauges, attached to a slick-line probe assembly with seating collar, were lowered and set into a seating nipple located in proximity above the perforated test interval to produce test interval, shut-in conditions. Shut-in conditions were used during the initial, test-interval equilibration phase and during recovery phases following constant-rate or head injection. They were also used during DST recovery following slug-injection testing. The slick-line probe assembly was raised a short distance (e.g., 10 ft) above the tubing-string seating nipple to produce open test zone conditions for supporting the injection phases of the test characterization sequence. Figure 2.2 shows a drawing of the downhole pressure probe assembly positioning during active injection (shut-in tool open) and during recovery (shut-in tool closed) phases of testing. A picture of the actual pressure probe assembly, with seating collar, is shown in Appendix B Figure B.2.

Table 2.1. Summary of Single-Well, Hydrologic Test Methods Used for Reservoir Zone Characterization (modified from Reidel et al. 2002)

Test Method	Hydrologic Parameter[(a)]					Relative Test Scale		
	T	**K_h**	**S**	**L**	**P_{sf}**	**Local**	**Intermed.**	**Large**
Slug	√	√				√	√	
DST Recovery	√	√			√	√	√	
Constant-Rate Injection – Buildup & Recovery	√	√	√	x	√		√	√
Constant-Head Injection Buildup & Recovery	√	√	√	x	√		√	√
Test History Matching	√	√	√	x	√		√	√

(a) Nomenclature

T = test-interval transmissivity (injectivity)

K_h = equivalent hydraulic conductivity; equal to T divided by test-interval length

S = storativity; dimensionless

L = leakage response

P_{sf} = static formation pressure

Note: √ = provides quantitative information

x = only provides inferential/qualitative information

Clean brine water from surrounding deep wells was used for the injection phases of hydraulic test characterization. The brine water was stored in two 500-barrel-capacity surface tanks, and the brine water was pumped during testing from the bottom of the surface tanks to minimize entrainment of gas during the injection process. Surface injection rates and pressures were monitored and controlled using a multiple-line, flow-control system contained within an instrumented trailer shown in Appendix B Figure B.3. The multiple, flow-control system had the capability of controlling and resolving injection flow rates to ~0.01 gpm. A standard oil-field lubricator was mounted on the wellhead to produce a surface seal around the slick line, which was attached to the downhole pressure probe assembly. Surface pressure transducers mounted on the wellhead and surface injection flow system provided real-time monitoring of injection pressures during phases when injection was performed at pressures above land surface conditions. A surface injection pressure of +50 psig was arbitrarily selected as the designed maximum surface injection pressure to ensure that minimum threshold formation fracture pressures were not exceeded during testing.

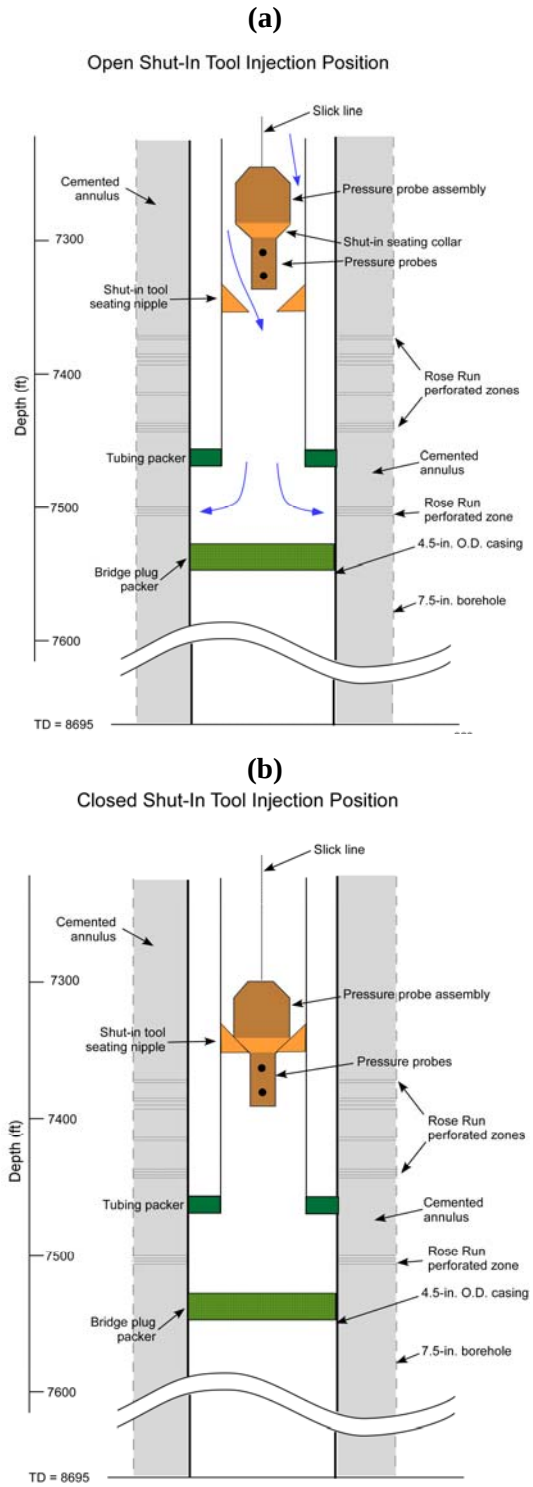

Figure 2.2. Drawing of Downhole Pressure Probe Assembly Deployment During Injection (a) Shut-in Tool Open, and During Recovery (b) Shut-In Tool Closed

2.3 Reservoir Zone Test Methods

The following is a general discussion of the various characterization and analytical methods used during the field borehole testing program and is taken from similar discussions presented in Spane.[(a)] Table 2.1 lists hydrogeologic parameters and relative investigative scale for the reservoir zone test methods used during testing of CO_2 No. 1 Well. Pertinent and specific test information pertaining to actual testing performed is presented in Section 3, "Hydrologic Test Results."

2.3.1 Slug/DST Methods

Because of their ease of implementation and relatively short duration, slug and/or DST (drill-stem) tests are commonly used to provide initial estimates of hydraulic properties (e.g., range and spatial/vertical distribution of hydraulic conductivity, K). Hydraulic properties determined using slug testing are representative of conditions relatively close to the borehole. For this reason, slug-test results are normally used to provide initial test-interval hydraulic-property characterization and provide information that can be used to design subsequent hydrologic tests having greater areas of investigation (e.g., slug interference [Novakowski 1989; Spane 1996], and constant-rate pumping or injection tests [Butler 1990; Spane 1993]).

To conduct this test, a known volume of test water is either instantaneously removed from (slug withdrawal) or added to (slug injection) the test interval. Because of the limitations imposed by the shut-in tool using a slick-line probe manipulation, only slug injection tests were actually viable for tests conducted at CO_2 No. 1 Well. The test was prepared by filling the test tubing string with test-system fluid to land surface with the pressure probe seated in the seating nipple, and the test interval effectively shut-in and isolated from the tubing string. The filling of the tubing string to the land surface represented an unknown over-pressure above test-interval conditions. The slug injection test was initiated by raising the pressure probe assembly a short distance (e.g., 10 ft) above the tubing-string seating nipple, initiating the slug injection of test-system fluid into the test interval. The open borehole/test system recovery following opening the shut-in tool represents the slug-test phase of the test. Analysis of the recovery response provides an estimate of the test-interval transmissivity (T), average hydraulic conductivity (K), and storativity (S). Estimates for storativity, however, are less certain, due to the test method's lower sensitivity to S. (Note: the effects of well skin, s_K, were not accounted for separately and were included within the estimate of S). The slug-test responses were analyzed with type-curve and deconvolution procedures discussed in Butler (1997) and Peres et al. (1989), respectively. Analyses of slug-test type curves presented in this report were generated using the Kansas Geological Survey (KGS) software program described in Liu and Butler (1995). Other relevant papers discussing the analysis of the slug-test phase of DST tests are provided in Ramey et al. (1975), Karasaki et al. (1988), and Ostrowski and Kloska (1989).

The lowering of the pressure probe assembly into the tubing seating nipple effectively reduces wellbore storage in the test response and accelerates recovery to static formation conditions. The recovery occurring during the subsequent closed shut-in tool period represents the DST recovery phase of

---

(a) FA Spane. 2004. "The Ohio River Valley CO_2 Storage Project -Results of the Mountaineer AEP#1 Borehole Field Testing Characterization Program FY-2004." Letter Report to Neeraj Gupta, Battelle, August 24, 2004.

the test. Normally, the DST shut-in recovery is initiated after the fluid-column recovery during the slug test has reached a value between 50 and 70 percent of the applied initial slug stress (i.e., in comparison to static formation conditions). Because memory gauge pressure probes were used during testing, an arbitrary open borehole (slug-injection) period of ~1 hour was used for most tests, which was followed by an arbitrary 1- to 2-hour DST (shut-in) recovery monitoring period. An analysis of the recovery buildup during later stages of the DST can be used to provide estimates of T, K, S, s_K, and (if pre-test trend conditions accounted for) static formation pressure conditions. DST results were analyzed using standard procedures presented in Earlougher (1977). Other relevant discussions pertaining to the recovery (shut-in) phase of DST testing are also presented in Correa and Ramey (1987) and Karasaki (1990).

2.3.2 Constant-Rate Injection Test

During constant-rate injection tests, test system water is injected into the test interval and regulated to maintain a constant, uniform rate. The pressure response within the borehole is monitored during the active injection (buildup) phase and during the subsequent recovery (fall-off) period following termination of injection. The analysis of the buildup and recovery pressure response within the test borehole provides a means for estimating hydraulic properties of the reservoir tested, as well as for discerning formational and non-formational flow conditions (e.g., wellbore storage, skin effects, presence of boundaries and leakage). Standard analytical methods used to analyze constant-rate tests include type-curve matching and straight-line methods.

Type-curve-matching methods are best applied to observation well data and not to injection wells because of the additional head losses that occur at the injection well. They can be used for single, injection well analyses, however, if certain assumptions pertaining to well efficiency (i.e., well-skin effects = 0) or the test interval (e.g., S is known) are made. This is the standard approach taken for single-well injection-test analysis within the petroleum industry. Type-curve-matching methods commonly used in the analysis of constant-rate test responses include those described in Theis (1935), Hantush (1964), Novakowski (1990), and Moench (1997). Analyses using constant-rate test type curves presented in this report were generated using the WTAQ program described in Moench (1997).

For straight-line analysis methods, the rate of change of water levels within the test system during injection and/or recovery is analyzed to estimate hydraulic properties of the test interval. Because well effects are constant with time during constant-rate tests, straight-line methods can be used to analyze quantitatively the water-level response at the injection well and any nearby observation wells. The semilog, straight-line analysis techniques commonly used are based either on the Cooper and Jacob (1946) method (for buildup analysis) or the Horner (1951) method for recovery analysis. It should be noted that the Horner method, which is commonly used in the petroleum industry, is identical to the Theis (1935) recovery method used in groundwater hydrology. These methods are theoretically restricted to the analysis of test responses from wells that fully penetrate nonleaky, homogeneous, isotropic, confined aquifers. Straight-line methods, however, may be applied under nonideal well and aquifer conditions if infinite-acting, radial flow conditions exist. Infinite-acting, radial flow conditions are indicated during testing when the change in pressure, at the point of observation, increases proportionately to the logarithm of time.

Log-log plots of water level or pressure versus time have traditionally been used for diagnostic purposes to examine pumping test drawdown or injection-test buildup data. Since the mid-1980's, the derivative of the well water-level response or pressure change has also been used as a diagnostic tool. Use of derivatives has been shown to improve significantly the diagnostic and quantitative analysis of various hydrologic test methods (Bourdet et al. 1989; Spane 1993; Spane and Wurstner 1993). The improvement in test analysis is attributed to the sensitivity of pressure derivatives to various test/formation/boundary conditions. As noted in Spane and Wurstner (1993), specific applications for which derivatives are particularly useful include the following:

- identifying formation-response characteristics (nonleaky or leaky; confined or unconfined aquifer) and boundary conditions (impermeable or constant head)
- assisting in the selection of the appropriate type-curve solution through combined type-curve/derivative plot matching
- determining when infinite-acting, radial flow conditions are established and, therefore, when straight-line analysis methods are applicable.

Figure 2.3 shows selected examples of log-log drawdown and derivative responses that are characteristic of some commonly encountered formation conditions during constant-rate pumping tests. The plots are equally applicable for injection buildup and recovery analysis. Spane (1993) provides a summary discussion on the use of standard and derivative-based analytical methods for constant-rate tests.

It should be noted that constant-rate injection tests were not used extensively as initially planned for test zone characterization at CO_2 No. 1 Well. This was because of the lower-than-expected permeability conditions for the test intervals and dependence on memory-based downhole pressure recording systems. As a result, after the first test zone characterization, constant-head (pressure) injection tests were used as the primary characterization test method for reservoir property determination. This test method is described below.

2.3.3 Constant-Head (Pressure) Injection Test

As noted previously due to unanticipated lower test-interval injection rates and dependence on memory gauges for test zone monitoring, the originally planned constant-rate injection tests were modified and constant-head (pressure) injection tests were employed for the majority of test zones at CO_2 No. 1 Well. To initiate the constant-head injection test, the following sequential steps were employed:

- With the downhole shut-in tool in the closed position, test system brine water was added to inside the test tubing string to land surface.
- The shut-in tool was opened by raising the downhole pressure probe assembly a short distance above the tubing shut-in tool seating nipple (e.g., 10 ft).
- The surface wellhead/lubricator was shut-in/closed and the designed, test injection pressure (e.g., +50 psi above surface conditions) was rapidly reached and then maintained throughout the duration of the injection-test period.

- At the end of the injection period the pressure probe assembly was rapidly lowered into the tubing, shut-in tool seating nipple, thereby stopping injection into the test zone and initiating pressure recovery (fall-off).

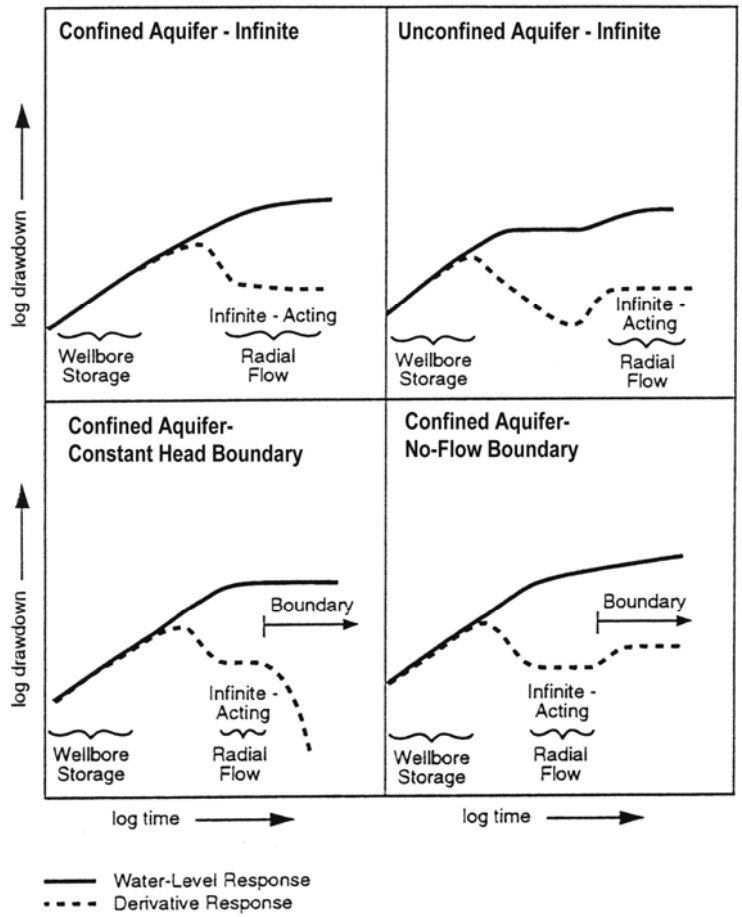

Figure 2.3. Characteristic Log-Log Drawdown and Drawdown Derivative Plots for Various Hydrogeologic Formation and Boundary Conditions (adapted from Spane and Wurstner 1993)

Because injection rates varied only slightly during the course of the active injection period, the pressure recovery following the termination of injection can be analyzed using the same analysis methods previously cited in Section 2.3.2 for constant-rate injection tests. When discharge variation is significant, however, special procedures, e.g., superposition/multi-rate analysis methods (see Earlougher 1977 and Horne 1990) can be used to obtain reliable analytical results.

In addition to analysis of pressure recovery following constant-pressure injection, the small decline of injection rates that occurred during the constant-pressure injection phase was examined. Theoretically, the magnitude of the observed discharge for the given injection pressure and its decline with time provides a means of determining the transmissivity, T, and to a lesser extent, storativity, S, of the interval

tested. The method used for analyzing these tests is based on the solution presented originally by Jacob and Lohman (1952). Because of the observed uniformity in low injection rates during testing and relatively high sensitivity of injection rates to unrecognized well-skin effects, this method was not used a primary analysis method. It was used, however, in most cases as a corroborative check on results obtained for the more quantitative recovery-based analysis methods.

2.3.4 Test History Matching

When a series of hydrologic characterization tests are conducted in a relatively continuous fashion, the entire testing response sequence can be analyzed as a *test history match*. This approach is particularly useful for validating the flow model used and for situations when the analysis of individual tests may be uncertain (e.g., due to small test recovery percentages). This technique relies on superimposing the predicted test responses of subsequent test responses, which can be used to match the entire composite test sequence. This analytical matching technique also provides a quantitative method for determining the *best-estimate* values for hydraulic properties of the tested interval, which incorporates the investigative scales of the various hydrologic test methods. For testing at CO_2 No. 1 Well, a test history match for the series of hydrologic tests conducted for each test zone interval was used as a means of identifying the best-estimate values for T, S, and well skin. Software based on the KGS model (Liu and Butler 1995) for slug-injection testing and the WTAQ model (Moench 1997) for constant-rate injection and injection-test recovery were used in preparing the superimposed test-history simulations. These simulations were then used to match the observed test-interval response for the entire hydrologic test sequence. The application of superposition of test responses in this report is similar to the approach presented previously in Enachescu and Ostrowski (1993) for analyzing hydrologic test sequences.

2.3.5 Property Conversions/Calculations/Assumptions

The test methods described above provide direct estimates for transmissivity, T, for the interval tested. Hydraulic conductivity, K, was calculated by dividing the value for T by the assumed contributing sandstone layer thickness, b. It was assumed for analytical purposes that the perforated interval, L, fully penetrated and was equivalent in length to the contributing sandstone layer thickness. As noted by Lohman (1979), both T and K are functions of fluid and formation properties, while intrinsic permeability, k, is only a property of the formation. The standard relationship between K and k is shown below:

$$K = k\,(\gamma_{fw}/\mu_{fw}) \tag{2.1}$$

where γ_{fw} is the formation fluid specific-weight density, and μ_{fw} is the formation fluid dynamic viscosity.

For analyses performed for tests conducted within CO_2 No. 1 Well, the γ_{fw} was calculated based on observed or projected, equilibrated downhole pressure measurements for the test interval for the measured downhole temperature and assumed formation water salinity conditions. These fluid-specific weight calculations were also corroborated using a computer problem HEADCO (Spane and Mercer 1985), which can be used to calculate γ_{fw}, given formation fluid temperature, pressure, and salinity conditions. The μ_{fw} was calculated based on the relationships presented in Meehan (1980a), which also takes into account observed/assumed temperature, pressure, and salinity conditions.

At standard temperature and pressure conditions (STP: temperature = 60˚F; pressure = 14.696 lb/in^2), γ_{fw}, = 62.3664 lb/ft^3 and μ_{fw} = 1.1295 cp (2.359 × 10^{-5} lb-sec/ft^2), assuming fresh-water conditions (i.e., ρ = 0.999014 g/cm^3), a k value of 1 darcy (1.0624 × 10^{-11} ft^2) would be equivalent to a K value of 2.43 ft/d under STP conditions. For comparison purposes, for typical test conditions encountered at the CO_2 No. 1 Well with an assumed formation water salinity of ~250,000 ppm, a temperature ~140˚F, and a pressure ~3,600 lb/in^2, the calculated formation density and viscosity are γ_{fw} = 74.46 lb/ft^3, and μ_{fw} = 0.878 cp. Under these CO_2 No. 1 Well test conditions, a permeability (k) of 1 darcy would be equivalent to a K value of ~3.12 ft/d for these specified test conditions. This is the conversion relationship for converting K to k in this report.

Depending on the particular hydrologic test method, storativity, S, is either determined directly from the test analysis results or assumed or calculated from independent physical relationships. As indicated below, S is equal to the product of the formation specific storage, S_s, and test thickness, b

$$S = S_s\, b = b\, \gamma_{fw}\, (c_f + n\, c_{fw}) \tag{2.2}$$

where c_f is the rock matrix compressibility, n is the formation porosity, and c_{fw} is the formation fluid compressibility.

For example purposes, as indicated in Newman (1973), the c_f for a sandstone having a formation porosity of 10 percent under 75 percent lithostatic pressure conditions is ~5 × 10^{-6} psi^{-1}, and the c_{fw}, estimated from relationships presented in Earlougher (1977) and Meehan (1980b) for the CO_2 No. 1 Well test example conditions listed above (i.e., 250,000 ppm salinity, pressure of ~3600 psi, and temperature of ~140˚F), yields a value of ~1.9 × 10^{-6} psi^{-1}. Using these derived values of compressibility and fluid density produces an S_s estimate of 2.7 × 10^{-6} ft^{-1}. This estimate is within the range of S_s values listed for sandstones, as reported in Shestakov (2002) and serves as the initial estimate for calculating S for test methods requiring this input for analysis (e.g., slug-injection tests), or for calculating combined wellbore storage/well-skin effects.

Wellbore storage, C_D, is an important parameter for recovery phases following injection tests conducted at CO_2 No. 1 Well. For open well tests, C_D is related to S and well test system parameters by the following relationship reported in Spane and Wurstner (1993):

$$C_D = r_c^2 / 2(r_w^2\, S) \tag{2.3}$$

where r_c is the radius of the test tubing/casing where fluid change is occurring, and r_w is the radius of the well/borehole.

As noted, Equation 2.3 is strictly for situations where test recovery occurs in an open borehole condition. For cases where recovery occurs using a downhole shut-in tool (as during recovery phases following injection tests at CO_2 No. 1 Well), C_D must be modified to represent the closed-system response condition. As noted in Bredehoeft and Papadopulos (1980), for closed-in recovery response, r_c^2 is replaced by the following:

$$r_c^2 = (V_{ts}\, c_{ts}\, \gamma_{fw})/\pi \tag{2.4}$$

where V_{ts} is the volume of closed, in-well test system, and c_{ts} is the compressibility of the closed, in-well test system; commonly equal to c_w.

It should be noted that during the well drilling and completion process, formation damage can occur, which represents a zone around the well of altered formational permeability. This zone of altered formational permeability is referred to as a *skin effect* or "well skin" (Earlougher 1977; Ramey 1970, 1982). For cases where well skin, s_K, is present, Equation 2.3 can be re-written to account for the added wellbore storage effect caused by well skin as:

$$C_D e^{2sk} = r_c^2 / 2(r_w^2\, Se^{2sk}) \tag{2.5}$$

Estimates for well skin in this report were determined by dividing the value derived for Se^{2sk} from test analysis by the calculated value for S (Equation 2.2) as indicated below:

$$s_K = -\ln (Se^{2sk}/S)/2 \tag{2.6}$$

Equation 2.6 provided estimates for s_K that were nearly identical to values derived using standard petroleum engineering relationships, as summarized in Earlougher (1977).

The *radius of investigation* of the hydrologic tests is variable and a function of the 1) duration and magnitude of the stress applied, 2) formation of hydraulic and storage properties, and 3) test system/formation fluid compressibility. Of these parameters, the presence of gas and its large influence on total fluid compressibility greatly limits the radius of investigation of the imposed hydrologic test. Radius of investigation relationships are commonly expressed in terms of *detecting* the pressure perturbation effects of an outside boundary. Horne (1990) provides the following area of investigation, A_i, relationship for detecting a closed (no-flow) circular reservoir boundary surrounding a test well, expressed in standard petroleum industry units:

$$A_i > 2.64E\text{-}4(k\, t)/(ø\, \mu\, c_t) \tag{2.7}$$

and,

$$r_i > (A_i/\pi)^{½} \tag{2.8}$$

As emphasized by Horne (1990), this is the radius at which a boundary would begin to be manifest at the test well. If the *actual* detection of a boundary is used as a parameter criterion, therefore, the radius of investigation relationship expressed in Equations 2.7 and 2.8 represent maximum distance estimates. It should be noted that the pressure perturbation imposed by a hydrologic test affects a larger region (i.e., *area or radius of influence*), but the more restrictive radius of investigation is a more meaningful parameter for assessing actual characterization distances.

3.0 Hydrologic Test Results

The following provides a discussion of the detailed hydrologic field-testing program conducted at CO_2 No. 1 Well. The primary objective of the field-testing program was for quantitative determination of *in situ* hydraulic and storage properties of candidate reservoir horizons previously identified regionally for potential CO_2 sequestration. The principal hydraulic/storage parameters characterized during testing include the following: transmissivity (T), hydraulic conductivity (K), intrinsic permeability (k), and storativity (S), which can be used to calculate porosity. In addition to acquiring hydraulic and storage property information, the test program was designed to also provide information concerning the static-reservoir-formation pressure for the respective test-interval depths.

In this section, a description of the tests and associated hydraulic characterization results for the various test zones are provided. Appendix A Tables A.1 through A.5 provide the detailed test summary and activities for the respective individual test zones characterized at CO_2 No. 1 Well between July 19 and August 6, 2007. Table 3.1 present the analytical results for the various hydraulic tests and best-estimate values for each of the reservoir test intervals. A discussion of the hydrologic tests and analytical methods results used during the reservoir test characterization is presented in Section 2.3. In all, five individual reservoir zones were characterized. Two of the five reservoir zone tests represent composite tests of the entire perforated sections within the Cambrian Basal sandstone and Rose Run sandstone, respectively. In addition, three individual reservoir zone tests were performed for perforated intervals located near the base, middle, and top of the Rose Run sandstone to address vertical permeability distribution and hydraulic communication within this geologic formation.

3.1 Basal Sandstone

As noted in Section 1.2, the Basal sandstone was perforated after the 4.5-in. O.D. well casing was cemented within the 7.875-in. drilled borehole. In all six depth intervals (8,526 to 8,531 ft, 8,536 to 8,542 ft, 8,554 to 8,576 ft, 8,578 to 8,587 ft, 8,602 to 8,604 ft, and 8,608 to 8,613 ft) were perforated on July 18, 2007. The perforated zones were chemically treated with an HCL acid injection wash, followed by fluid removal by swabbing for formation zone development.

The perforated depth intervals in the Basal sandstone occur within the upper 87 ft of the stratigraphic formation (i.e., formation contacts: 8,526 to 8,634 ft). The six perforated intervals were hydrologically tested collectively and not tested individually, as were zones within the overlying Rose Run formation. The composite 49-ft perforated interval was isolated within the cemented well casing on July 20, 2007, using an overlying test tubing-string packer set ~20 ft above the top perforated depth interval. The shut-in tool seating nipple location within the test tubing string was located at a depth of 8,483 ft. Following termination of acid wash and swabbing activities for test zone development at 1130 hours (Eastern Daylight Time [EDT]), July 20, 2007, the downhole, memory-based, pressure-probe assembly was lowered to a depth of 8,473 ft to monitor an open borehole equilibration period before injection testing. The pre-injection monitoring period continued until initiation of constant-rate injection testing that occurred at 1715 hours (EDT), July 20, 2007. The constant-rate injection test was conducted at an injection rate of 2 gpm during the beginning phases of the test. After ~300 minutes of injection at 2 gpm,

the test tubing string was filled to the land surface, and the wellhead was subsequently shut in to accommodate positive, pressure head injection. Surface injection pressures increased rapidly to +380 psi, and injection rates were lowered to injection rates of ≤ 0.03 gpm to halt a further increase in observed surface injection pressure. The test was aborted at 2245 hours (EDT) July 20, 2007, after it was surmised from the very low injection rates that the downhole shut-in tool mechanism had detached and set into the seating nipple causing shut-in, test-zone conditions. The shut-in test-zone recovery following the aborted constant-rate injection test continued for ~29 hours, while efforts were made to modify the downhole test equipment to prevent premature termination of future injection testing.

Table 3.1. CO_2 No. 1 Well: Hydrologic Testing/Analysis Summary: Basal Sandstone (Perforated Zone: 8,526 to 8,613 ft bKB[(a)])

Test Type	Hydraulic Properties					Analytical Method
	T ft^2/d	**K**[(b)] ft/d	**k**[(c)] md	**S**	s_K	
Injection-Test Recovery	0.073	0.0015	0.5	2.8E-2	0	Horner Plot
	0.073	0.0015	0.5	2.5E-2	0	Semi-Log Agarwal Recovery
	0.073	0.0015	0.5	2.8E-2	0	Injection-Test Recovery Type Curve/Derivative Plot
Constant-Head/ Discharge	(0.073)	(0.0015)	(0.5)	(2.8E-2)	(0)	Lohman—Corroborative Check
Slug-Injection Test	0.064	0.0013	0.4	1.5E-2	0	Type Curve/Derivative Plot
Test History Match	0.073	0.0015	0.5	2.8E-2	0	Superposition Simulation
Best Estimate	0.073	0.0015	0.5	2.8E-2	0	Test History Match

Note: shaded test methods indicate tests having higher reliability for formation hydraulic-property characterization.

(a) **ft bKB**: feet below original Kelly Bushing datum

(b) **K** = T/b; assumed contributing thickness, b; assigned equal to the perforated interval length, L = 49 ft

(c) **k** = K (μ/γ)

At the end of the recovery period, the downhole pressure probe assembly was raised 23 ft above the seating nipple depth (8,483 ft) at 0946 hours (EDT), July 22, 2007, effectively opening the shut-in tool and composite perforated test interval. Twenty-four minutes following opening of the downhole shut-in tool, an injection test was initiated at 1008 hours (EDT), July 22, 2007. During the course of the injection test, the downhole pressure probe assembly was removed and the modified shut-in tool re-installed to a test-probe depth location of 8,456 ft. The injection test was terminated at 1901 hours (EDT) July 22, 2007, which marked the beginning of the shut-in recovery test. The injection-test recovery continued until 0703 hours (EDT), July 23, 2007, when the shut-in tool was re-opened for performance of a slug-injection test. Testing for the composite Basal sandstone perforated interval was completed at 0956 hours (EDT), July 23, 2007.

Figure 3.1 shows the downhole pressure history response during the testing sequence performed during the Basal sandstone test characterization. A detailed discussion of hydrologic tests and analytical results for the various test methods is provided below. Because of the test complexities and equipment malfunctions previously discussed, no effort was made in analyzing the initial, aborted injection test. An analytical summary of individual hydrologic tests and associated analysis plots are presented in Table 3.1 and Appendix C, respectively.

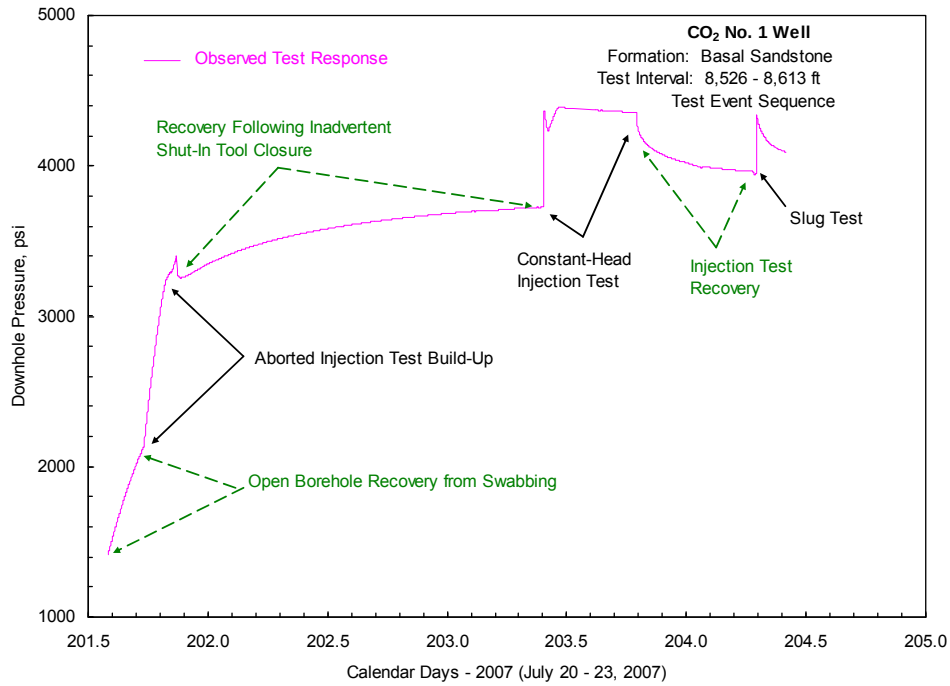

Figure 3.1. CO_2 No. 1 Well Test Event Pressure History Plot: Basal Sandstone

3.1.1 Constant-Head Injection Test

With the shut-in tool in the open position (i.e., downhole pressure probe positioned 23 ft above the seating nipple), an injection test for the Basal sandstone test zone was initiated at 1008 hours (EDT) on July 22, 2007. The test was implemented by injecting surface-tank brine water into the test tubing-string at initial injection rates of ~ 2 gpm to rapidly fill the test system to the land surface. After 60 minutes of constant-rate injection, the test tubing string was filled to the land surface and then maintained at that level as a constant-head injection test for the remainder of the injection test. Injection flow rates diminished only slightly during the course of the constant-head injection-test phase and during the last 5 hours of the test, varying from 0.92 to 0.62 gpm (weighted average = 0.83 gpm). As shown in Figure 3.1, even though the surface injection pressure was maintained at the top of the tubing string at the land surface, the downhole pressure decreased slightly (~35 psi) during the constant-head injection phase of the test. This slight decrease in downhole pressure is attributed to the injection of slightly lower density injection fluid, in comparison to that existing initially within the test tubing string. In total, 555 gallons of fluid were injected into the test tubing-string system during the 537-min injection test. Given the observed downhole pressure at the end of the injection test of 4,354.52 psi and the elevation

difference between the top of the tubing string and the downhole pressure probe depth setting (8,464 ft), an average fluid density of 1.188 g/cm^3 was calculated for the test-system fluid at the end of the test. This fluid density was used for analysis and parameter-conversion purposes for the Basal sandstone tests.

Under uniform fluid-column density conditions, the decline in observed injection rate can be analyzed with standard constant-head analysis methods (Section 2.33) to provide hydraulic/storage property estimates for the composite Basal sandstone perforated test interval. However, because of the complexities presented by the variable density and fluid-column conditions, more emphasis was placed on analysis of the recovery rather than injection phase of the test. This is because of the relative stabilization of surface injection rates during the last 10 hours of the injection test, and the more powerful diagnostic capabilities provided by composite recovery derivative analysis. Recovery pressures were monitored for ~12 hours following termination of injection testing at 1901 hours (EDT), July 22, 2007. The pressure recovery was recorded with the downhole shut-in tool closed, which isolates the test interval at test-formation depths and greatly reduces the effect of wellbore storage during the recovery period. The shut-in recovery was accomplished by lowering the pressure probe assembly into the shut-in tool seating nipple (Figure 2.2b). Because the injection rates were relatively uniform during the constant-head injection phase of the test, the pressure recovery data can be analyzed using constant-rate injection-test methods that are identified in Section 2.3.2. This analysis approach is consistent with previous discussions by Lohman (1979) for analyzing recovery responses following constant-head tests.

Appendix C Figure C.1 shows a diagnostic log-log plot of the observed recovery and recovery data derivative. The recovery data is plotted versus the Agarwal Equivalent Time function (Agarwal 1980), which adjusts the recovery data for the duration of the preceding injection (pressure buildup) test phase. Examination of Appendix C Figure C.1 indicates that infinite-acting radial flow conditions (i.e., horizontal derivative) were established only near the end of the recovery period (i.e., >100 minutes). In addition, because of the relatively low permeability of the test interval, closing of the shut-in tool caused a small positive pressure perturbation during the initial phase of test recovery. This is indicated in the diagnostic plot. Test data reflective of infinite-aquifer response characteristics can be analyzed with standard semi-log, straight-line solutions, as discussed previously in Spane (1993) and Spane and Wurstner (1993).

Appendix C Figure C.2 shows the analysis results using the Horner (1951) straight-line analysis method. The straight-line analysis provided the following estimated results: T = 0.073 ft^2/day, and K = 0.0015 ft/day (k = 0.5 milli-darcies). The K value of 0.0015 ft/day was calculated by dividing T by the estimated 49-ft contributing sandstone layer thickness, b. It is assumed that the contributing sandstone layer thickness coincides with the perforated test-interval length, L, (i.e., 8,526 to 8,531, 8,536 to 8,542, 8,554 to 8,576 ft, 8,578 to 8,587 ft, 8,602 to 8,604 ft, and 8,608 to 8,613 ft). Of particular note is the relatively large value estimated for S of 0.028 derived from the test analysis. This is considerably higher than a calculated test-zone value of 1.3E-4, which is based on assumed brine water and rock formation compressibility relationships (Section 2.3.5). This higher-than-expected value for S is attributed to a higher fluid compressibility because of the presence of gas within the test system and/or surrounding test formation. Without knowing the percentage of free and saturated gas within the surrounding test interval, it is not possible to assess well skin, s_K, conditions. Because of this uncertainty, a skin factor (s_K) of 0 was assigned to the combined storativity/skin parameter (i.e., $Se^{2sK} = S$). In

addition, a static formation pressure of 3,949.89 psi was calculated for the Basal sandstone test interval based on projecting the test recovery slope to infinite-recovery time conditions, i.e., Horner Time, (t + t')/t' = 1 (Note: probe depth = 8,483 ft). Given an estimated test system fluid density of 1.188 g/cm^3, this equates to a calculated static formation pressure of 3,972 psi for the top of the perforated test interval (i.e., 8,526 ft).

Appendix C Figure C.3 shows the analysis results using the semi-log, straight-line analysis method described in Agarwal (1980), which accounts for the duration of the pumping time using the Agarwal Equivalent Time Function, (t × t')/(t + t'). The straight-line analysis provided identical hydraulic-property results as the Horner plot analysis: T = 0.073 ft^2/day, and K = 0.0015 ft/day (k = 0.5 milli-darcies), and nearly identical value for S of 0.025.

To examine the relative *goodness-of-fit* of these straight-line analysis method estimates, the calculated parameters from the straight-line analysis methods were used initially in the analytical WTAQ model (Moench 1997) to calculate an associated recovery fall-off type-curve response. These values were adjusted slightly in iterative fashion until a visual best match to observed pressure recovery and recovery derivative response was obtained. A reasonable match was obtained with this approach, which essentially coincided with the values obtained from the semi-log analysis results. Appendix C Figure C.4 shows the results of the composite type-curve and derivative plot analysis using the following characterization parameters: T = 0.073 ft^2/day; K = 0.0015 ft/day; S = 2.8E-2; and S_k = 0. It should also be noted that to improve the early-time analysis fit, a dimensionless wellbore-storage parameter, C_D, value of 0 was used. This C_D value is indicative of the high surrounding formational fluid compressibility as it compares to the wellbore/test system compressibility.

Based on the recovery analysis results, the observed injection-rate data were examined semi-quantitatively for possible corroboration of formation hydraulic-property estimates. As previously noted, standard constant-head injection analytical methods can not be used directly in analyzing the Basal sandstone injection-rate test data because of the occurrence of variable injection head/pressure and variable inflow fluid density conditions that violate the analytical assumptions inherent in these methods. As a corroborative check, however, the analytical model based on the constant-head discharge solution presented originally by Jacob and Lohman (1952) was used to simulate injection rates vs. time based on 1) the results obtained from the composite type-curve and derivative plot analysis of recovery test data and 2) a calculated imposed constant-head injection pressure (above static formation pressure conditions) of 404.62 psi. Appendix C Figure C.5 shows the results of the predicted surface-discharge measurements, based on listed input parameters. As indicated, the predicted injection rates compare reasonably well with the observed data and provide additional corroboration of the estimated hydraulic/storage properties derived from the injection-test recovery analysis.

3.1.2 Slug-Injection Test

Following completion of the monitored recovery following termination of the injection test, a slug-injection test was initiated by opening the downhole shut-in tool at 0703 hours (EDT), July 23, 2007. This was accomplished by raising the pressure probe assembly a short distance above the tubing-string seating nipple. Prior to slug test initiation, the tubing string was filled with brine test water to near land

surface, which produced an over-pressure of 391.51 psi above observed pre-slug-test pressure conditions. The slug-injection recovery continued for 173 minutes and was terminated at 0956 hours. No DST recovery test was implemented because of test schedule requirements for testing the overlying Rose Run formation.

The pressure recovery observed during opening of the downhole shut-in tool represents a slug-injection test and can be analyzed with the analytical methods described in Section 2.3.1. The derivative plot of the slug-test response shown in Appendix C Figure C.6 indicates a departure and lowering of the derivative response. This is consistent with encountering a more compressible formation fluid (i.e., gas) away from the well. Appendix C Figure C.6 shows the analysis composite slug-test type curve and derivative plot for a homogeneous formation condition with no well skin present. As indicated, the slug-test analysis provided similar hydraulic and storage property estimates as the larger scale injection test: T = 0.064 ft^2/day, and K = 0.0013 ft/day (0.4 milli-darcies), and S of 0.015.

3.1.3 Test History Match

Figure 3.2 shows the sequence of hydrologic test events and associated downhole pressure response for the Basal sandstone test-interval characterization. To determine the *best-estimate* values for transmissivity and storativity for the test interval, the series of hydrologic characterization tests (injection test and injection-test recovery [fall-off] and the subsequent slug-injection test) were analyzed compositely as a collective testing sequence. The test history sequence analysis was performed with the test history matching procedure discussed in Section 2.3.4, which relies on the KGS (Liu and Butler 1995) and WTAQ (Moench 1997) analytical models. The property estimates derived from the injection-test recovery type-curve and derivative analysis served as initial input values for the test history matching procedure. It should be noted that the recovery following the constant-head injection test was modeled as a constant-rate injection test, using the weighted average injection rate determined during this phase of the test. The simulation shows both constant-head and constant-rate pressure simulations for the active injection-test phase. As noted in Section 2.3.3, the pressure buildup from a constant-rate injection test should be equivalent to the pressure applied during a constant-head pressure at the end of the injection phase (i.e., if the weighed average injection rate is used).

Figure 3.2 shows the coincidence of the simulated and observed responses. No improvement in the visual match was obtained through property adjustments. The initial input values obtained from the injection-test recovery analysis, therefore, are considered to represent the best-estimate property values: T = 0.073 ft^2/day, K = 0.0015 ft/day (k = 0.5 millidarcies), S = 2.8E-2, s_K = 0, and a static formation pressure of 3,949.89 psi at probe depth (i.e., 8,483 ft; projected static formation pressure of 3,972 psi for the top of the perforated test interval (i.e., 8,526 ft). For sensitivity analysis assessment, the best-estimate time history match simulation is shown in comparison to two simulations for varying test-interval hydraulic-property conditions in Figure 3.3. The comparisons were developed using the constant-rate injection approach during the active injection-test phase. As indicated, significant differences in the pressure history sequences are realized using hydraulic-property values one-half and twice the best-estimate value for test zone transmissivity (, i.e., T = 0.073 ft^2/d). This significant sensitivity exhibited to varying hydraulic-property conditions provides additional corroboration to the calculated best-estimate solution. Similar variations in test history response occurred when varying S and s_K (not shown).

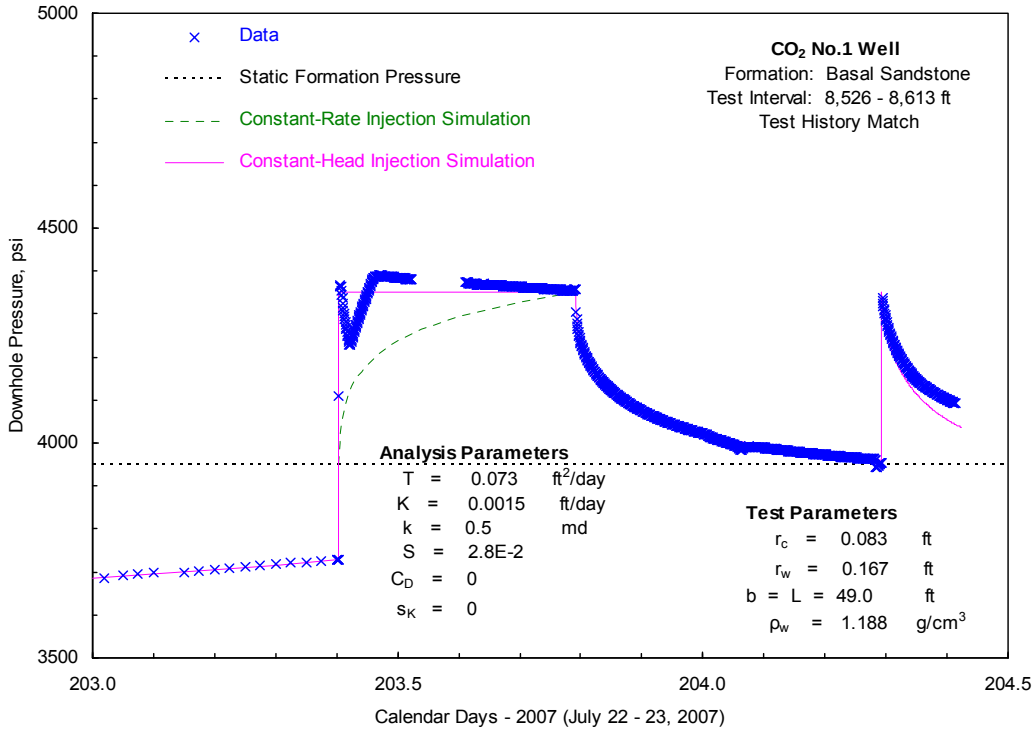

Figure 3.2. CO_2 No. 1 Well Test History Analysis Match: Basal Sandstone

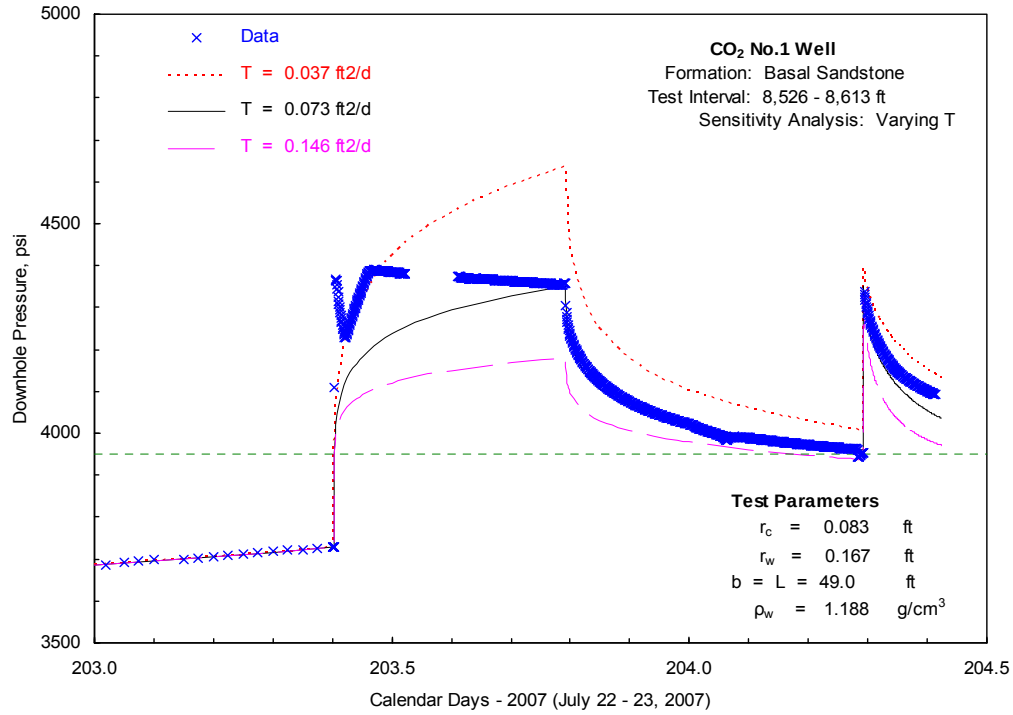

Figure 3.3. CO_2 No. 1 Well Test History Sensitivity Analysis: Basal Sandstone

3.2 Rose Run #1

As noted in Section 1.2, following hydraulic test characterization of the underlying Basal sandstone formation, a bridge plug packer was set above the Basal sandstone at a depth of 7,530 ft, and the Rose Run sandstone was perforated. In all, five Rose Run depth intervals were perforated on July 23, 2007: 7,377 to 7,380 ft, 7,387 to 7,396 ft, 7,416 to 7,418 ft, 7,435 to 7,446 ft, and 7,506 to 7,509 ft. The perforated zones were chemically treated with a HCL acid-injection wash, followed by fluid removal by swabbing for formation zone development.

Rose Run #1 includes only the lowest perforated Rose Run sandstone interval (7,506 to 7,509 ft) and occurs near the base of the stratigraphic unit. The 3-foot perforated interval was isolated within cemented well casing on July 25, 2007, with a bridge plug packer set at a depth of 7,530 ft and an overlying test tubing-string packer set at a depth of 7,463 ft. The shut-in tool seating nipple location within the test tubing string was located at a depth of 7,010 ft. Shut-in equilibration and hydraulic test characterization were delayed in an attempt to secure a wireline cable of sufficient length to support real-time surface monitoring of downhole pressures during testing. The real-time wireline system failed during installation within the tubing string on July 26, 2007. Subsequently, all hydrologic tests were performed with a slick-line, downhole, memory-based, pressure recording system. This system was lowered to the shut-in tool depth at 1750 hours, EDT, and after a brief ~20 minute open test system equilibration period, an injection test was initiated at 1810 hours (EDT) on July 26, 2007. The injection test was terminated at 0842 hours (EDT) July 27, 2007, which marked the beginning of shut-in recovery. Injection recovery continued until 0722 hours (EDT), July 28, 2007 when a slug-injection/DST recovery test was initiated by closing the downhole shut-in tool. Testing for this Rose Run perforated test interval was completed at 1001 hours (EDT), July 28, 2007.

Figure 3.4 shows the downhole pressure history response during the testing sequence performed during the Rose Run #1 test characterization. A detailed discussion of hydrologic tests and analytical results for the various test methods is provided below. An analytical summary of individual hydrologic tests and associated analysis plots are presented in Table 3.2 and Appendix C, respectively. Examination of the pressure response below the lower bridge plug during testing (Appendix D Figure D.2, indicates no hydraulic communication between the isolated test interval and underlying perforated zones within the Basal sandstone during the course of characterization of Rose Run #1.

3.2.1 Constant-Head Injection

With the shut-in tool in the open position (i.e., downhole pressure probe positioned 20 ft above the seating nipple), an injection test for Rose Run #1 test zone was initiated at 1810 hours on July 26, 2007. The test was implemented by injecting surface-tank brine water into the test tubing-string at initial inject rates of ~ 5 gpm to rapidly fill the test system to land surface. After 10 minutes of injection, the test tubing string was filled to land surface and the surface wellhead closed to maintain above-ground-level injection pressures. The surface injection pressure was slowly increased to +50 psi and then maintained at this constant-pressure (head) condition for the remainder of the test. Injection flow rates diminished during the course of constant-head phase of the injection test, from 0.20 gpm (at the beginning) to 0.07 gpm at the end of the test, (weighted average = 0.094 gpm). As shown in Figure 3.4, even though the surface injection pressure was maintained at a uniform +50 psi, the downhole pressure increased slightly

(~28 psi) during the constant-head injection phase of the test. This slight increase in downhole pressure is attributed to the injection of slightly higher-density, surface-tank brine water during the course of the test. In total, 245 gallons of fluid were injected into the test tubing-string system during the 872-min injection test. Given the observed downhole pressure at the end of the injection test of 3679.59 psi (at a surface injection pressure of +50 psi) and elevation difference between the wellhead surface pressure sensor location and the downhole pressure probe depth setting (6,998 ft), an average fluid density of 1.197 g/cm^3 was calculated for the test system fluid at the end of the test. This fluid density was used for analysis and parameter conversion purposes for Rose Run #1 tests.

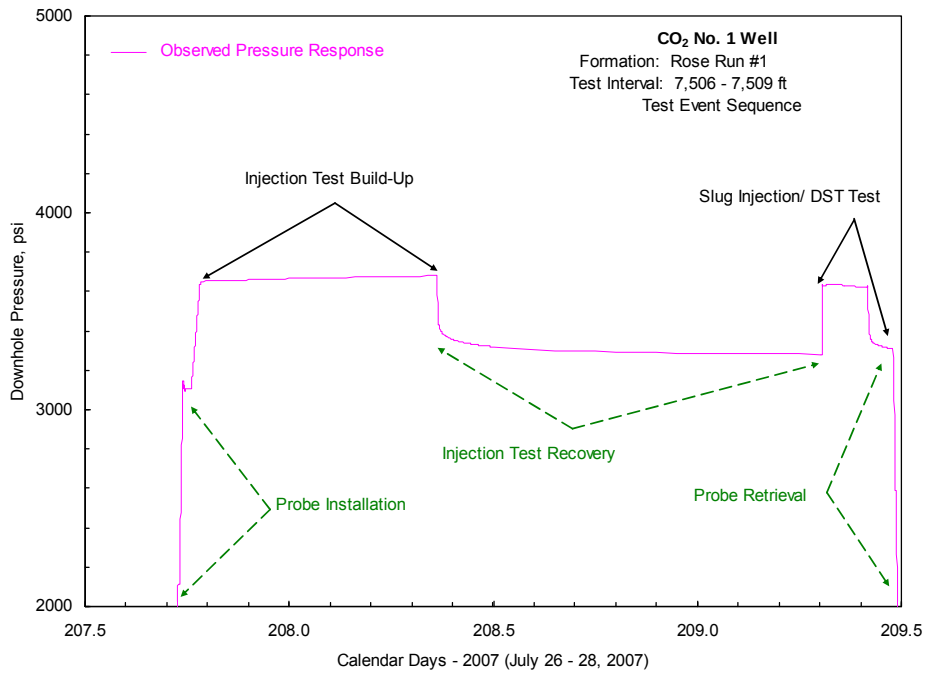

Figure 3.4. CO_2 No. 1 Well Test Event Pressure History Plot: Rose Run #1

Under uniform fluid-column density conditions, the decline in observed surface discharge can be analyzed using standard constant-head analysis methods (Section 2.33) to provide hydraulic/storage property estimates for the Rose Run #1 interval. Because of the complexities presented by the variable density, fluid-column conditions, more emphasis was place on analyzing the recovery rather than the injection phase of the test. This is because of the relative stabilization of surface injection rates during the last 10 hours of the injection test and the more powerful diagnostic capabilities provided by composite recovery derivative analysis. Recovery pressures were monitored for ~22.5 hours following termination of injection testing at 0842 hours (EDT), July 27, 2007. The pressure recovery was recorded with the downhole shut-in tool closed, which isolates the test interval at test formation depths and greatly reduces the effect of wellbore storage during the recovery period. The shut-in recovery was accomplished by lowering the pressure probe assembly into the shut-in tool seating nipple (Figure 2.2b). Because the injection rates were relatively uniform during the constant-head injection phase of the test, the pressure recovery data can be analyzed with constant-rate injection-test methods that are identified in Section 2.3.2. This analysis approach is consistent with previous discussions by Lohman (1979) for analyzing recovery responses following constant-head tests.

Table 3.2. CO_2 No. 1 Well: Hydrologic Testing/Analysis Summary: Rose Run #1 (Perforated Zone: 7,506 to 7,509 ft bKB[a])

Test Type	Hydraulic Properties					Analytical Method
	T ft^2/d	**K**[b] ft/d	**k**[c] md	**S**	s_K	
Injection-Test Recovery	0.023	0.008	2.6	8.1E-6	+0.3	Horner Plot
	0.023	0.008	2.6	8.1E-6	+0.4	Semi-Log Agarwal Recovery
	0.023	0.008	2.6	8.1E-6	+0.4	Injection-Test Recovery Type Curve/Derivative Plot
Constant-Head/ Discharge	(0.023)	(0.008)	(2.6)	(8.1E-6)	(+0.4)	Lohman—Corroborative Check
Slug-Injection/ DST Recovery	0.021	0.007	2.2	8.1E-6	+0.6	Horner Plot
Test History Match	0.023	0.008	2.6	8.1E-6	+0.4	Superposition Simulation
Best Estimate	0.023	0.008	2.6	8.1E-6	+0.4	Test History Match

Note: shaded test methods indicate tests having higher reliability for formation hydraulic-property characterization.

(a) **ft bKB**: feet below original Kelly Bushing datum
(b) **K =** T/b; assumed contributing thickness, b; assigned equal to the perforated interval length, L = 3 ft
(c) **k** = K (μ/γ)

Appendix C Figure C.7 shows a diagnostic log-log plot of the observed recovery and recovery data derivative. The recovery data are plotted versus the Agarwal Equivalent Time function (Agarwal 1980), which adjusts the recovery data for the duration of the preceding injection (pressure buildup) test phase. Examination of Appendix C Figure C.7 indicates that infinite-acting radial flow conditions (i.e., horizontal derivative) were established after approximately 60 minutes into the recovery period. This rather rapid transition into infinite-acting conditions is a function of using the downhole shut-in tool during recovery. Test data reflective of infinite-aquifer response characteristics can be analyzed with standard semi-log, straight-line solutions, as discussed previously in Spane (1993) and Spane and Wurstner (1993). Another diagnostic feature evident in the recovery plot is the transitional, non-radial flow condition between the wellbore storage and infinite-acting radial flow regions of the plot. This transitional region is believed attributable to the perforation and/or partial penetration completion aspect of the test well, and may represent the progression of flow from imposed non-radial (e.g., spherical-flow) to formational radial-flow conditions. Alternate models that may produce similar transitional derivative plot patterns include lateral variation in formation/fluid characteristics and double-porosity behavior (e.g., Gringarten 2008).

Appendix C Figure C.8 shows the analysis results obtained from the Horner (1951) straight-line analysis method. The straight-line analysis provided the following estimated results: T = 0.023 ft^2/day, and K = 0.008 ft/day (k = 2.6 milli-darcies). The K value of 0.008 ft/day was calculated by dividing T by

the estimated 3-ft contributing sandstone layer thickness, b. It is assumed that the contributing sandstone layer thickness coincides with the perforated test-interval length, L, (i.e., 7,506 to 7,509 ft). A small positive skin factor of +0.3 (indicative of minor borehole damage/well skin effects) was calculated with the relationship expressed in Equation 2.6 and assuming a test-interval storativity value of 8.7 E-6, based on formational and fluid compressibility estimates described in Section 2.3.5. As shown in the figure, a static formation pressure of 3,263.77 psi was calculated for the Rose Run #1 test interval based on projecting the test recovery slope to infinite-recovery time conditions, i.e., Horner Time, $(t + t')/t' = 1$ (Note: probe depth = 7,010 ft). Given an estimated test-system fluid density of 1.197 g/cm^3, this equates to a calculated static formation pressure of 3,521 psi for the top of the perforated test interval (i.e., 7,509 ft).

Appendix C Figure C.9 shows the analysis results using the semi-log, straight-line analysis method described in Agarwal (1980), which accounts for the duration of the pumping time, using the Agarwal Equivalent Time Function, $(t \times t')/(t + t')$. The straight-line analysis provided identical results as the Horner plot analysis: T = 0.023 ft^2/day, and K = 0.008 ft/day (k = 2.6 milli-darcies), and $s_K = +0.4$.

To examine the relative *goodness-of-fit* of these straight-line analysis method estimates, the calculated parameters from the straight-line analysis methods were used initially in the analytical model WTAQ (Moench 1997) to calculate an associated recovery fall-off type-curve response. These values were adjusted slightly in iterative fashion until a visual best match to observed pressure recovery and recovery derivative response was obtained. It should be noted that the analytical model used does not include the capability of modeling transitional flow periods (e.g., spherical to radial flow). Because of this limitation, emphasis was placed on matching early-time (wellbore storage and well-skin regions) and later-time radial-flow dominant time periods. A reasonable match was obtained with this approach. Appendix C Figure C.10 shows the results of the composite type-curve and derivative plot analysis using the following characterization parameters: T = 0.023 ft^2/day; K = 0.008 ft/day; S = 8.1E-6; and $S_k = +0.4$. It should also be noted that the analysis result for the dimensionless wellbore-storage parameter, C_D, of 20 is slightly higher than that estimated from test-system volumes and compressibility relationships. This slightly higher analysis value may be indicative of incorporating a small amount of air into the test system during either pre-zone development (swabbing) and/or the injection-test process.

Based on the recovery analysis results, the observed injection-rate data were examined semi-quantitatively for possible corroboration of formation hydraulic-property estimates. As previously noted, standard constant-head injection analytical methods can not be used directly in analyzing the Rose Run #1 injection-rate test data because of the occurrence of variable injection head/pressure and variable inflow fluid density conditions that violate the analytical assumptions inherent in these methods. As a corroborative check, however, the analytical model based on the constant-head discharge solution presented originally by Jacob and Lohman (1952) was used to simulate injection rates vs. time based on the results obtained from the composite type-curve and derivative plot analysis of recovery test data and a calculated imposed constant-head injection pressure (above static formation pressure conditions) of 415.82 psi. Appendix C Figure C.11 shows the results of the predicted surface discharge measurements, based on listed input parameters. As indicated, the predicted injection rates compare reasonably well with the observed data and provide additional corroboration of the estimated hydraulic/storage properties derived from the injection-test recovery analysis.

3.2.2 Slug-Injection/DST

Following completion of the monitored recovery following termination of the injection test, a slug-injection/DST test was initiated by opening the downhole shut-in tool at 0722 hours (EDT), July 28, 2007, by raising the pressure probe assembly a short distance above the tubing-string seating nipple. The tubing string was filled with brine test water to near land surface before test initiation, which produced an over-pressure of 352.078 psi above pre-slug-test pressure conditions. The downhole pressure response did not exhibit a typical recovery fall-off pattern during the initial 60 minutes. This lack of pressure fall-off is attributed to the presence of gas or gas bubble within the tubing-string fluid system, which may have been an artifact from the earlier long-duration constant-head injection test. During the last 95 minutes of the open slug-injection-test period, a pressure recovery decline of 12.645 psi was observed. The DST recovery phase of the test was initiated at 1001 hours (EDT), July 28, 2007, by lowering the pressure probe assembly into the tubing-string seating nipple. The DST recovery phase continued for 89 minutes and was terminated at 11:30 hours (EDT) on July 28, 2007. A typical DST recovery response pattern was exhibited during this phase of the test.

Because of the recovery complexities exhibited during the initial period of the slug injection test, no efforts were made to analyze this phase of the test. Also, because of the injection flow-rate and flow-period uncertainties, no quantitative analysis of the DST recovery data was possible. A qualitative analysis was attempted for the DST recovery data, however, using several analysis assumptions. Appendix C Figure C.12 shows a diagnostic log-log plot of the observed recovery and recovery data derivative. The recovery data are plotted versus Agarwal Equivalent Time function (Agarwal 1980), which adjusts the recovery data for the duration of the preceding injection (pressure buildup) test phase. This flow period is uncertain, but was taken to represent the last 95.6 minutes of the slug-injection period that exhibited pressure decline. The plot pattern is very similar to the diagnostic recovery plot exhibited for the constant-head injection recovery (Appendix C Figure C.7). Examination of Appendix C Figure C.12 indicates that infinite-acting radial flow conditions (i.e., horizontal derivative) were approached or established very near the end of the monitored recovery period. Test data reflective of infinite-aquifer response characteristics can be analyzed with standard semi-log, straight-line solutions, as discussed previously in Section 3.2.1. Another diagnostic feature evident in the recovery plot is the transitional, non-radial flow condition between the wellbore storage and infinite-acting radial flow regions of the plot. As noted previously, this transitional region is believed attributable to the perforation completion of the test well and most likely represents the progression of flow from imposed non-radial flow to formational radial-flow conditions.

Appendix C Figure C.13 shows the qualitative analysis results using the Horner (1951) straight-line analysis method. The straight-line analysis provided the following estimated results: T = 0.021 ft^2/day, and K = 0.007 ft/day (k = 2.2 milli-darcies). These values were obtained by assuming that the actual constant injection rate that occurred during the slug-injection phase of the test is proportional to the recorded average surface injection rate that occurred for the pressure applied (i.e., Q = 0.94 gpm; ΔP = 415.82 psi) during the previous constant-head injection test. Based on this proportionality, an injection rate of 0.080 gpm was calculated for the slug-injection/DST recovery. A small positive skin factor of +0.6 was calculated with the equation relationships presented in Earlougher (1977) and

assuming a test-interval storativity value of 8.7 E-6. These values are very similar to those obtained for the more quantitative constant-head injection-test recovery as presented in Section 3.2.1.

As shown in the figure, a static formation probe pressure of 3,287.73 psi was calculated for the Rose Run #1 test interval based on projecting the test recovery slope to infinite-recovery time conditions, i.e., Horner Time, (t + t')/t' = 1 (Note: probe depth = 7,010 ft). This static probe pressure value is ~24 psi greater than the static pressure indicated for the previous injection-test recovery analysis following the constant-head injection. The projected DST recovery static pressure reading, however, is highly impacted by the uncertainties associated with the slug-injection flow period, as well as the recovery trend from the previous test. For these reasons, it is not considered representative of actual static formation conditions.

3.2.3 Test History Match

Figure 3.4 shows the sequence of hydrologic test events and associated downhole pressure response for the Rose Run #1 test-interval characterization. To determine the *best-estimate* values for transmissivity and storativity for the test interval, the series of hydrologic characterization tests (injection test and injection-test recovery [fall-off] and the subsequent slug-injection/DST tests) were analyzed compositely as a collective testing sequence. The test history analysis was performed with the test history matching procedure discussed in Section 2.3.4, which relies on the KGS (Liu and Butler 1995) and WTAQ (Moench 1997) analytical models. The property estimates derived from the injection-test recovery type-curve and derivative analysis served as initial input values for the test history matching procedure. It should be noted that the recovery following the constant-head injection test was modeled as a constant-rate injection test using the weighted average injection rate determined during this phase of the test. The simulation shows both constant-head and constant-rate pressure simulations for the active injection-test phase. As previously discussed in Section 2.3.3, the pressure buildup from a constant-rate injection test should be equivalent to the pressure applied during a constant-head pressure at the end of the injection phase (i.e., if the weighed average injection rate is used).

Figure 3.5 shows the coincidence of the simulated and observed responses. No improvement in the visual match was obtained through property adjustments. The initial input values obtained from the injection-test recovery analysis, therefore, are considered to represent the best-estimate property values: T = 0.023 ft^2/day, K = 0.008 ft/day (k = 2.6 millidarcies), S = 8.1E-6, s_K = +0.4, and a static formation pressure of 3,263.77 psi at probe depth (i.e., 7,010 ft; projected static formation pressure of 3,521 psi for the top of the perforated test interval, i.e., 7,509 ft). For sensitivity analysis assessment, the best-estimate time history match simulation is shown in comparison to two simulations for varying test-interval hydraulic-property conditions in Figure 3.6. The comparisons were developed using the constant-rate injection approach during the active injection-test phase. As indicated, significant pressure history sequences are realized using hydraulic-property values one-half and twice the best-estimate value for test zone transmissivity (i.e., T = 0.023 ft^2/d). This significant sensitivity exhibited to varying hydraulic-property conditions provides additional corroboration to the calculated best-estimate solution. Similar variations in test history response occurred when varying S and s_K (not shown).

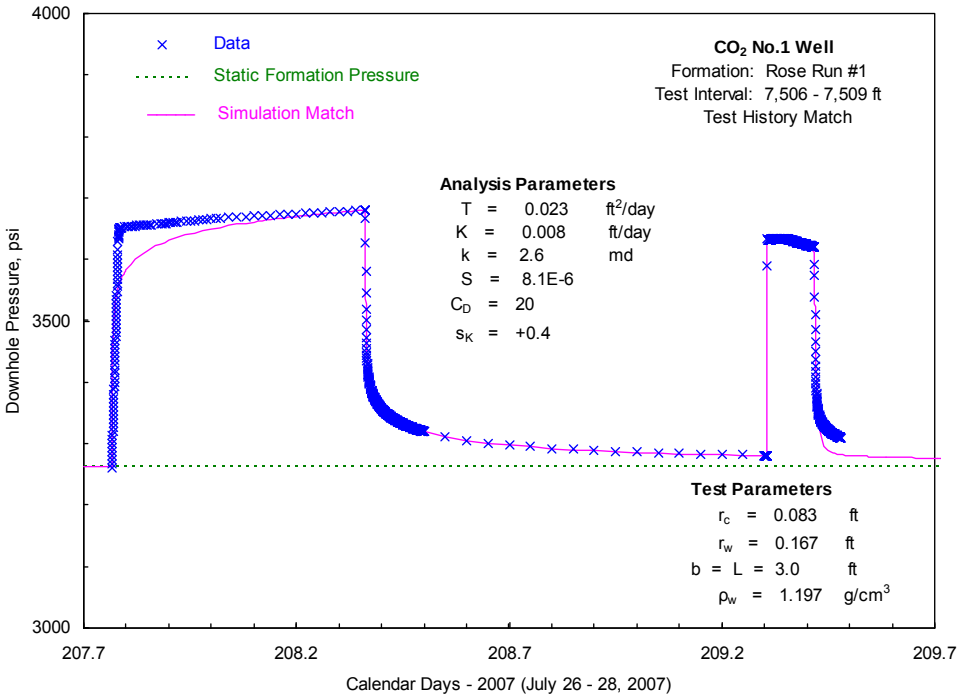

Figure 3.5. CO_2 No. 1 Well Test History Analysis Match: Rose Run #1

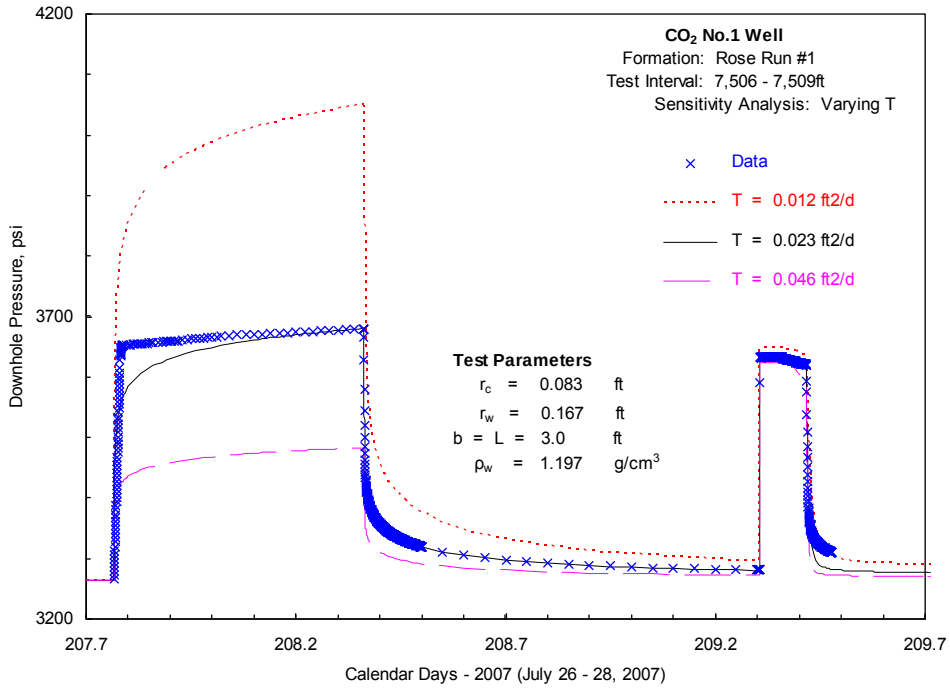

Figure 3.6. CO_2 No. 1 Well Test History Sensitivity Analysis: Rose Run #1

3.3 Rose Run #2

Following completion of hydraulic test characterization of the underlying Rose Run #1 test interval, the bridge plug and tubing-string packer were released and re-set at a depth of 7,482 ft and 7,410 ft, respectively, to support hydraulic test characterization of Rose Run #2. The Rose Run #2 zone isolated by the packers includes two perforated intervals that are positioned stratigraphically within the middle section of the Rose Run sandstone: 7,416 to 7,418 ft, and 7,435 to 7,446 ft. The 13-ft perforated interval was isolated within cemented well casing on July 29, 2007, with the bridge plug and an overlying test tubing-string packer system. The shut-in tool seating nipple location within the test tubing string was located at a depth of 7,380 ft. The downhole pressure probe assembly was lowered to 10 ft above the seating-nipple depth location (7,370 ft) at 1315 hours, EDT, and after a brief 45-minute open test system equilibration pressure period, an injection test was initiated at 1400 hours (EDT) on July 29, 2007. The injection test was terminated at 1000 hours (EDT) July 30, 2007, which marked the beginning of shut-in recovery. Injection-test recovery continued until 0925 hours (EDT), July 31, 2007 for performance of a slug-injection/DST test. Following completion of the slug-injection/DST test, a second constant-pressure injection test was initiated at 1217 hours (EDT) July 31, 2007. The second injection test was terminated at 2002 hours (EDT), July 31, 2007, which marked the beginning of the shut-in recovery. Recovery monitoring continued until 0658 hours (EDT), August 1, 2007, which marked the end of hydraulic test characterization of Rose Run #2.

Figure 3.7 shows the downhole pressure history response during the testing sequence performed during the Rose Run #2 test characterization. A detailed discussion of hydrologic tests and analytical results for the various test methods is provided below. An analytical summary of individual hydrologic tests and associated analysis plots are presented in Table 3.3 and Appendix C, respectively. Examination of the pressure response below the lower bridge plug during testing (Appendix D Figure D.3, indicates no hydraulic communication between the isolated test interval and the underlying Rose Run #1 perforated zone during the course of characterization of Rose Run #2.

3.3.1 Constant-Head Injection

Because of anticipated, higher permeability conditions, the first injection test for Rose Run #2 was initially designed to be conducted as a multi-step, constant-rate injection test. With the shut-in tool in the open position (i.e., downhole pressure probe positioned 10 ft above the seating nipple), the first step of the multi-stage, constant-rate injection test was initiated at 1400 hours on July 29, 2007. The test was implemented by injecting surface-tank brine water into the open test tubing-string at an initial inject rate of 5 gpm. After 10 minutes of injection, the test tubing string was filled to land surface and the surface wellhead closed to maintain above-ground-level injection pressures. The decision was made at that time to convert the constant-rate injection test to a constant-head (pressure) injection test. The surface injection pressure was slowly increased to +50 psi over a 5-min period and then maintained at this constant-pressure (head) condition for the remainder of the test (total injection test time = 1,261 minutes). As shown in Figure 3.7, even though the surface injection pressure was maintained at a relatively uniform +50 psi, the downhole pressure exhibited a steady increase in pressure (~200 psi) during the first half of the constant-head injection phase of the test. This observed increase in downhole pressure is attributed to the injection of slightly higher-density, surface-tank brine water during the initial period of the constant-head injection test. In total, 1,688 gallons of brine water were injected into the test tubing-string system

during the 1,261-min injection test. During the last 1,000 minutes of the injection test, injection rates fluctuated, but generally declined from 1.6 to 0.98 gpm (weighted average = 1.218 gpm). Given the observed downhole pressure at the end of the injection test of 3,824.70 psi (at a surface injection pressure of +50 psi) and distance from the wellhead surface pressure sensor location to the downhole probe depth setting (distance = 7,378 ft), an average density of 1.181 g/cm^3 was calculated for the test system fluid at the end of the test. This fluid density was used for analysis and parameter conversion purposes for all Rose Run #2 injection #1 related tests.

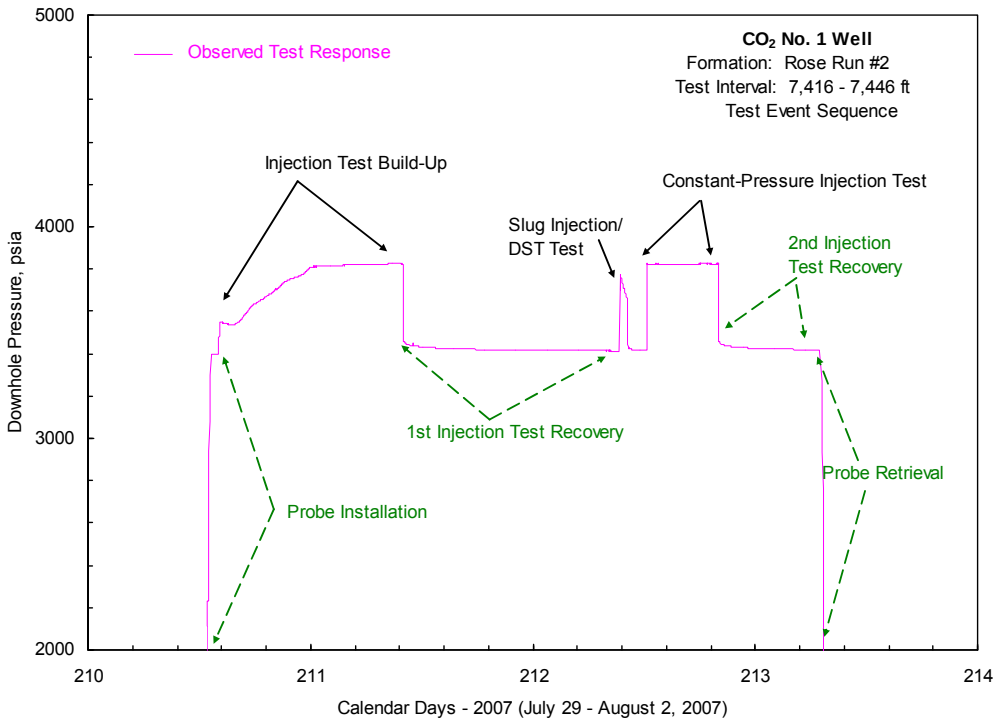

Figure 3.7. CO_2 No. 1 Well Test Event Pressure History Plot: Rose Run #2

Under uniform fluid-column density conditions, the decline in observed surface discharge can be analyzed using standard constant-head analysis methods (Section 2.33) to provide hydraulic/storage property estimates for the Rose Run #2 interval. Because of the complexities presented by the variable density, fluid-column conditions, more emphasis was placed on analyzing the recovery rather than injection phase of the test. This is because of the relative stabilization of surface injection rates during the last 16 hours of the injection test and the more powerful diagnostic capabilities provided by composite recovery derivative analysis. Recovery pressures were monitored for ~23.25 hours following termination of injection testing at 1000 hours (EDT), July 30, 2007. The pressure recovery was recorded with the downhole shut-in tool closed, which isolates the test interval at test formation depths and greatly reduces the effect of wellbore storage during the recovery period. The shut-in recovery was accomplished by lowering the pressure probe assembly into the shut-in tool seating nipple (Figure 2.2b). Because the injection rates were relatively uniform during the last 10 hours of the constant-head injection phase of the test, the pressure recovery data can be analyzed using constant-rate injection-test methods that are

identified in Section 2.3.2. This analysis approach is consistent with previous discussions by Lohman (1979) for analyzing recovery responses following constant-head tests.

Table 3.3. CO_2 No. 1 Well: Hydrologic Testing/Analysis Summary: Rose Run #2 (Perforated Zone: 7,416 to 7,446 ft bKB[a])

Test Type	Hydraulic Properties					Analytical Method
	T ft^2/d	**K**[b] ft/d	**k**[c] md	**S**	s_K	
Injection-Test #1 Recovery	0.906	0.070	22.4	3.5E-5	+12.6	Horner Plot
	0.902	0.069	22.2	3.5E-5	+12.5	Semi-Log Agarwal Recovery
	0.906	0.070	22.4	3.5E-5	+12.8	Injection-Test Recovery Type Curve/Derivative Plot
Injection-Test #2 Recovery	0.889	0.068	21.8	3.5E-5	+13.6	Horner Plot
	0.894	0.069	22.1	3.5E-5	+13.8	Semi-Log Agarwal Recovery
	0.892	0.069	22.1	3.5E-5	+13.7	Injection-Test Recovery Type Curve/Derivative Plot
Composite Constant-Head/ Discharge	(0.890)	(0.069)	(21.9)	(3.5E-5)	(+13.7)	Lohman—Corroborative Check
Slug-Injection Test	0.78	0.060	19.2	3.5E-5	+12.7	Type Curve/Derivative Plot
DST Recovery	(1.11)	(0.085)	(27.2)	(3.5E-5)	(+16.2)	Horner Plot (Note: infinite-acting, radial flow conditions were not achieved; estimate results are qualitative.)
Test History Match	0.891	0.069	22.1	3.5E-5	+13.8	Superposition Simulation
Best Estimate	0.891	0.069	22.1	3.5E-5	+13.8	Test History Match

Note: shaded test methods indicate tests having higher reliability for formation hydraulic-property characterization.

(a) **ft bKB**: feet below original Kelly Bushing datum
(b) **K** = T/b; assumed contributing thickness, b; assigned equal to the perforated interval length, L = 13 ft
(c) **k** = K (μ/γ)

Appendix C Figure C.14 shows a diagnostic log-log plot of the observed recovery and recovery data derivative following the first injection test. The recovery data are plotted versus the Agarwal Equivalent Time function (Agarwal 1980), which adjusts the recovery data for the duration of the preceding injection (pressure buildup) test phase. Examination of Appendix C Figure C.14 indicates that infinite-acting radial flow conditions (i.e., horizontal derivative) were established after approximately 150 minutes into the recovery period. This rather rapid transition into infinite-acting conditions is a function of using the downhole shut-in tool during recovery. Test data reflective of infinite-aquifer response characteristics can be analyzed with standard semi-log, straight-line solutions, as discussed previously in Spane (1993) and

Spane and Wurstner (1993). Another diagnostic feature evident in the recovery plot is the transitional, non-radial flow condition between the wellbore storage and infinite-acting radial flow regions of the plot. This transitional region is believed attributable to the perforation and/or partial penetration completion aspect of the test well, and may represent the progression of flow from imposed non-radial (e.g., spherical-flow) to formational radial-flow conditions. Alternate models that may produce similar transitional derivative plot patterns include lateral variation in formation/fluid characteristics and double-porosity behavior (e.g. Gringarten 2008). This derivative pattern is similar to the diagnostic recovery response exhibited for the underlying Rose Run #1.

Appendix C Figure C.15 shows the analysis results using the Horner (1951) straight-line analysis method. The straight-line analysis provided the following estimated results: T = 0.906 ft^2/day, and K = 0.070 ft/day (k = 22.4 milli-darcies). The K value of 0.070 ft/day was calculated by dividing T by the estimated 13-ft contributing sandstone layer thickness, b. It is assumed that the contributing sandstone layer thickness coincides with the perforated test-interval length, L, (i.e., 7,416 to 7,418 ft, and 7,435 to 7,446 ft). A positive skin factor of +12.6 (indicative of moderate borehole damage/well skin effects) was calculated with equation relationships presented in Earlougher (1977) and assuming a test-interval storativity value of3.5 E-5, based on formational and fluid compressibility estimates described in Section 2.3.5. As shown in the figure, a static formation pressure of 3,406.73 psi was calculated for the Rose Run #2 test interval based on projecting the test recovery slope to infinite-recovery-time conditions, i.e., Horner Time, $(t + t')/t' = 1$ (Note: probe depth = 7,380 ft). Given an estimated test system fluid density of 1.181 g/cm^3, this equates to a calculated static formation pressure of 3,425 psi for the top of the perforated test interval (i.e., 7,416 ft).

Appendix C Figure C.16 shows the analysis results using the semi-log, straight-line analysis method described in Agarwal (1980), which accounts for the duration of the pumping time, using the Agarwal Equivalent Time Function, $(t \times t')/(t + t')$. The straight-line analysis provided nearly identical results as the Horner plot analysis: T = 0.902 ft^2/day, and K = 0.069 ft/day (22.2 milli-darcies), and $s_K = +12.5$.

To examine the relative *goodness-of-fit* of these straight-line analysis method estimates, the calculated parameters from the straight-line analysis methods were used initially in the analytical model WTAQ (Moench 1997) to calculate an associated recovery fall-off type-curve response. These values were adjusted slightly in iterative fashion until a visual best match to observed pressure recovery and recovery derivative response was obtained. It should be noted that the analytical model used does not include the capability of modeling transitional flow periods (e.g., spherical to radial flow). Because of this limitation, emphasis was placed on matching early-time (wellbore storage and well skin regions) and later-time radial flow dominant time periods. A reasonable match was obtained with this approach. Appendix C Figure C.17 shows the results of the composite type-curve and derivative plot analysis using the following characterization parameters: T = 0.906 ft^2/day; K = 0.070 ft/day; S = 3.5E-5; and $S_k = +12.8$. It should also be noted that the analysis result for the dimensionless wellbore-storage parameter, C_D, of 7.5 is slightly higher than that estimated from test system volumes and compressibility relationships. This slightly higher analysis value may be indicative of incorporation of air into the test system during the injection-test process.

Because of the variability in test conditions that were exhibited during the first injection test, a shorter-duration injection test and recovery were included at the end of the test characterization following completion of a slug-injection/DST test (described in Section 3.3.2). Unlike the first test, the second injection test was conducted as a constant-head injection test from the beginning of the test by filling the test tubing-string to the surface with the test interval in a shut-in condition. The constant-head injection test was initiated at 1217 hours (EDT), July 31, 2007, by opening the shut-in tool (i.e., raising the pressure probe assembly 10 ft above the seating nipple location) and simultaneously initiating injection. The surface injection pressure was maintained at a closed-in, surface wellhead pressure of +50 psi for the entirety of the injection test. After 1,261 minutes, the constant-head injection test was terminated at 2002 hours (EDT), July 31, 2007. As shown in Figure 3.7, true constant-head conditions were established and maintained for the entirety of the second injection test. In total, 538 gallons of brine water were injected into the test tubing-string system during the 465-min injection test. Injection rates remained nearly constant during the course of the test, declining slightly from 1.2 to 1.05 gpm during the injection test (weighted average = 1.139 gpm). Given the observed downhole pressure at the end of the injection test of 3,824.50 psi (at a surface injection pressure of +50 psi) and distance from the wellhead surface pressure sensor location to the downhole probe depth setting (distance = 7,378 ft), an average density of 1.181 g/cm^3 was calculated for the test system fluid at the end of the test. This fluid density is identical to the value determined during injection-test #1 and was also used for analysis and parameter conversion purposes for all Rose Run #2 tests.

The recovery pressure response was monitored for ~11 hours and was terminated at 0658 hours (EDT), August 1, 2007. The pressure recovery was recorded with the downhole shut-in tool closed, which isolates the test interval at test formation depths and greatly reduces the effect of wellbore storage during the recovery period. Because the injection rates were essentially uniform during the course of the entire constant-head injection last, the pressure recovery data can be analyzed with constant-rate injection-test methods that are identified in Section 2.3.2. This analysis approach is consistent with previous discussions by Lohman (1979) for analyzing recovery responses following constant-head tests.

Appendix C Figure C.18 shows a diagnostic log-log plot of the observed recovery and recovery data derivative following the second injection test using the Agarwal Equivalent Time function (Agarwal 1980). A comparison of this diagnostic recovery plot with the recovery plot following injection-test #1 (Appendix C Figure C.14) indicates essentially identical behavior (i.e., over the recovery time period observed). This close similarity in diagnostic behavior indicates that test system fluid variations and increasing downhole pressures during the first phase of injection-test #1 had little impact on the recovery response following this test. Because of this close diagnostic plot similarity, similar recovery analysis results would be expected for injection-test #2 recovery results. Examination of Appendix C Figure C.18 indicates that infinite-acting radial flow conditions (i.e., horizontal derivative) were established after approximately 150 minutes into the recovery period. Test data reflective of infinite-aquifer response characteristics can be analyzed with standard semi-log, straight-line solutions, as discussed previously in Spane (1993) and Spane and Wurstner (1993).

Appendix C Figure C.19 shows the analysis results using the Horner (1951) straight-line analysis method for injection-test #2 recovery. The straight-line analysis provided the following estimated results: T = 0.889 ft^2/day, and K = 0.068 ft/day (k = 21.8 milli-darcies). The K value of 0.068 ft/day was

calculated by dividing T by the estimated 13-ft contributing sandstone layer thickness, b. It is assumed that the contributing sandstone layer thickness coincides with the perforated test-interval length, L, (i.e., 7,416 to 7,418 ft, and 7,435 to 7,446 ft). A positive skin factor of +13.6 (indicative of moderate borehole damage/well-skin effects) was calculated with equation relationships presented in Earlougher (1977) and assuming a test-interval storativity value of 3.5 E-5, based on formational and fluid compressibility estimates described in Section 2.3.5. As shown in the figure, a static formation pressure of 3,415.35 psi was calculated for the Rose Run #2 test interval based on projecting the test recovery slope to infinite-recovery time conditions, i.e., Horner Time, $(t + t')/t' = 1$ (Note: probe depth = 7,380 ft). Given an estimated test system fluid density of 1.181 g/cm^3, this equates to a calculated static formation pressure of 3,434 psi for the top of the perforated test interval (i.e., 7,416 ft). Because of the relative stability in downhole test-interval pressure conditions before initiation of injection-test #2, this projected static formation pressure is considered to provide the best estimate of static formation conditions.

Appendix C Figure C.20 shows injection-test #2 recovery analysis results using the semi-log, straight-line analysis method described in Agarwal (1980), which accounts for the duration of the pumping time, using the Agarwal Equivalent Time Function, $(t \times t')/(t + t')$. The straight-line analysis provided nearly identical results as the Horner plot analysis: T = 0.894 ft^2/day, and K = 0.069 ft/day (k = 22.1 milli-darcies), and $s_K = +13.8$.

To examine the relative *goodness-of-fit* of these straight-line analysis method estimates, the calculated parameters from the straight-line analysis methods were used initially in the analytical model WTAQ (Moench 1997) to calculate an associated recovery fall-off type-curve response. As for the analysis of injection-test #1, these values were adjusted slightly in iterative fashion until a visual best match to the observed injection-test #2 recovery and recovery derivative response was obtained. It should be noted that the analytical model used does not include the capability of modeling transitional flow periods (e.g., spherical to radial flow). Because of this limitation, emphasis was placed on matching early-time (wellbore storage and well skin regions) and later-time radial flow dominant time periods. A reasonable match was obtained with this approach. Appendix C Figure C.21 shows the results of the composite type-curve and derivative plot analysis using the following characterization parameters: T = 0.892 ft^2/day; K = 0.069 ft/day; S = 3.5E-5; and $S_k = +13.7$. It should also be noted that the analysis result for the dimensionless wellbore-storage parameter, C_D, of 6.0 is slightly higher than that estimated from test system volumes and compressibility relationships. This slightly higher analysis value may be indicative of incorporation of air into the test system during the injection-test process.

As a means of supporting the previous calculated recovery analysis results, the observed injection-rate data during injection-test #2 were analyzed for possible corroboration of formation hydraulic-property estimates. As a means of extending the plot analysis, observed discharge data obtained during the second half of injection-test #1 (i.e., the last 600 minutes) were included (when downhole injection pressures were relatively stable) to produce a combined, extended injection-test analysis plot. The analytical model based on the constant-head discharge solution presented originally by Jacob and Lohman (1952) was using to simulate injection rates vs. time based on the results obtained from the composite type-curve and derivative plot analysis of injection-test #2 recovery. The injection rates were calculated based on an imposed constant-head injection pressure (above static formation pressure conditions) of 410.82 psi. Appendix C Figure C.22 shows the results of the predicted surface discharge measurements,

based on listed input parameters. As indicated the predicted injection rates compare well with the observed data and provide additional corroboration of the estimated hydraulic/storage properties derived from the injection-test recovery analyses. For comparative purposes, an injection-rate profile is also shown for the same hydraulic/storage parameters without the presence well-skin damage. As indicated, the level of well-skin damage has a significant impact on transient injection rates.

3.3.2 Slug-Injection/DST

Following completion of the monitored recovery following termination of the injection-test #1, a slug-injection/DST test was initiated by opening the downhole shut-in tool at 0925 hours (EDT), July 31, 2007, by raising the pressure probe assembly a short distance above the tubing-string seating nipple. The tubing string was filled with brine test water to near land surface before opening the shut-in tool, which produced an over-pressure of 363.233 psi above pre-slug-test pressure conditions. The slug-injection recovery continued for 50 minutes and was terminated at 1015 hours. The slug-injection test was terminated, and the DST recovery phase of the test was initiated by lowering the pressure probe assembly into the tubing-string seating nipple, which closed the shut-in tool. The DST recovery phase continued for 92 minutes and was terminated at 1147 hours (EDT) on July 31, 2007. A typical DST recovery response pattern was exhibited during this phase of the test.

The pressure recovery observed during the period after opening of the downhole shut-in tool during the DST test represents a slug-injection test and can be analyzed with the analytical methods described in Section 2.3.1. The slug data and derivative plot of the slug-test response shown in Appendix C Figure C.23 indicates only a ~35 percent recovery of the applied over-pressure. For independent, quantitative analysis, at least a 50-percent recovery is required. To analyze the available slug-test data, hydraulic properties and skin conditions observed from the recovery phases of the injection test were used as initial parameter inputs and then adjusted iteratively until visually acceptable type curve and derivative plot matches were obtained. Appendix C Figure C.23 shows the final composite analysis slug-test type curve and derivative plot match. As indicated, the slug-test analysis provided slightly lower hydraulic properties for the indicated well-skin condition: T = 0.78 ft^2/day, and K = 0.060 ft/day (k = 19.2 milli-darcies), and s_K of +12.6.

Appendix C Figure C.24 shows a diagnostic log-log plot of the observed DST recovery and recovery data derivative. The plot pattern is very similar to the diagnostic recovery plot exhibited for the constant-head injection-test recoveries (Appendix C Figures C.12 and C.18). The DST derivative plot, however, indicates that late-time, infinite-acting, radial flow conditions were never established during the DST recovery monitoring period. This indicates that straight-line solutions cannot be used quantitatively. In an effort to provide qualitative property estimates, the DST recovery data were analyzed with this analytical method. Appendix C Figure C.25 shows the qualitative analysis results using the Horner (1951) straight-line analysis method. The straight-line analysis provided slightly higher hydraulic and well-skin conditions: T = 1.11 ft^2/day, K = 0.085 ft/day (k = 27.2 milli-darcies), and s_K = +16.2. These values were obtained by assuming that the constant injection rate that occurred during the slug-injection phase of the test is proportional volumetrically to the recorded decline in downhole pressure that occurred during this phase of the test (i.e., Q = 0.770 gpm; ΔP = 124.11 psi).

As shown in the figure, a static formation probe pressure of 3,414.47 psi was calculated for the Rose Run #2 test interval based on projecting the test recovery slope to infinite-recovery time conditions, i.e., Horner Time, (t + t')/t' = 1 (Note: probe depth = 7,380 ft). This static probe pressure value is very similar to the projected value obtained from the recovery of injection-test #2, which is considered to be most representative of actual static formation conditions.

3.3.3 Test History Match

Figure 3.7 shows the sequence of hydrologic test events and associated downhole pressure response for the Rose Run #2 test-interval characterization. To focus efforts to determine the *best-estimate* values for transmissivity and storativity for the test interval, the series of hydrologic tests conducted in the later characterization phase were examined. The first injection test and associated test recovery were not included in the test history match evaluation because of the complexities that occurred during the first half of the injection test. The collective testing sequence used in the test history match included the slug-injection and DST recovery, and injection-test #2 and associated injection-test recovery (fall-off). The test history analysis was performed with the test history matching procedure discussed in Section 2.3.4, which relies on the KGS (Liu and Butler 1995) and WTAQ (Moench 1997) analytical models. The property estimates derived from the injection-test #2 recovery type-curve and derivative analysis served as initial input values for the test history matching procedure. It should be noted that the recovery following the constant-head injection test was modeled as a constant-rate injection test using the weighted average injection rate determined during this phase of the test. The figure shows both constant-head and constant-rate pressure simulations for the active injection-test#2 phase. As previously discussed in Section 2.3.3, the pressure buildup from a constant-rate injection test should be equivalent to the pressure applied during a constant-head pressure at the end of the injection phase (i.e., if the weighed average injection rate is used).

Figure 3.8 shows the coincidence of the simulated and observed responses. No significant improvement in the visual match was obtained through property adjustments of the initial input values. The hydraulic and storage properties values used for the final time history simulation match represent the best-estimate property values for the Rose Run #2 test zone: T = 0.891 ft^2/day, K = 0.069 ft/day (k = 21.9 milli-darcies), S = 3.5E-5, s_K = +13.8. The best-estimate value for static formation pressure of 3,415.35 psi at probe depth (i.e., 7,380 ft; projected static formation pressure of 3,434 psi for the top of the perforated test interval i.e., 7,416 ft). For sensitivity analysis assessment, the best-estimate time history match simulation is shown in comparison to two simulations for varying test-interval hydraulic-property conditions in Figure 3.9. The comparisons were developed using the constant-rate injection approach during the active injection-test phase. As indicated, significant pressure history sequences are realized using hydraulic-property values one-half and twice the best-estimate value for test zone transmissivity (i.e., T = 0.891 ft^2/d). This significant sensitivity exhibited to varying hydraulic-property conditions provides additional corroboration to the calculated best-estimate solution. Similar variations in test history response occurred when varying S and s_K (not shown).

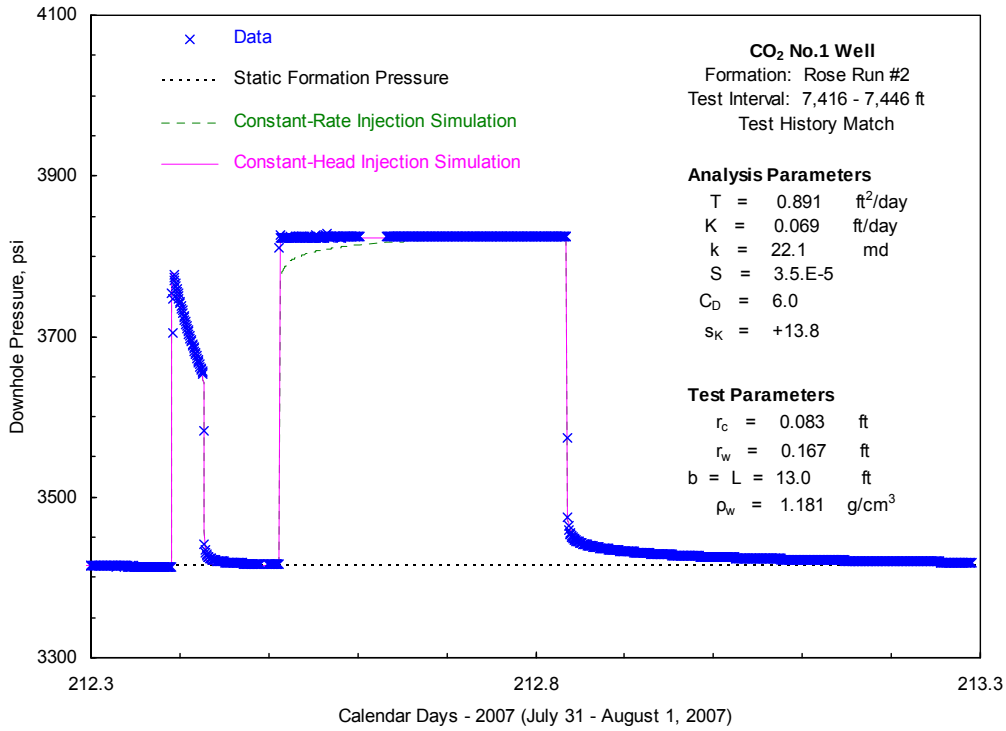

Figure 3.8. CO_2 No. 1 Well Test History Analysis Match: Rose Run #2

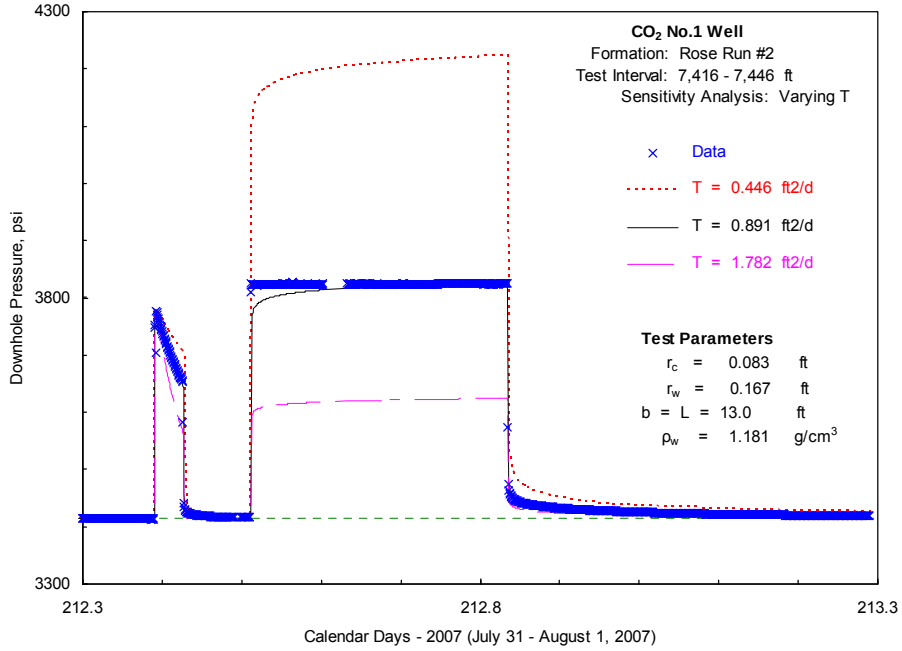

Figure 3.9. CO_2 No. 1 Well Test History Sensitivity Analysis: Rose Run #2

3.4 Rose Run #3

Following completion of hydraulic test characterization of the underlying Rose Run #2 test interval, the bridge plug and tubing-string packer were released and re-set at a depth of 7,404 ft and 7,326 ft, respectively, to support hydraulic test characterization of Rose Run #3. The Rose Run #3 zone isolated by the packers includes two perforated intervals that are positioned stratigraphically within the upper section of the Rose Run sandstone: 7,377 to 7,380 ft, and 7,387 to 7,396 ft. The 12-ft perforated interval was isolated within cemented well casing on August 1, 2007, using the bridge plug and an overlying test tubing-string packer system. The shut-in tool seating nipple location within the test tubing string was located at a depth of 7,315 ft. The downhole pressure probe assembly was lowered into the seating nipple to initiate shut-in equilibration of the test zone, at 1010 hours, EDT. After an 86-minute closed test-system equilibration pressure period, a constant-head injection test was initiated at 1137 hours (EDT) on August 1, 2007. The injection test was terminated at 0736 hours (EDT) August 2, 2007, which marked the beginning of shut-in recovery. Injection-test recovery continued until 0746 hours (EDT), August 3, 2007 when a slug-injection/DST test was initiated. DST recovery monitoring continued until 1147 hours, August 3, 2007, which marked the end of hydraulic test characterization of Rose Run #3.

Figure 3.10 shows the downhole pressure history response during the testing sequence performed during the Rose Run #3 test characterization. A detailed discussion of hydrologic tests and analytical results for the various test methods is provided below. An analytical summary of individual hydrologic tests and associated analysis plots are presented in Table 3.4 and Appendix C, respectively. Examination of the pressure response below the lower bridge plug during testing (Appendix D Figure D.4) indicates that there was observable hydraulic communication between the isolated test interval and the underlying Rose Run #2 perforated zone during the course of characterization of Rose Run #3. The lack of a definitive "leakage" response for diagnostic test derivative plots, however, suggests that the level of hydraulic communication exhibited with the underlying test zone did not adversely impact hydraulic-property characterization of Rose Run #3.

3.4.1 Constant-Head Injection

In preparation for conducting a constant-head injection test for Rose Run #3, the test tubing-string was filled to the surface with the test interval in a shut-in condition. The constant-head injection test was initiated at 1136 hours (EDT), August 1, 2007, by opening the shut-in tool (i.e., raising the pressure probe assembly 18 ft above the seating nipple location) and simultaneously initiating injection. The surface injection pressure was maintained at a closed-in, surface wellhead pressure of +50 psi for the entirety of the injection test. After 1,200 minutes, the constant-head injection test was terminated at 0736 hours (EDT), August 2, 2007. As shown in Figure 3.10, true constant-head conditions were established and maintained for the entirety of the constant-head injection test. In total, 265 gallons of brine water were injected into the test tubing-string system during the 20-hr injection test. Injection rates remained relatively constant during the course of the test, declining slightly from 0.28 to 0.17 gpm during the last 18 hours of the injection test (weighted average = 0.22 gpm). Based on the observed downhole pressure at the end of the injection test of 3778.59 psi (at a surface injection pressure of +50 psi) and elevation difference between the wellhead surface pressure sensor location and the downhole pressure probe depth setting (distance = 7,305 ft), an average density of 1.179 g/cm^3 was calculated for the test system fluid at

the end of the test. This fluid density was used for analysis and parameter conversion purposes for all Rose Run #3 tests.

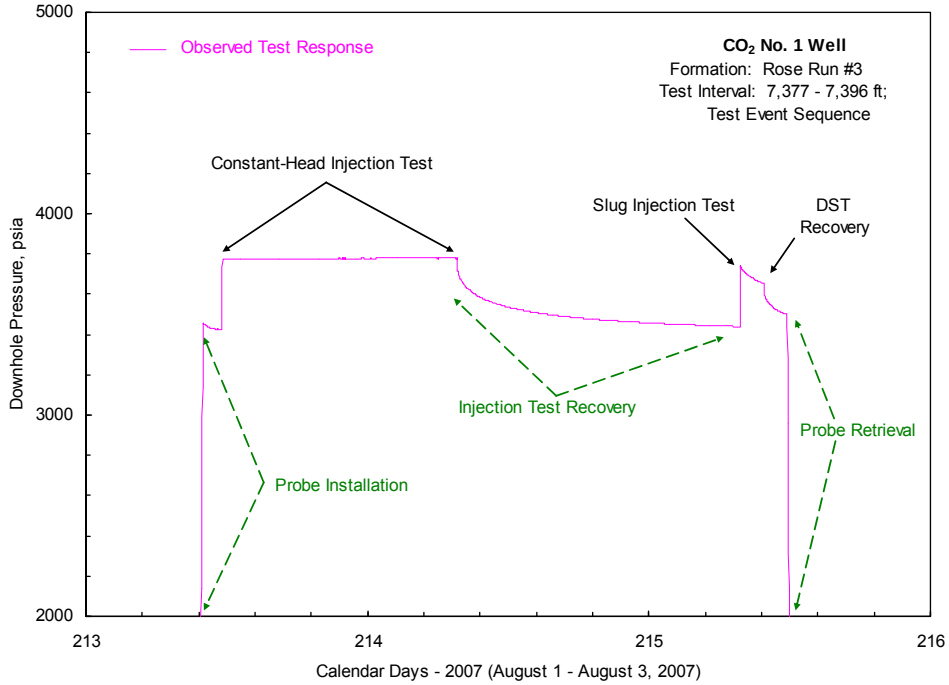

Figure 3.10. CO_2 No. 1 Well Test Event Pressure History Plot: Rose Run #3

Recovery pressure monitoring continued for ~24 hours following completion of injection testing, and was terminated at 0746 hours (EDT), August 3, 2007. The pressure recovery was recorded with the downhole shut-in tool closed, which isolates the test interval at test formation depths and greatly reduces the effect of wellbore storage during the recovery period. The shut-in recovery was accomplished by lowering the pressure probe assembly into the shut-in tool seating nipple (Figure 2.2b). Because the injection rates were relatively uniform during the constant-head injection phase of the test, the pressure recovery data can be analyzed using constant-rate injection-test methods that are identified in Section 2.3.2. This analysis approach is consistent with previous discussions by Lohman (1979) for analyzing recovery responses following constant-head tests.

Appendix C Figure C.26 shows a diagnostic log-log plot of the observed injection-test recovery and recovery data derivative. The recovery data is plotted versus Agarwal Equivalent Time function (Agarwal 1980), which adjusts the recovery data for the duration of the preceding injection (pressure buildup) test phase. Examination of Appendix C Figure C.26 indicates that infinite-acting radial flow conditions (i.e., horizontal derivative) were established only during the later-stages of the recovery period (i.e., after approximately 400 minutes). In addition, because of the relatively low permeability of the test interval, closing of the shut-in tool caused a small positive pressure perturbation during the initial phase of test recovery. This is indicated in the diagnostic plot. Test data reflective of infinite-aquifer response characteristics can be analyzed with standard semi-log, straight-line solutions, as discussed previously in Spane (1993) and Spane and Wurstner (1993). It should be noted that the recovery derivative plot for

Rose Run #3 is also diagnostically similar to the pattern exhibited for the underlying Basal sandstone test zone, which as previously noted was believed influenced by the presence of gas.

Table 3.4. CO_2 No. 1 Well: Hydrologic Testing/Analysis Summary: Rose Run #3 (Perforated Zone: 7,377 to 7,396 ft bKB[(a)])

Test Type	Hydraulic Properties					Analytical Method
	T ft^2/d	**K**[(b)] ft/d	**k**[(c)] md	**S**	s_K	
Injection-Test Recovery	0.019	0.002	0.6	1.8E-2	0	Horner Plot
	0.019	0.002	0.6	1.6E-2	0	Semi-Log Agarwal Recovery
	0.019	0.002	0.6	1.8E-2	0	Injection-Test Recovery Type Curve/Derivative Plot
Constant-Head/ Discharge	0.017	0.001	0.4	1.8E-2	0	Lohman Analysis
Slug-Injection Test	0.036	0.003	1.0	1.2E-3	0	Type Curve/Derivative Plot
DST Recovery	0.019	0.002	0.6	1.8E-2	0	Injection-Test Recovery Type Curve/Derivative Plot—Corroborative Check
Test History Match	0.019	0.002	0.6	1.8E-2	0	Superposition Simulation
Best Estimate	0.019	0.002	0.6	1.8E-2	0	Test History Match

Note: shaded test methods indicate tests having higher reliability for formation hydraulic-property characterization.

(a) **ft bKB**: feet below original Kelly Bushing datum
(b) **K** = T/b; assumed contributing thickness, b; assigned equal to the perforated interval length, L = 12 ft
(c) **k** = K (μ/γ)

Appendix C Figure C.27 shows the analysis results obtained from the Horner (1951) straight-line analysis method. The straight-line analysis provided the following estimated results: T = 0.019 ft^2/day, and K = 0.002 ft/day (0.6 milli-darcies). The K value of 0.002 ft/day was calculated by dividing T by the estimated 12-ft contributing sandstone layer thickness, b. It is assumed that the contributing sandstone layer thickness coincides with the perforated test-interval length, L, (i.e., 7,377 to 7,380 ft, and 7,387 to 7,396 ft). Of particular note is the relatively large value estimated for S of 0.018 derived from the test analysis. This is considerably higher than a calculated test zone value of 3.24E-5, which is based on assumed brine water and rock formation compressibility relationships (Section 2.3.5). This higher-than-expected value for S is attributed to higher fluid compressibility within the test system and/or surrounding test formation. Without knowing the percentage of free and/or saturated gas within the surrounding test interval, it is not possible to assess well skin, s_K, conditions. Because of this uncertainty, a skin factor (s_K) of 0 was assigned to the combined storativity term (i.e., $Se^{2sK} = S$). As shown in the figure, a static formation pressure of 3,384.07 psi was calculated for the Rose Run #3 test interval based on projecting the test recovery slope to infinite-recovery time conditions, i.e., Horner Time, (t + t')/t' = 1 (Note: probe

depth = 7,315 ft). Given an estimated test system fluid density of 1.179 g/cm^3, this equates to a calculated static formation pressure of 3,416 psi for the top of the perforated test interval (i.e., 7,377 ft).

Appendix C Figure C.28 shows the analysis results using the semi-log, straight-line analysis method described in Agarwal (1980), which accounts for the duration of the pumping time, using the Agarwal Equivalent Time Function, $(t \times t')/(t + t')$. The straight-line analysis provided nearly identical results as the Horner plot analysis: T = 0.019 ft^2/day, and K = 0.002 ft/day (0.6 milli-darcies), and S = 0.016.

To examine the relative *goodness-of-fit* of these straight-line analysis method estimates, the calculated parameters from the straight-line analysis methods were used initially in the analytical model WTAQ (Moench 1997) to calculate an associated recovery fall-off type-curve response. These values were adjusted slightly in iterative fashion until a visual best match to observed pressure recovery and recovery derivative response was obtained. It should be noted that the early-time recovery data ≤ 1 minutes were adversely impacted by shut-in tool closure. Because of this test complexity, emphasis was placed on matching recovery test data after this effect was dissipated. No significant improvement in the composite type-curve and derivative plot matching process was obtained in adjusting parameter values obtained from the straight-line analyses. Appendix C Figure C.29 shows the results of the composite type-curve and derivative plot analysis using the characterization parameters obtained from the straight-line analyses.

Based on the recovery analysis results, the observed injection-rate data were also examined quantitatively for possible corroboration of formation hydraulic-property estimates. Because downhole pressures were maintained at nearly constant-pressure conditions for the majority of the test, a higher level of analysis reliability was expected for this test, i.e., in contrast to some of the previous test zone constant-head tests. The analytical model based on the constant-head discharge solution presented originally by Jacob and Lohman (1952) was using to simulate injection rates vs. time based on the results obtained from the composite type-curve and derivative plot analysis of recovery test data and a calculated imposed constant-head injection pressure above pre-test pressure conditions of 366.78 psi. The pre-test pressure, rather than projected static formation pressure was used for the analysis because of the low test-interval permeability and lack of recovery to static conditions before test initiation. Appendix C Figure C.30 shows the results of the predicted surface discharge measurements, based on listed input parameters. As indicated, the predicted injection rates compare reasonably well with the observed data, but a slightly better fit to the observed discharge rates was realized by lowering the test zone transmissivity from 0.019 to 0.017 ft^2/day.

3.4.2 Slug-Injection/DST

Following completion of the recovery following termination of the injection test, a slug-injection/DST test was initiated by opening the downhole shut-in tool at 0746 hours (EDT), August 3, 2007, by raising the pressure probe assembly a short distance above the tubing-string seating nipple. Before opening the shut-in tool, the tubing string was filled with brine test water to near land surface, which produced an over-pressure of 312.49 psi above pre-slug-test pressure conditions. The downhole pressure response exhibited a typical recovery fall-off pattern during the initial 120 minutes of the test, with a pressure decline of 89 psi observed during the course of the test. The DST recovery phase of the test was initiated at 0947 hours (EDT), August 3, 2007, when the shut-in tool was closed by lowering the

pressure probe assembly into the tubing-string seating nipple. The DST recovery phase continued for an additional 120 minutes and was terminated at 11:47 hours (EDT) on August 3, 2007. A typical DST recovery response pattern was exhibited during this phase of the test.

The pressure recovery observed during the period after opening the downhole shut-in tool during the DST test represents a slug injection test and can be analyzed with the analytical methods described in Section 2.3.1. The slug data and derivative plot of the slug-test response shown in Appendix C Figure C.31 indicate only a ~30 percent recovery of the applied over-pressure. For independent, quantitative analysis, at least a 50-percent recovery is required. To analyze the available slug-test data, hydraulic properties and skin conditions observed from the recovery phases of the injection test were used as initial parameter inputs and then adjusted iteratively until visually acceptable type curve and derivative plot matches were obtained. Appendix C Figure C.31 shows the final composite analysis slug-test type curve and derivative plot match. As indicated, the slug-test analysis provided slightly higher hydraulic properties and slightly lower storativity value: T = 0.036 ft^2/day, and K = 0.003 ft/day (1.0 milli-darcies), and S = 1.2E-3. The departure in the observed data derivative and predicted derivative plot is believed attributable to either not accounting for the pre-test pressure trend or slightly higher S conditions (i.e., test-fluid compressibility) with distance from the test well.

Appendix C Figure C.32 shows a diagnostic log-log plot of the observed DST recovery and recovery data derivative. The plot pattern is nearly identical to the diagnostic recovery plot exhibited for the constant-head injection-test recoveries (Appendix C Figures C.26 and C.29). The DST derivative plot, however, indicates that late-time, infinite-acting, radial flow conditions were never established during the DST recovery monitoring period. This indicates that straight-line solutions cannot be used quantitatively to analyze the DST recovery data. In an effort to provide qualitative property corroboration, the DST recovery data were compared to predicted type-curve and derivative plot using the previously determined hydraulic and storage property estimates obtained from the injection-test recovery analyses. Appendix C Figure C.33 shows the corroborative match of the observed DST recovery data using this approach. As indicated, a consistent observed versus predicted recovery result was obtained. These values were obtained by assuming that the constant injection rate that occurred during the slug-injection phase of the test is proportional volumetrically to the recorded decline in downhole pressure that occurred during this phase of the test (i.e., Q = 0.235 gpm; ΔP = 88.96 psi) during the previous slug-injection test.

3.4.3 Test History Match

Figure 3.10 shows the sequence of hydrologic test events and associated downhole pressure response for the Rose Run #3 test-interval characterization. To determine the *best-estimate* values for transmissivity and storativity for the test interval, the series of hydrologic characterization tests (injection test and injection-test recovery [fall-off] and the subsequent slug-injection/DST tests) were analyzed compositely as a collective testing sequence. The test history analysis was performed with the test history matching procedure discussed in Section 2.3.4, which relies on the KGS (Liu and Butler 1995) and WTAQ (Moench 1997) analytical models. The property estimates derived from the injection-test recovery type-curve and derivative analysis served as initial input values for the test history matching procedure. It should be noted that the recovery following the constant-head injection test was modeled as a constant-rate injection test using the weighted average injection rate determined during this phase of the

test. The simulation shows both constant-head and constant-rate pressure simulations for the active injection-test phase. As previously discussed in Section 2.3.3, the pressure buildup from a constant-rate injection test should be equivalent to the pressure applied during a constant-head pressure at the end of the injection phase (i.e., if the weighed average injection rate is used).

Figure 3.11 shows the coincidence of the simulated and observed responses. No improvement in the visual match was obtained through property adjustments. The initial input values obtained from the injection-test recovery analysis, therefore, are considered to represent the best-estimate property values: T = 0.019 ft^2/day, K = 0.002 ft/day (k = 0.6 milli-darcies), S = 1.8E-2, and a static formation pressure of 3,384.07 psi at probe depth (i.e., 7,315 ft; projected static formation pressure of 3,415.71 psi for the top of the perforated test interval i.e., 7,377 ft). For sensitivity analysis assessment, the best-estimate time history match simulation is shown in comparison to two simulations for varying test-interval hydraulic-property conditions in Figure 3.12. The comparisons were developed using the constant-rate injection approach during the active injection-test phase. As indicated, significant pressure history sequences are realized using hydraulic-property values one-half and twice the best-estimate value for test zone transmissivity (i.e., T = 0.019 ft^2/d). This significant sensitivity exhibited to varying hydraulic-property conditions provides additional corroboration to the calculated best-estimate solution. Similar variations in test history response occurred when varying S and s_K (not shown).

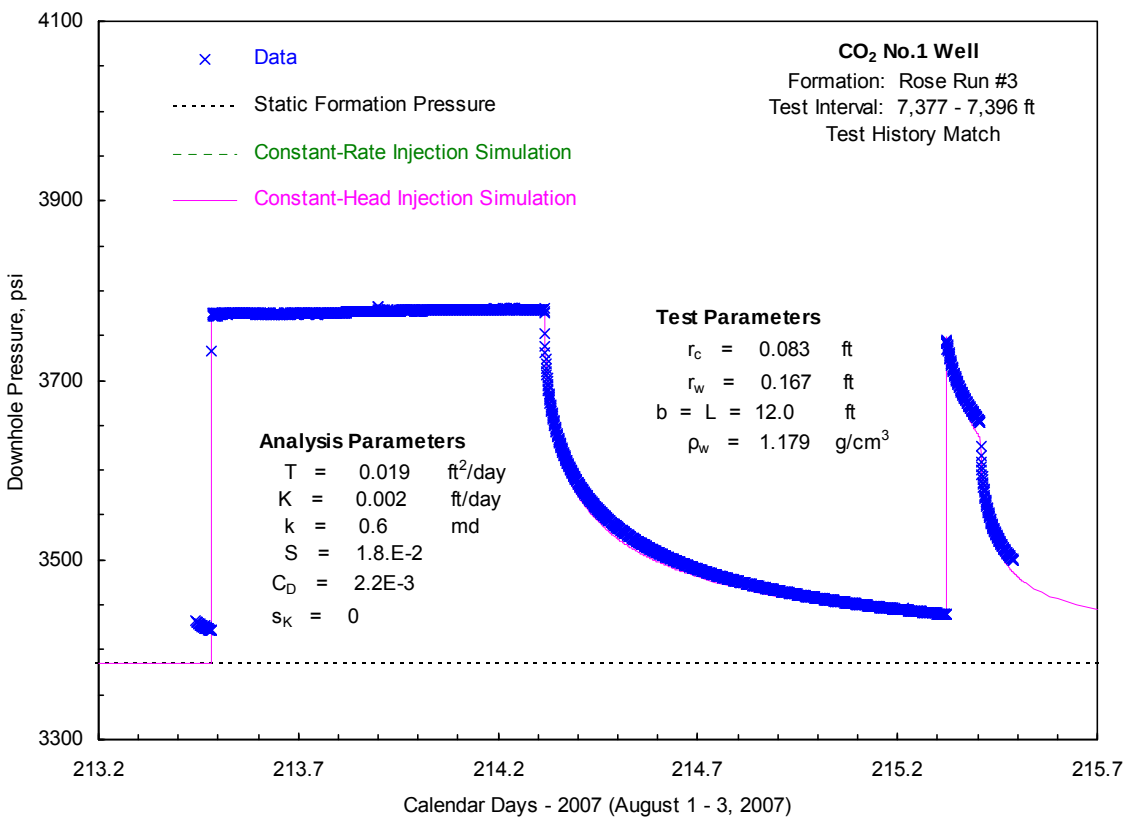

Figure 3.11. CO_2 No. 1 Well Test History Analysis Match: Rose Run #3

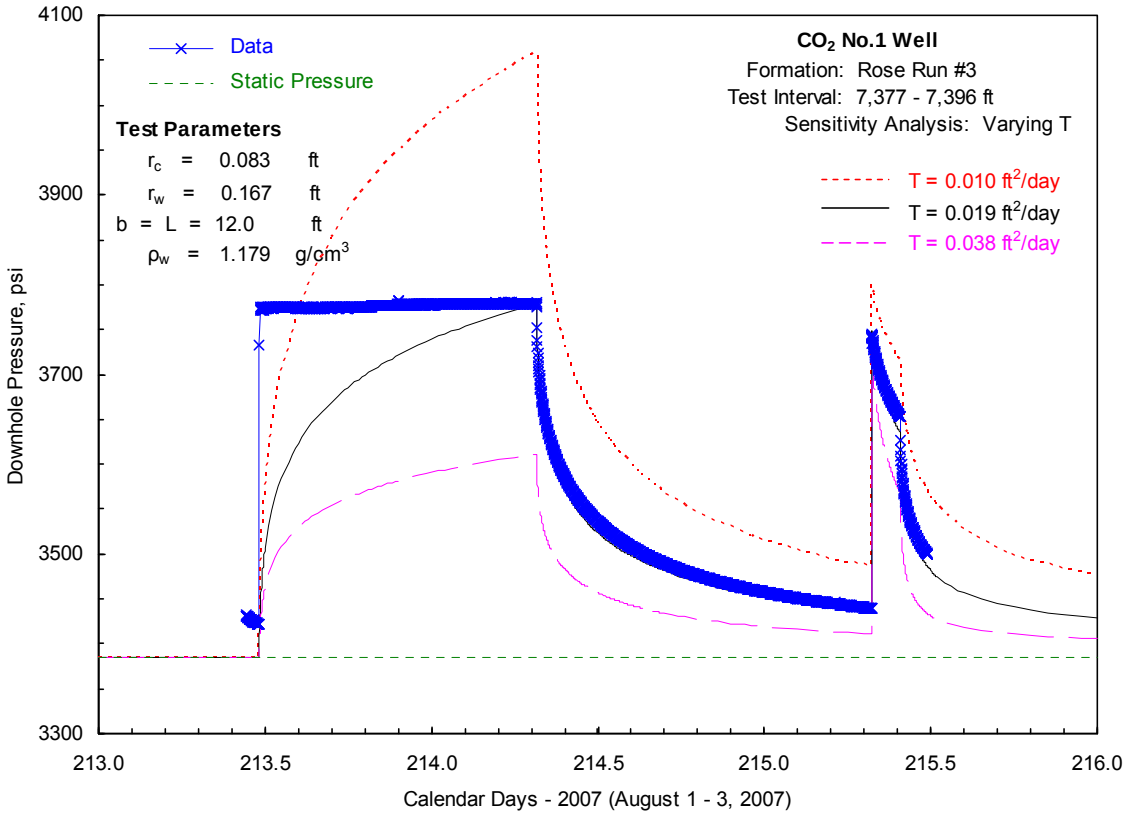

Figure 3.12. CO_2 No. 1 Well Test History Sensitivity Analysis: Rose Run #3

3.5 Composite Rose Run

Following completion of the hydraulic test characterization of Rose Run #3 test interval, the bridge plug and tubing-string packer were released and re-set at a depth of 7,530 ft and 7,326 ft, respectively, to support composite hydraulic test characterization of all perforated Rose Run test zones (i.e., Rose Run #1, #2, and #3). The composite Rose Run test zone isolated by the packers includes five separate perforated intervals that are positioned stratigraphically within the upper, middle, and lower-section of the Rose Run sandstone: 7,377 to 7,380 ft, 7,387 to 7,396 ft, 7,416 to 7,418 ft, 7,435 to 7,446 ft, and 7,506 to 7,509 ft. The 28-ft perforated interval was isolated within cemented well casing on August 3, 2007, using the bridge plug and an overlying test tubing-string packer system. The shut-in tool seating nipple location within the test tubing string was located at a depth of 7,315 ft. The downhole pressure probe assembly was lowered into the seating nipple to initiate test zone, shut-in equilibration at 1510 hours (EDT), August 3, 2007. After a 135-minute closed test-system equilibration pressure period, a constant-head injection test was initiated at 1725 hours (EDT). The injection test was terminated at 1734 hours (EDT) August 4, 2007, which marked the beginning of shut-in recovery. Injection-test recovery continued until 0633 hours (EDT), August 6, 2007, for performance of a slug-injection/DST test. DST recovery monitoring continued until 1033 hours, August 6, 2007, which marked the end of hydraulic test characterization of composite Rose Run test zone.

Figure 3.13 shows the downhole pressure history response during the testing sequence performed during the composite Rose Run test characterization. The primary objective of the composite Rose Run test was to provide additional corroboration of the individual hydraulic test zone characterizations conducted within the Rose Run. A detailed discussion of hydrologic tests and analytical results for the various test methods is provided below. Examination of the pressure response below the lower bridge plug during testing (Appendix D Figure D.5, indicates that there was no observable hydraulic communication between the isolated test interval and the underlying, much deeper, Basal sandstone perforated intervals.

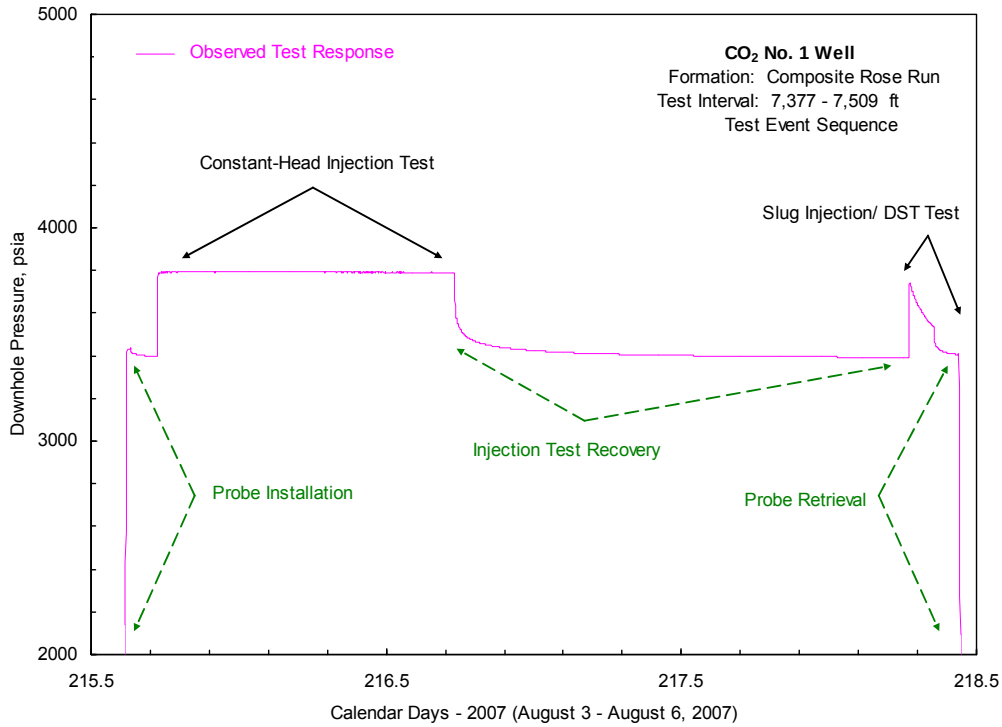

Figure 3.13. CO_2 No. 1 Well Test Event Pressure History Plot: Composite Rose Run

3.5.1 Constant-Head Injection

In preparation for conducting a constant-head injection test for composite Rose Run test zone, the test tubing-string was filled to the surface with the test interval in a shut-in condition. The constant-head injection test was initiated at 1725 hours (EDT), August 3, 2007, by opening the shut-in tool (i.e., raising the pressure probe assembly 15 ft above the seating nipple location) and simultaneously initiating injection. The surface injection pressure was maintained at a closed-in, surface wellhead pressure of +50 psi for the entirety of the injection test. After 1,449 minutes, the constant-head injection test was terminated at 1734 hours (EDT), August 4, 2007. As shown in Figure 3.13, true constant-head conditions were established and maintained for the entirety of the constant-head injection test. In total, 1,450 gallons of brine water were injected into the test tubing-string system during the ~24-hr injection test. Injection rates steadily decreased from 2.1 to 1.1 gpm during the initial 250 minutes of the injection test and then remained relatively constant, declining only slightly from 1.1 to 0.83 gpm during the last 1,200 minutes

of the injection test (weighted average = 0.99 gpm). Based on the observed downhole pressure at the end of the injection test of 3,790.30 psi (at a surface injection pressure of +50 psi) and the elevation difference between the wellhead surface pressure sensor location and the downhole pressure probe depth setting (distance = 7,308 ft), an average density of 1.182 g/cm^3 was calculated for the test system fluid at the end of the test. This fluid density was used for analysis and parameter conversion purposes for all composite Rose Run tests.

Recovery pressure monitoring continued for ~37 hours following completion of injection testing, and was terminated at 0633 hours (EDT), August 6, 2007. The pressure recovery was recorded with the downhole shut-in tool closed, which isolates the test interval at test formation depths and greatly reduces the effect of wellbore storage during the recovery period. The shut-in recovery was accomplished by lowering the pressure probe assembly into the shut-in tool seating nipple (Figure 2.2b). Because the injection rates were relatively uniform during the majority of the constant-head injection phase of the test, the pressure recovery data can be analyzed theoretically using constant-rate injection-test methods that are identified in Section 2.3.2. This analysis approach is consistent with previous discussions by Lohman (1979) for analyzing recovery responses following constant-head tests.

Appendix C Figure C.34 shows a diagnostic log-log plot of the observed injection-test recovery and recovery data derivative. The recovery data are plotted versus Agarwal Equivalent Time function (Agarwal 1980), which adjusts the recovery data for the duration of the preceding injection (pressure buildup) test phase. Examination of Appendix C Figure C.34 suggests that infinite-acting radial flow conditions (i.e., horizontal derivative) were never fully established during the entire extended recovery period, and after approximately 30 minutes of recovery time, the derivative plot starts a steady decline. This decline is attributed to commingling and in-well flow between widely separated Rose Run perforated intervals during the intermediate-time recovery. Ideally, composite testing of multi-layered systems having no significant formational cross-flow and hydraulically connected primarily within the well test interval should provide an equivalent, single-layer transmissivity value that is equal to the combined transmissivities of the various individual layers. However, as noted by Wikramaratna (1985), this is only valid when the transmissivity and storativity values (i.e., T_i and S_i, respectively) of the individual layers are proportional in their contribution to the equivalent, single-layer T and S values:

$$S_i = \alpha_i S \tag{3.1}$$

$$T_i = \beta_i T \tag{3.2}$$

and,

$$\alpha_i = \beta_i \tag{3.3}$$

When the proportionality contributions of individual layers are not equal, as they relate to the composite single-layer T and S, then Wikramaratna (1985) notes that their associated response to composite testing will not be uniform during the test and can be considerably different at various stages of the test period (i.e., early, intermediate, and late-time). For cases examined by Wikramaratna (1985) where an individual layer made up the majority of the composite test zone S (as is the case for Rose Run #3), test durations of

several days were required before individual layers responded proportionally to their individual transmissivity values, i.e., T_i. The required time is indicated when infinite-acting, radial flow conditions have been established during the test. As noted above, derivative plot analysis indicates that these conditions were not established during the injection-test recovery. Other pertinent discussions pertaining to hydraulic testing of multi-layered systems connected within the test interval (i.e., commingled zones) are presented in a number of papers, including Raghaven et al. (1974), Kucuk et al. (1986), and Gao (1987).

Because infinite-acting radial flow conditions were not established during the injection recovery period, the Horner and semi-log straight-line analysis methods are not appropriate and, therefore, were not attempted. Force-fitting of straight-line analyses on the curvilinear recovery plots (not shown) would underestimate the composite, single-layer T for the combined three Rose Run zones tested. Similarly, no log-log analyses of injection-test recovery or injection rate vs. time were attempted because of the inherent analytical assumptions requiring that multi-layer test responses be commensurate with their T_i contribution percentages. Figure C.35, however, shows a comparison of the observed injection rates during constant-head injection testing for the composite Rose Run and three individual Rose Run test zones. The constant-head magnitudes were similar for each of the tests, so no quantitative corrections were made for this test comparison. As shown, the three individual Rose Run test zones show typical injection rate profiles vs. time, which are a function of their individual T, S, and s_K characteristics. In contrast, the composite Rose Run exhibits a profile that does not mirror or reflect the summation of the individual test zones and cuts-across the profile exhibited by Rose Run #2, the predominant zone of transmissivity, but relatively low storativity. This cross-cutting profile supports the previous discussion that the predominance and contribution to composite test response was variable for each of the three zones during the course of composite Rose Run zone testing. It would be expected that with extended injection-test time that the composite test time would eventually merge with the Rose Run #2 zone response and then increase to a level equivalent to injection rates of all three Rose Run zones. This would occur when infinite-acting radial flow conditions were established for the multi-layer system.

3.5.2 Slug-Injection/DST

Following completion of monitoring injection-test recovery, a slug-injection/DST test was initiated by opening the downhole shut-in tool at 0633 hours (EDT), August 6, 2007, by raising the pressure probe assembly a short distance above the tubing-string seating nipple. Before opening the shut-in tool, the tubing string was filled with brine test water to near land surface, which produced an over-pressure of 349.65 psi above pre-slug-test pressure conditions. The downhole pressure response exhibited a typical recovery fall-off pattern during the initial 120 minutes of the test, with a pressure recovery decline of 116 psi observed during the course of the test. The DST recovery phase of the test was initiated at 0833 hours (EDT), August 6, 2007, by lowering the pressure probe assembly into the tubing-string seating nipple and closing the shut-in tool. The DST recovery phase continued for an additional 120 minutes and was terminated at 1033 hours (EDT). A typical DST recovery response pattern was exhibited during this phase of the test.

The pressure recovery observed during the period after opening the downhole shut-in tool during the DST test represents a slug-injection test and can theoretically be analyzed with the analytical methods

described in Section 2.3.1 for homogeneous formation conditions. These analytical methods, however, are not appropriate for analyzing multi-layered test zones that do not exhibit equivalent single-layer formation response characteristics. As discussed previously, the injection test and injection-test recovery data exhibit response characteristics reflective of commingled multi-layer systems. As an initial step in examining the slug-injection-test results, the composite Rose Run test response was plotted in Appendix C Figure C-36 in comparison to slug-test responses observed for the individual Rose Run test zones #1, #2, and #3. Individual test zones exhibiting higher T values generally recover more rapidly (i.e., for single-phase fluid systems) and would plot proportionally farther to the left in the test figure. This plotting relationship is generally consistent with the individual Rose Run test zone results shown, with an additional time-lag for Rose Run #3 attributed to the significantly higher test zone S (i.e., higher compressibility due to the presence of gas). In addition, based on the earlier test-zone characterizations, Rose Run #2 was calculated to contain approximately 95 percent of the combined T value for Rose Run perforated test intervals. It would be expected, therefore, that the composite Rose Run test results should be nearly identical to those exhibited for Rose Run #2. This nearly identical relationship is also indicated in Appendix C Figure C-36.

Because slug tests are an open-borehole test response, the impact of wellbore storage effects is predominant. As noted in Wikramaratna (1985), wellbore storage tends to diminish the impact of multi-layer formational conditions on test response. Because of this, an analysis of the composite Rose Run slug-injection test was attempted using the homogeneous formation type curve and derivative plot approach discussed in Section 2.3.1. The analysis parameters calculated for Rose Run #2 were used as an initial basis for analyzing the composite Rose Run test results and then adjusted iteratively (primarily S and s_K) in an attempt to visually match the slug-test data and data derivative. The entire data and data derivative set could not be matched using this approach, which suggests that even though wellbore storage diminishes the impact of multi-layer formation effects, these effects still significantly impacted the slug-test response results. Appendix C Figure C.37 shows the attempted type-curve and derivative plot analysis match of the composite Rose Run test, using Rose Run #2 values as analysis parameters.

Appendix C Figure C.38 shows a diagnostic log-log plot of the composite Rose Run DST recovery and recovery data derivative. The plot pattern is nearly identical to the diagnostic recovery plot exhibited for the constant-head injection-test recovery (Appendix C Figure C.34). As discussed previously in Section 3.5.2, the lack of establishing infinite-acting, radial flow conditions and the presence of multi-layer commingled zone conditions eliminate the possibility of analyzing the DST recovery test using standard analysis methods described in Section 2.3.1. As a result, no additional effort was initiated for composite Rose Run test results.

4.0 Predicted Injection Rates

This section discusses predicted transient injection rates for the Basal sandstone and the Rose Run sandstone at selected surface injection pressures. The predicted injection rates are based on the best estimate hydraulic/storage properties (i.e., transmissivity and storativity) determined from the hydrologic tests performed on the respective test formations, as discussed in Section 3. Based on the best estimate hydraulic/storage properties, transient injection rates were calculated for selected constant surface injection pressures using the analytical solution originally presented in Jacob and Lohman (1952).

The predicted injection rates are also based on several assumptions:

- The perforated test intervals within CO_2 Well No. 1 fully capture and intersect all of the permeable test sections within the respective geologic formations.
- The test formation is fully developed and exhibits no formation damage (i.e., well skin) due to the drilling and well completion process.
- The selected surface injection pressures did not exceed the downhole fracture gradient conditions.

While some thin permeable layers within test formations may not be accessible by the perforated intervals within the cemented casing string, the depth intervals perforated were designed to intersect most of the significant permeable layers/horizons within the formations based on the interpretation of wireline geophysical survey results. It is anticipated that the majority of the permeable layers contributing to the composite formation transmissivity (i.e., ≥90 percent) were intersected and characterized by the completed hydraulic tests. The predicted injection rates, therefore, would be expected to be slightly lower than (i.e., ≤10 percent) the potential maximum injection rate if the test formation was completely perforated over its entire thickness.

Several of the test intervals (e.g., Rose Run #2) exhibited positive well skins indicative of low to moderate formation damage. Since formation damage can be reduced by additional well-development procedures, it was not included for the transient injection-rate predictions (i.e., well skin: $s_K = 0$).

The maximum allowable surface injection pressure (i.e., below downhole fracture gradient conditions was calculated based on the following equation relationship provided in the Ohio Administrative Code (2008) governing saltwater injection wells:

$$P_{inj} = (0.75 - \rho g)\ d \tag{4.1}$$

where P_{inj} is the maximum allowable surface injection pressure (psi), ρg is the fluid pressure-density gradient (psi/ft), and d is the depth to the highest perforation within the injection zone (ft). Based on a

fluid pressure-density gradient value of 0.52 psi/ft (Wickstrom, personal communication, 2008[(a)]), a maximum allowable surface injection pressure of 1,961 psi and 1,697 psi were calculated for the Basal sandstone and composite Rose Run test formations, respectively.

4.1 Basal Sandstone

Table 4.1 and Figure 4.1 show the predicted surface injection rates versus continuous injection times for the Basal sandstone at CO_2 Well No. 1 for the indicated surface injection pressures. The predictions are based on the best estimate values for transmissivity and storativity of 0.073 ft^2/day and 2.8E-2, respectively (see Table 3.1). It should be noted that an additional 405 psi of pressure is imposed on the injection zone by filling the injection system to land surface above static formation conditions. This additional pressure is based on a fluid density of 1.188 g/cm^3, which was calculated while the Basal sandstone within CO_2 Well No. 1 was being tested, as discussed in Section 3.1. This additional pressure was added to the indicated surface injection pressures for calculating the predicted injection rates versus time.

As shown in Table 4.1 and Figure 4.1, predicted injection rates are extremely low, ranging between 0.60 and 2.16 gpm, after 100 days of continuous injection for the indicated surface injection pressure range of 250 to 1,960 psi, respectively. The low predicted injection rates are primarily a function of the low transmissivity value calculated for the Basal sandstone at CO_2 Well No. 1.

4.2 Rose Run

Table 4.2 and Figure 4.2 show the predicted surface injection rates versus continuous injection times for the composite Rose Run at CO_2 Well No. 1 for the indicated surface injection pressures. For the Rose Run sandstone, three perforated test intervals were tested individually. The predicted injection rates for the composite Rose Run represent a summation of individual perforated interval transmissivity and storativity, which is consistent with the principle of superposition within confined aquifer systems. The predictions are based on the best estimate values for transmissivity and storativity of 0.933 ft^2/day and 1.8E-2, respectively (see Table 3.2 through Table 3.4). It should be noted that an additional 411 psi of pressure is imposed on the injection zone by filling the injection system to land surface above static formation conditions. This additional pressure is based on an average fluid density of 1.181 g/cm^3, which was calculated during testing of the Rose Run test interval that contains the majority (i.e., >90 percent) of the composite Rose Run transmissivity (i.e., Rose Run #2). This additional pressure was added to the indicated surface injection pressures for calculating the predicted injection rates versus time.

As shown in Table 4.2 and Figure 4.2, predicted injection rates range from 6.01 to 19.19 gpm after 100 days of continuous injection for the indicated surface injection pressure range of 250 to 1,700 psi, respectively.

(a) Larry Wickstrom. 2008. "Concerning Maximum Allowable Surface Injection Pressures." Personal communication, September 17, 2008.

Table 4.1. Predicted Transient Injection Rates for the Basal Sandstone at CO_2 No. 1 Well, at Selected Surface Injection Pressures

Surface Injection Pressure [a] psi	Predicted Injection Rates (gpm) at Selected Continuous Injection Times [b]					
	0.01 days	0.1 days	1.0 days	10 days	100 days	1000 days
250	3.04	1.64	1.06	0.77	0.60	0.49
500	4.20	2.27	1.46	1.06	0.83	0.67
750	5.36	2.89	1.87	1.35	1.05	0.86
1000	6.52	3.52	2.27	1.64	1.28	1.05
1250	7.68	4.15	2.67	1.94	1.51	1.23
1500	8.85	4.77	3.08	2.23	1.74	1.42
1750	10.01	5.40	3.48	2.52	1.97	1.61
1960	10.98	5.93	3.82	2.77	2.16	1.76

(a) Note: an additional 405 psi of pressure is imposed on the injection zone by filling the injection system to land surface above static formation conditions, with brine fluid at a fluid density of 1.188 g/cm^3; this is additive to the indicated surface injection pressure.

(b) Predicted injection rates based on the indicated surface injection pressures and based on the best-estimate hydraulic/storage property values indicated in Table 3.1 for the Basal sandstone at CO_2 No. 1 Well.

Table 4.2. Predicted Transient Injection Rates for the Composite Rose Run at CO_2 No. 1 Well, at Selected Surface Injection Pressures

Surface Injection Pressure [a] psi	Predicted Injection Rates (gpm) at Selected Continuous Injection Times [b]					
	0.01 days	0.1 days	1.0 days	10 days	100 days	1000 days
250	18.38	12.34	9.17	7.27	6.01	5.12
500	25.34	17.01	12.64	10.02	8.28	7.05
750	32.29	21.68	16.11	12.76	10.55	8.99
1000	39.25	26.35	19.58	15.51	12.82	10.92
1250	46.20	31.02	23.05	18.25	15.10	12.86
1500	53.16	35.69	26.52	21.01	17.37	14.79
1700	58.72	39.42	29.29	23.21	19.19	16.34

(a) Note: an additional 411 psi of pressure is imposed on the injection zone by filling the injection system to land surface above static formation conditions, with brine fluid at a fluid density of 1.181 g/cm^3; this is additive to the indicated surface injection pressure.

(b) Predicted injection rates based on the indicated surface injection pressures and based on the summation of best-estimate values for hydraulic/storage property values indicated in Table 3.2 through Table 3.4 for Rose Run test intervals at CO_2 No. 1 Well.

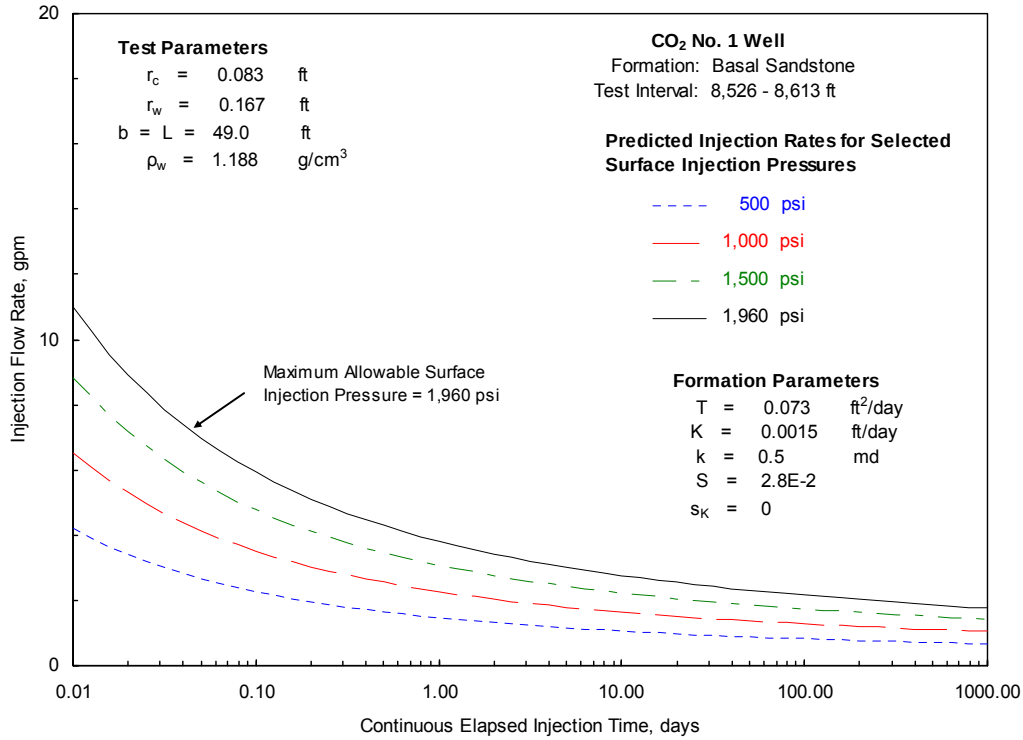

Figure 4.1. Comparison of Predicted Transient Injection Rates for the Basal Sandstone at CO_2 No. 1 Well at Selected Surface Injection Pressures

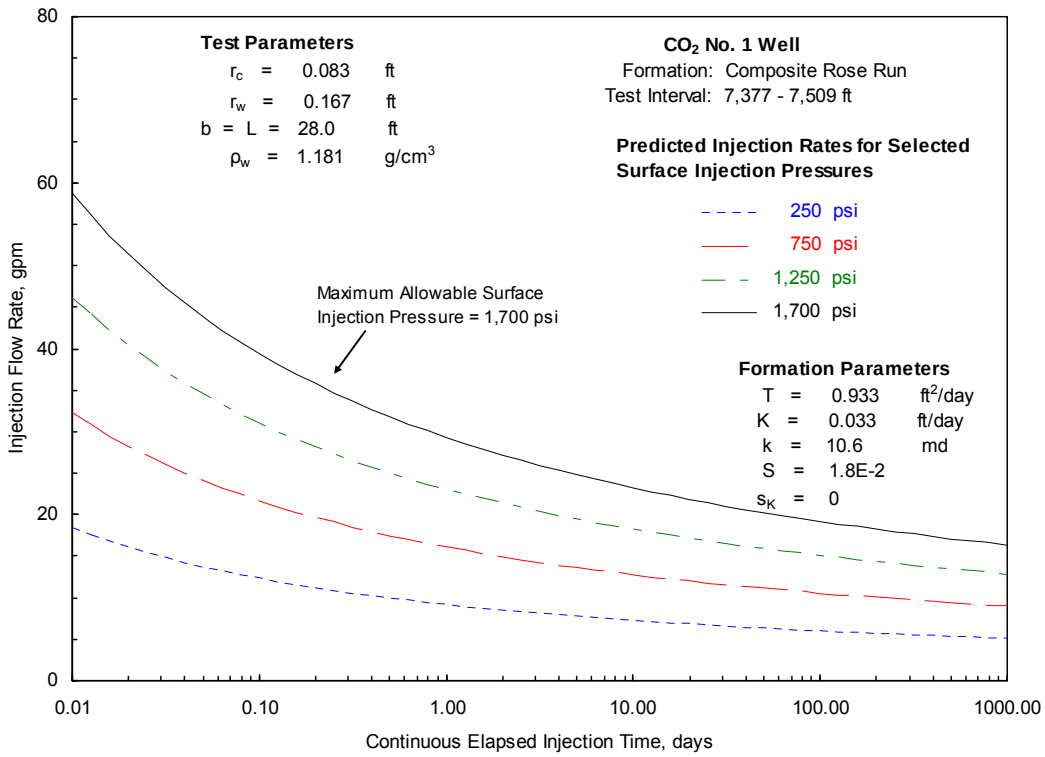

Figure 4.2. Comparison of Predicted Transient Injection Rates for the Composite Rose Run at CO_2 No. 1 Well at Selected Surface Injection Pressures

5.0 Conclusions

Field-test characterization activities conducted within selected test intervals (7,377 to 7,509 ft, and 8,526 to 8,613 ft) of the Ohio Geological Survey CO_2 No. 1 Well between July 19 and August 6, 2007, provided significant site-specific characterization information concerning the sequestration potential of CO_2 fluids within regionally recognized reservoir horizons. The characterization information obtained from the field-test program includes hydraulic and storage property information specifically for selected test horizons within the Cambrian Basal Sandstone and Rose Run formations. The principal hydraulic/storage parameters quantified during testing include transmissivity, hydraulic conductivity, permeability (intrinsic), and storativity. The field-test activities were completed using a hydrologic test sequence approach that included short-duration, slug-injection/DST recovery tests, used in conjunction with longer duration injection test and injection-test recovery characterizations. Hydrologic tests were analyzed individually using standard analytical methods and collectively using a combined test history matching approach. The combination of individual and test-sequence analysis provides a better means of determining best-estimate property values for the respective test intervals.

The perforated test intervals were isolated within the cemented well casing using a lower bridge-plug packer and an overlying tubing string packer. Downhole memory gauges were used to monitor downhole pressures within the isolated test interval and well interval below the bridge-plug packer. A surface-based pressure probe was used on the wellhead to monitor closed-system annular pressures outside the test tubing string. This pressure monitoring system provided capabilities for not only monitoring test-zone responses, but also for assessing test-zone isolation integrity and potential hydraulic communication with underlying perforated intervals. Except for a few minor test-equipment malfunctions, the test system performed well, and intervals were isolated and tested successfully.

Testing complexities identified for some of the zones during the characterization phase include 1) high test system/formation fluid compressibility due to the presence of gas (Basal sandstone, Rose Run #3), moderate well-skin effects (Rose Run #2), 2) multi-layer, commingled reservoir conditions (composite Rose Run), and 3) transitional, non-radial flow conditions possibly imposed by the partial penetration/perforation well completion (Rose Run #1 and #2). All test zones, except for the composite Rose Run, were successfully characterized with standard analytical methods. Average hydraulic-property values obtained from field testing are generally comparable and within the range of small-scale values obtained from wireline CMR survey results and discrete sidewall cores obtained over the perforated intervals tested. It is also interesting to note that the transmissivity summation value for the perforated Rose Run test intervals (0.93 ft^2/day) is very similar to the transmissivity estimate reported by Spane et al. (2006) of 0.79 ft^2/day for the Rose Run at a deep characterization borehole located ~100 miles south of CO_2 No. 1 Well. This well (Mountaineer AEP #1) was also characterized using similar borehole packer tests. No successful test results for the Basal sandstone were completed within this borehole for comparison with test results obtained from the CO_2 No. 1 Well. Qualitative open borehole tests for this stratigraphic horizon at AEP #1, however, suggest relatively low permeability conditions for the Basal sandstone unit.

The radius of investigation of the hydrologic tests for boundary detection is variable and a function of the 1) duration and magnitude of the stress applied, 2) formation of hydraulic and storage properties, and 3) test

system/formation fluid compressibility. Of these parameters, the presence of gas and its large influence on total fluid compressibility greatly limits the radius of investigation of the imposed hydrologic test. For the individual test-zone injection tests conducted at CO_2 No. 1 Well that were not impacted by the presence of high compressibility fluid (gas) conditions, radii of investigations are estimated to have ranged from ~25 ft (Rose Run #1) to ~90 ft (Rose Run #2). Test zones exhibiting high test system/formation fluid compressibility conditions (i.e., Basal sandstone and Rose Run #3) are assumed of have radii of investigations of 10 ft or less. The radius of investigation for the shorter duration slug-injection/DST recovery tests would be considerably less than for the longer duration injection tests. The relative correspondence of hydraulic properties obtained from the smaller scale slug-injection/DST recovery tests with the larger scale, longer duration injection tests, however, suggests a degree of formational uniformity for the test intervals in the immediate vicinity of the CO_2 No. 1 Well.

More detailed description of the salient characterization test findings is provided below for the two test formations.

5.1 Basal Sandstone

Six discrete, perforated depth intervals within the Basal sandstone (8,526 to 8,531 ft, 8,536 to 8,542 ft, 8,554 to 8,576 ft, 8,578 to 8,587 ft, 8,602 to 8,604 ft, and 8,608 to 8,613 ft) were hydrologically tested collectively. The perforated depth intervals occur within the upper 87 ft of this stratigraphic formation (i.e., formation contacts: 8,526 to 8,634 ft). Collectively, the Basal Sandstone perforated intervals exhibited relatively low hydraulic properties: T = 0.073 ft^2/day, K = 0.0015 ft/day, and k = 0.5 milli-darcies. The high storativity value of S = 2.8E-2 is an indication of the presence of gas within the test system or surrounding formation. Because of the high storativity and associated compressibility, the radius of investigation for the larger scale injection test is limited and estimated to be approximately 10 ft or less.

Table 5.1 and Figure 5.1 present a comparison of the average field-test-derived k estimate (0.5 milli-darcies) as it relates to the range of small-scale k values obtained from the wireline CMR and the PressureXpress survey test results, and discrete sidewall cores that were obtained over the entire Basal sandstone unit. As indicated, the average field-test k value falls within the k range obtained for four discrete sidewall core permeability measurements (0.0052 to 0.84 milli-darcies) obtained within the perforated test interval. The wireline CMR survey results for the perforated test interval average 2.6 milli-darcies (range: 1E-5 to 17.7 milli-darcies), which is a factor of 5 greater than the field-test-derived value of 0.5 milli-darcies. The wireline PressureXpress test results for six discrete depth intervals within the Basal sandstone ranged from 0.01 to 0.06 milli-darcies, which is significantly lower than the field-test-derived average estimate.

5.2 Rose Run

Three perforated test zones situated at the base (Rose Run #1), middle (Rose Run #2), and top (Rose Run #3) of the Rose Run were hydrologically tested individually. The perforated depth intervals that were tested include Rose Run #1 (7,506 to 7,509 ft), Rose Run #2 (7,416 to 7, 418 and 7,435 to 7,446 ft), and Rose Run #3 (7,377 to 7,380 ft and 7,387 to 7,396 ft). Based on the results of these tests, ~95 percent of the composite transmissivity is contained within the middle Rose Run test interval (Rose Run #2). Based on examination of the pressure response monitored below the bottom isolation packer, only the top and middle Rose Run test

zones exhibited a slight degree of formational hydraulic connection. The top test interval (Rose Run #3) exhibited a high test system/formation fluid compressibility indicative of the presence of gas. It is interesting to note that the Basal sandstone test zone, which also has perforated intervals located in the upper section of this unit, also exhibited highly compressible fluid conditions. This is consistent with an anticipated occurrence of gas within multiphase reservoir settings.

Table 5.1. Intrinsic Permeability Test Zone Comparison by Characterization Method

Stratigraphic Unit	Test Zone[a]	Perforated Interval ft	Characterization Method			
			Packer Tests[b] k, md	**CMR Survey[c]** k, md	**PressureXpress Survey[d]** k, md	**Sidewall Core Laboratory Tests[e]** k, md
Rose Run	Rose Run #3 (upper)	7,377–7,380 7,387–7,396	0.6	0.7 (0.1–3.1)	<0.01 (two tests)	0.004–0.8 (three core tests)
	Rose Run #2 (middle)	7,416–7,418 7,435–7,446	22.1	5.1 (0.05–16.3)	3.86–5..67 (two tests)	0.8–26.6* (two core tests)
	Rose Run #1 (lower)	7,506–7,509	2.6	0.7 (0.02–1.8)	0.22 (one test)	1.4 (one core test)
Basal Sandstone	(total)	8,526–8,531 8,536–8,542 8,554–8,576 8,578–8,587 8,602–8,604 8,608–8,613	0.5	2.6 (1E-5–17.7)	0.01–0.06 (six tests)	0.0052–0.84 (four core tests)

(a) Relative position within stratigraphic unit indicated in parentheses.

(b) k = K (μ/γ); K = T/b; assumed contributing thickness, b; assigned equal to the perforated interval length, L.

(c) k = determinations every 0.5 ft; range and average value calculated just over perforated interval.

(d) k calculated from discrete PressureXpress survey mobility measurements using an assumed formation fluid dynamic viscosity value of 0.878 cp (see Section 2.3.5).

(e) k = Klinkenberg laboratory measurements; * indicated core value for Rose Run #2 located 1 ft above a test-zone perforated interval.

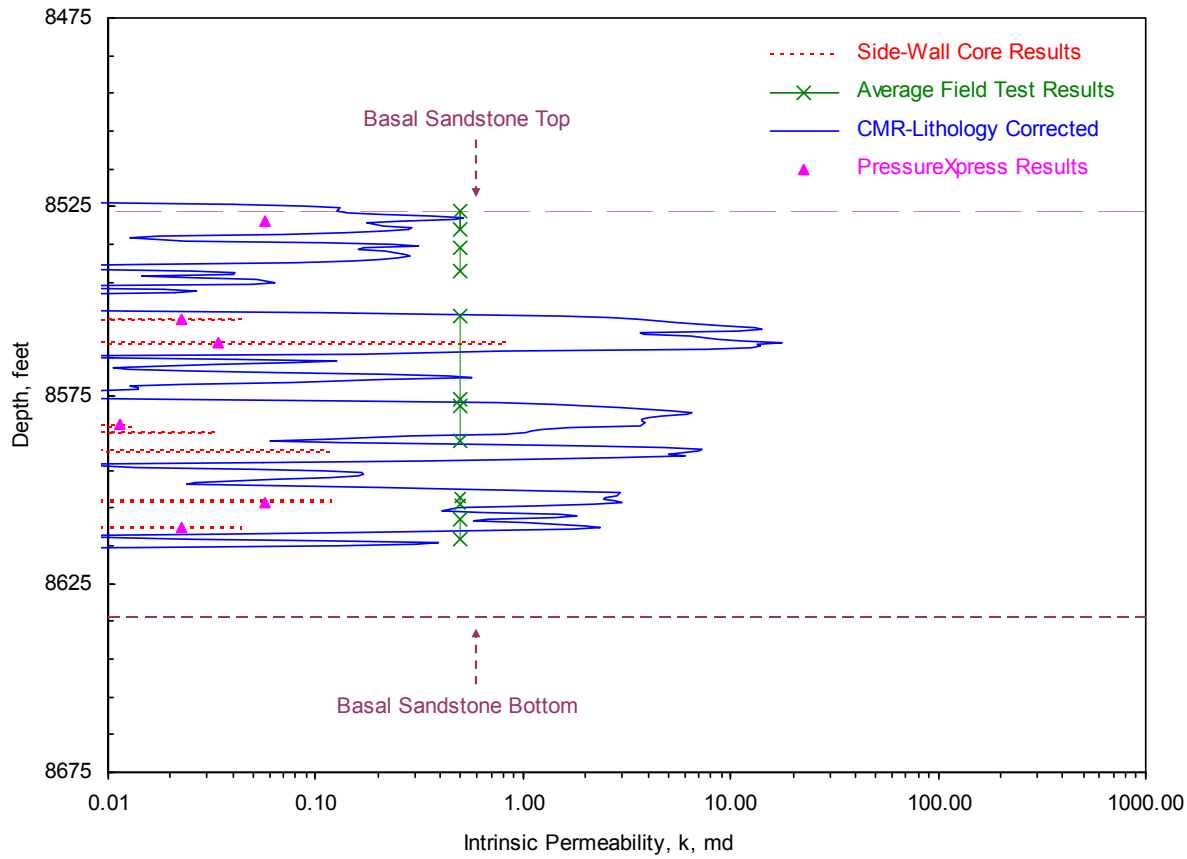

Figure 5.1. Permeability Comparison Plot: Field Testing, CMR and PressureXpress Surveys, and Sidewall-Core Sample Results: Basal Sandstone

In addition to the individual zone tests, the three Rose Run test zones were tested compositely. The test response of the composite Rose Run test is consistent with a multi-layer reservoir where the individual layers are hydraulically connected primarily at the wellbore (commingled) with little cross-formational connection. The response of the Rose Run as a multi-layer rather than as an equivalent single-layer reservoir is attributed primarily to the disparate contribution ratio of each layer to the composite Rose Run hydraulic diffusivity (i.e., T/S). As noted previously, the composite summation transmissivity value for the perforated Rose Run test intervals (0.93 ft^2/day) is very similar to the transmissivity estimate reported by Spane et al. (2006) of 0.79 ft^2/day for Rose Run at a deep characterization borehole located ~100 miles south of CO_2 No. 1 Well.

Table 5.1 and Figure 5.2 present a comparison of the average field-test-derived k estimate values for the three Rose Run test zones as they compare to the range of small-scale k values obtained from wireline CMR and PressureXpress survey results, and discrete sidewall cores obtained over the entire Rose Run Formation. As indicated, the average field-test k value for the lower and middle Rose Run test zones (i.e., Rose Run #1 and #2) generally fall within the upper or slightly above the k range obtained from discrete sidewall core permeability measurements and wireline CMR and PressureXpress survey results. For Rose Run #1 (with a average field-test-derived k estimate of 2.6 milli-darcies), the one sidewall core permeability measurement and

one PressureXpress test result available for the perforated interval provided a value of 1.4 and 0.22 milli-darcies, respectively. The CMR survey results for the tested interval ranged from 0.02 to 1.8 milli-darcies and averaged 0.7 milli-darcies. For Rose Run #2 (with an average field-test-derived k estimate of 22.1 milli-darcies), the two sidewall core permeability measurements and two PressureXpress test results available for or within proximity to the perforated interval provided a k estimate range of 0.8 and 26.6 milli-darcies, and 3.86 and 5.67 milli-darcies, respectively. The CMR survey results for the tested interval ranged from 0.05 to 16.3 milli-darcies and averaged 5.1 milli-darcies. The reason for the slightly higher average k estimate for the field tests in comparison to the averaged CMR survey and PressureXpress results is not known. The lower k values from the small-scale CMR survey and PressureXpress test results, however, may be attributed to the presence of low-to-moderate skin effects that were detected during the field-test characterization.

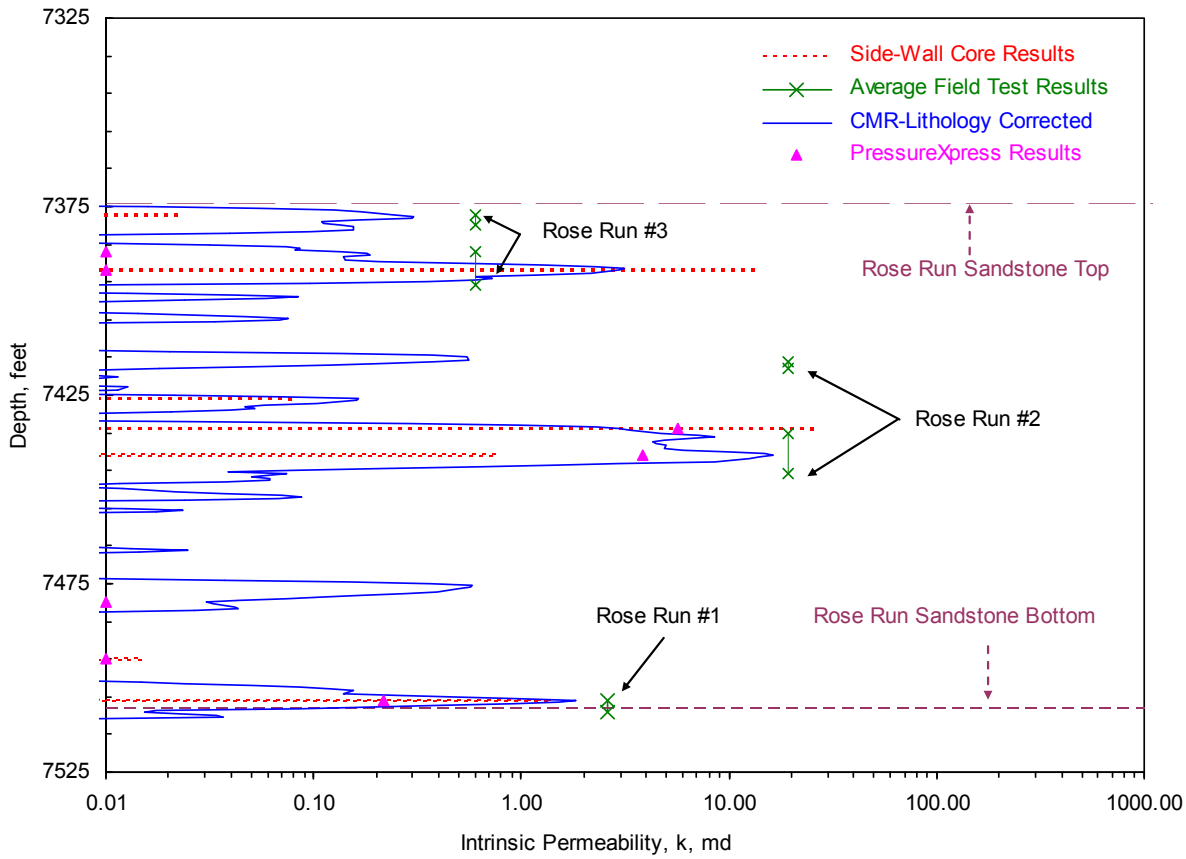

Figure 5.2. Permeability Comparison Plot: Field Testing, CMR and PressureXpress Surveys, and Sidewall-Core Sample Results: Rose Run Sandstone

For Rose Run #3, the three sidewall core permeability measurements and two PressureXpress test results available for the perforated interval provided a wide range varying between 0.004 and 13.8 milli-darcies, and less than 0.01 milli-darcies, respectively. The CMR results for the tested interval ranged more narrowly between 0.1 and 3.1 milli-darcies and averaged 0.7 milli-darcies. The average CMR-derived k value of 0.7

milli-darcies for the Rose Run #3 perforated test interval is nearly identical to the average field-test-derived k estimate of 0.6 milli-darcies.

The relative correspondence between the average k wireline CMR values and the larger scale average field-test k estimates for the various Rose Run test intervals (Figure 5.1) suggests that there is little scale-dependence between these two test-methods, and suggests that the test intervals are relatively homogeneous away from the test well over the test radius-of-investigation. The relative correspondence of average k values for field tests and wireline CMR surveys suggests that the CMR may be a viable reconnaissance borehole indicator for identifying the distribution and presence of permeability within the targeted sandstone reservoir formations. A similar conclusion was reported in Spane et al. (2006) for the Rose Run characterization relationships observed at the Mountaineer AEP #1 borehole.

6.0 References

Agarwal RG. 1980. "A new method to account for producing time effects when drawdown type curves are used to analyze pressure buildup and other test data." *SPE Paper 9289*, Society of Petroleum Engineers, Dallas, Texas.

Bourdet DJ, A Ayoub, and YM Pirard. 1989. "Use of pressure derivative in well-test interpretation." *SPE Formation Evaluation*, June:293–302.

Bredehoeft JD, and SS Papadopulos. 1980. "A method for determining the hydraulic properties of tight formations." *Water Resources Research* 16(1):233–238.

Butler JJ, Jr. 1990. "The role of pumping tests in site characterization: some theoretical considerations." *Ground Water* 28(3):394–402.

Butler JJ, Jr. 1997. *The design, performance, and analysis of slug tests*. Lewis Publishers, CRC Press, Boca Raton, Florida.

Cooper HH, Jr., and CE Jacob. 1946. "A generalized graphical method for evaluating formation constants and summarizing well-field history." *American Geophysical Union, Transactions* 27(4):526–534.

Correa AC, and HJ Ramey, Jr. 1987. "A method for pressure buildup analysis of drillstem tests." *SPE Paper 16802,* Society of Petroleum Engineers, paper presented at the 62nd Annual Technical Conference and Exhibition of the Society of Petroleum Engineers, Dallas, Texas, September 27–30, 1987.

Earlougher RC, Jr. 1977. *Advances in well test analysis*. Monograph Vol. 5, Society of Petroleum Engineers, Richardson, Texas.

Enachescu C and LP Ostrowski. 1993. "Special aspects of applying constant rate analysis approach in low-permeability formations." *SPE Paper 25877,* Society of Petroleum Engineers, paper presented at the SPE Rocky Mountain Regional/Low Permeability Reservoirs Symposium of the Society of Petroleum Engineers, Denver, Colorado, April 12–14, 1993.

Gao, C-T. 1987. "Determination of parameters for individual layers in multilayer reservoirs by transient well tests." *SPE Formation Evaluation,* Society of Petroleum Engineers, March 1987:43–65.

Gringarten, AC. 2008. "From straight lines to deconvolution; the evolution of the state of the art in well test analysis." *SPE 102079,* Society of Petroleum Engineers, paper presented at the 2006 SPE Annual Technical Conference and Exhibition, San Antonio, Texas, September 24–27, 2006.

Gupta N. 2003. *Phase III novel concepts research in geologic storage of CO_2: the Ohio River Valley CO_2 storage project - reservoir testing field work plan*. National Energy Technology Laboratory Interim Report; addendum December 2003.

Hantush MS. 1964. "Hydraulics of wells." *Advances in Hydroscience* (VT Chow, ed) 1:282–433, Academic Press, New York.

Horner DR. 1951. "Pressure build-up in wells." In: *Proceedings of the Third World Petroleum Congress*, The Hague, Session II:503-523.

Horne RN. 1990. *Modern well test analysis: a computer-aided approach*. Petroway, Inc., Palo Alto, California.

Jacob CE, and SW Lohman. 1952. "Non-steady flow to a well of constant drawdown in an extensive aquifer." *Transact American Geophysical Union* 33(4):559–569.

Karasaki K. 1990. "A systematized drillstem test." *Water Resources Research* 26(12):2913–2919.

Karasaki K, JCS Long, and PA Witherspoon. 1988. "Analytical models of slug tests." *Water Resources Research* 24(1):115–126.

Kucuk, F, M Karakas, and L Ayestaran. 1986. "Well testing and analysis techniques for layered reservoirs." *SPE Formation Evaluation,* Society of Petroleum Engineers, August:342–354.

Liu WZ, and JJ Butler, Jr. 1995. *The KGS model for slug tests in partially penetrating wells (Version 3.0)*. Kansas Geological Survey Computer Series Report 95-1, Lawrence, Kansas.

Lohman, SW. 1979. "Ground-water hydraulics." *U.S. Geological Survey Professional Paper 708*, Washington, DC.

Meehan DN. 1980a. "Estimating water viscosity at reservoir conditions." *Petroleum Engineer* July:117–118.

Meehan DN. 1980b. "A correlation for water compressibility." *Petroleum Engineer* July:125-126.

Moench AF. 1997. "Flow to a well of finite diameter in a homogeneous, anisotropic water-table aquifer." *Water Resources Research* 33(6):1397–1407.

Newman GH. 1973. "Pore-volume compressibility of consolidated, friable, and unconsolidated reservoir rocks under hydrostatic loading." *Journal of Petroleum Technology* February:129–134

Novakowski KS. 1989. "Analysis of pulse interference tests." *Water Resources Research* 25(11):2377-2387.

Novakowski KS. 1990. "Analysis of aquifer tests conducted in fractured rock: a review of the physical background and design of a computer program for generating type curves." *Ground Water* 27(1):99-107.

Ohio Administrative Code. 2008. "Operating, monitoring, and reporting of saltwater injection wells." Ohio Division of Mineral Resources Management – Oil and Gas, Chapter 1501:9-3-07. Available at: http://codes.ohio.gov/oac/1501%3A9-3. Accessed 09-26-2008.

Ostrowski LP, and MB Kloska. 1989. "Use of pressure derivatives in analysis of slug test or DST flow period data." *SPE Paper 18595,* Society of Petroleum Engineers, paper presented at the SPE Production Operations Symposium, March 13–14, 1989.

Peres AM, M Onur, and AC Reynolds. 1989. "A new analysis procedure for determining aquifer properties from slug test data." *Water Resources Research* 25(7):1591–1602.

Raghaven R, HN Topaloglu, WM Cobb, and HJ Ramey, Jr. 1974. "Well-test analysis for wells producing from two commingled zones of unequal thickness." *SPE 4559,* Society of Petroleum Engineers, paper presented at the SPE-AIME 48th Annual Fall Meeting, Las Vegas, Nevada, September 30–October 3, 1973.

Ramey HJ Jr. 1970. "Short-time well test data interpretation in the presence of skin effect and wellbore storage." *Journal of Petroleum Technology, AIME* 249:97-104.

Ramey HJ Jr. 1982. "Well-loss function and the skin effect: a review." *Geological Society of America Special Paper 189*:265-271.

Ramey HJ Jr., RG Agarwal, and I. Martin. 1975. "Analysis of 'slug test' or DST flow period data." *Journal of Canadian Petroleum Technology* July–September:37–47.

Reidel SP, VG Johnson, and FA Spane. 2002. *Natural gas storage in basalt aquifers of the Columbia Basin, Pacific Northwest USA: A guide to site characterization*. PNNL-13962, Pacific Northwest National Laboratory, Richland, Washington.

Shestakov VM. 2002. "Development of relationship between specific storage and depth of sandy and clay formations." *Environmental Geology* 42:127-129.

Spane FA, Jr. 1993. *Selected hydraulic test analysis techniques for constant-rate discharge tests*. PNL-8539, Pacific Northwest Laboratory, Richland, Washington.

Spane FA, Jr. 1996. "Applicability of slug interference tests for hydraulic characterization of unconfined aquifer: (1) Analytical assessment." *Ground Water* 34(1):66-74.

Spane FA, Jr. and RB Mercer. 1985. *HEADCO: A program for converting observed water levels and pressure measurements to formation pressure and standard hydraulic head*. RHO-BW-ST-71 P, Rockwell Hanford Operations, Richland, Washington.

Spane FA, Jr. and SK Wurstner. 1993. "DERIV: A program for calculating pressure derivatives for use in hydraulic test analysis." *Ground Water* 31(5):814-822.

Spane, FA, PD Thorne, N. Gupta, P. Jagucki, TS. Ramakrishnan, and N. Mueller. 2006. "Results Obtained from Reconnaissance-Level and Detailed Reservoir Characterization Methods Utilized for Determining Hydraulic Property Distribution Characteristics at Mountaineer AEP #1"; PNNL-SA-48622; Proceedings, International Symposium on Site Characterization for CO_2 Geological Storage, CO2SC 2006, Lawrence Berkeley National Laboratory, Berkeley, California, March 20-22, 2006.

Theis CV. 1935. "The relationship between the lowering of the piezometric surface and the rate and duration of discharge of a well using ground-water storage." *American Geophysical Union, Transactions*, 2:519-524; reprinted in Society of Petroleum Engineers, "Pressure Transient Testing Methods", SPE Reprint Series (14):27-32, Dallas, Texas.

Wikramaratna, RS. 1985. "On the components of flow resulting from abstraction in a two-layered confined aquifer with no cross flow." *Water Resources Research* 21(7):985-989.

Appendix A

Detailed Test Summary/Activity Tables for the CO_2 No. 1 Well

Appendix A: Detailed Test Summary/Activity Tables for the CO_2 No. 1 Well

A.1 CO_2 No. 1 Well Test Summary/Activity Log: Basal Sandstone

A.2 CO_2 No. 1 Well Test Summary/Activity Log: Rose Run #1

A.3 CO_2 No. 1 Well Test Summary/Activity Log: Rose Run #2

A.4 CO_2 No. 1 Well Test Summary/Activity Log: Rose Run #3

A.5 CO_2 No. 1 Well Test Summary/Activity Log: Composite Rose Run

Table A.1. CO_2 No. 1 Well Test Summary/Activity Log: Basal Sandstone

Formation	Perforated Test-Interval Depth, ft bKB[(a)]	Borehole Test Activity	Test Date/Time[(b)]	Comments*
Basal Sand	8,526–8,531 8,536–8,542 8,554–8,576 8,578–8,587 8,602–8,604 8,608–8,613	Swab Development of Basal Sand Perforated Zones	7/19/07 (15:30–18:30) 7/20/07 (08:00–11:30)	Total volume of fluid ***removed*** from interval ≈ 3,970 gallons (94.5 barrels); pH increased from 1 to 6 and fluid weight density from 8.5 to 10.3 lb/gal during the course of fluid removal.
		Aborted Injection Test	7/20/07 (17:18–20:52)	Injection rate at ~2 gpm and then test aborted due to inadvertent closing of downhole shut-in tool; Injection Vol.: 430 gal Max. Surface Inj. Pressure: < 0 psi Max. Downhole Obs. Pressure: 3,405 psi Avg. Fluid Weight Density: ~9.8 lb/gal.
		Constant-Pressure Injection Test	7/22/07 (10:08–19:01)	Injection rates varied from 2.42 to 0.61 gpm during the course of the test; Injection Vol.: 555 gal Max. Surface Inj. Pressure: 3 psi Max. Downhole Obs. Pressure: 4,355 psi Avg. Fluid Weight Density: ~9.8 lb/gal.
		Slug Injection Test	7/23/07 07:03–09:56	Injection Vol.: 85 gal Max. Surface Inj. Pressure: < 0 psi Max. Downhole Obs. Pressure: 4,340 psi Avg. Fluid Weight Density: ~9.8 lb/gal.
		Basal Sand Test-Interval Summary: **Total Injection Volume: 1,070 gallons** **Total Injection Period: 15.3 hours** **Maximum Surface Injection Pressure: 3 psi** **Maximum Observed Downhole Pressure: 4,355 psi**		

(a) **ft bKB**: feet below original Kelly Bushing datum; note: packers used to isolate perforated test intervals within cemented well-casing string.

(b) Observed surface test time; EDT

* Note: **Injection Volume** represents volume injected into test system during the active injection period; the actual volume injected into the test zone may be slightly less than this amount. **Maximum Surface Injection Pressure** represents the maximum surface pressure observed during the injection test; **Maximum Observed Downhole Injection Pressure** represents the maximum pressure observed with the downhole pressure gauge located in proximity/above the top perforated test interval.; except for Rose Run #1 where probe depth setting was ~495 above top perforated interval. **Average Fluid Weight Density** represents the average of the injection fluid weight density measured at the surface during the test.

Table A2. CO_2 No. 1 Well Test Summary/Activity Log: Rose Run #1

Formation	Perforated Test-Interval Depth, ft bKB[(a)]	Borehole Test Activity	Test Date/Time[(b)]	Comments*
Rose Run #1	7,506–7,509	Constant-Pressure Injection Test	7/26/07 (18:10) - 7/27/07 (08:42)	After test system fill-up, the test was maintained at a constant surface pressure of 50 psi. Injection rates varied from 0.2 to 0.07 gpm during the course of the constant-pressure injection test: Injection Vol.: 245 gal Max. Surface Inj. Pressure: 50 psi Max. Downhole Obs. Pressure: 3,680 psi Avg. Fluid Weight Density: ~9.8 lb/gal.
		Slug-Injection Test	7/28/07 (07:22–10:01)	Injection Vol.: 5 gal Max. Surface Inj. Pressure: < 0 psi Max. Downhole Obs. Pressure: 3,635 psi Avg. Fluid Weight Density: ~9.8 lb/gal.
		Rose Run #1 Test-Interval Summary: **Total Injection Volume: 250 gallons** **Total Injection Period: 17.2 hours** **Maximum Surface Injection Pressure: 50 psi** **Maximum Observed Downhole Pressure: 3,680 psi**		

(a) **ft bKB**: feet below original Kelly Bushing datum; note: packers used to isolate perforated test intervals within cemented well-casing string

(b) Observed surface test time; EDT

* Note: **Injection Volume** represents volume injected into test system during the active injection period; the actual volume injected into the test zone may be slightly less than this amount. **Maximum Surface Injection Pressure** represents the maximum surface pressure observed during the injection test; **Maximum Observed Downhole Injection Pressure** represents the maximum pressure observed with the downhole pressure gauge located in proximity/above the top perforated test interval.; except for Rose Run #1 where probe depth setting was ~495 above top perforated interval. **Average Fluid Weight Density** represents the average of the injection fluid weight density measured at the surface during the test.

Table A.3. CO_2 No. 1 Well Test Summary/Activity Log: Rose Run #2

Formation	Perforated Test-Interval Depth, ft bKB[(a)]	Borehole Test Activity	Test Date/Time[(b)]	Comments*
Rose Run #2	7,416–7,418 7,435–7,446	Constant-Pressure Injection-Test #1	7/29/07 (14:00)–7/30/07 (10:00)	After test system fill-up, the test was maintained at a constant surface pressure of 50 psi. Injection rates varied from 3.2 to 1.0 gpm during the course of the constant-pressure injection test: Injection Vol.: 1,688 gal Max. Surface Inj. Pressure: 51 psi Max. Downhole Obs. Pressure: 3,825 psi Avg. Fluid Weight Density: ~9.8 lb/gal.
		Slug Injection Test	7/31/07 (09:25–10:15)	Injection Vol.: 45 gal Max. Surface Inj. Pressure: < 0 psi Max. Downhole Obs. Pressure: 3,785 psi Avg. Fluid Weight Density: ~9.8 lb/gal.
		Constant-Pressure Injection-Test #2	7/31/07 (12:17–20:03)	After test system fill-up, the test was maintained at a constant surface pressure of 50 psi. Injection rates varied from 1.2 to 1.0 gpm during the course of the constant-pressure injection test: Injection Vol.: 530 gal Max. Surface Inj. Pressure: 50 psi Max. Downhole Obs. Pressure: 3,825 psi Avg. Fluid Weight Density: ~9.8 lb/gal.
		Rose Run #2 Test-Interval Summary: **Total Injection Volume: 820 gallons** **Total Injection Period: 28.6 hours** **Maximum Surface Injection Pressure: 50 psi** **Maximum Observed Downhole Pressure: 3,825 psi**		

(a) **ft bKB**: feet below original Kelly Bushing datum; note: packers used to isolate perforated test intervals within cemented well-casing string

(b) Observed surface test time; EDT

* Note: **Injection Volume** represents volume injected into test system during the active injection period; the actual volume injected into the test zone may be slightly less than this amount. **Maximum Surface Injection Pressure** represents the maximum surface pressure observed during the injection test; **Maximum Observed Downhole Injection Pressure** represents the maximum pressure observed with the downhole pressure gauge located in proximity/above the top perforated test interval.; except for Rose Run #1 where probe depth setting was ~495 above top perforated interval. **Average Fluid Weight Density** represents the average of the injection fluid weight density measured at the surface during the test.

Table A.4. CO_2 No. 1 Well Test Summary/Activity Log: Rose Run #3

Formation	Perforated Test-Interval Depth, ft bKB[(a)]	Borehole Test Activity	Test Date/Time[(b)]	Comments*
Rose Run #3	7,377–7,380 7,387–7,396	Constant-Pressure Injection Test	8/1/0 (11:36)- 8/2/07 (07:36)	After test system fill-up, the test was maintained at a constant surface pressure of 50 psi. Injection rates varied from 0.55 to 0.17 gpm during the course of the constant-pressure injection test: Injection Vol.: 265 gal Max. Surface Inj. Pressure: 50 psi Max. Downhole Obs. Pressure: 3,780 psi Avg. Fluid Weight Density: ~9.8 lb/gal.
		Slug Injection Test	8/3/07 (07:46–9:47)	Injection Vol.: 30 gal Max. Surface Inj. Pressure: < 0 psi Max. Downhole Obs. Pressure: 3,745 psi Avg. Fluid Weight Density: ~9.8 lb/gal.
		Rose Run #3 Test-Interval Summary: **Total Injection Volume: 295 gallons** **Total Injection Period: 22.0 hours** **Maximum Surface Injection Pressure: 50 psi** **Maximum Observed Downhole Pressure: 3,780 psi**		

(a) **ft bKB**: feet below original Kelly Bushing datum; note: packers used to isolate perforated test intervals within cemented well-casing string

(b) Observed surface test time; EDT

* Note: **Injection Volume** represents volume injected into test system during the active injection period; the actual volume injected into the test zone may be slightly less than this amount. **Maximum Surface Injection Pressure** represents the maximum surface pressure observed during the injection test; **Maximum Observed Downhole Injection Pressure** represents the maximum pressure observed with the downhole pressure gauge located in proximity/above the top perforated test interval.; except for Rose Run #1 where probe depth setting was ~495 above top perforated interval. **Average Fluid Weight Density** represents the average of the injection fluid weight density measured at the surface during the test.

Table A.5. CO_2 No. 1 Well Test Summary/Activity Log : Composite Rose Run

Formation	Perforated Test-Interval Depth, ft bKB[(a)]	Borehole Test Activity	Test Date/Time[(b)]	Comments*
Composite Rose Run	7,377–7,380 7,387–7,396 7,416–7,418 7,435–7,446 7,506–7,509	Swab Development of Composite Rose Run Perforated Zone	7/24/07 (16:00–18:15) - 7/25/07 (07:00–13:05)	Set bridge plug at 7,530 ft and initiated development of composite Rose Run perforated interval. Total volume of fluid ***removed*** from interval ≈ 10,330 gallons (246 barrels); pH increased from 1 to 5 and weight from 8.6 to 10.1 lb/gal during the course of fluid removal.
		Constant-Pressure Injection Test	8/3/07 (17:25)–8/4/07 (17:34)	After test system fill-up, the test was maintained at a constant surface pressure of 50 psi. Injection rates varied from 2.12 to 0.82 gpm during the course of the constant-pressure injection test: Injection Vol.: 1,450 gal Max. Surface Inj. Pressure: 50 psi Max. Downhole Obs. Pressure: 3,790 psi Avg. Fluid Weight Density: ~9.8 lb/gal.
		Slug Injection Test	8/6/07 (06:33–8:33)	Injection Vol.: 65 gal Max. Surface Inj. Pressure: < 0 psi Max. Downhole Obs. Pressure: 3,740 psi Avg. Fluid Weight Density: ~9.8 lb/gal.
		Composite Rose Run Test-Interval Summary: **Total Injection Volume: 1,515 gallons** **Total Injection Period: 26.2 hours** **Maximum Surface Injection Pressure: 50 psi** **Maximum Observed Downhole Pressure: 3,790 psi**		

(a) **ft bKB**: feet below original Kelly Bushing datum; note: packers used to isolate perforated test intervals within cemented well-casing string

(b) Observed surface test time; EDT

* Note: **Injection Volume** represents volume injected into test system during the active injection period; the actual volume injected into the test zone may be slightly less than this amount. **Maximum Surface Injection Pressure** represents the maximum surface pressure observed during the injection test; **Maximum Observed Downhole Injection Pressure** represents the maximum pressure observed with the downhole pressure gauge located in proximity/above the top perforated test interval.; except for Rose Run #1 where probe depth setting was ~495 above top perforated interval. **Average Fluid Weight Density** represents the average of the injection fluid weight density measured at the surface during the test.

Appendix B

Selected Pictures of Test Equipment Used at the CO_2 No. 1 Well

Appendix B: Selected Pictures of Test Equipment Used at the CO_2 No. 1 Well

B.1 Schlumberger Perforation Tool

B.2 Shut-In Tool Seating Collar (a) and (b) Combined Pressure Probe Assembly

B.3 Injection Trailer (a) with Multiple, Flow-Line Control Instrumentation (b)

Figure B.1. Schlumberger Perforation Tool

(a)

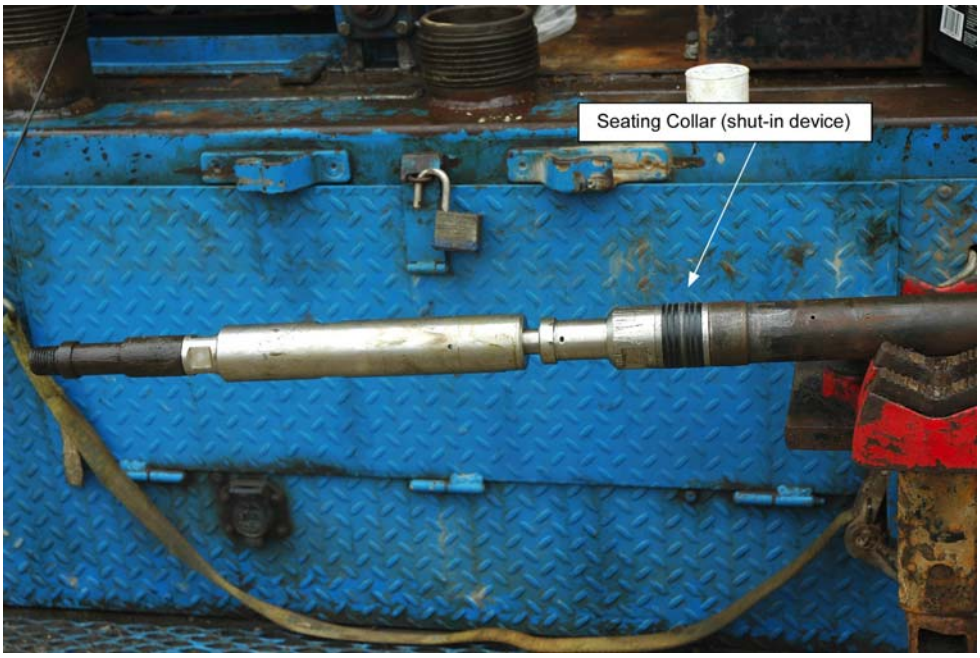

(b)

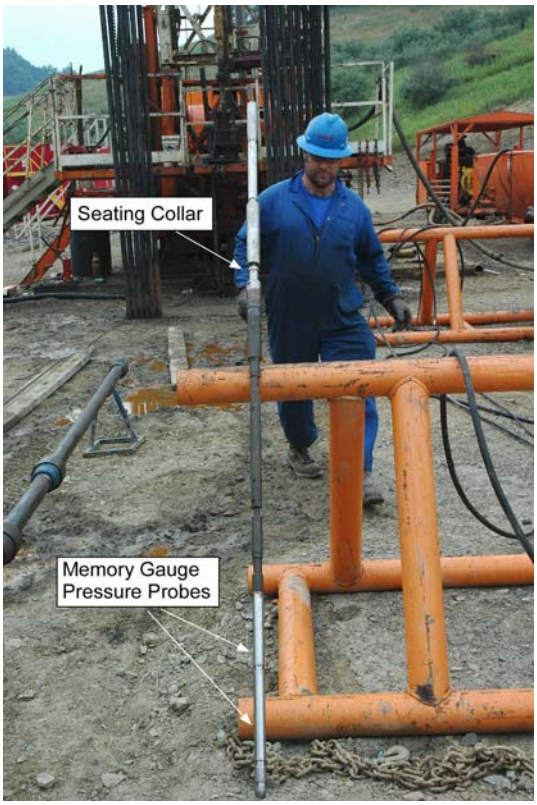

Figure B.2. Shut-In Tool Seating Collar (a) and Combined Pressure Probe Assembly (b)

(a)

(b)

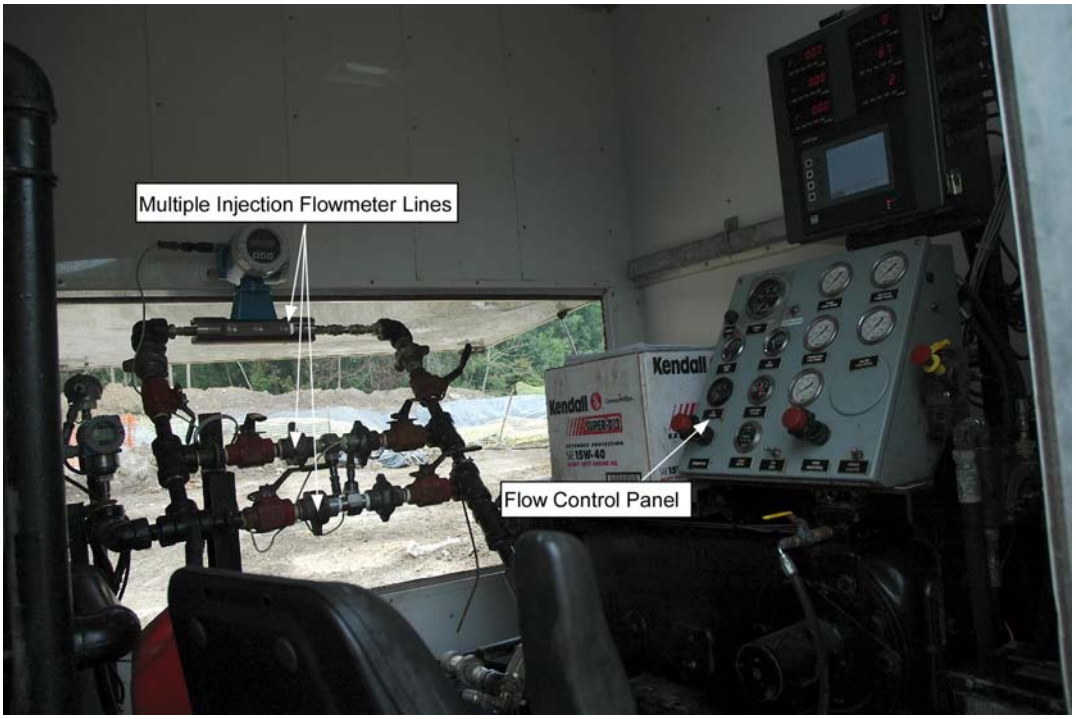

Figure B.3. Injection Trailer (a) with Multiple, Flow-Line Control Instrumentation (b)

Appendix C

Selected Analysis Figures for CO_2 No. 1 Well

Appendix C: Selected Analysis Figures for CO_2 No. 1 Well

C.1 Diagnostic Derivative Plot Analysis of Injection Recovery Test: Basal Sandstone; 8,526 to 8,613 ft

C.2 Horner Plot Analysis of Injection Recovery Test: Basal Sandstone; 8,526 to 8,613 ft

C.3 Semi-Log Plot Analysis of Injection Recovery Test: Basal Sandstone; 8,526 to 8,613 ft

C.4 Composite Type Curve and Derivative Plot Analysis of Injection Recovery Test: Basal Sandstone; 8,526 to 8,613 ft

C.5 Corroborative Injection-Rate Analysis for Constant-Head Injection Test: Basal Sandstone; 8,526 to 8,613 ft

C.6 Composite Type Curve and Derivative Plot Analysis of Slug Injection Test: Basal Sandstone; 8,526 to 8,613 ft

C.7 Diagnostic Derivative Plot Analysis of Injection Recovery Test: Rose Run #1: 7,506 to 7,509 ft

C.8 Horner Plot Analysis of Injection Recovery Test: Rose Run #1: 7,506 to 7,509 ft

C.9 Semi-Log Plot Analysis of Injection Recovery Test: Rose Run #1: 7,506 to 7,509 ft

C.10 Composite Type Curve and Derivative Plot Analysis of Injection Recovery Test: Rose Run #1: 7,506 to 7,509 ft

C.11 Corroborative Injection-Rate Analysis for Constant-Head Injection Test: Rose Run #1: 7,506 to 7,509 ft

C.12 Diagnostic Derivative Plot Analysis of DST Recovery Test: Rose Run #1: 7,506 to 7,509 ft

C.13 Horner Plot Analysis of DST Recovery Data: Rose Run #1: 7,506 to 7,509 ft

C.14 Diagnostic Derivative Plot Analysis of Injection-Test #1 Recovery: Rose Run #2: 7,416 to 7,446 ft

C.15 Horner Plot Analysis of Injection-Test #1 Recovery: Rose Run #2: 7,416 to 7,446 ft

C.16 Semi-Log Plot Analysis of Injection-Test #1 Recovery: Rose Run #2: 7,416 to 7,446 ft

C.17 Composite Type Curve and Derivative Plot Analysis of Injection-Test #1 Recovery: Rose Run #2: 7,416 to 7,446 ft

C.18 Diagnostic Derivative Plot Analysis of Injection-Test #2 Recovery: Rose Run #2: 7,416 to 7,446 ft

C.19 Horner Plot Analysis of Injection-Test #2 Recovery: Rose Run #2: 7,416 to 7,446 ft

C.20 Semi-Log Plot Analysis of Injection-Test #2 Recovery: Rose Run #2: 7,416 to 7,446 ft

C.21 Composite Type Curve and Derivative Plot Analysis of Injection-Test #2 Recovery: Rose Run #2: 7,416 to 7,446 ft

C.22 Corroborative Injection-Rate Analysis for Combined Constant-Head Injection Tests: Rose Run #2: 7,416 to 7,446 ft

C.23 Composite Type Curve and Derivative Plot Analysis of Slug Injection Test: Rose Run #2: 7,416 to 7,446 ft

C.24 Diagnostic Derivative Plot Analysis of DST Recovery Test: Rose Run #2: 7,416 to 7,446 ft

C.25 Horner Plot Analysis of DST Recovery Data: Rose Run #2: 7,416 to 7,446 ft

C.26 Diagnostic Derivative Plot Analysis of Injection-Test Recovery: Rose Run #3: 7,377 to 7,396 ft

C.27 Horner Plot Analysis of Injection-Test Recovery: Rose Run #3: 7,377 to 7,396 ft

C.28 Semi-Log Plot Analysis of Injection-Test Recovery: Rose Run #3: 7,377 to 7,396 ft

C.29 Composite Type Curve and Derivative Plot Analysis of Injection-Test Recovery: Rose Run #3: 7,377 to 7,396 ft

C.30 Injection-Rate Analysis for Constant-Head Injection Test: Rose Run #3: 7,377 to 7,396 ft

C.31 Composite Type Curve and Derivative Plot Analysis of Slug Injection Test: Rose Run #3: 7,377 to 7,396 ft

C.32 Diagnostic Derivative Plot Analysis of DST Recovery Test: Rose Run #3: 7,377 to 7,396 ft

C.33 Corroborative Type Curve and Derivative Plot Analysis of DST Recovery Data: Rose Run #3: 7,377 to 7,396 ft

C.34 Diagnostic Derivative Plot Analysis of Injection-Test Recovery: Composite Rose Run: 7,377 to 7,509 ft

C.35 Rose Run Test Zone Constant-Head Injection-Test Comparison

C.36 Rose Run Test Zone Slug-Injection-Test Comparison

C.37 Composite Type Curve and Derivative Plot Analysis of Slug Injection Test: Composite Rose Run: 7,377 to 7,509 ft

C.38 Diagnostic Derivative Plot Analysis of DST Recovery Test: Composite Rose Run: 7,377 to 7,509 ft

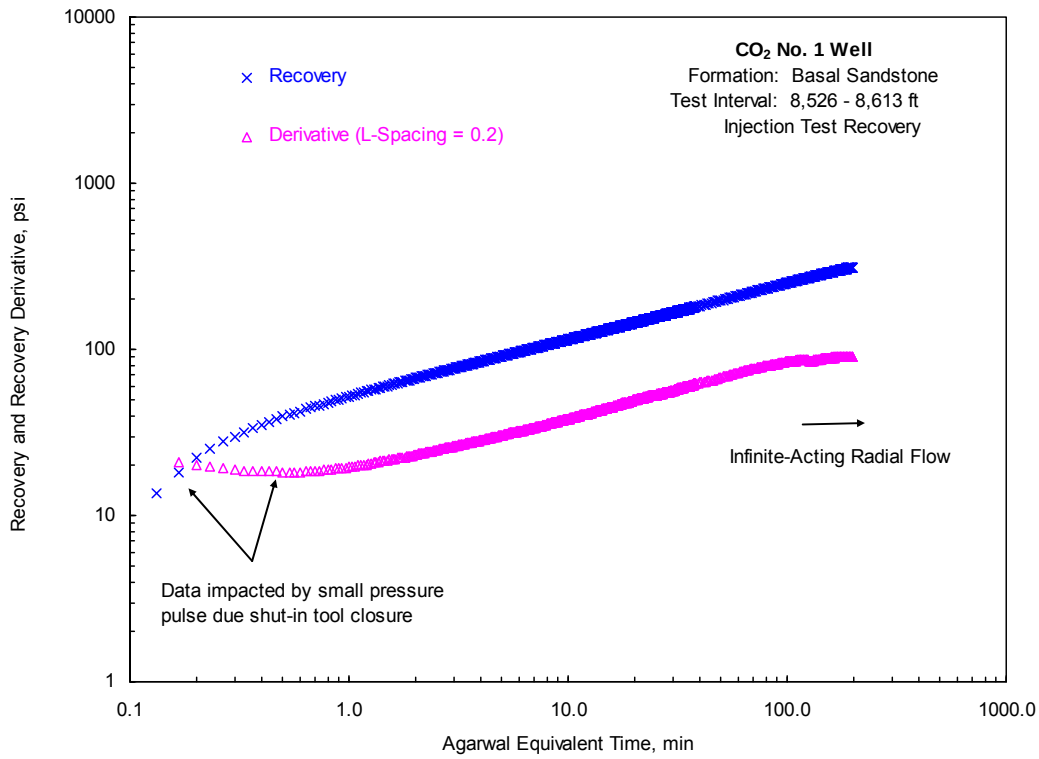

Figure C.1. Diagnostic Derivative Plot Analysis of Injection Recovery Test: Basal Sandstone; 8,526 to 8,613 ft

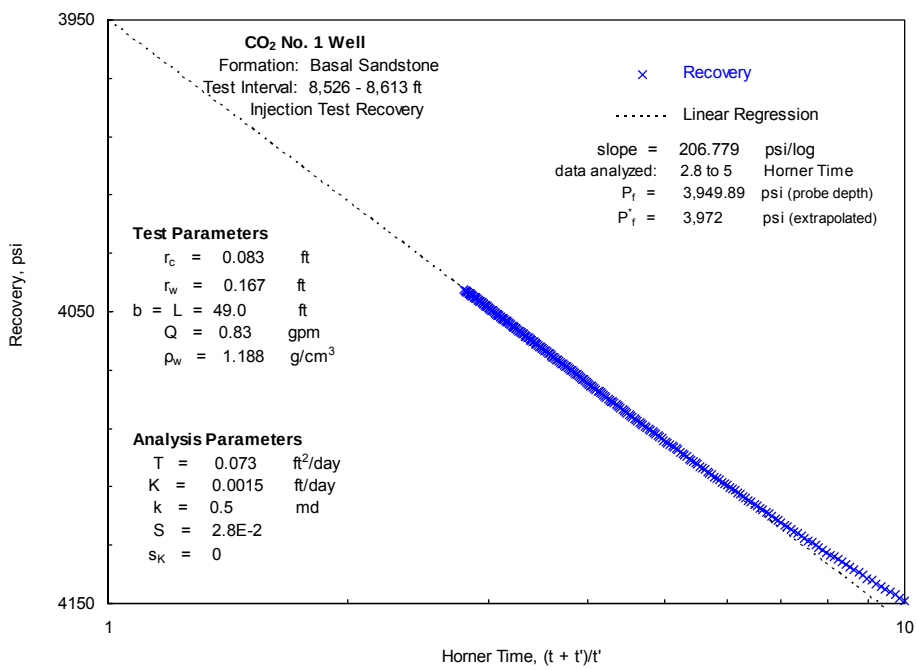

Figure C.2. Horner Plot Analysis of Injection Recovery Test: Basal Sandstone; 8,526 to 8,613 ft

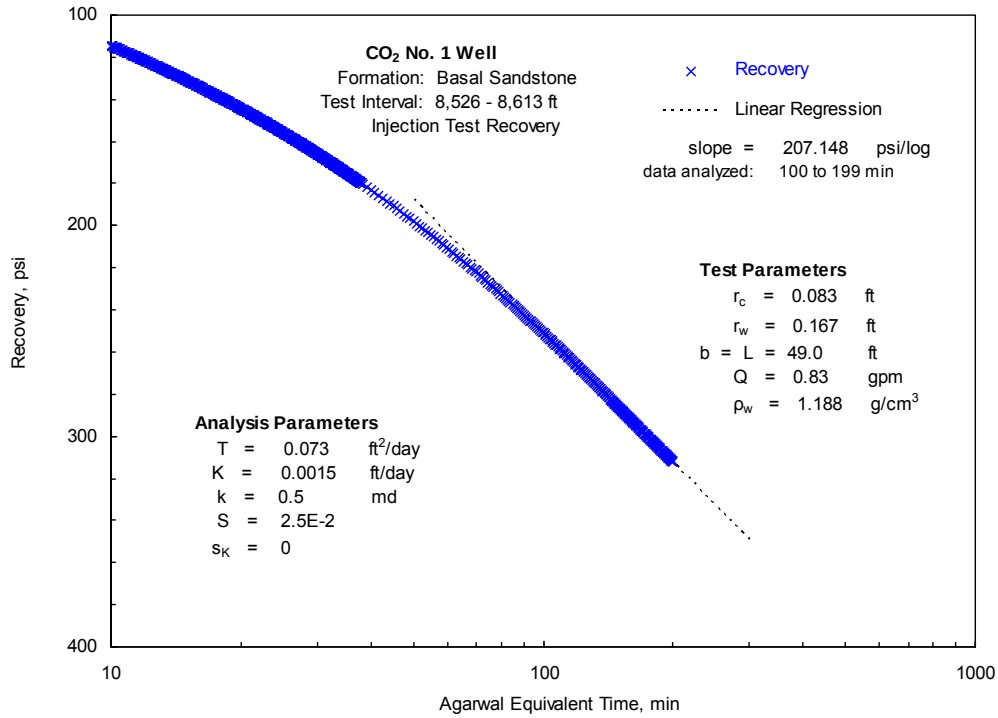

Figure C.3. Semi-Log Plot Analysis of Injection Recovery Test: Basal Sandstone; 8,526 to 8,613 ft

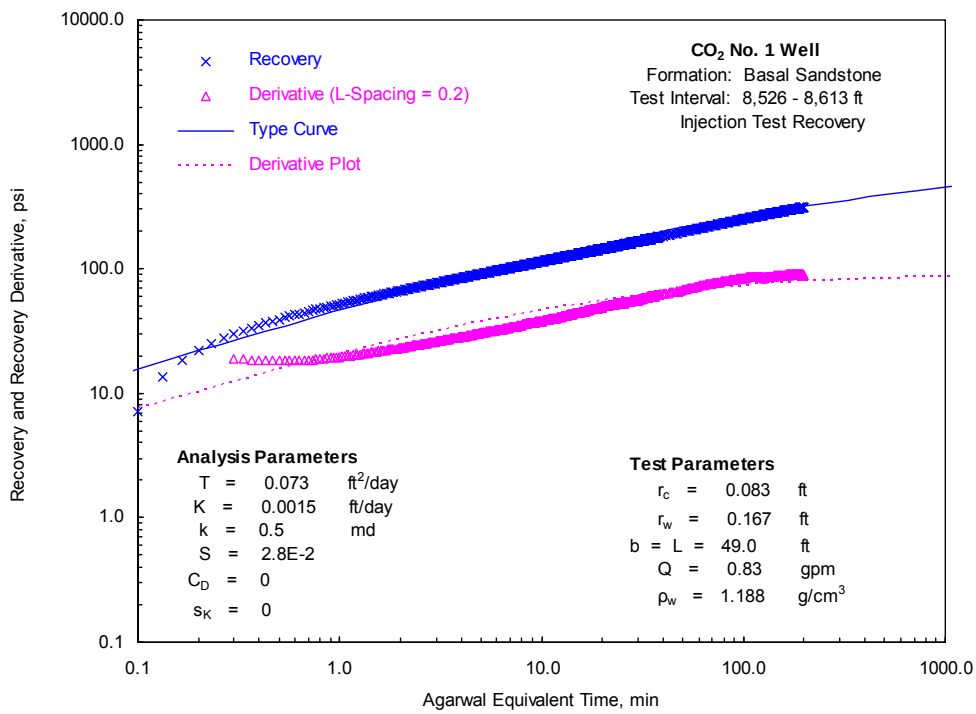

Figure C.4. Composite Type-Curve and Derivative Plot Analysis of Injection Recovery Test: Basal Sandstone; 8,526 to 8,613 ft

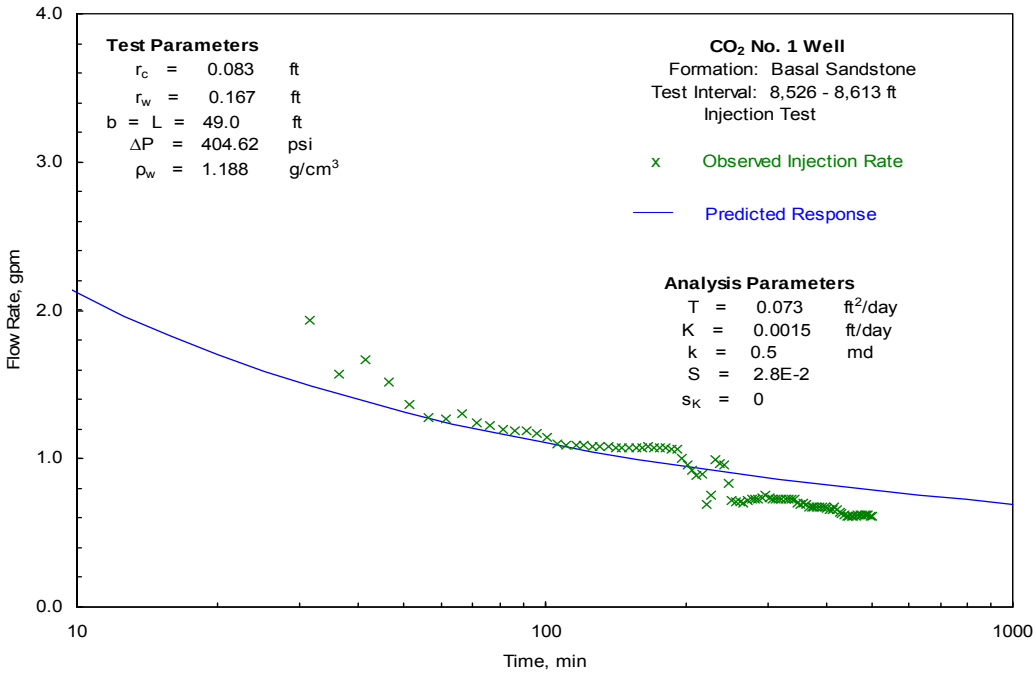

Figure C.5. Corroborative Injection-Rate Analysis of Constant-Head Injection Test: Basal Sandstone: 8,526 to 8,613 ft

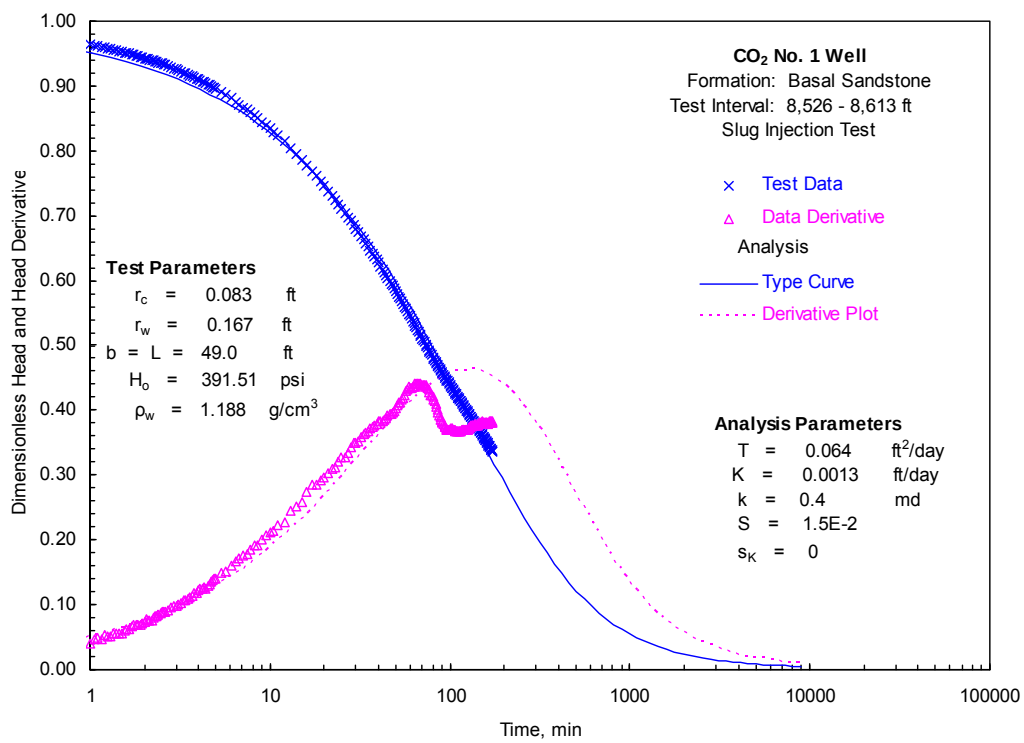

Figure C.6. Composite Type-Curve and Derivative Plot Analysis of Slug Injection Test: Basal Sandstone; 8,526 to 8,613 ft

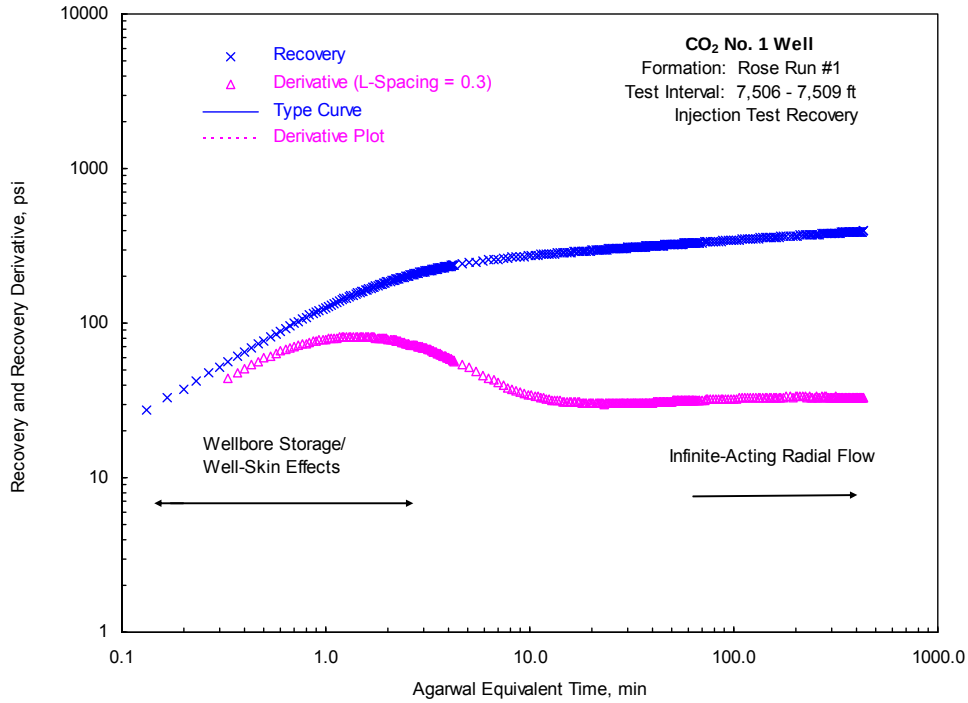

Figure C.7. Diagnostic Derivative Plot Analysis of Injection Recovery Test: Rose Run #1: 7,506 to 7,509 ft

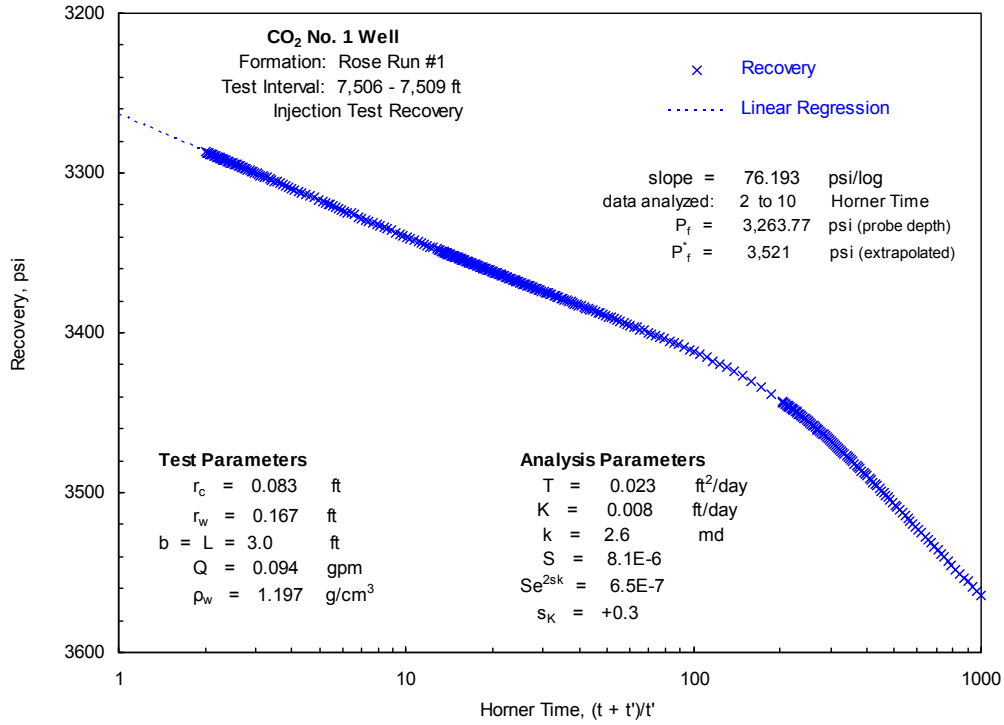

Figure C.8. Horner Plot Analysis of Injection Recovery Test: Rose Run #1: 7,506 to 7,509 ft

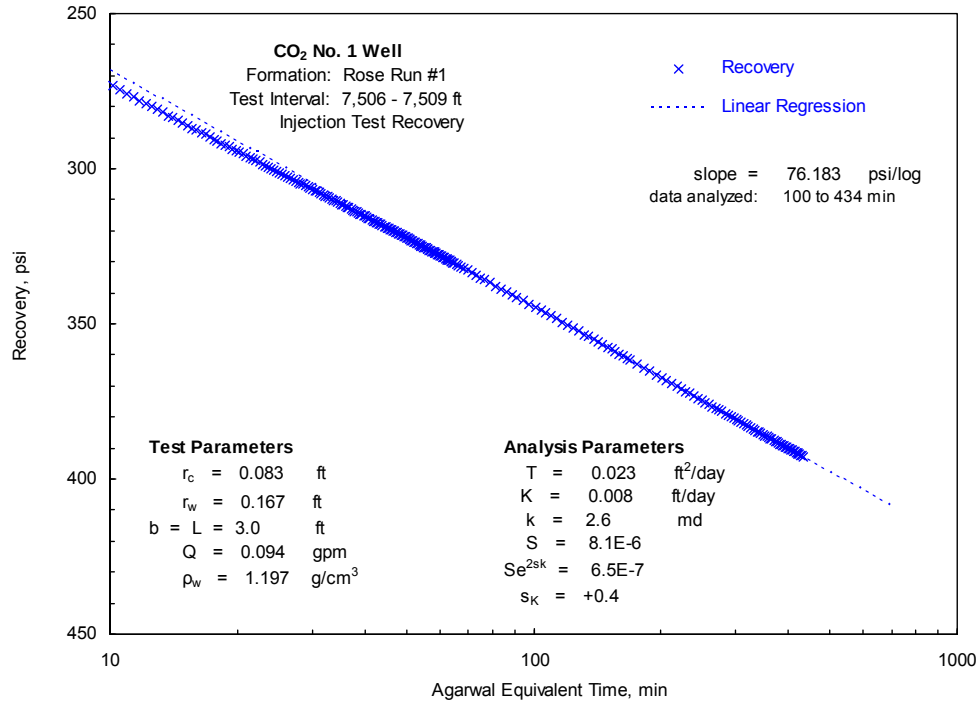

Figure C.9. Semi-Log Plot Analysis of Injection Recovery Test: Rose Run #1: 7,506 to 7,509 ft

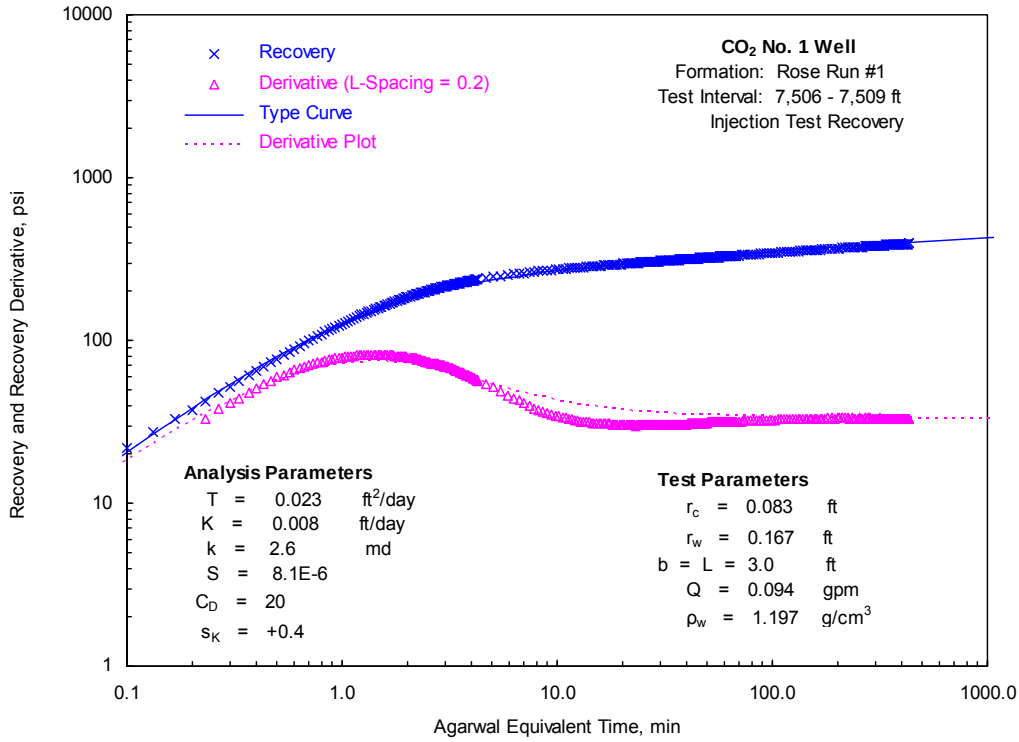

Figure C.10. Composite Type-Curve and Derivative Plot Analysis of Injection Recovery Test: Rose Run #1: 7,506 to 7,509 ft

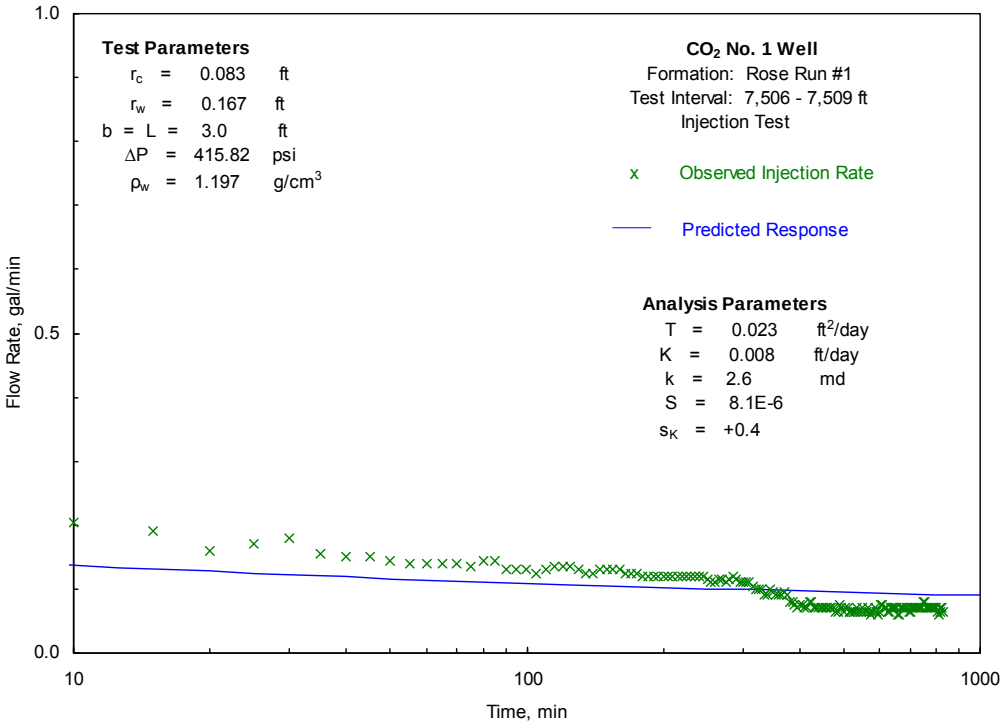

Figure C.11. Corroborative Injection-Rate Analysis of Constant-Head Injection Test: Rose Run #1: 7,506 to 7,509 ft

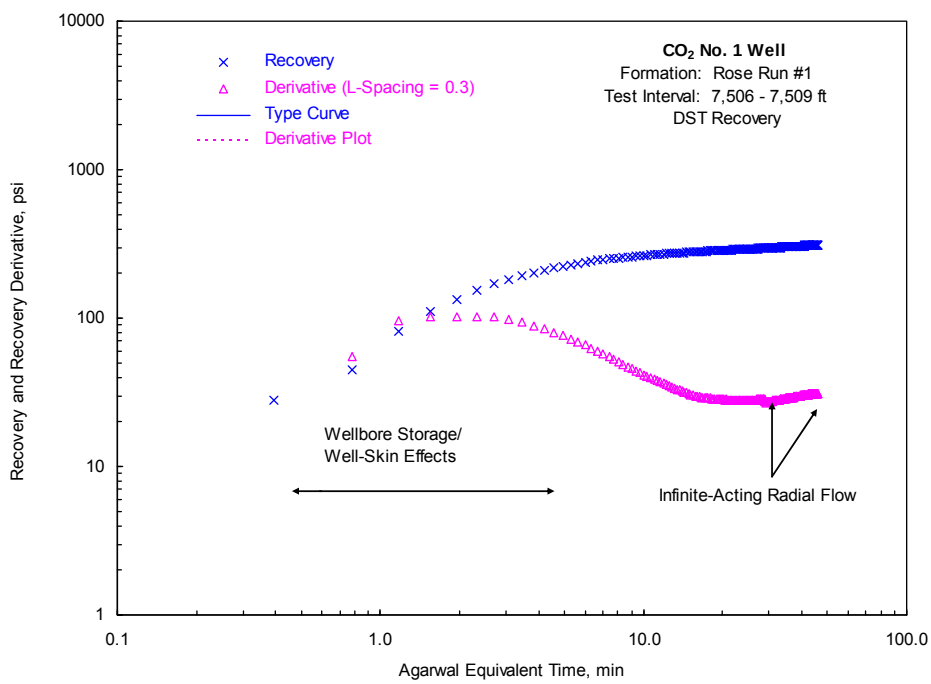

Figure C.12. Diagnostic Derivative Plot Analysis of DST Recovery Test: Rose Run #1: 7,506 to 7,509 ft

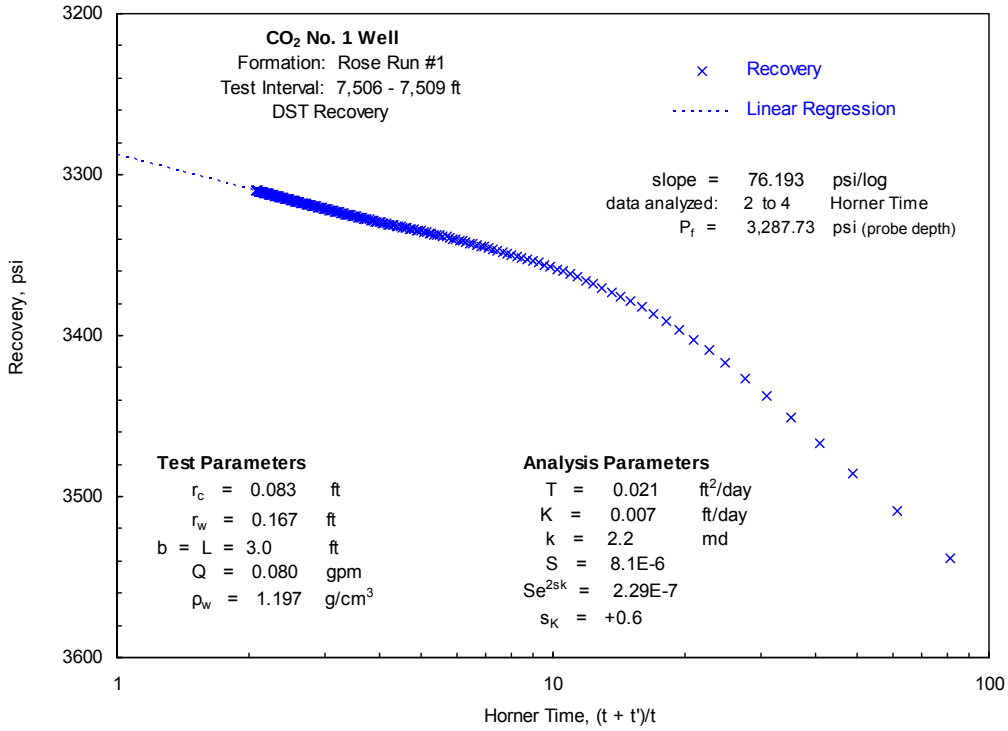

Figure C.13. Horner Plot Analysis of DST Recovery Data: Rose Run #1: 7,506 to 7,509 ft

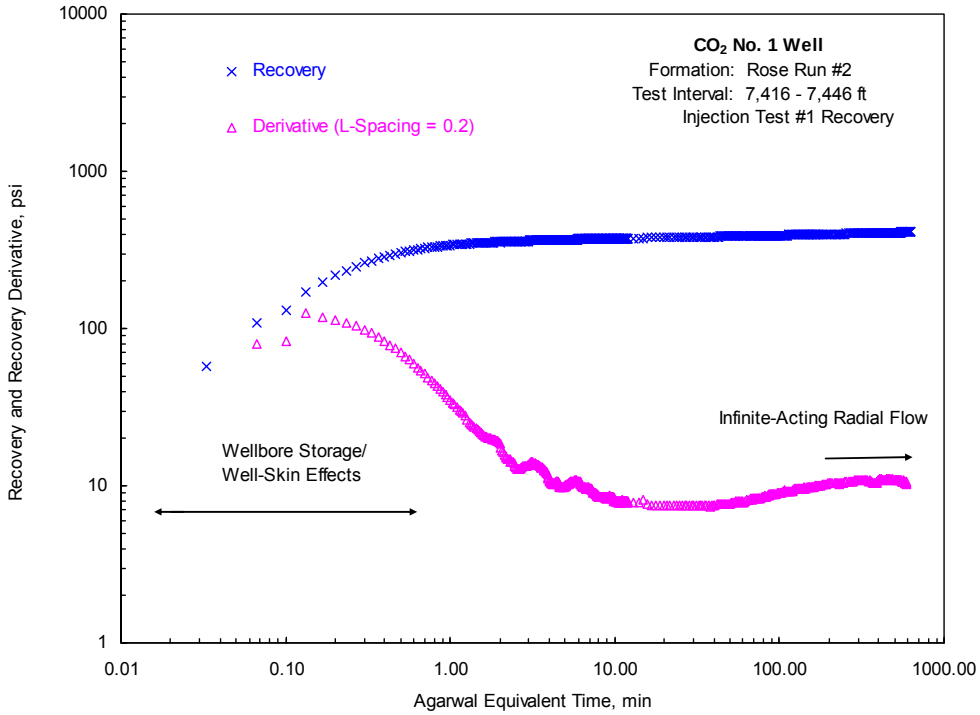

Figure C.14. Diagnostic Derivative Plot Analysis of Injection-Test #1 Recovery: Rose Run #2: 7,416 to 7,446 ft

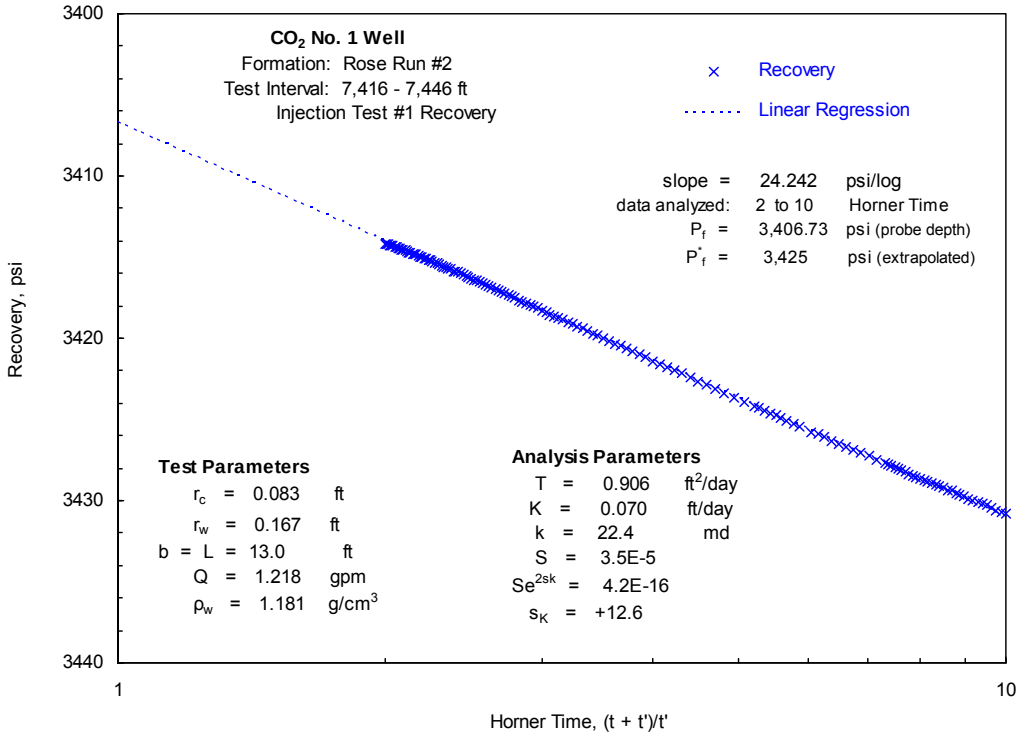

Figure C.15. Horner Plot Analysis of Injection-Test #1 Recovery: Rose Run #2: 7,416 to 7,446 ft

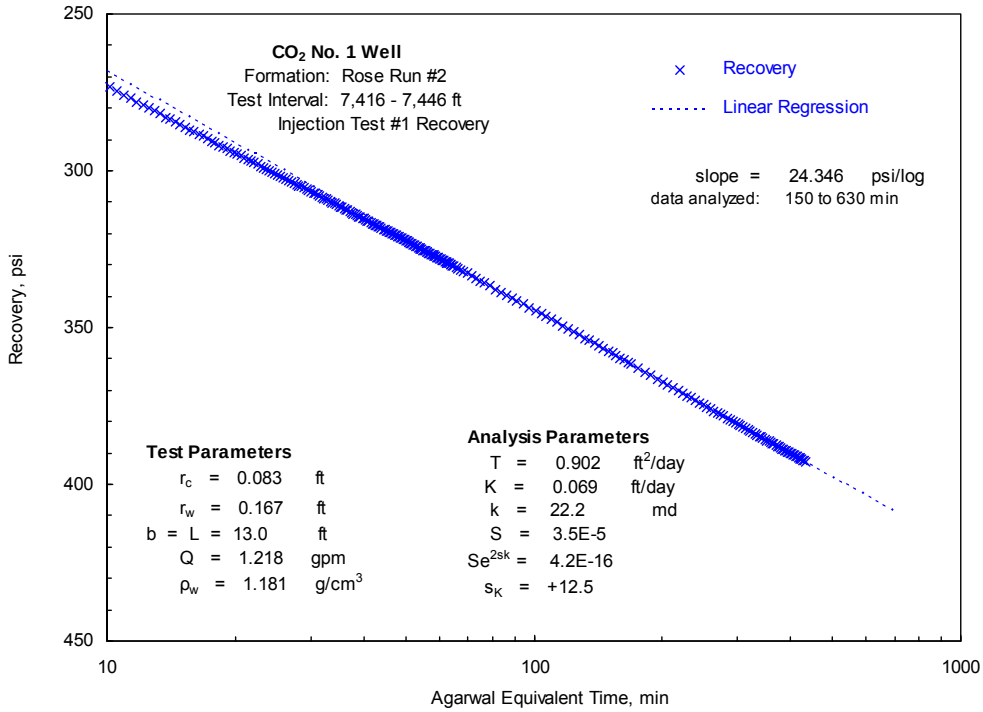

Figure C.16. Semi-Log Plot Analysis of Injection-Test #1 Recovery: Rose Run #2: 7,416 to 7,446 ft

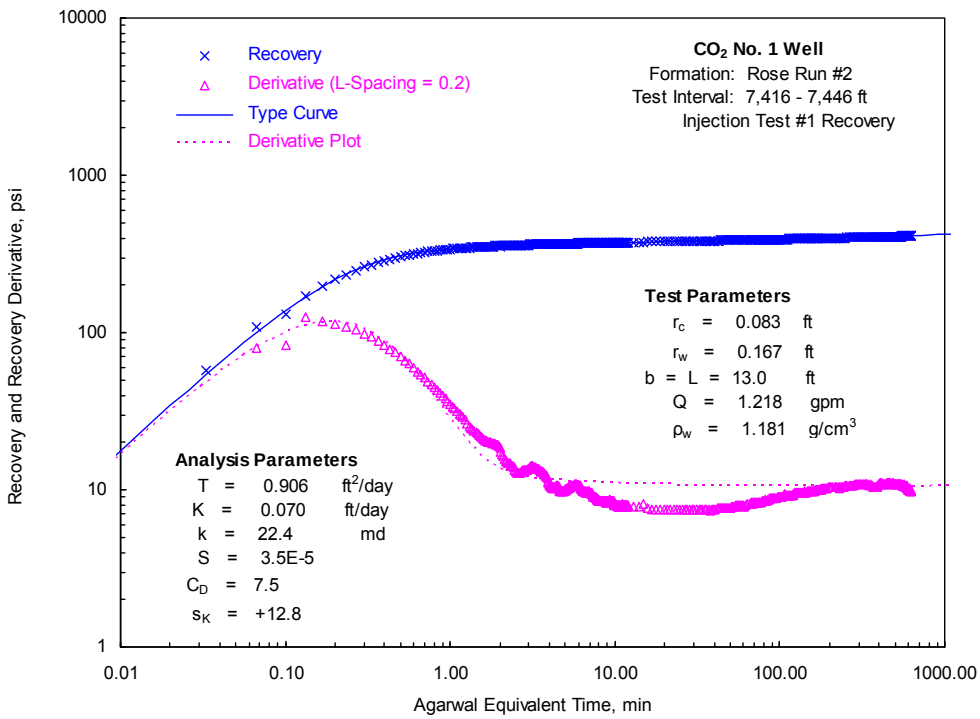

Figure C.17. Composite Type-Curve and Derivative Plot Analysis of Injection-Test #1 Recovery: Rose Run #2: 7,416 to 7,446 ft

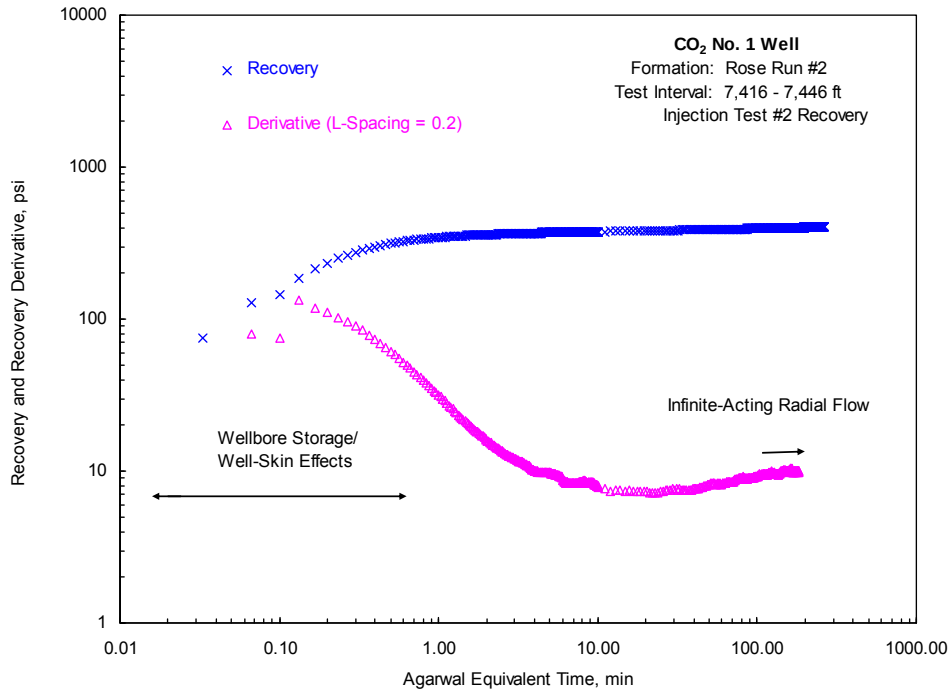

Figure C.18. Diagnostic Derivative Plot Analysis of Injection-Test #2 Recovery: Rose Run #2: 7,416 to 7,446 ft

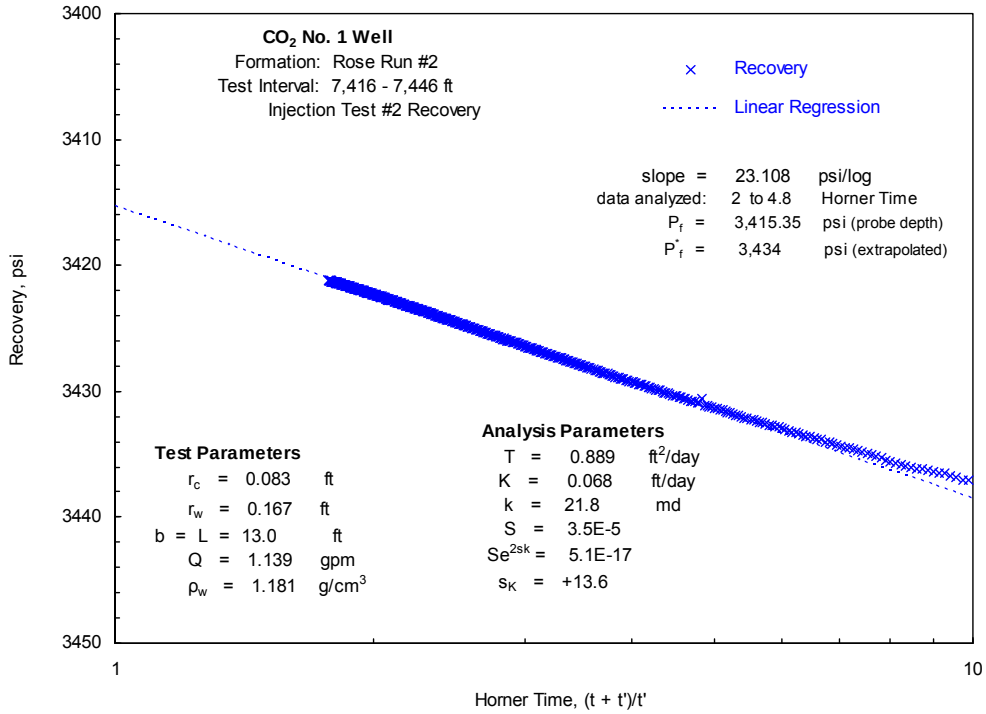

Figure C.19. Horner Plot Analysis of Injection-Test #2 Recovery: Rose Run #2: 7,416 to 7,446 ft

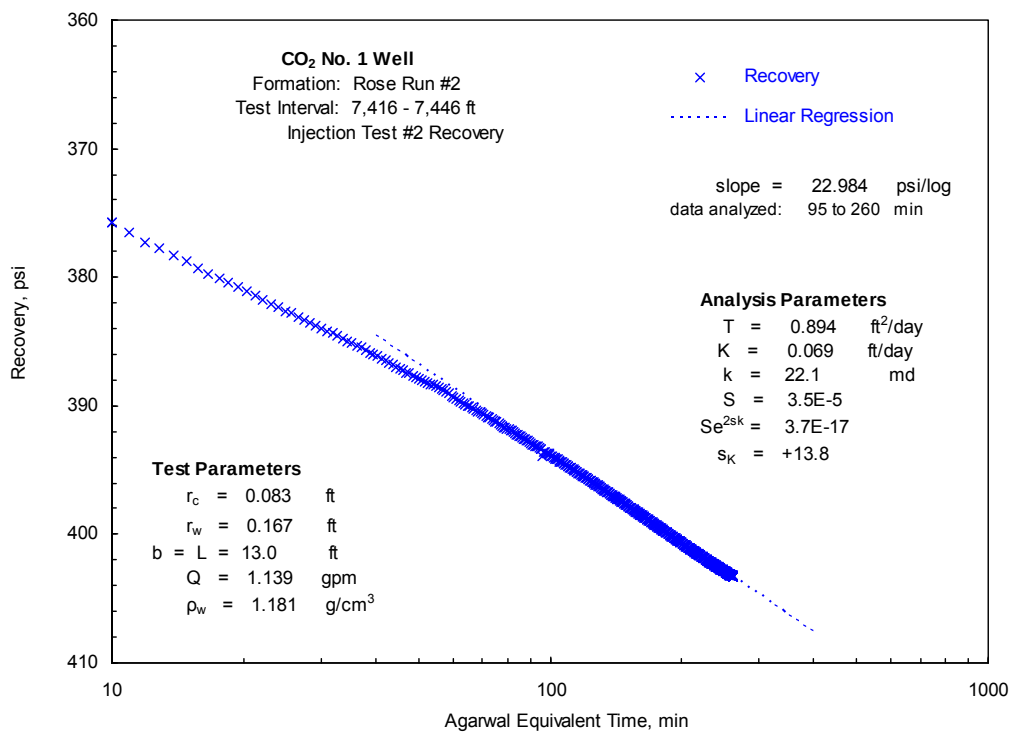

Figure C.20. Semi-Log Plot Analysis of Injection-Test #2 Recovery: Rose Run #2: 7,416 to 7,446 ft

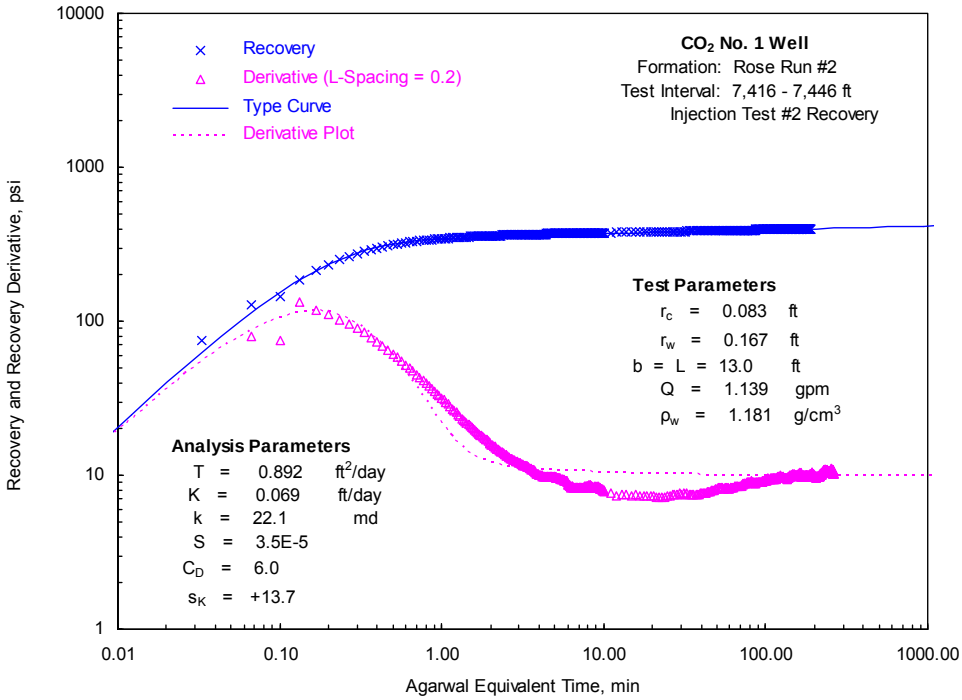

Figure C.21. Composite Type-Curve and Derivative Plot Analysis of Injection-Test #2 Recovery: Rose Run #2: 7,416 to 7,446 ft

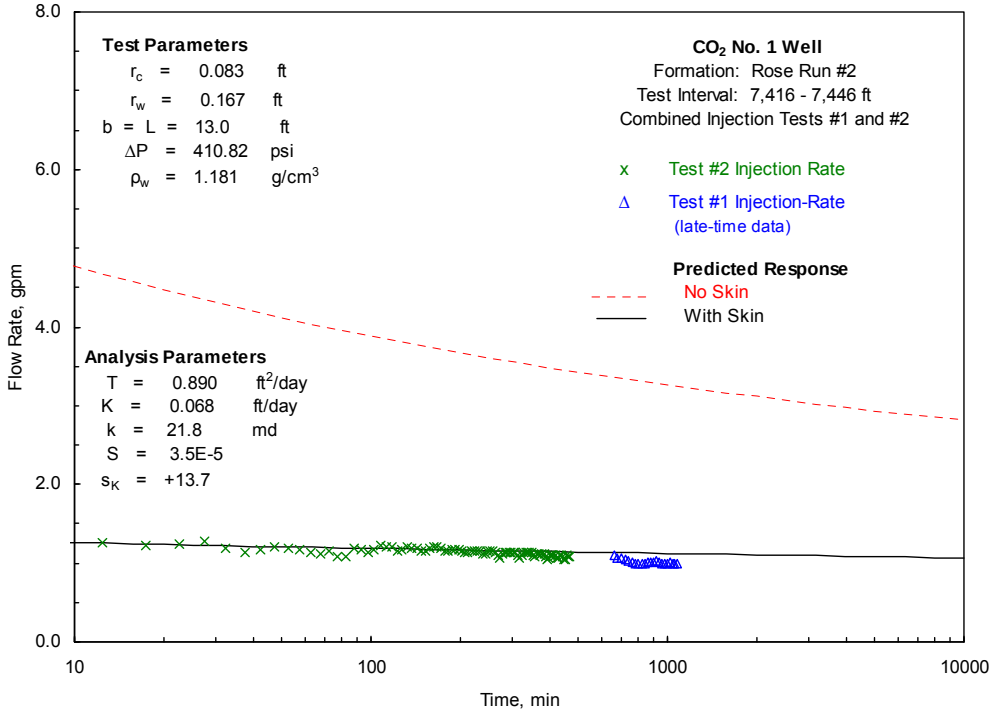

Figure C.22. Corroborative Injection-Rate Analysis for Combined Constant-Head Injection Tests: Rose Run #2: 7,416 to 7,446 ft

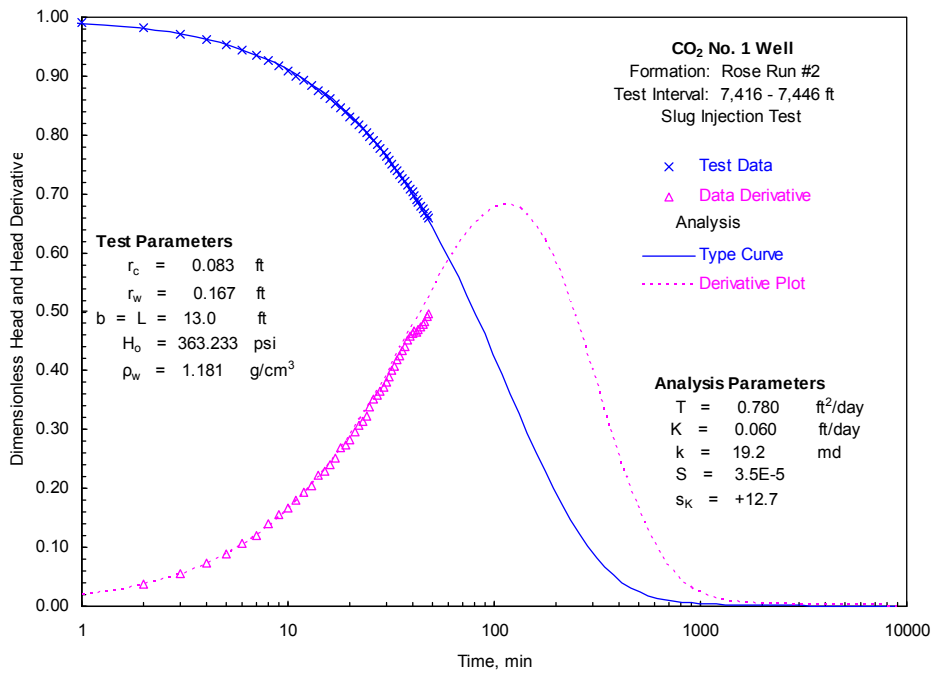

Figure C.23. Composite Type-Curve and Derivative Plot Analysis of Slug-Injection Test: Rose Run #2: 7,416 to 7,446 ft

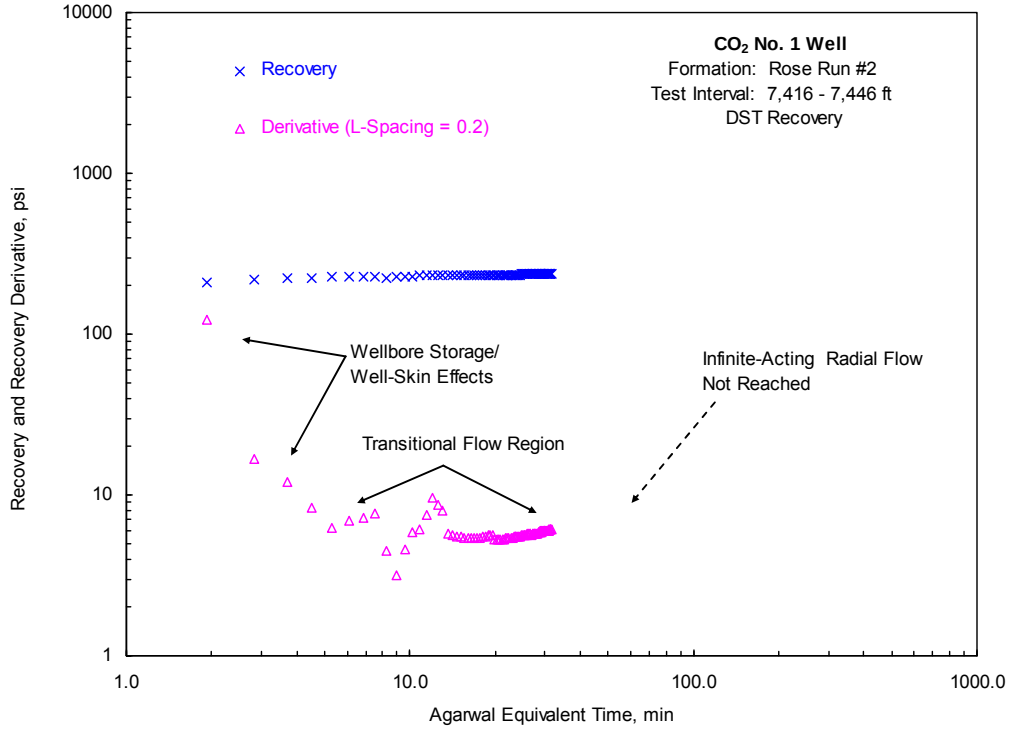

Figure C.24. Diagnostic Derivative Plot Analysis of DST Recovery Test: Rose Run #2: 7,416 to 7,446 ft

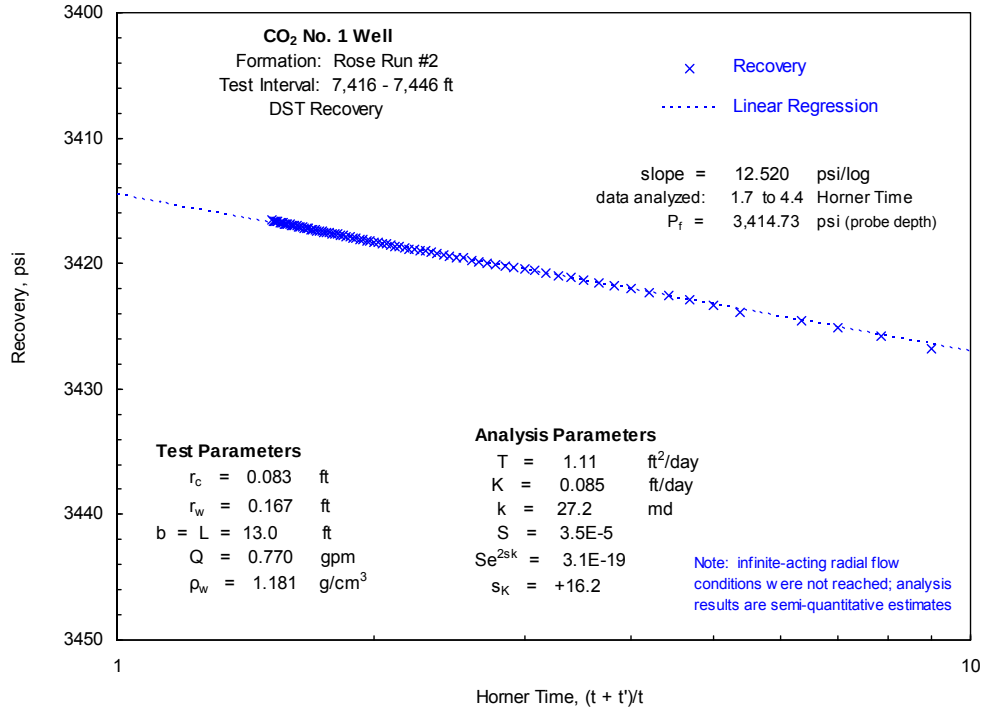

Figure C.25. Horner Plot Analysis of DST Recovery Test: Rose Run #2: 7,416 to 7,446 ft

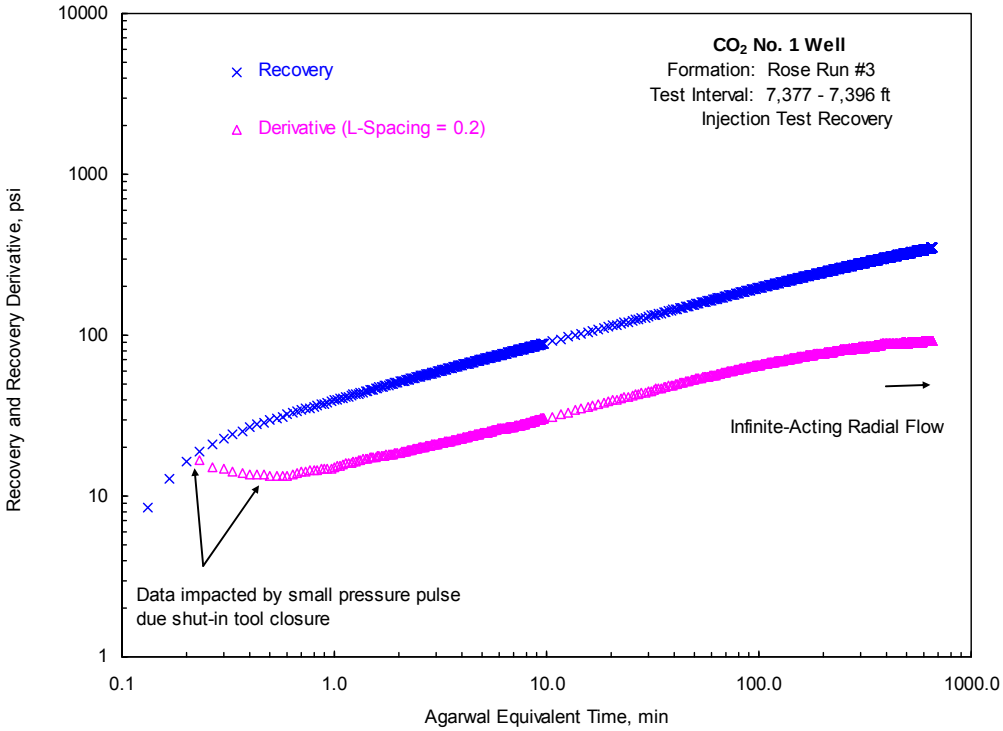

Figure C.26. Diagnostic Derivative Plot Analysis of Injection-Test Recovery: Rose Run #3: 7,377 to 7,396 ft

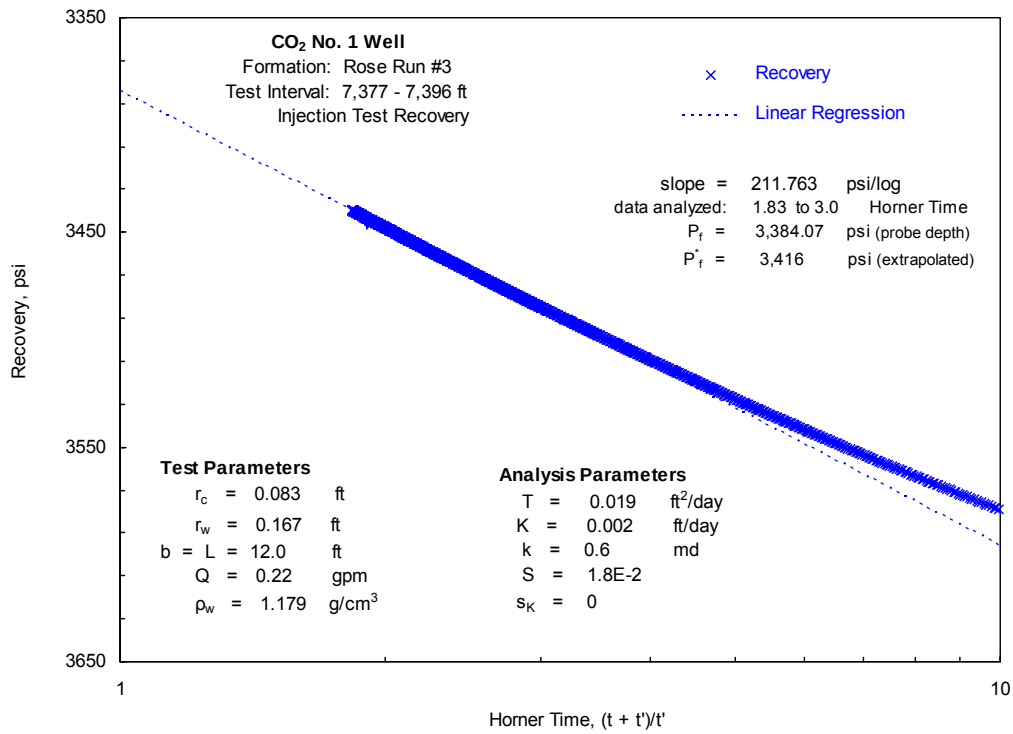

Figure C.27. Horner Plot Analysis of Injection-Test Recovery: Rose Run #3: 7,377 to 7,396 ft

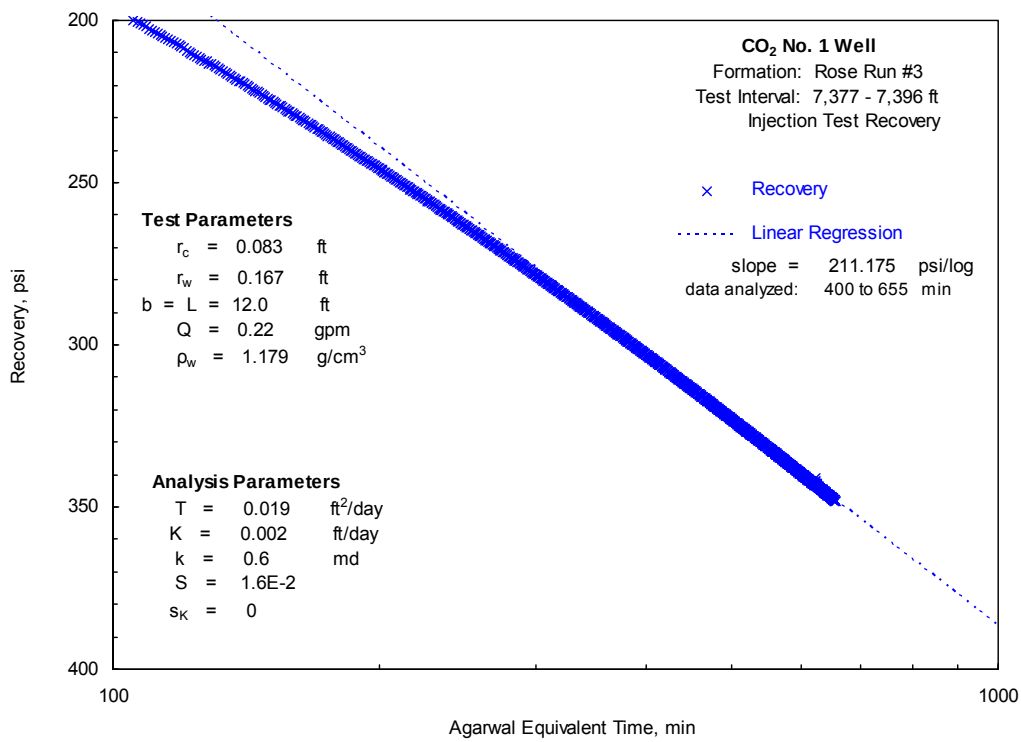

Figure C.28. Semi-Log Plot Analysis of Injection-Test Recovery: Rose Run #3: 7,377 to 7,396 ft

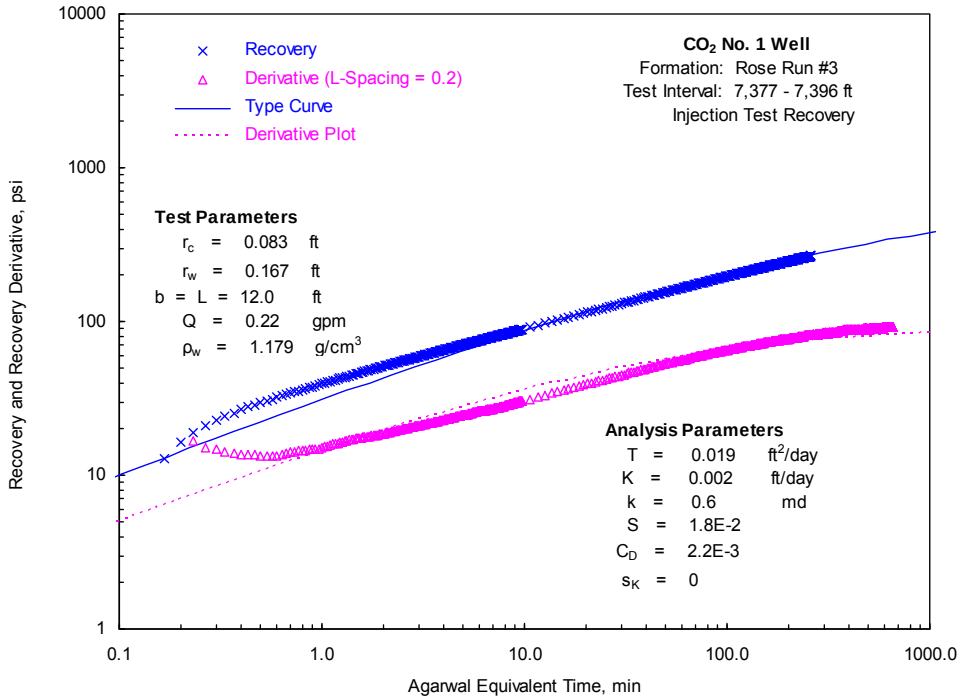

Figure C.29. Composite Type-Curve and Derivative Plot Analysis of Injection-Test Recovery: Rose Run #3: 7,377 to 7,396 ft

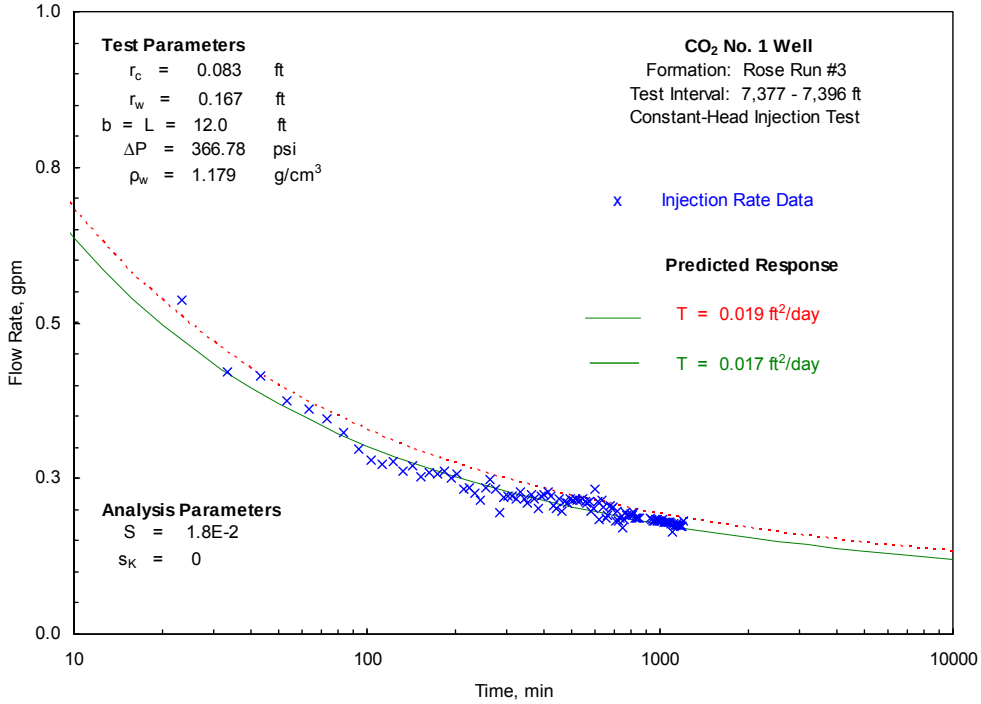

Figure C.30. Injection-Rate Analysis for Constant-Head Injection Test: Rose Run #3: 7,377 to 7,396 ft

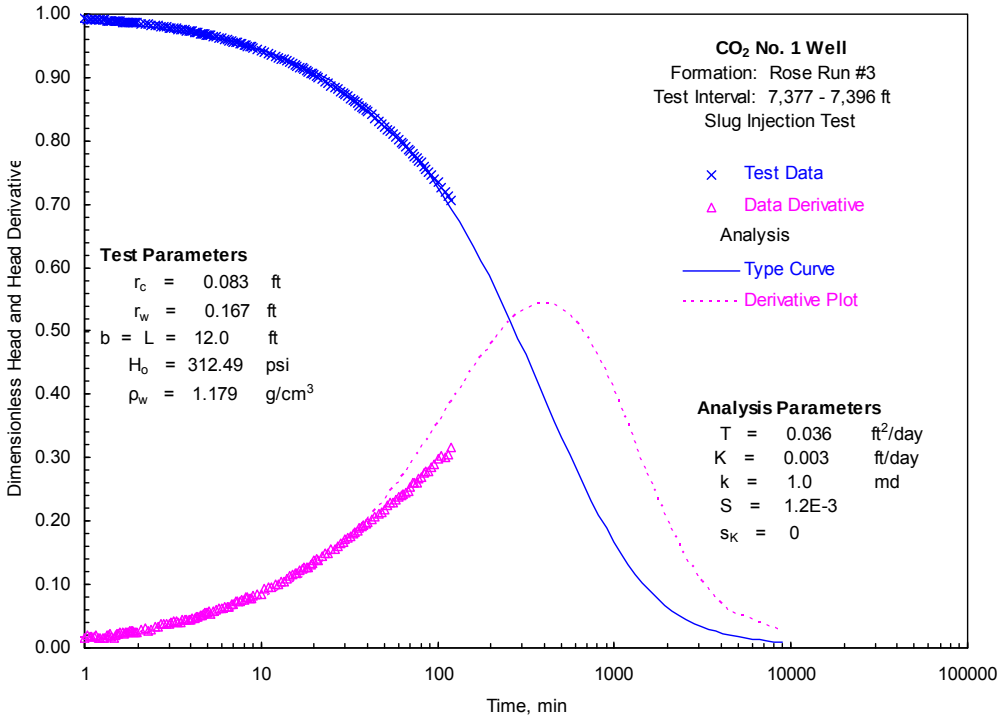

Figure C.31. Composite Type-Curve and Derivative Plot Analysis of Slug Injection Test: Rose Run #3: 7,377 to 7,396 ft

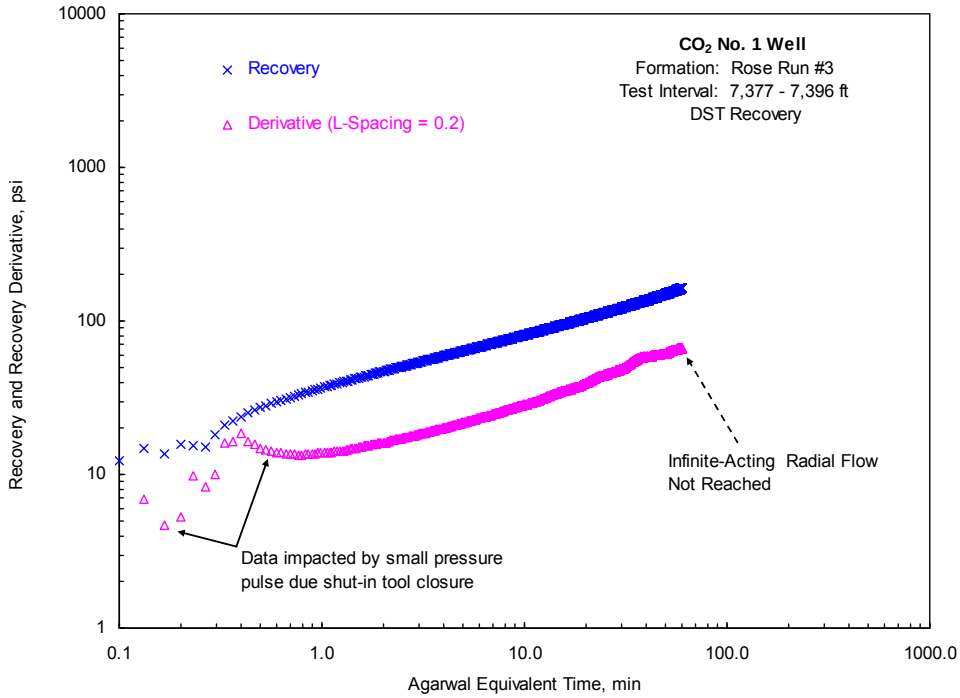

Figure C.32. Diagnostic Derivative Plot Analysis of DST Recovery Test: Rose Run #3: 7,377 to 7,396 ft

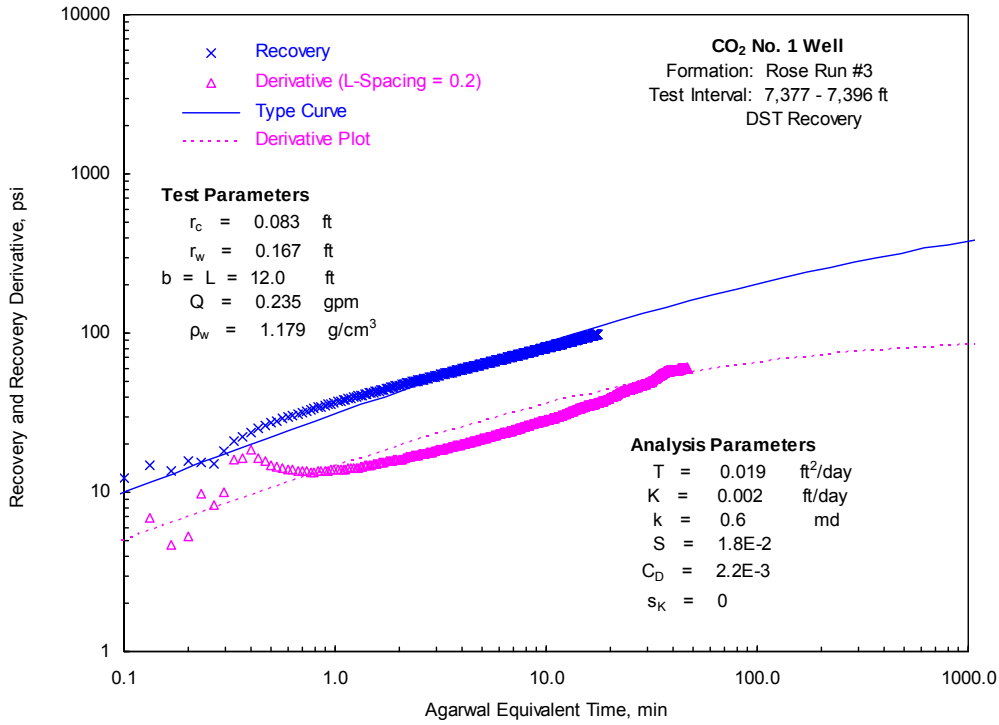

Figure C.33. Corroborative Type Curve and Derivative Plot Analysis of DST Recovery Test: Rose Run #3: 7,377 to 7,396 ft

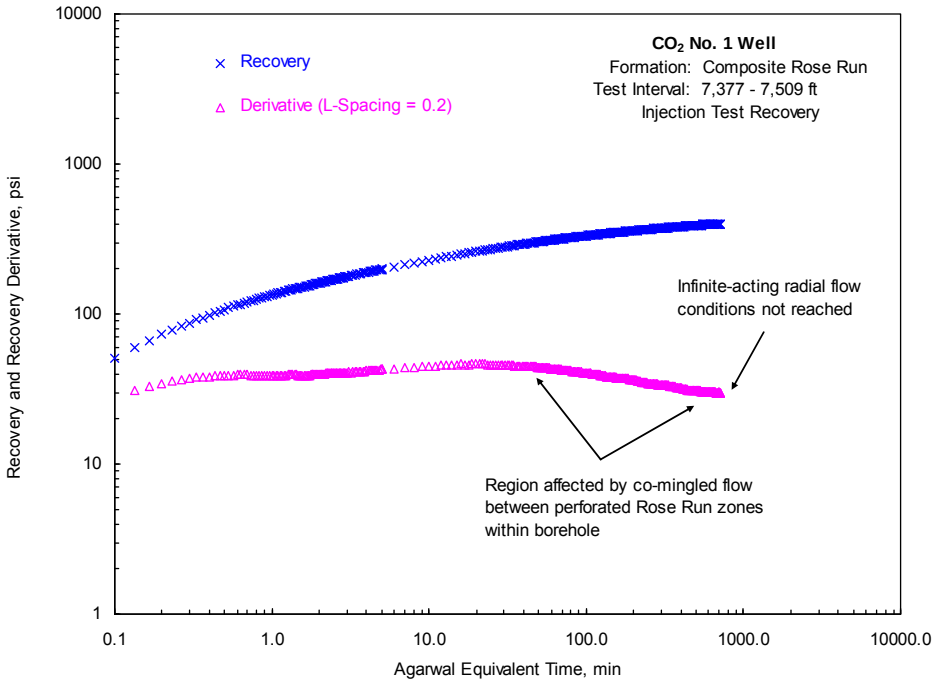

Figure C.34. Diagnostic Derivative Plot Analysis of Injection-Test Recovery: Composite Rose Run: 7,377 to 7,509 ft

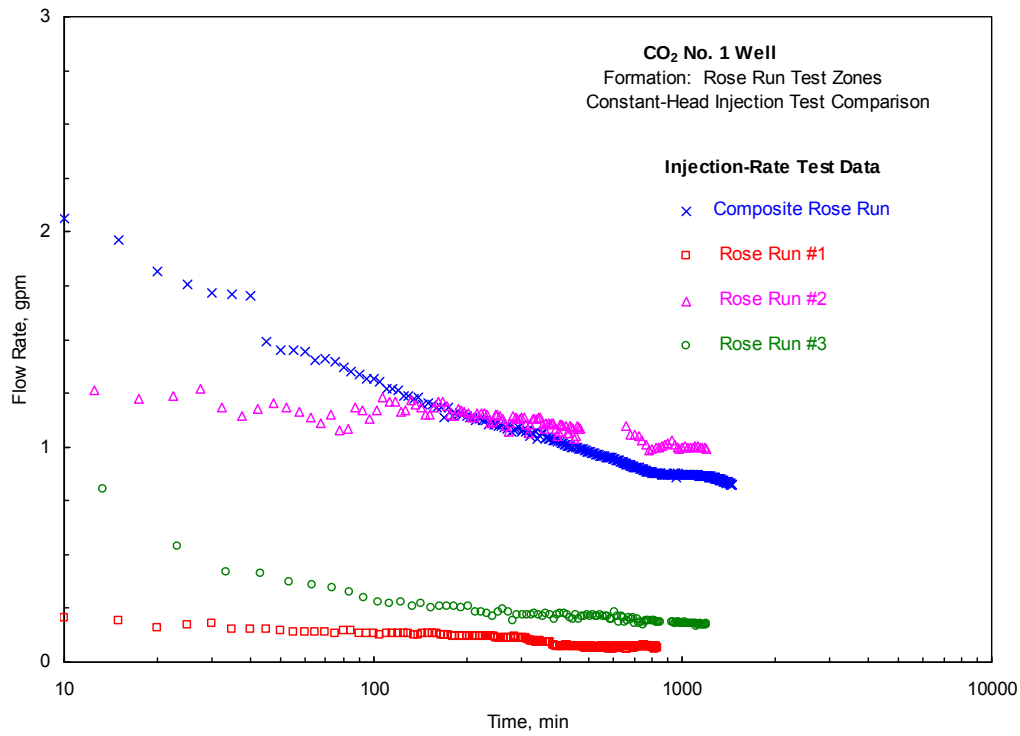

Figure C.35. Rose Run Test Zone Constant-Head Injection-Test Comparison

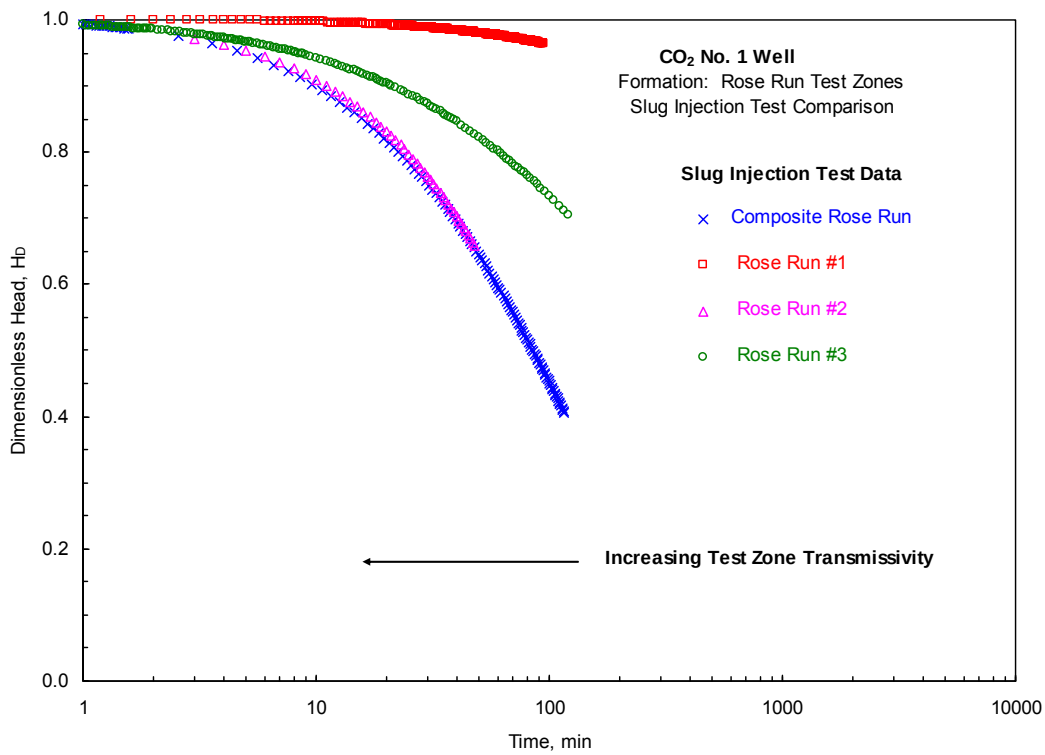

Figure C.36. Rose Run Test Zone Slug-Injection-Test Comparison

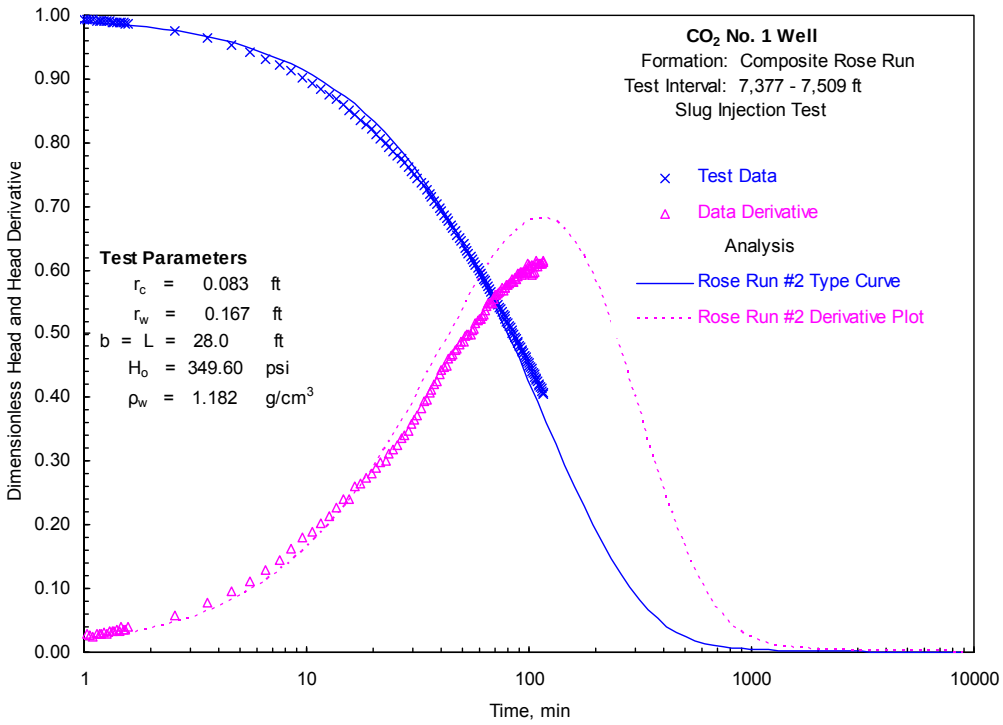

Figure C.37. Composite Type-Curve and Derivative Plot Analysis of Slug Injection Test: Composite Rose Run: 7,377 to 7,509 ft

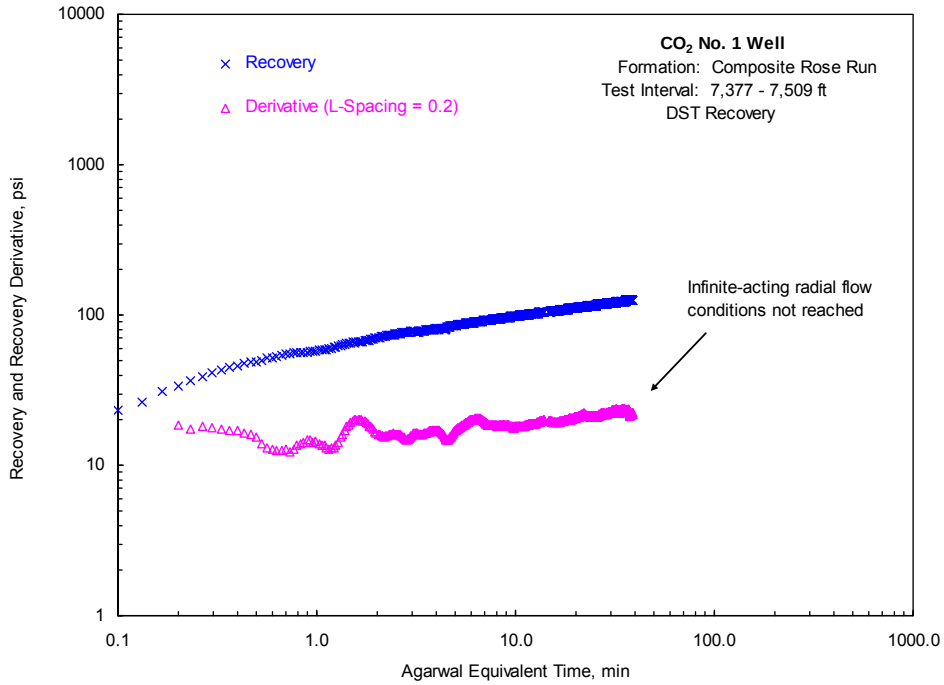

Figure C.38. Diagnostic Derivative Plot Analysis of DST Recovery Test: Composite Rose Run: 7,377 to 7,509 ft

Appendix D

Lower Bridge Plug Pressure Plots for CO_2 No. 1 Well

Appendix D: Lower Bridge Plug Pressure Plots for CO_2 No. 1 Well

D.1 Below Packer Pressure Response During Testing of all Rose Run Test Intervals

D.2 Below Packer Pressure Response During Testing of Rose Run #1

D.3 Below Packer Pressure Response During Testing of Rose Run #2

D.4 Expanded Below Packer Pressure Response During Testing of Rose Run #3

D.5 Below Packer Pressure Response During Testing of the Composite Rose Run

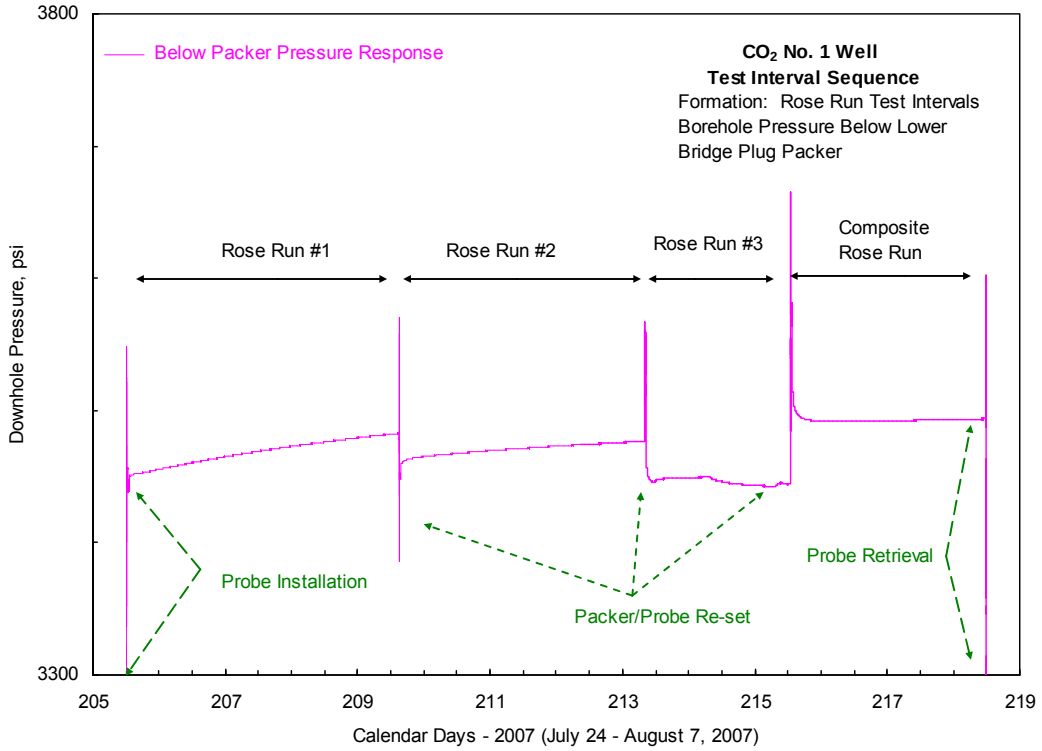

Figure D.1. Below Packer Pressure Response During Testing of all Rose Run Test Intervals

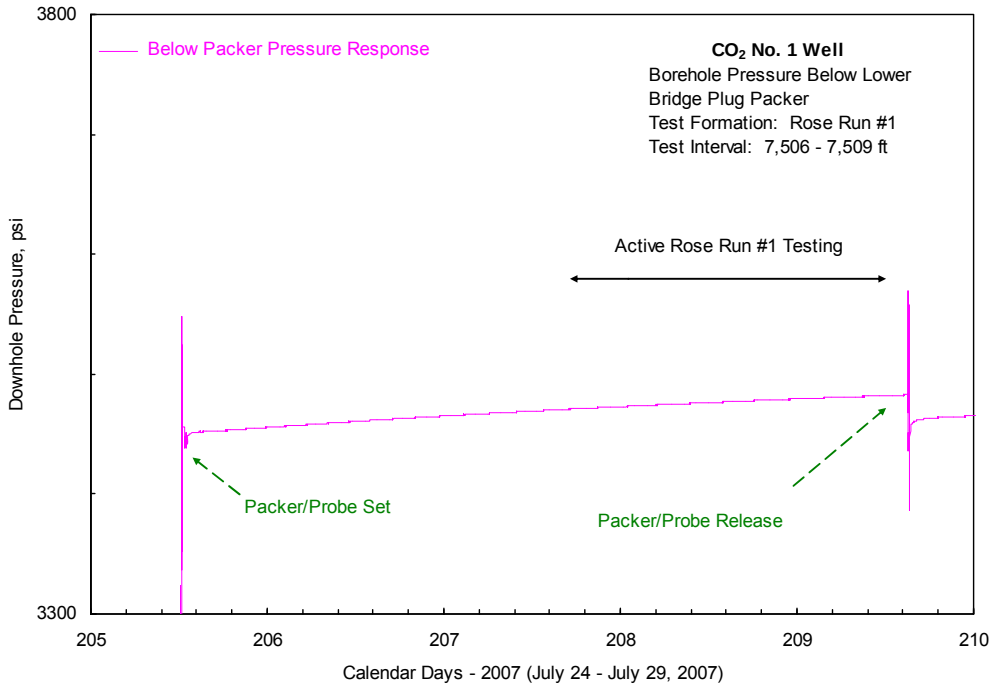

Figure D.2. Below Packer Pressure Response During Testing of all Rose Run #1

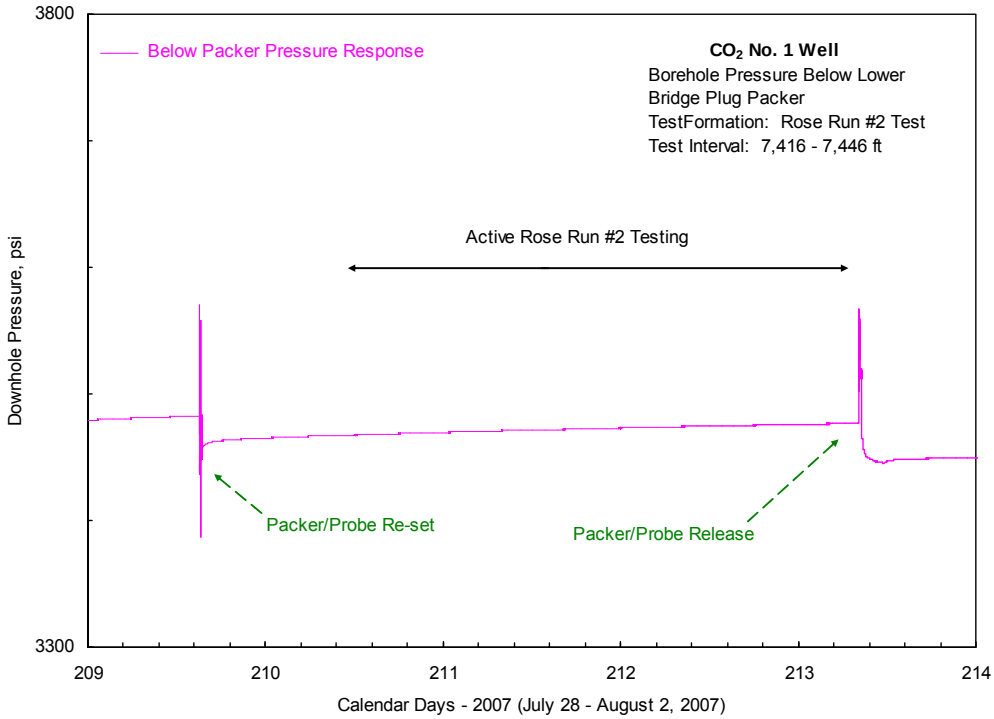

Figure D.3. Below Packer Pressure Response During Testing of all Rose Run #2

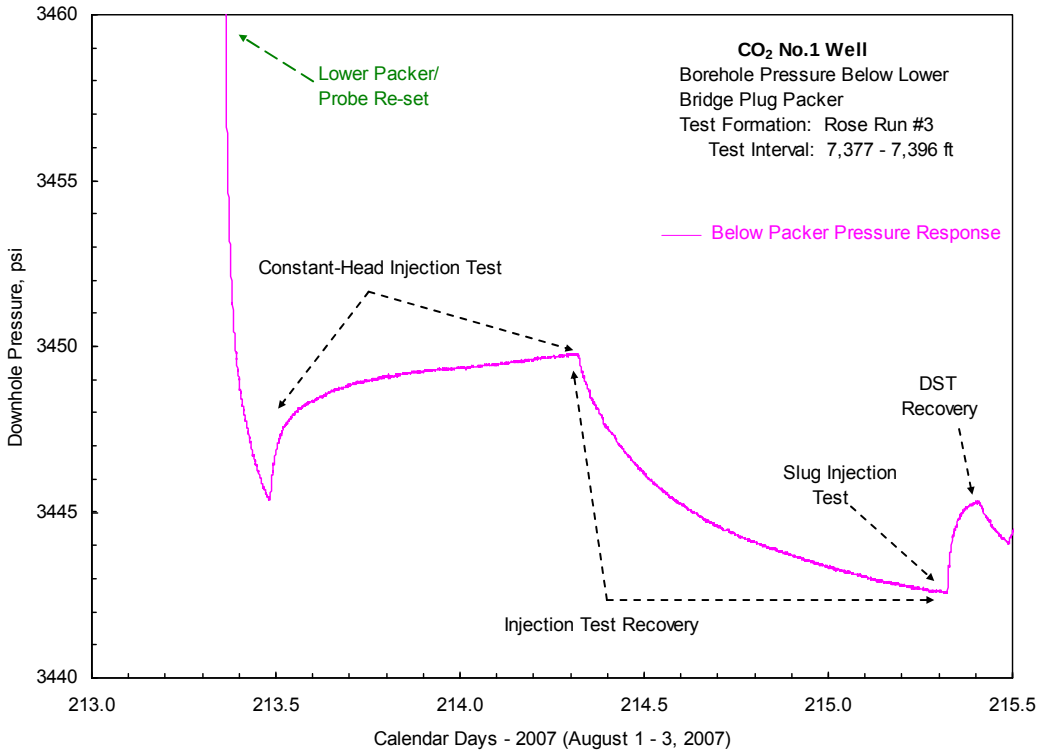

Figure D.4. Expanded Below Packer Pressure Response During Testing of all Rose Run #3

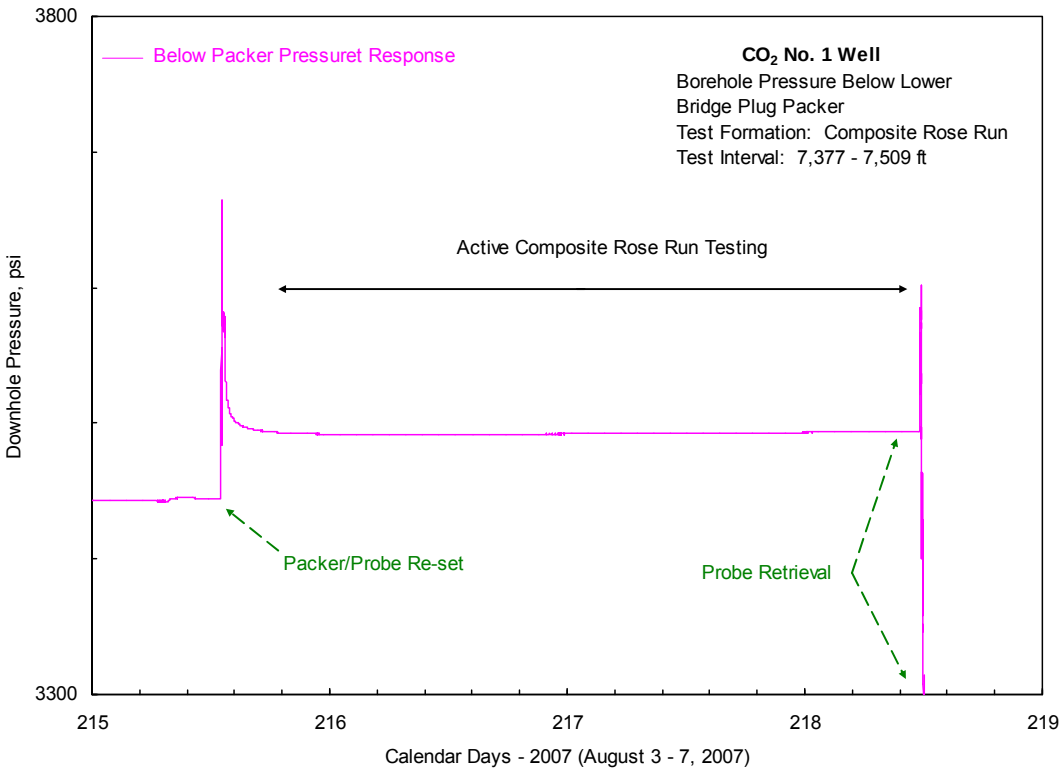

Figure D.5. Below Packer Pressure Response During Testing of the Composite Rose Run

Distribution

HARDCOPY DISTRIBUTION

No. of
Copies

6 Larry Wickstrom
Division Chief and State Geologist
Ohio Division of Geological Survey
2045 Morse Rd., Bldg. C
Columbus, Ohio 43229

ELECTRONIC REPORT DISTRIBUTION LIST

Battelle-Columbus
Dave Ball
balld@battelle.org

Jackie Gerst
GerstJ@battelle.org

Neeraj Gupta
gupta@battelle.org

Erica Howat
HowatE@battelle.org

Danielle Meggyesy
meggyesyd@battelle.org

Joel Sminchak
sminchak@battelle.org

Battelle—Pacific Northwest Division
Robert Dahowski
bob.dahowski@pnl.gov

Pete McGrail
Pete.McGrail@pnl.gov

Frank Spane
frank.spane@pnl.gov

Paul Thorne
paul.thorne@pnl.gov

Ohio Division of Geological Survey
Ron Riley
Ron.Riley@dnr.state.oh.us

Larry Wickstrom
Larry.Wickstrom@dnr.state.oh.us

APPENDIX 5

List of geophysical logs, mud log, and associated files (See DVD for files)

3415725334_DS_SCH_4952_8700_N_136_TH100.tif
3415725334_GR-C-R-L_SCH_128_1187_N_136_BR80.tif
3415725334_GR-C-R-L-AZ_SCH_1200_4950_N_136_BR75.tif
3415725334_GR-C-R-T_SCH_4952_8700_N_136_TH71.tif
3415725334_GR-C-T-D-N-P-PE_SCH_1190_4950_N_136_BR80.tif
3415725334_GR-C-T-D-N-P-PE_SCH_4952_8700_N_136_TH72.tif
3415725334_GR-F_SCH_3100_4900_N_79_TH100.tif
3415725334_GR-PF_SCH_8526_8556_N_NA_TH45.tif
3415725334_GR-S_SCH_4900_8650_N_100_TH100.tif
3415725334_GR-T-C-D-PE-N-P_SCH_128_1210_N_136_BR70.tif
3415725334_GR-T-P-PERM-CMR_SCH_6200_8700_N_136_TH71.tif
3415725334_GR-V-S-T_SCH_6200_8700_N_136_TH72.tif
3415725334_GR-VD-CB-CCL_SCH_6400_8655_N_NA_TH100.tif
3415725334_PR_SCH_4952_8700_N_136_TH72.tif
3415725334_TT-MI_SCH_6200_8700_N_136_TH100.tif
3415725334_Battelle_Ohio-Geological-Survey_CO2-1_CMR_Elan_out2.las
3415725334.las
MAIN_CMR_096LUP.DLIS
MAIN_FMI_DSI_124LUP.DLIS

- **Mudlog**
  - OhGeolSurv#1CO2MudLog.xls
  - OhGeolSurv#1CO2MudLogPart2.xls
- **pds**
  - Battelle_Ohio-Geological-Survey_CO2-1_CMR_Elan_montage_ondep.pds
  - Battelle_Ohio-Geological-Survey_CO2-1_FracCADE_4930-3090.pds
  - Battelle_Ohio-Geological-Survey_CO2-1_FracCADE_ondepth.pds
  - Battelle_Ohio-Geological-Survey_CO2-1_OH-Composite-4930-3090.pds
  - Battelle_Ohio-Geological-Survey_CO2-1_Sonic_4930-3090.pds
  - Battelle_Ohio-Geological-Survey_CO2-1_Sonic_LQC-4930-3090.pds
  - Battelle_Ohio-Geological-Survey_CO2-1_Sonic_ondepth.pds
  - OCDO1 Perfs DAY 21.PDS

Pressure express_battelle_ohio_geological_survey_co2_1_assembled_doccument.pdf